



# Thèse de Doctorat

*Mention Sciences agronomiques et écologiques  
Spécialité Sciences de la mer : biologie et écologie*

présentée à l'*Ecole Doctorale en Sciences Technologie et Santé (ED 585)*

de l'**Université du Littoral Côte d'Opale**

par

**Carolin Julie Neven**

pour obtenir le grade de Docteur de l'Université du Littoral Côte d'Opale

*Different perspectives on zooplankton functioning in the Southern North Sea and the English Channel in relation to lower and higher trophic levels*

Soutenue le 13.12.2024, après avis des rapporteurs, devant le jury d'examen :

M<sup>me</sup> Lidia Yebra, Professeur HDR,  
Instituto Español de Oceanografía  
M. Christophe Lebigre, Cadre Scientifique, HDR, Ifremer  
M. Lars Stemmann, Professeur, Sorbonne Université  
M. Rachid Amara, Professeur, Université du  
Littoral Côte d'Opale  
M. Paul Marchal, Professeur, Ifremer  
M<sup>me</sup> Carolina Giraldo, Cadre de Recherche, Ifremer

Rapporteur  
Rapporteur  
Examineur  
Président du Jury  
Directeur de thèse  
Co-directrice de thèse





## Acknowledgments

This thesis was founded by the Ifremer Scientific Direction through the project "FORESEA" and the research allocation flagship program from the region Hauts de France, who I would like to thank. In this context, I would like to especially thank Mathieu Doray who coordinates the FORESEA project, that also facilitated me the participation at the ICES Zooplankton Production Symposium in Hobart, Tasmania that was an experience that I highly appreciated. I would like to further express my gratitude to the research federation "SFR Campus de la mer" and the graduate school IFSEA that benefits from a France 2030 grant (ANR-21-EXES-0011) operated by the French National Research Agency for financing the stable isotope analysis (SFR Campus de la mer) and the participation at a formation in statistics (SFR Campus de la mer, IFSEA).

Merci à vous Carolina et Paul d'avoir m'accepter en thèse au début, pour votre accompagnement et pour avoir toujours été très humaine. J'ai beaucoup apprécié votre façon à pas mettre trop de pression, que vous été toujours disponible et qu'on a toujours pu parler pour résoudre de situations compliquées. Merci pour ces trois ans et pour avoir m'aider à avancer et me développer scientifiquement !

Je voudrais également remercier Philippe Soudant pour avoir été mon encadrant en distance. Merci pour tes commentaires et ton input !

Merci aussi à ceux qui on s'engagé pour mon Comité de Suivi de Thèse. Merci pour votre temps et vos conseils : Sébastien Lefebvre, Philippe Koubbi, Fabrice Pernet, Inga Kirstein, Cédric Meunier, Eric Goberville, Christophe Loots et Marie Vagner.

Je voudrais également remercier tout le labo, pour ces trois ans agréables. Merci pour votre accueil, pour être toujours prêt à aider dans des moments dans lesquelles j'ai me battu avec l'administration française, j'ai eu besoin d'une traduction, d'une fourrure pour le carnaval ou j'ai eu autres petites questions. J'ai beaucoup apprécié le moment des horoscopes pendant les pauses café, les pots (un truc génial qui n'existe pas comme ça en Allemagne) et les batailles dans le couloir. Merci d'avoir pris en compte ma barrière de langue et d'avoir

m'appris des belles expressions françaises ! Merci aussi pour ton effort Clémence de pratiquer l'Allemand et à toi Dudus pour avoir fait tomber chaque jour plusieurs fois mon stylo !

Merci à toi Kirsteen, que t'a toujours pris le temps pour discuter et pour me monter le moral quand ça allé pas. Vive les aquariums !!!!

Merci Arnaud et Ghassen pour me partager vos expériences et connaissance ! J'ai beaucoup aimé discuter avec vous et nos échanges ! Je te remercie aussi Ghassen d'avoir m'a laisser utiliser ton algorithme évolutionnaire qui m'a débloqué pendant les travaux pour mon premier chapitre !

Aussi merci à toi Christophe pour avoir m'accepter dans ton labo et pour avoir réagi dans une façon super dans le moment des e-mails concernant le bien-être des poissons !

Sébastien, merci à toi pour avoir t'impliquer autant dans ma thèse, pour tes suggestions, nos discussions et pour ton temps !

Merci aussi aux participants des campagnes IBTS 2008, 2021, 2022 et de la CGFS 2021 qui étaient impliqué dans la collecte de mes échantillons ! Dans ce contexte, un grand merci à Elvire Antajan, Alice Delegrange, Adeline Le Bris, Vincent Cornille, Stéphanie Lelièvre, Josselin Caboche, Valérie Lefebvre qui ont facilité la détermination de mesozooplankton and ichthyoplankton de la IBTS 2008, 2021 et 2022 et CGFS 2021. Également merci à Camille Blondel et Vincent Duquesne qui ont analysé les nutriments dessous, le POM et le chlorophylle a. Clémence Couvreur et Rémy Cordier, merci pour la préparation d'échantillons des isotope stables ! L'analyse des lipides n'aurait pas été possible sans l'aide précieuse de Claudie Quere et Valérian Le Roy.

Merci pour les discussions qui m'ont aidé à développer le première chapitre : merci à Arnaud Auber, David Devreker, Mathieu Doray, Philippe Koubbi et Eric Goberville ! Également merci à Kirsteen MacKenzie, Alain Lefebvre and David Devreker par rapport à nos discussions qui ont aidé à développer le deuxième chapitre et à Philippe Soudant et Fabrice Pernet pour votre collaboration et input par rapport tout ce qui concerne les acides gras (troisième chapitre) !

Quand j'ai commencé ma thèse j'ai pensé que je connaissais R. Au moins un petit peu. Après j'ai me rendu compte que qu'est-ce que j'ai connu c'était ggplot2. Dans ce contexte, je te remercie énormément Stéphane Karasiewicz pour avoir m'apprié comment coder en R, comment trouble shoot et comment organiser ses scripts, outputs etc. Sans ton accompagnement au début, je ne sais pas comment j'aurais fait. Dans ce contexte aussi merci à vous Paul et Carolina pour avoir initié cet accompagnement, c'était vraiment super !

Parlons on du R et de stat, je voudrais te dire une grand merci Raphael Girardin pour prendre le temps de me dépanner plein de fois, pour regarder avec moi les détails des GLM, GLMM, GAM et GAMM et pour être dispo pour tous ces questions autour ces modèles !!!

Une circonstance que j'ai beaucoup apprécié pendant ma thèse c'est d'être si proche au Laboratoire Environment Ressources. Merci beaucoup à vous, Alain Lefebvre, David Devreker et Guillaume Wacquet pour notre collaborations et discussions qui m'ont permis d'intégrer le phytoplancton dans cette thèse, un fait que j'ai beaucoup apprécié.

Une personne qui était vraiment très importante dans ces trois années de thèse surtout au début, c'était toi Lola. Merci beaucoup pour toute ton aide, pour m'expliquer toutes les choses administratives pendant mon début en France, pour tes conseille qui m'ont beaucoup servie pendant ces trois années et pour ton amitié, le café après le marché et les soirées aux Vieux Singe !

Fedi, although you have been far away, you have been with me especially during the moments that have been very difficult. Ich möchte dir von ganzem Herzen dafür danken. Auch für deine Heiterkeit und deine Verrücktheit! Ich hoffe, in den Jahren die da kommen, haben wir mehr Zeit, die freudigen Zeiten des Lebens zusammen zu geniessen!

Marvin, ich hab dich lieb! Danke, dass du immer da bist, egal wann und wofür, für deinen Humor, deine Verplantheit und dein grosses Herz!

Marvin, Manuel, Elena, danke für eure Freundschaft, dass ich weiss, dass wir uns sehen, wenn ich nach Mühleim komme und dass ich auf euch zählen kann, wenn es hart auf hart kommt!

Merci, aussi à vous Maia, Momo, Line, Sarah et Elise. Je suis très contente d'avoir vous rencontré et les moments qu'on a passé ensemble ce dernier temps m'ont fait beaucoup du bien dans un moment qui n'était pas facile.

Danke an euch Hanni und Andrea, die ihr mir immer eine Unterstützung gewesen seid in all den Jahren während meines Studiums. Es ist mir eine enorme Hilfe zu Wissen, dass ich immer zu euch kommen kann, wenn mir nach Meer ist und mich die Fluchtgedanken packen! Danke!

Last but not least, je voudrais remercier mes parents, qui étaient toujours là pour moi et qui me soutient n'importe lequel chemin je choisis. Surtout à toi maman, je ne sais pas si j'aurais eu le déclic pour ma discussion générale sans nos discussions !

Am Ende möchte ich vor allem euch danken, Mama und Papa. Danke für eure Unterstützung in diesen drei herausfordernden Jahren, dafür, dass ihr mich bei allem unterstützt was ich mir vornehme, dass ihr mich auffangt, ich immer nach Hause kommen kann und vor allem für eure Geduld und Liebe in diesen letzten Monaten!

***“The first law of ecology is  
that everything is connected to everything.”***

In “The Closing Circle”,

Barry Commoner (1971)

# Table of contents

Table of contents.....	i
List of Figures and Tables .....	v
Figures.....	v
Tables.....	xiii
List of Abbreviations.....	xv
General Introduction.....	1
Understanding of ecosystem functioning .....	1
The role of plankton in marine ecosystem functioning .....	2
Need for understanding of zooplankton functioning in the context of climate change.....	5
Studying zooplankton functioning in the ecosystem .....	6
Study area.....	8
North Sea .....	9
English Channel.....	13
Higher trophic levels.....	14
Herring.....	14
Sardine.....	19
Plaice.....	24
Several perspectives of zooplankton diversity in the context of MBEF.....	28
CHAPTER 1 - 1. Perspective – Taxonomical composition.....	31
1.1 Introduction.....	32
1.2 Materials & Methods.....	36
1.2.1 Data .....	36
1.2.2 Data projection on an optimized grid .....	40
1.2.3 Determining assemblages by means of fuzzy clustering .....	44
1.2.4 Environmental drivers of taxa distribution .....	50
1.2.5 Inter-annual comparison.....	51



1.3	Results.....	52
1.3.1	PCA on potential abiotic and biotic drivers.....	52
1.3.2	Characterization of the assemblages found.....	54
1.3.3	Inter-annual comparison between zooplankton assemblages in relation to the SNS-EEC environment.....	63
1.4	Discussion .....	67
1.4.1	Zooplankton assemblages and environmental conditions .....	67
1.4.2	Inter-annual changes in zooplankton assemblages .....	76
1.5	Conclusion .....	77
CHAPTER 2 - 2. Perspective – Size structure .....		79
2.1.	Introduction .....	81
2.2.	Materials & Methods.....	85
2.2.1.	Sampling .....	85
2.2.2.	Isotope analysis .....	86
2.2.3.	Statistical analysis.....	87
2.3.	Results.....	91
2.3.1.	Environmental conditions .....	91
2.3.2.	Size structuration planktonic food web .....	92
2.3.3.	Predicted values of planktonic size classes .....	93
2.3.4.	Proportion of different plankton size classes to larval diet .....	97
2.4.	Discussion .....	101
2.4.1.	Structuration of the planktonic food web in the EEC during winter .....	101
2.4.2.	Feeding regime of herring and plaice larvae.....	104
2.4.3.	Herring larvae .....	105
2.4.4.	Plaice larvae.....	107
2.5.	Perspectives.....	110
2.5.1.	Biological perspectives .....	110

2.5.2.	Further refinements .....	111
2.5.3.	Additional analysis.....	111
2.6.	Conclusion .....	112
CHAPTER 3 - 3. Perspective – Biochemical composition .....		113
3.1.	Introduction .....	115
3.2.	Materials & Methods.....	118
3.2.1.	Sampling .....	118
3.2.2.	Lipid analysis.....	119
3.2.3.	Phytoplankton community composition.....	122
3.2.4.	Zooplankton community composition .....	122
3.2.5.	Statistical analyses.....	123
3.3.	Results.....	125
3.3.1.	Biological parameters of sardines .....	125
3.3.2.	Taxonomic composition of zoo- and phytoplankton .....	126
3.3.3.	Spatial pattern of the FA profile of zooplankton and sardine .....	128
3.3.4.	Spatial segregation patterns .....	130
3.3.5.	Factors influencing trophic transfer of EFA.....	131
3.4.	Discussion .....	134
3.4.1.	Potential drivers of spatial variability of FA profiles - plankton community composition and biological parameters of sardines .....	135
3.4.2.	Spatial variability in FA profiles of zooplankton and sardine.....	136
3.4.3.	Factors influencing the trophic transfer of EFA .....	138
3.4.4.	Spatial separation of sardines in the English Channel .....	141
3.5.	Conclusion .....	143
General Discussion .....		145
4.1	Insights and possible inferences from multitrophic spatial variation .....	146
4.2	From nutrients to higher trophic levels - The planktonic food web .....	148

4.3	Implication of spatial variation for modelling .....	150
4.3.1	Traits.....	152
4.4	Conclusion .....	154
	References.....	156
	French Summary - Résumé .....	clxxxvii
	Appendix.....	ccii
	List of Figures Appendix.....	ccii
	List of Tables Appendix.....	ccix
	Appendix I – Chapter 1.....	ccxi
	Appendix II – Chapter 2.....	ccxxvi
	Appendix III – Chapter 3.....	ccxxxvii
3.1	Phytoplankton community composition .....	ccxxxvii
3.2	GLMM sardine morphological and physiological parameters. ....	ccxxxviii
3.2.1	Verification .....	ccxxxviii
3.2.2	Summary results.....	ccxlv
3.3	Differences in environmental parameters between the basins.....	ccxlvii
3.4	GLMM and GAM to evaluate factors influencing trophic transfer - Model selection process.....	ccxlviii
3.4.1	EPA.....	ccxlviii
3.4.2	DHA.....	cclviii
3.4.3	ARA .....	cclxvii
3.5	Principal Component Analysis Zooplankton (PCA).....	cclxxvi
3.6	Complete FA profiles of zooplankton and sardine .....	cclxxvi
3.7	Phytoplankton community .....	cclxxx

# List of Figures and Tables

## Figures

**Figure 1 Role of zooplankton in marine ecosystems and resulting ecosystem services.** By feeding on phytoplankton and microplankton zooplankton channels energy to small pelagic fish that in turn transfer energy and nutrients to higher trophic levels like piscivorous fish and marine mammals. Furthermore, sinking carcasses and fecal pellets are an energy source for benthic communities. This central role in the energy transfer makes zooplankton a crucial part for the ecosystem service food production, which is indicated in the schema with a “1”. Zooplankton contribute to carbon export to the deep sea which functions as potential carbon sink, by the excretion of fecal pellets, sinking of carcasses, diurnal vertical migration and by facilitating the existence of subsequent trophic levels that themselves might export carbon due to sinking carcasses. Thus, zooplankton contribute to climate regulation indicated with a “2”. Excretion of nutrients like dissolved organic carbon and nitrogen and ammonium as well as decomposition of zooplankton fecal pellets by bacteria contribute to nutrient recycling that in turn promotes primary production. This ecosystem service is indicated with a “3”. All silhouette pictures used were obtained from <https://www.phylopic.org/>. The chlorophyte silhouette was created by Sergio A. Muñoz-Gomez and of *Mytilus* spp. by Harold N. Eyster. . 3

**Figure 2 Plankton classed by size.** Silhouette images used in this figure were obtained from <https://www.phylopic.org/>. The amphipod silhouette (mesoplankton) was created by Collin Gross..... 4

**Figure 3 Bathymetric map of study area (English Channel and Southern North Sea) in a bigger spatial context.** Pointed line indicates transition between Northern and Southern North Sea. .... 9

**Figure 4 Circulation pattern of different water masses of the North Sea.** Blue names indicate rivers, red names indicate orientation points to divide the North Sea in a Southern and a Northern part. Adapted from OSPAR Commission (2000)..... 10

**Figure 5 English Channel.** Bathymetric map of the English Channel. Blue names indicate rivers terminating in the Eastern English Channel. Arrow indicates main flow direction from the Celtic Sea towards the Dover Strait. .... 13

**Figure 6 Adult Herring (*Clupea harengus*).** Photograph Pierre Porché, Ifremer. .... 14

**Figure 7 Feeding, spawning and nursery areas of Autumn Spawning North Sea Herring.** A: Drifting routes of herring larvae from the spawning grounds of the different spawning components in the northwestern, western and southern North Sea to the main nursery areas in the eastern North Sea. Adapted from Corten (2013); B: Annual migration of adult herring between feeding and spawning areas. Red arrow indicates migration route of Downs herring. Adapted from Corten (2001)..... 15

**Figure 8 Larvae of herring (*Clupea harengus*) of stage 1 to 4.** Stage 1: yolk sac stage, stage 2: pre-flexion stage, stage 3: flexion stage, stage 4: post flexion. Graphic from Joly et al. (2021). ..... 16

**Figure 9 Stock development over time for North Sea Autumn Spawning Herring in Subarea 4 and divisions 3.4 and 7.d.** Fishing pressure above the  $F_{MSY}$  indicates overexploitation of the stock. Spawning stock biomass (SSB) below  $MSY B$  trigger indicates the SSB being too low for the stock to be in a good ecological state. Adapted from ICES (2024a)..... 18

**Figure 10 Adult sardine (*Sardina pilchardus*).** Photograph Ifremer. .... 19

**Figure 11 A: European North Atlantic sardine stocks.** Adapted from ICES (2022a); B: Egg abundance in eggs/10 m<sup>3</sup> obtained from the surveys EVHOE (Bay of Biscay) and CGFS (English Channel) conducted by Ifremer in 2019. Graphic from <https://campagnes.flotteoceanographique.fr/series/11/>; C: Distribution of juvenile sardines of the Northern stock. Graphic from Campanella and van der Kooij (2021)..... 20

**Figure 12 Stock development over time of sardine (*Sardina pilchardus*) in Subarea 7 (Southern Celtic Seas and English Channel).** Upper panel: Catches since 2002, including catches below minimum size (BMS) and discards; lower panel: Biomass index obtained from the PELTIC survey (Western English Channel). Horizontal orange lines indicate biomass index for 2023 and the average for 2021 – 2022. Adapted from ICES (2024c)..... 23

**Figure 13 Adult plaice (*Pleuronectes platessa*).** Photograph Pierre Porché, Ifremer. .... 24

**Figure 14 Approximate position of spawning grounds of plaice (*Pleuronectes platessa*) in the Eastern English Channel and the Southern North Sea reflected by egg abundance.** Graphic from Bolle et al. (2009)..... 25

**Figure 15 Larvae of plaice (*Pleuronectes platessa*) at different developmental stages.** Stage 1: yolk sac stage, stage 2 pre-flexion stage, stage 3: post-flexion stage, stage 4: metamorphosis, juvenile. Photographs Michele Pernak. .... 26

**Figure 16 Stock development over time for plaice in the Eastern English Channel (Division 7.d).** Fishing pressure above the  $F_{MSY}$  indicates overexploitation of the stock. Spawning stock biomass (SSB) below MSY B trigger indicates the SSB being too low for the stock to be in a good ecological state. Adapted from ICES (2024d)..... 27

**Figure 17 Stock development over time for North Sea plaice (Subarea 4 and Subdivision 20).** Fishing pressure above the  $F_{MSY}$  indicates overexploitation of the stock. Spawning stock biomass (SSB) below MSY B trigger indicates the SSB being too low for the stock to be in a good ecological state. Adapted from ICES (2024e)..... 28

**Figure 18 IBTS sampling stations.** A: Mesozooplankton (IBTS 2008), black dots indicate locations delineating the geographical distinction between the Southern and Northern North Sea, furthermore the position of the sandbank Dogger Bank is indicated; B: Fish larvae (IBTS 2008); C: Fish eggs (IBTS 2008); D: Mesozooplankton (IBTS 2022); E: Fish larvae (IBTS 2022). ..... 37

**Figure 19 Number of sampling stations per cell for the 2008 dataset.** A: Grid with the optimal grid cell size of 0.83 x 0.83 degrees; B: Number of sampling stations for mesozooplankton per grid cell; C: Number of sampling stations for fish larvae per grid cell; D: Number of sampling stations for fish eggs per grid cell; E: Number of sampling stations salinity, temperature and depth; F: Number of sampling stations of water samples for phytoplankton community analysis; G: water samples for concentration of material in suspension and chlorophyll a. .. 43

**Figure 20 Overview steps for assemblage definition.** ..... 46

**Figure 21 Highest membership values per cell of clustering using different k.** Fuzzy clustering evaluates the strength of affiliation of a cell to each cluster, which is expressed by a membership value. High membership values indicate coherent regions, low membership values indicate regions of low coherence. A,B: three clusters (maximized silhouette width), C,D: four clusters (minimized Kelly-Gardner-Sutcliffe penalty and maximized Mantel correlation), E,F: five clusters (quasi minimized Kelly-Gardner-Sutcliffe penalty, quasi maximized Mantel correlation and quasi maximized silhouette width). ..... 49

**Figure 22 Potential drivers of zooplankton assemblages.** A: Abiotic parameters displayed in a two-dimensional space constituted by the first and second dimensions of the PCA; B: Values of coordinates of first dimension of the PCA on abiotic parameters per grid cell. The more positive a value the higher the concentration of nutrients, and the lower temperature, depth and salinity and vice versa; C: Values of coordinates of second dimension of the PCA on abiotic

parameters per grid cell; D: Phyto- and microplankton displayed in a two-dimensional space constituted by the first and second dimensions of the PCA; E: Values of coordinates of first dimension of the PCA on phyto-microplankton per grid cell. High values indicate high proportion of nanoflagellates and others (*Phaeocystis globosa*, *Heterosigma* spp., *Eutreptiella* spp., *Mediophyceae*, *Crysohyceae* and *Cryptophyceae*), low values indicate high importance of diatoms; F: Total abundance of phyto- and microplankton per grid cell. .... 53

**Figure 23 Assemblages and total zooplankton abundance.** A: Clusters/assemblages based on mesozooplankton and ichthyoplankton sampled during the International Bottom Trawl survey in January and February 2008; B: Indicator species per cluster/assemblage with respective indicator value and adjusted p-value; C: Total mean abundance of zooplankton (meso- and ichthyoplankton) per grid cell. .... 54

**Figure 24 PCA applied to zooplankton taxa.** A: Taxa displayed in a two-dimensional space of the PCA; B: Assemblages/cluster displayed in the same two-dimensional space as in A. Numbers indicate grid cell ID. .... 55

**Figure 25 Proportional taxa composition per assemblage.** Each bar corresponds to an assemblage: C-T: Channel-Thames assemblage. R-Sch: Rhein-Scheldt assemblage; GB-N: German Bight-Norfolk assemblage; Central: Central assemblage; N-Bc: Northern-British coast assemblage. A: Mesozooplankton; B: Fish larvae other than herring; C: Herring larvae; D: Fish eggs..... 57

**Figure 26 Mean abundance of the most important taxa per cluster.** From left to right: mesozooplankton, fish larvae other than herring, three different size classes of herring larvae, and fish eggs. Each row represents one assemblage. Only the most structuring taxa were displayed (excluded taxa: *Centropages* spp., *Euterpina* spp., *Lotidae* (eggs) and *Solea solea* (eggs)). .... 58

**Figure 27 Zooplankton assemblages using the 2008 data and the small sampling extent.** . 63

**Figure 28 Comparison of relative community composition between 2008 and 2022 in the clustering output from 2008 (Figure 27).** Fish larvae are displayed in two lines with the line positioned in the middle displaying all fish larvae other than herring larvae and the lowest line representing herring larvae of three different size classes. .... 64

**Figure 29 Difference in abundance between 2008 and 2022 per grid cell.** Abundance in 2008 was subtracted from abundance in 2022 per cell. A: Heatmap displaying increase or decrease per taxon and cell. Difference in abundance of mesozooplankton in ind/m<sup>3</sup>. Difference in

abundance of fish larvae in ind/1000m<sup>3</sup>; B: Difference of total abundance of mesozoo- and ichthyoplankton per grid cell. .... 66

**Figure 30 Anomaly analysis.** A: Temperature; B: Salinity; C: Chlorophyll a concentration; D: Herring larvae density index in billions per area. Measurements were taken in the area between 49°N and 55°N during January and February. .... 67

**Figure 31 Sampling stations.** A: Sampling stations of herring larvae (blue squares), plaice larvae (yellow dots) and different plankton size classes (red triangles). Blue names indicate the location of the rivers terminating in the EEC; B: Sampling stations for temperature, salinity and depth. .... 86

**Figure 32 Environmental parameters.** A: Surface temperature; B: Surface salinity, C: Depth. .... 91

**Figure 33 Biplot of carbon ( $\delta^{13}\text{C}$ ) and nitrogen ( $\delta^{15}\text{N}$ ) stable isotope signatures for different plankton size classes and fish larvae.** A: Mean and standard deviation per size class and larval species; B: Raw values per sampling station (one sample per station and plankton size class and between 8 to 10 larvae per station)..... 93

**Figure 34 Predicted values of  $\delta^{13}\text{C}$  by the gam\_micro\_carbon model.** Map displays predicted values at nano-microplankton sampling stations. .... 95

**Figure 35 Predicted values of  $\delta^{15}\text{N}$  by the gam\_micro\_nitrogen model.** Map displays predicted values at nano-microplankton sampling stations..... 96

**Figure 36 Predicted values of  $\delta^{15}\text{N}$  and  $\delta^{13}\text{C}$ .** A: Predictions of the gam\_meso\_nitrogen model. Maps display predicted values at nano-microplankton sampling stations; B: Predictions of the gam\_meso\_carbon model. Maps display predicted values at nano-microplankton sampling stations..... 97

**Figure 37 Spatial distribution of ontogenetic stages per species.** A: Mean and standard deviation of occurrence of ontogenetic stages of herring at stations situated in the center of the Eastern English Channel and in an area of riverine influence; B: Map displaying sampling stations of herring larvae with colors indicating stations associated to the center of the Eastern English Channel (gray) and in the area of riverine influence (orange), location of Seine and Somme estuaries are indicated; C: Mean and standard deviation of occurrence of ontogenetic stages of plaice at stations situated in the center of the Eastern English Channel and in an area of riverine influence; D: Map displaying sampling stations of plaice larvae with colors indicating



stations associated to the center of the Eastern English Channel (gray) and to the area of riverine influence (orange)..... 98

**Figure 38 Proportion (% diet) of plankton size classes to larval diet.** Boxplots represent median and 95 % credible interval of the posterior distribution of the MixSIAR models predicting the contribution of each size class to herring (blue) and plaice (orange) larvae diet. Minor refers to a posteriori aggregated size classes (20 – 125  $\mu\text{m}$  and 200 – 500  $\mu\text{m}$ ) due to minor contribution of these size classes to larval diet. A: Global model; B: Spatial model for the overall population; C: Output of the spatial model for a station representing stations situated in the center of the Eastern English Channel; D: Output of the spatial model for a station representing stations of riverine influence..... 100

**Figure 39 Proportion (% diet) of plankton size classes to diet of plaice larvae ontogenetic stages.** Boxplots represent median and 95 % credible interval of the posterior distribution of the MixSIAR models predicting the contribution of each size class to stage 1 (green), stage 2 (yellow) and stage 3 (violet) plaice larvae diet. A: Stage-space model not discriminating for stations; B: Output of the stage-space model for a station representing stations situated in the center of the Eastern English Channel; C: Output of the stage-space model for a station representing stations influenced by river discharge..... 101

**Figure 40 Abundance of *O. dioica* derived from the IBTS survey taking place in January – February 2008 (A) and 2022 (B).** ..... 108

**Figure 41 Location of sampling stations during CGFS 2021.** A: Blue dots indicate sampling stations of sardine; red dots indicate sampling stations of zooplankton serving for lipid analysis; red triangles represent sampling stations serving for lipid analysis and taxonomic analysis; green dots indicate sampling stations of phytoplankton; B: Sampling stations of environmental parameters (surface temperature, salinity, depth). Blue dots indicate sampling stations situated in the Western English Channel, red dots indicate sampling stations situated in the Eastern English Channel..... 119

**Figure 42 PCA taxonomic composition of zooplankton (500 – 1000  $\mu\text{m}$ ), first and second principal components.** A: Taxa (the darker the taxon, the higher its contribution to the first component); only taxa with a contribution higher than 2% are displayed); B: Sampling stations (the bigger the dot the higher its contribution to the first component); blue and red dots were located in the Western English Channel (WEC) or the Eastern English Channel (EEC), respectively; numbers represent sampling station id..... 127

**Figure 43 PCA taxonomic composition of phytoplankton, first and second principal components.** A: Taxa (the darker the taxon, the higher its contribution to the first component); only taxa with a higher contribution than 1 % are depicted; pink, green and black dots represent dinoflagellate, diatom and other species, respectively; B: Sampling stations (the bigger the dot the higher its contribution to the first component); blue and red dots were located in the Western English Channel (WEC) or the Eastern English Channel (EEC), respectively; numbers represent sampling station id; C: Relative abundance of diatoms (green) and dinoflagellates (pink) to total abundance per station (size of pie charts represent abundance in cells/l). ..... 128

**Figure 44 Principal component analysis (PCA) on the fatty acid profiles of sardines (A, B) and zooplankton (500 - 1000  $\mu$ m) (C,D) collected in the Western English Channel (blue) and Eastern English Channel (red).** Panel A and C display FA in the two dimensional plane of the first and second component. The darker the taxon, the higher its contribution to the first component. Panel B and D display sampling stations. The bigger the dot the higher its contribution to the first component. Numbers represent sampling station id..... 131

**Figure 45 Factors influencing trophic transfer of eicosapentanoic acid (EPA) revealed by the GAM.** The relation of EPA % in zooplankton and sardine and all significant factors influencing trophic transfer revealed by the GAM model are displayed. Significance level is displayed in the heading of the respective plots: \*\*\* (P<0.001), (P<0.01), \* (P<0.05). ..... 133

**Figure 46 Factors influencing trophic transfer of docosahexaenoic acid (DHA) revealed by the GLMM.** For DHA also the relation to zooplankton DHA and region is shown although not significant. Significance level is displayed in the heading of the respective plots: \*\*\* (P<0.001), (P<0.01), \* (P<0.05). ..... 133

**Figure 47 Factors influencing trophic transfer of arachidonic acid (ARA) revealed by the GLMM.** The relation of ARA % in zooplankton and sardine and all significant factors influencing trophic transfer revealed by the GAM model are displayed. Significance level is displayed in the heading of the respective plots: \*\*\* (P<0.001), (P<0.01), \* (P<0.05). ..... 134

**Figure 48 Interannual comparison of sardine fatty acid profile.** Upper four panels showing PCAs applied to data sampled in autumn 2021 in the context of the present thesis. Lower four panels show PCAs applied data sampled by Mathieu-Resuge et al. (2024) in autumn 2020. A, E: FA displayed in the two dimensional plane of the first and second component of a PCA applied to the **mean fatty acid profile per station**; C,G: FA displayed in the two dimensional

plane of the first and second component of a PCA applied to **individual FA profiles of all sardines** sampled; Maps indicate the position of sampling stations on the first component of the PCA by color. Each map corresponds to the PCA presented to its left. .... 142

## Tables

<b>Table 1 Outcomes of GLMM evaluating possible biotic and abiotic drivers of taxa distribution from two PCAs (dimensions = principal components).</b> The n and y in the column cluster indicate if cluster was retained in the most appropriate model or not (n=no and y=yes). Significance: *** (P<0.001), ** (P<0.01), * (P<0.05), · (P<0.1). N indicates the number of sampling stations used in the model. AIC (Akaike’s Information Criterion) was the parameter used for model selection with smaller AIC for the models of the same taxon indicating better explanation of variance. Estimates indicate significant and non-significant positive or negative correlation between a dimension and taxon abundance. Non-significant correlations were not displayed in the table. ....	62
<b>Table 2 Results of GLMM testing for differences in abundance of dominant taxa between the assemblages independent of year and with regard to inter-annual differences in the same assemblage.</b> .....	65
<b>Table 3 River discharge of the Seine river during January and February from 2014 to 2021.</b> .....	92
<b>Table 4 Summary of hierarchical GAMs to predict stable isotope values of trophic sources at larvae sampling stations.</b> The table presents intercept values of size classes with standard error (S.E.), and p-values of the spatial term integrated in the model as a smoothed term. Further estimated degrees of freedom (edf) of the smooth term, the adjusted R <sup>2</sup> , deviance explained and samples used (n) per model are displayed.....	94
<b>Table 5 Biological parameters of sardine.</b> Data are presented for each region (Eastern English Channel (EEC), Western English Channel (WEC)) and by sex, along with the corresponding number of collected individuals. Mean values and standard deviations are provided for length, weight, triglyceride-sterol ratio (TAG-ST), and Le Cren’s condition index.....	125
<b>Table 6 Results GLMM testing inter-regional differences of sardines.</b> Estimates with standard error (S.E.) indicate significant and non-significant positive or negative correlation between a covariate and the proportion of the respective parameter of sardines. Significance: *** (P<0.001), ** (P<0.01), * (P<0.05). AIC (Akaike’s Information Criterion). n indicates the number of individuals used in the model. ....	126
<b>Table 7 Fatty acid trophic markers and most important fatty acids (FA) for zooplankton and sardine.</b> Values are reported as mean ± standard deviation by region (Eastern English Channel (EEC), Western English Channel (WEC)). n indicates number of stations. The FA listed in this	

table represent the 20 most important FA with regard to percentage and including FATM and essential FA. A complete table can be found in Annex III (**Table A 8, 9**). ..... 129

**Table 8 Factors influencing trophic transfer of essential fatty acids (EFA).** Estimates with standard error (S.E.) indicate significant and non-significant positive or negative correlation between a covariate and the proportion of the respective fatty acid (FA) in sardine. Significance: \*\*\* (P<0.001), \*\* (P<0.01), \* (P<0.05); AIC (Akaike's Information Criterion); type: model used; n: number of sampling stations; (s): parameters integrated in the model as a spatial smoother; edf: estimated degrees of freedom for the smoothed terms. .... 132

## List of Abbreviations

<b>AIC</b>	Akaike's Information Criterion
<b>ARA</b>	arachidonic acid
<b>CGFS</b>	Channel Ground Fish Survey
<b>CUFES</b>	Continous Underway Fish Egg Sampler
<b>DHA</b>	docosahexaenoic acid
<b>EEC</b>	Eastern English Channel
<b>EFA</b>	essential fatty acid
<b>EPA</b>	eicosapentanoic acid
<b>FA</b>	fatty acid
<b>FAME</b>	fatty acid methyl ester
<b>FATM</b>	fatty acid trophic markers
<b>GAM</b>	generalized additive model
<b>GLMM</b>	generalized linear mixed model
<b>GOV</b>	Grand Ouverture Verticale
<b>HGAM</b>	hierarchical generalized additive models
<b>HPTLC</b>	high-performance thin-layer chromatography
<b>IBTS</b>	International Bottom Trawl Survey
<b>MBEF</b>	Multitrophic Biodiversity Ecosystem Functioning
<b>MIK</b>	Method Isaac Kid
<b>MixSIAR</b>	Stable isotope mixing models
<b>MUFA</b>	monounsaturated fatty acids
<b>NSASH</b>	North Sea Autumn Spawning Herring
<b>PCA</b>	Principal component analysis
<b>POM</b>	particulate organic matter
<b>PUFA</b>	polyunsaturated fatty acids
<b>SAF</b>	saturated fatty acids
<b>SIA</b>	Stable isotope analysis
<b>SNS</b>	Southern North Sea
<b>SNS-EEC</b>	Southern North Sea - Eastern English Channel
<b>TAG-ST</b>	triglyceride-sterol ratio
<b>TEF</b>	trophic enrichment factor
<b>Ucrit</b>	maximal swimming speed
<b>WEC</b>	Western English Channel



## General Introduction

### Understanding of ecosystem functioning

Understanding ecosystem functioning is needed to comprehend the environment in which we live and on which we depend. Ecosystem functioning is a wide term that encompasses ecosystem properties and services. Thereby ecosystem properties (or processes) describe the energy stock and flow in an ecosystem, as well as their stability over time (Srivastava and Vellend, 2005; Pacala and Kinzig, 2013). Ecosystem services depend on ecosystem properties and are defined as “conditions and processes through which natural ecosystems, and the species that make them up, sustain and fulfil human life.” (Daily, 1997). Air and water purification, maintenance of soil fertility, pollination, aesthetic beauty, climate regulation, maintenance of atmospheric composition and food provisioning are examples of ecosystem services (Christensen *et al.*, 1996; Daily, 1997). Provision of seafood is thereby among the most exploited ecosystem services and overall marine ecosystem services are estimated to represent a value of \$50 trillion per year (Costanza *et al.*, 2014; Lomartire *et al.*, 2021).

Being part of ecosystems, anthropogenic influence on the environment is a natural process but the intensity of some anthropogenic pressures like greenhouse gas emissions and other pollution, fisheries, eutrophication or habitat modification affect the functioning of ecosystems and therewith also the provision of ecosystem services (Pauly *et al.*, 1998; Smith, 2003; Millennium Ecosystem Assessment, 2005; Halpern *et al.*, 2008; Cardinale *et al.*, 2012; IPCC, 2014). Thus, management measures have to be realized to adapt or mitigate anthropogenic pressures in a way that ecosystem functioning is maintained (Lomartire *et al.*, 2021). Due to the complexity and interrelatedness of ecosystem compartments, management measures should consider and be based on the ecosystem as a whole as aimed at in ecosystem-based management (Brussard *et al.*, 1998; McLeod *et al.*, 2005). A critical step of ecosystem management is the development of a thorough ecosystem understanding, however (Brussard *et al.* 1998), which remains an immense challenge due to the complexity and temporal dynamics of ecosystems. In order to contribute to a better understanding of marine ecosystem functioning the present thesis focused on zooplankton that play a crucial role in marine ecosystems (Richardson, 2008).



## The role of plankton in marine ecosystem functioning

Plankton are organisms that live suspended in the water column. As autotrophic primary producers, phytoplankton sequester carbon, are estimated to produce 50 - 70 % of the atmospheric oxygen (Walker, 1980; Behrenfeld *et al.*, 2001), and constitute the energetic and nutritional foundation of the oceans. By grazing on phytoplankton, zooplankton regulate biogeochemical cycles, water quality, and the biological carbon pump, ultimately affecting the climate (**Figure 1**). In addition, zooplankton transfers energy and nutrients, such as proteins and long chain polyunsaturated fatty acids, to higher trophic levels like small pelagic fish (Richardson, 2008; Arts *et al.*, 2009; De Troch *et al.*, 2012). Small pelagic fish such as herring or sardine, occupy an intermediate trophic level between planktonic organisms and higher trophic levels like piscivorous fish, marine mammals, seabirds and human beings (Cury *et al.*, 2000; Richardson, 2008; Beaugrand *et al.*, 2014; Olin *et al.*, 2022) (**Figure 1**). Understanding the functioning of zooplankton communities within the ecosystem, particularly its interactions with both phytoplankton and higher trophic levels, is central to understand, predict and manage marine ecosystems and finally for the implementation of ecosystem-based-management (Tam *et al.*, 2017; Lomartire *et al.*, 2021).

## General Introduction

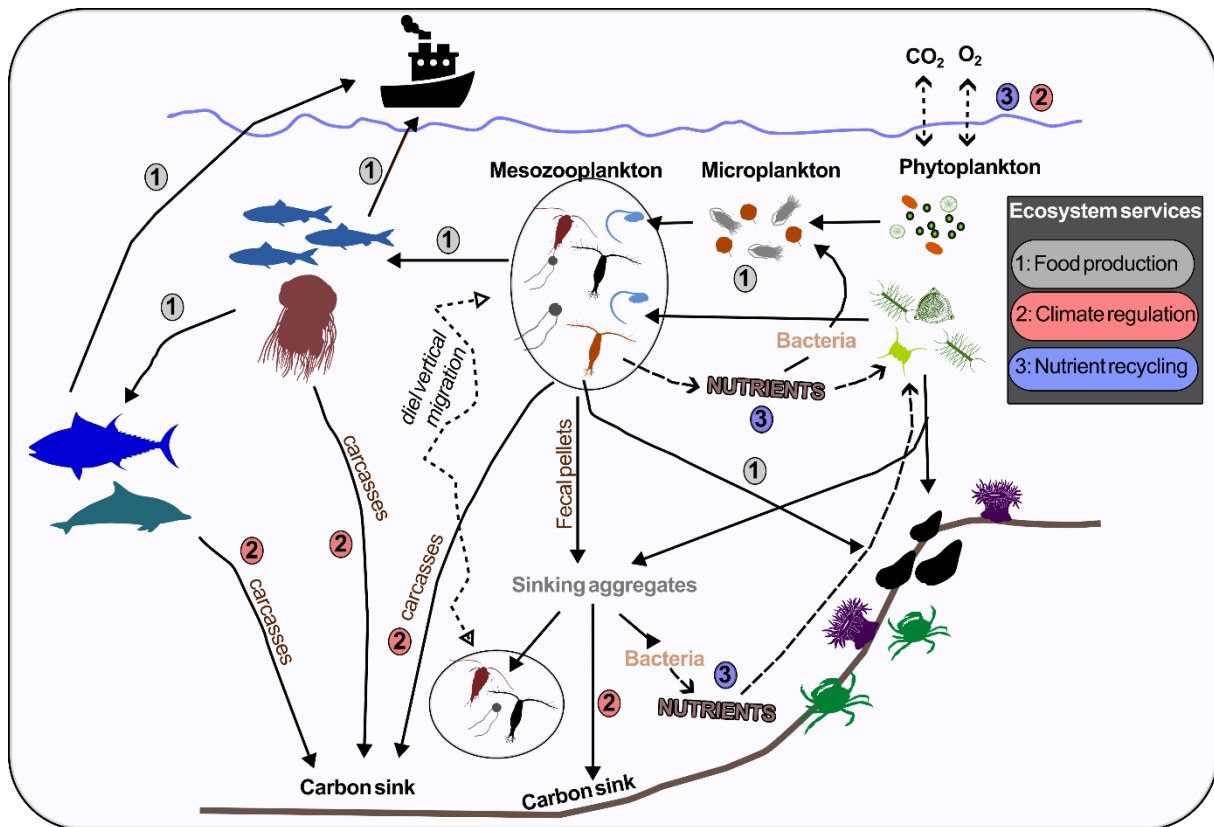


**Figure 1 Role of zooplankton in marine ecosystems and resulting ecosystem services.** By feeding on phytoplankton and microplankton zooplankton channels energy to small pelagic fish that in turn transfer energy and nutrients to higher trophic levels like piscivorous fish and marine mammals. Furthermore, sinking carcasses and fecal pellets are an energy source for benthic communities. This central role in the energy transfer makes zooplankton a crucial part for the ecosystem service food production, which is indicated in the schema with a “1”. Zooplankton contribute to carbon export to the deep sea which functions as potential carbon sink, by the excretion of fecal pellets, sinking of carcasses, diurnal vertical migration and by facilitating the existence of subsequent trophic levels that themselves might export carbon due to sinking carcasses. Thus, zooplankton contribute to climate regulation indicated with a “2”. Excretion of nutrients like dissolved organic carbon and nitrogen and ammonium as well as decomposition of zooplankton fecal pellets by bacteria contribute to nutrient recycling that in turn promotes primary production. This ecosystem service is indicated with a “3”. All silhouette pictures used were obtained from <https://www.phylopic.org/>. The chlorophyte silhouette was created by Sergio A. Muñoz-Gomez and of *Mytilus* spp. by Harold N. Eyster.

However, behind the group of zooplanktonic organisms lies a complex diversity in terms of size (ranging from pico to mega), taxonomy, life history traits and behaviours (Teodosio and Barbosa, 2020), allowing for complex interactions within the ecosystem. Zooplankton include both unicellular and multicellular organisms (Boyce *et al.*, 2015), spanning 15 phyla and accounting for approximately 40 % of the world’s marine biomass (Hatton *et al.*, 2021). Zooplankton can be divided into holoplankton, which spend their entire life cycle as plankton,

## General Introduction

and meroplankton, which only remain planktonic during their egg and larval stages. Many benthic organisms, such as bivalves, crustaceans, polychaetes, and echinoderms, have meroplanktonic eggs and larvae. Fish eggs and larvae also belong to this category and are referred to as ichthyoplankton (Teodosio and Barbosa, 2020). In terms of size (**Figure 2**), zooplankton span over seven orders of magnitude, ranging from pico-plankton (0.2 - 2  $\mu\text{m}$ ) to nano- (2 - 20  $\mu\text{m}$ ), micro (20 - 200  $\mu\text{m}$ ), meso- (200 - 2000  $\mu\text{m}$ ), macroplankton (2 - 20 cm) and megaplankton (20 - 200 cm), with the latter including organisms like large jellyfish (Boyce *et al.*, 2015).

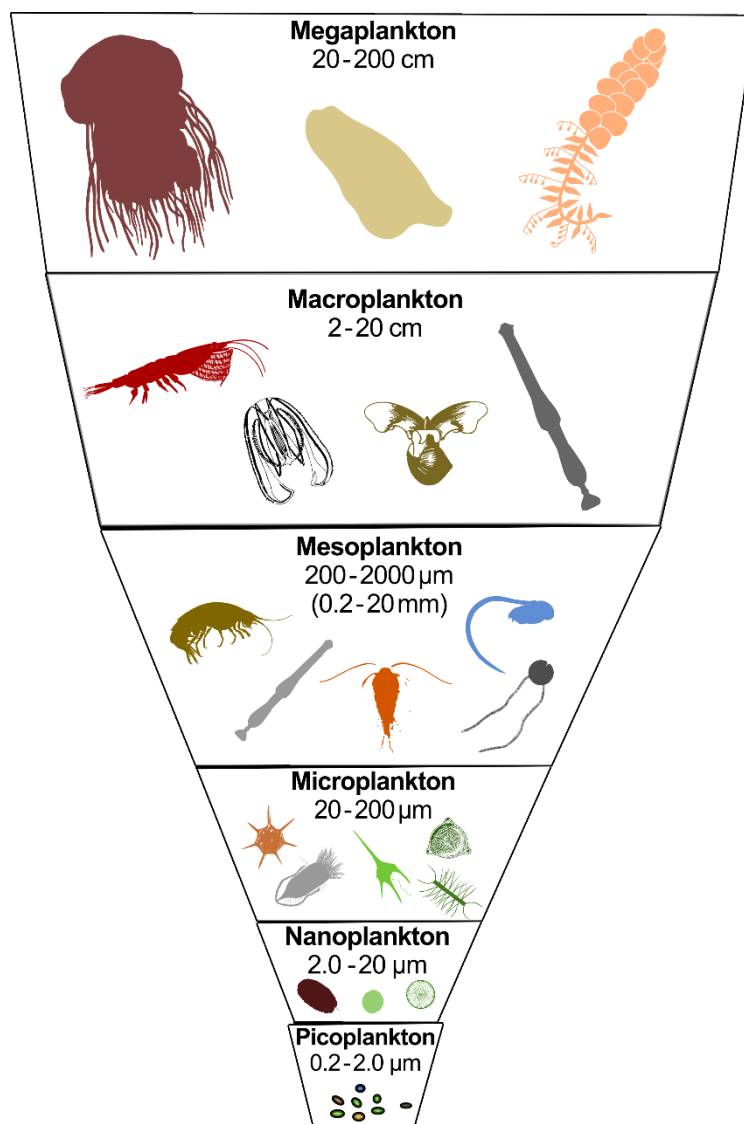


**Figure 2 Plankton classed by size.** Silhouette images used in this figure were obtained from <https://www.phylopic.org/>. The amphipod silhouette (mesoplankton) was created by Collin Gross.

Zooplanktonic organisms exhibit a range of feeding modes, including heterotrophic and mixotrophic behaviours, herbivorous, omnivorous or carnivorous feeding modes, and diverse feeding strategies. For ambush-feeders, predator-prey encounters depend on prey's motility and prey may be encountered passively, intercepted directly, or detected remotely before being actively captured. Other organisms are filter-feeders, using a feeding current targeting remotely detected prey, or passing water through filtering structures that screen prey particles. Other filter-feeders capture prey unselectively, using structures such as tentacles. In contrast, cruise-feeding predators are motile and actively move toward prey detected remotely. These different feeding strategies influence trophic interactions and planktonic community dynamics, as each approach favours prey of distinct characteristics. Furthermore, zooplankton organisms display a range of survival strategies including chemical and morphological defence mechanisms, diurnal vertical migration, dormancy and starvation tolerance, to cope with predators or unfavourable conditions. Reproduction among zooplankton is equally diverse, with organisms reproducing asexually, hermaphroditically or sexually. Sexual reproduction varies between broadcast spawners and species that carry eggs attached to their body. Fertilization takes place externally and internally and in some cases, sexual reproduction leads to spawning aggregations, which can attract predators and thus influence zooplankton community dynamics (Litchman *et al.*, 2013).

Given the complexity of zooplankton and their interactions, it becomes clear that understanding their role within the ecosystem, especially in relation to spatio-temporal variations of abiotic and biotic drivers, is a significant challenge.

### **Need for understanding of zooplankton functioning in the context of climate change**

Ocean warming is affecting and is expected to continue influencing zooplankton community composition, planktonic food webs, and overall zooplankton biomass (Richardson, 2008; Schmidt *et al.*, 2020; Heneghan *et al.*, 2023) with potential consequences for ecosystem functioning. When summarizing general trends of the effect of ocean warming on zooplankton, it is crucial to keep in mind that strong regional variations exist (Richardson, 2008; Chust *et al.*, 2014; Heneghan *et al.*, 2023). Warming has been observed to influence the phenology of various zooplankton taxa (Edwards and Richardson, 2004) and to drive

biogeographical shifts (Beaugrand *et al.*, 2002b) that modify community compositions (Beaugrand *et al.*, 2002b; Edwards and Richardson, 2004; Richardson, 2008). Additionally, increased water temperatures have been found to decrease zooplankton body size, either by direct effects on the individuals or by favouring smaller species (Daufresne *et al.*, 2009; Brosset *et al.*, 2016). As ocean warming also affects phytoplankton, zooplankton is further influenced indirectly through bottom-up effects. Increased stratification can reduce nutrient replenishment of surface waters leading to a reduction in phytoplankton biomass and size, which in turn can result in decreased zooplankton biomass (Richardson, 2008; Chust *et al.*, 2014). A shift from large sized phytoplankton cells to picophytoplankton will further alter planktonic food web structures. Smaller phytoplankton favours filter-feeders and carnivores, while omnivorous zooplankton are disadvantaged leading to a reduction in their biomass (Heneghan *et al.*, 2023). Furthermore, a decline in the nutritional quality of phytoplankton is predicted, particularly in terms of long-chain polyunsaturated fatty acids (Litzow *et al.*, 2006; Galloway and Winder, 2015; Hixson and Arts, 2016; Vagner *et al.*, 2019; Schmidt *et al.*, 2020). As zooplankton are important prey for larval and adult fish such as herring and sardine, changes in zooplankton communities will influence higher trophic levels through the transfer of energy and nutrients, potentially affecting fisheries (Brosset *et al.*, 2017). In the North Sea, a reduction in euphausiids, copepod size, and abundance of the copepod *Calanus finmarchicus* has contributed to a long-lasting decline in cod recruitment (Beaugrand and Kirby, 2010; Bedford *et al.*, 2020). Similarly, decreased zooplankton biomass in the Northern Californian Current has been linked to reduced growth and survival rates of juvenile salmon and herring (Mackas *et al.*, 2013; Daly *et al.*, 2017). In the Mediterranean, the decline in size and condition of sardine and anchovy have been attributed to community change from larger to smaller species with lower lipid content (Feuilloley *et al.*, 2020).

### **Studying zooplankton functioning in the ecosystem**

A mechanistic understanding of the changes in zooplankton communities and their effects on the ecosystem is crucial for developing adequate management measures and to predict how zooplankton and the ecosystem in which they are embedded will respond to a changing environment. However, acquiring this level of understanding is challenging due to the diversity and complexity of zooplankton and their interactions within the ecosystem. Ecosystem

## General Introduction

models often oversimplify zooplankton, which can lead to inaccuracies in model output and predictions (Girardin *et al.*, 2018; Bracis *et al.*, 2020; Chenillat *et al.*, 2021; Ito *et al.*, 2023; Ratnarajah *et al.*, 2023; Thorpe, 2024). Grazing by zooplankton on phytoplankton is often modelled using a simple biomass-based relationship. However, incorporating the size composition of both phyto- and zooplankton, as well as the proportion of herbivores versus omnivores in the zooplankton community, can provide a more realistic representation of this trophic interaction and decrease model uncertainty (Chenillat *et al.*, 2021). The impact of a predator, like plaice larvae, on a zooplankton community can vary depending on whether the larvae are specialist or generalist feeders. Specialist or generalist feeders will respond differently to changes in the zooplankton community due to different strengths of trophic interactions (Thébault and Loreau, 2006). Thus, while simplification of zooplankton diversity is often necessary to limit computational burden, it is essential to recognize the diversity of zooplankton in terms of taxonomy, size and behaviour. Trait-based approaches appeared as a good compromise between simplification and maintenance of the zooplankton diversity required to understand zooplankton functioning in the ecosystem (Mlambo, 2014; Hébert *et al.*, 2017; Benedetti *et al.*, 2019). Traits are characteristics of organisms related to behaviour, physiology or morphology (Litchman *et al.*, 2013; Mlambo, 2014). Trait information for most zooplankton taxa is scarce, however (Hébert *et al.*, 2021; Ratnarajah *et al.*, 2023), except for certain groups like copepods (Benedetti *et al.*, 2015; Ratnarajah *et al.*, 2023). Furthermore, the choice of traits adequate to represent zooplankton in a study requires a clear definition of the ecosystem function of interest and prior knowledge on the ecosystem and zooplankton studied (Hooper *et al.*, 2005; Litchman *et al.*, 2013; Hébert *et al.*, 2017; McQuatters-Gollop *et al.*, 2019; Bedford *et al.*, 2020). A theoretical framework investigating diversity in relation to ecosystem functioning is Multitrophic Biodiversity Ecosystem Functioning (MBEF) (Thompson *et al.*, 2012). This framework aims at creating a link between community ecology and ecosystem ecology using trophic relationships. Community ecology focuses on the composition and distribution of taxa, providing mechanistic insights into drivers of community dynamics and health. However, community ecology often concentrates on small parts of the ecosystem (e.g., specific trophic levels) and does not fully integrate and connect this knowledge with the entire ecosystem. Conversely, ecosystem ecology examines stocks and flows of energy and nutrients, and biomass distributions to understand the functioning of the ecosystem as a whole, but it tends to overlook species composition and interaction. Food web ecology can

connect these approaches by incorporating taxonomic details, interspecific links and relationships, body mass and body size while quantifying these relationships through trophic energy flows (Thompson *et al.*, 2012).

Considering zooplankton crucial role as intermediate trophic level, MBEF appears promising to investigate zooplankton functioning in the ecosystem by allowing the integration of zooplankton diversity in relation to lower and higher trophic levels. Thus, this approach was chosen to investigate zooplankton in the present thesis considering phytoplankton as lower and fish (larvae or adults) as higher trophic levels.

Zooplankton composition and function will vary in space due to spatial variation in biotic drivers like benthic communities and abiotic drivers such as temperature, distribution of water masses, stratification and nutrient concentration (Hooper *et al.*, 2005; Thompson *et al.*, 2012; Grandremy *et al.*, 2023). Furthermore, marine environments can be spatially distinguished with regard to migration routes, feeding and spawning grounds and nursery areas for example. Thus, assessing spatial variation in zooplankton functioning and investigating its drivers is important to understand ecosystem processes and to inform ecosystem-based management (Bedford *et al.* 2020).

## Study area

Shelf and coastal seas display high productivity due to high rates of primary production and elevated diversity of primary producers nourished by riverine and oceanic nutrient inputs (Thomas *et al.*, 2005; Sharples *et al.*, 2013). These areas provide 90 % of global fish catches (Pauly *et al.*, 2002; Sharples *et al.*, 2013) but suffer from intense anthropogenic pressures.

The North Sea was proposed to have experienced several regime shifts in the past (Beaugrand, 2004; Alvarez-Fernandez *et al.*, 2012; Boersma *et al.*, 2015) and recent studies suggest that the zooplankton community is changing in this area (Bedford *et al.*, 2020; Semmouri *et al.*, 2023). Less information is known about zooplankton communities and their sensitivity to environmental pressures in the English Channel but regime shifts are also proposed to have occurred in this region based on data from a stationary long-term sampling station in the Western English Channel (Reygondeau *et al.*, 2015).

The Southern North Sea and the English Channel, which harbour key spawning and nursery grounds for several fish species like herring (*Clupea harengus*), plaice (*Pleuronectes platessa*),

sardine (*Sardina pilchardus*), cod (*Gadus morhua*), sole (*Solea solae*) and whiting (*Merlangius merlangus*), were chosen as study area of the present thesis (Coombs *et al.*, 2005; Bolle *et al.*, 2009; Kanstinger and Peck, 2009; Martin *et al.*, 2009; Corten, 2013) (**Figure 3**).

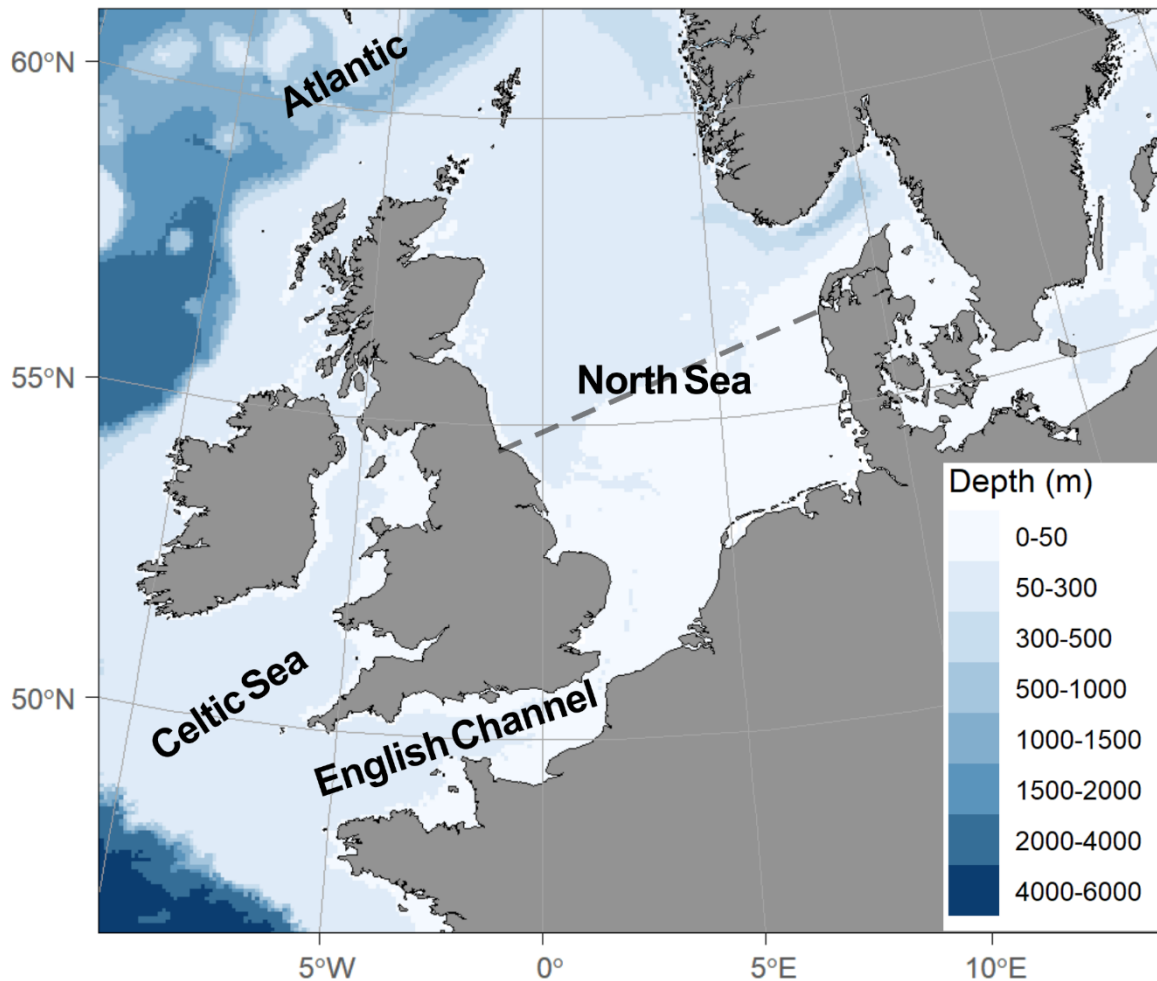


**Figure 3** Bathymetric map of study area (English Channel and Southern North Sea) in a bigger spatial context. Pointed line indicates transition between Northern and Southern North Sea.

## North Sea

The North Sea is a European shelf sea being connected to the Atlantic Ocean in the North and to the English Channel in the South (OSPAR Commission, 2000; Krause *et al.*, 2003; Winther and Johannessen, 2006). It can be divided in a northern and southern part due to its bathymetry, hydrology (OSPAR Commission, 2000; Krause *et al.*, 2003; Lenhart *et al.*, 2004) and ecology (Beaugrand *et al.*, 2001; Lenhart *et al.*, 2004) with a proposed border between Middlesbrough and Esbjerg (Lenhart *et al.*, 2004) or the river Humber and Skagen (Krause *et al.*, 2003) (**Figure 4**).



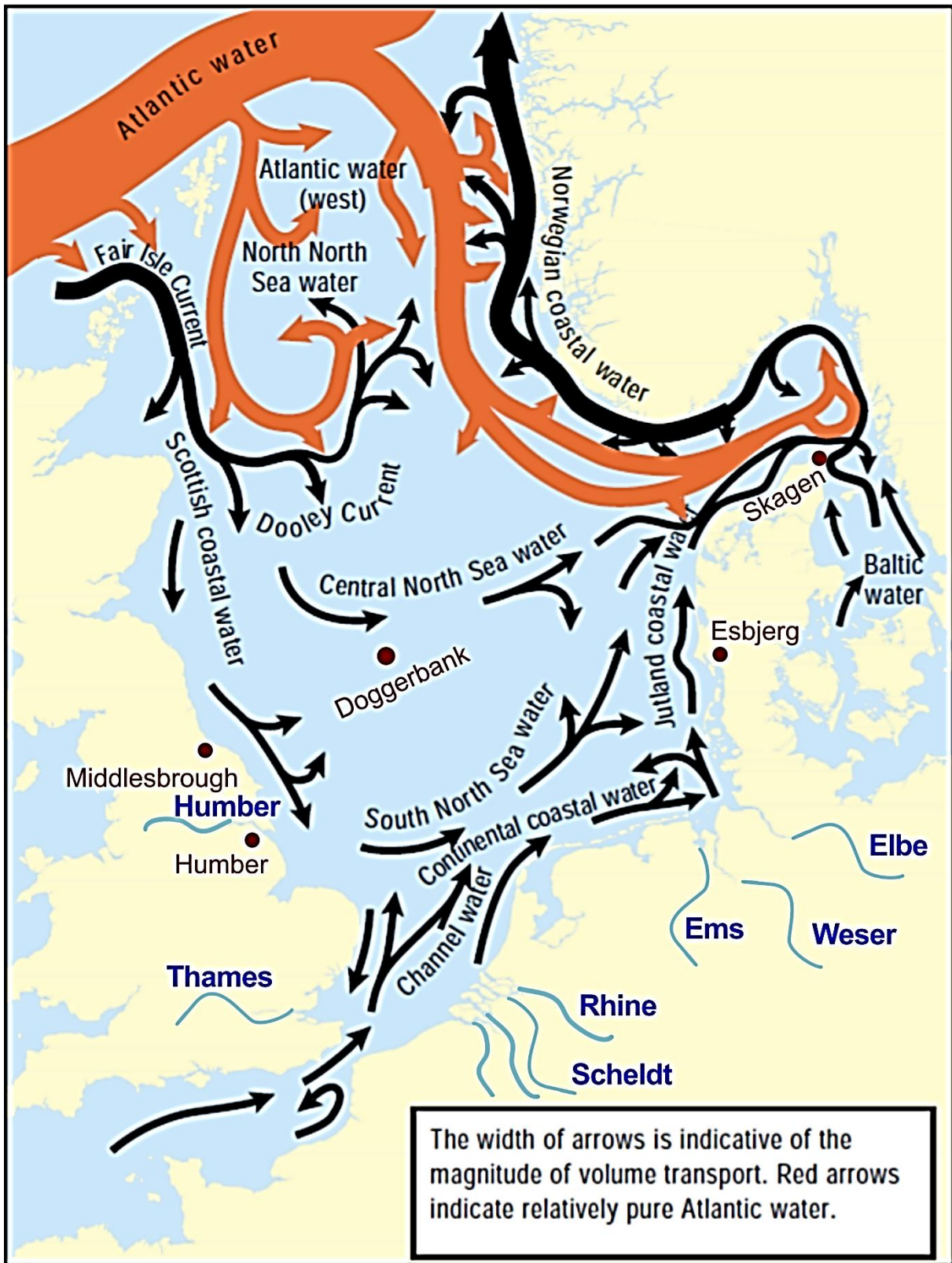


**Figure 4** Circulation pattern of different water masses of the North Sea. Blue names indicate rivers, red names indicate orientation points to divide the North Sea in a Southern and a Northern part. Adapted from OSPAR Commission (2000).

## General Introduction

Due to the domination of Atlantic water and its greater depth, the Northern North Sea is a rather oceanic system (Thomas *et al.*, 2005). It displays depth between approximately 100 to 150 m at the shelf and exceeds 700 m in the Norwegian trench (OSPAR Commission, 2000; Thomas *et al.*, 2005; Winther and Johannessen, 2006). Stratification of the deeper basins of the Northern North Sea allows for sinking of particulate organic matter (POM) to the subsurface layer and export of dissolved inorganic carbon to the North Atlantic ocean (Lenhart *et al.*, 2004; Thomas *et al.*, 2005).

The Southern North Sea (SNS) by contrast is shallow with depth less than 50 m south of the Dogger Bank (Thomas *et al.*, 2005) and it is mainly controlled by riverine input as the Atlantic water entering via the Dover Strait in the south accounts for only 10 % of total Atlantic water input in the North Sea (OSPAR Commission, 2000; Lenhart *et al.*, 2004; Thomas *et al.*, 2005) (**Figure 4**). Furthermore, only a minor fraction of the Atlantic water inflow in the North reaches the area beyond the Dogger Bank (approx. 55°N3°E) (Turrell, 1992; Lenhart *et al.*, 2004; Thomas *et al.*, 2005). Due to the continuously mixed water POM does not sediment and is mineralized within the water column leading to a high turnover of carbon and nutrients (Lenhart *et al.*, 2004; Thomas *et al.*, 2005).

Rivers entering the SNS are the Elbe, Weser, Rhine, Meuse, Scheldt, Thames and Humber (**Figure 4**). River discharge from the Dutch and Belgian coast (Rhine, Meuse, Scheldt) including the Dutch Wadden Sea, account for 91-97 km<sup>3</sup> per year, whereas the discharge coming from the English east coast encompassing the rivers Tyne, Tees, Humber and Thames and from the Danish and German coasts account for 32 km<sup>3</sup> per year, respectively (OSPAR Commission, 2000). Although the Northern North Sea receives with around 300 km<sup>3</sup> higher freshwater inputs than the SNS (OSPAR Commission, 2000; Lenhart *et al.*, 2004), the influence of freshwater in the northern area is of minor importance, as freshwater is retained in a current flowing along the Norwegian coast and thus does not mix with the rest of the basin (Svendsen *et al.*, 1991; Thomas *et al.*, 2005). By contrast, the freshwater input in the much smaller, shallower and continuously stirred SNS is mixed with marine water masses, thus exerting a higher influence on the ecosystem (Thomas *et al.*, 2005). Overall, North Sea water is a varying mixture of North Atlantic water and freshwater run-off (OSPAR Commission, 2000). The circulation and distribution of water masses are determining factors for the biology and ecology of the North Sea (Williams *et al.*, 1993; OSPAR Commission, 2000; Krause *et al.*, 2003; Lenhart *et al.*, 2004). Svendsen *et al.* (1991) described the accepted general mean pattern of

## General Introduction

North Sea circulation and distribution of water masses (**Figure 4**) that can be distinguished by their salinity (Krause *et al.*, 2003). Atlantic water enters the North Sea in the North by the Fair Isle current and over the eastern Shetland shelf area (Otto *et al.*, 1990; Turrell, 1992). Only a small fraction of this Atlantic water protrudes further south as 'Scottish Coastal water'. Atlantic water flowing towards the center transforms to 'Central North Sea water' (OSPAR Commission, 2000; Krause *et al.*, 2003) and is directed eastwards by the Dogger Bank (Otto *et al.*, 1990). East of the Dogger Bank part of the 'Central North Sea water' is flowing into the SNS (Svendsen *et al.*, 1991; Krause *et al.*, 2003). 'Scottish Coastal water' flows along the British coast into the SNS, where it mixes with fresh water (decreasing salinity to 34 - 34.75) and becomes the 'Southern North Sea water'. This water mass prevails in the open SNS. Entering the North Sea via the Dover Strait, the saline 'Channel Water' dominates in the Southern Bight. Flowing northwards along the east coast, the 'Channel Water' is mixed with freshwater inputs, transforming it to 'Continental Coastal water', displaying a lower but more variable salinity (31-34) compared to the 'Southern North Sea water' (OSPAR Commission, 2000; Krause *et al.*, 2003).

Being a temperate shelf Sea, the North Sea displays a pronounced seasonal cycle caused by varying solar radiation. Furthermore, the influence of Atlantic water fluctuates seasonally, partially retreating during summer and occupying a wider area in winter. Thus, hydrological fluctuations contribute to the seasonal dynamics of plankton communities in this area (Krause *et al.*, 2003).

## English Channel

The English Channel is a shallow epicontinental sea, bordering with the Celtic Sea in the west and the SNS in the east (Dauvin, 2012) (**Figure 5**).

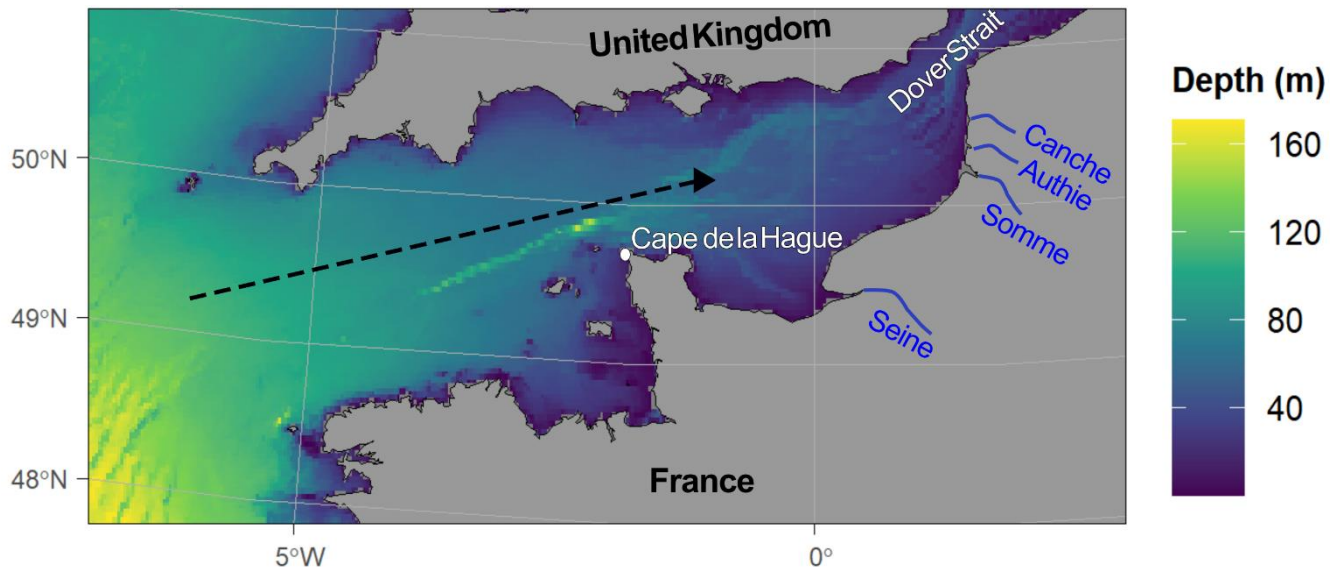


**Figure 5 English Channel.** Bathymetric map of the English Channel. Blue names indicate rivers terminating in the Eastern English Channel. Arrow indicates main flow direction from the Celtic Sea towards the Dover Strait.

Entering the English Channel from the west, Atlantic water flows north-eastwards, constituting the main water mass circulation although strong tidal currents create local gyres (Richirt et al., 2021 and references therein). Based on differing hydrologic and oceanographic features, the English Channel can be divided in a western and an eastern part roughly separated at the Cap de la Hague (Stanford and Pitcher, 2004; Dauvin, 2012). Whereas the Western English Channel (WEC) is more saline due to the influence of Atlantic water, the Eastern English Channel (EEC) is characterized by important fresh water inputs from the rivers Seine and Somme creating a northward flowing coastal current of desalinated water (Brylinski et al., 1991; Dauvin, 2012) (**Figure 5**). The Seine accounts for two thirds of the drainage area of the English Channel (Pawson, 1995). Furthermore, differing depth profiles influence stratification and temperature. The WEC displays a depth of around 100 m at its entrance deepening to 174 m in its central trench, while the EEC is rather shallow with a depth of 40 m in the Dover Strait (Dauvin, 2012; Stanford and Pitcher, 2004). This results in seasonal occurrence of stratification in summer in the WEC whereas water in the EEC remains mixed throughout the year (Dauvin, 2012; Stanford and Pitcher, 2004). Compared to the WEC, the EEC is generally warmer in summer and colder in winter (Stanford and Pitcher, 2004). These distinct hydrologic and oceanographic features were found to cause differences in biological

features regarding fish stocks and benthic invertebrates for instance (Araùjo et al., 2005; Cabioch and Gentil, 1977; Dupont et al., 2007).

## Higher trophic levels

In the present thesis, I mainly focused on three economically and ecologically important fish species, which consume zooplankton at various stages of their development: sardine, herring and plaice. Some consideration will also be given to the early stages of other fish species/taxa (e.g., Ammoditidae, Gadidae, Gobiidae) in chapter 1. Herring and sardine belong to the group of small pelagic fish and therefore represent an important intermediate trophic level due to their abundance, schooling behavior, energy density and planktivorous feeding mode which they sustain throughout their life span (Cury *et al.*, 2000; Rosa *et al.*, 2010; Garrido *et al.*, 2015; ICES, 2022a). Plaice is a benthic flatfish species that feeds on benthos and channels energy to several piscivorous predators (Ellis *et al.*, 1996; van der Veer *et al.*, 2000; Martin *et al.*, 2009; Girardin *et al.*, 2018). The larvae of all three species are planktivorous. As a result of data availability, I focused on specific ontogenetic stages for these species: adults (sardine) and larvae (herring, plaice).

## Herring

Atlantic herring (*Clupea harengus*) is a pelagic species of the Clupeidae family found mostly associated to the continental shelf (Whitehead, 1986) (**Figure 6**). Herring maximal size is reported to be 40 cm but most fish in the North Sea measure 20 – 30 cm. Their maximum life span is 7 – 10 years (ICES, 2004).



**Figure 6 Adult Herring (*Clupea harengus*).** Photograph Pierre Porché, Ifremer.

## Geographical distribution of species and stocks

Atlantic herring occur in the Northern Atlantic from the northern Bay of Biscay to Greenland into the Barents Sea in the east and from South Carolina to Labrador in the west (Whitehead, 1985, 1986). The North Sea Autumn Spawning Herring (NSASH) stock, who lives their entire lifespan in the North Sea, is structured in four different spawning components (Orkney-Shetland, Buchan, Banks, Downs) which are characterized by different growth rates, migration routes, spawning times, spawning grounds and recruitment patterns (Dickey-Collas *et al.*, 2010) (**Figure 7**). During spring and early summer, all spawning components gather on feeding grounds located in the western North and Central North Sea (Corten, 2001) (**Figure 7B**). The Downs component, which this thesis will focus on, was the first of the four NSASH components to collapse due to overexploitation in the 1960's and took the longest to recover (Dickey-Collas *et al.*, 2009). In recent years, however, the contribution of the Downs component to the overall NSASH stock increased and it is now considered larger than the contribution of the other three NSASH components (ICES, 2023a).

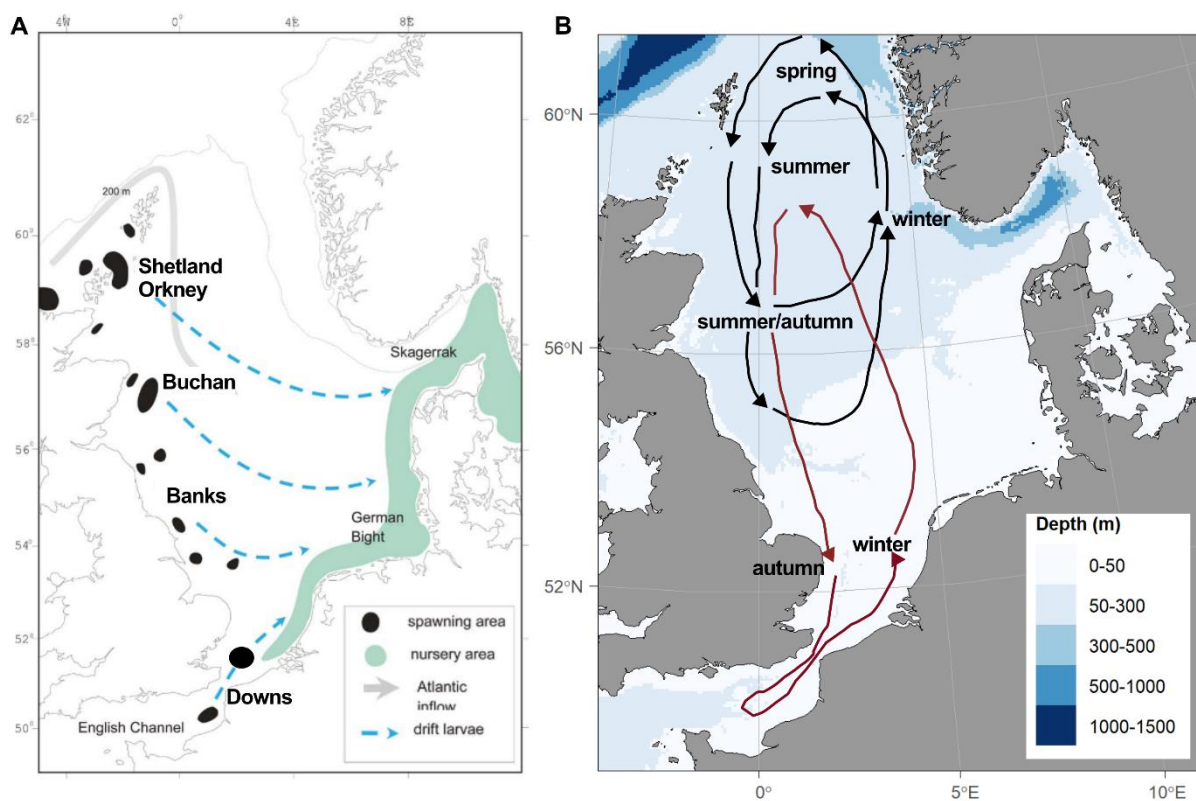


**Figure 7 Feeding, spawning and nursery areas of Autumn Spawning North Sea Herring.** A: Drifting routes of herring larvae from the spawning grounds of the different spawning components in the northwestern, western and southern North Sea to the main nursery areas in the eastern North Sea. Adapted from Corten (2013); B: Annual migration of adult herring between feeding and spawning areas. Red arrow indicates migration route of Downs herring. Adapted from Corten (2001).

### Reproduction and life cycle

Herring are determinate single batch demersal spawners that attach their eggs to gravel beds on distinct spawning grounds (Geffen, 2009). They attain maturity at an age of 2 – 3 years (ICES, 2004). The Downs component migrates to the EEC and the Southern Bight of the North Sea to spawn between November and January (Schmidt *et al.*, 2009). During spawning migration herring stop feeding (Slotte, 1999; Van Ginderdeuren *et al.*, 2014a; McBride *et al.*, 2015) as gonads occupy the major part of their abdominal cavity. Thus, gonad development, migration and routine metabolism are fuelled by energy storages accumulated during the feeding period (McBride *et al.*, 2015). Herring larvae (**Figure 8**) of the Downs component are drifted to the nursery areas along the Dutch coasts and in the German Bight (**Figure 7A**). Juveniles leave the nursery areas to join adults on the feeding grounds between ages 1 - 3 (Dickey-Collas, 2005).

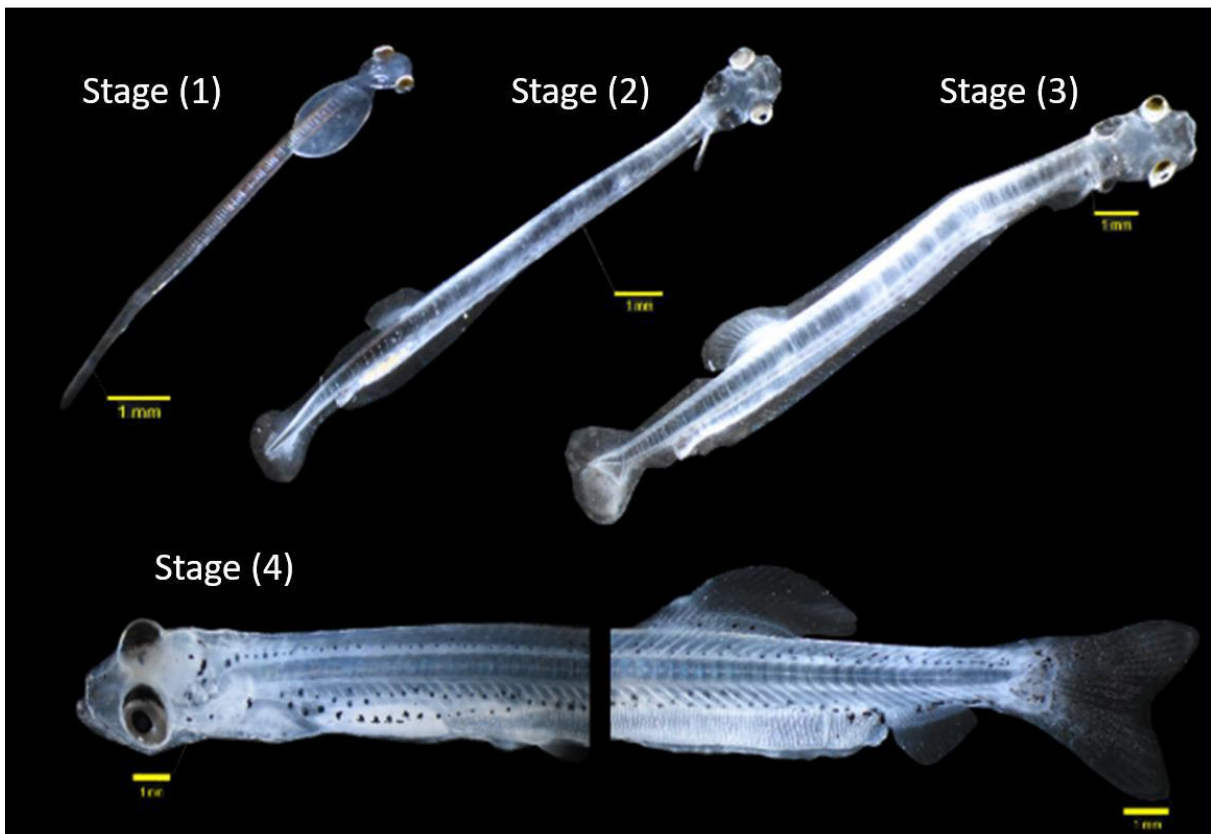


**Figure 8** Larvae of herring (*Clupea harengus*) of stage 1 to 4. Stage 1: yolk sac stage, stage 2: pre-flexion stage, stage 3: flexion stage, stage 4: post flexion. Graphic from Joly *et al.* (2021).

### **Trophic role in the ecosystem**

Herring display trophic plasticity depending on feeding conditions. Their prey spectrum varies with size, location, season and year (Dickey-Collas *et al.*, 2010). Although herring are mainly planktivorous, using particulate- and filter-feeding, they also prey on nektonbenthos, zoobenthos and juvenile fish (Batty *et al.*, 1990; Gibson and Ezzi, 1992; Casini *et al.*, 2004; Dickey-Collas *et al.*, 2010). In the North Sea, *Calanus spp.*, *Temora spp.*, *Pseudocalanus spp.*, *Oikopleura spp.*, *Sagitta spp.*, amphipods, juvenile Ammodytidae, fish eggs and larvae are the major constituents of adult herring diet (Segers *et al.*, 2007). With regard to higher trophic levels, adult NSASH channel energy to gadoids and marine birds (ICES, 2008; Lindegren *et al.*, 2011), while juveniles are mostly preyed on by mackerel and horse mackerel (ICES, 2007, 2008). Historically herring have been the main prey for bluefin tuna that disappeared from the North Sea in the early 1950s (Dickey-Collas *et al.*, 2010).

Herring larvae start feeding three days post hatch (Joly *et al.*, 2021). A variety of planktonic organisms ranging from micro- to mesozooplankton organisms contribute to their diet, with the copepods genera *Para-* and *Pseudocalanus* proposed to be major prey organisms (Alvarez-Fernandez *et al.*, 2015; Denis *et al.*, 2016; Bils *et al.*, 2022). Further details on herring larval feeding are given in chapter 1 and 2.

### **Fisheries**

Herring is further an economically important species with landings for human consumption in the entire North Sea accounting for 421 000 tonnes in 2023. In the SNS and the EEC catches accounted for 41 075 tonnes in 2023 (ICES, 2023a). Herring has a long history of exploitation, including stock collapse due to recruitment overfishing and the quasi-extinction of the Downs population in the mid-1970s (Geffen, 2009; Payne *et al.*, 2009; Dickey-Collas *et al.*, 2010). Since 1996 a recovery plan was implemented to reduce fishing mortality and the stock of autumn spawners is seen as recovered with regard to the biomass threshold that is supposed to secure recruitment (Dickey-Collas *et al.*, 2010) (**Figure 9**).



## General Introduction

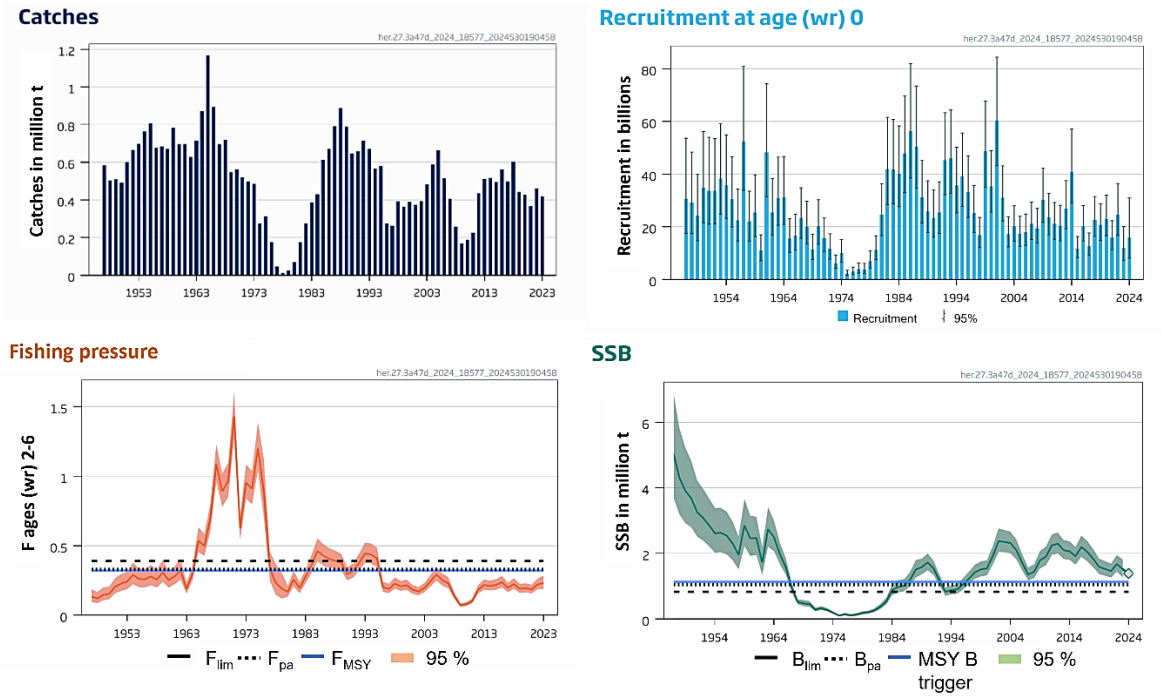


**Figure 9** Stock development over time for North Sea Autumn Spawning Herring in Subarea 4 and divisions 3.4 and 7.d. Fishing pressure above the  $F_{MSY}$  indicates overexploitation of the stock. Spawning stock biomass (SSB) below MSY B trigger indicates the SSB being too low for the stock to be in a good ecological state. Adapted from ICES (2024a).

Since 2002, however, North Sea herring has experienced sustained poor recruitments despite spawning stock biomass above MSY (Maximum Sustainable Yield) level (Payne *et al.*, 2009; ICES, 2024b). Increased larval mortality due to increased temperature and a regime shift in the planktonic communities in the North Sea, possibly combined with other factors (e.g., predation, poor hatching conditions) were evoked as possible drivers of these low recruitments (Corten, 2013).

## Sardine

Atlantic sardine or European pilchard (*Sardina pilchardus*) (**Figure 10**) (afterwards referred to as sardine) is a coastal pelagic species of the family Clupeidae (Nunes *et al.*, 2011; Garrido *et al.*, 2015). Although being able to attain an age of 14 years with a length of 27.2 cm (Silva *et al.*, 2008) Atlantic sardine is often considered as short lived (Neves *et al.*, 2021) or moderate lived (7 - 8 years) (Silva *et al.*, 2006) species.



**Figure 10** Adult sardine (*Sardina pilchardus*). Photograph Ifremer.

### Geographical distribution of species and stocks

Sardines are found in the Northeast Atlantic, from the North Sea to Mauritania/Senegal, with the Azores being their western distributional limit which extends eastward to the Mediterranean and the Black Seas (Parrish *et al.*, 1989). Within its distributional range, sardines are divided into several populations and stocks, though definitions vary depending on the methods or discriminant features used (Neves *et al.*, 2021). In European Atlantic waters, three stocks are differentiated: the Northern stock in the Celtic Sea and the English Channel (ICES area 7), the Central stock in the Bay of Biscay, and the Southern stock spanning from the Cantabrian Sea to the Gulf of Cadiz (ICES, 2017; Neves *et al.*, 2021) (**Figure 11A**). This thesis will focus on the Northern stock, and more specifically its English Channel component.

## General Introduction

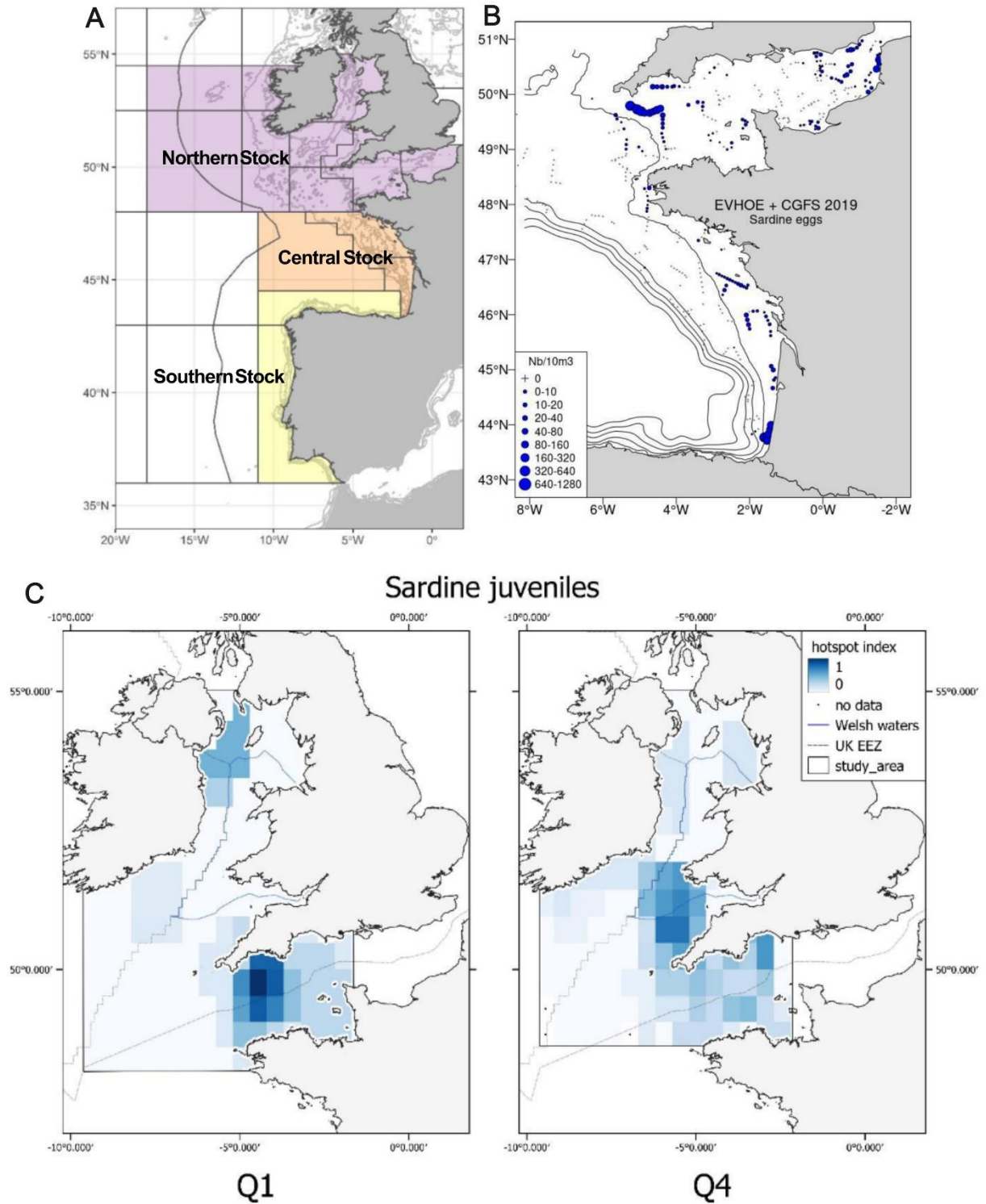


**Figure 11 A: European North Atlantic sardine stocks.** Adapted from ICES (2022a); B: Egg abundance in eggs/10 m<sup>3</sup> obtained from the surveys EVHOE (Bay of Biscay) and CGFS (English Channel) conducted by Ifremer in 2019. Graphic from <https://campagnes.flotteoceanographique.fr/series/11/>; C: Distribution of juvenile sardines of the Northern stock. Graphic from Campanella and van der Kooij (2021).

### Reproduction and life cycle

Sardines are indeterminate multiple batch spawners releasing pelagic eggs several times during the spawning season. For indeterminate batch spawners, potential annual fecundity is not fixed before the onset of spawning (Murua and Saborido-Rey, 2003) and gamete production relies on both stored energy and energy directly acquired from feeding (Bandarra *et al.*, 1997). Sexual maturity is attained mainly in the age-groups 0-1 year (Silva *et al.*, 2006). Two peaks of spawning were observed in the English Channel with one from May – July and a second one in autumn (October) (Coombs *et al.*, 2005; Stratoudakis *et al.*, 2007). Despite clear spawning seasonality, residual spawning takes place year around (Stratoudakis *et al.*, 2007). In contrast to herring, no distinct spawning grounds are defined for sardines in the English Channel (Coombs *et al.*, 2005) but data coming from the CGFS survey conducted in autumn indicate the westernmost part, the Baie de Somme and the eastern part of the EEC being regions of increased egg abundance (**Figure 11B**). Information about nursery areas only exist for the WEC. While juveniles were especially abundant in the center of the WEC from January to April, from September to December the spatial distribution was less distinct (Campanella and van der Kooij, 2021) (**Figure 11C**).

### Trophic role in the ecosystem

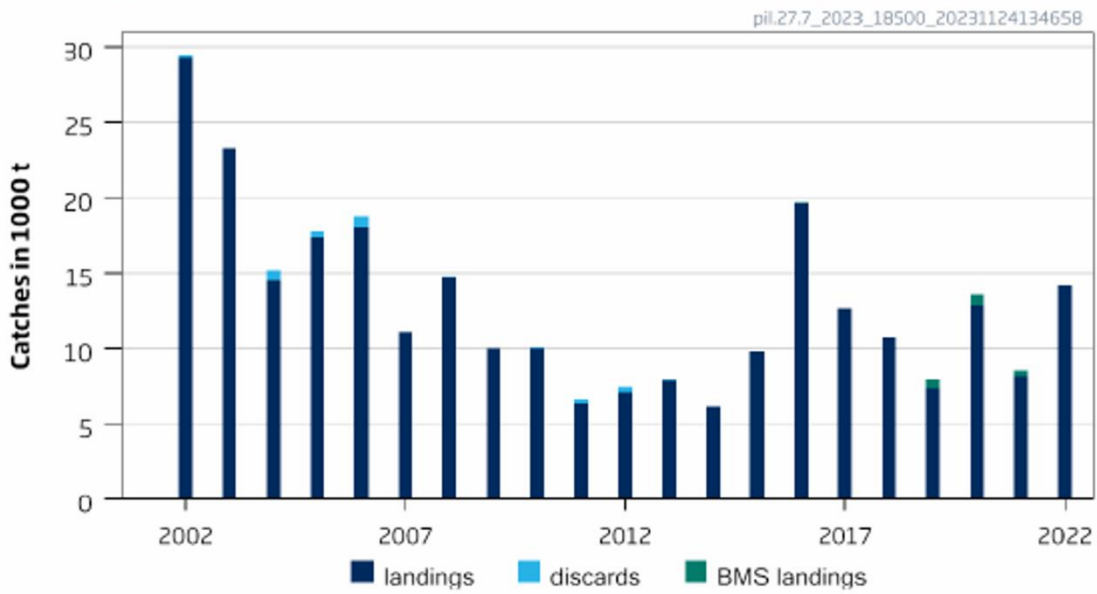
Sardines display an opportunistic feeding behavior that varies ontogenetically, spatially and temporally (Garrido *et al.*, 2007a; Costalago *et al.*, 2015; Garrido *et al.*, 2015; El Mghazli *et al.*, 2020). They switch between filter-feeding and therewith preying on small copepods, micro- and phytoplankton and particulate feeding ingesting mesozooplankton and fish eggs. Thus, their diet encompasses a wide range of prey sizes (Bode *et al.*, 2004; Garrido *et al.*, 2007a; Nikolioudakis *et al.*, 2012). Feeding mode in sardine is not considered density-dependent but influenced by the prey size available (Garrido *et al.*, 2007a).

Sardines serve themselves as prey for many piscivorous taxa such as harbour porpoise (*Phocoena phocoena*), bottlenose dolphin (*Tursiops truncatus*), striped dolphin (*Stenella coeruleoalba*), white-sided dolphin (*Lagenorhynchus acutus*) and common dolphin (*Delphinus delphis*), with the latter extracting 6000 to 9000 tonnes of sardines annually in Galician waters (Marçalo *et al.*, 2018; ICES, 2022a).

### **Fisheries**

Sardine fisheries have strong socio-economic interests and are one of the most valuable fisheries in the Atlantic (De Leonardis and Macciola, 2004; Neves *et al.*, 2021) with annual landings from the Bay of Biscay and the Iberian Peninsula above 100 000 tonnes since the late 1970 (Silva *et al.*, 2015a). Looking at European sardine catches during the last decade, a decline can be observed and nearly all stocks are recognized as fully or heavily exploited (FAO, 2018, 2019; ICES, 2018). Biomass of the European Southern stock for instance decreased by 71 % between 2006 and 2013 due to a period of low recruitment (ICES, 2018). A comparable decrease in biomass together with a decrease in size and condition was observed in the Mediterranean, increasing the risk of over exploitation (FAO, 2018). By contrast, off Morocco and Mauritania, stock biomass appears to be stable and total catch increased by 4 and 17 % in 2016 - 2017, respectively (FAO, 2019). The Northern Stock is a non-quota stock without implementation of management measures at international level (ICES, 2022b). The stock and exploitation status in relation to the maximum sustainable yield (MSY) is not assessed but according to the reference point used in the precautionary approach ( $I_{stat}$ ) the stock biomass is above a critical limit (ICES, 2024c) (**Figure 12**). In the English Channel sardine landings varied between 6157 and 29 287 tonnes between 2002 and 2019 (ICES, 2022b) (**Figure 12**).

## Catches



## Biomass Index

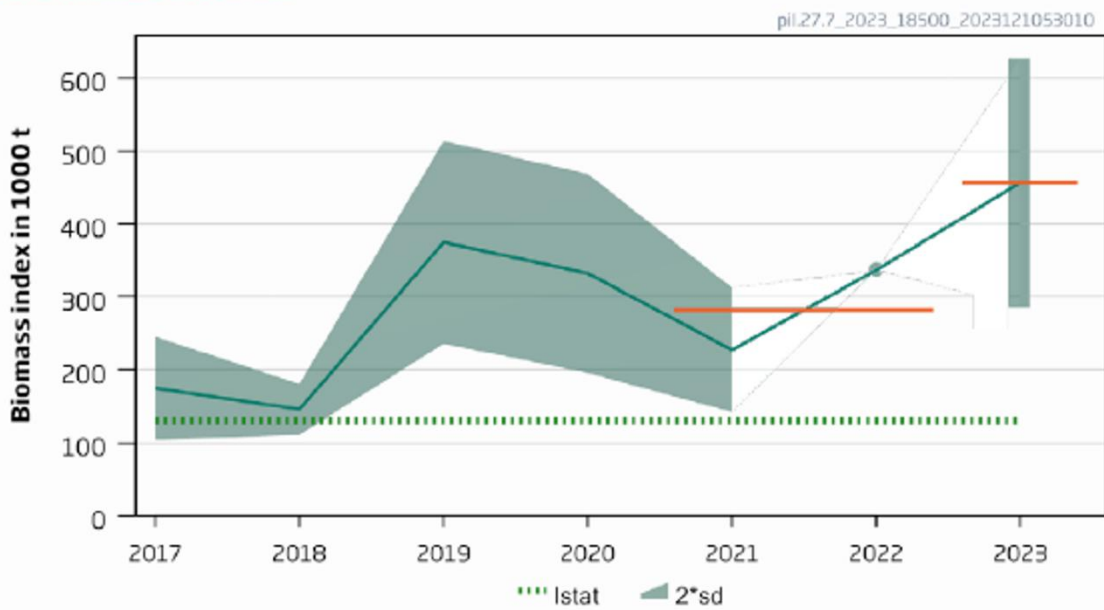


**Figure 12 Stock development over time of sardine (*Sardina pilchardus*) in Subarea 7 (Southern Celtic Seas and English Channel).** Upper panel: Catches since 2002, including catches below minimum size (BMS) and discards; lower panel: Biomass index obtained from the PELTIC survey (Western English Channel). Horizontal orange lines indicate biomass index for 2023 and the average for 2021 – 2022. Adapted from ICES (2024c).

## Plaice

Plaice (*Pleuronectes platessa*) (**Figure 13**) is a benthic flatfish species mostly living on sandy habitats and belonging to the family of Pleuronectidae (Zijlstra *et al.*, 1982; Berghahn, 1986). They can attain a maximum length of 1 m and an age of 50 years (Muus and Nielsen, 1999).



**Figure 13** Adult plaice (*Pleuronectes platessa*). Photograph Pierre Porché, Ifremer.

### Geographical distribution of species and stocks

The biogeographical distribution of plaice ranges from the western Mediterranean Sea, along the European coast to the White Sea, Iceland and Greenland (Nielsen, 1986). Plaice in the North Sea and the English Channel are managed as three different stocks, one associated to the WEC, one to the EEC and the third being the North Sea stock although individuals of all management components mix spatially at some point of their life cycle (ICES, 2021). Tagged animals in the EEC were found in the WEC and North Sea (ICES, 2021) and the assessment of the North Sea stock includes 50 % of the mature specimen of the EEC stock due to its presence in the North Sea during the first annual quarter (ICES, 2023b). Several spawning populations exist that mix during feeding in summer and separate for spawning migration in winter (De Veen, 1978; Hunter *et al.*, 2004).

### Reproduction and life cycle

Plaice are determinate multiple batch spawners, spawning several batches of pelagic eggs during the spawning season while feeding is nearly completely ceased during the spawning period (Urban and Alheit, 1988; Rijnsdorp, 1989; Sauger *et al.*, 2023). Males attain maturity at 2 to 3 years and females between the age of 4 to 5. Possibly resulting from an evolutionary response to fishing mortality, a shift to earlier maturation was found in the early 1980s (Rijnsdorp and Van Beek, 1991; Rijnsdorp *et al.*, 1991; Grift *et al.*, 2003). Plaice spawn offshore on distinct spawning grounds to which they display fidelity (**Figure 14**). During spawning migration tidal currents are used selectively by ascending in mid-water to move downstream with the tide and staying at the bottom during opposing tide (Harding, 1978). On the spawning grounds in the WEC, EEC and the Southern Bight spawning starts in December and January while spawning on the spawning grounds south of the Dogger Bank occurs in February and March (Houghton and Harding, 1976; Arnold and Metcalfe, 1996; Bolle *et al.*, 2009; Loots *et al.*, 2010; Hufnagl *et al.*, 2013; Lelièvre *et al.*, 2014) (**Figure 14**).

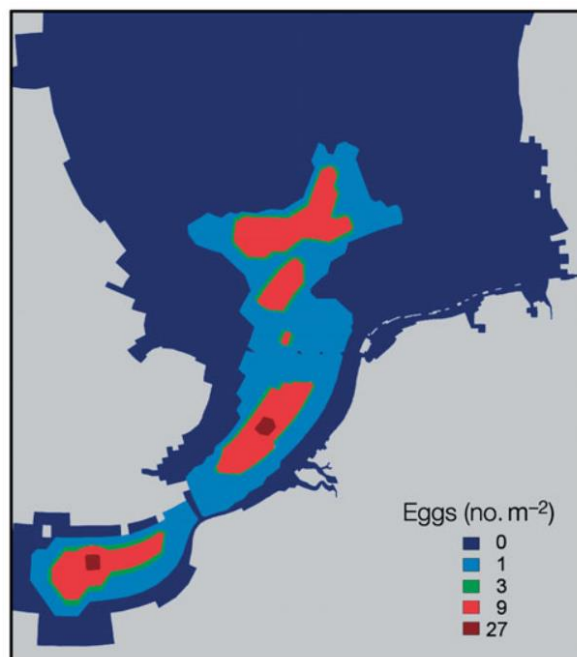


**Figure 14** Approximate position of spawning grounds of plaice (*Pleuronectes platessa*) in the Eastern English Channel and the Southern North Sea reflected by egg abundance. Graphic from Bolle *et al.* (2009).

Depending on the spawning ground, larvae are transported to different coastal nursery areas located along the coasts in the EEC and Southern North Sea (Bolle *et al.*, 2009). After



## General Introduction

metamorphosis from a round to a flat body (**Figure 15**), plaice settle preferentially on sand habitats (Zijlstra *et al.*, 1982; Berghahn, 1986). Close to attaining adulthood plaice move from coastal into deeper areas (De Veen, 1978; Hunter *et al.*, 2003).

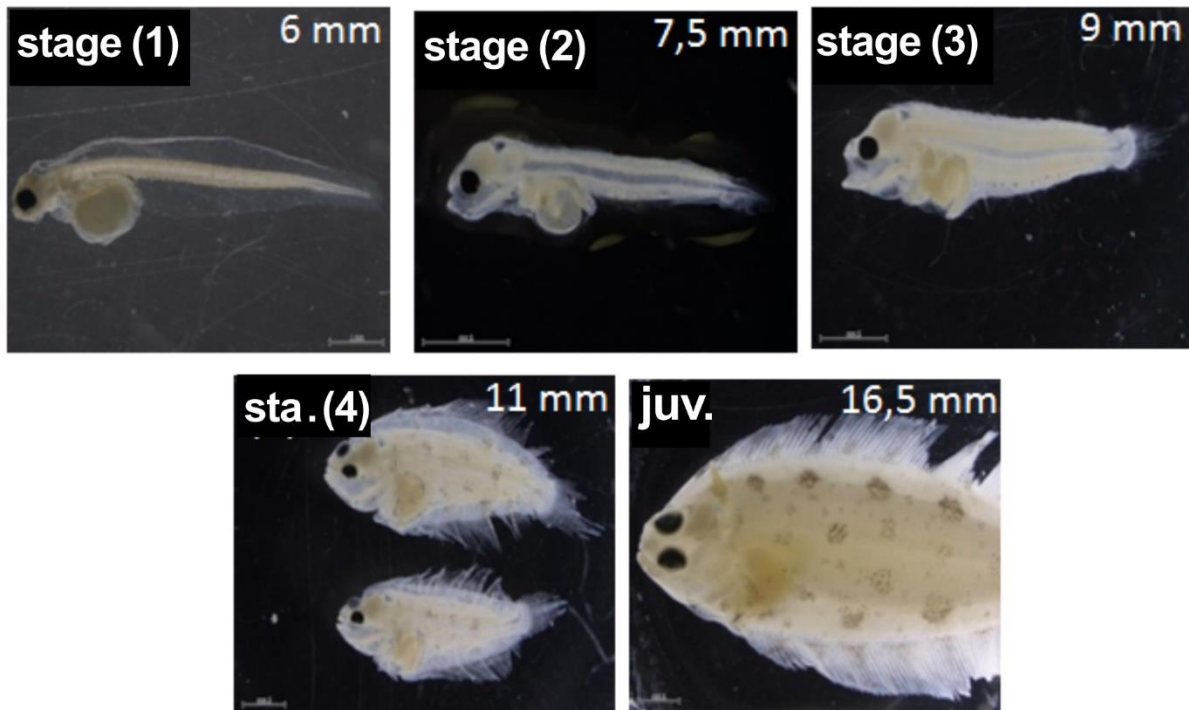


**Figure 15 Larvae of plaice (*Pleuronectes platessa*) at different developmental stages.** Stage 1: yolk sac stage, stage 2 pre-flexion stage, stage 3: post-flexion stage, stage 4: metamorphosis, juvenile. Photographs Michele Pernak.

### Trophic role in the ecosystem

Plaice are important predators for benthic invertebrates like annelid polychaetes, bivalves, coelenterates, crustaceans and echinoderms and of small fish. In the English Channel they live in competition for food with crustaceans, whiting (*Merlangius merlangus*) and other demersal fish (Martin *et al.*, 2009; Girardin *et al.*, 2018). While adult and juvenile plaice are preyed upon by cod, common skate, starry ray, dogfish, cormorants and grey seals (Hammond *et al.*, 1994; Ellis *et al.*, 1996; van der Veer *et al.*, 2000), plaice eggs are eaten by herring and sprat (Segers *et al.*, 2007).

Plaice larvae mainly feed on the appendicularian species *Oikopleura dioica* (Shelbourne, 1953, 1957, 1962; Last, 1978). Further details about plaice larvae feeding will be given in chapters 1 and 2.

## Fisheries

The EEC plaice stock is overexploited with the spawning stock biomass being below the MSY reference point indicating a critical ecological state of the stock (ICES, 2024d) (**Figure 16**). The North Sea plaice stock suffered from overexploitation until approximately 2008 but fishing effort was adapted and is now below  $F_{MSY}$ . The ecological state of the stock was critical from beginning of the 1990's until the 2000's. Afterwards the stock recovered and was in a good ecological state during the last two decades with regard to the MSY reference point (ICES, 2024e) (**Figure 17**). In the first quarter of 2022 25 543 tonnes of plaice were caught in the North Sea of which 283 tonnes were attributed to the stock of the EEC (ICES, 2023b). In the EEC the landings in 2022 accounted for 1601 tonnes (ICES, 2023b).

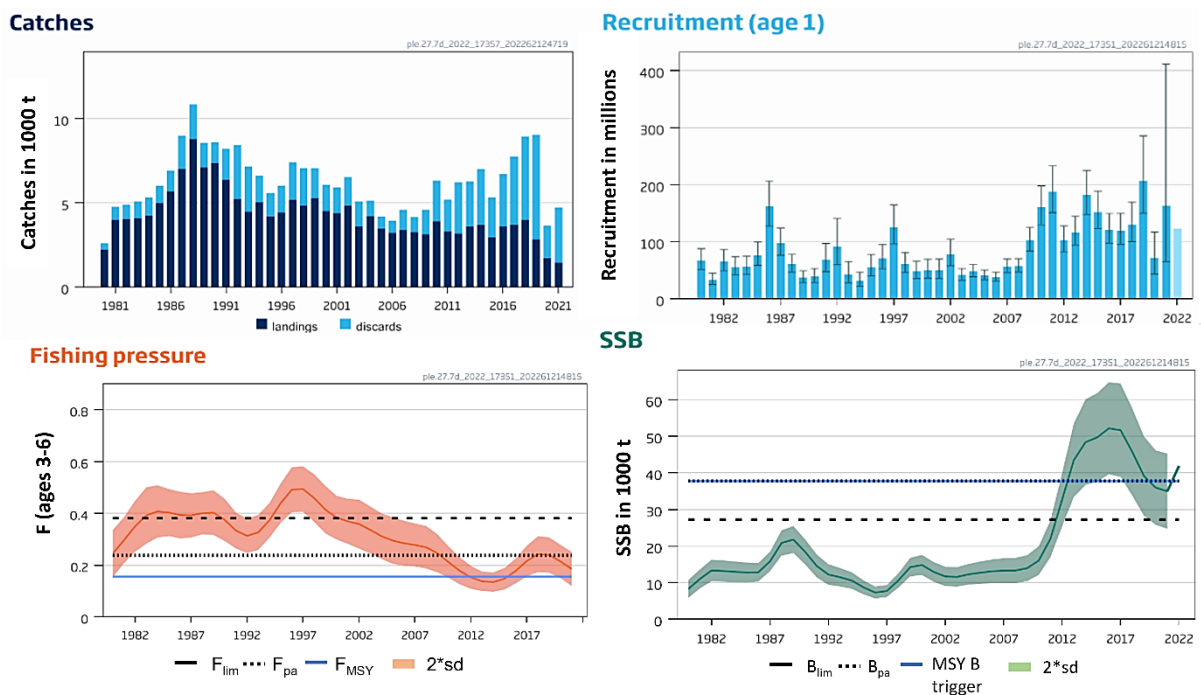


**Figure 16** Stock development over time for plaice in the Eastern English Channel (Division 7.d). Fishing pressure above the  $F_{MSY}$  indicates overexploitation of the stock. Spawning stock biomass (SSB) below MSY B trigger indicates the SSB being too low for the stock to be in a good ecological state. Adapted from ICES (2024d).

## General Introduction

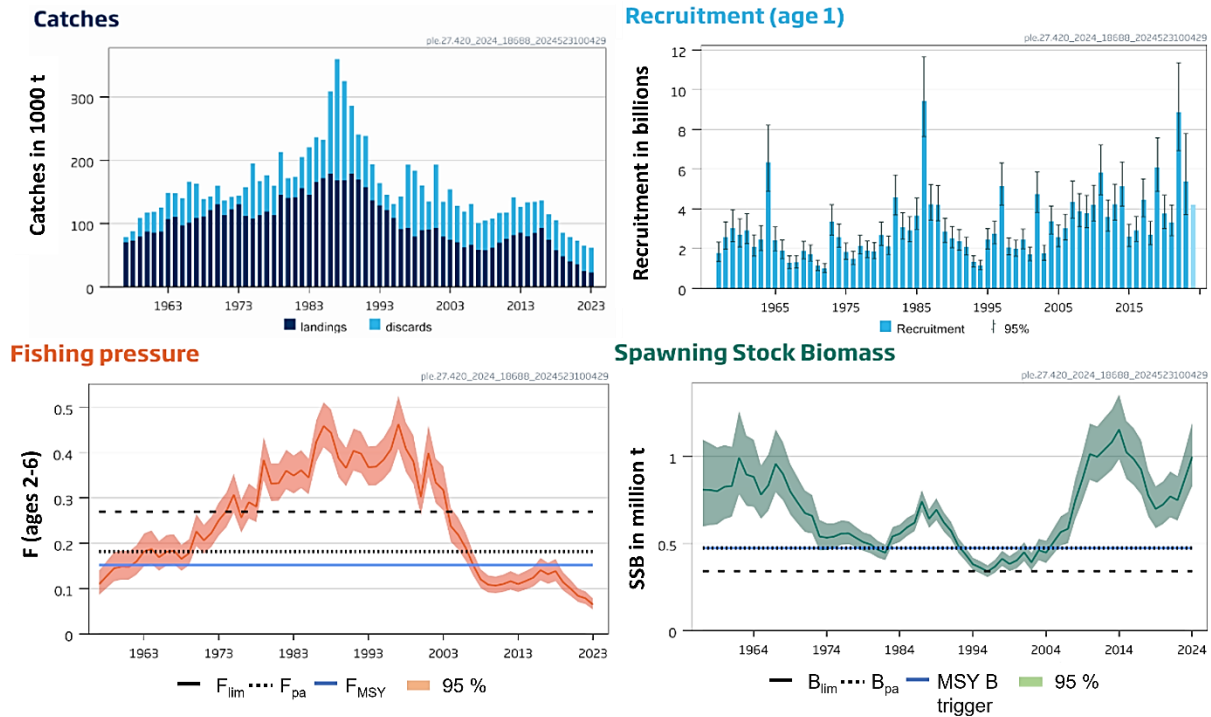


**Figure 17** Stock development over time for North Sea plaice (Subarea 4 and Subdivision 20). Fishing pressure above the  $F_{MSY}$  indicates overexploitation of the stock. Spawning stock biomass (SSB) below MSY B trigger indicates the SSB being too low for the stock to be in a good ecological state. Adapted from ICES (2024e)

## Several perspectives of zooplankton diversity in the context of MBEF

Trophic potential is defined by both prey quantity and quality (Schoo *et al.*, 2012). When considering zooplankton as prey for higher trophic levels, food availability and quality are influenced not only by the taxonomic composition and abundance of zooplankton but also by their biochemical stoichiometry and size. Zooplankton taxa vary with regard to their carbon content: gelatinous zooplankton have a low carbon content of 0.5 %, while crustaceans and microzooplankton contain 12 % and 15 % of carbon, respectively (Heneghan *et al.*, 2023). Furthermore, the proportion of essential fatty acids, largely contributing to prey nutritional quality, is driven by a combination of phylogenetic and environmental factors (Persson and Vrede, 2006).

Size was suggested to be a ‘master trait’ in ecology as it determines metabolic rates and productivity that in turn are related to abiotic variables like temperature. Thus, size represents an indirect way to measure energy and nutrient transfer in relation to abiotic conditions

## General Introduction

(Brown *et al.*, 2004; Giraldo *et al.*, 2024). Furthermore, size plays a determining role in predator-prey interactions and mortality rates (Anderson, 1988; Cohen *et al.*, 1993). Fish larvae depend on distinct prey size due to the size of their mouth gape, for instance (Last, 1978). Thus, considering not only taxonomic diversity but also size and biochemical diversity within the MBEF framework may be necessary for a more mechanistic understanding of zooplankton diversity in the ecosystem.

Thus, the aim of the present thesis was to contribute to a better understanding of ecosystem functioning by studying zooplankton functioning in the English Channel and the Southern North Sea within the MBEF framework. I considered several aspects of zooplankton diversity in relation to lower and higher trophic levels, accounting for spatial variation and potential abiotic drivers.

### **Perspective 1: Taxonomical composition**

In the first chapter, I investigated the spatial distribution of zooplankton and ichthyoplankton taxa during winter in the EEC and SNS in relation to biotic and abiotic drivers with the aim to better understand and assess zooplankton winter assemblages and spatial variability of feeding conditions for winter spawned fish larvae.

The principal question in chapter 1 was: Which mesozooplankton and ichthyoplankton assemblages are present in the SNS-EEC during winter and which abiotic and biotic factors drive their composition and distribution?

### **Perspective 2: Plankton size structure: an isotopic approach**

In the second chapter, I investigated the size structure of plankton ranging from nano- to mesoplankton and their contribution to the diet of herring and plaice larvae in the EEC using stable isotopes.

The principal questions of chapter 2 were: What is the size structure of plankton in the EEC with regard to their isotopic signature during winter? Which plankton size classes are characteristic for plaice and herring larval diet?

**Perspective 3: Biochemical composition: a fatty acid approach**

In the third chapter, I focused on the biochemical composition of mesozooplankton with regard to fatty acids (FA) and their transfer to higher trophic levels represented by sardine. The FA profiles of mesozooplankton and sardine were analysed in combination with the taxonomical composition of zooplankton and phytoplankton in the entire English Channel accounting for spatial variation in relation to environmental drivers.

The principal question asked in this chapter was: How does the FA profile of zooplankton and sardine vary spatially in the English Channel and what are the drivers of the spatial variability in the trophic transfer of these essential nutrients between these two trophic levels?

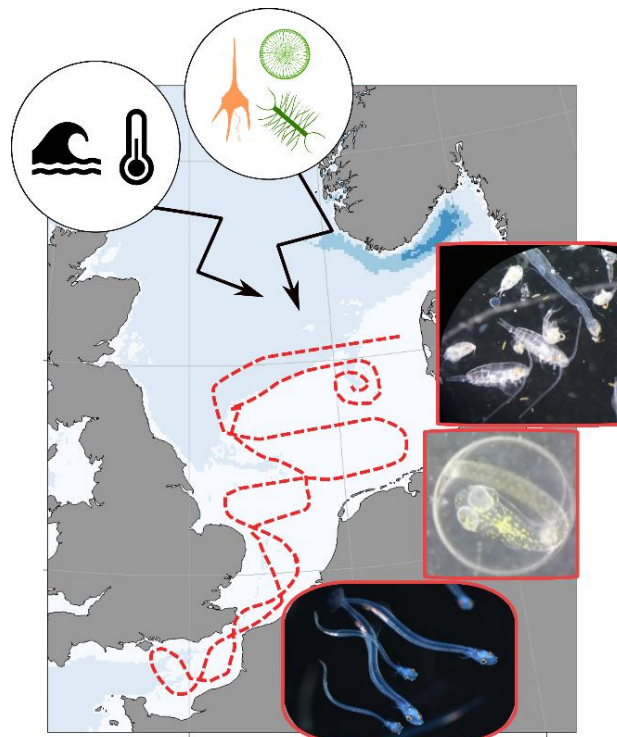
## CHAPTER 1 - 1. Perspective – Taxonomical composition

Historically, the word plankton was used to refer to organisms that were thought to be randomly and uniformly distributed in space (Hensen, 1887; Lussenhop, 1974; Lomartire *et al.*, 2021). Today, we know that plankton display distinct vertical and horizontal distribution patterns that are driven by biotic and abiotic factors (Krause *et al.*, 1995; Hays *et al.*, 2001; Grandremy *et al.*, 2023). As the composition and distribution of zooplankton communities can influence lower and higher trophic levels through grazing, nutrient recycling and energy transfer (Legendre and Rassoulzadegan, 1995; Sommer and Lewandowska, 2011; Pitois *et al.*, 2012), the first chapter aimed at understanding the spatial distribution of meso- and ichthyoplankton during winter in the SNS and the EEC, a period for which information concerning zooplankton remain limited.

The work in this chapter was published in the scientific journal PLOS ONE (in press):

### Winter distribution of zooplankton and ichthyoplankton assemblages in the North Sea and the English Channel

Carolin Julie Neven, Carolina Giraldo, Raphaël Girardin, Alain Lefebvre, Sébastien Lefebvre, Christophe Loots, Cédric Leo Meunier, Paul Marchal



# Winter distribution of zooplankton and ichthyoplankton assemblages in the North Sea and the English Channel

---

## 1.1 Introduction

In temperate regions, the annual abundance of zooplankton organisms follows a seasonal cycle. This cycle starts with a phytoplankton spring bloom facilitating an increase of zooplankton abundance and biomass characterized by a succession from herbivorous to predatory taxa (Sommer *et al.*, 2012; Teodosio and Barbosa, 2020). Depending on hydrological conditions and community structure, a second abundance peak may occur in autumn facilitated by the phytoplankton autumn bloom growing on remineralized nutrients and terminating the productive period (Teodosio and Barbosa, 2020). But what happens outside of these periods? How and where do zooplankton organisms survive or live during low primary production and winter conditions? Some insight is coming from studies on overwintering strategies and seasonality of marine copepods (Hay *et al.*, 1991; Hay, 1995; Halsband and Hirche, 2001; Engel and Hirche, 2004; Halsband-Lenk *et al.*, 2004; Wesche *et al.*, 2007). Whereas the copepod *Acartia clausi* was found to undergo a reproductive dormancy probably regulated by intrinsic factors as egg production increased irrespective of environmental conditions, *Temora longicornis* and *Centropages typicus* can reproduce throughout winter (Wesche *et al.*, 2007) albeit reproduction rate may be driven by prey availability and temperature, respectively (Dam and Lopes, 2003; Wesche *et al.*, 2007). Some species like *T. longicornis* seem to display a mixed strategy consisting of hibernal (winter) reproduction and production of resting eggs (Halsband and Hirche, 2001; Engel and Hirche, 2004; Wesche *et al.*, 2007). Further overwintering strategies of zooplankton are diapause, seasonal vertical migration, building of energy storage, reduced growth and metabolic rate, for instance (Varpe, 2012). Zooplankton overwintering stocks are of importance as their size and distribution were found to influence year-to-year variations in the general abundance and distribution of zooplankton in the North Sea (Colebrook, 1984, 1987) functioning like a seed (Hay *et al.*, 1991) ready to flourish as soon as conditions are adequate. Evidence suggests that depending on the

size and composition of the zooplankton overwintering stock the phytoplankton spring bloom might be exploited differently with regard to time, biomass, phytoplankton species and size classes (Sommer and Lewandowska, 2011). As discussed by Nielsen and Richardson (1989) small overwintering populations might leave a major part of the spring bloom unexploited. High initial copepod overwintering stocks by contrast might introduce top-down control earlier during the spring bloom development, prolonging the time span of nutrient availability for phytoplankton by remineralization. This might have further consequences for plankton succession and carbon sequestration (Sterner, 1986; Nielsen and Richardson, 1989; Spilling *et al.*, 2018). Although overwintering strategies are complex and our understanding remains limited (Wesche *et al.*, 2007), spatial and temporal variation of zooplankton overwintering stocks can be expected. Temperature and prey availability are control mechanisms of overwintering. Thus, ocean warming (Edwards and Richardson, 2004; Wiltshire and Manly, 2004; Boersma *et al.*, 2015) and observed changes in the phenology, composition and abundance of primary producers (Edwards *et al.*, 2002; Hawkins *et al.*, 2003; Edwards and Richardson, 2004) might have taxa-specific influences on zooplankton overwintering (Wesche *et al.*, 2007). This in turn, might have potential consequences for phytoplankton spring bloom succession (Sommer and Lewandowska, 2011; Friedland *et al.*, 2016).

Zooplankton were extensively studied in the North Sea (e.g. Alvarez-Fernandez *et al.*, 2012; Beaugrand *et al.*, 2014, 2001; Fransz *et al.*, 1991; Friedland *et al.*, 2016; Hawkins *et al.*, 2003), albeit winter populations have been less studied than spring-summer assemblages, despite growing acknowledgment of the importance of this period (Colebrook, 1984; Fransz *et al.*, 1991; Sommer and Lewandowska, 2011; Hufnagl *et al.*, 2015; Dudeck *et al.*, 2021; Akimova *et al.*, 2023). Furthermore, studies describing spatial distribution of single species or assemblages in detail remain scarce, spatially limited or describe the distribution of zooplankton at the end of the last century. Krause and Martens (1990) and Krause *et al.* (1995) assessed the zooplankton community of the entire North Sea sampled during winter 1987 and provided maps displaying the distribution of abundance and biomass for each taxon found. With regard to abundance three overall patterns of taxa distribution were revealed constituting the affiliation to Northern North Sea water, the central North Sea or coastal neritic areas (Krause *et al.*, 1995). With regard to biomass, centers of relatively high biomass were localized in the SNS associated to eastern river deltas, off the British coast towards the Dogger Bank and in the Skagerrak region (Krause and Martens, 1990). Van Ginderdeuren *et al.* (2014) described



the zooplankton assemblage in the Belgian part of the North Sea in winter 2009 as single neritic zooplankton assemblage dominated by *T. longicornis* and *A. clausi* with presence of oceanic species depended on Atlantic water inflow. In a recent study, Dudeck et al. (2021) evaluated data sampled from 1991 to 2013 in the EEC and the Southern Bight to investigate temporal change in size and overall abundance of zooplankton considering potential spatial variation. Whereas zooplankton individual size displayed a decreasing trend, zooplankton abundance was found to increase with no difference among the four regions defined based on zooplankton congregations. A similar pattern was found in the Bay of Biscay where there was a decline in zooplankton body size but an increase in abundance leading to no changes in the overall biomass (Grandremy *et al.*, 2023). None of these studies, however, defined and concurrently described the defined zooplankton assemblages and their spatial distribution in the SNS and EEC (SNS-EEC), and ichthyoplankton (fish larvae and eggs) was never included comprehensively. Furthermore, although being a period of relatively low prey abundance (Krause and Martens, 1990), several fish species spawn in winter in the SNS-EEC (Munk and Nielsen, 2005; Martin *et al.*, 2008; Coppin *et al.*, 2009). The SNS-EEC harbor spawning sites, larval drifting routes and nursery areas and constitute therewith an important area for winter spawning fish, particularly for herring (*Clupea harengus*) and plaice (*Pleuronectes platessa*) (Martin *et al.*, 2008; Bolle *et al.*, 2009; Coppin *et al.*, 2009). The Downs herring spawning component, for instance, spawns in the EEC and Southern Bight of the North Sea from November until February (Coppin *et al.*, 2009; Dickey-Collas *et al.*, 2009) and larvae hatching in the EEC are transported to eastern North Sea nursery grounds (Bolle *et al.*, 2009). The Downs population has recovered after almost disappearing in the late 1970es, and it is now a major contributor to the overall North Sea herring recruitment (ICES, 2022b, 2023a). Fluctuations in Downs herring year class strength are driven by favorable environmental conditions combined with match-mismatch dynamics (Cushing, 1990; Nash and Dickey-Collas, 2005; Peck *et al.*, 2012). In particular, Downs herring larvae feed on overwintering plankton, and the lack of knowledge about the distribution and composition of these prey was mentioned as a major gap in understanding their survival (Akimova *et al.*, 2023).

A large scale approach aiming at the definition of plankton assemblages in the North Atlantic and its adjacent Seas using seasonally integrated data indicated the existence of several plankton assemblages in the SNS (Kléparsi *et al.*, 2021). Although the data used in this study did not cover the Southern Bight and EEC and detailed information about the assemblages in

the SNS-EEC remained limited, this study gives rise to the hypothesis that different zooplankton assemblages may exist in this area during winter. With the aim to shed light on the described knowledge gap, the present study intends to investigate the spatial distribution of winter zooplankton assemblages integrating mesozooplankton and ichthyoplankton in the SNS-EEC, and to discuss them with regard to potential environmental drivers. Understanding the distribution and composition of assemblages can be complex (Gabaldón *et al.*, 2019) as they might be influenced by several factors like abiotic condition (e.g. temperature, oxygen, depth) (Luo *et al.*, 2014), predation (Maes *et al.*, 2005; Daewel *et al.*, 2014) and food availability (Luo *et al.*, 2014). Also food quality was shown to influence zooplankton abundance (Nobili *et al.*, 2013; Meunier *et al.*, 2016). The dissolved N/P ratio in the sea water was shown to reflect the phytoplankton quality in terms of prey for herbivorous zooplankton, as the N/P ratio in phytoplankton varies with the ratio of dissolved nutrients in surrounding sea water (Sterner and Elser, 2017). Phytoplankton displaying an N/P ratio close to the Redfield ratio of 16:1 were found to represent food of higher quality for copepod species (Nobili *et al.*, 2013). These examples show that factors shaping assemblages are diverse and we aim to elucidate their relationships with the assemblages found by using a comprehensive set of potential environmental drivers.

Analyzing mesozooplankton and ichthyoplankton data concomitantly is methodologically challenging as these different zooplankton compartments are surveyed using different sampling schemes, resulting in datasets with distinct sampling resolution and coverage. In this study, we propose the use of a geostatistical method developed in agronomics (Tisseyre *et al.*, 2018) to define a common spatial grid adapted to the data and allowing for common analysis of those datasets. Using a clustering approach, we then defined zooplankton assemblages and assessed inter-annual variation of the spatial extent and composition of the assemblages found. As present knowledge about hibernal zooplankton assemblage composition and distribution is scarce, the outcome of the present study will allow to recognize potential future changes of zooplankton assemblage composition and distribution and help to better understand spring plankton succession/development in the context of climate change.

## 1.2 Materials & Methods

### 1.2.1 Data

All zooplankton and most environmental data used in this study were sampled in January-February during the first quarter International Bottom Trawl Survey (IBTS) in 2008 and 2022, onboard of the French Thalassa Research Vessel from the French Oceanographic fleet. Additional details on sampling protocols are given below and are accessible using the survey's DOI (2008: 10.17600/8040010, 2022: 10.17600/18001811).

In 2008 (27.01.2008 to 21.02.2008) data collection included taxa-specific abundance of zooplankton (mesozooplankton, ichthyoplankton (eggs, larvae), taxa-specific phyto- and microplankton abundance and environmental parameters (particulate organic matter (POM), chlorophyll a, nitrate ( $\text{NO}_3^-$ ), nitrite ( $\text{NO}_2^-$ ), ammonium ( $\text{NH}_4^+$ ), phosphate ( $\text{PO}_4^{3-}$ ), silicate ( $\text{Si(OH)}_4$ ), temperature, salinity, depth) (**Figure 18A-C**, Annex I **Figure A 1**). The ratio of nitrogen (sum of nitrite, nitrate and ammonium) and phosphate and the sum of nitrate and nitrite was calculated for further analysis. In 2022 (17.01.22 – 09.02.22) a more restricted spectrum of ecosystem and environmental parameters was assessed over a smaller spatial extent (**Figure 18D-E**). Data available for 2022 were mesozooplankton, fish larvae, temperature, salinity, depth and chlorophyll a concentration.

For the implementation of an anomaly analysis salinity and temperature data for the period 1998 to 2022 and chlorophyll a data available for the period 2008 – 2022 were downloaded from the ICES (<https://www.ices.dk/data/dataset-collections/Pages/default.aspx>) and Datras database (<https://datras.ices.dk>). Data of the herring larval index (1992 – 2022) were accessed from the 2023 report of the ICES working group HAWG (ICES, 2023a).

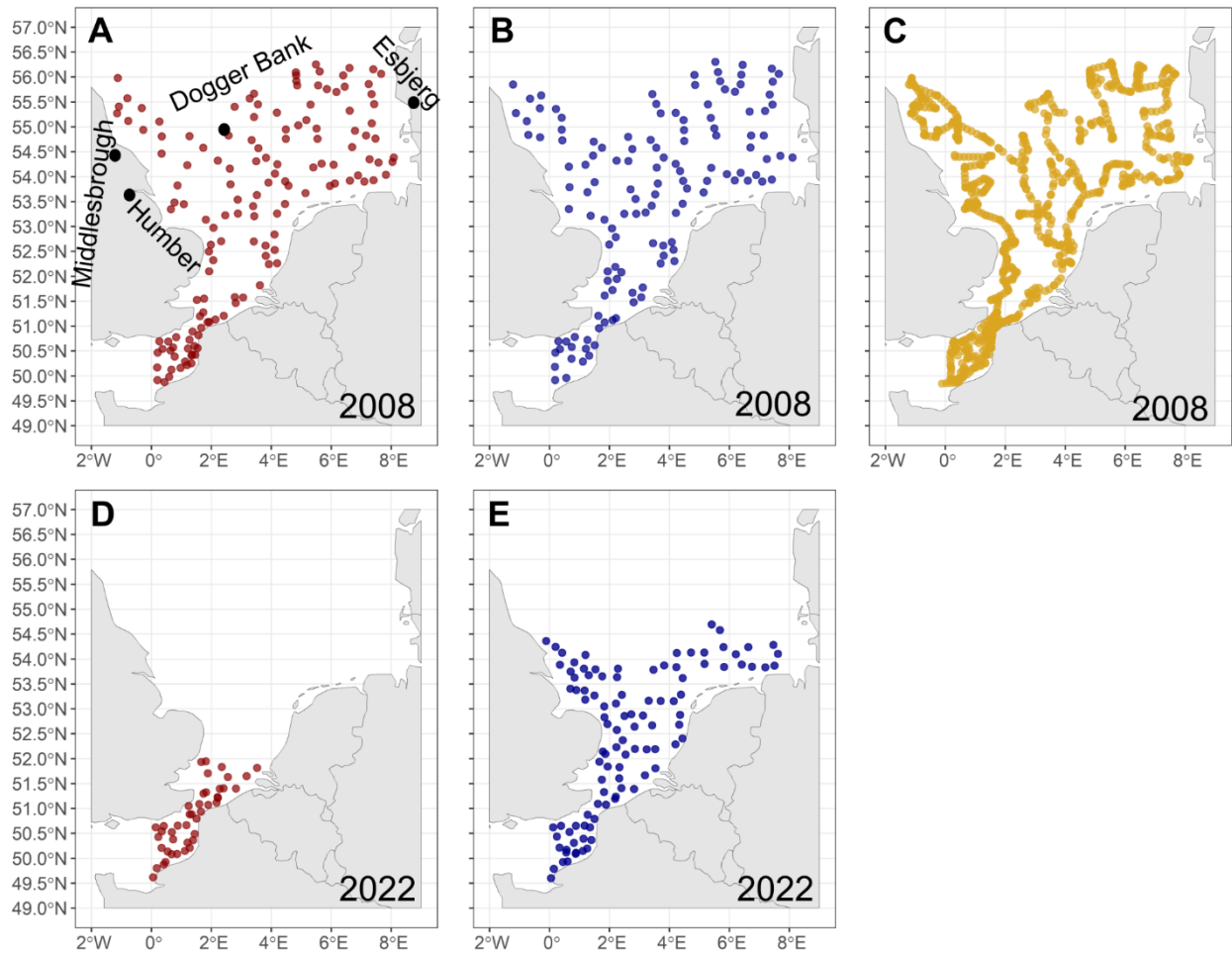


**Figure 18 IBTS sampling stations.** A: Mesozooplankton (IBTS 2008), black dots indicate locations delineating the geographical distinction between the Southern and Northern North Sea, furthermore the position of the sandbank Dogger Bank is indicated; B: Fish larvae (IBTS 2008); C: Fish eggs (IBTS 2008); D: Mesozooplankton (IBTS 2022); E: Fish larvae (IBTS 2022).

### 1.2.1.1 Zooplankton taxa and abundance

#### *Mesozooplankton*

In 2008 and 2022, a total of respectively 142 and 43 mesozooplankton samples were taken using a WP2 net (mesh size 200  $\mu\text{m}$ ) which was vertically hauled from 3 m above bottom to surface. Sampling took place during night and daytime and no significant differences were found between night and day samples.

Species determination was assisted by a ZooScan (Grosjean *et al.*, 2004; Gorsky *et al.*, 2010). Briefly, a ZooScan allows scanning zooplankton samples as pictures, which are subsequently used by a machine-learning algorithm for species determination. The machine-learning algorithm used in 2008 was Plankton Identifier ([37](http://www.obs-</a></p>
</div>
<div data-bbox=)

vlfr.fr/~gaspari/Plankton\_Identifier/index.php) and Eco-Taxa (<http://ecotaxoserver.obs-vlfr.fr>) in 2022. Both algorithms are based on the ZooProcess software and produce comparable results. Samples stored in 1% formalin were rinsed and specimens were divided in two size classes (A: 200-500 µm, B: >500 µm) to increase determination success of the method. To further enhance determination exactness, samples were fractionated by means of the Motoda method (Motoda, 1959; Grosjean *et al.*, 2004). Finally, specialists in zooplankton taxonomy validated ZooScan taxonomic classification output. Since the ZooScan is able to detect organisms with an equivalent circular diameter of at least 300 µm (Gorsky *et al.*, 2010), only the mesozooplankton size fraction >300 µm was retained in this study. In 2008, 46 groups of specimen were determined with the finest taxonomic determination level being genus (Annex I **Table A 1**) and multiples accounted for 6.6 % of all pictures. In 2022, 62 taxa were found with the finest taxonomic level being species (Annex I **Table A 2**). Multiples accounted for 8.1 % of all pictures. Taxonomic resolution was adapted to the resolution of the 2008 data set to facilitate inter-annual comparison reducing the number of taxa to 44. Depth integrated mesozooplankton abundance was calculated as individuals per m<sup>3</sup>. The water volume filtered by the WP2 bongonet was derived using equation (1), where  $V$  is the filtered volume of seawater in m<sup>3</sup>,  $T$  the number of turns of the volume meter,  $0.3$  the conversion factor provided by the manufacturer of the volume meter and  $D$  the net diameter ( $D=0.57$  m).

$$V = T * 0.3 * \left[ \pi * \left( \frac{D}{2} \right)^2 \right] \quad (1)$$

The abundance per taxon and station ( $Ab$  in individuals per m<sup>3</sup>) was calculated using equation (2), with  $N$  being the number of individuals identified per size class (A and B),  $F$  the fraction of the sample after application of the Motoda method (e.g.  $\frac{1}{16}$ ) and  $V$  the volume filtered per station / sample.

$$Ab = \frac{\left( \frac{NA}{FA} + \frac{NB}{FB} \right)}{V} \quad (2)$$

### **Fish larvae**

In 2008 and 2022, a total of respectively 130 and 103 fish larvae samples were collected. Sampling took place after sunset and was realized using a MIK (Method Isaac Kid) with a mesh

size of 500 µm. At the sampling station the MIK was descended to the bottom and ascended diagonally covering the entire water column for a duration of 10 min. Samples were analyzed for species abundance in the laboratory using a Stereo Microscope (Olympus SZX16 with a 7x – 115x zoom range). The abundance per taxon and station (in individuals per 1000 m<sup>3</sup>) was calculated by dividing the number of individuals per station by the volume filtered. The volume filtered was calculated by means of equation 1.

A total of eight taxonomic groups were found in 2008, of which four could be identified to species level (Annex I **Table A 1**). In 2022 a total of 14 taxonomic groups were found, including 11 species, one genus and two families (Annex I **Table A 2**). Herring larvae (*C. harengus*) were separated into three size classes to allow for spatial analysis of larvae with different prey composition. Class 6-12 mm represented the yolk sac and preflexion stage (Joly *et al.*, 2021), class 13–20 mm represented a critical stage with regard to a change in prey selection (Checkley, 1982; Denis *et al.*, 2016), and class 21–42 mm covered the postflexion stage (Joly *et al.*, 2021). No size specific data was available for the other taxonomic groups of fish larvae.

### ***Fish eggs***

In contrast to mesozooplankton and fish larvae samples, fish eggs were sampled continuously during the route of the research vessel. Seawater was pumped from three meters below sea surface by means of the Continuous Underway Fish Egg Sampler (CUFES) (Checkley Jr *et al.*, 1997). In total 861 samples were taken in 2008. Samples were stored in 1% formol. Taxonomic determination was realized using a Stereo Microscope (Olympus SZX16 with a 7x – 115x zoom range). The abundance per taxon (in individuals per m<sup>3</sup>) was calculated by dividing the number of individuals per sample by the water volume filtered.

In 2008, the eggs of five taxonomic groups (Annex I **Table A 1**) were collected of which two were identified to species level.

### **1.2.1.2 Phyto- and microplankton**

In 2008, phyto- and microplankton taxa composition and taxa abundance were determined using inverse-microscopy. The abundance per taxon and station (in cells per liter) was calculated by dividing the number of individuals per station by the volume filtered.

To simplify later analysis taxa abundance of diatoms, dinoflagellates, flagellates, nanoflagellates, ciliates, chlorophytes and others was summed. The group of others contained

the taxa *Phaeocystis globosa*, *Heterosigma spp.*, *Eutreptiella spp.*, Mediophyceae, Crysophyceae and Cryptophyceae. These groups represented the overall diversity of phyto- and microplankton and its spatial distribution sufficiently for the purpose of the present study.

## 1.2.2 Data projection on an optimized grid

### 1.2.2.1 Estimation of optimal grid size

The optimal grid cell size was determined using the most comprehensive and spatially-extended 2008 dataset. As mesozooplankton, fish larvae and fish egg datasets differed in their sampling extent as well as in their sampling resolution, a common sampling area and spatial grid was defined, building on an approach initially developed in agronomics (Tisseyre *et al.*, 2018) and to our best knowledge, for the first time applied to marine ecological data. The area of analysis (polygon) was restricted to the dataset covering the smallest sampling area (fish egg data set). Within the polygon 141 mesozooplankton samples, 129 fish larvae and 861 fish egg samples remained for further analysis. The optimal grid cell size ( $L_{opt}$ ) was then defined as cell size that reduced the undesirable nugget variance (derived from a semi-variogram) to a minimum, whilst minimizing the resulting decrease in the informative variance component of the spatial structure (Bellehumeur *et al.*, 1997; Tisseyre *et al.*, 2018). In detail,  $L_{opt}$  was defined as the cell length, which optimizes the structural information in a grid cell, by maximizing the sum of two components. The first component is the proportion of nugget variance that is removed (PNR). The second component is the proportion of sill variance that is retained (PS). This relationship was specified in formula 3, where  $fv$  is the amount of information per grid cell of size  $v$  (area),  $P_{NR}$  is the proportion of initial noise that is removed and  $P_S$  is the proportion of remaining spatially structured variance.

$$fv = PNR + P_S \quad (3)$$

Tisseyre *et al.* (2018) showed that, with an exponential variogram model, equation (3) could be simplified as a function of the length of the raster cell ( $L$ ), the range ( $a$ ) estimated from the variogram model, and the sampling rate ( $r$ ) in the study area (equation (4)).

$$fv = \exp\left(-\frac{L}{2a}\right) + 1 - \frac{1}{rL^2} \quad (4)$$

To calculate  $L_{opt}$ , we calculated the first derivative of  $f_v$  relative to  $L$  ( $f_v'$ ), and numerically sought the value of  $L$  for which  $f_v'$  was null:

$$f_v' = -\frac{1}{2a} * \exp\left(-\frac{L}{2a}\right) + \frac{2}{rL^3} \quad (5)$$

As the sampling resolution of the mesozooplankton and fish larvae datasets ( $n=141$ ,  $n=129$ , respectively) was much lower than that of the fish egg dataset ( $n=861$ ), only the taxa of the former two datasets were considered to derive  $L_{opt}$ . To solve equation  $f_v' = 0$ , the ranges ( $a$ ) of all mesozooplankton and fish larvae groups with a higher occurrence than 10 % and contributing to 95 % of cumulative frequency of abundance in the polygon were calculated. Non-stationarity data (variogram not displaying sill) with a spatial trend accounting for more than 20% ( $R^2 \geq 0.2$ ) of the variation were detrended using the least-square regression method. The trend was modelled by fitting a linear or quadratic regression to the spatial coordinates. If the regression model was significant with a  $R^2$  higher than 0.2 the empirical variogram was calculated on the residuals (Loots *et al.*, 2010). In case linear and quadratic regression models were significant with a similar  $R^2$ , quadratic residuals were chosen for geostatistical analysis (Annex I **Figure A 2**). Finally, it was not possible to fit an exponential variogram model for certain taxa, owing to the spatial structure of their distribution. In case an exponential variogram model could not be fitted to the empirical variogram (8 taxa from 22), the respective taxonomic group was excluded from the grid cell size definition process. In a next step,  $f_v'$  was solved for all taxonomic groups with a nugget effect higher than zero (7 taxa from 14) using an evolutionary algorithm running 500 iterations testing 1000 numbers per cycle. Finally, it was verified that the received taxon specific  $L_{opt}$ s were bigger than the minimum distance between stations and smaller than the practical range (Tisseyre *et al.*, 2018).

After having defined taxon-specific- $L_{opt}$  (79.9 – 123.3 km) (Annex I **Figure A 3**), we sought a compromise value for which  $L_{opt}$  was close to the maximum taxon-specific- $L_{opt}$  of all taxa, and for which the number of empty grid cells was kept to a minimum. For this purpose, the median value of the taxon-specific- $L_{opt}$  was calculated resulting in an  $L_{opt}$  of 91.58 km producing a maximal information content per cell that differed by less than 1.7 % from the information content obtained using taxon-specific- $L_{opt}$ . The minimum number of sampling



## CHAPTER 1 - 1. Perspective – Taxonomical composition

stations per cell was one for mesozooplankton and fish larvae and two for the egg dataset (**Figure 19**). One cell of central position did not contain sampling stations and thus was excluded from further analyses. The Lopt of 91.58 km was subsequently applied to project information from both the 2008 and 2022 datasets.

All analyses were performed in R version 4.2.1 using the package “gstat” (Pebesma, 2004) and “sp” (Pebesma and Bivand, 2005) for the geostatistical analyses and the package “raster” (Hijmans, 2012) for definition of empty cells per grid cell size.

CHAPTER 1 - 1. Perspective – Taxonomical composition

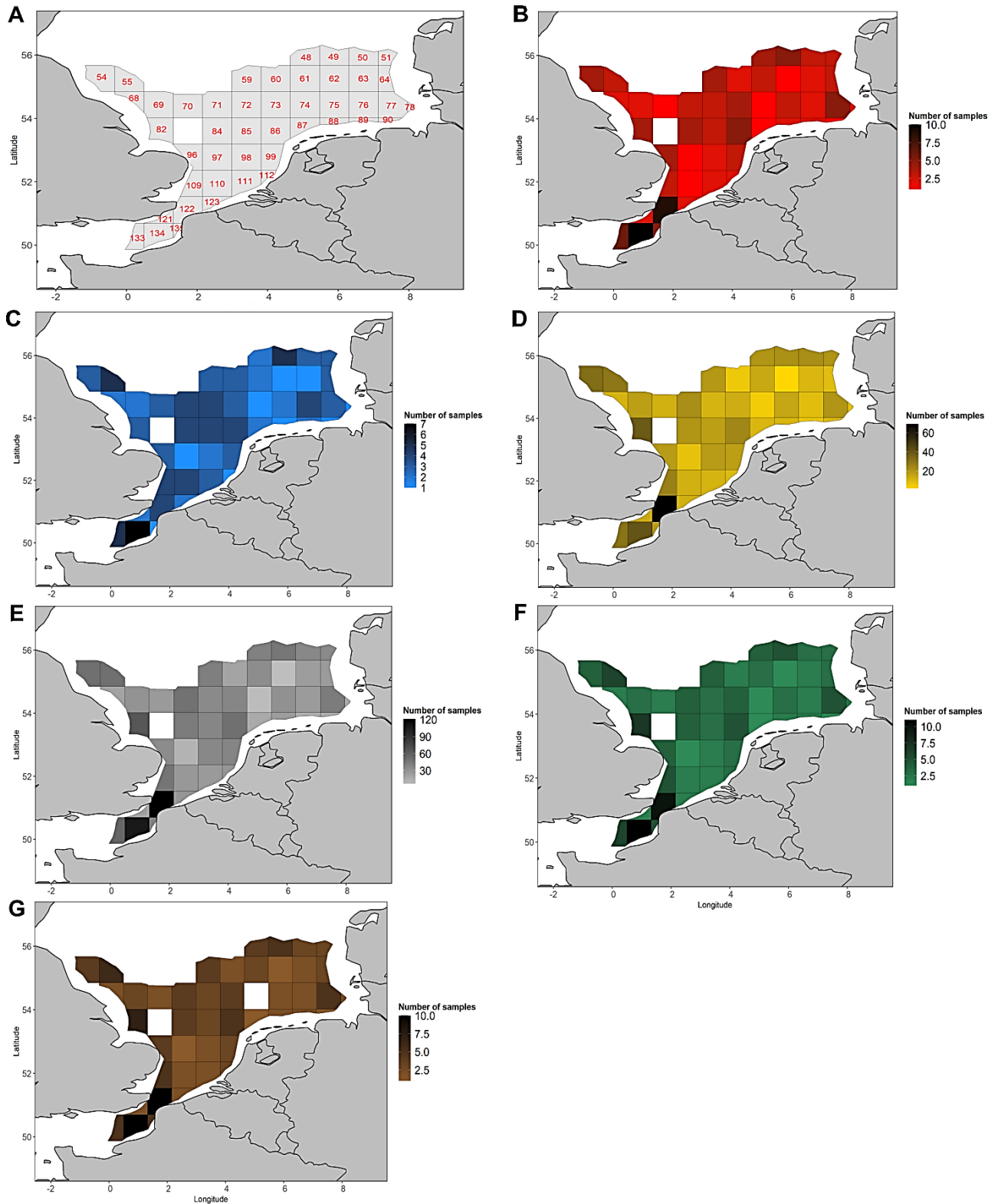


**Figure 19** Number of sampling stations per cell for the 2008 dataset. A: Grid with the optimal grid cell size of 0.83 x 0.83 degrees; B: Number of sampling stations for mesozooplankton per grid cell; C: Number of sampling stations for fish larvae per grid cell; D: Number of sampling stations for fish eggs per grid cell; E: Number of sampling stations for salinity, temperature and depth; F: Number of sampling stations of water samples for phytoplankton community analysis; G: water samples for concentration of material in suspension and chlorophyll a.

### 1.2.2.2 Planktonic abundance and environmental parameters per grid cell

The abundance ( $x$ ) of all zooplankton taxa per sampling station was transformed with the  $\log(x+1)$  function. This transformation allowed to downscale the high variability among the abundances of the different taxa (Clarke and Warwick, 2001). Using a bootstrap with the number of iterations set to 10000, the mean abundance per grid cell was calculated for log-transformed and raw data of each taxon. The mean of log-transformed data was used for clustering whereas the mean derived from raw data was used for the determination of indicator taxa (**Figure 20**) and to investigate the relation to environmental drivers later on (see chapter 1.2.4). The mean of non-transformed and  $\log(x+1)$  transformed environmental parameters and phyto-microplankton abundance was calculated using the same method. Using the bootstrap method reduced the bias resulting from a differing number of sampling or measuring stations per grid cell (Nahorniak *et al.*, 2015).

Summing the mean abundance of all taxa collected in a grid cell, the total mean zooplankton (mesozooplankton and ichthyoplankton) abundance and the total mean phyto-microplankton abundance per grid cell were calculated.

### 1.2.3 Determining assemblages by means of fuzzy clustering

An overview of the methodological steps for the assemblage definition is given in **Figure 20**. In order to define assemblages based on the most important taxa with regard to abundance (McKnight *et al.*, 2019), whilst considering the ecological meaning of rarer specimens, taxa were separated into dominant and secondary. A taxon was considered dominant when its relative abundance was higher than 0.5 %, and secondary otherwise (Souissi *et al.*, 2001). Dominant taxa were used for clustering. Secondary taxa were included in the calculation of indicator taxa (Dufrêne and Legendre, 1997). Indicator taxa were determined by means of the IndVal method (Dufrêne and Legendre, 1997), which reveals taxa with a high fidelity and specificity for a cluster. Cluster-specific taxa display a high abundance in a cluster compared to the others. Taxa with a high fidelity for a cluster occur in a high number of grid cells belonging to that cluster. All indicator taxa considered, had a higher indicator value than 0.25 (Dufrêne and Legendre, 1997; Souissi *et al.*, 2001).

The broad zooplankton taxonomic groups Copepoda, Calanoida, and Crustacea nauplius were excluded from the clustering analysis, although dominant, to assure that each taxon only contributed once to the clustering analysis and to keep the finest taxonomic resolution

possible. The mentioned groups regroup taxa that are building a taxonomic group on their own in our data set. An example is the genus *Temora*, which is sorted by the software as proper group but individuals of this genus can also be found in the groups Copepoda and Calanoida. For the same reasons the taxa Cyclopoida and Calanoida were excluded from the clustering analysis applied to the 2022 dataset.

Prior to clustering, the grid cell mean of mesozooplankton and ichthyoplankton taxa (calculated on log-transformed data) were transformed to relative abundance by means of the Hellinger transformation (Borcard *et al.*, 2011; Frelat *et al.*, 2022), to enhance the joint analysis of the different data sets (Frelat *et al.*, 2022) (**Figure 20**). Furthermore, it allowed assigning the same weight to mesozooplankton and ichthyoplankton in the clustering analysis by rendering the contribution of abundant and rare species to the distance matrix similar (Legendre and Gallagher, 2001; Borcard *et al.*, 2011; Legendre and Legendre, 2012). Hellinger distance (Borcard *et al.*, 2011) was chosen as distance metric in this study.

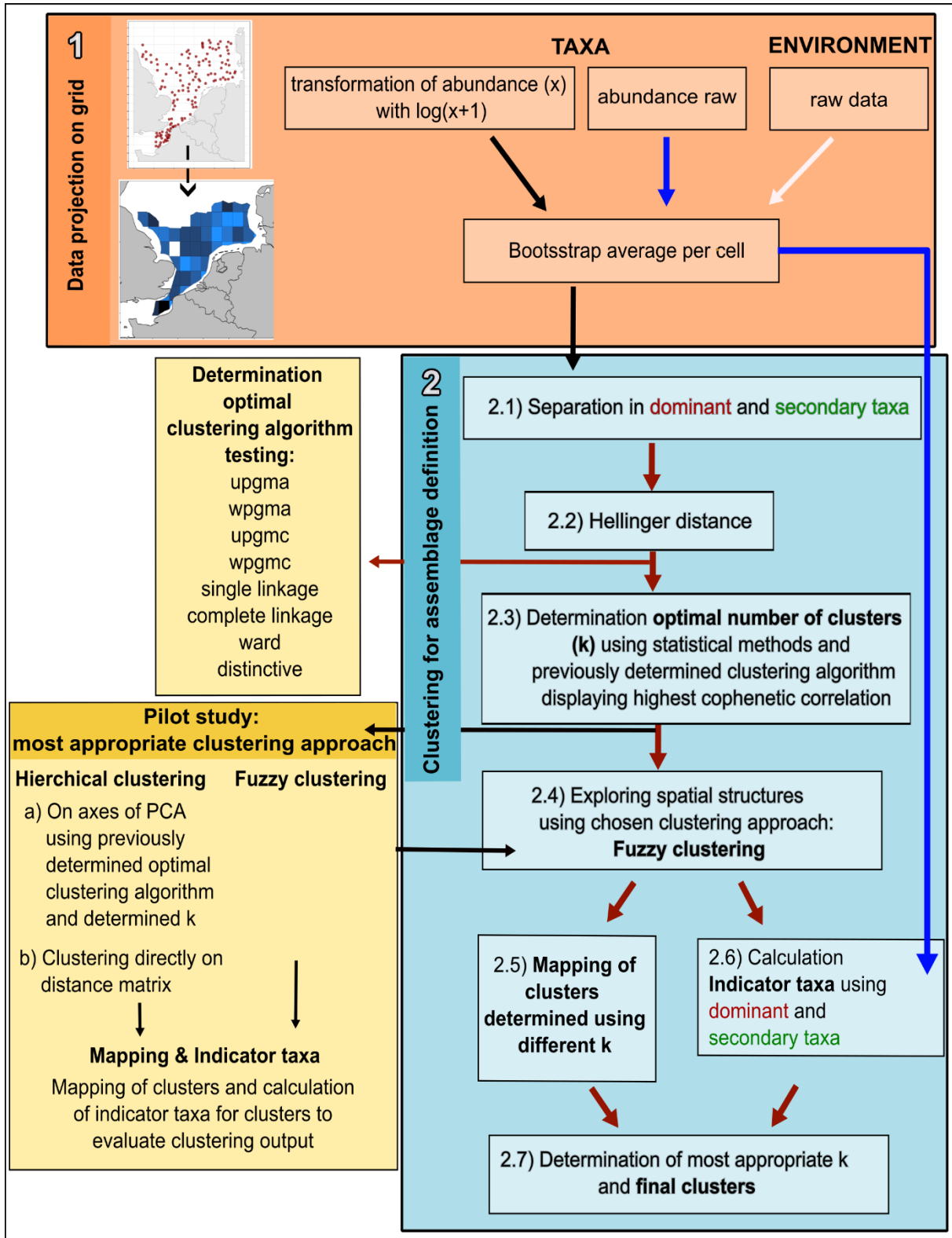


Figure 20 Overview steps for assemblage definition.

### 1.2.3.1 Pilot study – clustering method and number of clusters

To evaluate the most appropriate clustering approach for the present dataset a pilot study was conducted applying a hierarchical and a fuzzy clustering method (Borcard *et al.*, 2011) to the 2008 dataset and by mapping and evaluating clustering output. Hierarchical clustering was applied on principal components of a Principal Component Analysis (PCA) using all dominant taxa and directly implemented on the data (**Figure 20**).

Hierarchical clustering can be implemented using different clustering algorithms. The algorithm representing the original distance matrix most adequately should be used (Borcard *et al.*, 2011). The most appropriate algorithm was determined testing eight different clustering algorithms (unweighted pair-group method using arithmetic averages, unweighted pair-group method using centroids, weighted pair-group method using arithmetic averages, weighted pair-group method using centroids, Ward's method, single linkage, complete linkage, divisive hierarchical method) using Shepard-like diagrams (Borcard *et al.*, 2011; Hattab *et al.*, 2015).

After having chosen the adequate clustering algorithm the number of clusters needs to be defined as clustering methods require an *a priori* definition of the number of clusters (k) or the cut-off level (Kreft and Jetz, 2010). To make this choice more objective, Kreft and Jetz (2010) proposed the use of statistical methods for the definition of the optimal k. Using three different methods namely the Silhouette widths, the Mantel correlation between the distance matrix and binary matrix computed from the dendrogram (Borcard *et al.*, 2011) and the Kelly-Gardner-Sutcliffe penalty function (Hattab *et al.*, 2015) resulted in different optimal k. To evaluate the k most appropriate to the data set, clustering was conducted using all statistically derived k. The resulting clusters were mapped and their ecological meaning evaluated assessing the existence of indicator taxa and considering the spatial coherence of the clusters (membership value and spatial distribution).

Analysis was conducted using the package "labdsv" and a p-value of 0.05 adjusted after Benjamini and Hochberg (Benjamini and Hochberg, 1995).

### 1.2.3.2 Fuzzy clustering

Based on the pilot study, the fuzzy c-means clustering method was chosen as most appropriate for the present data. In fuzzy clustering each cell is affiliated to each cluster and strength of affiliation to a cluster is expressed by the membership value. The sum of per-cell membership values over all clusters equals 1. To assess the coherence of the assemblage, maps displaying the maximum membership value per cell were produced indicating cells of strong affiliation (high membership value) and therefore coherent clusters and cells of weak affiliation (low membership value) and therefore less coherent regions (**Figure 21**). Fuzzy clustering was implemented with a membership exponent of 1.2 using the function `fanny()` from the “cluster” package (Borcard *et al.*, 2011; Maechler *et al.*, 2023).

The number of clusters ( $k$ ) was determined as described above. The statistical methods used proposed  $k$  values of 4 and 3 (Annex I **Figure A 4**). Restricting clustering to a number of 3 produced a continuous region of lower membership values towards the center of the study area (**Figure 21A**). As this region of lower membership values turned into a cluster when allowing for 4 clusters (**Figure 21C**), setting  $k$  to 4 was judged more appropriate to describe zooplankton assemblages present in the study area than setting  $k$  to 3. The blurred pattern of lower membership values resulting from a  $k$  of 4 and 5 indicated (**Figure 21C,D**), that a  $k$  higher than 5 would not reveal further spatially-coherent clusters. As indicator species were found for clusters one to five, a distinctively lower mesozooplankton abundance was observed in cluster 5 compared to cluster 1 and abundance of herring larvae (6-12 mm) was distinctively higher in cluster 5 compared to cluster 1 (see Results section), a  $k$  of 5 was chosen as the most appropriate number of clusters.

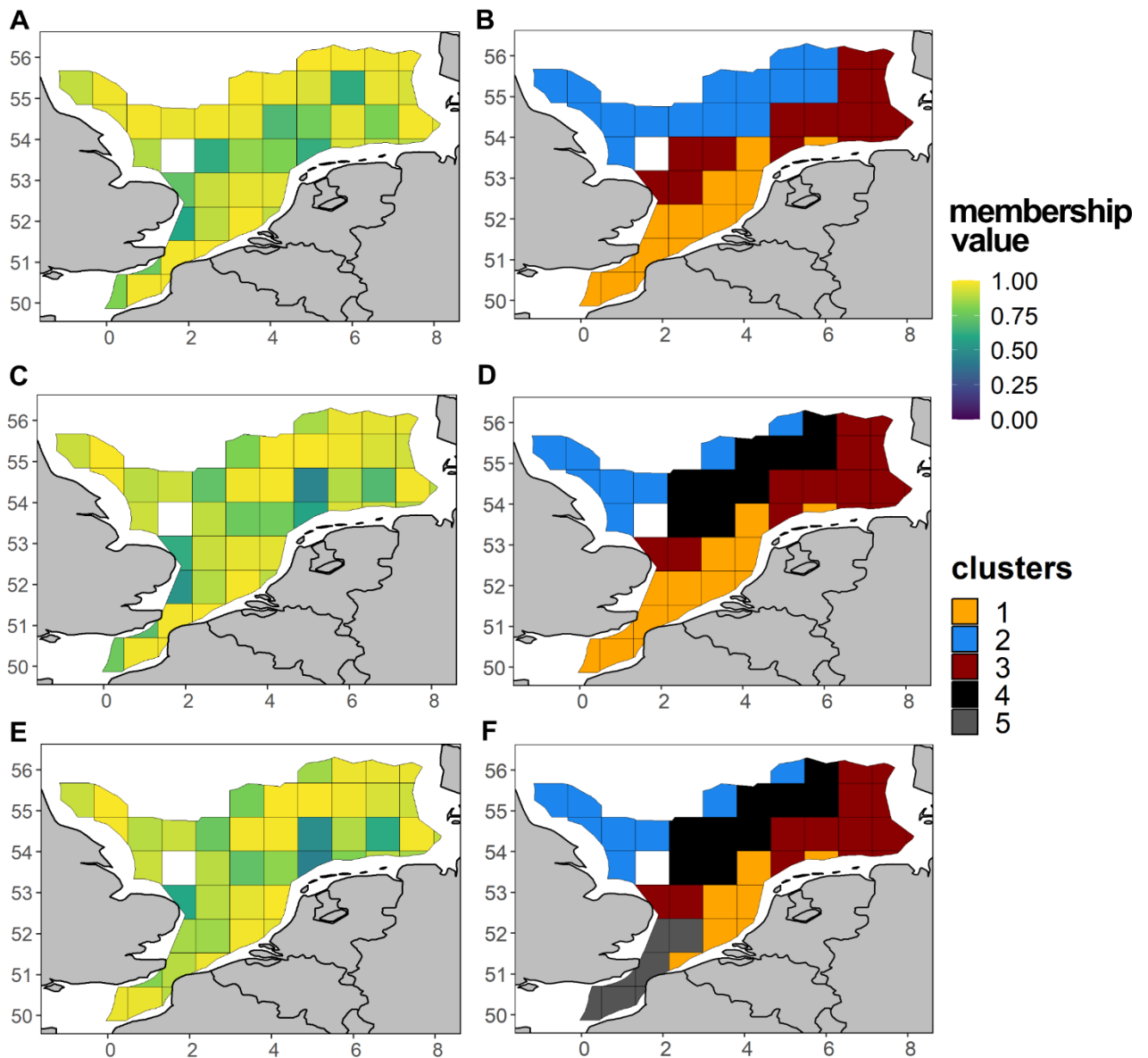


**Figure 21 Highest membership values per cell of clustering using different  $k$ .** Fuzzy clustering evaluates the strength of affiliation of a cell to each cluster, which is expressed by a membership value. High membership values indicate coherent regions, low membership values indicate regions of low coherence. A,B: three clusters (maximized silhouette width), C,D: four clusters (minimized Kelly-Gardner-Sutcliffe penalty and maximized Mantel correlation), E,F: five clusters (quasi minimized Kelly-Gardner-Sutcliffe penalty, quasi maximized Mantel correlation and quasi maximized silhouette width).

Clustering analysis was conducted in R version 4.1.2 using the packages “cluster” (Maechler *et al.*, 2023), “vegan” (Oksanen *et al.*, 2001) and “maptree” (White and Gramacy, 2022) and results were mapped by means of the packages “sf” (Pebesma, 2018), “sp” (Pebesma and Bivand, 2005), “EchoR” (Schramm, 2022) and “ggplot2” (Wickman, 2016).



To characterize the assemblages, the mean abundance of the taxa per assemblage was calculated using the non-transformed grid cell mean and visualized using barplots. Additionally, Principal Component Analysis (PCA) was applied to  $\log(x+1)$  and Hellinger transformed grid cell means of zooplankton abundance using the package “FactoMineR” (Lê *et al.*, 2008). PCA allows to reduce the dimensionality of a dataset. The position of variables with regard to the new dimensions created by the PCA, reveals patterns and relationships between variables and individuals. Thereby each new dimension explains a percentual proportion of the variance in the dataset and the most explaining ones are kept for interpretation.

#### **1.2.4 Environmental drivers of taxa distribution**

A generalized linear mixed model (GLMM) was used to evaluate potential drivers of zooplankton distribution and therewith assemblage composition. If available, the relation of one mesozooplanktonic and one ichthyoplanktonic (fish larvae) indicator taxon per assemblage with potential environmental drivers was tested. To synthesize the environmental parameters measured, two PCAs were applied on log-transformed, centered and scaled grid cell means of abiotic (temperature, salinity, depth, sum of nitrate and nitrite, ammonium, phosphate, silicate, POM, chlorophyll a) on one side and to hellinger-transformed grid cell means of biotic parameters (abundance of 7 phyto-microplankton groups), on the other side. The N/P ratio was used as supplementary variable due to its correlation to nitrogen and phosphate. The dimensions (principal components) of the PCAs explaining the majority of the variance were used as explanatory variables in the GLMM model. As principal components are orthogonal to each other, no problems of correlation between the dimensions of the same PCA in the model can be encountered. Potential correlations between the principal components originating from the two different PCAs were tested. To consider the spatial component, assemblages (cluster) were integrated as random effect. GLMMs were applied to untransformed grid cell means of zooplankton taxa abundance. Starting with the most complete model, the parameters were reduced in a step-by-step procedure excluding non-significant covariates. The most parsimonious model was chosen with regard to the smallest Akaike’s Information Criterion (AIC) and significant ANOVA. The fulfillment of model assumptions was verified using the “DHARMA” package (Hartig, 2022). To simplify interpretation the most parsimonious model with variables coded as independent was chosen

if AIC, Anova and the fulfillment of assumptions allowed to do so. Models were run using the package “glmmTMB” (Brooks *et al.*, 2017). Depending on data distribution, a “gamma” or “tweedie” distribution was used.

The most complete model coding variables as interactions was constructed as follows:

Model = glmmTMB(taxon\_abundance ~ Dim.1abiotic\* Dim.1biotic + Dim.2abiotic\* Dim.1biotic + (1|cluster), family = distrib), with distrib equal to tweedie () or Gamma(link="log").

This model tested also the separate effect of the independent variables.

### 1.2.5 Inter-annual comparison

The distribution and composition of the assemblages found in 2008 were compared to data sampled in 2022 as zooplankton data coming from the same campaign were available for these two years. As the sampling extent of mesozooplankton sampled in 2022 was the smallest among data sets (**Figure 18D**), this sampling extent defined the area (polygon) serving for the inter-annual comparison. The clustering approach described above was applied to the spatially restricted data set of 2008. A k of 2 was found the most appropriate choice (Annex I **Figure A 5**). 2008 clustering (**Figure 27**) was then applied to calculate the mean abundance of the dominant (in terms of dominant and secondary) taxa sampled in 2022 per cluster. Inter-annual differences between the total abundance of mesozooplankton and fish larvae respectively and of the most dominant taxa per cluster were assessed by means of GLMM. Spatial autocorrelation was considered by integrating coordinates grouped by year as random effect fitted with an exponential function. Models were run using the “glmmTMB” package in R. Depending on data distribution a “log-normal” or “tweedie” distribution was used. The model applied to single taxa and total abundance was constructed as follows:

Model = glmmTMB(taxon\_abundance ~ cluster + cluster:year + exp(coordinates + 0|year),  
family=tweedie())

or

Model = glmmTMB(log(taxon\_abundance) ~ cluster + cluster:year + exp(coordinates + 0|year), family=gaussian())

With the aim to place the two years examined in a broader inter-annual context, an anomaly analysis with data of salinity, temperature (1998 – 2022), chlorophyll a concentration (2008 - 2022) and the herring larvae density index (1992 – 2022) sampled during the first quarter IBTS was conducted. Due to data availability, the region between 49°N and 55°N was used for the anomaly analysis.

## 1.3 Results

### 1.3.1 PCA on potential abiotic and biotic drivers

The first two dimensions of the PCA applied to abiotic variables (**Figure 22A-C**) explained 64 % of the total variance (48 % and 16 %, respectively). The first dimension (A1) represented an inverse relationship between dissolved nitrogen (sum of nitrate and nitrate, ammonium), silicate and POM on the positive side and temperature, depth and salinity on the negative side. Thus, a grid cell displaying a high value of dimension one was characterized by high POM, nitrogen and silicate concentration and low temperature, depth and salinity (**Figure 22B**). The second dimension (A2) represented chlorophyll a and phosphate concentration (**Figure 22A**), with higher values representing cells with high phosphate and chlorophyll a concentration (**Figure 22C**). The first dimension of the PCA applied to phyto- and microzooplankton (B1) explained 77 % of the variance (**Figure 22D**). It represented the abundance and distribution of diatoms, nanoflagellates and the group of others (*Phaeocystis globosa*, *Heterosigma spp.*, *Eutreptiella spp.*, Mediophyceae, Crysohyceae and Cryptophyceae) with higher values indicating abundance of nanoflagellates and others whereas lower values indicated importance of diatoms (**Figure 22E**).

CHAPTER 1 - 1. Perspective – Taxonomical composition

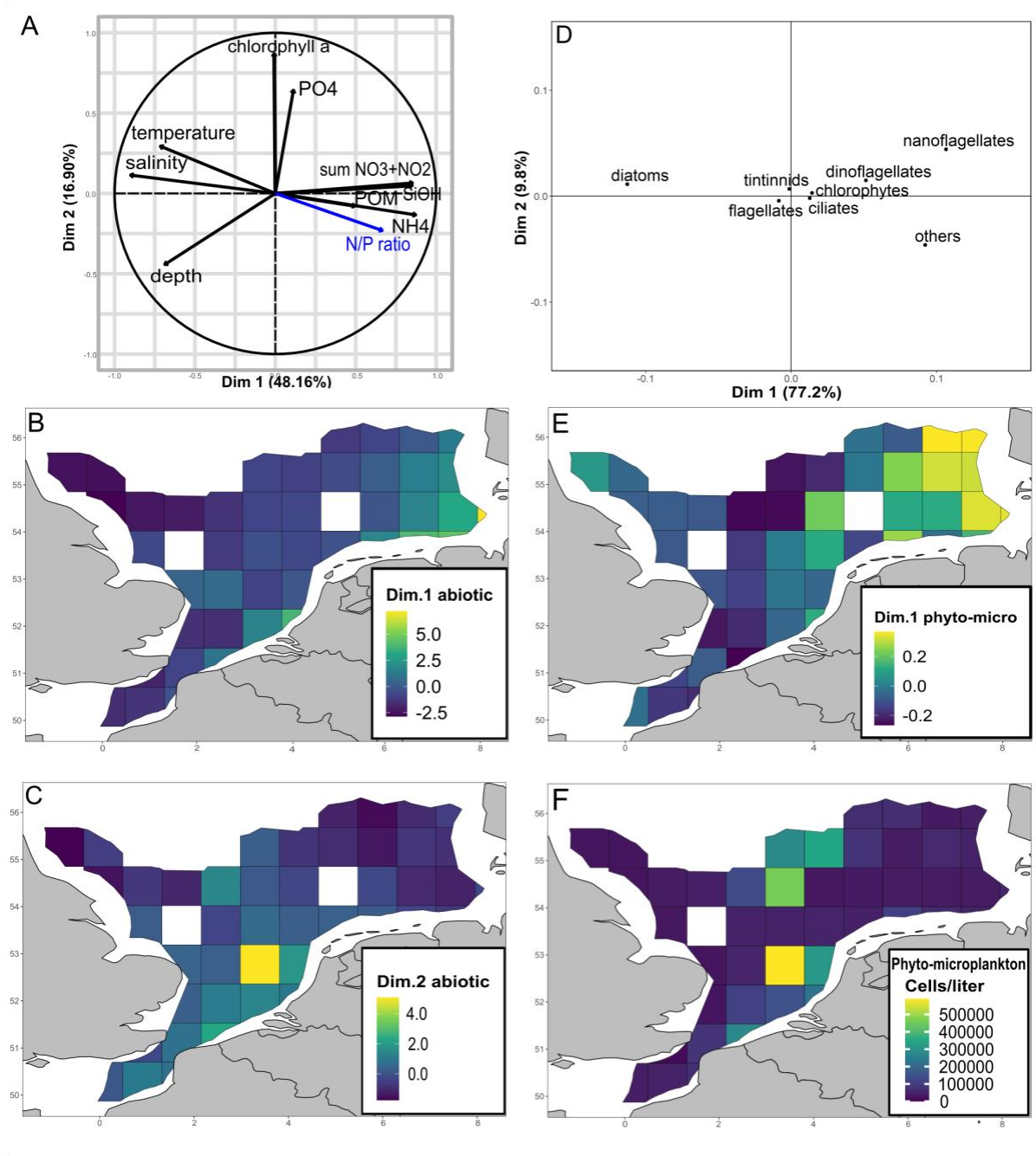


**Figure 22 Potential drivers of zooplankton assemblages.** A: Abiotic parameters displayed in a two-dimensional space constituted by the first and second dimensions of the PCA; B: Values of coordinates of first dimension of the PCA on abiotic parameters per grid cell. The more positive a value the higher the concentration of nutrients, and the lower temperature, depth and salinity and vice versa; C: Values of coordinates of second dimension of the PCA on abiotic parameters per grid cell; D: Phyto- and microplankton displayed in a two-dimensional space constituted by the first and second dimensions of the PCA; E: Values of coordinates of first dimension of the PCA on phyto-microplankton per grid cell. High values indicate high proportion of nanoflagellates and others (*Phaeocystis globosa*, *Heterosigma* spp., *Eutreptiella* spp., *Mediophyceae*, *Crysophyceae* and *Cryptophyceae*), low values indicate high importance of diatoms; F: Total abundance of phyto- and microplankton per grid cell.

### 1.3.2 Characterization of the assemblages found

The 2008 dataset was the most extensive in terms of spatial extent, observations and environmental variables available, and we first provide detailed results of the assemblages found with that dataset, their environmental conditions and the overall pattern. The assemblages found in 2008 and 2022 with a reduced spatial extent are compared subsequently.

A total of five clusters was determined in the SNS-EEC representing five zooplankton assemblages (mesozoo- and ichthyoplankton) within the study area (**Figure 23A**). These assemblages were named as follows: cluster 1 will be referred to as ‘Rhine-Scheldt assemblage’, cluster 2 as ‘Northern-British coast assemblage’, cluster 3 as ‘German Bight-Norfolk assemblage’, cluster 4 as ‘Central assemblage’ and cluster 5 as ‘Channel-Thames assemblage’. As each assemblage was associated to a certain region the name of the assemblages was used together with the term region when referring to the location of the respective assemblage.

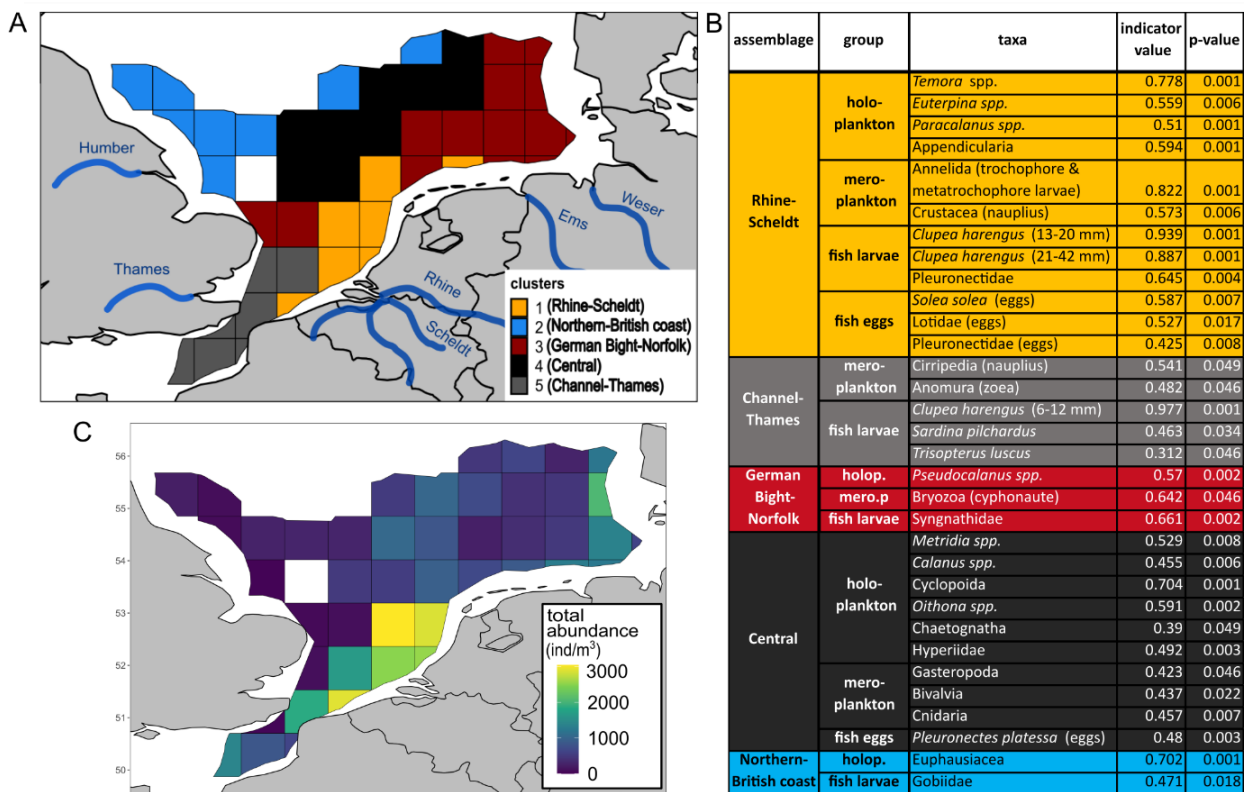


**Figure 23 Assemblages and total zooplankton abundance.** A: Clusters/assemblages based on mesozooplankton and ichthyoplankton sampled during the International Bottom Trawl survey in January and February 2008; B: Indicator species per cluster/assemblage with respective indicator value and adjusted p-value; C: Total mean abundance of zooplankton (meso- and ichthyoplankton) per grid cell.

### 1.3.2.1 Zooplanktonic and environmental profiles per assemblage

In the following the overall pattern of characteristics within and among the assemblages will be described (Figure 23-26).

For an overall comparison of the zooplankton assemblages a PCA was applied to zooplankton data (Figure 24). The first two dimensions explained 47.9 % of the variance. PCA revealed an overall segregation between northern (Northern-British coast, Central) and southern assemblages (Rhine-Scheldt, Channel-Thames), with the Northern-British coast assemblage and the Central assemblage being located on the negative side of dimension one and the Channel-Thames assemblage and the Rhine-Scheldt assemblage on the positive side. This corresponded to the relative abundance of certain taxa with *Oithona* spp., Gobiidae larvae, *Metridia* spp. and *Calanus* spp. characterizing northern assemblages whereas southern assemblages were related to eggs of *Solea solea*, *Centropages* spp., small and medium sized herring larvae and *Temora* spp. (Figure 24-26). The German Bight-Norfolk assemblage was positioned on both sides of the first dimension what corresponded to the observation that *Pseudocalanus* spp. was part of the dominant taxa in contrast to the remaining assemblages (Figure 24-26).

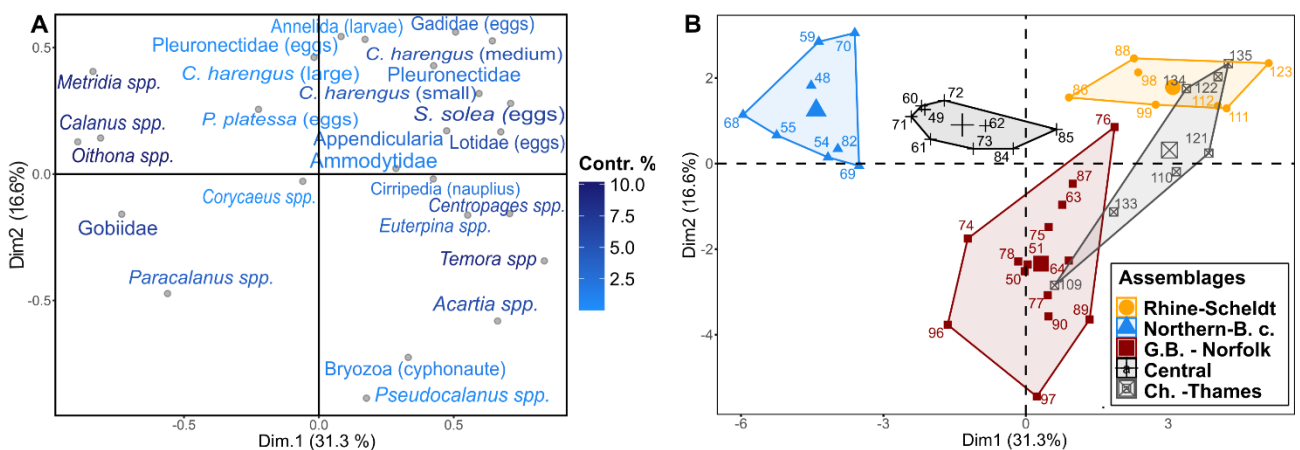
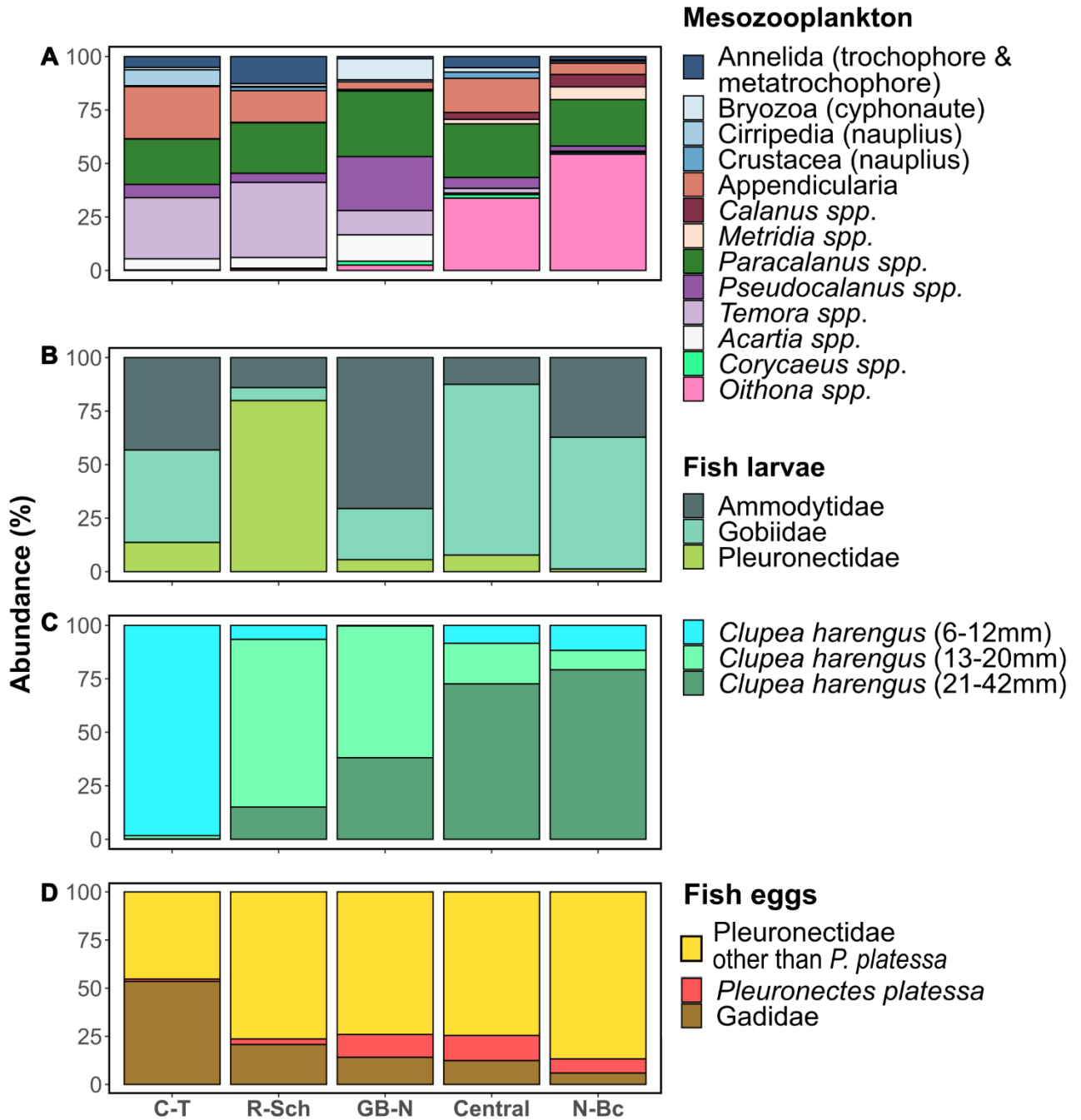


Figure 24 PCA applied to zooplankton taxa. A: Taxa displayed in a two-dimensional space of the PCA; B: Assemblages/cluster displayed in the same two-dimensional space as in A. Numbers indicate grid cell ID.

The **Channel-Thames assemblage** was characterized by small herring larvae (6 and 12 mm), Cirripedia nauplius larvae, zoea larvae of the infra-order Anomura, larvae of *S. pilchardus* and *Trisopterus luscus* that were revealed as indicator taxa (Figure 23B, Annex I Figure A 8). The larval assemblage was dominated by the smallest size class of herring larvae (97 %) that

displayed with a mean abundance of 508 individuals per 1000 m<sup>3</sup> the highest abundance among assemblages (**Figure 26**).

The Channel-Thames region was characterized by negative values of dimension 1 of the abiotic PCA (A1) meaning warmer temperature, average salinity, low nitrogen, silicate and POM concentration and average values on dimension 2 (A2) i.e., phosphate and chlorophyll concentration (**Figure 22**). The phyto- and microplankton community was characterized by diatoms that accounted for 74 % of total abundance (negative values on dimension 2 of the biotic PCA (B1)) (**Figure 22**, Annex I **Figure A 6**). The N/P ratio was with  $20 \pm 7$  slightly elevated with regard to the Redfield ratio.



**Figure 25 Proportional taxa composition per assemblage.** Each bar corresponds to an assemblage: C-T: Channel-Thames assemblage. R-Sch: Rhein-Scheldt assemblage; GB-N: German Bight-Norfolk assemblage; Central: Central assemblage; N-Bc: Northern-British coast assemblage. A: Mesozooplankton; B: Fish larvae other than herring; C: Herring larvae; D: Fish eggs.



## CHAPTER 1 - 1. Perspective – Taxonomical composition

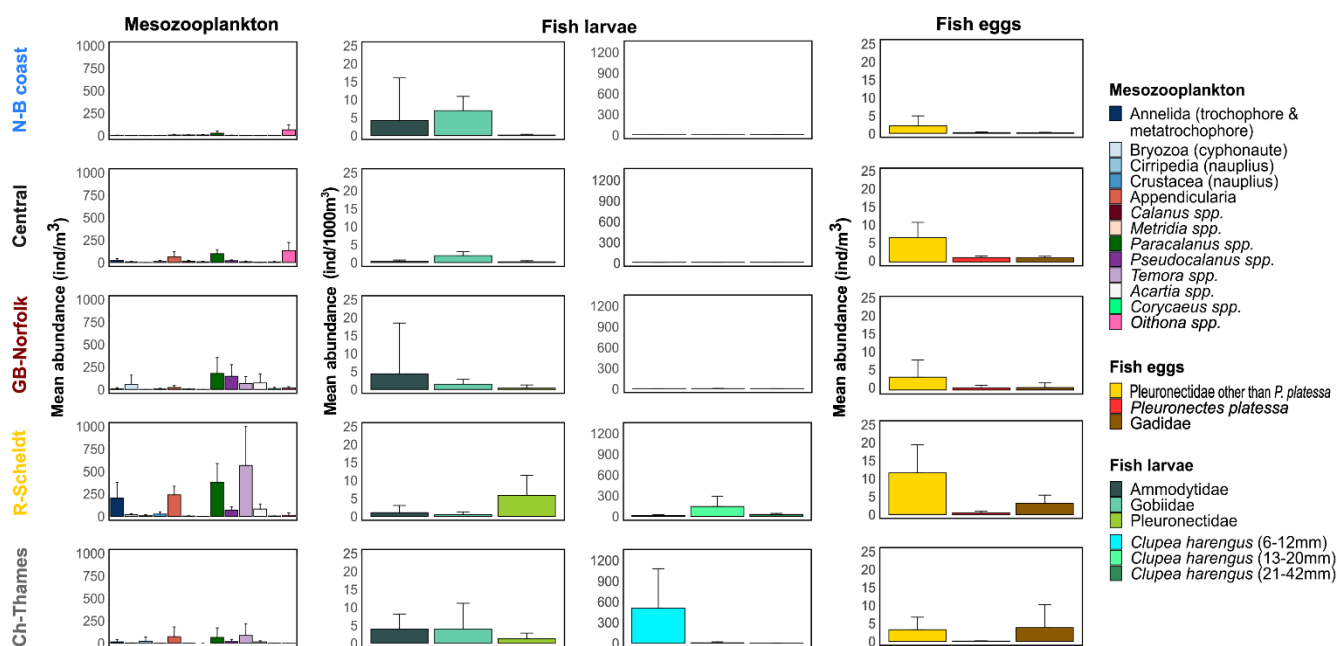


**Figure 26** Mean abundance of the most important taxa per cluster. From left to right: mesozooplankton, fish larvae other than herring, three different size classes of herring larvae, and fish eggs. Each row represents one assemblage. Only the most structuring taxa were displayed (excluded taxa: *Centropages* spp., *Euterpina* spp., *Lotidae* (eggs) and *Solea solea* (eggs)).

The **Rhine-Scheldt assemblage** was characterized by 15 indicator taxa and covered the region with highest total zooplankton abundance (**Figure 23C, 26**). Mesoplanktonic indicator taxa were trochophore and metatrochophore larvae of the phylum Annelida, Crustacea nauplii, *Temora* spp., Appendicularia, *Euterpina* spp., Calanoida, and *Paracalanus* spp. Indicator taxa belonging to the ichthyoplankton were *C. harengus* size class 13-20 mm, *C. harengus* size class 21-42 mm, Pleuronectidae larvae, *S. solea* eggs, Lotidae eggs and Pleuronectidae eggs (**Figure 23B**). The Rhine-Scheldt region was characterized by elevated abundance of phyto- and microplankton (**Figure 22F**) corresponding to positive values on A2 meaning elevated chlorophyll a concentration (**Figure 22C**). The phyto-microplankton assemblage was dominated by diatoms (58%) and the group of others (33%) (average value on B1) (**Figure 22E**, Annex I **Figure A 6**). Positive values on A1 represented elevated concentration of POM, nitrogen, phosphate and silicate and average temperature, salinity and depth (**Figure 22A**). The N/P ratio of  $17 \pm 12$  indicated rather balanced nutrient availability with regard to the Redfield ratio (Annex I **Figure A 7**).

The **German Bight-Norfolk assemblage** was characterized by cyphonaute larvae of the phylum Bryozoa, the copepod genus *Pseudocalanus* and fish larvae of the family Syngnathidae. The east of the German Bight-Norfolk assemblage covered a region of elevated zooplankton abundance (**Figure 23C, 26**).

The German Bight-Norfolk region was characterized by positive values on A1 meaning cold temperature, shallow depth and low salinity as well as elevated concentrations of POM, nitrogen and silicate. Negative values on A2 represented low concentration of phosphate and chlorophyll a (**Figure 22**). A low concentration of phosphate (Annex I **Figure A 7**) and an elevated concentration of nitrogen resulted in an elevated N/P ratio of  $21 \pm 11$  (Annex I **Figure A 7**). The phyto- microplankton was dominated by diatoms (42 %), others (28 %) and nanoflagellates (17 %) (positive values on B1) whereby nanoflagellates and dinoflagellates (10 %) displayed the highest share among assemblages (**Figure 22, Annex I Figure A 6**).

Ten indicator taxa characterized the **Central assemblage**: Cyclopoida, *Oithona spp.*, *Metridia spp.*, Hyperiidae, Cnidaria, *Calanus spp.*, Bivalvia, Gasteropoda and Chaetognatha, and one being *P. platessa* eggs (**Figure 23B**). The Central region displayed average depth, salinity, temperature, silicate and POM concentration (values around zero on A1). Values around zero on A2 mean average chlorophyll a and phosphate concentration (**Figure 22**). Nitrogen was low resulting in an N/P ratio of  $6 \pm 3$  (**Figure 22, Annex I Figure A 7**). Total phyto-microplankton abundance was elevated (**Figure 22F**) and dominated by diatoms (81%) (negative value on B1) (**Figure 22, Annex I Figure A 6**).

Two indicator taxa were revealed for the **Northern-British coast assemblage**, namely the order Euphausiacea and Gobiidae larvae (**Figure 23**). Overall zooplankton abundance was low in the assemblage (**Figure 23C, 26**).

With regard to environmental conditions, this region was characterized by deep depth, elevated salinity and warm temperature and low concentrations of POM, nitrogen, silicate (negative values on A1) and phyto-microplankton abundance (**Figure 22**). Negative values on A2 mean low chlorophyll a concentration (Annex I **Figure A 7**). N/P ratio was low ( $8 \pm 3$ ). Diatoms dominated the phyto-microplankton assemblage as indicated by negative values on B1.

### 1.3.2.2 Drivers of species distribution

The two first dimensions of the PCA applied to abiotic parameters (A1, A2) and the first dimension of the PCA applied to the biotic variables (B1) were used as fixed explanatory variables in the GLMM. Biotic and abiotic drivers explaining taxa distribution differed between the indicator taxa tested (**Table 1**). Overall, A2 significantly explained the abundances of 6 out of the 10 taxa tested to a different extent whereas A1 and B1 contributed to the explanation of the distribution of 4 out of the 10 taxa tested. For 6 out of 10 taxa the random effect cluster was retained in the most appropriate model (**Table 1**). This means that an unexplained spatial gradient remained once environmental variables included. The most extreme case was Euphausiacea with a significant random cluster effect while no significant environmental drivers were evidenced. For the remaining taxa (*Temora spp.*, *Pseudocalanus spp.*, *Oithona spp.*, Gobiidae larvae), the fixed variables alone were sufficient to explain the specificity of the taxa to the assemblages, meaning that any spatial effects were accounted for through the selected environmental variables.

The distribution of small herring larvae characterizing the Channel-Thames region was explained by an interactive effect of A1 and B1 with a higher importance of B1 indicated by its revelation as significant (**Table 1**). This means that the abundance of small herring larvae was positively correlated to nanoflagellates and other phytoplankton that were the major drivers for this taxon but that in regions of low nanoflagellate and other phyto-microplankton abundance elevated nutrient and POM concentration still positively influenced small herring larvae abundance. The distribution of Cirripedia nauplius larvae and medium sized herring larvae were solely driven by chlorophyll a concentration (and possibly phosphates) in accordance with the elevated chlorophyll a concentration in the Channel-Thames and Rhine-Scheldt region. *Temora spp.* and *Pseudocalanus spp.* were further taxa positively correlated to chlorophyll a concentration (and possibly phosphates) but additional groups of variables explained their distribution and abundance. *Temora spp.* was additionally correlated to nutrient and POM concentration (A1) and *Pseudocalanus spp.* to nutrient and POM concentration (A1) and abundance of nanoflagellates and the group of other phyto-microplankton (B1) corresponding to the characteristics of the Rhine-Scheldt and the German Bight-Norfolk region, respectively. Syngnathidae larvae, *Oithona spp.* and Gobiidae larvae were negatively correlated to chlorophyll a and phosphate concentration (A2). The abundance and distribution of Syngnathidae larvae was further correlated to nitrogen and POM

concentration (A1) and diatom abundance (B1) was revealed as further driver of Gobiidae larvae. The drivers of these two taxa corresponded to the conditions in the German Bight-Norfolk and Northern-British coast region. Beside low chlorophyll a and phosphorous concentration *Oithona spp.* were negatively correlated to A1 and thus further driven by elevated salinity, temperature, depth.

CHAPTER 1 - 1. Perspective – Taxonomical composition

**Table 1 Outcomes of GLMM evaluating possible biotic and abiotic drivers of taxa distribution from two PCAs (dimensions = principal components).** The *n* and *y* in the column cluster indicate if cluster was retained in the most appropriate model or not (*n*=no and *y*=yes). Significance: \*\*\* ( $P<0.001$ ), \*\* ( $P<0.01$ ), \* ( $P<0.05$ ), · ( $P<0.1$ ). *N* indicates the number of sampling stations used in the model. AIC (Akaike's Information Criterion) was the parameter used for model selection with smaller AIC for the models of the same taxon indicating better explanation of variance. Estimates indicate significant and non-significant positive or negative correlation between a dimension and taxon abundance. Non-significant correlations were not displayed in the table.

Taxa	Intercept	Estimates								cluster	N	AIC
		Dim1-abiotic (A1)		Dim2-abiotic (A2)		Dim1-phyto (B1)		Dim1-abiotic (A1) x Dim1-phyto (B1)				
		+	-	+	-	+	-	+	-			
		NO <sub>2</sub> -+NO <sub>3</sub> <sup>-</sup> , NH <sub>4</sub> <sup>+</sup> Si(OH) <sub>4</sub> , POM	temperature, salinity, depth	Chlorophyll a, PO <sub>4</sub> <sup>3-</sup>		nanofalgellates, others, dinoflagellates	diatoms					
<i>Temora spp.</i>	3.54	0.62***		1.17***						n	44	407
herring larvae (medium-sized)	0.71			0.34·						y	44	212
<i>Pseudocalanus spp.</i>	3.55	0.46***		0.38*		2.43**				n	44	408
Syngnathidae larvae	-3.42	0.15·			-0.89**					y	44	48
<i>Oithona spp.</i>	3.26		-0.43***		-1.06**					n	44	312
<i>Metridia spp.</i>	-1.09						-2.64·			y	44	154
Euphausiacea	-2.58									y	44	61
Gobiidae larvae	0.71				-0.74***			-3.52***		n	44	194
Cirripedia nauplius larvae	-0.33			1.27*						y	44	139
herring larvae (small-sized)	0.76					6.61*		-4.22*		y	44	203

### 1.3.3 Inter-annual comparison between zooplankton assemblages in relation to the SNS-EEC environment

#### 1.3.3.1 Spatial extent and distribution of assemblages

Using a smaller spatial extent, clustering with data from 2008 resulted in regions slightly different (cell 122) from clustering utilizing the full spatial extent (**Figure 23, 27**). As the distribution of the assemblages in 2008 nevertheless related to those found when using the full spatial extent, the same nomenclature will be applied with the orange assemblage corresponding to the Rhine-Scheldt and the grey assemblage corresponding to the Channel-Thames assemblage.

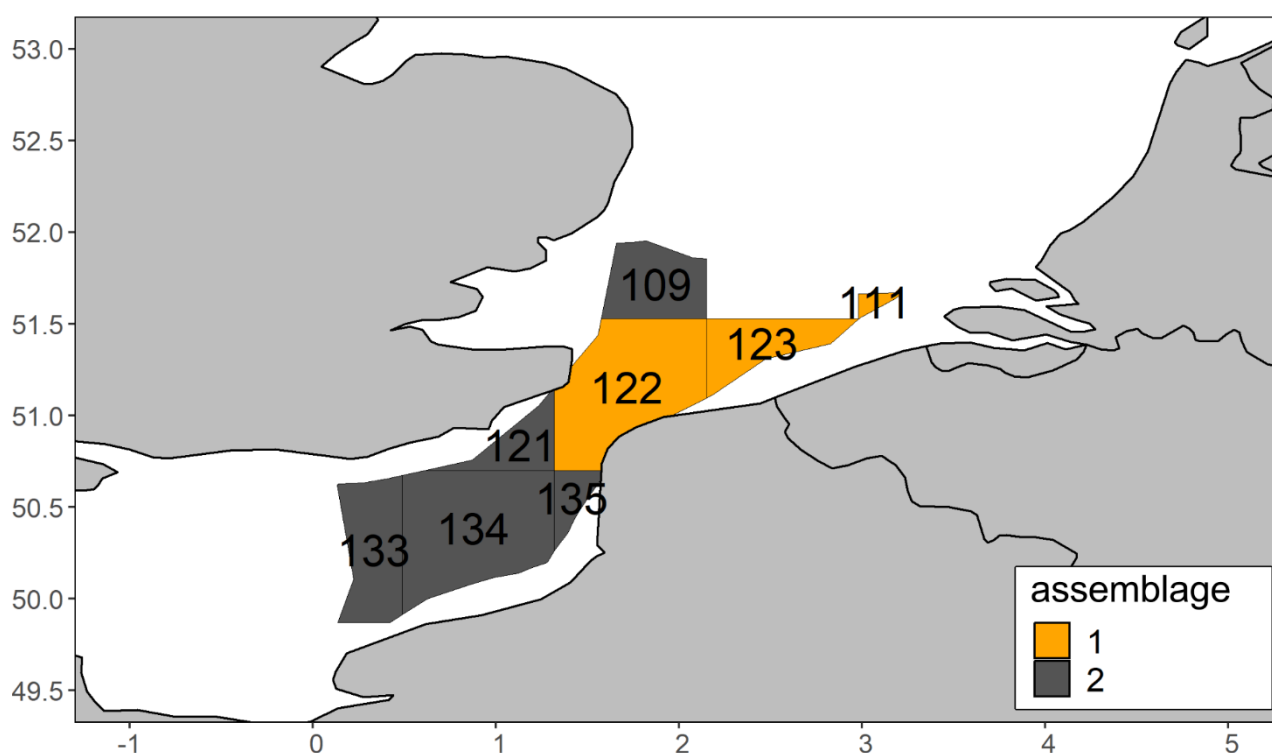


*Figure 27 Zooplankton assemblages using the 2008 data and the small sampling extent.*

#### 1.3.3.2 Inter-annual differences of assemblage composition and environmental condition

When comparing 2008 and 2022 zooplankton assemblages remained overall stable with regard to taxa composition, relative and absolute abundance.

With regard to relative abundance Appendicularia were not part of the dominant taxa in 2022 in the Channel-Thames region, in contrast to 2008 as relative abundance decreased (**Figure**

28). The relative contribution of *Temora* spp. was higher in this assemblage in 2022 compared to 2008 (Figure 28). In both assemblages the relative contribution of medium sized herring larvae was higher in 2022 than in 2008.

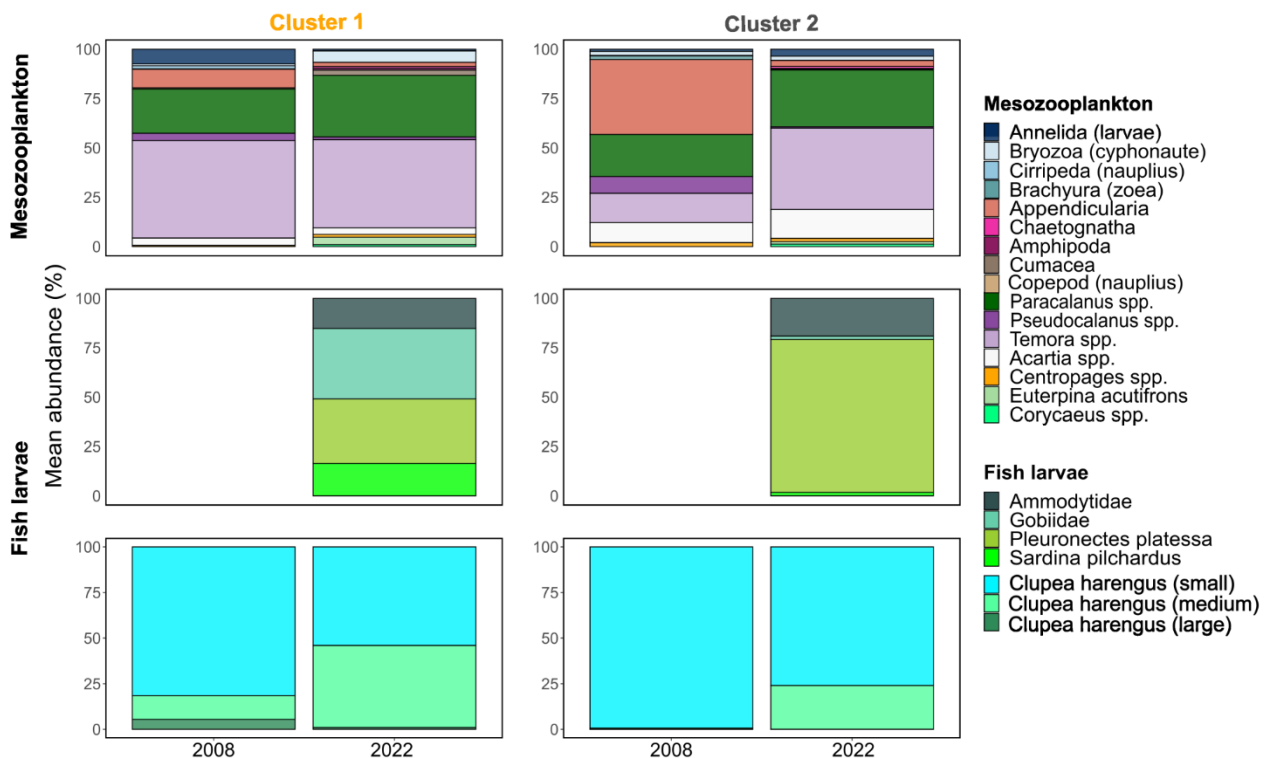


Figure 28 Comparison of relative community composition between 2008 and 2022 in the clustering output from 2008 (Figure 27). Fish larvae are displayed in two lines with the line positioned in the middle displaying all fish larvae other than herring larvae and the lowest line representing herring larvae of three different size classes.

With regard to absolute abundance (Figure 29, Annex I Figure A 8), the GLMM (Table 2) revealed a lower abundance of Appendicularians in the Rhine-Scheldt assemblage in 2022 compared to 2008. The absolute abundance of all other taxa tested remained stable. A striking difference was observed with regard to fish larvae abundance other than herring that was high enough to be considered in the clustering process in 2022 but not in 2008. This indicates a higher larval abundance of fish larvae other than herring in 2022. Furthermore, GLMM detected a higher total larvae abundance in the Channel-Thames region in 2022 than in 2008. A heatmap displaying the inter-annual differences of taxa per grid cell did not reveal a great inter-annual variability of taxa abundance and supported the differences and similarities revealed by the GLMM between the two years (Figure 29).

The total mean abundance of mesozooplankton and abundance of medium sized herring larvae was higher in the Rhine-Scheldt than in the Channel-Thames assemblage in both years (Table 2).

**Table 2 Results of GLMM testing for differences in abundance of dominant taxa between the assemblages independent of year and with regard to inter-annual differences in the same assemblage.**

	<i>Predictors</i>	(Intercept)	Rhine-Scheldt	Channel-Thames * year2022	Rhine-Scheldt* year2022	dispersion parameter	n
<b><i>Temora spp.</i></b>	<i>Estimates</i>	0.71	3.37	1.97	1.39	0.00	77
	<i>std. Error</i>	0.73	1.13	1.00	1.28		
	<b>p</b>	0.33	<b>0.00</b>	0.05	0.28		
<b><i>Paracalanus spp.</i></b>	<i>Estimates</i>	2.02	1.71	-0.10	1.19	0.00	77
	<i>std. Error</i>	0.54	0.91	0.77	1.07		
	<b>p</b>	<b>&lt;0.001</b>	0.06	0.90	0.26		
<b>Appendicularia</b>	<i>Estimates</i>	1.77	2.06	-1.24	-2.57	0.21	77
	<i>std. Error</i>	0.69	1.01	0.98	1.22		
	<b>p</b>	<b>0.01</b>	<b>0.04</b>	0.21	<b>0.04</b>		
<b><i>Acartia spp.</i></b>	<i>Estimates</i>	1.31	1.26	0.38	0.50	0.00	77
	<i>std. Error</i>	0.48	0.79	0.68	0.92		
	<b>p</b>	<b>0.01</b>	0.11	0.58	0.59		
<b>herring larvae (small)</b>	<i>Estimates</i>	4.67	-0.41	-0.30	0.43	13.80	57
	<i>std. Error</i>	1.13	1.17	0.93	1.35		
	<b>p</b>	<b>&lt;0.001</b>	0.73	0.75	0.75		
<b>herring larvae (medium)</b>	<i>Estimates</i>	-0.73	4.32	2.32	0.35	5.84	57
	<i>std. Error</i>	1.15	1.36	1.19	1.35		
	<b>p</b>	0.52	<b>0.002</b>	0.05	0.79		
<b>total abundance mesozooplankton</b>	<i>Estimates</i>	4.47	1.70	0.25	0.30	0.13	
	<i>std. Error</i>	0.50	0.68	0.69	0.84		77
	<b>p</b>	<b>&lt;0.001</b>	<b>0.01</b>	0.72	0.72		
<b>total abundance fish larvae</b>	<i>Estimates</i>	3.34	1.75	1.95	0.78	0.00	
	<i>std. Error</i>	0.58	1.03	0.82	1.22		57
	<b>p</b>	<b>&lt;0.001</b>	0.09	<b>0.02</b>	0.53		

The statistical evaluation of inter-annual changes by means of GLMM was limited by sampling size for several species. Models integrating cluster and the interaction between cluster and year as predictive variables did not meet model assumptions for *Temora spp.*, *Paracalanus spp.* and medium sized herring larvae. The output of these models could be verified, however,



CHAPTER 1 - 1. Perspective – Taxonomical composition

by running simplified models testing cluster and year separately allowing us to display the output of the complete model in **Table 2**, nonetheless.

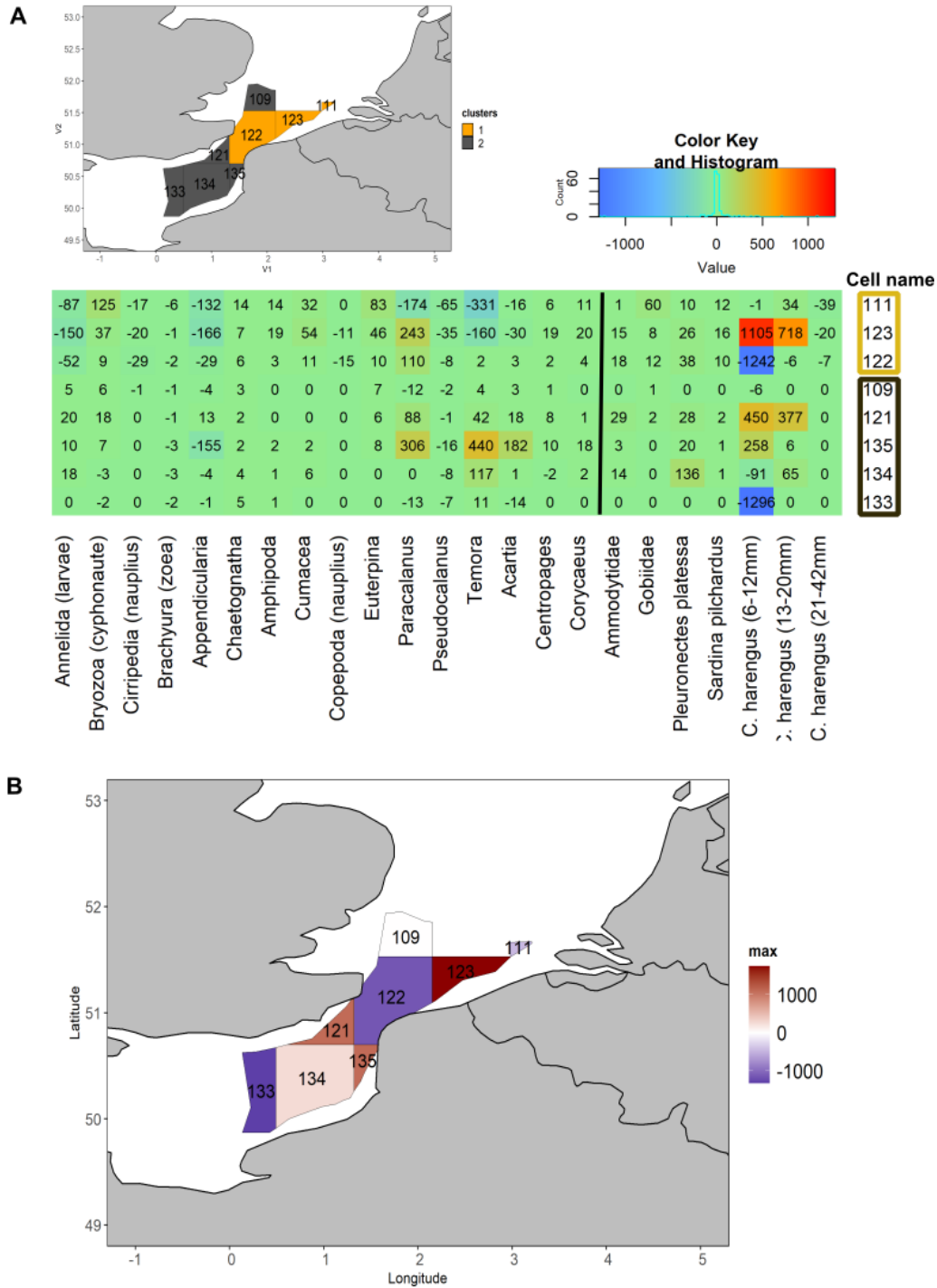


**Figure 29** Difference in abundance between 2008 and 2022 per grid cell. Abundance in 2008 was subtracted from abundance in 2022 per cell. A: Heatmap displaying increase or decrease per taxon and cell. Difference in abundance of mesozooplankton in ind/m<sup>3</sup>. Difference in abundance of fish larvae in ind/1000m<sup>3</sup>; B: Difference of total abundance of mesozoo- and ichthyoplankton per grid cell.

An anomaly analysis revealed no exceptional conditions in 2008 or 2022 with regard to temperature, salinity, chlorophyll a and herring larvae density (**Figure 30**). In comparison with

2022 both years displayed a slight negative temperature anomaly and a comparable negative anomaly in the herring larvae density index which was found to be negative from 2003 to 2022 with only two exceptions.

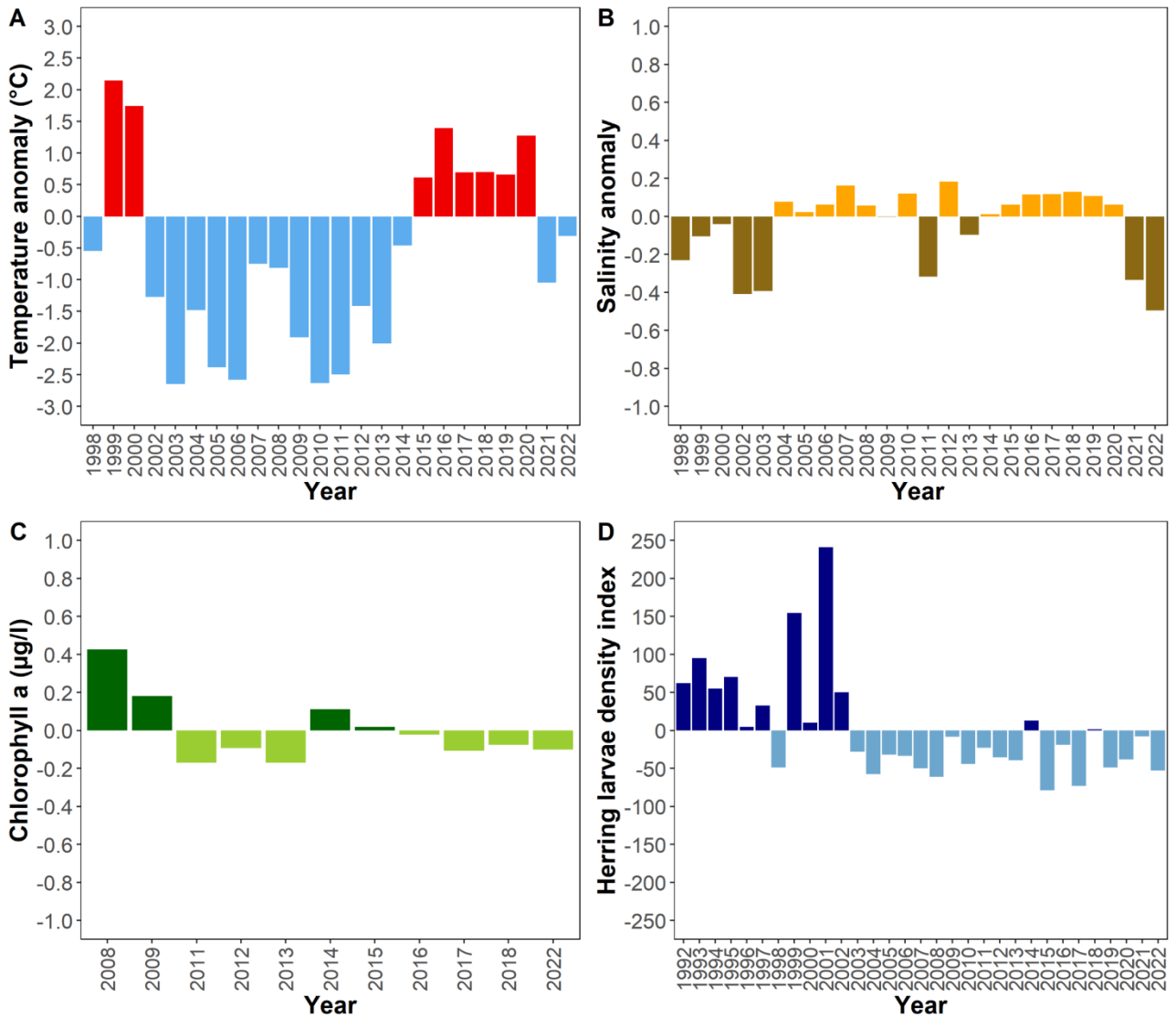


**Figure 30 Anomaly analysis.** A: Temperature; B: Salinity; C: Chlorophyll a concentration; D: Herring larvae density index in billions per area. Measurements were taken in the area between 49°N and 55°N during January and February.

## 1.4 Discussion

### 1.4.1 Zooplankton assemblages and environmental conditions

Five zooplankton assemblages were found in the SNS-EEC during winter, which differed with regard to taxa abundance and indicator taxa. The spatial distribution of the assemblages

appeared related to chlorophyll a concentration, dissolved N/P ratios, phyto- and microplankton composition, advection and fish spawning grounds. In the following, we will first discuss the overall pattern of zooplankton distribution with regard to environmental drivers and secondly the composition of the assemblages separated in their mesozooplankton and ichthyoplankton component with a major focus on indicator taxa.

#### 1.4.1.1 Overall patterns and environmental drivers

The assemblage distribution and composition displayed two overall patterns representing a north south gradient and being related to total zooplankton abundance. The north south gradient was indicated by the dominance of *Oithona spp.* in the northern assemblages (Northern-British coast and Central) and of *Temora spp.* in the southern assemblages (Channel-Thames and Rhine-Scheldt) suggesting the influence of different water masses on the zooplankton assemblages. The northern assemblages can be hypothesized to be influenced by Northern North Sea water and the Central North Sea as further indicated by the presence of *Metridia spp.*, Euphausiacea and Gobiidae larvae. *Oithona spp.* were found to display higher abundance in the Northern and Central North Sea in autumn thus elevated abundance in the SNS might indicate advection from the North and/or Center (Hay *et al.*, 1991). Due to high abundance of *Metridia spp.* around the Orkney isles the presence of this genera was proposed to indicate the presence of Atlantic water in the North Sea (Fransz *et al.*, 1991; Krause *et al.*, 1995). The finding that the spatial component was the major driver of *Metridia spp.* among the variables tested might be interpreted as further indication of advection. Also Euphausiacea and Gobiidae larvae are known to have a northern distribution during winter and can be hypothesized to be transported by advection into the SNS (Miller, 1986; Krause *et al.*, 1995) (see below). Southern assemblages further characterized by herring and Pleuronectidae larvae (**Figure 25**) were most probably influenced by Channel water and Southern North Sea water which are richer in nitrogen and silicate due to riverine input (OSPAR Commission, 2000) (**Figure 22B**, Annex I **Figure A 7**) and which represent drifting routes of herring and plaice larvae (Arnold and Metcalfe, 1996; Bolle *et al.*, 2009; Dickey-Collas *et al.*, 2009) (see below).

The German Bight-Norfolk region was not associated to the north south gradient (**Figure 24**). It was characterized by *Pseudocalanus spp.* and differed with regard to phyto-microplankton and nutrient composition from the other assemblages.

The second pattern was related to the distribution of total zooplankton abundance. Total zooplankton abundance was elevated in the Rhine-Scheldt and the German Bight-Norfolk assemblage and seemed to be driven by phyto-microplankton biomass (chlorophyll a), phyto-microplankton and nutrient composition. Elevated phyto-microplankton abundance in the Central assemblage did not result in increased zooplankton abundance. Relatively high abundance of phyto-microplankton in the Rhine-Scheldt and the Central assemblages during winter in comparison to the other regions was in accordance with the findings of Dudeck *et al.* (2021), Hay *et al.* (1991), Krause *et al.* (1995), Nielsen *et al.* (1993), Nielsen and Richardson (1989) and Groß *et al.* (2022). The low zooplankton abundance despite elevated phyto-microplankton abundance in the Central assemblage might be due to lower phytoplankton biomass, differing phyto-microplankton composition and differences in dissolved N/P ratio compared to the Rhine-Scheldt region. Lower chlorophyll a concentration in the Central compared to the Rhine-Scheldt region indicated lower biomass in the former. Whereas diatoms dominated in the Central assemblage, the Rhine-Scheldt assemblage was more diverse as characterized by a mixture of diatoms and the group of other phyto-microplankton. The N/P ratio in the Rhine-Scheldt region was close to the Redfield ratio, which may indicate favorable phytoplankton quality for zooplankton, which was not the case in the Central region during the study period.

The German Bight-Norfolk region displayed elevated zooplankton abundance despite low phyto-microplankton abundance, chlorophyll a and phosphorus concentrations and an elevated dissolved N/P ratio. The low phosphorus concentration found in this region was in accordance with Eberlein (1994) and the proportion of nanoflagellates was also reported by Wesche *et al.* (2007) who observed dominance of small flagellates with regard to phytoplankton biomass in winter around Helgoland. The main proportion of total zooplankton abundance was constituted by *Para-* and *Pseudocalanus spp.* As revealed by the GLMM abundance of *Pseudocalanus spp.* was related to nanoflagellates, the group of other phyto-microplankton, POM, chlorophyll a and phosphate. This indicated that *Pseudocalanus spp.* might be able to profit from the prey composition in this assemblage, despite low prey quantity. Both *Para-* and *Pseudocalanus spp.* are known to feed on small prey in the size range of flagellates and dinoflagellates (Poulet, 1973; Suzuki *et al.*, 1999) and *Pseudocalanus spp.* were reported to feed on flagellates, dinoflagellates and detritus (Peters *et al.*, 2006). Furthermore, the elevated load of POM could result in a detritus based food web with

flagellates and dinoflagellates as intermediate food-level, upgrading prey quality in this region (Klein Breteler *et al.*, 1999). Another hypothesis takes into account the low temperature in the German Bight-Norfolk region, which by decreasing metabolic costs, could facilitate zooplankton organisms to better deal with low food abundance.

#### 1.4.1.2 Mesozooplankton

The **Northern-British coast region** was the assemblage displaying lowest total zooplankton abundance. This was in accordance with the lower total biomass concentration along the British coast reported by (Pitois and Fox, 2006). A possible explanation might be the deep depth of this region as using GAM, Dudeck *et al.* (2021) found a negative relationship between zooplankton abundance and depth. As shown by the PCAs on potential environmental drivers, greater depth was related to higher relative salinity and temperature and lower nitrogen concentration indicating a potential multifactor explanation for the low abundance observed in this assemblage. The abundance of the indicator taxon Euphausiacea might indicate the presence of Scottish coastal water in this region. A transport of Euphausiacea by Scottish coastal water to this part of the SNS was also hypothesized by Krause *et al.* (1995) who found a similar distribution of this taxon in winter 1987. A further indication of advection was the finding that all fixed variables tested to explain the distribution of abundance of this taxon were not found significant but the spatial component of the model explained spatial distribution of Euphausiacea. This could indicate that the distribution and presence of this taxon in the Northern-British coast assemblage was mostly due to advection to this precise area but not due to the preference for or avoidance of the variables tested.

An almost similar finding was made for *Metridia spp.* an indicator taxa of the **Central assemblage** and known as indicator taxa for Atlantic water as discussed above. *Oithona spp.*, a further indicator taxon (Ndah *et al.*, 2022) of the Central assemblage, was driven by elevated salinity, temperature, deeper depth and low nutrient and chlorophyll a concentration as revealed by the GLMM. These set of drivers reflect the off-shore distribution of this taxon that was absent or very low in abundance in the southern assemblages and the German Bight-Norfolk region, areas characterized by coastal characteristics like shallow depth and increased nutrient concentration, for instance (Annex I **Figure A 7, 9**). As proposed for other taxa displaying higher abundance in the Central North Sea (Krause *et al.*, 1995), the absence or lower abundance of *Oithona spp.* in the southern assemblages might be the result of water

mass circulation. Northwards flowing water masses namely Channel and Southern North Sea water might prevent the protrusion of this genus further south in the SNS. Correlation to elevated salinity, temperature and deep depth might be a further indication of advection of this taxon from the Central and Northern North Sea as for example from the Dogger Bank region. In this area the egg-carrying strategy of Cyclopoid copepods (Deschamps *et al.*, 2024) was hypothesized to be advantageous as pelagic eggs might encounter high mortality rates due to elevated predation risks by the benthic suspension feeder community in this shallow and well mixed area (Nielsen and Sabatini, 1996). Although chlorophyll a concentration was lower in this assemblage than in the Rhine-Scheldt region, the concentration of chlorophyll a in the Central region was not the lowest in the study area. Thus, the negative correlation of *Oithona spp.* to chlorophyll a concentration appears surprising but could be due to the low explanatory power of A2 axis (16 %) that represented chlorophyll a and phosphate. The finding of Chaetognatha and Cnidaria as indicator species for the Central assemblage was in accordance with Krause *et al.* (1995). They hypothesize that hibernal primary production in the Dogger Bank region in winter 1988 (Nielsen and Richardson, 1989; Hay *et al.*, 1991; Nielsen *et al.*, 1993; Krause *et al.*, 1995) facilitated maintenance of secondary production sufficient to sustain predators like cnidarians (*Aglantha digitale*, *Pleurobrachia pileus*) and Chaetognaths. The **Rhine-Scheldt assemblage** appeared to be characterized by taxa associated with elevated phyto-microplankton abundance, biomass and the balanced N/P ratio. Appendicularians, micro- to macrophagous filter feeders (Lombard *et al.*, 2011), were found to reproduce in the Southern Bight (Wyatt, 1973). *T. longicornis* was reported to reproduce year around (Halsband and Hirche, 2001) with highest production repeatedly observed in hibernating females (Fransz *et al.*, 1990; Wesche *et al.*, 2007) and to display increased egg production when food concentration is high (Dam and Lopes, 2003; Wesche *et al.*, 2007). Moreover, high nutrient levels and chlorophyll a concentration were revealed as drivers of *Temora spp.* abundance and distribution. The dominance of *Temora spp.* in this assemblage was further in accordance with other investigations (Rae and Fraser, 1941; Fransz *et al.*, 1991; Krause *et al.*, 1995; Van Ginderdeuren *et al.*, 2014b; Dudeck *et al.*, 2021) pointing to the importance of this taxon in this region during winter. Also, the presence of crustacean larvae and annelid trochophore and metatrochophore larvae might be due to adequate feeding conditions promoting reproduction of these meroplanktonic taxa during winter. Polychaete-larvae were found in similar abundance at a similar location in winter 1987 (Krause *et al.*, 1995).

The mesozooplankton assemblage of the **Channel-Thames** region was characterized by meroplanktonic taxa and displayed a mesozooplankton composition very similar to the Rhine-Scheldt assemblage but with lower total abundances. Cirripedia larvae, Anomura larvae and ichthyoplankton taxa (see below) were indicator taxa for this region. Cirripedia larvae might find adequate feeding conditions as their abundances were positively related to chlorophyll a concentration that was of average concentration in this region (Annex I **Figure A 7, 9**).

The **German Bight-Norfolk assemblage** differed from northern and southern assemblages and was characterized by *Pseudocalanus spp.* and a relatively high proportion of nanoflagellates and dinoflagellates with regard to phyto-microplankton composition. As discussed above, *Pseudocalanus spp.* were positively correlated to nanoflagellate abundances. Furthermore, evidence suggests that *Pseudocalanus spp.* might be able to cope with low prey abundance as it displays a certain resilience to food shortage (Corkett and McLaren, 1970; Paffenhöfer and Harris, 1976; Walve and Larsson, 1999; Cotonnec *et al.*, 2003) which could be of advantage in this region of low primary production. However, *Pseudocalanus spp.* were also positively correlated to high concentrations of chlorophyll a and phosphate although chlorophyll a and phosphate were found in low concentrations in this region. This apparently contradictory result could be due to the low explanatory power of A2 axis (16 %) that represented chlorophyll a and phosphate. A further explanation could be the fact that this genus was also present in the Rhine-Scheldt assemblage although in lower abundance.

A common feature of all assemblages was the dominance of *Paracalanus spp.*, in accordance with other studies (Rae and Rees, 1947; Krause *et al.*, 1995).

The North Sea mesozooplankton community is estimated to consist of 112 species (Brylinski, 2009; Van Ginderdeuren *et al.*, 2014b), while this study considered 43 taxa of which was none determined until species level. It should be noted that we used different levels of taxonomic resolution to keep a maximum of information, an approach applied by several other studies (Krause *et al.*, 1995; Kléparski *et al.*, 2021). Nonetheless, we expect the use of a finer taxonomic resolution to result in similar assemblages but to potentially strengthen the distinction of the assemblages found (Krause *et al.*, 1995). Predicting future changes in the study area during winter, e.g. in response to climate change, is an interesting aspect which future studies should focus on. To that purpose, a taxonomic resolution at species level would be necessary as each species has characteristics of its own, e.g., biology, sensitivity to

environmental and community changes (Beaugrand *et al.*, 2013) and may play a specific role in the food web (Semmour *et al.*, 2023).

### 1.4.1.3 Ichthyoplankton

Winter zooplankton assemblages also differed with regard to ichthyoplankton. Based on the present study the southern assemblages, Channel-Thames and Rhine-Scheldt, can be judged particularly important for the offspring of several fish species as they harbor spawning and nursery areas and drifting routes. This was specifically true for plaice and herring larvae for which the study period represented peak spawning time (Harding, 1978; Martin *et al.*, 2008; Coppin *et al.*, 2009; Corten, 2013). By contrast common dab (*Limanda limanda*), flounder (*Platichthys flesus*), sole (*S. solea*), whiting (*Merlangius merlangus*) and cod (*Gadus morhua*) were at the beginning of their spawning period indicating the potential for higher inter-annual variability in the contribution of these species to the assemblages. The smallest size class of herring larvae outnumbered the larval assemblage in the **Channel-Thames region**, a region harboring several spawning grounds of Downs herring (Coppin *et al.*, 2009; Dickey-Collas *et al.*, 2009). The drift of herring larvae spawned in the EEC can explain the finding of the size classes 13 – 20 mm and 21 – 42 mm being an indicator taxa of the Rhine-Scheldt assemblage (Dickey-Collas *et al.*, 2009; Denis *et al.*, 2016). Although larval drift and retention is inter-annually highly variable (Dickey-Collas *et al.*, 2009; Denis *et al.*, 2016), the arrival of larvae bigger than 12 mm in the Southern Bight and smaller larvae being rather situated in the EEC at the moment of the first quarter IBTS survey appears to be a recurring pattern (Denis *et al.*, 2016; Akimova *et al.*, 2023). Thus, we hypothesize that small herring larvae are a reoccurring characteristic component of the Channel-Thames assemblage with larger herring larvae being associated to the Rhine-Scheldt region. Environmental drivers differed between the two size classes with the small larvae being predominantly correlated to the abundance of nanoflagellates and the group of other phytoplankton and secondly to nitrogen, silicate and POM concentration whereas medium sized larvae were marginally related to chlorophyll a concentration indirectly corresponding to the elevated zooplankton abundance in the Rhine-Scheldt assemblage. The high explicative power of the spatial component for the abundance of medium sized larvae might be interpreted as indicator of larval drift being a further driver of this taxon's distribution. Nevertheless, an inter-annual variability of the contribution of the different herring larvae size classes to the Channel-Thames and Rhine-Scheldt assemblages



has to be expected. A region corresponding to the South of the Rhine-Scheldt assemblage (French and Belgium coast) was considered advantageous with zooplankton biomass in December comparable to the Buchan/Banks areas in September and low proportions of starved larvae (Akimova *et al.*, 2023). Prey of medium sized herring larvae like *Paracalanus spp.* and *Temora spp.* (Denis *et al.*, 2016) were of high abundance in the Rhine-Scheldt assemblage. Interestingly, Dickey-Collas *et al.* (2009) found a positive relation between the retention of herring larvae close to their spawning grounds (meaning larval drift not surpassing the Rhine-Scheldt delta) and the recruitment index of Downs herring. This indicates that although elevated plankton abundance was found in the entire Rhine-Scheldt assemblage in the present study this might not been the case in earlier years investigated by the mentioned authors (1988 – 2003). Or, that due to spatial variation of plankton or other factors influencing larval feeding within the assemblage the area until the Rhine-Scheldt delta provides better feeding conditions than the rest of this assemblage. Small herring larvae characterizing the Channel-Thames region were likely distributed in the vicinity of spawning areas. The correlation of these larvae with nanoflagellates could indicate a higher abundance of microzooplanktonic prey (Legendre and Rassoulzadegan, 1995) but a direct relation to prey abundance could not be revealed in this study due to the lack of detailed microzooplankton data.

Pleuronectidae larvae, an indicator taxon of the **Rhine-Scheldt assemblage**, most probably consisted of plaice larvae (*P. platessa*) with regard to the main spawning period (Harding, 1978; Munk and Nielsen, 2005). These larvae most probably originated from the spawning grounds in the EEC and Southern Bight, where spawning starts in December and January, respectively (Arnold and Metcalfe, 1996; Bolle *et al.*, 2009; Hufnagl *et al.*, 2013), and which are mainly connected to the nurseries in the Scheldt estuary (Hufnagl *et al.*, 2013) and along the Dutch Wadden Sea (Bolle *et al.*, 2009). As plaice larvae were found to nearly exclusively prey on Appendicularians in the study area (Last, 1978; Hufnagl *et al.*, 2013), it can be hypothesized that the Rhine-Scheldt assemblage is suitable for drifting plaice larvae with regard to prey provision as abundance of Appendicularians accounted for 15 % of the mesozooplankton assemblage in this region. As larvae of both the EEC and the SNS spawning grounds provide larvae to the Rhine-Scheldt assemblage we assume that plaice larvae will constitute a reoccurring member of this assemblage despite the inter-annual variability in larval drift predicted by Bolle *et al.* (2009). Eggs of plaice characterized the Central assemblage

which is in accordance with the location of the spawning ground south of the Dogger Bank (Loots *et al.*, 2010; Hufnagl *et al.*, 2013; Lelièvre *et al.*, 2014) for which spawning was reported to peak during February and March (Arnold and Metcalfe, 1996). Pleuronectidae eggs other than plaice were revealed as indicator species of the Rhine-Scheldt assemblage. They were most probably belonging to common dab (*L. limanda*) and flounder (*P. flesus*) as egg distribution corresponded to spawning periods and spawning grounds (Htun-Han, 1978; Van der Land, 1991; Martin *et al.*, 2008; Coppin *et al.*, 2009; Lelièvre *et al.*, 2012).

Further indicator species of the Rhine-Scheldt region were the eggs of *S. solea* and Lotidae which was in accordance with the spawning areas of these taxa. Spawning grounds of Lotidae species like *Ciliata mustela* are located along the eastern coast of the SNS with centers off the Belgian and Dutch coast up to the Frisian islands with a spawning period reported to start in January (Martin *et al.*, 2008). Sole spawns in the EEC, the Thames estuary and along the Belgian coast (Mollet *et al.*, 2007; Lacroix *et al.*, 2013).

Although spawning grounds of sardine exist in the German and Southern Bight, sardine larvae were observed in summer (June – August) in these areas (Kanstinger and Peck, 2009; Munk *et al.*, 2024). Spawning in the EEC by contrast continued until October (July – October) (Coombs *et al.*, 2005). We can thus assume that the larvae characterizing the Channel-Thames assemblage, displaying a size between 16 – 40 mm, were drifted to the Channel-Thames region from the EEC.

Further north, the eastern part of the **German Bight-Norfolk region** appeared important for Syngnathidae larvae most probably *Syngnathus rostellatus* consistent with previous works (Muus and Nielsen, 1999; Munk and Nielsen, 2005, personal communication Patrick Polte).

Gobiidae larvae were found to be an indicator species of the **Northern-British coast assemblage**. The only species reported to reproduce in the North Sea during winter was *Pomatochistus minutus* with a spawning period from February to June off Scotland (Miller, 1986). One could thus hypothesize that larvae hatched off Scotland drifted into the Northern-British coast assemblages with the Scottish Coastal water mass.

Drivers of taxa distribution not considered in this study could further have influenced the distribution of the assemblages found. This was indicated by the finding that for six taxa the abundance in the assemblages could not be entirely explained with the explicative variables used as indicated by retention of the spatial component in the most appropriate model (**Table 1**). A possible driver not considered in this study is the effect of top-down control that might

be exerted by zooplanktonic taxa like fish larvae, carnivorous copepods and by planktivorous fish. Although the North Sea as a whole is considered as bottom-up controlled (Daewel *et al.*, 2014), top-down control exerted by planktivorous fish was proposed to play a role in subareas of the North Sea (Daewel *et al.*, 2014; Marques *et al.*, 2023) and especially during autumn and winter when secondary production is low (Maes *et al.*, 2005; Daewel *et al.*, 2014; Timmerman *et al.*, 2020). Whiting displayed an increased consumption of *T. longicornis* in the Channel-Thames and Rhine-Scheldt region in winter (Timmerman *et al.*, 2020) and calculated consumption of herring and sprat juveniles exceeded production of investigated copepod species in the Scheldt estuary during this season (Maes *et al.*, 2005).

### 1.4.2 Inter-annual changes in zooplankton assemblages

The overall mesozooplankton taxa composition and total abundance as well as herring larvae abundance were relatively stable between 2008 and 2022 despite the long time span elapsed between these two years. This finding gives further evidence for an inter-annual persistence or reoccurrence of elevated secondary production in the Rhine-Scheldt assemblage during winter as was reported by several other studies (Krause and Martens, 1990; Krause *et al.*, 1995; Dudeck *et al.*, 2021). The inter-annual comparison further supported the finding of medium sized herring larvae as indicator of the Rhine-Scheldt assemblage as abundance of this taxon was higher in this assemblage in both years. Overall, the only notable differences between the two periods were found in the Rhine-Scheldt assemblage with a lower abundance of Appendicularians in 2022 and in the Channel-Thames region with higher total fish larvae abundance in 2022. The decline of Appendicularians might be related by the increased abundance of plaice larvae (**Figure 28, 29**) known to feed mainly on *Oikopleura dioika* (Last, 1978; Hufnagl *et al.*, 2013). With regard to fish larvae, abundance of species other than herring (plaice, sardine, Gobiidae, Ammodytidae) was higher in 2022 compared to 2008. This is in accordance with an increasing abundance trend of ichthyoplankton in the North Sea observed between 1960 and 2019 (Holland *et al.*, 2023) and an increase in sardine larvae in the southern and south-eastern North Sea observed for several years (ICES, 2023a).

Other studies have found inter-annual differences in mesozooplankton abundance in the study area between 2008 - 2022. An increase in mesozooplankton abundance was observed by Dudeck *et al.* (2021) between 2010 - 2013 in both the EEC and the Southern Bight. Semmouri *et al.* (2023) described a decrease in abundance of *T. longicornis*, *A. clausi*,

*Centropages sp.* and *Calanus helgolandicus* from 2015 to 2022 in Belgian waters. With regard to mesozooplankton abundance before 2008 the present study was in accordance with the reported decreasing trend of zoo- and holoplankton (Pitois and Fox, 2006; Alvarez-Fernandez *et al.*, 2012; Bedford *et al.*, 2020). Compared to winter 1987 (Krause *et al.*, 1995) the abundance of *Acartia spp.* and *Pseudocalanus spp.* were distinctively lower, for instance. Thus, the stability observed when comparing 2008 and 2022 does not fully reflect the inter-annual variability occurring between these two years.

However, there are reasons to believe that the assemblages found in the big polygon in 2008 displayed a representative pattern of winter zooplankton assemblages in the study area. First, the assemblages were related to the distribution of different water masses and other work (see above) (Williams *et al.*, 1993; Krause *et al.*, 2003). Second, higher abundance of phytoplankton in the Dogger Bank region and of plankton in the Rhine-Scheldt assemblage were found in several years by several authors (Nielsen and Richardson, 1989; Hay *et al.*, 1991; Nielsen *et al.*, 1993; Krause *et al.*, 1995; Dudeck *et al.*, 2021; Groß *et al.*, 2022). Third, the overall distribution of taxa was similar to 2022. Fourth, 2008 did not display strong anomalies with regard to salinity, temperature, chlorophyll a and herring larval density.

## 1.5 Conclusion

The present study suggests the existence of five zooplankton assemblages in the Southern North Sea and Eastern English Channel during winter that vary with regard to productivity, taxa abundance and composition. Chlorophyll a concentration, dissolved N/P ratios, phyto- and microplankton composition, water masses and fish spawning grounds were revealed as major driver of assemblage distribution. The Rhine-Scheldt and German Bight-Norfolk assemblages harbored the greatest zooplankton overwintering stocks that might influence the grazing pressure on phytoplankton spring production. Furthermore, elevated phyto-microplankton abundance in the Central region indicated this assemblage being a center of early spring plankton production. The distribution of ichthyoplankton taxa within the assemblages corresponded to spawning grounds and drifting routes of fish species with the Channel-Thames and Rhine-Scheldt assemblages being of high importance for herring and plaice larvae.

Future studies would profit from the integration of taxonomical data of microplankton (<200µm) facilitating the distinction of developmental stages of copepods, for instance, that would enhance the understanding of fish larvae distribution with regard to prey availability (Denis *et al.*, 2016; Akimova *et al.*, 2023) and give further insight in overwintering strategies of zooplanktonic organisms. Anomaly analysis of environmental and biological parameters, comparison with zooplankton data sampled in 2022 and earlier work suggest that the 2008 assemblages are broadly representative of the mesozooplankton and ichthyoplankton spatial distribution. Nonetheless, the evaluation of spatial data from other years would clearly enhance and verify our understanding of hibernal zooplankton assemblages and their potential influence on seasonal plankton succession in the context of climate change.

## CHAPTER 2 - 2. Perspective – Size structure

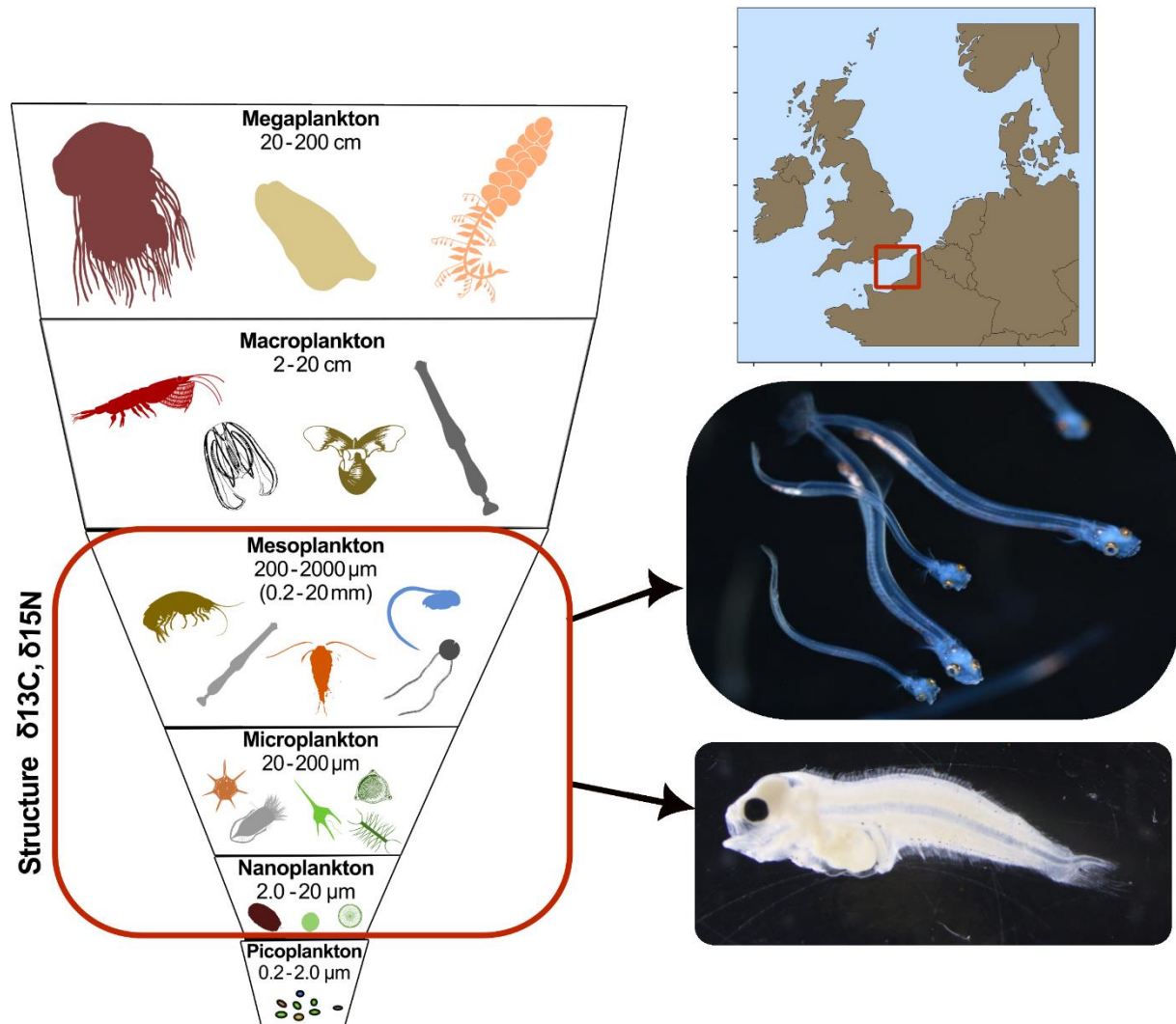
In the first chapter, I focused on a significant part of zooplankton organisms, namely holoplankton, meroplankton and ichthyoplankton. This facilitated a comprehensive insight in zooplankton assemblage composition and distribution in relation to the surrounding ecosystem. Assessing zooplankton communities in the most holistic way possible by incorporating a variety of zooplankton compartments is important for a comprehensive understanding of zooplankton functioning. Beside holoplankton like copepod species, meroplankton can constitute a dominant part of zooplankton assemblages, for instance (Lindley, 1998; Johns and Reid, 2001; Greve *et al.*, 2004) and are relevant for fish larval feeding (Denis *et al.*, 2016). Furthermore, meroplanktonic organisms were found to be indicator species of certain assemblages and seem to constitute reoccurring components of distinct winter assemblages as late polychaete-larvae were found in similar abundance at a similar location in winter 1987 (Krause *et al.*, 1995) as in winter 2008 (chapter 1). Although the composition of ichthyoplankton will be mainly influenced by spawning time, location, dispersal and predation (Hjort, 1914; Miller *et al.*, 1988; Bailey and Houde, 1989), fish larval distribution will further be determined by prey availability and the presence of predators (Miller *et al.*, 1988). Thus, the concurrent assessment of potential prey like mesozooplankton organisms and fish larvae might help to understand the distribution patterns of organisms and assemblages also with regard to the potential top-down influence of fish larvae on mesozooplankton composition through predation (Bollens, 1988; Munk and Nielsen, 1994). As both, fish eggs and larvae, and mesozooplankton constitute prey for predators like jellyfish (Purcell, 1985) and fish such as herring, sardine and sprat (Garrido *et al.*, 2007a; Segers *et al.*, 2007), incorporating mesozooplankton and ichthyoplankton in the same study further allows a more comprehensive insight in the feeding potential of zooplankton assemblages for higher trophic levels.

A plankton component that was only roughly considered in the first chapter, however, were microplankton. As discussed in chapter 1, the consideration of microplankton in plankton studies could be of interest for several reasons. Among others, microplankton represent an important part of the planktonic food web and are important for larval nutrition.

## CHAPTER 2 - 2. Perspective – Size structure

Thus, in the second chapter I aimed at investigating the planktonic food web including a wide plankton size range encompassing microplankton and using a direct approach allowing to assess the contribution of different plankton size classes to fish larval diet.

The work presented in this chapter is planned to be submitted for publication until my doctoral defence.



# Ontogenetic and spatial variation in the diet of herring and plaice larvae: Insights from stable isotope analysis

---

## 2.1. Introduction

Abundance and biomass of fish populations fluctuate in time mainly due to variability in the recruitment process (Houde, 2016). One bottleneck of year class strength is the survival of early life stages (Houde, 2008). Several theories exist regarding the factors that determine the survival of fish larvae pointing out the importance of larval feeding. Successful feeding allows the larvae to overcome the change from internal to external feeding, during which mortality is especially high (“critical period” hypothesis, Hjort, 1914), and to grow out of the size range most exposed to predation (“bigger is better” hypothesis, Anderson, 1988).

Larvae of herring (*C. harengus*) and plaice (*P. platessa*), are part of the same planktonic food web due to similar spawning periods and areas. The Downs component of North Sea herring spawns in the EEC from November to February (Coppin *et al.*, 2009; Dickey-Collas *et al.*, 2009) and plaice spawn from December to March (Harding, 1978; Munk and Nielsen, 2005). Beside herring larvae, which outnumber those of other fish species, plaice larvae are among the most abundant fish larvae during this period (Giraldo *et al.*, 2024; Neven *et al.*, *in press*, chapter 1). Successful larval feeding has been proposed to play an important role in the recruitment of both plaice and herring (Nash and Dickey-Collas, 2005; Hufnagl *et al.*, 2013, 2015; Illing *et al.*, 2018; Di Pane *et al.*, 2019).

The larval phase of a fish can be separated in several periods according to developmental stages ranging from the yolk-sac larvae to the juvenile fish. The first three larval stages of plaice are pelagic and feeding success during this pelagic phase was proposed as one factor influencing year-class strength (Bolle *et al.*, 2009; Di Pane *et al.*, 2019). Larvae attaining good condition before metamorphosis might more successfully compete for feeding resources on the nursery grounds. This might be of importance as in general the carrying capacity of feeding grounds was proposed to be limited with regard to prey availability (Di Pane *et al.*, 2019). Metamorphosis starts at stage 4 at a size of 9 to 11 mm transforming the bilaterally



symmetrical body form of pelagic larvae to a flat body form (Shelbourne, 1957; Hovenkamp, 1990; Silva *et al.*, 2015b). During metamorphosis larvae start to descend in the water column to finally settle down for a benthic life style in the nursery areas (Bolle *et al.*, 2009).

For herring, several studies suggest that the major factor influencing year-class strength is the survival of larvae before metamorphosis (<20 mm) (Nash and Dickey-Collas, 2005; Corten, 2013; Hufnagl *et al.*, 2015). This could be related to several critical periods during this developmental phase. Herring larvae open their mouth three days post hatch at a size of 8 to 9 mm and ingest first prey items, which likely serve as preparation for external feeding. Between 9 and 14 mm, the yolk sac is absorbed, larvae attain the pre-flexion stage (stage 2) relying entirely on external feeding. Metamorphosis starts at the end of stage 4 (post-flexion stage) when the larvae reach approximately 15 - 30 mm (Joly *et al.*, 2021). Based on fluctuations in quantities of liver reserves, Joly *et al.* (2021) suggested that the transition from pre-flexion to flexion and onset of metamorphosis are highly energy-demanding, making these periods particularly sensitive to feeding condition. Similarly, changes in larval condition and prey composition have been identified as critical period for herring larvae within the size range of 13 - 20 mm (Denis *et al.*, 2016, 2017).

Thus, understanding the feeding strategies of herring and plaice across different developmental stages is crucial for enhancing our knowledge of the variability in their recruitment. This is of particular interest for herring that displays a period of low recruitment since 2002 (ICES, 2023) and in the context of climate change. Climate change was shown to influence zooplankton community composition in the study area (Beaugrand *et al.*, 2014; Bedford *et al.*, 2020; Semmouri *et al.*, 2023), and might have consequences for the planktonic food web, potentially affecting the quantity and quality of fish larvae prey.

Several recent studies using different approaches advanced the knowledge about Downs herring larval feeding while knowledge about plaice larval feeding was mostly gained from earlier research. Studies considering the feeding of both larvae simultaneously are rare (but see Giraldo *et al.* (2024)).

Herring larvae are proposed to be omnivorous feeders feeding on a wide variety of prey (Denis *et al.*, 2016). Analysis of larval stomach contents using electron microscopy suggests a major contribution (~60 - 70%) of *Paracalanus parvus*, *Pseudocalanus elongatus* and invertebrate eggs with lower contributions (~20 - 40%) of copepod and cirripedia nauplii as well as the copepods *Euterpina acutifrons* and *T. longicornis* (Denis *et al.*, 2016). A strong correlation

between herring larval abundance and the abundance of *P. elongatus* was also observed by Alvarez-Fernandez et al. (2015) in the North Sea. Similar to stomach content analysis, stable isotope analysis suggests a major (~60 %) proportion of the copepods *Acartia clausi*, *Paracalanus spp.*, *Pseudocalanus spp.* and *Ditrichocorycaeus anglicus* to herring larval diet. Beside mesozooplankton organisms (200 - 500 µm), microplankton (20 - 200 µm), including protists (unicellular organisms) and multicellular organisms, were proposed to represent a relevant part of herring larval nutrition (Denis et al., 2016; Bils et al., 2022; Akimova et al., 2023). Depending on larval size, microplankton (20 - 200 µm) accounted for 4 - 38 % of the diet based on physiological modeling (Akimova et al., 2023). Microplanktonic prey included diatoms, dinoflagellates and ciliates (Denis et al., 2016; Akimova et al., 2023).

The major prey of plaice larvae in the study area from January to March is the appendicularian species *O. dioica* that was found to constitute ~80 to 100 % of the investigated stomach contents (Shelbourne, 1953, 1957, 1962; Last, 1978). Beside *O. dioica*, nauplii of *P. parvus* and *P. minutus*, other nauplii, polychaete larvae, gastropod veliger larvae and *T. longicornis* belonged to prey items ingested by larval plaice (Shelbourne, 1953; Last, 1978). A study based on stable isotopes suggests a contribution of *A. clausi*, *Paracalanus spp.*, *Pseudocalanus spp.* and *D. anglicus* to plaice larval diet (Giraldo et al., 2024). Comparing abundance of zooplankton taxa in stomach contents and in water samples, Shelbourne (1953) suggested that plaice displays selective feeding on distinct taxa. In other regions like the Irish Sea, Scottish coastal waters and around Plymouth, *O. dioica* was not found to dominate plaice larval diet, but the annelid larvae, *Evadne normanni*, mollusk larvae and small copepod species were found to be major prey items (Shelbourne (1962) and references therein). Although the importance of microplankton for fish larval nutrition is more and more recognized (Bils et al., 2022; Akimova et al., 2023), to our best knowledge no study exists investigating the role of microplankton in the feeding of plaice larvae.

Studying larval feeding is challenging as prey organisms are small and rapidly digested (de Figueiredo et al., 2005), stomach content can get lost during the sampling process due to regurgitation (Denis et al., 2016) and fish larvae as part of the planktonic food web might feed on a variety of different prey items of varying taxonomy and size (de Figueiredo et al., 2005; Denis et al., 2016). Stable isotope analysis (SIA) allows analyzing the structure of a trophic system with regard to trophic levels and food sources used by its members.  $\delta^{15}\text{N}$  can be used as an indicator for trophic position as the percentage of  $^{15}\text{N}$  relative to  $^{14}\text{N}$  in tissues increases

with increasing trophic position in a progressively and predictably manner (Schoo *et al.*, 2018). Between two trophic levels a fractionation of  $\delta^{15}\text{N}$  of around 3.4‰ (Minagawa and Wada, 1984) takes place with values in aquatic systems suggested to be around 2.3‰ (McCutchan Jr *et al.*, 2003). Due to different mechanisms of primary producers for the fixation of atmospheric carbon, dietary sources can be differentiated based on  $\delta^{13}\text{C}$  (Fry, 2006). Using SIA to study larval feeding delivers dietary information integrated in tissues over a certain period of time and is therewith complementary to stomach content analysis that represents a temporal snapshot of larval nutrition. SIA might further allow to assess the contribution of microplankton to larval diet that is digested rapidly due to small organism sizes (de Figueiredo *et al.*, 2005).

Considering plankton in terms of size rather than taxonomic composition has proven useful in trophic ecology. This is because the taxonomic composition varies between different size classes, such as nanoplankton, microplankton and mesoplankton (Reynolds, 2006). Size-based classification is also crucial because different developmental stages (and therefore sizes) of the same species can exhibit distinct stoichiometries and energy requirements, which influence their role in energy pathways and trophic interactions (Brooks and Dodson, 1965; Meunier *et al.*, 2016). For instance, smaller plankton may have different nutritional profiles compared to larger ones (Mayzaud *et al.*, 2011, 2016), affecting their availability and suitability as prey for various predators. This size-dependent variability can significantly impact predator-prey dynamics and energy transfer within the food web (Tesán-Onrubia *et al.*, 2023).

However, information about meso- and microplankton in the study area during winter are scarce (Hufnagl *et al.* (2015), chapter 1) and few studies exist delivering information about isotopic signature of small plankton size classes (Tesán-Onrubia *et al.*, 2023), leading to a lack of information necessary for the assessment of larval nutrition.

Different larval stages of fish species often exhibit distinct spatial patterns due to larval drift, although multiple stages may co-occur in the same areas (Neven *et al.*, *in press*, chapter 1). Understanding the spatial variability in larval dietary composition is essential to comprehensively assess how larval dispersal influences the survival of early life stages (Morote *et al.*, 2010). This includes accounting for how environmental parameters influence larval feeding condition and prey availability (Arula *et al.*, 2012; Shideler and Houde, 2014; Akimova *et al.*, 2023). The EEC is characterized by strong environmental gradients with regard to depth, salinity and temperature (Brylinski *et al.*, 1991; Giraldo *et al.*, 2017). Although on a larger

spatial scale the EEC was suggested to harbor a relatively homogenous mesozooplankton assemblage (Neven *et al.*, *in press*, chapter 1), a study building on a higher spatial resolution unveiled spatial variation in EEC plankton assemblage composition (Dudeck *et al.*, 2021).

The second chapter aims at gaining further insight into the prey composition and feeding strategies of herring and plaice larvae within a planktonic food web. By integrating both size-based and spatial considerations, we hope to better understand the complex interplay between larval development, environmental variability, and recruitment success. In detail, we intended to answer the following questions:

- a) Which plankton size classes are characteristic of larval diet?
- b) Does the contribution of different size classes to larval diet change with ontogenetic development (i.e. size/stage)?
- c) How does the contribution of different plankton size classes to larval diet vary with spatial location?
- d) Do herring and plaice larvae display similar feeding strategies with regards to their trophic niches?

## 2.2. Materials & Methods

### 2.2.1. Sampling

Sampling took place in January-February 2021 (15.01. - 08.02.2021) during the first quarter of the IBTS survey, onboard of the French Thalassa Research Vessel of the French Oceanographic fleet. Additional details on sampling protocols are accessible using the survey's DOI (10.17600/18001237).

Salinity and temperature were measured at the surface by means of a thermosalinometer, while depth was measured using a bathysonde (**Figure 31B**). Several size classes (microplankton, mesozooplankton) of plankton were sampled including larvae of herring and plaice (**Figure 31A**). The size class <20  $\mu\text{m}$  was collected at 11 stations using a Niskin bottle and a sieve to obtain the targeted size fraction. Microplankton (20 - 200  $\mu\text{m}$ ) was sampled at nine stations by means of phytoplankton nets with a mesh size of 20 and 80  $\mu\text{m}$ . The 20  $\mu\text{m}$  mesh size allowed to sample the fractions 20-50  $\mu\text{m}$  and 50-80  $\mu\text{m}$  that were separated by sieving the collector content through sieves with different mesh sizes. The fractions 50 - 80

$\mu\text{m}$  and 80 - 125  $\mu\text{m}$  were collected using an 80  $\mu\text{m}$  mesh size and size-adapted sieving. Mesozooplankton was collected by means of a WP2 and a bongo net (mesh size 200  $\mu\text{m}$  and 500  $\mu\text{m}$  respectively) at 12 stations and sieved with respective mesh sizes to obtain the size fractions 200 - 500 and 500 - 1000  $\mu\text{m}$ . All nets mentioned above were vertically hauled from 3 m above bottom to surface. All size fractions sampled were transferred on glass microfiber filters of the type GF/F of a diameter of 47 mm. Sampling of herring and plaice larvae was realized using a MIK net with a mesh size of 500  $\mu\text{m}$ . Per station 8 - 10 herring and plaice larvae were sampled. All samples were stored at  $-80^{\circ}\text{C}$  until further analysis.

To obtain information about riverine inputs during the study period, data of the daily discharge of the Seine river, which represents the river with the greatest catchment area in the study area, was downloaded from <https://www.hydro.eaufrance.fr/>.

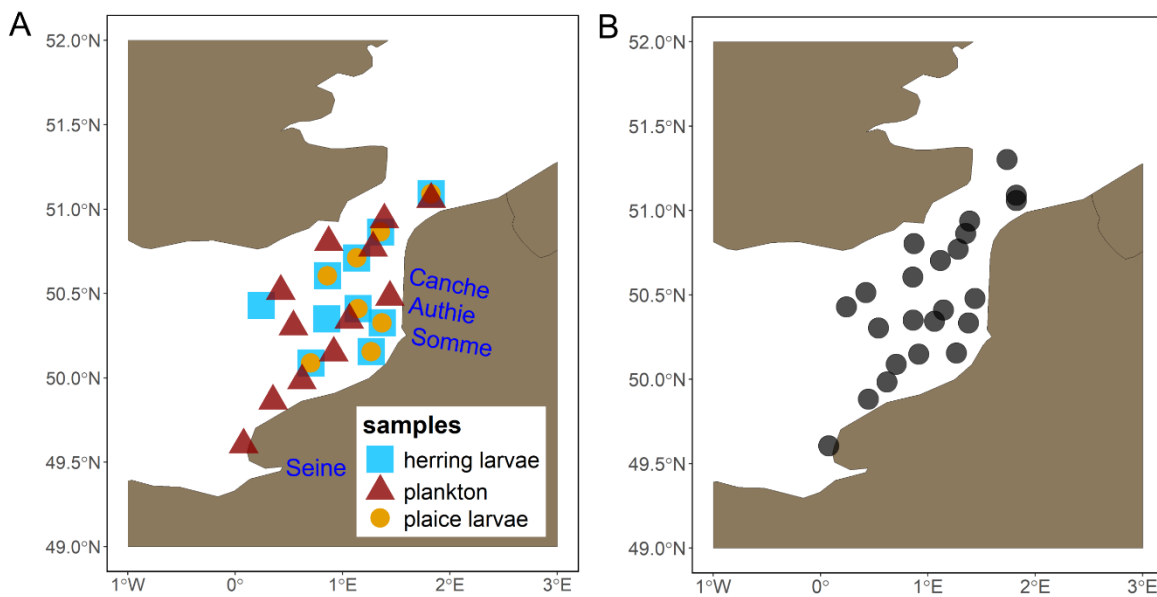


**Figure 31 Sampling stations.** A: Sampling stations of herring larvae (blue squares), plaice larvae (yellow dots) and different plankton size classes (red triangles). Blue names indicate the location of the rivers terminating in the EEC; B: Sampling stations for temperature, salinity and depth.

### 2.2.2. Isotope analysis

The stable isotope composition ( $\delta^{13}\text{C}$ ,  $\delta^{15}\text{N}$ ) from the different plankton size classes and fish larvae were used to gain information about the size structure and trophic relationships in the study area. Larvae were measured, individually stored in Eppendorf tubes, freeze-dried and

ground to a fine powder. All other plankton samples were freeze-dried, screened under a stereomicroscope to remove organisms not fitting the size class and to decide if samples of mesozooplankton should be acidified to remove sources of inorganic carbon. In case sand, shell debris and/or phytoplankton were detected on the filter, half of the sample was fumed with HCL before subsequent  $\delta^{13}\text{C}$  analysis to remove inorganic carbon. The other half of the sample was kept for  $\delta^{15}\text{N}$  analysis. Zooplanktonic sources of inorganic carbon such as cirripedia nauplius larvae or chaetognaths were not judged to bias the sample as samples consisted of a mixture of plankton organisms.

Isotope ratios were measured with a Thermo Delta V isotope mass ratio spectrometer, interfaced to a NC2500 elemental analyzer. The accuracy of the isotopic ratio measurements was verified by analyzing an in-house standard after every 10<sup>th</sup> sample with an overall standard deviation of 0.21‰ for  $\delta^{15}\text{N}$  and 0.09‰ for  $\delta^{13}\text{C}$ . Stable isotopes ratios were expressed in accordance with the classical  $\delta$  notation with:

$$\delta X = \left( \frac{R_{\text{sample}}}{R_{\text{standard}}} - 1 \right) * 10^3$$

where X corresponds to  $\delta^{13}\text{C}$  or  $\delta^{15}\text{N}$ , and R to the isotopic ratios ( $^{13}\text{C}/^{12}\text{C}$  or  $^{15}\text{N}/^{14}\text{N}$ , respectively) of the samples measured and of international standards (Vienna Pee Dee Belemnite for C and atmospheric nitrogen for N).

### 2.2.3. Statistical analysis

#### 2.2.3.1. Predicting source isotope signature at larvae sampling stations

Nano-, micro- and mesoplankton were not sampled at all larvae sampling stations. To explore the contribution of the different size classes to herring and plaice larval diet we predicted  $\delta^{13}\text{C}$  and  $\delta^{15}\text{N}$  values of the different plankton size classes (from <20 to 1000  $\mu\text{m}$ ) at the larvae sampling stations using hierarchical generalized additive models (HGAM) (Pedersen *et al.*, 2019). These models allowed to take into account spatial variation in the isotope data considering potential differences between size classes. Generalized additive models (GAM) allow to consider data with different distributions and non-linear relationships between a variable and its predictor by using smooth terms (Zuur, 2012). HGAM allows to explore if a non-linear relationship between a variable and a predictor varies within a group applying a smooth term per group level. In the present study we used two models per stable isotope, one predicting values of microplankton including all size classes <200  $\mu\text{m}$  and another

predicting values of mesozooplankton (>200 - 1000  $\mu\text{m}$ ). In these models all size classes taken together corresponded to ‘group’ that could be separated into different group levels represented by the size classes. This allowed to predict the isotope values of a group of size classes in a single model by allowing for different smooth terms per size class (group level).

Three different GAM models, each incorporating increasing levels of complexity to account for spatial variability by size class were compared. The simplest (simple) model, predicted  $\delta^{13}\text{C}$  or  $\delta^{15}\text{N}$  by a spatial component represented by the coordinates of the sampling stations. The simple model did not allow for group-level (size-classes) differences, thus predicting the overall variation of the isotopic signatures in space for nano-microplankton and mesozooplankton, respectively. The second model (intermediate) allowed for a differing intercept per group-level (size class). The third and most complex model (advanced) allowed for a differing intercept and spatial smooth term per group-level (size class).

**Simple:**  $\delta^{13}\text{C}$  or  $\delta^{15}\text{N} \sim \text{smooth}(\text{long}, \text{lat}) + \varepsilon$

with  $\varepsilon$  following gaussian or gamma distribution with as log, inverse or identity link function

**Intermediate:**  $\delta^{13}\text{C}$  or  $\delta^{15}\text{N} \sim \text{smooth}(\text{long}, \text{lat}) + \text{size class} + \varepsilon$

with  $\varepsilon$  following gaussian or gamma distribution with as log, inverse or identity link function

**Advanced:**  $\delta^{13}\text{C}$  or  $\delta^{15}\text{N} \sim \text{smooth}(\text{long}, \text{lat}, \text{by} = \text{size class}) + \text{size class} + \varepsilon$

with  $\varepsilon$  following gaussian or gamma distribution with as log, inverse or identity link function

The GAM models were run using the package “mcgv” (Wood, 2011). Each model was verified to meet model assumptions by plotting residuals versus fitted values, versus each group-level and by verifying overall residual distribution using the `gam.check()` function and the “Dharma” package (Hartig, 2022). Furthermore, it was verified if the spatial terms were significant. If assumptions were not met the model was revised by first, testing different smooth terms: tensor product interactions (ti), tensor product smooth (te), alternative tensor products (t2); second, testing different smoothing basis (e.g., tp, bs, ts), and finally, testing different distributions by applying gaussian and gamma distribution with identity, inverse and log functions. As  $\delta^{13}\text{C}$  data contained negative values that are not allowed when using log link

functions and gamma distributions, the value 30 was added as a constant to  $\delta^{13}\text{C}$  before modeling. After verifying that all models satisfied the required assumptions, the AIC values for the simple, intermediate, and advanced models were compared. The model with the lowest AIC was selected as the most appropriate. Models that failed to meet the assumptions following the revision process were excluded from the AIC comparison. In cases where the spatial pattern of the isotope modeled was similar between size classes (as indicated by similar intercepts and estimated degrees of freedom of the smooth terms) these size classes were grouped and the model was compared to models with ungrouped size classes using the AIC.

### **2.2.3.2. Stable isotope mixing models**

Stable isotope mixing models (MixSIAR) were used to assess the contribution of different size classes to the larvae's nutrition (Stock *et al.*, 2018). These models are based on the principle that the isotopic signature of a consumer reflects the mixture of the isotopic signatures of the consumed food sources, relative to their contribution to the consumer's diet. The mixture is adjusted for the isotopic fractionation taking place during digestion, metabolism and assimilation using trophic enrichment factors (TEF) (Post, 2002). Based on outputs of the GAM models serving for stable isotope value prediction, plankton in a size range of 20 - 125  $\mu\text{m}$  were aggregated to a single size class *a priori* as they displayed a similar spatial pattern and similar values in both isotopes. Model assumptions were verified by confirming that the consumer (larvae) isotopic signatures were in the isotopic space of the food sources (plankton size classes) after correction for trophic enrichment and by inspecting correlation coefficients between the isotopic values of prey sources.

MixSIAR models were applied using TEF values of 0.8 for carbon and 2.3 for nitrogen as previously proposed for zooplankton food webs (Schwamborn and Giarrizzo, 2015; Figueiredo *et al.*, 2020). Models were run in the "long" setting with the following parameters: 300 000 chain length, 200 000 k burn-ins, and thin number 100 for three parallel Markov Chain Monte Carlo (MCMC) chains. The Gelman-Rubin test and Geweke test (MixSIAR default) were used to assess convergence.

Several MixSIAR models were run to investigate different research questions:



**Global model:** The global model did not include any covariate and aimed to predict the global contribution of the different size classes per species.

**Spatial model:** The space model included ‘sampling station’ as a random effect, allowing for spatial variation in the proportion of plankton size classes contributing to larval nutrition.

**Stage-space model:** For plaice larvae, the space model indicated a spatial trend correlated with the spatial distribution of larval stages. Therefore, a third model was applied for plaice including ‘sampling station’ and ‘ontogenetic stage’ as covariates. Ontogenetic stage was used instead of larval size as a continuous variable because the latter did not converge due to restricted sample sizes.

For illustration purposes of larval diet composition, the 20 - 125  $\mu\text{m}$  and 200 - 500  $\mu\text{m}$  size classes were grouped *a posteriori* and displayed as ‘minor’ as their contribution to larval diet was minor compared to the remaining size classes.

Model outputs are presented as mean  $\pm$  SD. The entire posterior distribution can be found in Annex II (**Table A 3, 5**).

### **2.2.3.3. Ontogenetic stages larvae**

Larvae were categorized by developmental stage based on size, using literature on the size ranges for different ontogenetic stages of herring and plaice larvae. Herring larvae with a size of 6 - 10 mm were classed as stage 1, corresponding to yolk-sac larvae. Stage 2 larvae comprised larvae between >10 - 13 mm, corresponding to larvae in the pre-flexion stage. Stage 3 larvae represented by larvae with a size between >13 - 20 mm corresponded to the flexion stage (Joly *et al.*, 2021; Akimova *et al.*, 2023). Plaice stage 1 larvae, representing the yolk sac stage, included larvae of a size between 4 - 7 mm. Stage 2 larvae (pre-flexion feeding larvae) included larvae of a size between >7 - 8.5 mm. Stage 3 larvae, representing larvae before metamorphosis, corresponded to a size range of >8.5 - 11 mm (Hovenkamp, 1990; Silva *et al.*, 2015b).

## 2.3. Results

### 2.3.1. Environmental conditions

Seawater in the EEC during winter displayed a mean surface temperature of  $9.19 \pm 0.55$  °C and a mean surface salinity of  $34 \pm 0.9$ . The mean depth in the study area was  $34.7 \pm 7.7$  m (**Figure 32**).

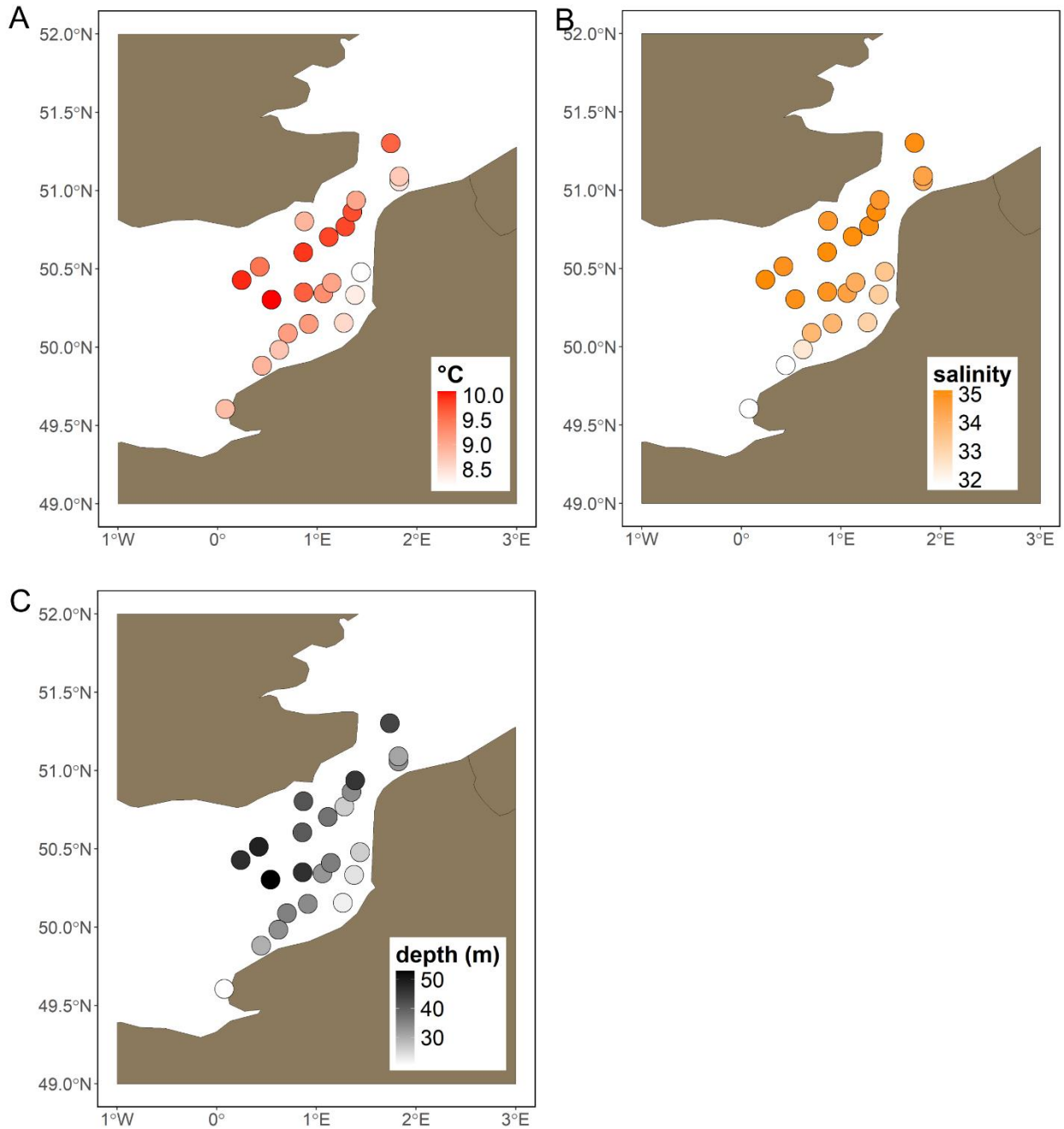


**Figure 32 Environmental parameters.** A: Surface temperature; B: Surface salinity, C: Depth.

The river runoff of the Seine river during the study period was compared approximatively with regard to its cumulated discharge during January and February between the years 2014 to 2021 (**Table 3**). The river discharge varied between ~121 000 and ~205 000 m<sup>3</sup>/sec. Compared to the other years the river discharge in January and February 2021 was elevated with 198 609 m<sup>3</sup>/sec comparable to the years 2014 and 2018.

**Table 3** River discharge of the Seine river during January and February from 2014 to 2021.

Year	River discharge (m <sup>3</sup> /sec)
2014	181 295
2015	160 954
2016	205 133
2017	121 259
2018	227 839
2019	131 129
2020	171 145
2021	198 609

### 2.3.2. Size structuration planktonic food web

Stable isotope values of microplankton size classes were highly variable (**Figure 33**). The smallest size class (<20 µm) displayed the largest variability with regard to δ<sup>15</sup>N values (between ~3‰ and ~27‰). δ<sup>13</sup>C values of this size class also differed from other size classes with mean values ~-28‰ compared to ~-21‰ for the other classes. The 50 - 80 µm, 80 - 125 µm and 200 - 500 µm size classes displayed similar stable isotopes values with δ<sup>13</sup>C ranging from ~-17‰ to ~-24‰ and δ<sup>15</sup>N values from ~3‰ to ~14‰. The 125 - 200 µm size class was close in the isotopic space to size classes between 20 and 200 µm, however with a higher variation in both δ<sup>15</sup>N and δ<sup>13</sup>C values. The 500 - 1000 µm size class could be distinguished from the other size classes with slightly lower δ<sup>13</sup>C and slightly higher δ<sup>15</sup>N stable isotopes. Fish larvae displayed less variation in stable isotope values and had a species-specific stable isotope signature. Similar to the 500 - 1000 µm size class they could be distinguished from plankton size classes due to slightly higher δ<sup>15</sup>N stable isotopes.

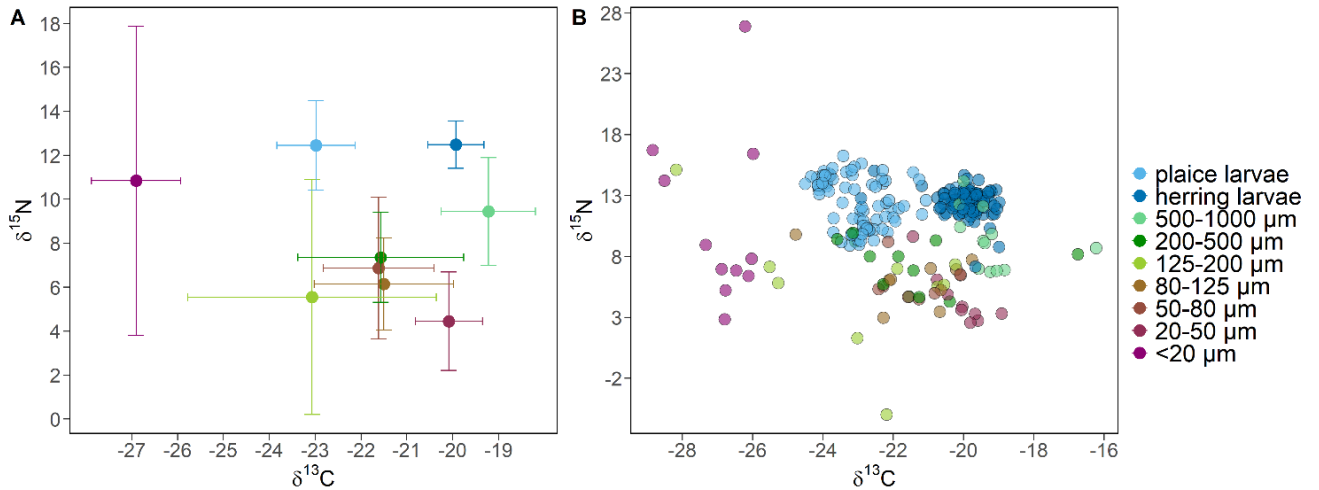


**Figure 33 Biplot of carbon ( $\delta^{13}\text{C}$ ) and nitrogen ( $\delta^{15}\text{N}$ ) stable isotope signatures for different plankton size classes and fish larvae.** A: Mean and standard deviation per size class and larval species; B: Raw values per sampling station (one sample per station and plankton size class and between 8 to 10 larvae per station).

### 2.3.3. Predicted values of planktonic size classes

GAMs revealed spatial variability in the isotopic signatures of the different plankton size-classes. Several size classes displayed similar spatial patterns (similar intercepts and estimated degrees of freedom of the smooth terms) and were grouped in the final model. These concerned the size classes between 20 - 125  $\mu\text{m}$  (i.e., size classes 20 - 50  $\mu\text{m}$ , 50 - 80  $\mu\text{m}$  and 80 - 125  $\mu\text{m}$ ) which were grouped in the model predicting  $\delta^{13}\text{C}$  (gam\_micro\_carbon) and all size classes between 20 - 200  $\mu\text{m}$  in the model predicting  $\delta^{15}\text{N}$  (gam\_micro\_nitrogen) (**Table 4**).

As a result of the model selection process, the following models were used for stable isotope predictions (**Table 4**):

$$\text{gam\_micro\_carbon} = \text{gam}(\delta^{13}\text{C} \sim \text{ti}(\text{long}, \text{lat}, \text{by} = \text{size class}) + \text{size class} + \epsilon$$

with  $\epsilon$  following gaussian distribution with a log link function

$$\text{gam\_micro\_nitrogen} = \text{gam}(\delta^{15}\text{N} \sim \text{ti}(\text{long}, \text{lat}, \text{by} = \text{size class}) + \text{size class} + \epsilon$$

with  $\epsilon$  following Gamma distribution with an inverse link function

$$\text{gam\_meso\_carbon} = \text{gam}(\delta^{13}\text{C} \sim \text{ti}(\text{long}, \text{lat}) + \text{size class} + \epsilon$$

with  $\epsilon$  following gaussian distribution with a log link function

$$\text{gam\_meso\_nitrogen} = \text{gam}(\delta^{15}\text{N} \sim \text{te}(\text{long}, \text{lat}) + \text{size class} + \epsilon$$

with  $\epsilon$  following gaussian distribution with a log link function

**Table 4 Summary of hierarchical GAMs to predict stable isotope values of trophic sources at larvae sampling stations.** The table presents intercept values of size classes with standard error (S.E.), and p-values of the spatial term integrated in the model as a smoothed term. Further estimated degrees of freedom (edf) of the smooth term, the adjusted  $R^2$ , deviance explained and samples used (n) per model are displayed.

model	size class ( $\mu\text{m}$ )	Intercept (S.E.)	p-value smooth terms	edf	$R^2$ (adj)	Deviance explained (%)	n
gam_micro_carbon	<20	-27.16 (0.4)	0.3	1	0.85	89	47
	20 - 125	6.40 (0.54)	0.04*	3.8			
	125 - 200	4.86 (0.80)	>0.001***	5.7			
gam_micro_nitrogen	<20	0.11 (0.01)	0.005**	4.8	0.75	70.8	46
	20 - 200	0.1 (0.02)	<0.001***	4.2			
gam_meso_carbon	200 - 500	-22.02 (0.29)	<0.001***	3.3	0.8	84	24
	500 - 1000	2.35 (0.34)					
gam_meso_nitrogen	200 - 500	7.36 (0.51)	0.02*	4.7	0.49	60	24
	500 - 1000	2.09 (0.72)					

As can be seen in **Figure 34**, the models predicting  $\delta^{13}\text{C}$  for microplankton revealed no or weak spatial variation of  $\delta^{13}\text{C}$  for the smallest size fraction (<20  $\mu\text{m}$ ) and the grouped size fraction 20 - 125  $\mu\text{m}$ , respectively. The size class 125 - 200  $\mu\text{m}$  displayed a tendency of lower  $\delta^{13}\text{C}$  values in a zone influenced by the discharge of the Seine river and higher values close to the English coast and the Dover Strait.

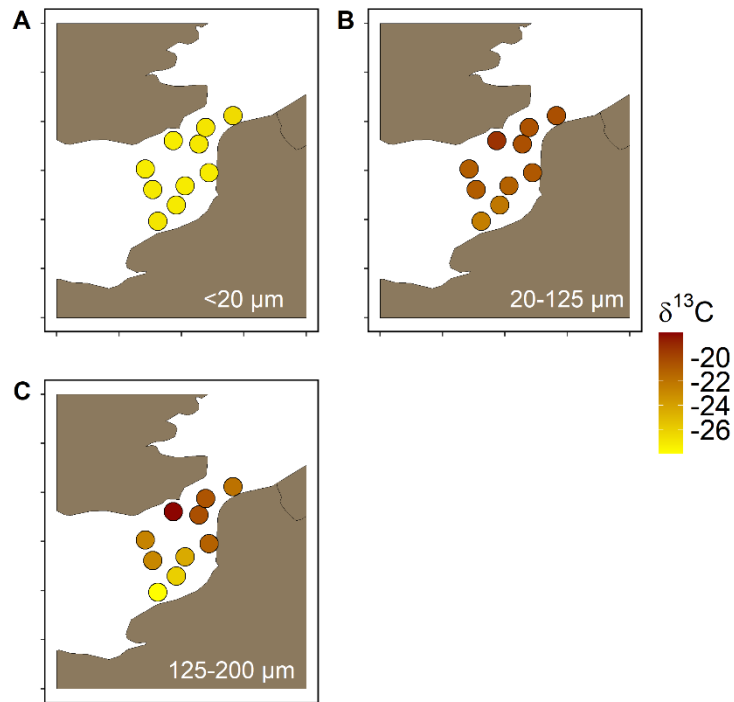


**Figure 34** Predicted values of  $\delta^{13}\text{C}$  by the *gam\_micro\_carbon* model. Map displays predicted values at nano-microplankton sampling stations.

The predictions of  $\delta^{15}\text{N}$  for the <math><20\ \mu\text{m}</math> size class revealed a difference between values in the EEC and the sampling station situated in the North Sea (**Figure 35**). Whereas  $\delta^{15}\text{N}$  values varied between  $\sim 6\text{‰}$  and  $\sim 12\text{‰}$  in the EEC without a distinct spatial pattern the  $\delta^{15}\text{N}$  value in the North Sea was higher with  $\sim 15\text{‰}$ .  $\delta^{15}\text{N}$  values of the grouped 20 - 200  $\mu\text{m}$  size class displayed the lowest  $\delta^{15}\text{N}$  values on the English side of the English Channel whereas the highest value was observed close to the Seine estuary.

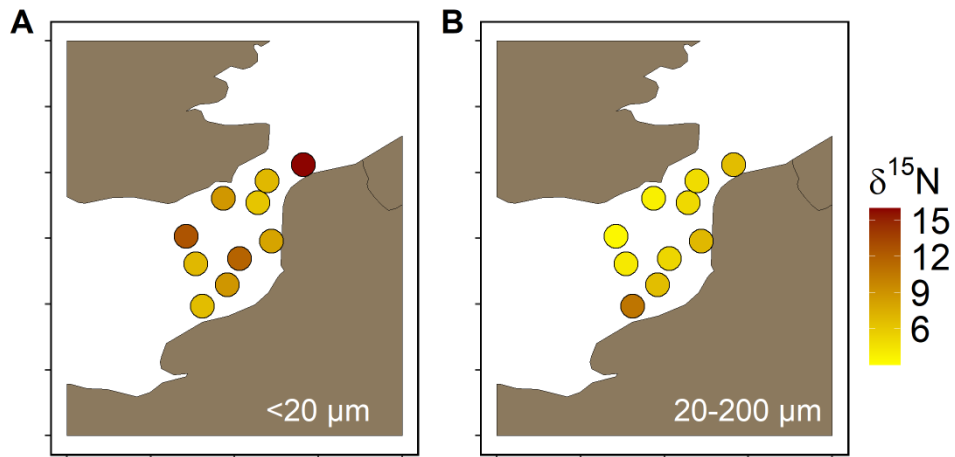


**Figure 35** Predicted values of  $\delta^{15}\text{N}$  by the *gam\_micro\_nitrogen* model. Map displays predicted values at nano-microplankton sampling stations.

The spatial variability of  $\delta^{13}\text{C}$  values for mesozooplankton (**Figure 36**) was low in the English Channel but displayed a higher value for both size classes at the sampling station situated in the North Sea. Spatial variability of  $\delta^{15}\text{N}$  values was similar between the 200 - 500 and 500 - 1000  $\mu\text{m}$  size class with the highest values close to the Seine estuary and the lowest values close to the English coast.

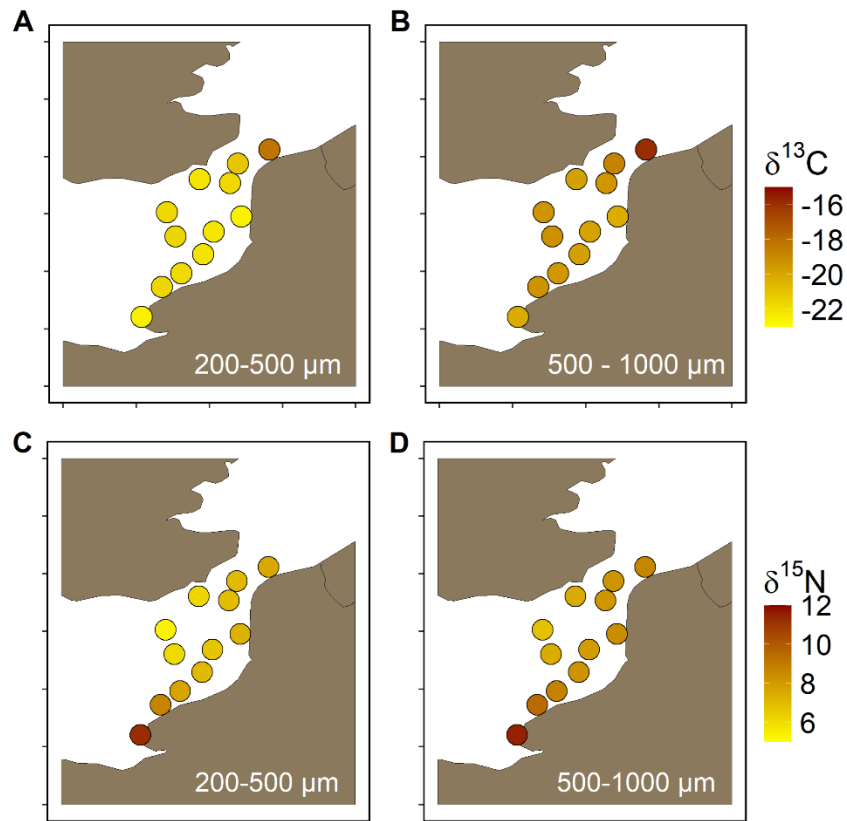


**Figure 36 Predicted values of  $\delta^{15}\text{N}$  and  $\delta^{13}\text{C}$ .** A: Predictions of the *gam\_meso\_nitrogen* model. Maps display predicted values at nano-microplankton sampling stations; B: Predictions of the *gam\_meso\_carbon* model. Maps display predicted values at nano-microplankton sampling stations.

## 2.3.4. Proportion of different plankton size classes to larval diet

### 2.3.4.1. Spatial distribution of ontogenetic stages

For herring, stage 2 larvae were the most abundant in the entire study area (**Figure 37A**). The distribution of plaice larvae developmental stages varied spatially between stations influenced by riverine inputs (mostly the rivers Seine and Somme) subsequently called river influenced stations, and those located in the center of the EEC (**Figure 37B,D**). At river influenced stations, a higher abundance of stage 3 larvae (river:  $5.5 \pm 3.3$  ind/1000 m<sup>3</sup> vs center:  $2.0 \pm 1.4$  ind/1000 m<sup>3</sup>) was observed whereas at stations in the center of the EEC the abundance of stage 1 larvae was slightly higher than at the river influenced stations (center:  $5.8 \pm 2.2$  ind/1000 m<sup>3</sup> vs river:  $4.0 \pm 1.4$  ind/1000 m<sup>3</sup>).



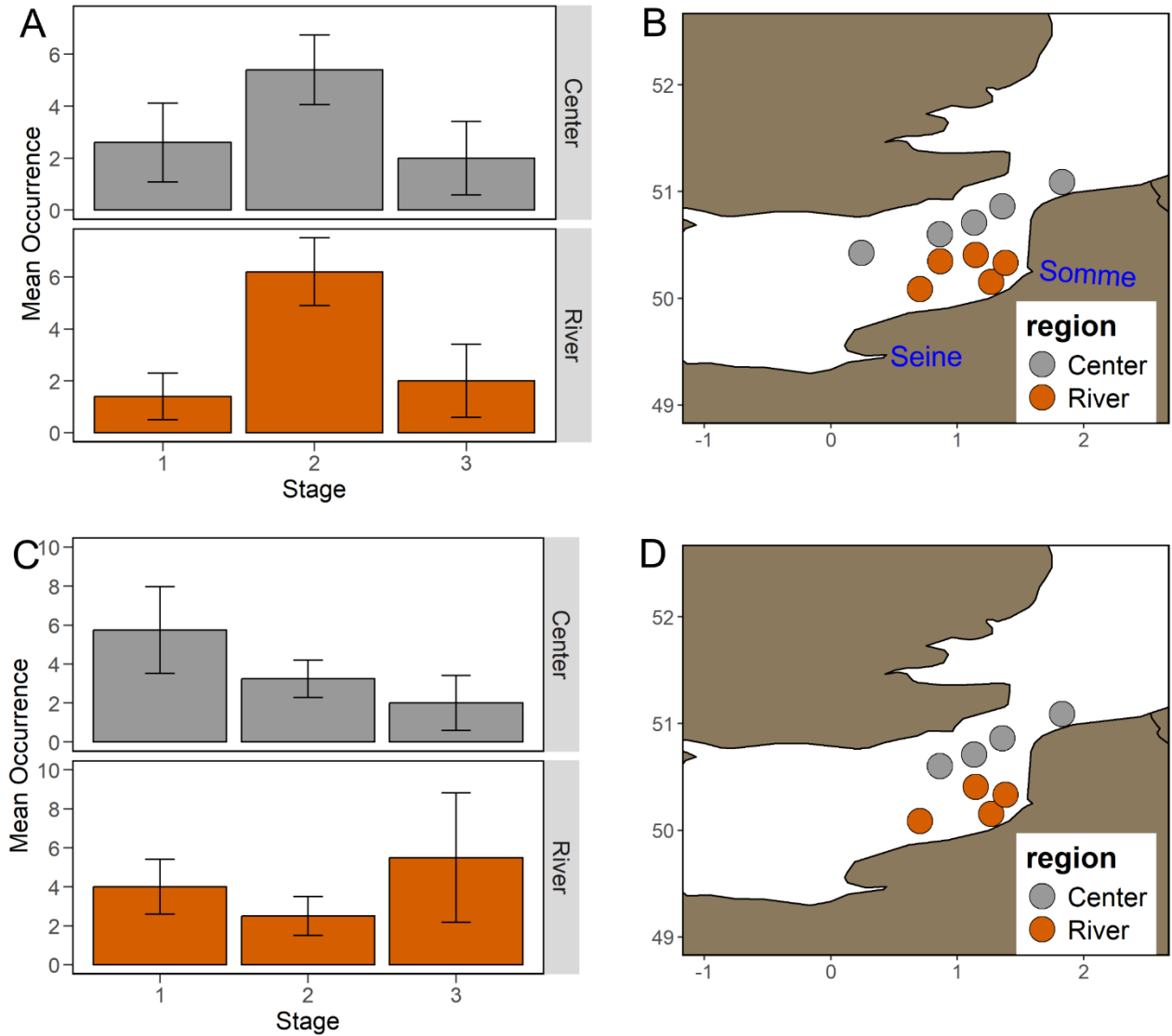


**Figure 37 Spatial distribution of ontogenetic stages per species.** A: Mean and standard deviation of occurrence of ontogenetic stages of herring at stations situated in the center of the Eastern English Channel and in an area of riverine influence; B: Map displaying sampling stations of herring larvae with colors indicating stations associated to the center of the Eastern English Channel (gray) and in the area of riverine influence (orange), location of Seine and Somme estuaries are indicated; C: Mean and standard deviation of occurrence of ontogenetic stages of plaice at stations situated in the center of the Eastern English Channel and in an area of riverine influence; D: Map displaying sampling stations of plaice larvae with colors indicating stations associated to the center of the Eastern English Channel (gray) and to the area of riverine influence (orange).

#### 2.3.4.2. MixSIAR analysis

Analysis of diet per species, comparing models with and without spatial covariates (global vs spatial model), revealed a strong spatial pattern in the diet (proportion of different size classes) for plaice, while no spatial variation was found in the diet of herring larvae (**Figure 38**).

For herring larvae, both models predicted a dominance of the 500 - 1000  $\mu\text{m}$  size class, constituting between  $66.4 \pm 6$  and  $78.5 \pm 8$  % to the overall diet. The second most dominant size class was  $<20 \mu\text{m}$  contributing between  $23.1 \pm 5$  and  $13 \pm 6$  %. The classes between 20  $\mu\text{m}$  and 500  $\mu\text{m}$  displayed minor contributions with a cumulative mean of less than 10 % in both models (**Figure 38A -B**).

For plaice, considering a spatial term changed the estimated dietary pattern for the overall population, highlighting the importance of the 125 - 200  $\mu\text{m}$  size class (global:  $11.1 \pm 11.7$  % vs spatial:  $36.9 \pm 19.1$  %) along with the size class  $<20 \mu\text{m}$  (global:  $50.8 \pm 6$  % vs spatial:  $39.6 \pm 8$  %) (**Figure 38A,B**). Diet composition varied between stations of riverine influence, dominated by the size class  $<20 \mu\text{m}$  ( $44.2 \pm 4$  to  $56.8 \pm 5$  %) and those located in the center of the EEC, dominated by the size class 125 - 200  $\mu\text{m}$  ( $40.4 \pm 8$  to  $62.0 \pm 8$  %) (**Figure 37D, Figure 38C,D**).

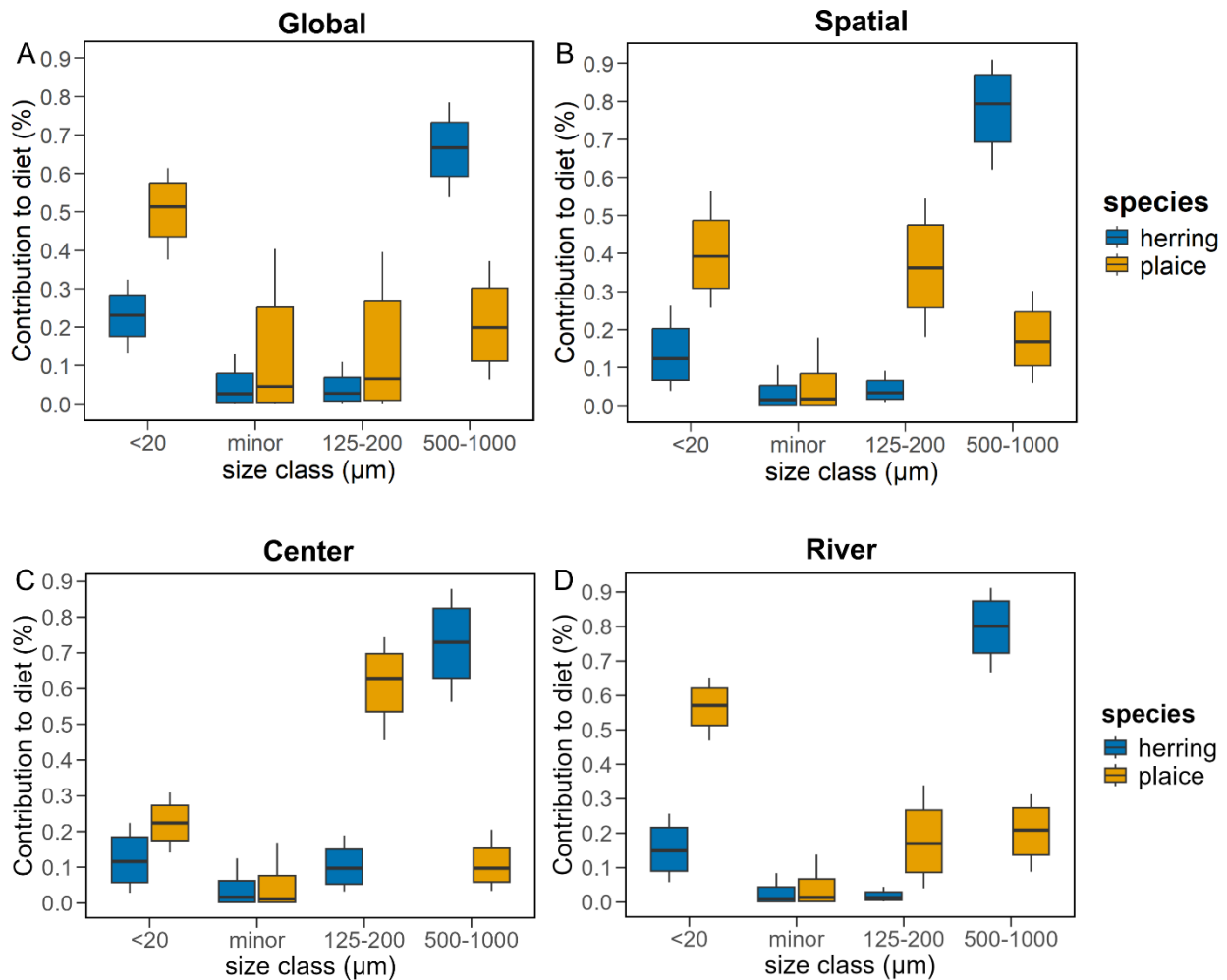


**Figure 38** Proportion (% diet) of plankton size classes to larval diet. Boxplots represent median and 95 % credible interval of the posterior distribution of the MixSIAR models predicting the contribution of each size class to herring (blue) and plaice (orange) larvae diet. Minor refers to a posteriori aggregated size classes (20 – 125  $\mu\text{m}$  and 200 – 500  $\mu\text{m}$ ) due to minor contribution of these size classes to larval diet. A: Global model; B: Spatial model for the overall population; C: Output of the spatial model for a station representing stations situated in the center of the Eastern English Channel; D: Output of the spatial model for a station representing stations of riverine influence.

As described above, the ontogenetic stage-frequency distribution and diet of plaice larvae varied spatially. Thus, a third model was run for plaice larvae, including a spatial and an ontogenetic component. Overall, diet composition was similar across the three developmental stages tested (**Figure 39**). Furthermore, the same spatial variation in diet composition was observed for all stages, with a higher contribution of the 125 - 200  $\mu\text{m}$  size class in the center of the EEC ( $29.3 \pm 15 - 59.0 \pm 18 \%$ ) and a higher contribution of plankton <20  $\mu\text{m}$  at river influenced stations ( $45.1 \pm 6 - 58.1 \pm 6 \%$ ). This indicated that differences in the ontogenetic stage frequency between the stations/regions had a minor influence on the spatial pattern observed in larval plaice diet composition.

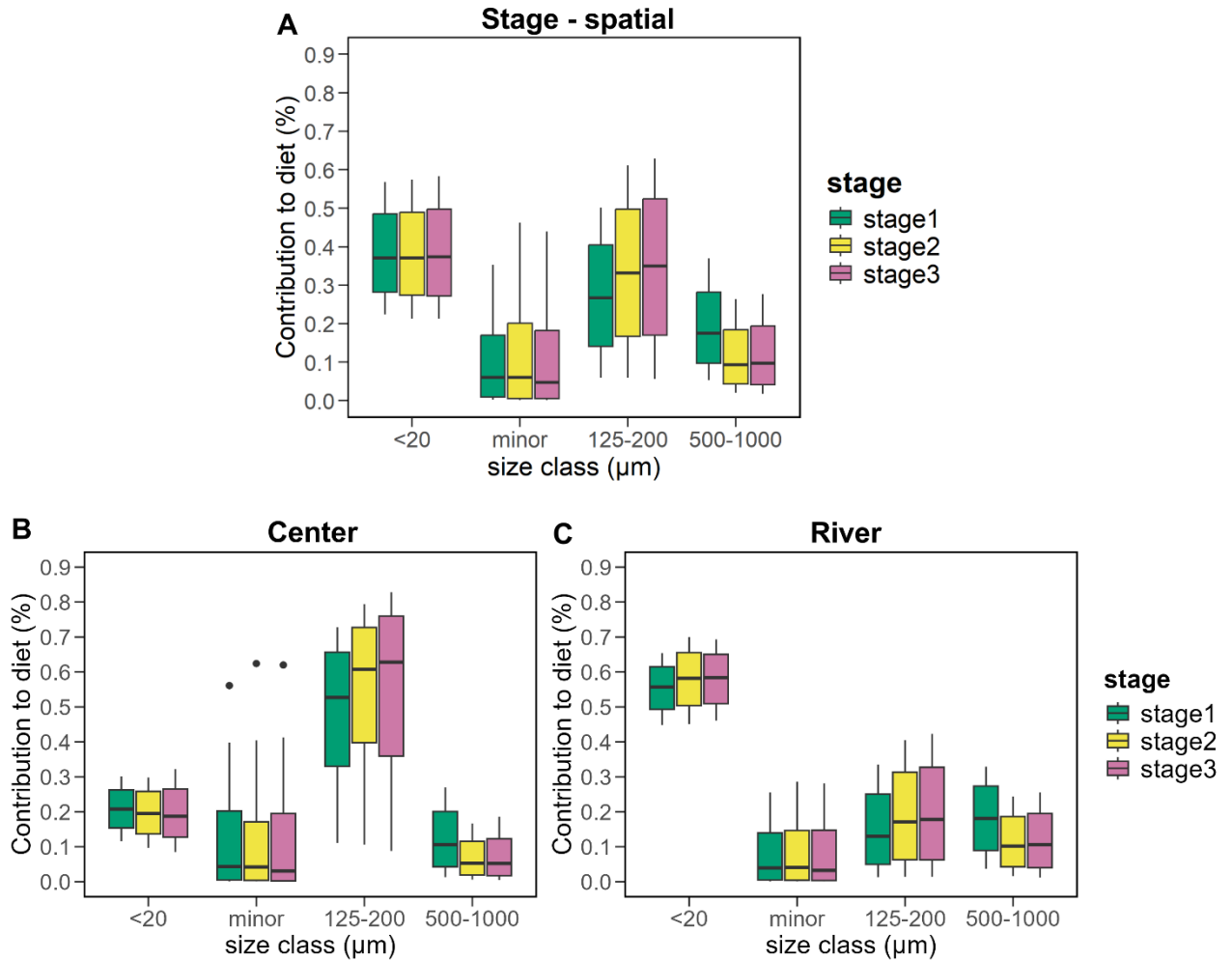


**Figure 39 Proportion (% diet) of plankton size classes to diet of plaice larvae ontogenetic stages.** Boxplots represent median and 95 % credible interval of the posterior distribution of the MixSIAR models predicting the contribution of each size class to stage 1 (green), stage 2 (yellow) and stage 3 (violet) plaice larvae diet. A: Stage-space model not discriminating for stations; B: Output of the stage-space model for a station representing stations situated in the center of the Eastern English Channel; C: Output of the stage-space model for a station representing stations influenced by river discharge.

## 2.4. Discussion

### 2.4.1. Structuration of the planktonic food web in the EEC during winter

The isotopic vertical structure of the planktonic food web in the EEC in winter was high with  $\delta^{15}\text{N}$  ranging from below zero to around 18‰. In comparison, the range of  $\delta^{15}\text{N}$  values for plankton in the Mediterranean (spring) ranged from above zero to 5‰ (Tesán-Onrubia *et al.*, 2023). However, the vertical size structure was less pronounced in the EEC than in the Mediterranean. Size classes between 50 to 500  $\mu\text{m}$  displayed similar isotopic signatures, with

$\delta^{13}\text{C}$  values ranging between -21.5‰ to -23‰, and  $\delta^{15}\text{N}$  values ranging between 6‰ and 8‰, along with high variability in isotopic values within each size class. In the Mediterranean food web, several microplankton and mesozooplankton size classes were characterized by clearly distinguished isotopic signatures (Tesán-Onrubia *et al.*, 2023). The isotopic signatures of the 500 - 1000  $\mu\text{m}$  size class and fish larvae were more distinct with slightly elevated  $\delta^{15}\text{N}$  values (~9‰ and 13‰, respectively) compared to the other plankton size classes (except <20  $\mu\text{m}$ ) indicating the affiliation to a higher trophic level and a mainly carnivorous feeding mode.

Low differentiation in isotopic signatures of microplankton size classes was in accordance with Bils *et al.* (2022) that investigated plankton samples from the study area in winter 2014. Comparing the structuration of the planktonic food web in the study area between seasons Giraldo *et al.* (2024) found less vertical structuration during winter and autumn than in spring and related these differences to the proportion of primary productivity and recycled matter fueling the planktonic food web. They hypothesized that higher primary production leads to a higher level of trophic divergence which results in a stronger vertical structuration of the food web (Kozak *et al.*, 2020; Décima, 2022; Giraldo *et al.*, 2024). Thus, the similar isotopic signature of 50 - 500  $\mu\text{m}$  size classes found in the present study might be due to low phytoplankton biomass that might result in a dominance of omnivory and thus low trophic divergence (Kozak *et al.*, 2020; Giraldo *et al.*, 2024) explaining the weak size-structuration observed. Although similar to the other microplankton size classes the isotopic signature of the 20 - 50  $\mu\text{m}$  plankton displayed slightly more enriched  $\delta^{13}\text{C}$  values and slightly lower  $\delta^{15}\text{N}$  values compared to other microplankton. This could be related to its taxonomic composition characterized by diatoms, dinoflagellates, silicoflagellates and ciliates and the fact that larger size classes were reported to no longer contain primary producers (Akimova *et al.*, 2023). The slightly elevated  $\delta^{15}\text{N}$  and lower  $\delta^{13}\text{C}$  values of the 500 - 1000  $\mu\text{m}$  size class, indicate a different feeding strategy that could be related to a higher proportion of carnivorous zooplankton in this size class (Akimova *et al.*, 2023). Overall, the values observed in the present study for plankton size classes larger than 20  $\mu\text{m}$  are comparable to the  $\delta^{15}\text{N}$  and  $\delta^{13}\text{C}$  values reported by Kürten *et al.* (2013) for mesozooplankton (200 - >1000  $\mu\text{m}$ ) in the North Sea.

Picoplankton and nanoplankton (<20  $\mu\text{m}$  size class) displayed mean  $\delta^{15}\text{N}$  values comparable to predators like fish larvae and strongly depleted  $\delta^{13}\text{C}$  values (~-27‰) separating it from the other plankton size classes in the isotopic space. While Bils *et al.* (2022) reported less depleted  $\delta^{13}\text{C}$  values (~-18‰) of POM, other studies observed similarly depleted  $\delta^{13}\text{C}$  values in the

study area ranging from around -25.8‰ to -15‰ (Kopp *et al.*, 2015; Giraldo *et al.*, 2024). Less depleted C values in the study of Bils *et al.* (2022) could be due to the mixture of POM sampled in the EEC and the Southern Bight as POM from the latter was shown to display less depleted  $\delta^{13}\text{C}$  values ( $\sim$ -14‰ - -21‰) (Bristow *et al.*, 2013; Kürten *et al.*, 2013). Despite different isotopic signatures, POM was more depleted in  $\delta^{13}\text{C}$  than microplankton ( $\sim$ 7‰) (Bils *et al.*, 2022), which was in accordance with the present study. POM represents a heterogeneous material including size classes  $<200\ \mu\text{m}$  (Harmelin-Vivien *et al.*, 2008). Size-fractionating POM revealed that the depleted  $\delta^{13}\text{C}$  values originated from the smallest size fraction ( $<5\ \mu\text{m}$ ) corresponding to pico- and nanoplankton along with detrital material (Rolff, 2000; Harmelin-Vivien *et al.*, 2008). This might explain why the next larger size class in the present study (20 - 50  $\mu\text{m}$ ) resembled the other microplankton profiles and was not associated with the  $<20\ \mu\text{m}$  size class. Several processes could explain the isotopic signature of the  $<20\ \mu\text{m}$  size class. Picoplankton and nanoplankton, might be utilizing a different carbon source than larger plankton. For instance, they could be relying more on dissolved organic carbon or recently produced organic matter that has a different isotopic signature. The depleted  $\delta^{13}\text{C}$  values of the  $<20\ \mu\text{m}$  size class could be further related to the presence of terrestrial organic material and/or sewage water coming from riverine discharge (Megens *et al.*, 2001; Harmelin-Vivien *et al.*, 2008; Bouaziz *et al.*, 2021; Tesán-Onrubia *et al.*, 2023). Sewage water is known to be depleted in  $\delta^{13}\text{C}$  with values between -23‰ to -29‰ (Bristow *et al.*, 2013). It could furthermore explain the  $\delta^{15}\text{N}$  values observed in the present study, that were elevated compared to other studies reporting values of around 3‰ to 9‰ (Kopp *et al.*, 2015; Liénart *et al.*, 2017; Bils *et al.*, 2022; Giraldo *et al.*, 2024). Sewage water displays  $\delta^{15}\text{N}$  value of 1 to 10 but depending on sewage treatment bacterial nitrification can lead to an elevation of  $\delta^{15}\text{N}$  (Bristow *et al.*, 2013; Tesán-Onrubia *et al.*, 2023). The French side of the EEC is influenced by several riverine inputs of the rivers Seine, Canche, Authie and Somme. Mixing with EEC water these river discharges build a water mass called “Fleuve côtier” which flows along the French coastline towards the North Sea (Brylinski *et al.*, 1991). Compared to other years the discharge of the river Seine which has the largest catchment area among the rivers terminating in the EEC (Pawson, 1995) was elevated. However, water salinity did not indicate that the riverine input spread throughout the entire area but remained in the zone of the “Fleuve côtier” (**Figure 32B**). Thus, the presence of terrestrial organic material and sewage water is unlikely

to be the only explanation for the isotopic profile of the <20  $\mu\text{m}$  size class that did not display a spatial pattern.

The EEC is an area with strong benthic-pelagic coupling (Kopp *et al.*, 2015; Giraldo *et al.*, 2017, 2024; Cresson *et al.*, 2020). An influence of benthic-pelagic coupling on the planktonic food web was indicated by the high variability of the  $\delta^{13}\text{C}$  values ranging from -28‰ to -16‰ (Kopp *et al.*, 2015). Material of benthic origin cannot explain the depleted  $\delta^{13}\text{C}$  values in the <20  $\mu\text{m}$  size class, however, as benthic algae and benthic feeding organisms are reported to display enriched  $\delta^{13}\text{C}$  values (Chouvelon *et al.*, 2012; Kopp *et al.*, 2015; Liénart *et al.*, 2020). Microphytobenthos displays elevated  $\delta^{15}\text{N}$  values (7‰ - 10‰) comparable to the values observed in the present study (Kostecki *et al.*, 2012; Day *et al.*, 2021) by contrast. An influence of resuspended microphytobenthos on the isotopic profile of the <20  $\mu\text{m}$  size class seems unlikely, however, as due to the depth profile and high turbidity in the EEC the abundance of microphytobenthos is expectably low. Overall, further investigations are needed to understand the isotopic signature of this size class.

In the present study, the 125 - 200  $\mu\text{m}$  size class displayed a wide range of both  $\delta^{13}\text{C}$  and  $\delta^{15}\text{N}$  values, with  $\delta^{15}\text{N}$  values below zero suggesting bacterial activity. Furthermore, this size class displayed a different spatial pattern of  $\delta^{13}\text{C}$  values compared to the other size classes, with more depleted values at the western stations of the study area and less depleted values towards the Dover Strait. Due to limited information available on this microplankton size class in the literature, any explanations for these observations would be highly speculative.

#### **2.4.2. Feeding regime of herring and plaice larvae**

Herring and plaice larvae displayed similar  $\delta^{15}\text{N}$  values, indicating their affiliation to the same trophic level, but differing  $\delta^{13}\text{C}$  values suggesting different feeding regimes. The contribution of size classes to the overall diet also differed between species, with herring larvae showing a higher dominance of the 500 - 1000  $\mu\text{m}$  size class, whereas plaice larval diet was dominated by the <20  $\mu\text{m}$  and 125 - 200  $\mu\text{m}$  size class. While no spatial variation in the proportion of size classes in herring larval diet was observed, the size class composition of plaice larvae diets varied spatially, with differences observed between larvae located at stations near riverine influence and those sampled in the center of the EEC. The distribution of developmental stages of plaice larvae displayed a spatial pattern with regard to river and center stations. The lack of marked differences in the isotopic signatures between different developmental stages

suggests however, only a minor influence on the spatial variability in plaice larvae diet composition.

### 2.4.3. Herring larvae

#### 2.4.3.1. Overall diet composition and spatial variation (global model and spatial model)

The isotopic values of Downs herring larvae sampled in winter 2021 were similar to values of larvae sampled in winter of earlier years (Bils *et al.*, 2022; Giraldo *et al.*, 2024). As a spatial pattern was found in the isotopic values of several prey size classes, sampling station was included in the spatial MixSIAR model thus, accounting for potential spatial variation in herring isotopic signatures. However, the spatial model did not indicate variation in herring diet that was always dominated by the 500 - 1000  $\mu\text{m}$  size class (global:  $\sim 66\%$ , spatial:  $\sim 80\%$ ). This suggests that either herring larvae consistently target and select the 500 - 1000  $\mu\text{m}$  size class independent of the location, or that this size class was the most dominant across the entire study area, and herring larvae behave as opportunistic predators. A larger prey size range has been reported in the literature for herring larvae. Based on mouth gape and feeding experiments (reviewed by Hufnagl and Peck (2011)), the maximum prey size of larvae smaller than 24 mm was 1600  $\mu\text{m}$ . Copepod species proposed to be important prey for herring larvae like *P. parvus* and *P. elongatus* display a size range of 700 - 1400  $\mu\text{m}$  (Conway, 2012) supporting that herring larvae preferentially feed on prey bigger than 500  $\mu\text{m}$ . This is in accordance with results from a previous study also using stable isotopes that revealed a dominance ( $\sim 60\%$ ) of prey between 1000 - 1500  $\mu\text{m}$  in herring diet. In the same study, size classes  $> 1500 \mu\text{m}$ , corresponding to bigger taxa like *T. longicornis*, *Centropages hamatus*, *C. helgolandicus*, Cumacea and Brachyura larvae, contributed to  $\sim 25\%$  to herring larval diet (Giraldo *et al.*, 2024). Although the contribution of prey  $> 1000 \mu\text{m}$  might be overestimated in the study of Giraldo *et al.* (2024) as prey  $< 1000 \mu\text{m}$  were not included (except of POM), it is possible that the dominance of the 500 - 1000  $\mu\text{m}$  size class found in the present study is slightly overestimated as prey of size classes bigger than 1000  $\mu\text{m}$  were not considered.

Evidence coming from studies using different approaches like stomach content analysis, SIA and physiological models suggests that beside mesozooplankton, microplankton (20 - 200  $\mu\text{m}$ ) are also important for herring larval diet (Denis *et al.*, 2016; Bils *et al.*, 2022; Akimova *et al.*,



2023). In the present study, microplankton accounted for around 10 % of larval diet, which fits within the range suggested by physiological modeling, which estimated microplankton contributions of 38 % and 4 % for 8 mm and 23 mm larvae (Akimova *et al.*, 2023). Akimova *et al.* (2023) further found that young herring larvae growth rate would decrease by 40% if only preying on copepods which together with the present study underlines the importance of including small plankton size classes when investigating larval diet. Interestingly, also the <20  $\mu\text{m}$  size class contributed to around 10 % to herring larval diet. As a direct ingestion of such small particles by a visual predator like herring larvae (Batty, 1987) appears unlikely, this may represent an indirect signal from consumers that fed on plankton in the 0 - 20  $\mu\text{m}$  range, such as appendicularians (Gaughan, 1991; Purcell *et al.*, 2005; Lombard *et al.*, 2011), which are known to be important in the diet of several fish larvae (Llopiz *et al.*, 2010). However, if these organisms are not a dominant part of their size class, their contribution to the herring larvae diet might be better represented by the isotopic signal of the size class they themselves feed on. Since no taxonomical data was available in this study, this hypothesis could not be verified. Overall, studies delivering information about the proportion of plankton size classes to herring larvae diet only considered a part of its potential prey size range. Future studies should include the entire size range from microplankton to mesozooplankton >1500  $\mu\text{m}$  to obtain a complete and representative impression of herring larvae diet prey size composition.

#### **2.4.3.2. Ontogenetic diet shifts**

Several studies proposed an ontogenetic diet change of herring larvae around 13 mm (Checkley, 1982; Denis *et al.*, 2016, 2017; Joly *et al.*, 2021). In the present study we did not explicitly investigate potential changes in prey size composition during ontogenetic development but visualizations of  $\delta^{13}\text{C}$  and  $\delta^{15}\text{N}$  against herring larvae size did not indicate strong variation of isotopic signatures within the size range investigated (Annex II **Figure A 15**). As in previous studies, a dominance of 11 -12 mm larvae might have prevented the detection of an ontogenetic diet change (Bils *et al.*, 2022). Integrating larval size or developmental stage in a MixSIAR model will be an interesting perspective for future research. However, a larger spatial sampling extent and an increased number of samples would be necessary to adequately cover the entire area of larval dispersion in the North Sea.

## 2.4.4. Plaice larvae

### 2.4.4.1. Overall diet composition (spatial model)

Accounting for spatial variation in the diet improved the dietary estimates and resulted in a more diverse diet in comparison to the global model. The <20  $\mu\text{m}$  and 125 - 200  $\mu\text{m}$  size classes dominated plaice larvae diet together accounting for  $\sim 80\%$ . The preferred prey size-class of plaice larvae is, to the best of our knowledge, not known. Larvae between 6 and 11 mm have a mouth width of 300  $\mu\text{m}$  to ca. 800  $\mu\text{m}$  (Last, 1978). Given that the 500 - 1000  $\mu\text{m}$  size class contributed to ca. 15 % to plaice larval diet, this suggests that while plaice larvae can feed on prey larger than 200  $\mu\text{m}$ , they preferentially consume smaller prey. This is supported by the size of prey items found in plaice larvae stomach contents. Ingested *O. dioica*, a prey reported to be essential in the diet of plaice larvae (Shelbourne, 1953, 1957, 1962; Last, 1978), was suggested to be dominated by individuals smaller than 500  $\mu\text{m}$  (Last, 1978). Theoretically, *O. dioica* might have been present in the size classes >125  $\mu\text{m}$  (Last, 1978; Fenaux *et al.*, 1986), as this species reproduces during winter in the study area (Wyatt, 1973). Other prey found in plaice larval stomachs like nauplii of *P. parvus*, *P. minutus* and polychaete larvae (Shelbourne, 1953; Last, 1978) should also be found in the 125 - 200  $\mu\text{m}$  size class (Conway, 2012, 2015; Mitsuzawa *et al.*, 2017). This suggests an importance of microplankton for larval plaice nutrition. Due to the lack of biomass data for the different size classes, we cannot exclude the possibility, however, that the contribution of the 125 - 200  $\mu\text{m}$  size class may be a result of higher biomass compared to the 500 - 1000  $\mu\text{m}$  size class.

Plaice larvae are suggested to be visual predators (Shelbourne, 1953) making feeding on particle sizes of <20  $\mu\text{m}$  unlikely. Thus, the elevated contribution of prey <20  $\mu\text{m}$  might represent feeding on *O. dioica* that are known to feed on pico- and nanoplankton (Lombard *et al.*, 2011). If this hypothesis holds true the current study would be in accordance with earlier findings reporting the dominance of this appendicularian species in plaice larval diet (Shelbourne, 1953, 1957, 1962; Last, 1978).

### 2.4.4.2. Spatial variation

A strong spatial pattern was found in the diet of plaice larvae. In the center of the English Channel, the 125 - 200  $\mu\text{m}$  size class dominated, with lower contributions of the <20  $\mu\text{m}$  and 500 - 1000  $\mu\text{m}$  size classes. In contrast, at river influenced stations, (**Figure 37D**), the <20  $\mu\text{m}$  size class constituted ca. 50 % of the larval diet. Assuming that this size class is a proxy for the

contribution of *O. dioica* (as discussed above), a higher proportion of this prey seems to be eaten in this area. This is in agreement with spatial variance of *O. dioica* abundance that was elevated in regions of riverine influence (**Figure 40**, chapter 1). Riverine input might result in a higher charge of organic matter in the <20  $\mu\text{m}$  size range and higher production of pico- and nanoplankton due to nutrient inputs that might benefit *O. dioica*.

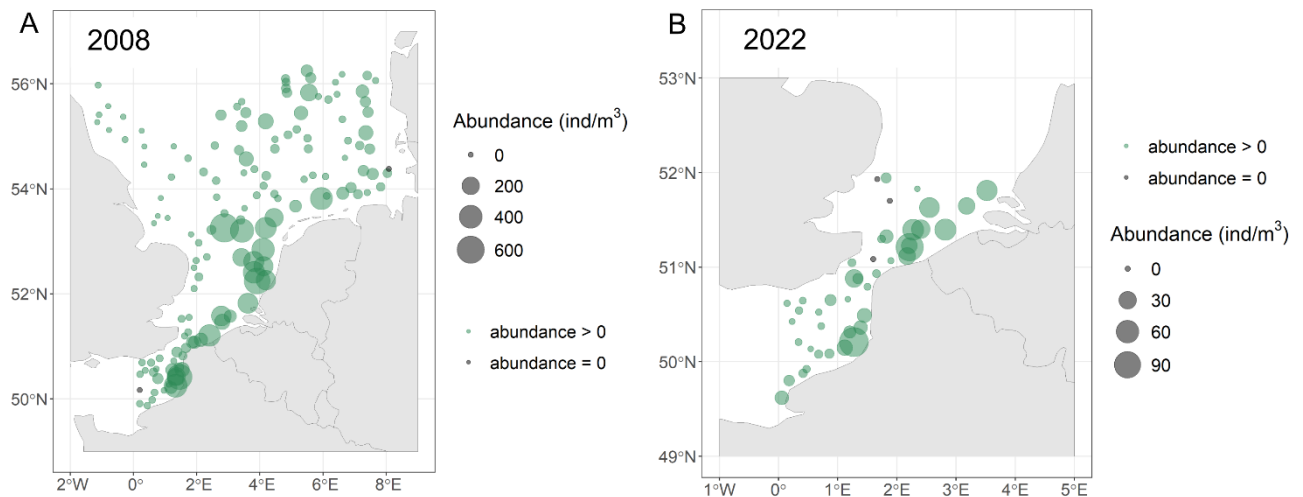


**Figure 40** Abundance of *O. dioica* derived from the IBTS survey taking place in January – February 2008 (A) and 2022 (B).

Consequently, the higher contribution of the 125 - 200  $\mu\text{m}$  size class in the center of the EEC likely reflects the presence of prey other than *O. dioica*, suggesting that plaice larvae feed on the most abundant prey within their preferred size class. By contrast, Shelbourne (1953) suggested that plaice larvae selectively target distinct prey items as the abundance of prey in stomach contents did not correspond to the abundance of zooplankton from water samples. This might suggest that plaice larvae selectively feed on *O. dioica* as soon as it is available but might switch to alternative prey when abundance of *O. dioica* is low. As in recent years, the dominance of *O. dioica* in terms of abundance appears to vary interannually (Neven *et al.*, *in press*, chapter 1) a spatial and interannual difference in the contribution of this species to plaice larvae diet might be expected.

Although appendicularians belong to gelatinous plankton they have a similar nutritional value with regard to carbon and nitrogen content (50.1 - 62.3 %, 11.3 - 14.9 % of dry weight respectively) as copepods (32.3 - 67.5 %, 5.1 - 13.1 % of dry weight respectively). They further display a fast generation time of (1 - 8 days) compared to copepods (~3 weeks), a slow

swimming speed and aggregate in swarms and patches making them easy to hunt for carnivorous zooplankton like fish larvae (Purcell *et al.*, 2005). Differing predation capacities might have led to herring larvae feeding mostly on larger crustacean zooplankton whereas plaice larvae select relatively smaller prey like *O. dioica*. Herring and plaice larval stages included in the present study display similar maximal swimming speeds ( $U_{crit}$ ) suggesting similar predatory competences between herring and plaice larvae before metamorphosis (Silva *et al.*, 2015b; Moyano *et al.*, 2016). Gaughan (1991) proposed the categorization of fish larvae into three categories with regard to their prey: (i) fish larvae feeding on copepods, (ii) on appendicularians or fish larvae and (iii) on other prey. Larvae of the family Pleuronectiformes are associated to the group of larvae feeding on appendicularians mostly based on the studies investigating larval diet in the EEC and SNS. Beside Pleuronectiformes a variety of other fish families such as tuna larvae feed on appendicularians (Llopiz *et al.*, 2010).

#### **2.4.4.3. Ontogenetic shifts in diet**

The abundance of different larval stages exhibited collinearity with the spatial pattern in diet size class composition with a higher proportion of smaller individuals in the center of the EEC and a higher proportion of larger larvae at river influenced stations. This pattern corresponds to the position of spawning grounds and nursery areas of plaice (Bolle *et al.*, 2009). Spawning grounds are mostly situated in the deeper regions in the middle of the EEC (Hufnagl *et al.*, 2013) whereas the river influenced stations are located closer to the nursery areas (Bolle *et al.*, 2009).

Although an influence of differing stage composition in the two regions cannot be excluded, MixSIAR models allowing for spatial variation and variation of diet composition per larval stage did not indicate an influence of plaice developmental stages on diet. This is in accordance with the fact that in the literature no ontogenetic shifts with regard to diet composition are reported except a size selectivity of larger individuals selecting for larger *O. dioica* (Shelbourne 1962). As *O. dioica* feeds on particles smaller than 20  $\mu\text{m}$  independent of body size (Lombard *et al.*, 2011) and plankton size classes used in the present study did represent a mixture of different organisms we might not have been able to detect this diet shift from smaller to bigger *O. dioica* individuals.

## 2.5. Perspectives

### 2.5.1. Biological perspectives

To better understand larval feeding regime and position in the planktonic food web, several aspects not addressed in this chapter could provide valuable perspectives for future research. Investigating these aspects would be necessary to draw conclusions about how larval feeding influences survival under varying conditions.

A better understanding of the feeding strategy of larvae with regard to specialist-generalist strategies is important to understand their position in the planktonic food web and their sensitivity to fluctuations in prey availability. Integrating biomass data of the different plankton size classes would allow to get insight in the feeding strategies of these two species and would further enhance the evaluation of the planktonic food web structure. Information about the carbon content of each size class could be used as prior in the MixSIAR analysis and give information about prey availability. Information about the taxonomic composition of plankton size classes would enhance the interpretation of the larval feeding regime by allowing to verify the information about the taxonomical composition of the different size classes derived from the literature. Taxonomical analysis would further allow to evaluate the hypothesis that plaice larvae selectively feed on *O. dioica* and a lower contribution of the <20 µm size class represents lower *O. dioica* abundance at the stations in the center of the EEC.

Additional studies on plaice larval nutrition from other regions and years, together with the evaluation of the planktonic food web would allow to investigate if *O. dioica* is the preferred feeding source of these larvae or if it is a particularity to plaice larvae from the EEC. This could provide further insight into the potential adaptation of plaice larvae to the dominance of herring larvae in this region during winter. Together with information on larval condition, interannual variation in feeding regimes could allow to evaluate the trophic flexibility of the two species, and their resilience and adaptability to changes in plankton community composition. Evaluating how a diet dominated by *O. dioica* affects plaice larvae condition could further reveal their specialization and dependence on this food source, ultimately providing insights into the interannual variability of plaice larval survival. Studies on predatory performance and behavior could help to explain why plaice larvae appear to prefer feeding on microplankton although the ingestion of mesozooplankton seems possible.

### 2.5.2. Further refinements

Although TEF has been found to be stable across a wide range of taxa, smaller size classes of plankton are less thoroughly investigated compared to groups like mesozooplankton (Pepin and Dower, 2007). As planktonic size groups encompass various feeding strategies from autotroph to heterotroph, from herbivores to carnivorous, it is challenging to estimate TEF adequately (Aberle and Malzahn, 2007; Bils *et al.*, 2022). For future methodological refinement, it could be useful to apply different TEF values proposed in the literature to assess the sensitivity of the current results to the choice of TEF. Additionally, TEF could be obtained from models like isoweb (Kadoya *et al.*, 2012) which predict TEF based on the isotope values of predator and prey and a given TEF distribution of possible values (Giraldo *et al.*, 2017).

### 2.5.3. Additional analysis

For the publication of this chapter certain aspects will be further explored. The spatial variability of the proportion of different size classes to plaice larval diet will be directly set in relation to potential environmental drivers like depth, salinity or temperature using GAM models applied to the MixSIAR output as predicted variable. Preliminary analysis of GAM models with abiotic parameters as covariate indicate that environmental parameters can explain a part of the spatial variability observed. Thus, those models could help to further understand spatial variability in isotopic values and to confirm the hypothesis that spatial variation is related to riverine input.

The 500 – 1000  $\mu\text{m}$  size class had an elevated  $\delta^{15}\text{N}$  compared to smaller plankton size classes, and can be assumed to contain a higher proportion of carnivorous taxa like Chaetognaths. A MixSIAR model could be used to investigate the proportion of different plankton size classes to the diet of these larger plankton organisms. This would enhance our understanding of the structure and trophic pathways in the planktonic food web.

Acidification of samples can be required as preliminary step in SIA to remove non-dietary, inorganic carbon in the samples. Reporting the differences in  $\delta^{13}\text{C}$  values of acidified and non-acidified plankton samples will deliver information on the impact of this preparational step on the analysis (Schlacher and Connolly, 2014).

## 2.6. Conclusion

The present study suggests different feeding strategies for herring and plaice larvae with regard to prey size. Furthermore, spatial variation of the isotopic signatures of different plankton size classes and in the contribution of plankton size classes to plaice larval nutrition were found. The isotopic signature of herring and plaice larvae was species specific and did not indicate any overlap in their isotopic niches. Whereas herring larvae preferentially fed on the 500 - 1000  $\mu\text{m}$  size class, the 125 - 200  $\mu\text{m}$  and <20  $\mu\text{m}$  size classes displayed the highest contributions in plaice larval diet. The contribution of the <20  $\mu\text{m}$  size class might support earlier findings reporting *O. dioica* as major prey item for plaice larvae in the EEC. Spatial variation in plaice larval dietary composition in relation to riverine inputs appeared to be linked to spatial variation in the abundance of this species. This study further suggests the importance of microplankton for plaice larvae nutrition. Initial analysis of ontogenetic diet changes in plaice larvae showed no variation in the contribution of different plankton size classes to their diet from stage 1 to stage 3. Further analysis of ontogenetic diet changes of herring and plaice larvae are needed for final conclusions. In accordance with previous studies, the size structuration of the planktonic food web in EEC during winter was weak with regard to similar isotopic signatures of several plankton size classes suggesting low trophic divergence when productivity is low. The second chapter underlines the importance of the consideration of all possible prey items and prey size classes in MixSIAR analysis in order to obtain representative estimations of diet composition.

## CHAPTER 3 - 3. Perspective – Biochemical composition

The role of zooplankton as trophic vector from primary producers to higher trophic levels is not only important with regard to energy transfer but also with regard to the transfer of nutrients such as amino acids or essential fatty acids.

Fatty acids are major constituents of lipids such as phospholipids or triglycerides and further serve as precursors of hormones (Dalsgaard *et al.*, 2003). They are constituted of a mostly straight chain of 14 – 24 carbon atoms that can be connected by simple or double bonds, with the number of the latter varying between zero to six. Each carbon chain is terminated by a methyl group at one end and a carboxyl (acid) group at the other. Fatty acids are most commonly named based on chain length and number and position of double bonds, with the fatty acids A:B(n-x) being constituted out of A carbon atoms, B double bonds and the first double bond being positioned at the x position relative to the methyl group. Furthermore, fatty acids can be separated in three different groups depending on the number of double bonds. Fatty acids only consisting of single bonds are called saturated fatty acids (SFA), while the presence of one double bond classes a fatty acids as monounsaturated fatty acid (MUFA). Fatty acids being composed of more than one double bond are referred to as polyunsaturated fatty acids (PUFA) (Budge *et al.*, 2006). While SFA and MUFA are mostly incorporated in storage lipids, PUFA are preferentially integrated in phospholipids and therewith represent a major constituent of cell membranes (Tocher, 2003; Pethybridge *et al.*, 2014).

As essential fatty acids are crucial for the physiological functioning of organisms, the transfer of these nutrients will impact ecosystem functioning. Like the efficiency of energy transfer, also the transfer of fatty acids will vary with environmental condition, phyto- and zooplankton composition and potentially with the physiological state of the consumer (Galloway and Winder, 2015; Schmidt *et al.*, 2020).

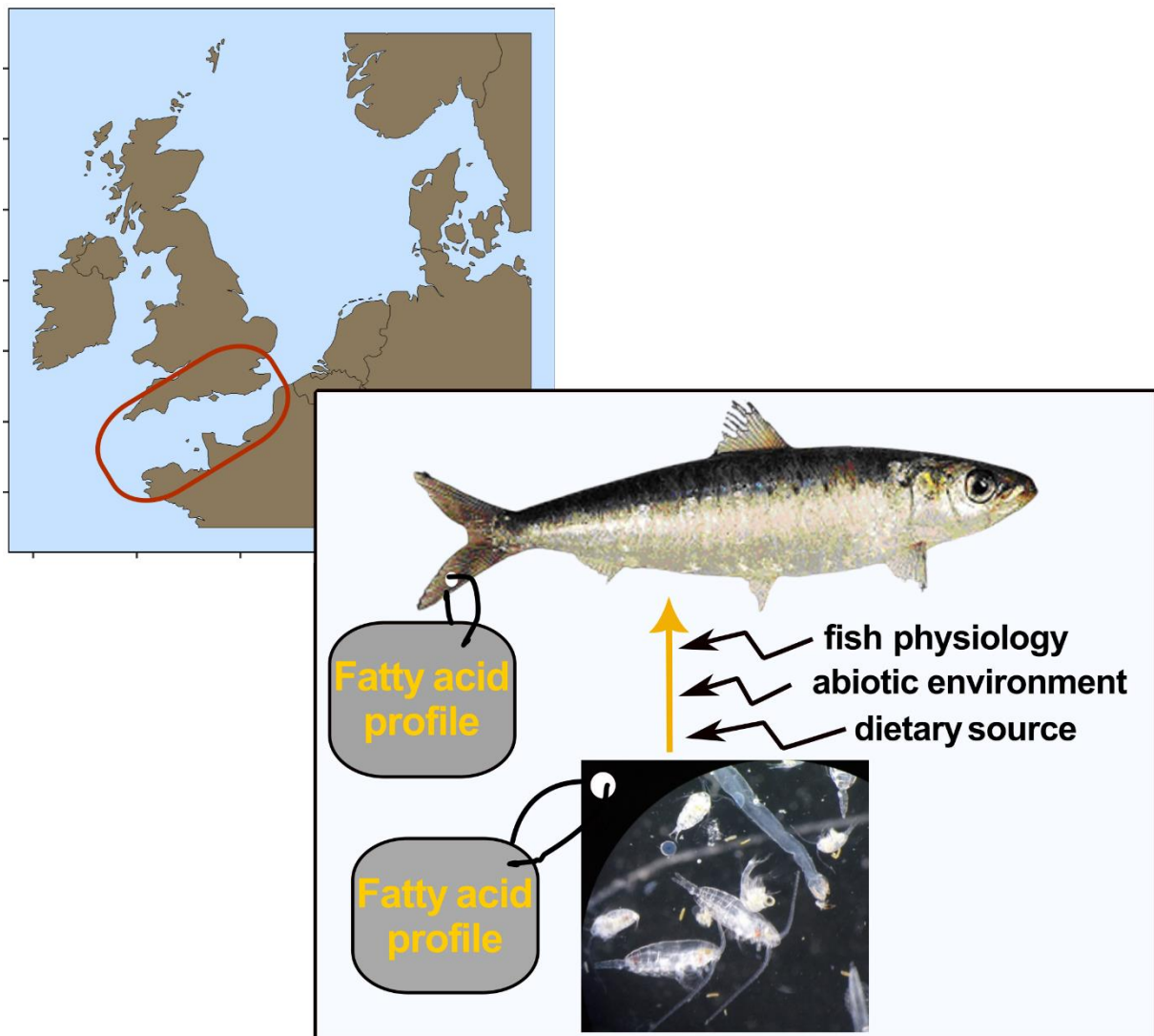
Thus, the third chapter aimed at investigating the spatial variability in the trophic transfer of fatty acids from zooplankton to small pelagic fish in relation to plankton community composition, environmental condition and fish physiology.



The work of the third chapter was presented in an oral presentation during the ICES Zooplankton Production Symposium 2024 and it is currently under review the ICES Journal of Marine Science:

## **Spatial variability in fatty acid profiles – Factors influencing trophic transfer of essential nutrients from plankton to the European sardine (*Sardina pilchardus*)**

Carolin Julie Neven, Philippe Soudant, Paul Marchal, Sébastien Lefebvre, Alain Lefebvre, Guillaume Wacquet, Claudie Quere, Fabrice Pernet & Carolina Giraldo



# Spatial variability in fatty acid profiles - Factors influencing the trophic transfer of essential nutrients from plankton to sardine

---

## 3.1. Introduction

Understanding the spatial distribution and variability in the trophic transfer of essential nutrients is crucial for a better grasp of ecosystem functioning (Brett and Müller-Navarra, 1997; Arts *et al.*, 2009; Budge *et al.*, 2014; Galloway and Winder, 2015). This information can enhance our comprehension of the spatial repartition of feeding grounds, fluctuations in fish stock recruitment (Garrido *et al.*, 2007b) and inform fisheries management (Pethybridge *et al.*, 2014) as well as the planification of marine protected areas. FA such as docosahexaenoic acid (22:6(n-3), DHA), eicosapentanoic acid (20:5(n-3), EPA), and arachidonic acid (20:4(n-6), ARA) are essential nutrients for most marine animals. These fatty acids are needed for proper physiological performance (Tocher, 2003; Wagner *et al.*, 2004; Chatelier *et al.*, 2006; Vagner *et al.*, 2015; Gladyshev *et al.*, 2018) and must be obtained from the diet as they cannot or only to a limited extent be synthesized by the animal itself (Henderson, 1993; Tocher, 2010; Vagner and Santigosa, 2011; Parrish *et al.*, 2012; Galloway and Winder, 2015; Sissener *et al.*, 2020).

In the marine realm essential fatty acids (EFA) are produced at the base of the food web, primarily by phytoplankton (Závorka *et al.*, 2023). Herbivorous zooplankton incorporate and accumulate FA from their phytoplanktonic prey, thereby channeling FA to the next trophic level including small pelagic fish, that in turn, serve as a vector of EFA to higher trophic levels (Cury *et al.*, 2000; Dalsgaard *et al.*, 2003; Costalago *et al.*, 2015; Mathieu-Resuge *et al.*, 2024). However, spatial variability in the distribution and in the trophic transfer (Brett and Müller-Navarra, 1997) of FA can be expected. The proportional composition of FA in phytoplankton varies with taxonomical composition and environmental condition (Galloway and Winder, 2015; Peltomaa *et al.*, 2019; Závorka *et al.*, 2023) as does the quality and ingestability of phytoplankton for predators with regard to cell morphology, colony architecture and

secondary metabolites (Brett and Müller-Navarra, 1997). The trophic transfer of FA is conservative - meaning the prey FA composition is largely retained in the predator - allowing the use of certain FA acids as trophic markers (FATM) (Dalsgaard *et al.*, 2003). Grazers and predators such as zooplankton and small pelagic fish may still contribute to the spatial variability in their FA profile via their taxonomical composition and physiological state combined with varying abiotic conditions leading to different feeding and energy storage/allocation strategies (Kattner and Krause, 1989; Kattner and Hagen, 1995, 2009; Nelson *et al.*, 2001; Dalsgaard *et al.*, 2003; Zlatanov and Laskaridis, 2007; Bertrand *et al.*, 2022). For instance, the FA composition of zooplankton sampled in the Puget Sound (USA) was mainly driven by taxonomic differences followed by season and region (Hiltunen *et al.*, 2022), and different temperature treatments provoked a species specific response in *Acartia clausi* and *Acartia tonsa* with regard to the FA profile of storage lipids (Werbrouck *et al.*, 2016). Kainz *et al.* (2004) studied plankton from different freshwater systems and found that FA composition differed between size classes (10-64  $\mu\text{m}$ , 100-200  $\mu\text{m}$ , 200-500  $\mu\text{m}$ , >500  $\mu\text{m}$ ), which they hypothesized to be related to variable taxonomic composition and size specific physiological requirements. The FA profile of higher trophic level species such as sardine (*S. pilchardus*), albacore tuna (*Thunnus alalunga*) and chub mackerel (*Scomber japonicus*), was found to be influenced by length beside phyto- and zooplankton community composition and biomass (Pethybridge *et al.*, 2015; Bertrand *et al.*, 2022; Ohshimo *et al.*, 2022). Length was proposed to influence trophic transfer through ontogenetic shifts in diet, length-dependent metabolic rate and energy allocation strategy with regard to growth and reproduction (Pethybridge *et al.*, 2015; Bertrand *et al.*, 2022; Ohshimo *et al.*, 2022). Thus, a contribution of all trophic levels to spatial variability in the distribution and trophic transfer of FA could be expected.

In this chapter, we hypothesized that the spatial pattern in FA distribution will differ between trophic levels due to differing locomotion abilities assuming that the English Channel provides a heterogeneous environment especially between the western and eastern basin (Dauvin, 2012). Zoo- and phytoplankton with limited mobility and no active horizontal migration, will experience similar environmental conditions. This lack of mobility, combined with small-scale variability in abiotic parameters and taxonomic composition, may result in a more heterogeneous spatial pattern in their FA profiles compared to small pelagic fish. Small pelagic fish occupy larger feeding areas and encounter more diverse environmental conditions and a variety of prey. They might hence work as spatial smoother, reducing spatial variability in the

availability of FA due to horizontal movement. The objectives of the present study were thus to (i) assess the spatial variability of the FA profile of zooplankton and sardine in the English Channel considering phytoplankton and zooplankton community composition and environmental parameters as potential drivers, and (ii) to better understand the trophic transfer of EFA from zooplankton to sardine with regard to the factors influencing this transfer such as prey FA composition, environmental parameters and fish physiological state.

The European sardine (*S. pilchardus*) belonging to the group of small pelagic fish, is a planktivorous species feeding on phyto- and zooplankton (Bode *et al.*, 2003, 2004; Garrido *et al.*, 2008a, 2008b; Nikolioudakis *et al.*, 2012) and channeling energy to seabirds, marine mammals and piscivorous fish (Campo *et al.*, 2006; Meynier *et al.*, 2008; Certain *et al.*, 2011). The FA profile of sardines was studied by several authors, with sardines coming from the Mediterranean (Šimat *et al.*, 2020), the Bay of Biscay (Mathieu-Resuge *et al.*, 2024), off the Portuguese coast (Garrido *et al.*, 2008b) and the waters off Morocco (Mkadem and Kaanane, 2020). Only recently, the FA profile of sardines in the English Channel were described for the first time by Mathieu-Resuge *et al.* (2024) in comparison to the FA profile of sardines from the Bay of Biscay and the Gulf of Lions. They found significant differences in the FA acid profile among regions that might be related to prey composition with sardines of the English Channel characterized by calanoid copepod trophic markers 20:1(n-9) and 20:1(n-11), whereas FATM indicated a diatom-based food web in the Bay of Biscay and a dinoflagellate-based food web in the Gulf of Lions. Since 2017, sardines in the English Channel and the Celtic Sea are considered as proper stock and are separated from the central stock covering the Bay of Biscay (ICES). However, information on this Northern sardine stock remains scarce (Menu *et al.*, 2023), as does information about the FA profile of zooplankton in the English Channel. In other sardine stocks like in the Bay of Biscay (Doray *et al.*, 2018; Véron *et al.*, 2020; Boëns *et al.*, 2021) and parts of the Mediterranean (Brosset *et al.*, 2017; Albo-Puigserver *et al.*, 2021), biomorphological changes with regard to a decrease in size-at-age, weight-at-age and condition-at-age were observed and food quantity and quality were suggested as possible drivers (Van Beveren *et al.*, 2014; Brosset *et al.*, 2015, 2016; Boëns *et al.*, 2021; Menu *et al.*, 2023). With regards to English Channel sardines, predictions based on an energetic model suggested an average decrease of 3.5 % in size and 12.4 % in weight since 2000 (Menu *et al.*, 2023). As ocean warming might cause a potential decrease in EFA in phytoplankton (Hixson

and Arts, 2016), the present study will deliver valuable information with regard to ongoing and future changes in trophic dynamics.

## 3.2. Materials & Methods

### 3.2.1. Sampling

Environmental, planktonic and fish samples were collected in the English Channel during the Channel Ground Fish Survey (CGFS, Giraldo et al. 2021, <https://doi.org/10.17600/18001250>) in 2021 on board of the R/V *Thalassa* in autumn (mid-September to mid-October). Fish samples were collected using a GOV (Grande Ouverture Verticale) bottom trawl towed for 30 min during daylight at a constant speed of 3.5 knots. Immediately after trawling, all fish were sorted, identified, and weighed. A subsample of minimum 5 sardine individuals was randomly selected at each station (total sardines= 249, total stations = 45) for subsequent lipid analysis (**Figure 41**). For those individuals, a small piece of dorsal muscle tissue was dissected. Sex, length and weight were recorded. Spawning activity was determined from sexual maturity of gametes with premature and mature gametes recorded as spawning individuals and immature and post-spawning gametes recorded as non-spawning individuals due to the visual similarity of the latter two stages. Furthermore, the Le Cren's condition index was calculated from length and weight measurements (Le Cren, 1951; Gubiani *et al.*, 2020). Full oceanographic profiles of the water column were conducted at each station using a conductivity, temperature, and depth (CTD) probe (total n = 122). Niskin bottles were used to characterize taxonomic composition of phytoplankton (n = 11). Mesozooplankton was collected from vertical hauls using a WP11 net (200 µm mesh size). Samples serving for lipid analysis were pre-filtered on a nylon mesh of 500 and 1000 µm to remove small zooplankton and phytoplankton colonies and zooplankton > 1000 µm. The remaining fraction (500 – 1000 µm) was filtered through pre-combusted (450°C for 4h) GF/F filters (n = 39). Samples serving for taxonomic determination (n = 11) were stored in a formalin solution while samples used for lipid analysis were immediately frozen at -80°C. The majority of samples, serving for different analyses, were collected at the same station. If this was not possible, information from the closest sampling stations were used to investigate the relation between the different trophic levels. This was assumed appropriate as these sampling stations were situated in close vicinity.

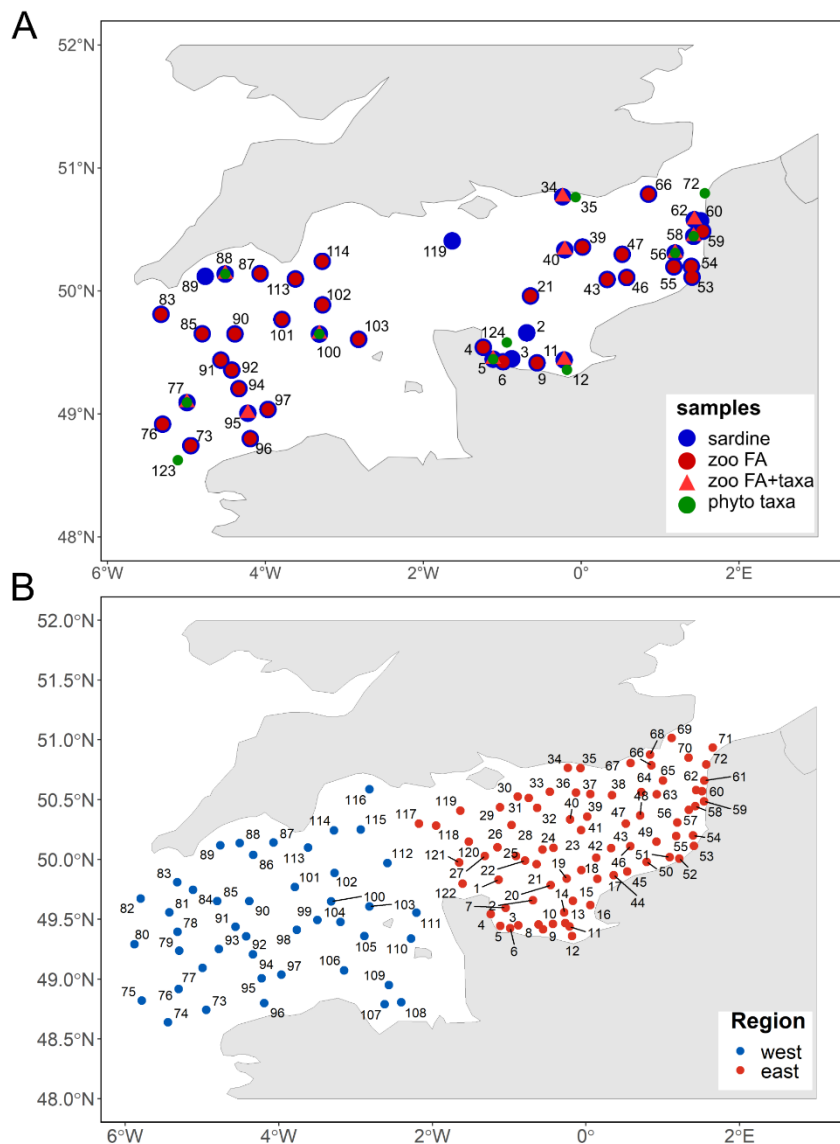


**Figure 41** Location of sampling stations during CGFS 2021. A: Blue dots indicate sampling stations of sardine; red dots indicate sampling stations of zooplankton serving for lipid analysis; red triangles represent sampling stations serving for lipid analysis and taxonomic analysis; green dots indicate sampling stations of phytoplankton; B: Sampling stations of environmental parameters (surface temperature, salinity, depth). Blue dots indicate sampling stations situated in the Western English Channel, red dots indicate sampling stations situated in the Eastern English Channel.

### 3.2.2. Lipid analysis

#### 3.2.2.1. Lipid extraction method

Dorsal muscles of sardine stored at  $-80^{\circ}\text{C}$  were ground with a Retsch homogenizer into liquid nitrogen. Approximately 250-300 mg of the homogenized powder was placed in pre-

combusted glass vials to which we added 6 ml of solvent mixture (CHCl<sub>3</sub>:MeOH, 2:1, v:v). As described in (Mathieu-Resuge *et al.*, 2023), lipid extracts were flushed under nitrogen gas, sonicated, vortexed and rested few hours to ensure complete lipid extraction. Approximately 250-300 mg of zooplankton were scrapped/recovered from filters stored at -80°C, suspended in 6 ml of solvent mixture (CHCl<sub>3</sub>:MeOH, 2:1, v:v) and proceeded as above.

### 3.2.2.2. Lipid class composition quantification

Neutral lipids (mostly reserve lipids) were analysed by high-performance thin-layer chromatography (HPTLC) on HPTLC glass plates (20×10mm) pre-coated with silica gel 60 from Merck (Darmstadt, Germany) and quantified by using a scanning densitometer (Automatic TLC Sampler 4 and TLC Scanner 3 respectively, CAMAG, Switzerland) as previously described in Haberkorn *et al.* (2010). Briefly, a preliminary run was carried out to remove possible impurities using hexane:diethyl ether (1:1), and the plate was activated for 30 min at 120 °C. Lipid samples (4 µl) were spotted on the plates by the CAMAG automatic sampler. The neutral lipids were separated using a double development with hexane:diethyl ether:acetic acid (20:5:0.5) as first solvent system followed with hexane:diethyl ether (93:3) as a second solvent system. Lipid classes appeared as black bands after dipping plates in a cupric sulfate (3 %), phosphoric acid solution (8 %) and heating for 20 min at 180 °C (charring). Eight neutral lipid classes (categorized as storage lipids: free fatty acids, sterol esters, glyceride ethers, monoacylglycerol, diacylglycerol, wax ester, and triacylglycerol; considered as structural lipids: sterols) were identified based upon standards (Sigma–Aldrich, France) and coloring techniques. The charred plates were read by scanning at 370 nm, and black bands were quantified by Visiocats software. Results were expressed as mg of each identified neutral lipid class per g of muscle/zooplankton wet weight. The triglyceride-sterol ratio (TAG-ST) was calculated, as this ratio allows to scale the amount of energy reserves (in form of triglycerides) by size (represented by sterols belonging to the structural lipids). Thus, the TAG-ST ratio represents a lipidic condition index.

### 3.2.2.3. Fatty acids analysis

A 500µL aliquot of sardine total lipid extract was, after adding C23:0 (2.3µg) as internal standard (free fatty acid form), evaporated and hydrolysed in 1 ml of KOH-MeOH (0.5 M) for

30 min at 80 °C, and then transesterified with 1.6 ml of MeOH:H<sub>2</sub>SO<sub>4</sub> (3.4 %; v/v) for 10 min at 100 °C to form fatty acid methyl ester (FAME). We extracted FAME by adding 800 µl of hexane and 1.5 ml of hexane-saturated distilled water, and by shaking and centrifuging 10 min at 1000 rpm. The denser aqueous phase was discarded and this step was repeated twice by adding only 1.5 ml of hexane-saturated distilled water. Finally, the samples were placed in the freezer at -20°C without removing the aqueous phase. After several hours, we quickly transferred the unfrozen upper organic phase into 2 ml vials, which are flushed with N<sub>2</sub> and stored in a refrigerator until GC-FID (Gas chromatography with downstream flame ionization detector) analysis.

As zooplankton lipids may contain high amount of wax ester, FAME preparation was performed differently to eliminate unsaponifiable compounds such as alcohol released from wax esters. One mL of zooplankton lipid extract was evaporated under N<sub>2</sub> flux. Fatty acids were saponified with 1 ml of KOH-MeOH (0.5 M) for 3 min at 90°C. After cooling, 0.5 ml of water and 0.4 ml of ethanol were added and sample was vortexed. To eliminate unsaponifiable compounds 2 ml of hexane were added. Samples were vortexed again, centrifuged 10 min at 1000 rpm and upper phase was discarded. This step was repeated twice with 1ml hexane. To release saponified fatty acids, 0.5 ml of 6N HCl was added. After vortexing, 2 ml of hexane was added and sample centrifuged 10 min at 1000 rpm and upper phase was transferred in a 7 ml vial. This step was repeated twice with 1ml hexane. Combined hexane upper phases with C23:0 (2.3µg) as internal standard were evaporated and then transesterified with 1.6 ml of MeOH:H<sub>2</sub>SO<sub>4</sub> (3.4 %; v/v) for 10 min at 100 °C to form FAME. Extraction of FAME was performed as above and stored in a refrigerator until analysis.

FAME composition of sardine muscle and zooplankton was determined using a gas chromatograph system (HP - Agilent 6890, Agilent Technologies, USA) equipped with a JW DB wax (30 m length x 0.25 mm i.d. x 0.25 µm film thickness), with an on-column injector at 60°C and a FID detector at 300°C. Peaks were identified by comparison with retention times of external known standards (Supelco 37 Component FAME Mix, PUFA No.1 and No.3, and Bacterial Acid Methyl Ester Mix from Sigma) using Chemstation software (Agilent). FAME content was converted into fatty acid content based on 23:0 internal standard. Total FA content was calculated as the sum of all identified FA. Data were expressed as a proportion of the total FA composition (%).



#### 3.2.2.4. Fatty acid trophic markers (FATM)

The following FATM were used to investigate the trophic structure from plankton to sardine. The presence of diatoms was inferred from 16:2(n-4), 16:3(n-4), 16:4(n-1) marking diatoms only, from 16:1(n-7) marking diatoms and Eustigmatophyceae and Pavlovophyceae and from a high ratio of EPA/DHA. FATM representing dinoflagellates were a low EPA/DHA ratio and high level of 18:5(n-3) (Graeve *et al.*, 1994; Auel *et al.*, 2002; Dalsgaard *et al.*, 2003; Remize *et al.*, 2022). The long-chain MUFA 20:1(n-9) and 22:1(n-11) were used as markers for the presence of *Calanus spp.* as polar herbivorous calanoid copepods like the genera *Calanus* and *Calanoides* biosynthesize these long-chain MUFA via chain elongation and integrate these FA in their energy storage (Kattner and Hagen, 1995; Hagen and Auel, 2001; Dalsgaard *et al.*, 2003).

#### 3.2.3. Phytoplankton community composition

Phytoplankton taxonomical composition was analyzed using an image acquisition system building on optical microscopy. Samples were digitized using an 8-bit grayscale Benchtop B2 Series FlowCam® Model VS-IV (Yokogawa Fluid Imaging Technologies, Inc., Scarborough, ME, USA), with a 4× objective lens coupled with a 300 µm-depth flow-cell. The images were analyzed using “EcoTransLearn” which is an R-package that facilitates the use of Transfer Learning methods to automatically classify digital images for ecological studies (<https://github.com/IFREMER-LERBL/EcoTransLearn>, Wacquet and Lefebvre, 2022). For further details see Annex III section 3.1.

#### 3.2.4. Zooplankton community composition

Taxonomic species determination was assisted by using a ZooScan (Grosjean *et al.*, 2004; Gorsky *et al.*, 2010) and the machine-learning web-application Eco-Taxa (<http://ecotaxoserver.obs-vlfr.fr>). Samples stored in 1 % formalin were rinsed and specimens were divided in three size classes (200 - 500 µm, 500 - 1000 µm, >1000 µm). To further enhance determination exactness, samples of the size class 200 - 500 µm were additionally fractionated by means of the Motoda method (Motoda, 1959; Grosjean *et al.*, 2004). For further details see chapter 1.2.1.1).

### 3.2.5. Statistical analyses

All statistical analyses were conducted with the R software environment v4.1.2 and results were considered significant when  $p$  was equal to or lower than 0.05.

#### 3.2.5.1. Spatial differences of environmental and sardine biological parameters

Differences in environmental drivers between the EEC and WEC, were assessed using a Student's  $t$ -test, provided that normality and homoscedasticity of data were satisfied. If data did not meet parametric assumptions, logarithmic or square-root transformations were applied. When parametric testing was not feasible, the Wilcoxon test was chosen as non-parametric alternative.

GLMM (Zuur *et al.*, 2013) were used to investigate differences in length, weight, TAG-ST ratio and Le Cren's condition index between the EEC and WEC. Each parameter was modeled as a function of the fixed covariates region (categorical with two levels) and of a fixed interaction term between region and sex (categorical with two levels) to take into account the different sex ratios between the regions. A spatial component was added as mixed effect to take into account spatial autocorrelation using an exponential variogram model ( $\exp(\text{pos}|0, \text{group})$ ).

In all models a gaussian distribution was used with a log or identity link function depending on model conversions and quality with regard to residuals. Model assumptions were verified by inspecting residuals using the "DHARMA" package. Furthermore, we assessed residuals for spatial dependency. GLMM were run using the "glmmTMB" package (Brooks *et al.*, 2017).

The model was constructed as follows:

Model = parameter  $\sim$  + region + region:sex +  $\exp(\text{pos}|0, \text{group}) + \epsilon$  with  $\epsilon$  following gaussian distribution with a log or identity link function

For details about model verification please see Appendix III 3.2.

#### 3.2.5.2. Assessments of spatial patterns in FA profile and taxonomic composition

PCA was used to assess spatial patterns in (i) FA profiles of sardine and zooplankton (500 - 1000  $\mu\text{m}$ ), and (ii) taxonomic composition of zooplankton and phytoplankton communities.

The quantity of wax esters was used as supplementary variable in the PCA applied to zooplankton FA and the outcome of the PCA applied to both zooplankton and sardine FA was interpreted with regard to FATM. For zooplankton taxonomical data PCA was applied to the size class also investigated for their FA profile (500 - 100  $\mu\text{m}$ ) and to a non-size differentiated dataset to investigate the potential spatial patterns in the entire zooplankton community sampled. Phyto- and zooplankton data was Hellinger-transformed prior to PCA. PCA was computed using the function PCA of the “FactoMineR” package (Lê *et al.*, 2008).

### 3.2.5.3. Factors influencing trophic transfer

GLMM and GAM (Zuur, 2012; Zuur *et al.*, 2013) were used to evaluate the influence of environmental and physiological parameters on the trophic transfer of EFA between zooplankton and sardines. In both models a beta distribution with a logit link function was chosen as this distribution is adequate for proportional data (between 0 and 1). Proportion of EFA in sardines was modeled as a function of the fixed covariates Le Cren’s condition index (continuous), spawning activity (categorical with two levels, see chapter 3.2.1) and region (categorical with two levels). The covariate ‘region’ was used as proxy for the environmental state in the model as environmental parameters (temperature, salinity, depth) were strongly correlated and differed significantly between the WEC and EEC (Annex III section 3.3). Other physiological and biometrical parameters of sardine like the TAG-ST ratio and length were not included in the model to avoid colinear issues with spawning activity (Annex III **Figure A 50**). We investigated the transfer of three EFA namely EPA, DHA and ARA as relative values. First a GLMM was conducted to account for spatial autocorrelation as random effect using an exponential variogram model ( $\text{exp}(\text{pos}|0, \text{group})$ ). The model was constructed as follows:

Model = EFAsardine (%)  $\sim$  EFAzooplankton (%) + LeCren’s index + spawning activity + region +  $\text{exp}(\text{pos}|0, \text{group}) + \epsilon$  with  $\epsilon$  following beta distribution with a logit link function

Quantile residuals were investigated against each covariate using the “DHARMA” package (Hartig, 2022) (see Appendix III 3.4). In case a non-linear pattern was detected in the residuals of the second quantile, the transfer of the respective FA was investigated using a GAM applying a spline based function (function *s* of the “mcgv” package (Wood, 2011)) to the

covariates for which a non-linear pattern was detected previously. The GAM model was constructed as follows:

Model = EFAsardine (%) ~ EFAzooplankton (%) + LeCren's index + spawning activity + region +  $\epsilon$  with  $\epsilon$  following beta distribution with logit as link function

GLMM and GAM were run using the “glmmTMB” package (Brooks *et al.*, 2017) and the “mgcv” package (Wood, 2011), respectively. Model assumptions were verified by inspecting residuals using the “DHARMA” package (see Appendix III 3.4 for information about model selection and verification steps). Furthermore, we assessed residuals for spatial dependency.

### 3.3. Results

#### 3.3.1. Biological parameters of sardines

Sardines collected in the WEC were significantly smaller and lighter than sardines in the EEC but did not differ regarding condition (TAG-ST ratio and Le Cren's index). Further inter-regional differences were observed with regard to the sex ratio and spawning activity. More females were caught in the East (females: 69, males: 48), whereas males were more numerous than females in the West (males: 71, females: 58). Females and males differed significantly in terms of length and weight but not with regard to TAG-ST ratio and Le Cren's condition index (**Table 5, 6**). A PCA applied to the FA profile of males and females did not indicate intersexual differences in the overall FA profile (**Figure A 52**). More spawning individuals were found in the EEC (~95 % of all individuals) than in the WEC (~68 %).

**Table 5 Biological parameters of sardine.** Data are presented for each region (Eastern English Channel (EEC), Western English Channel (WEC)) and by sex, along with the corresponding number of collected individuals. Mean values and standard deviations are provided for length, weight, triglyceride-sterol ratio (TAG-ST), and Le Cren's condition index.

region	sex	n	length (cm) mean $\pm$ S.D.	weight (g) mean $\pm$ S.D.	TAG-ST mean $\pm$ S.D.	Le Cren's index mean $\pm$ S.D.
EEC		117	21.31 $\pm$ 2.53	87.25 $\pm$ 26.05	80.16 $\pm$ 36.2	0.98 $\pm$ 0.01
	Female	69	22.02 $\pm$ 1.88	94.61 $\pm$ 20.84	83.88 $\pm$ 35.63	0.99 $\pm$ 0.1
	Male	48	20.28 $\pm$ 2.98	76.67 $\pm$ 29.2	75.08 $\pm$ 36.72	0.96 $\pm$ 0.09
WEC		129	18.21 $\pm$ 2.68	49.52 $\pm$ 20.66	69.5 $\pm$ 62.41	1.03 $\pm$ 0.1
	Female	58	18.59 $\pm$ 2.77	53.38 $\pm$ 22.20	74.15 $\pm$ 62.87	1.02 $\pm$ 0.1
	Male	71	17.90 $\pm$ 2.58	46.37 $\pm$ 18.89	65.61 $\pm$ 62.19	1.04 $\pm$ 0.1

**Table 6 Results GLMM testing inter-regional differences of sardines.** Estimates with standard error (S.E.) indicate significant and non-significant positive or negative correlation between a covariate and the proportion of the respective parameter of sardines. Significance: \*\*\* ( $P < 0.001$ ), \*\* ( $P < 0.01$ ), \* ( $P < 0.05$ ). AIC (Akaike's Information Criterion). *n* indicates the number of individuals used in the model.

		length	weight	TAG-ST ratio	Le Cren's index
Intercept (S.E.)		19.07 (0.5) ***	4.0 (0.07) ***	72.34 (9.10) ***	0.02 (0.01)
Estimates (S.E.)	region	2.56 (0.68) ***	0.49 (0.09) ***	9.95 (12.21)	-0.03 (0.02)
	regionWEC:sex	-1.2 (0.31) ***	-0.19 (0.06) **	-10.3 (8.79)	0.02 (0.02)
	regionEEC:sex	-0.81 (0.38) *	0.12 (0.04) **	-5.01 (9.66)	-0.03 (0.02)
AIC		1058	2151	2632	-429
n		245	245	245	245

### 3.3.2. Taxonomic composition of zoo- and phytoplankton

#### 3.3.2.1. Zooplankton

The taxonomic composition of zooplankton was analyzed at 11 stations mostly corresponding to regions or sampling stations of phytoplankton. Zooplankton of the size ranges 300 - 500  $\mu\text{m}$ , 500 - 1000  $\mu\text{m}$  and >1000  $\mu\text{m}$  represented respectively 90 %, 9 % and 1 % of the overall 300 - 1000+  $\mu\text{m}$  abundance. The first three principal components of a PCA implemented with taxonomic data of the size class 500 - 1000  $\mu\text{m}$  explained 24.5 %, 15.9 % and 11.8 % of the variance, respectively. Differences were observed in the community composition between the WEC and the EEC (**Figure 42**). These differences were also obtained when using a non-size differentiated dataset including all samples (Annex III **Figure A 53**). Stations of the western basin were located on the negative side of the first dimension whereas stations of the eastern basin were mostly located on the positive side. Taxa contributing mostly to this differentiation were *Candacia spp.*, *Calanus spp.*, Euphausiacea larvae and Euphausiacea for the WEC and *Acartia spp.* and *T. longicornis* for the EEC (**Figure 42**). When using all size classes *P. parvus*, annelid larvae and *E. acutifrons* characterized the eastern basin whereas the presence of *Calanus spp.*, crustacea larvae, *Candacia spp.*, *Corycaeus spp.* and Oithonidae characterized the western basin (Annex III **Figure A 53**).

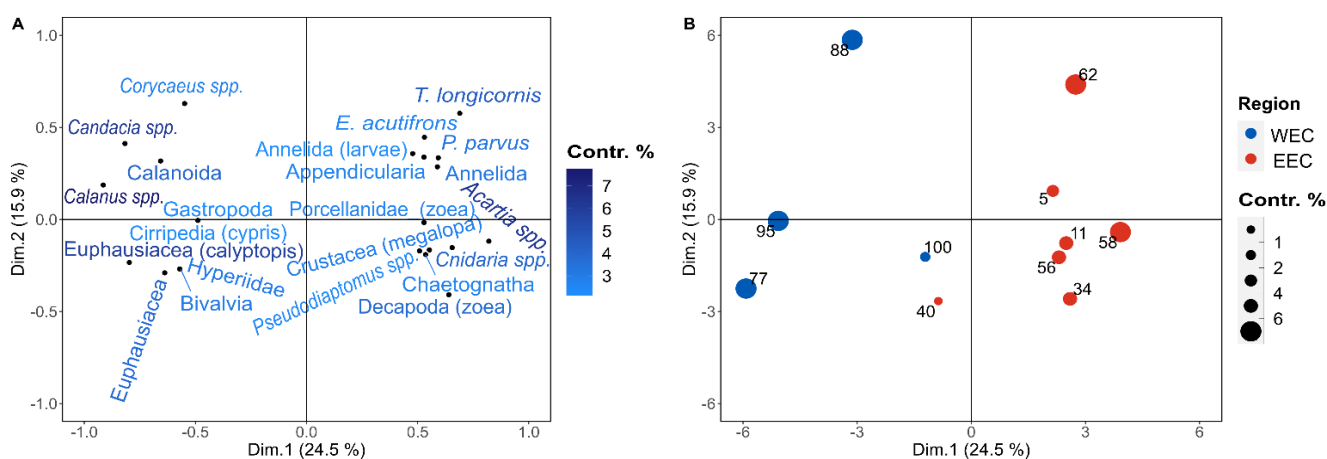


**Figure 42** PCA taxonomic composition of zooplankton (500 – 1000 µm), first and second principal components. A: Taxa (the darker the taxon, the higher its contribution to the first component); only taxa with a contribution higher than 2% are displayed); B: Sampling stations (the bigger the dot the higher its contribution to the first component); blue and red dots were located in the Western English Channel (WEC) or the Eastern English Channel (EEC), respectively; numbers represent sampling station id.

### 3.3.2.2. Phytoplankton

Phytoplankton taxonomic composition and abundance between the EEC and the WEC was analyzed at 11 stations. Differences in phytoplankton taxonomic composition between the EEC and the WEC were revealed by the first two axes of a PCA, representing 48.4 % of the overall variance (**Figure 43A,B**). Diatom species dominated in the EEC whereas diatoms and dinoflagellates characterized the WEC. Taxa that contributed the most to overall abundance and that were characteristic for the EEC were *Chaetoceros spp.*, *Guinardia spp.*, *Leptocylindrus spp.* and *Rhizosolenia spp.* (**Figure 43A,B**, Annex III **Figure A 55**). The WEC was characterized by *Thalassionema spp.*, *Thalassiosira spp.* and *Dytilum spp.* Phytoplankton abundance was higher in the East than in the West mostly driven by stations situated at the French coast close to the Dover Strait (**Figure 43C**). Station 123 might deviate from the east-west pattern due to its position. It is the westernmost station and likely has the highest offshore influence from the Atlantic. Compared to other stations sampled in the EEC, Station 56 is the most offshore, potentially reflecting an offshore to inshore gradient.

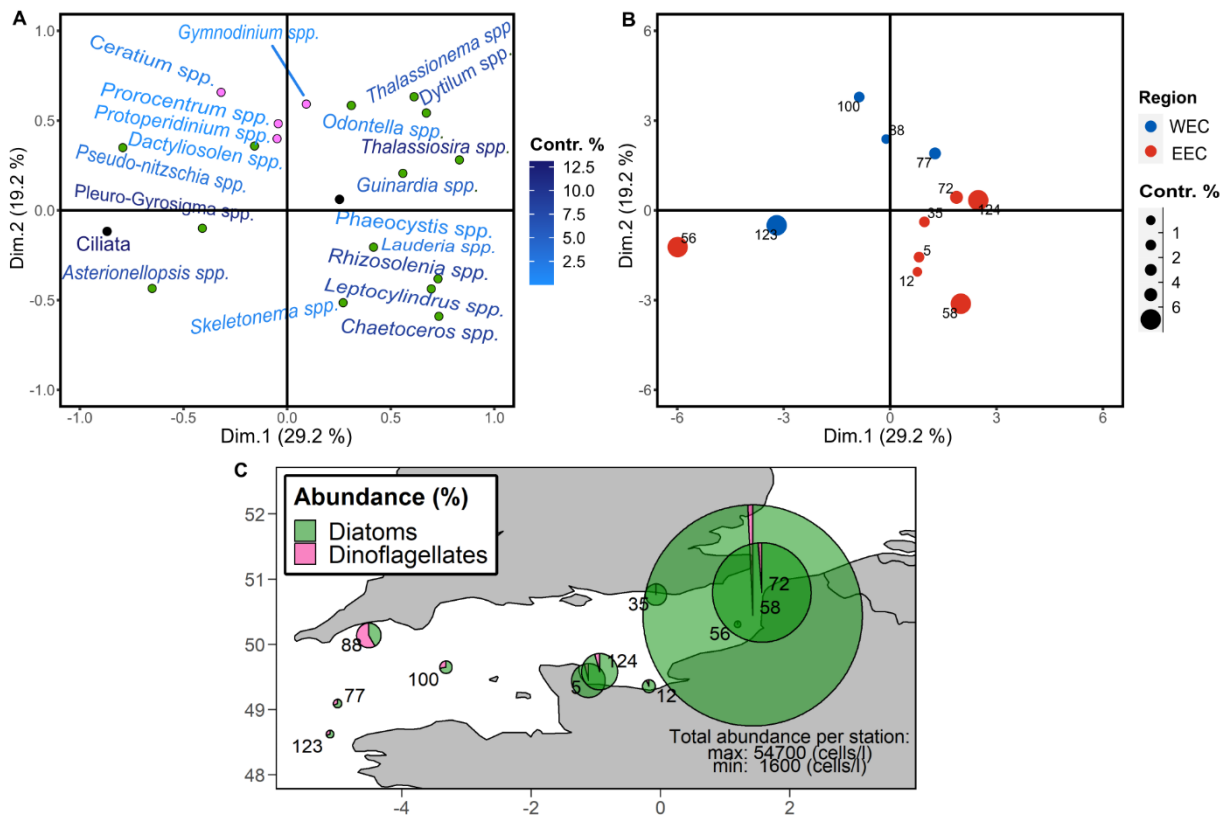


**Figure 43 PCA taxonomic composition of phytoplankton, first and second principal components.** A: Taxa (the darker the taxon, the higher its contribution to the first component); only taxa with a higher contribution than 1 % are depicted; pink, green and black dots represent dinoflagellate, diatom and other species, respectively; B: Sampling stations (the bigger the dot the higher its contribution to the first component); blue and red dots were located in the Western English Channel (WEC) or the Eastern English Channel (EEC), respectively; numbers represent sampling station id; C: Relative abundance of diatoms (green) and dinoflagellates (pink) to total abundance per station (size of pie charts represent abundance in cells/l).

### 3.3.3. Spatial pattern of the FA profile of zooplankton and sardine



For sardines, a total number of 45 FA were identified. Overall, SFA were dominated by palmitic acid (16:0, ~21 %) (Table 7). The dominant MUFA was oleic acid (18:1(n-9), ~9 %) followed by palmitoleic acid (16:1(n-7), ~4 %) and 18:1(n-7) (~3 %). PUFA were dominated by DHA (~22 %) followed by EPA (~11 %).

For zooplankton, we identified 43 FA. As for sardines, 16:0 was the dominant SFA (~16 %), whereas 16:1(n-7) (~4 %) and 18:1(n-9) (~4 %) were the most abundant MUFA. PUFA were dominated by DHA (~23 %) and EPA (~18 %) (Table 7).

Tables showing the complete set of FA of sardines and zooplankton are provided in Annex III (Table A 8, 9).

CHAPTER 3 - 3. Perspective – Biochemical composition

**Table 7 Fatty acid trophic markers and most important fatty acids (FA) for zooplankton and sardine.** Values are reported as mean  $\pm$  standard deviation by region (Eastern English Channel (EEC), Western English Channel (WEC)). *n* indicates number of stations. The FA listed in this table represent the 20 most important FA with regard to percentage and including FATM and essential FA. A complete table can be found in Annex III (Table A 8, 9).

		WEC n = 20 mean $\pm$ S.D.	EEC n = 19 mean $\pm$ S.D.		WEC n = 129 mean $\pm$ S.D.	EEC n = 117 mean $\pm$ S.D.
<b>Saturated FA (%)</b>						
14:0		6.7 $\pm$ 2.3	4.6 $\pm$ 1.9		3.7 $\pm$ 1.0	3.9 $\pm$ 1.1
16:0		16.0 $\pm$ 1.0	15.6 $\pm$ 1.2		20.9 $\pm$ 2.1	21.5 $\pm$ 1.2
18:0		3.6 $\pm$ 1.1	5.2 $\pm$ 1.0		5.0 $\pm$ 0.6	6.0 $\pm$ 0.8
<i>Total SFA</i>		28.6 $\pm$ 1.2	28.5 $\pm$ 1.9		31.6 $\pm$ 0.9	33.5 $\pm$ 0.9
<b>Monounsaturated FA (%)</b>						
16:1(n-7)		3.6 $\pm$ 1.0	5.4 $\pm$ 1.5		3.7 $\pm$ 1.0	5.1 $\pm$ 1.4
18:1(n-9)		4.3 $\pm$ 1.3	3.3 $\pm$ 1.3		7.9 $\pm$ 3.2	11.5 $\pm$ 2.9
18:1(n-7)					2.4 $\pm$ 0.5	3.3 $\pm$ 0.6
20:1(n-11)		0.1 $\pm$ 0.0	0.5 $\pm$ 0.4		0.3 $\pm$ 0.2	0.1 $\pm$ 0.1
20:1(n-9)		0.8 $\pm$ 0.5	0.3 $\pm$ 0.2		2.1 $\pm$ 1.2	1.7 $\pm$ 0.5
22:1(n-11)		1.8 $\pm$ 1.6	0.1 $\pm$ 0.1		1.9 $\pm$ 1.6	0.1 $\pm$ 0.2
22:1(n-9)		0.2 $\pm$ 0.1	0.1 $\pm$ 0.1		0.5 $\pm$ 0.2	0.5 $\pm$ 0.3
<i>Total MUFA</i>		13.9 $\pm$ 2.9	14.2 $\pm$ 2.8		21.4 $\pm$ 3.3	24.1 $\pm$ 2.5
<b>Polyunsaturated FA (%)</b>						
16:2(n-4)		0.4 $\pm$ 0.2	0.7 $\pm$ 0.5		0.2 $\pm$ 0.2	0.4 $\pm$ 0.3
16:3(n-4)		0.2 $\pm$ 0.1	0.7 $\pm$ 0.7		0.1 $\pm$ 0.2	0.4 $\pm$ 0.3
16:4(n-1)		0.7 $\pm$ 0.3	1.4 $\pm$ 0.7		0.2 $\pm$ 0.3	0.5 $\pm$ 0.4
18:2(n-6)		1.9 $\pm$ 0.6	0.9 $\pm$ 0.2		1.2 $\pm$ 0.4	0.6 $\pm$ 0.2
18:3(n-3)		1.1 $\pm$ 0.8	1.2 $\pm$ 0.6		1.1 $\pm$ 0.3	0.7 $\pm$ 0.3
18:4(n-3)		4.7 $\pm$ 2.2	2.7 $\pm$ 1.3		2.1 $\pm$ 0.6	1.6 $\pm$ 0.5
18:5(n-3)		0.3 $\pm$ 0.2	0.1 $\pm$ 0.1			
20:4(n-6)		0.8 $\pm$ 0.3	1.5 $\pm$ 0.4		1.1 $\pm$ 0.4	1.3 $\pm$ 0.3
20:5(n-3)		16.1 $\pm$ 2.4	20.9 $\pm$ 2.2		10.5 $\pm$ 2.3	12.7 $\pm$ 1.9
22:4(n-6)		0.1 $\pm$ 0.1	0.2 $\pm$ 0.1		0.2 $\pm$ 0.2	0.3 $\pm$ 0.2
22:6(n-3)		25.8 $\pm$ 3.7	20.8 $\pm$ 3.4		25.7 $\pm$ 6.8	18.9 $\pm$ 5.3
EPA/DHA		0.6 $\pm$ 0.3	1.1 $\pm$ 0.3		0.4 $\pm$ 0.1	0.7 $\pm$ 0.1
<i>Total PUFA</i>		56.1 $\pm$ 3.3	54.9 $\pm$ 2.5		46.3 $\pm$ 3.7	41.8 $\pm$ 2.5



### 3.3.4. Spatial segregation patterns

PCA was used to compare the overall FA signatures of sardine and zooplankton (500 - 1000  $\mu\text{m}$ ) (**Figure 44**). The first two components explained 59.4 % of the variance in sardine FA, and 49.0 % of the variance in zooplankton FA profiles. A clear spatial segregation pattern was visible for both zooplankton and fish. Zooplankton from the West was characterized by a higher proportion of the Calanus-markers 22:1(n-11) (~1.8 % of total FA) and 20:1(n-9) (~0.8 % of total FA) when compared to samples from the East (~0.1 % and 0.3 % of total FA, respectively). Presence of wax-esters in zooplankton was associated with the WEC. Similarly, diatom vs dinoflagellates markers in zooplankton (16:2(n-4), 16:3(n-4), 16:4(n-1), 16:1(n-7), 18:5(n-3), ratio EPA/DHA) suggest a dominance of silica-rich diatoms-based food web in the East and a more dinoflagellate-based food web in the West (**Table 7**).

Sardines displayed similar patterns. Both Calanus-markers were associated to western stations. The proportion of 22:1(n-11) was more than twice as high in western sardines (WEC: ~1.92 % of total FA) than in eastern sardines (EEC: ~0.11 % of total FA). The differing dominance of diatoms and dinoflagellates between the eastern and the western basin was indicated by the respective markers. The dinoflagellate marker 18:5(n-3) was not detected in the FA profile of sardines.

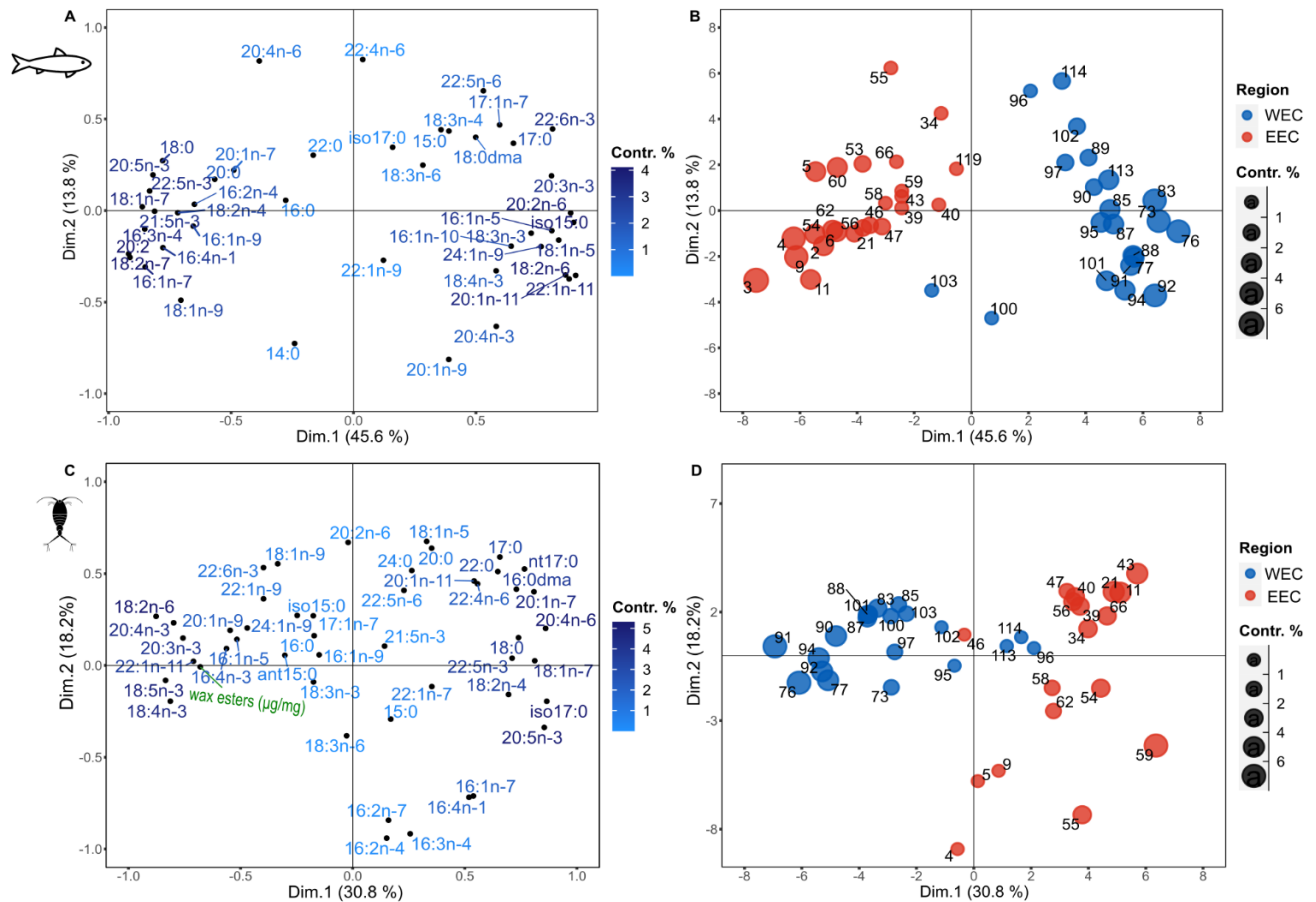


**Figure 44** Principal component analysis (PCA) on the fatty acid profiles of sardines (A, B) and zooplankton (500 - 1000  $\mu\text{m}$ ) (C, D) collected in the Western English Channel (blue) and Eastern English Channel (red). Panel A and C display FA in the two dimensional plane of the first and second component. The darker the taxon, the higher its contribution to the first component. Panel B and D display sampling stations. The bigger the dot the higher its contribution to the first component. Numbers represent sampling station id.

### 3.3.5. Factors influencing trophic transfer of EFA

Factors influencing the trophic transfer of EPA, DHA and ARA from zooplankton to sardine were investigated using GLMM and GAM (Table 8, Figure 45 - 47, Annex III Table A 7).

Proportions of EFA were significantly higher in non-spawning than in spawning fish. The proportions of EPA and ARA, were significantly higher in the EEC then in the WEC. Proportions of EPA and ARA were positively correlated with their proportion in 500 - 1000  $\mu\text{m}$  zooplankton. Sardine and zooplankton DHA proportions were not significantly correlated. Le Cren's condition index significantly influenced the proportion of EPA but was not correlated to sardine's DHA and ARA proportions.

Including a spatial component as a random effect in the GLMM reduced the spatial autocorrelation in the residuals and decreased the AIC of the models, though it did not entirely remove spatial autocorrelation. This could be due to the insufficient number of sampling stations. For the same reason it was not possible to use a generalized additive mixed model with a spatial component as a random effect. As this study focuses on large scale patterns (EEC vs WEC) the model outcome can still be considered reliable. For further details please see Appendix III 3.4.

**Table 8 Factors influencing trophic transfer of essential fatty acids (EFA).** Estimates with standard error (S.E.) indicate significant and non-significant positive or negative correlation between a covariate and the proportion of the respective fatty acid (FA) in sardine. Significance: \*\*\* ( $P < 0.001$ ), \*\* ( $P < 0.01$ ), \* ( $P < 0.05$ ); AIC (Akaike's Information Criterion); type: model used; n: number of sampling stations; (s): parameters integrated in the model as a spatial smoother; edf: estimated degrees of freedom for the smoothed terms.

		EPA	DHA	ARA
<b>Intercept (S.E.)</b>		-1.97 (0.12) ***	-1.07 (0.3) ***	-4.26 (0.17) ***
<b>Estimates (S.E.)</b>	<b>zooplankton FA</b>	(s) ***	0 (0.00)	0.17 (0.04) ***
	<b>Le Cren's index</b>	0.23 (0.12) *	-0.26 (0.22)	-0.04 (0.15)
	<b>spawning</b>	-0.26 (0.03) ***	-0.19 (0.06) ***	-0.29 (0.04) ***
	<b>region</b>	-0.19 (0.04) ***	0.35 (0.19)	-0.15 (0.04) ***
<b>edf</b>	2.9			
<b>AIC</b>	-1212.2	-671.9	-2075.5	
<b>type</b>	GAM	GLMM	GLMM	
<b>n</b>	233	233	234	

CHAPTER 3 - 3. Perspective – Biochemical composition

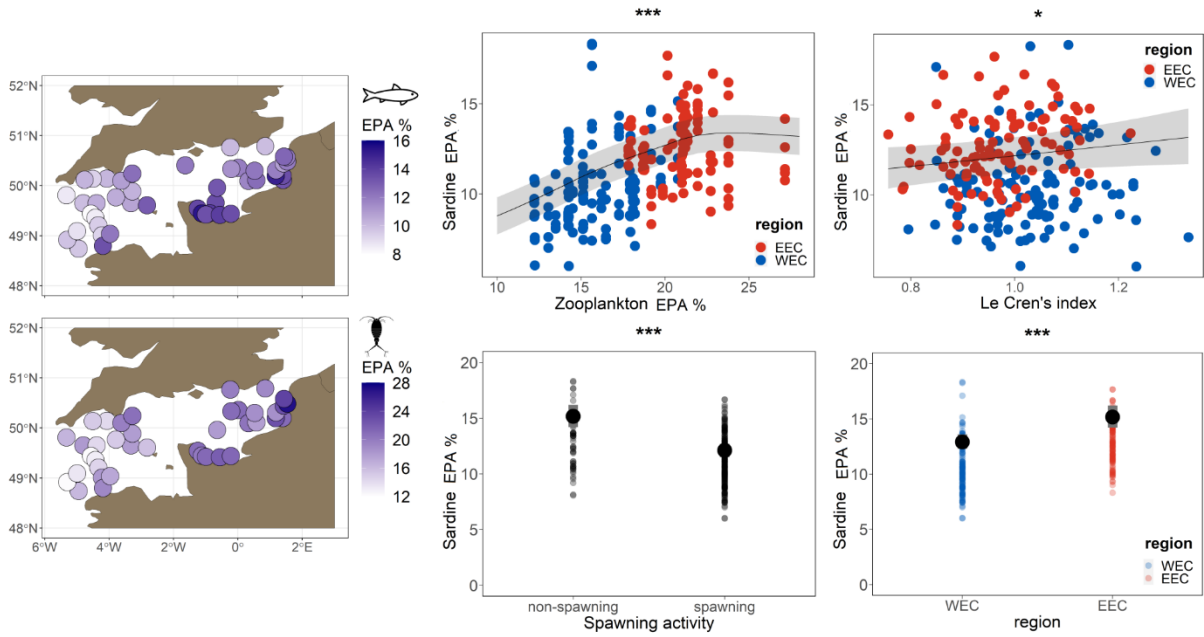


**Figure 45** Factors influencing trophic transfer of eicosapentanoic acid (EPA) revealed by the GAM. The relation of EPA % in zooplankton and sardine and all significant factors influencing trophic transfer revealed by the GAM model are displayed. Significance level is displayed in the heading of the respective plots: \*\*\* ( $P < 0.001$ ), ( $P < 0.01$ ), \* ( $P < 0.05$ ).

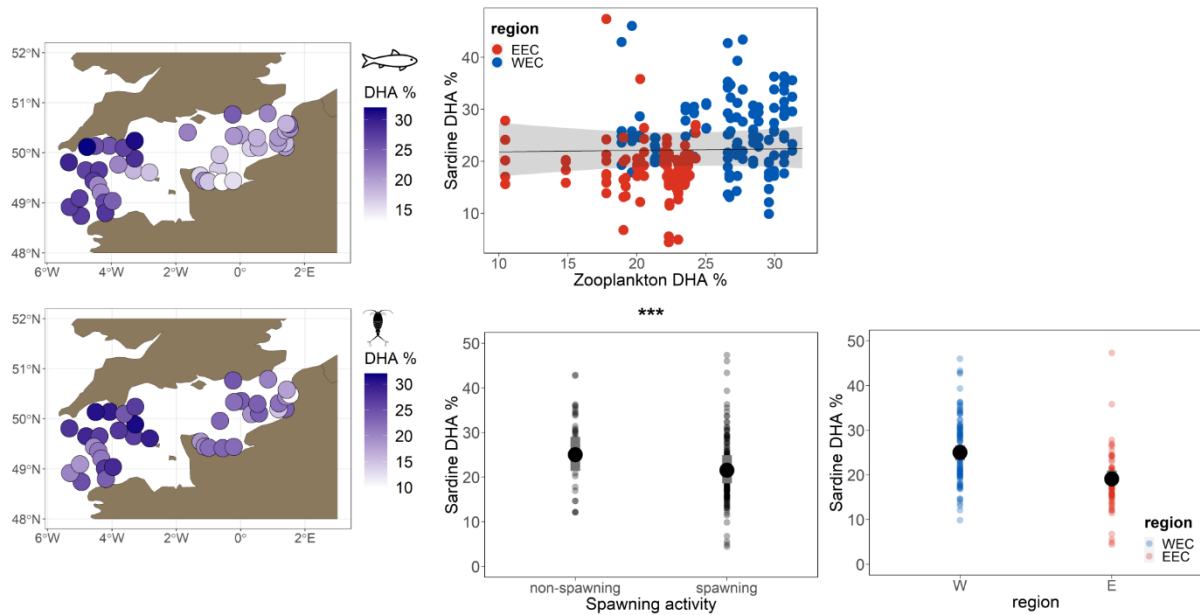


**Figure 46** Factors influencing trophic transfer of docosahexaenoic acid (DHA) revealed by the GLMM. For DHA also the relation to zooplankton DHA and region is shown although not significant. Significance level is displayed in the heading of the respective plots: \*\*\* ( $P < 0.001$ ), ( $P < 0.01$ ), \* ( $P < 0.05$ ).

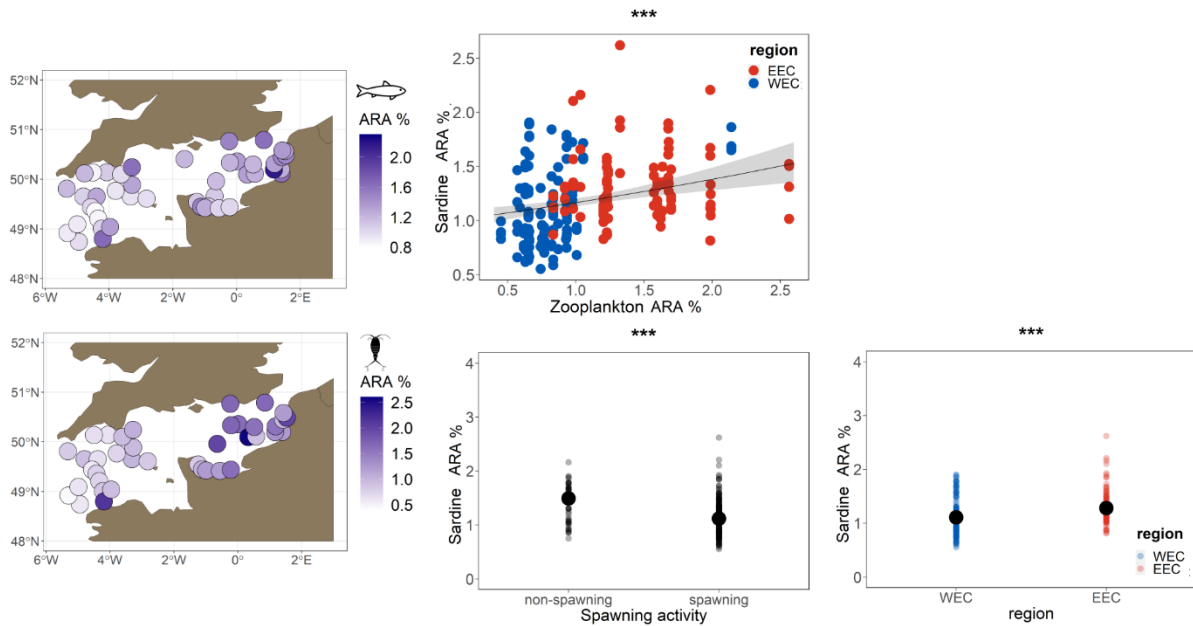


**Figure 47** Factors influencing trophic transfer of arachidonic acid (ARA) revealed by the GLMM. The relation of ARA % in zooplankton and sardine and all significant factors influencing trophic transfer revealed by the GAM model are displayed. Significance level is displayed in the heading of the respective plots: \*\*\* ( $P < 0.001$ ), ( $P < 0.01$ ), \* ( $P < 0.05$ ).

### 3.4. Discussion

Spatial variability in the FA composition of zooplankton and sardine was observed with FA profiles differing between the eastern and the western basins of the English Channel. This pattern aligns with the spatial variability in the taxonomical composition of phyto- and zooplankton and the differing environmental conditions indicating a strong bottom-up control of the transfer of essential fatty acids.

Dietary proportion of DHA, ARA and EPA in zooplankton together with spawning activity, region and condition were revealed as factors influencing the trophic transfer of these EFA from zooplankton to sardine. Together with differences in length, weight and spawning activity between the EEC and WEC, this suggests that the morphological and physiological characteristics of sardines might have further contributed to the observed spatial pattern in overall sardine FA profiles.

### 3.4.1. Potential drivers of spatial variability of FA profiles - plankton community composition and biological parameters of sardines

Phyto- and zooplankton community composition differed between the EEC and WEC possibly due to differences in hydrologic conditions (Beaugrand *et al.*, 2000). Dinoflagellate species displayed a higher contribution to the community in the WEC compared to the EEC, a finding that was also reported by other studies for the autumn period (Hoch and Garreau, 1998; Widdicombe *et al.*, 2010; White *et al.*, 2015).

The zooplankton community of the WEC was rather oceanic as indicated by the presence of taxa like *Calanus spp.*, *Candacia spp.* and Euphausiacea (Fransz *et al.*, 1991). The EEC by contrast was characterized by taxa associated to coastal regions like *T. longicornis* (Fransz *et al.*, 1991; Krause *et al.*, 1995), *P. parvus* (Krause *et al.*, 1995), *E. acutifrons* (Sautour and Castel, 1993) and *Acartia spp.*, with the latter genus including several species that are found at low salinities (Fransz *et al.*, 1991).

The WEC is deeper and influenced by Atlantic water whereas the EEC is shallower with a higher turbulence (Stanford and Pitcher, 2004; Dauvin, 2012) favoring diatom species instead of dinoflagellates (e. g. Margalef, 1978). Furthermore, the EEC is characterized by high riverine discharge leading to high nutrient input and areas of low salinity with the Seine estuary accounting for two thirds of the drainage area of the entire English Channel (Brylinski *et al.*, 1991; Stanford and Pitcher, 2004; Dauvin, 2012; Lefebvre and Devreker, 2020). This most probably led to a significantly lower salinity in the EEC than in the WEC observed during the study period. Although significant, mean differences of salinity and surface temperature between the basins were small (16.6 vs. 17 °C; ~35 vs. 34) (Annex III section 3.3).

Biometrical and physiological parameters of sardines differed between the basins. Sardines in the EEC were longer and heavier than in the WEC. This was related to the sex ratio sampled that was characterized by a higher contribution of females in the EEC that were longer and heavier than males. The smaller mean length in the WEC could also have been related to ontogenetic stage as well, considering that non-spawning individuals were smaller than spawners and that the proportion of spawning individuals was lower in the WEC than in the EEC (Annex III **Figure A 23**, **Figure A 50**). The differences in length and weight observed between the two basins were not explained by dissimilar feeding conditions, since both lipidic and morphological condition indices did not vary significantly between regions and sex.

### 3.4.2. Spatial variability in FA profiles of zooplankton and sardine

The distinct difference in the FA profile of sardine and zooplankton found between the EEC and WEC aligned with the spatial differences in phyto- and zooplankton community composition. FATM indicated the presence of *Calanus spp.*, wax-ester producing species and the presence of dinoflagellates in the WEC whereas diatom FATM appeared to be characteristic for the EEC. The use of wax-esters as energy storage is known in herbivorous calanoid copepods such as *Calanus spp.* (Kattner and Krause, 1989; Dalsgaard *et al.*, 2003) and Euphausiacea (Lee *et al.*, 2006). Small calanoid copepods as those characterizing the EEC are hypothesized to not have the need to produce lipid storages in form of wax esters considering their omnivorous life style (Kattner and Hagen, 2009; Benedetti *et al.*, 2015). Thus, the association of wax-esters to the WEC appears to be in accordance with the zooplankton taxonomical characteristics of the two basins.

In previous studies, the FA composition of phyto- and zooplankton communities were found to be mainly driven by their taxonomy, as well as diet in the case of zooplankton (Persson and Vrede, 2006; Gladyshev *et al.*, 2010; Galloway and Winder, 2015; Hiltunen *et al.*, 2015, 2022; Mathieu *et al.*, 2022). Thus, we suggest that the spatial pattern in the zooplankton FA composition observed was related to the phyto- and zooplankton community composition (Gladyshev *et al.*, 2010; Galloway and Winder, 2015; Hiltunen *et al.*, 2022). In case food quality might be the reason for the observed changes in length and weight of sardines in the Mediterranean and the Bay of Biscay (Menu *et al.*, 2023) this might indicate that compositional changes in the phyto- and zooplankton communities might drive changes in food quality with regard to FA.

The FA profile of sardines displayed the same spatial pattern as zooplankton, with the FA profile of individuals differing between the WEC and the EEC. As discussed above FATM in the muscle FA profile suggested a strong bottom-up control by dietary availability on the transfer of FA. This was further supported by the taxonomical composition of other zooplankton size classes (300 - 500  $\mu\text{m}$ , >1000  $\mu\text{m}$ ) that serve as sardine prey (Garrido *et al.*, 2007a, 2015) and that were not analyzed for their FA profile but followed the same spatial east-west pattern (Annex III **Figure A 53**). Sardines display an opportunistic feeding behavior that varies ontogenetically, spatially and temporally (Garrido *et al.*, 2007a, 2015; Costalago *et al.*, 2015; El Mghazli *et al.*, 2020). The importance and role of phytoplankton in sardine diet is still under debate (Bode *et al.*, 2003, 2004; Garrido *et al.*, 2008a, 2008b; Nikolioudakis *et al.*, 2012;

Giraldo *et al.*, 2024) and the spatial pattern in the phytoplankton trophic markers might be the result of direct or indirect ingestion of phytoplankton via herbivorous zooplankton.

An influence of diet on sardine FA composition was also suggested by other studies based on FATM and taxonomic information about prey composition (Bertrand *et al.*, 2022; Mathieu-Resuge *et al.*, 2024). Field studies directly comparing prey FA composition with sardine FA composition are rare (Shirai *et al.*, 2002; Garrido *et al.*, 2008b). Thus, the present study provides additional evidence for a strong bottom-up control of the transfer of FA from zooplankton to small pelagic fish.

Environmental conditions and biometrical and physiological characteristics of sardines could have further contributed to the spatial separation of sardines FA profile. Length might influence FA composition via energy allocation strategy with regard to reproduction and growth (Pethybridge *et al.*, 2015; Ohshimo *et al.*, 2022). As discussed, above non-spawning individuals were more abundant in the WEC and they were smaller compared to their spawning counterparts. Thus, one could hypothesize that more individuals allocated energy towards growth in the WEC than in the EEC. Maturity at length data for sardines in the EC would help to verify this hypothesis. Length might further influence FA composition via ontogenetic prey selectivity. We did not observe a decrease of EPA/DHA ratio with length as was found by Bertrand *et al.* (2022) with regard to age and that was proposed to be related to a diet shift towards more macrozooplankton in older individuals. Nevertheless, a different feeding strategy of smaller individuals more abundant in the WEC could explain the dissimilar FA compositions.

Evidence suggests that temperature, salinity and depth might affect FA composition of fish (Kemp and Smith, 1970; Farkas *et al.*, 1980; Olsen *et al.*, 1999; Cordier *et al.*, 2002; Hunt *et al.*, 2011; Voronin *et al.*, 2022). A higher proportion of long-chain PUFA in the cell membrane of fish at colder temperature has been proposed to serve as 'homeoviscous adaptation' allowing the fish to maintain membrane fluidity (Arts and Kohler, 2009). The universal validity of this mechanisms has been questioned however (Gladyshev *et al.*, 2018). Depth adaptation with regard to FA is proposed to concern membrane fluidity by a similar principle as in homeoviscous adaptation in terms of temperature (Radnaeva *et al.*, 2017; Voronin *et al.*, 2022). A distinct differing characteristic between the WEC (~81 m) and EEC (~38 m) was the depth profile that could have led to a colder environment experienced by sardine in the WEC despite similar basin surface temperature. Sardines are known to undertake diurnal vertical



migrations (Giannoulaki *et al.*, 1999; Zwolinski *et al.*, 2007) that make them reside close to the seabed during night as found for sardines living off the Portuguese coast (Zwolinski *et al.*, 2007). Studies that have shown an influence of depth on the FA composition of fish mostly focused on abyssal or mesopelagic fish that inhabit greater depth than experienced by sardines in the English Channel, however (Voronin *et al.*, 2021, 2022). Thus, an influence of a deeper depth profile and potentially lower temperature experienced by sardine in the WEC on the muscle fatty acid composition remains highly speculative. Salinity was found to influence the proportion of DHA of phospholipids in fish liver, muscle and gill (Cordier *et al.*, 2002; Hunt *et al.*, 2011). Most studies that observed an effect of salinity on PUFA composition investigated fish species that frequent low salinity zones like estuaries, however (Cordier *et al.*, 2002; Khériji *et al.*, 2003; Hunt *et al.*, 2011). Furthermore, fish were exposed to acclimation from freshwater to saltwater (Khériji *et al.*, 2003; Hunt *et al.*, 2011) and therewith to a magnitude of salinity variation that was remarkably higher (~28 - 40) than in the present study (~35 vs. 34).

Thus, due to the small differences of mean surface temperature and salinity between the basins an environmental effect on the transfer of EFA in this region is likely rather indirect, mediated through differing hydrological conditions and nutrient regimes (Lefebvre and Devreker, 2020) influencing phyto- and zooplankton dynamics, composition and quality.

### **3.4.3. Factors influencing the trophic transfer of EFA**

The GLMM and GAM models used to investigate factors influencing the trophic transfer of DHA, EPA and ARA further support a bottom-up control and an influence of sardine's physiological state on the trophic transfer. This corroborates earlier studies suggesting that the predator FA profile is not only driven by prey FA composition (Garrido *et al.*, 2007b; Gladyshev *et al.*, 2018; Yasuda *et al.*, 2021).

EPA and ARA were significantly correlated with zooplankton FA proportions, while DHA was not. This could be related to a stronger regulation of this physiologically important EFA by the organism making a link to trophic sources more complex.

Spawning activity was negatively correlated to the proportion of all three EFA tested. The study period was within the autumn reproduction period of sardine in the English Channel (Coombs *et al.*, 2005, 2010; Stratoudakis *et al.*, 2007; Menu *et al.*, 2023). DHA, EPA and ARA are known to be important for fish embryo and larvae development (Koven *et al.*, 1990;

Izquierdo, 1996; Bruce *et al.*, 1999; Tocher, 2010) and are incorporated into sardines oocytes leading to a decrease of the concentration of these FA in the muscle (Garrido *et al.*, 2007b, 2008b). With regard to relative values of FA, similar patterns were observed in Japanese sardine (*Sardinops melanostictus*). In this species proportions of DHA and ARA were lower during the spawning season than during the non-spawning period, and the proportion of EPA decreased with decreasing total muscle lipid content, indicating a decrease of this FA during spawning with regard to absolute values (Yasuda *et al.*, 2021). However, not only EFA were found to be influenced by spawning activity. MUFAs and certain SFA (14:0, 16:0, 18:0) in oocytes were observed to be correlated to the mother's muscle concentration as well (Garrido *et al.*, 2007b). In contrast to PUFA the incorporation of MUFA and SFA were not conserved meaning that the 18:1(n-9) oocyte concentration, for instance, decreased with the muscle concentration whereas the concentration of DHA was independent from the muscle concentration and was always higher in the oocyte (Garrido *et al.*, 2007b). Concentration of 20:1(n-9) and 22:1(n-11) were lower in the oocytes than in the muscle, a finding that was also reported for other species (Sargent and Tocher, 2002; Garrido *et al.*, 2007b; Huynh *et al.*, 2007). Thus, spawning activity might influence the overall FA profile of sardines not only with regard to the three EFA tested. The inclusion of both female and male sardine data in the models (Annex III **Table A 7**) and in a PCA analysis on the overall FA profile (Annex III **Figure A 52**) did not show any influence of sex on the results. This is in accordance with Garrido *et al.* (2008b) who did not find differences between sexes in the FA composition (absolute values) and reported a similar seasonality of the FA composition of both sex.

Spawning activity and the TAG-ST ratio were related (Annex III **Figure A 50**), with non-spawning individuals having a lower TAG-ST ratio meaning lower fat reserves than spawning individuals. Thus, the correlation of spawning activity and the three EFA tested could also represent a relationship to this lipidic condition index. DHA and ARA decreased with increasing TAG-ST ratio (Annex III **Figure A 51**). A negative correlation of DHA and ARA proportion to lipid content was also observed in Japanese sardine (Yasuda *et al.*, 2021) and the proportion of total n-3 PUFA decreased with total lipid content in *Perca fluviatilis* (Mairesse *et al.*, 2006). This observation was suggested to be related to the proportion of structural to neutral lipids (Mairesse *et al.*, 2006; Gladyshev *et al.*, 2018; Yasuda *et al.*, 2021). Fish in poor condition can be expected to have a higher proportions of structural lipids than fish in good condition with a higher share of neutral storage lipids. Thus, the relative values of EFA which are most

prominent in the structural phospholipids might decrease in fish of good condition because the share of storage lipids increases although the absolute values of EFA might not. EPA did not display a negative relationship with the TAG-ST ratio. This finding was similar to Japanese sardine in which the proportion of EPA did not decrease during the spawning period in contrast to DHA and ARA (Yasuda *et al.*, 2021). Yasuda *et al.* (2021) propose a stronger transfer of DHA and ARA to the ovaries as a possible explanation. A study comparing the concentration of the different EFA in sardine muscle and oocytes would not support this suggestion for European sardine (Garrido *et al.*, 2007b). Due to the diverse physiological roles of EPA, ARA and DHA (Tocher, 2003), other physiological processes like immune or stress response might explain the difference in the relation to lipidic condition observed what could be further investigated in future studies (Gladyshev *et al.*, 2018). EPA was also positively correlated to the morphological condition index although the p-value of 0.047 and the values predicted indicate a modest correlation (**Figure 45**) that we judge not robust enough for further interpretation.

In the present study, the FA profile of total muscle lipids was used meaning that lipids were not separated in polar and neutral lipids. This might have been a shortcoming with regard to the interpretation of the influence of physiological or environmental factors on the proportion of FA in sardine, as physiological signals might have been confounded with dietary signals (Bertrand *et al.*, 2022; Mathieu-Resuge *et al.*, 2024). As the FA profile of total lipids is the profile relevant to trophic transfer throughout the food chain, however, the use of total muscle lipids was reasonable given the aim of the present study.

In this regard it would be interesting to include other tissues than muscle in future studies (Sissener, 2018) also with regard to stable isotope analysis that could allow for a temporal insight of the spatial feeding pattern of sardine.

#### **3.4.4. Spatial separation of sardines in the English Channel**

The spatial separation pattern of sardine FA profile, combined with the association of FATM to either the WEC or EEC indicates that sardines only resided and fed on one side of the English Channel during the study period and the preceding weeks corresponding to the incorporation time of the FA profile. This might explain why sardines did not smoothen the spatial variability found in zooplankton FA profiles. To get insight in the inter-annual variability of this pattern, a PCA was applied to mean and individual FA profiles of sardines sampled in the English Channel in autumn 2020 (**Figure 48**) obtained from Mathieu-Resuge *et al.* (2024). The FA profile of these animals displayed the same east-west pattern, with individuals sampled in the WEC characterized by Calanus-markers, whereas sardines caught in the EEC were associated to diatom FATM. This indicates that the residing of sardines only in one of the two basins during autumn might be a reoccurring pattern.

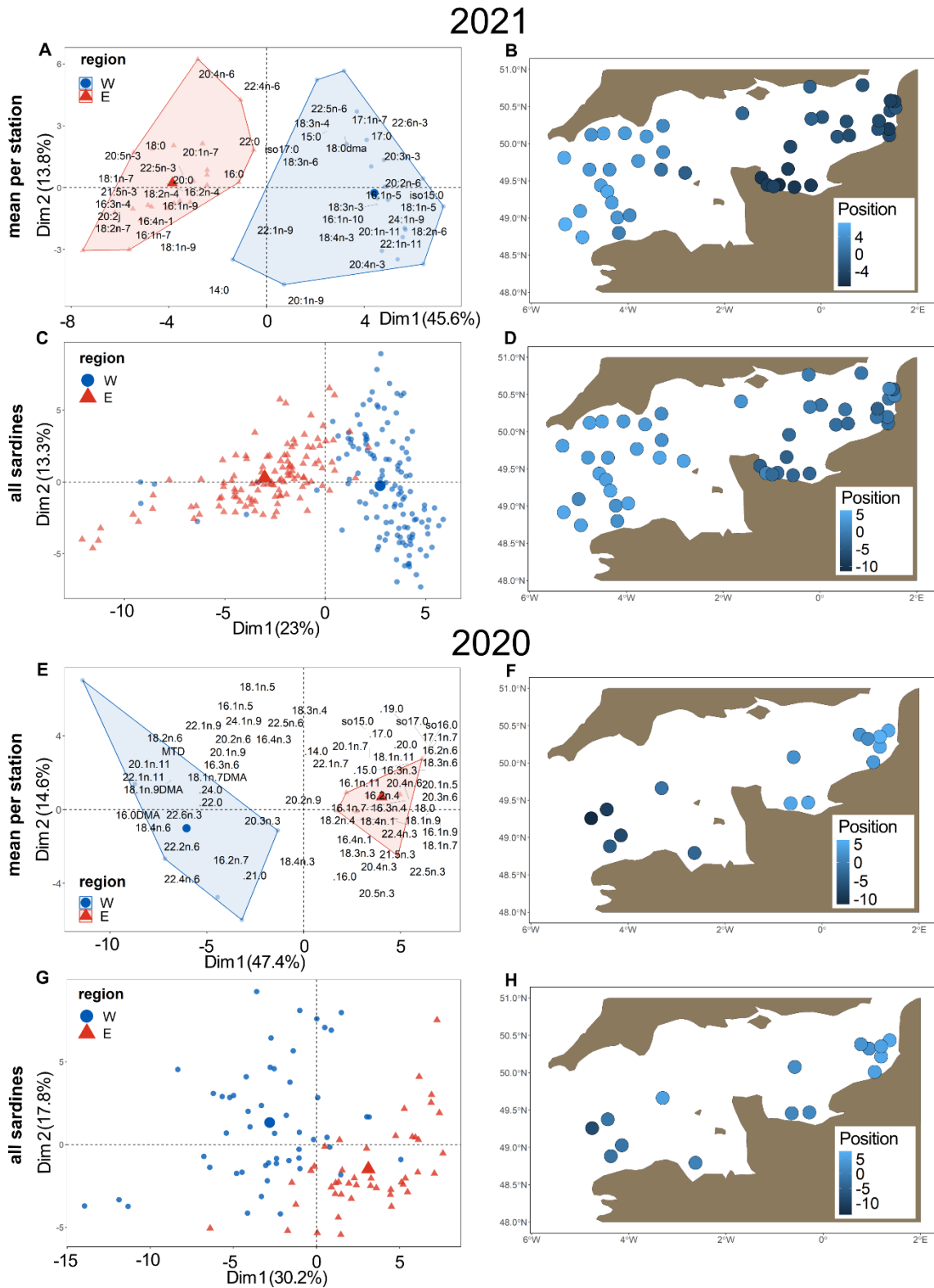


**Figure 48 Interannual comparison of sardine fatty acid profile.** Upper four panels showing PCAs applied to data sampled in autumn 2021 in the context of the present thesis. Lower four panels show PCAs applied data sampled by Mathieu-Resuge et al. (2024) in autumn 2020. A, E: FA displayed in the two dimensional plane of the first and second component of a PCA applied to the **mean fatty acid profile per station**; C, G: FA displayed in the two dimensional plane of the first and second component of a PCA applied to **individual FA profiles of all sardines** sampled; Maps indicate the position of sampling stations on the first component of the PCA by color. Each map corresponds to the PCA presented to its left.

Since 2017, sardines in the Celtic Sea and the English Channel are considered separately from the Bay of Biscay and are defined as a single stock based on a higher growth rate and the presence of all life stages (eggs, larvae, recruits and adults) in ICES sub-area 7 suggesting a self-sustaining stock unit (ICES, 2017). There is little information about sardines from the English Channel. The finding that sardines from the North Sea and the WEC did not differ genetically (Laurent *et al.*, 2007; Kasapidis *et al.*, 2012) does not indicate the presence of different populations in the WEC and EEC. However, differences within the same species between the WEC and EEC have been reported for sole (*Solea solea*) and cod (*Gadus morhua*) regarding abundance trends (Araújo *et al.*, 2006; ICES, 2023b). Cod individuals residing in the WEC and EEC are managed as part of different fish stocks, with the west affiliated to the Celtic Sea stock and the east being affiliated to the North Sea stock (Araújo *et al.*, 2006; ICES, 2023b). These two species are benthic or demersal; thus, the characteristic pattern of sardines in the two basins in autumn provides a unique case for a pelagic species. Dauvin (2012) proposed to separate the English Channel in a western and eastern part mainly based on differences in benthic communities (Luczak and Spilmont, 2012). Other studies such as Beaugrand *et al.* (2000), also found differences between the two basins regarding the plankton community which was in accordance to the present study. Data spanning several years and seasons are necessary to further verify and better understand the spatial pattern of sardine in the English Channel. Nevertheless, the spatial pattern of FA in sardines corresponds to the spatial separation pattern found for other species and ecosystem compartments. It further fits into the larger context of biogeographical studies (Spalding *et al.*, 2007; Longhurst, 2010), which affiliated the WEC and EEC to different ecoregions, biomes and provinces. This might suggest that evaluations of sardine biometrical parameters considering the predicted decrease of length and weight (Menu *et al.*, 2023) should be conducted separately for the WEC and EEC due to potential local patterns arising from differences in prey composition and therewith potentially prey quality.

### 3.5. Conclusion

A strong spatial separation pattern of fatty acid profiles of zooplankton and sardine has been found between the WEC and EEC in autumn 2021. Similar spatial patterns in the taxonomic composition of phyto- and zooplankton and FATM as well as correlation of EFA in sardine muscle and zooplankton indicated a strong bottom-up control of the trophic transfer of FA

mostly driven by taxonomical compositions. Beside the strong bottom-up control of trophic transfer, the physiological state of sardine with regard to spawning, energy allocation strategy and condition was indicated to influence trophic transfer which should be taken into account for the use of FATM and with potential consequences for higher trophic levels. Sardines did not smooth spatial variability in FA profiles indicating a residence of individuals either in the WEC or EEC immediately prior and during the study period. This further suggests differences between the two basins of the English Channel, a finding relevant to inform ecosystem models and management strategies. The potential of small pelagic fish as spatial smoothers in other regions would be an interesting topic for future studies as would be a study using absolute instead of relative values to evaluate the spatial variability in FA profiles. This would complete the present study with regard to the assessment of bioavailability of FA and food quality also with regard to ongoing changes in recent sardine populations.

## General Discussion

In the present thesis, we explored three different perspectives on zooplankton functioning in the ecosystem using an integrated approach that considers both lower and higher trophic levels within the context of multitrophic biodiversity ecosystem functioning. We investigated the taxonomic composition and abundance of zooplankton in the Southern North Sea, the isotopic size structure of zooplankton in the Eastern English Channel and the fatty acid profile of zooplankton in the entire English Channel accounting for spatial distribution and variability. The mesozooplankton and ichthyoplankton assemblages defined in the Southern North Sea and the Eastern English Channel during winter indicated spatial patterns in the potential top-down effect of zooplankton on phytoplankton spring bloom and in the potential bottom-up effect of zooplankton with regard to fish larvae (chapter 1). Whereas the Rhine-Scheldt region and the Channel-Thames region were important assemblages for herring and plaice larval feeding, the Rhine Scheldt region followed by the German Bight harbored the highest hibernal zooplankton stocks which indicated a potential for fast zooplankton stock increase and top-down influence on phytoplankton succession. Abiotic and biotic drivers such as dissolved nutrients and phyto-microplankton composition were revealed as drivers for spatial distribution of zooplankton indicator species. The assessment of the isotopic signature of plankton size classes spanning from nanoplankton to mesozooplankton in the EEC during winter (chapter 2) indicated low trophic divergence of microzooplankton but a more distinct isotopic signature of zooplankton organisms of a size of 500 - 1000  $\mu\text{m}$  and of herring and plaice larvae. The contribution of plankton size classes to herring and plaice larvae diet suggested a different trophic niche of these larval species and spatial variation in the contribution of plankton size classes to plaice larval diet. Chapter 3 revealed spatial differences in the biochemical composition of zooplankton and sardines with regard to the fatty acid composition between the WEC and EEC. Similar spatial patterns in the taxonomical composition of phyto- and zooplankton suggested a strong bottom-up effect in the trophic transfer of fatty acids from zooplankton to sardines, which was further influenced by fish physiological state with regard to energy allocation strategy and condition.

Independent of the perspective, all studies revealed spatial patterns in ecosystem functioning, as spatial variability in zooplankton characteristics seemed to be related to both lower and



higher trophic levels. Thus, investigating zooplankton in the context of multitrophic biodiversity ecosystem functioning contributed to a more mechanistic understanding of zooplankton diversity as part of, and in relation to, other components of the ecosystem, knowledge essential for ecosystem modelling and ecosystem-based management.

### 4.1 Insights and possible inferences from multitrophic spatial variation

Observing concurrent spatial variation in zooplankton characteristics, lower and higher trophic levels as well as abiotic factors in different marine areas, provided insights into the spatial patterns observed and could facilitate drawing conclusions about zooplankton characteristics in other marine regions. Chapters 1 and 3 indicated that spatial variability in zooplankton taxonomical and biochemical composition was related to phyto- and zooplankton composition. The difference in FA composition between the WEC and EEC corresponded to the differences in the proportion of dinoflagellates, diatoms and *Calanus spp.* between these regions. This suggests that the FA composition of zooplankton assemblages in the SNS-EEC might also vary, as the German-Bight Norfolk region displayed a higher percentage of dinoflagellates than the other regions, the proportion of diatoms varied between the assemblages (Annex I **Figure A 6**), and *Calanus spp.* were of highest proportion in the Northern- and Central assemblage. The Channel-Thames and the Northern assemblage displayed similar proportions of dinoflagellates. Depending on the dominant driver of zooplankton FA composition, this suggests that the spatial variance in the FA composition of zooplankton in the SNS-EEC could be lower than the taxonomical variance, resulting in a lower number of zooplankton assemblages based on the FA profiles, with implications for spatial variability in zooplankton functioning. A better understanding of the extent to which FA composition is driven by phyto- and zooplankton taxonomical composition and environmental parameters would improve the prediction of spatial variability in FA composition in zooplankton in other regions like the SNS-EEC. This could be achieved by using partial redundancy analysis as continuation of the analyses in chapter 3.

As seen in chapter 3 spatial variability in zooplankton FA profiles influences higher trophic levels. The concordance of FA profiles of zooplankton and sardines revealed a spatial pattern in sardine feeding and was against the hypothesis of spatial smoothing of FA composition by

small pelagic fish. Knowledge about the FA profile of zooplankton in the SNS could therefore be valuable for studying the spatial pattern of feeding of small pelagic fish species and their influence on the transfer of FA to subsequent trophic levels. Juveniles of sprat and herring feed in the Rhine-Scheldt area during winter to subsequently join adult fish in the North Sea (Maes *et al.*, 2005). This might lead to a temporal smoothing effect of potential differences in zooplankton FA composition between the Rhine-Scheldt area and other parts of the North Sea. Adult herring feed in the Northern and Central North Sea (Corten, 2001) and stop feeding during their spawning migration towards the Southern Bight and the EEC (Slotte, 1999; Van Ginderdeuren *et al.*, 2014a; McBride *et al.*, 2015). This large-scale migration might in the context of marine functional connectivity enrich the FA availability and composition for piscivorous predators in the SNS-EEC as herring might provide a different FA profile than fish feeding in the south due to differences between northern and southern phyto- and zooplankton communities (Krause and Martens, 1990; Williams *et al.*, 1993; Beaugrand *et al.*, 2001, 2019; Kléparski *et al.*, 2021). This might also be relevant with regard to FA quantity. The biological transport of energy from the Atlantic to the Norwegian coast by Norwegian spring-spawning herring was found to account for  $1.3 \times 10^6$  tonnes and to strongly influence the coastal ecosystem for example regarding the population and fisheries of the lobster *Homarus gammarus* (Varpe *et al.*, 2005).

Given the importance of FA for fish larval development (Koven *et al.*, 1990; Izquierdo, 1996; Bruce *et al.*, 1999; Tocher, 2010), knowledge on the FA composition of zooplankton in the Channel-Thames and Rhine-Scheldt assemblages could enhance our understanding of larval survival, as the present thesis indicated these two areas being important feeding grounds for herring and plaice larvae. As discussed in chapter 1, larval retention and dispersal between these assemblages is hypothesized to influence the survival of herring larvae (Dickey-Collas *et al.*, 2009). Akimova *et al.* (2023) investigated the feeding potential for herring larvae in this area with regard to size-dependent zooplankton biomass. Information on the FA composition of the 500 - 1600  $\mu\text{m}$  size class (chapter 2) of the two assemblages might complement this information with regard to herring larvae food quality. Furthermore, quantity and quality of zooplankton in the SNS-EEC might be of interest with regard to adult herring feeding. Due to the starvation of Downs herring during spawning migration they depend on adequate feeding possibilities for resourcing after gamete release. Downs herring overwinter in the SNS before they return to their feeding grounds in spring (Corten, 2001) but information on the timing

and area where Downs herring start feeding post spawning is scarce. Although, other herring races have been reported to leave spawning grounds shortly after gamete release (Skaret *et al.*, 2002), feeding around the spawning grounds in the SNS-EEC does occur including cannibalisms on herring eggs as revealed by stomach content analyses in our laboratory (unpublished data). Cannibalism on herring eggs has also been observed in herring spawning off southern Norway, although the proportion of cannibalistic animals was low (10 %) and only considered late spawning individuals (Skaret *et al.*, 2002). While herring eggs represent an abundant and easily available food source, demersal feeding is considered risky, due to decreased escape possibilities near bottom and presence of predators around the spawning grounds (Axelsen *et al.*, 2000). One could hypothesize that the availability of zooplankton adequate for adult herring diet with regard to taxonomical composition and prey quality in the SNS-EEC would decrease cannibalism but information about feeding after spawning of Downs herring in relation to zooplankton assemblage composition would be necessary to further evaluate on this topic.

Beside taxonomical composition, the size structure of planktonic food webs influences prey availability of larval fish. Chapter 2 showed that isotopic signatures of several size classes of plankton were very similar indicating low trophic divergence related to low primary production. By contrast, other regions or seasons with higher primary production were reported to display higher trophic divergence (Kozak *et al.*, 2020; Giraldo *et al.*, 2024). As we found different levels of primary production in the SNS-EEC (chapter 1) we might expect that in regions with higher hibernial phytoplankton production, higher trophic divergence might be present resulting in a more distinct isotopic signature of plankton size classes. This might have consequences for larval feeding and planktonic food web structure and productivity.

## **4.2 From nutrients to higher trophic levels - The planktonic food web**

The SNS ecosystem was proposed to be mainly driven by riverine nutrient inputs (Clark and Frid, 2001; Thomas *et al.*, 2005). In chapter 1 we could see that the concentration of nutrients like phosphate and nitrogen species varied spatially in relation to river discharge and different origins of water masses. Different configurations/structures of planktonic food webs exist related to availability of dissolved nutrients. High concentrations of dissolved nutrients,

## General Discussion

particularly nitrates, favor the so called “herbivorous food web”, consisting of large phytoplankton cells that facilitate direct ingestion by herbivorous mesozooplankton that in turn transfer the energy towards small pelagic fish and fish larvae (Legendre and Rassoulzadegan, 1995). Under low nutrient availability, primary production is driven by recycling of dissolved organic matter by bacteria leading to small phytoplankton cells and the microbial loop as trophic regime. Here, nano- and pico-phytoplankton and bacteria are fed on by ciliates, microflagellates and heterotrophic dinoflagellates (Tian *et al.*, 2003; Pepin and Dower, 2007). Legendre and Rassoulzadegan (1995) propose that in between these two trophic extremes, a multivorous planktonic food web exists, in which both herbivorous and microbial pathways play an important role. Therein large phytoplankton cells would be favored by nitrate and grazed by herbivorous copepods that excrete ammonium and dissolved organic nitrogen (DON). Ammonium and DON favor the remineralization of ammonium by bacteria and therewith protozoan bacteria grazers while autochthonous ammonium favors the production of small phytoplankton cells (Legendre and Rassoulzadegan, 1995). Planktonic food webs with high primary production and dominance of large phytoplankton cells tend to have shorter food chain length and to be dominated by herbivor-omnivor organisms whereas low primary production due to oligotrophic conditions and a dominance of small phytoplankton tend to result in longer food chain length with higher levels of carnivory (Décima, 2022). Thus, the assessment of spatial variation in dissolved nutrient concentration could not only be used to infer the nutritional quality of phytoplankton as zooplankton food (chapter 1), but might also indicate and/or explain planktonic food web structure. Knowledge about the planktonic food web structure might help to assess fish larvae feeding potential with regard to the biomass and composition of different plankton size classes. Furthermore, it is a relevant factor for ecosystem productivity (Schmidt *et al.*, 2020; Décima, 2022) with regard to carbon export to the benthic community and therewith the strength of benthic-pelagic coupling (Marquis *et al.*, 2011) that plays an important role in the EEC (Kopp *et al.*, 2015; Cresson *et al.*, 2020). The direct link between nutrient concentration and planktonic food web structure might further help to better understand and manage anthropogenic impacts coming from sewage and agriculture nutrient inputs. Also FA composition in phytoplankton was shown to be directly (Jónasdóttir, 2019) and indirectly (Strandberg *et al.*, 2022) driven by dissolved nitrogen and phosphorous either by mechanisms like reduced synthesis of n-3 PUFAs or due to a taxonomical change in the phytoplankton community

composition. Thus, incorporating information about dissolved nutrients in plankton studies might help to understand taxonomical and biochemical plankton community composition with regard to ecosystem functioning.

### 4.3 Implication of spatial variation for modelling

The understanding of ecosystem functioning needed for ecosystem-based management can be improved using ecosystem and trophic models that allow to extend the information derived from observation and experiments (Ratnarajah *et al.*, 2023). Due to their immense taxonomic, trophic and size diversity, representing plankton adequately in numerical models is highly challenging (Chenillat *et al.*, 2021). In its simplest way zooplankton is represented as a single trophic level with simple nutrient-phyto-zooplankton relationships (Chenillat *et al.*, 2021; Frelat *et al.*, 2022; Ratnarajah *et al.*, 2023). More advanced models use plankton functional types like autotrophs, heterotrophs, calcifiers and prey or traits to facilitate the incorporation of zooplankton diversity while maximizing computational efficiency (Serra-Pompei *et al.*, 2020; Chenillat *et al.*, 2021; Ratnarajah *et al.*, 2023). In their review Ratnarajah *et al.* (2023) conclude that zooplankton are not represented in an adequate manner in most numerical models although even small changes in zooplankton parametrization can strongly influence model outputs with regard to community structure, food web pathways and spatial variability (Bracis *et al.*, 2020; Chenillat *et al.*, 2021; Ratnarajah *et al.*, 2023; Thorpe, 2024). Zooplankton display complex species-specific behaviors, life cycles and high trophic plasticity with organisms capable of changing from herbivorous to omnivorous feeding, making the collection of comprehensive information about zooplankton challenging. Trait information is lacking for most zooplankton organisms although some groups like copepods, euphausiacea and ciliates are comparatively well studied (Benedetti *et al.*, 2015; Hébert *et al.*, 2017; Ratnarajah *et al.*, 2023). Furthermore, spatial information about community composition, abundance and biomass is needed for model parametrization but also as reference for comparison and model validation (Maar *et al.*, 2018; Dudeck *et al.*, 2021; Ratnarajah *et al.*, 2023; Grandremy *et al.*, 2024).

At the expense of temporal resolution, the present thesis delivers spatial large-scale (chapter 3), intermediate-scale (chapter 1) and small-scale (chapter 2) information about zooplankton in the SNS and EC that complements existing information and informs model parametrization

## General Discussion

and validation. Including higher and lower trophic levels allowed a more mechanistic understanding of the spatial patterns observed with regard to potential drivers and bottom-up effects. Zooplankton in the North Sea has been thoroughly studied. Most studies have focused on productive seasons like spring and autumn, from a macro-ecological perspective, considering large scale drivers like hydrology and temperature to understand what controls inter-annual zooplankton dynamics (Fransz *et al.*, 1991; Krause *et al.*, 1995, 2003; Beaugrand *et al.*, 2002a, 2013; Beaugrand, 2004; Bedford *et al.*, 2020). Other studies have used a small-scale approach by focusing on distinct regions like the German Bight or Belgic waters (Fransz and van Arkel, 1983; Van Ginderdeuren *et al.*, 2014b; Boersma *et al.*, 2015; Semmouri *et al.*, 2023). In chapter one, the intermediate-scale approach allowed for the detection and description of small-scale patterns, specifically identifying five zooplankton assemblages in the Southern North Sea ecoregion. Concurrently, this approach was broad enough to account for spatial differences in zooplankton composition around fish spawning grounds and fish larvae dispersal routes. Furthermore, together with Dudeck *et al.* (2021) this chapter is to the best of our knowledge the only recent spatial investigation focusing on winter zoo- and phytoplankton communities in the North Sea. The third chapter revealed differences in the biochemical and taxonomical composition of mesozooplankton between the WEC and EEC. A comparison of zooplankton communities between the WEC and EEC has to the best of our knowledge not been realized yet although these two basins were proposed to belong to different ecosystems (Beaugrand *et al.*, 2000; Dauvin, 2012; Luczak and Spilmont, 2012). Most of the information about zooplankton in the WEC comes from the stationary long-term monitoring at the L4 station off Plymouth (Rodríguez *et al.*, 2000; John *et al.*, 2001; Eloire *et al.*, 2010; Reygondeau *et al.*, 2015). Studies on zooplankton in the EEC are scarce (Graham and Harding, 1938; Dauvin *et al.*, 1998; Bedford *et al.*, 2020; Dudeck *et al.*, 2021). Thus, together with chapters one and two the present thesis delivers valuable information about the zooplankton taxonomic, size structure and biochemical composition in this area. The spatial variability observed could be useful for *a priori* model parametrization, such as considering spatial separation of sardines between the WEC and EEC. Furthermore, considering the SNS as a single ecoregion harboring one zooplankton community in ecosystem models might not be appropriate, especially during the winter season. This is because significant spatial variation in zooplankton composition, and particularly in abundance, was found, which could potentially influence larval feeding success and phytoplankton succession. In the context of

modeling, the present thesis emphasizes the need for spatially resolved zooplankton monitoring in the EEC, as chapter three proposes difference in the zooplankton community between the WEC and EEC, suggesting that monitoring in the WEC is not representative of zooplankton in the eastern basin. Information on zooplankton in the EEC is further relevant as this basin harbors spawning grounds and nursery areas of several fish species and some fish species like sardine (chapter 3) and plaice seem affiliated to and are managed in this region (Araújo *et al.* 2006; ICES 2023). This thesis only coarsely assessed the distribution of microplankton in the SNS-EEC but highlighted the importance of microplankton in plaice larval diet. As discussed above and noted by other studies (Pepin and Dower, 2007; Kürten *et al.*, 2013; Schoo *et al.*, 2018), microplankton plays an important role in planktonic food webs. Spatial information on microplankton composition and biomass is necessary to adequately incorporate this component of marine ecosystems into numerical models (Maar *et al.*, 2018).

### 4.3.1 Traits

In the present thesis we used a combined approach of zooplankton taxonomy and biological traits with regard to zooplankton size and FA profile. Using these traits helped to assess the link between plankton size classes and larvae of herring and plaice and multitrophic spatial differences between the WEC and EEC. The combined investigation of zooplankton taxonomy and FA composition in relation to phytoplankton and sardine reveals additional zooplankton characteristics that link zooplankton to the ecosystem, and contribute to a more mechanistic understanding of zooplankton functioning. Abundance of diatoms, dino- and nanoflagellates as well as phytoplankton biomass were revealed as drivers of the spatial distribution of assemblage's indicator taxa (chapter 1). This was in accordance with the spatial distribution of mesozooplankton in the Bay of Biscay that also displayed distinct spatial patterns apparently related to primary production and trophic phyto-zooplankton relationships (Grandremy *et al.*, 2023). Major differences in the FA profile of zooplankton and sardine were related to the proportion of dinoflagellates and diatoms in the phytoplankton community and to the presence of *Calanus spp.* Overall, the link between phytoplankton, zooplankton and sardine appears to be related to the transfer of FA, energy storage and hibernation strategies, the feeding mode and reproductive strategy. Depending on zooplankton taxa, FA are nearly exclusively obtained from phytoplankton but can also be synthesized *de-novo* and modulated to a certain extent by certain taxa like *Calanus spp.* that build lipid storages in form of wax-

## General Discussion

esters (Kattner and Hagen, 1995; Hagen and Auel, 2001; Dalsgaard *et al.*, 2003). Lipid storages in form of wax-esters were proposed to be present in species that are capable of hibernation (Cavallo and Peck, 2020). Whereas *Pseudocalanus spp.* and *Paracalanus spp.* appear to be able to adapt to the high POM load in the German Bight by filter-feeding, ambush- or cruise-feeding organisms might be disadvantaged in this region. Hibernation might facilitate *Temora spp.* to profit from primary production in the Rhine-Scheldt region. Thus, trying to understand the link between potential drivers of zooplankton distribution and biochemical composition reveals a link between zooplankton traits and ecosystem functioning. Litchman *et al.* (2013) proposed three groups of zooplankton traits related to feeding, reproduction and survival categorizing the traits discussed above. They argue that due to energy allocation trade-offs an organism cannot maximize the performance of all traits simultaneously. This results in so called trait trade-offs creating distinct trait combinations in an organism. An animal that invests energy into growth will have to allocate this energy from reproduction for instance. A zooplanktonic ambush-feeder will experience lower encounter rates with mating partners and will potentially develop reproduction strategies different from cruise-feeding organisms. Based on a literature review, Benedetti *et al.* (2015) obtained trait information of copepods in the Mediterranean and conducted clustering with these traits based on the idea of Litchman *et al.* (2013). The resulting trait clusters appear to be promising to enhance mechanistic understanding of zooplankton distribution, community structure and functioning in the ecosystem as distinct combinations of feeding modes, energy storage and reproduction strategies were found. The first cut-off level differentiated carnivores and omnivore/herbivores copepods. Only at the second cut-off level body size distinguished small carnivorous and large carnivorous copepods, indicating that body size alone might be insufficient to understand and model plankton food webs (Moloney and Field, 1991; Ward *et al.*, 2014). Using trophic, survival and reproductive trait-combinations resulting from trait trade-offs to represent zooplankton in numerical models might thus be an interesting avenue for further research (Thorpe, 2024) as these traits might more adequately represent zooplankton diversity and mechanistic functioning within the ecosystem. Observing zooplankton in the context of multitrophic biodiversity ecosystem functioning seems to be a promising approach to assess these traits together with experimental work.

Although trait-based approaches are likely to enhance mechanistic understanding of zooplankton communities in the ecosystem, most trait-based information cannot be derived



or assigned without taxonomical knowledge. Taxonomical knowledge might further be necessary to choose the adequate traits or be required itself to explain observed dynamics and processes (Bedford *et al.*, 2020). The inverse abundance trend of *Calanus finmarchicus* and *Calanus helgolandicus* with a decrease of *C. finmarchicus* and an increase of *C. helgolandicus* in the North Sea (Beaugrand *et al.*, 2003; Reid *et al.*, 2003; Bonnet *et al.*, 2005) was not reflected by the temporal fluctuations of the abundance of small and big copepods for example (Bedford *et al.*, 2020). Thus, species-specific information or other traits like energy/lipid content were needed to understand the decreasing recruitment success of cod (*Gadus morhua*) (Beaugrand and Kirby, 2010). Overall, taxonomical information should be acknowledged as basis for trait-based approaches (Mlambo, 2014) and when seen as complementary these approaches hold big potential to progress a mechanistic understanding of zooplankton that is needed for ecosystem and fisheries models and for the realization of ecosystem-based management.

## 4.4 Conclusion

The present thesis suggests the existence of distinct spatial patterns in pelagic shelf-sea ecosystems ranging from phytoplankton to small pelagic fish. This underlines the usefulness of spatially resolved plankton monitoring for better ecosystem understanding and management.

Investigating zooplankton in a multitrophic context was shown to be powerful to get insight into zooplankton functioning within the ecosystem and to develop hypotheses to explain the patterns and relationships observed. This approach should be extended to assess inter-seasonal and inter-annual variability.

Assessing zooplankton from several perspectives might be necessary to understand and detect zooplankton functioning in the ecosystem also with regard to climate change. The observed decrease of size and condition of sardines and anchovies in the Mediterranean and in the Bay of Biscay was proposed to be related to feeding distress (Brosset *et al.*, 2015, 2016; Queiros *et al.*, 2019; Menu *et al.*, 2023). The consideration of different zooplankton community characteristics was necessary to acquire a mechanistic understanding of this relationship. Food quantity and quality can vary due multiple factors, such as a decrease in overall or taxa specific zooplankton abundance (Beaugrand and Kirby, 2010; Menu *et al.*,

## General Discussion

2023), shifts in the zooplankton community from larger to smaller taxa (Brosset *et al.*, 2016), or a decline in prey quality, including the energy density of prey organisms (Heneghan *et al.*, 2023; Menu *et al.*, 2023). Increasing temperature due to ocean warming might result in a decrease of zooplankton individual size due to a direct (Daufresne *et al.*, 2009; Dudeck *et al.*, 2021) or indirect effect via stratification that might reduce nutrient availability and therewith effects plankton food web structure (Lewandowska *et al.*, 2014). Furthermore, climate change might alter the FA production in phytoplankton, potentially reducing FA availability for higher trophic levels (Litzow *et al.*, 2006; Galloway and Winder, 2015; Hixson and Arts, 2016; Vagner *et al.*, 2019; Schmidt *et al.*, 2020). Thus, monitoring and assessing zooplankton communities and assemblages using a multi-characteristic approach is essential to account for zooplankton diversity, with regard to their links and roles in the ecosystem (Heneghan *et al.*, 2023), and the potential effects of climate change on various zooplankton characteristics.

## References

- Aberle, N., and Malzahn, A. M. 2007. Interspecific and nutrient-dependent variations in stable isotope fractionation: experimental studies simulating pelagic multitrophic systems. *Oecologia*, 154: 291–303.
- Akimova, A., Peck, M. A., Börner, G., Van Damme, C., and Moyano, M. 2023. Combining modeling with novel field observations yields new insights into wintertime food limitation of larval fish. *Limnology and Oceanography*: 1865–12391.
- Albo-Puigserver, M., Pennino, M. G., Bellido, J. M., Colmenero, A. I., Giráldez, A., Hidalgo, M., Gabriel Ramírez, J., *et al.* 2021. Changes in Life History Traits of Small Pelagic Fish in the Western Mediterranean Sea. *Frontiers in Marine Science*, 8. <https://www.frontiersin.org/articles/10.3389/fmars.2021.570354>.
- Alvarez-Fernandez, S., Lindeboom, H., and Meesters, E. 2012. Temporal changes in plankton of the North Sea: community shifts and environmental drivers. *Marine Ecology Progress Series*, 462: 21–38.
- Alvarez-Fernandez, S., Licandro, P., Van Damme, C. J. G., and Hufnagl, M. 2015. Effect of zooplankton on fish larval abundance and distribution: a long-term study on North Sea herring (*Clupea harengus*). *ICES Journal of Marine Science*, 72: 2569–2577.
- Anderson, J. T. 1988. A Review of Size Dependent Survival During Pre-Recruit Stages of Fishes in Relation to Recruitment. *J. Northwest Atl. Fish. Sci*, 8: 55–56.
- Araújo, J. N., Mackinson, S., Stanford, R. J., Sims, D. W., Southward, A. J., Hawkins, S. J., Ellis, J. R., *et al.* 2006. Modelling food web interactions, variation in plankton production, and fisheries in the western English Channel ecosystem. *Marine Ecology Progress Series*, 309: 175–187.
- Arnold, G. P., and Metcalfe, J. D. 1996. Seasonal migrations of plaice (*Pleuronectes platessa*) through the Dover Strait. *Marine Biology*, 127: 151–160.
- Arts, M., Brett, M. T., and Kainz, M. J. (Eds). 2009. *Lipids in Aquatic Ecosystems*. Springer New York, New York, NY. <https://link.springer.com/10.1007/978-0-387-89366-2>.
- Arts, M. T., and Kohler, C. C. 2009. Health and condition in fish: the influence of lipids on membrane competency and immune response. *In Lipids in Aquatic Ecosystems*, pp. 237–256. Ed. by M. Kainz, M. T. Brett, and M. T. Arts. Springer, New York, NY. [https://doi.org/10.1007/978-0-387-89366-2\\_10](https://doi.org/10.1007/978-0-387-89366-2_10).
- Arula, T., Kotta, J., Lankov, A., Simm, M., and Pölme, S. 2012. Diet composition and feeding activity of larval spring-spawning herring: Importance of environmental variability. *Journal of Sea Research*, 68: 33–40.
- Auel, H., Harjes, M., da Rocha, R., Stübing, D., and Hagen, W. 2002. Lipid biomarkers indicate different ecological niches and trophic relationships of the Arctic hyperiid amphipods *Themisto abyssorum* and *T. libellula*. *Polar Biology*, 25: 374–383.
- Axelsen, B. E., Nøttestad, L., Fernö, A., Johannessen, A., and Misund, O. A. 2000. 'Await' in the pelagic: dynamic trade-off between reproduction and survival within a herring school splitting vertically during spawning. *Marine Ecology Progress Series*, 205: 259–269.
- Bailey, K. M., and Houde, E. D. 1989. Predation on Eggs and Larvae of Marine Fishes and the Recruitment Problem. *In Advances in Marine Biology*, pp. 1–83. Ed. by

## References

- J. H. S. Blaxter and A. J. Southward. Academic Press. <https://www.sciencedirect.com/science/article/pii/S006528810860187X>.
- Bandarra, N. M., Batista, I., Nunes, M. I., Empis, J. M., and Christie, W. W. 1997. Seasonal Changes in Lipid Composition of Sardine (*Sardina pilchardus*). *Journal of Food Science*, 62: 40–42.
- Batty, R. S. 1987. Effect of light intensity on activity and food-searching of larval herring, *Clupea harengus*: a laboratory study. *Marine Biology*, 94: 323–327.
- Batty, R. S., Blaxter, J. H. S., and Richard, J. M. 1990. Light intensity and the feeding behaviour of herring, *Clupea harengus*. *Marine Biology*, 107: 383–388.
- Beaugrand, G., Ibañez, F., and Reid, P. C. 2000. Spatial, seasonal and long-term fluctuations of plankton in relation to hydroclimatic features in the English Channel, Celtic Sea and Bay of Biscay. *Marine Ecology Progress Series*, 200: 93–102.
- Beaugrand, G., Ibañez, F., and Lindley, J. 2001. Geographical distribution and seasonal and diel changes in the diversity of calanoid copepods in the North Atlantic and North Sea. *Marine Ecology Progress Series*, 219: 189–203.
- Beaugrand, G., Ibañez, F., Lindley, J., Philip, C., and Reid, P. 2002a. Diversity of calanoid copepods in the North Atlantic and adjacent seas: species associations and biogeography. *Marine Ecology Progress Series*, 232: 179–195.
- Beaugrand, G., Reid, P. C., Ibañez, F., Lindley, J. A., and Edwards, M. 2002b. Reorganization of North Atlantic Marine Copepod Biodiversity and Climate. *Science*, 296: 1692–1694. American Association for the Advancement of Science.
- Beaugrand, G., Ibañez, F., and Lindley, J. A. 2003. An overview of statistical methods applied to CPR data. *Progress in Oceanography*, 58: 235–262.
- Beaugrand, G. 2004. The North Sea regime shift: Evidence, causes, mechanisms and consequences. *Progress in Oceanography*, 60: 245–262.
- Beaugrand, G., and Kirby, R. R. 2010. Climate, plankton and cod. *Global Change Biology*, 16: 1268–1280.
- Beaugrand, G., Mackas, D., and Goberville, E. 2013. Applying the concept of the ecological niche and a macroecological approach to understand how climate influences zooplankton: Advantages, assumptions, limitations and requirements. *Progress in Oceanography*, 111: 75–90.
- Beaugrand, G., Harlay, X., and Edwards, M. 2014. Detecting plankton shifts in the North Sea: a new abrupt ecosystem shift between 1996 and 2003. *Marine Ecology Progress Series*, 502: 85–104.
- Beaugrand, G., Conversi, A., Atkinson, A., Cloern, J., Chiba, S., Fonda-Umani, S., Kirby, R. R., *et al.* 2019. Prediction of unprecedented biological shifts in the global ocean. *Nature Climate Change*, 9: 237–243.
- Bedford, J., Ostle, C., Johns, D. G., Atkinson, A., Best, M., Bresnan, E., Machairopoulou, M., *et al.* 2020. Lifeform indicators reveal large-scale shifts in plankton across the North-West European shelf. *Global Change Biology*, 26: 3482–3497.
- Behrenfeld, M. J., Randerson, J. T., McClain, C. R., Feldman, G. C., Los, S. O., Tucker, C. J., Falkowski, P. G., *et al.* 2001. Biospheric Primary Production During an ENSO Transition. *Science*. <https://www.science.org/doi/10.1126/science.1055071>.
- Bellehumeur, C., Legendre, P., and Marcotte, D. 1997. Variance and spatial scales in a tropical rain forest: changing the size of sampling units. *Plant Ecology*, 130: 89–98.

## References

- Benedetti, F., Gasparini, S., and Ayata, S.-D. 2015. Identifying copepod functional groups from species functional traits. *Journal of Plankton Research*, 38: 159–166.
- Benedetti, F., Jalabert, L., Sourisseau, M., Becker, B., Cailliau, C., Desnos, C., Elineau, A., *et al.* 2019. The Seasonal and Inter-Annual Fluctuations of Plankton Abundance and Community Structure in a North Atlantic Marine Protected Area. *Frontiers in Marine Science*, 6: 214.
- Benjamini, Y., and Hochberg, Y. 1995. Controlling the false discovery rate: a practical and powerful approach to multiple testing. *Journal of the Royal statistical society: series B (Methodological)*, 57: 289–300. Wiley Online Library.
- Berghahn, R. 1986. Determining abundance, distribution, and mortality of 0-group plaice (*Pleuronectes platessa* L.) in the Wadden Sea. *Journal of Applied Ichthyology*, 2: 11–22.
- Bertrand, M., Brosset, P., Soudant, P., and Lebigre, C. 2022. Spatial and ontogenetic variations in sardine feeding conditions in the Bay of Biscay through fatty acid composition. *Marine Environmental Research*, 173: 105514.
- Bils, F., Aberle, N., Van Damme, C. J. G., Peck, M. A., and Moyano, M. 2022. Role of protozooplankton in the diet of North Sea autumn spawning herring (*Clupea harengus*) larvae. *Marine Biology*, 169: 90.
- Bode, A., Carrera, P., and Lens, S. 2003. The pelagic foodweb in the upwelling ecosystem of Galicia (NW Spain) during spring: natural abundance of stable carbon and nitrogen isotopes. *ICES Journal of Marine Science*, 60: 11–22.
- Bode, A., Alvarez-Ossorio, M. T., Carrera, P., and Lorenzo, J. 2004. Reconstruction of trophic pathways between plankton and the North Iberian sardine (*Sardina pilchardus*) using stable isotopes. *Scientia Marina*, 68: 165–178.
- Boëns, A., Grellier, P., Lebigre, C., and Petitgas, P. 2021. Determinants of growth and selective mortality in anchovy and sardine in the Bay of Biscay. *Fisheries Research*, 239: 105947.
- Boersma, M., Wiltshire, K. H., Kong, S.-M., Greve, W., and Renz, J. 2015. Long-term change in the copepod community in the southern German Bight. *Journal of Sea Research*, 101: 41–50.
- Bolle, L. J., Dickey-Collas, M., Beek, J. K. L. van, Erftemeijer, P. L. A., Witte, J. I., Veer, H. W. van der, and Rijnsdorp, A. D. 2009. Variability in transport of fish eggs and larvae. III. Effects of hydrodynamics and larval behaviour on recruitment in plaice. *Marine Ecology Progress Series*, 390: 195–211.
- Bollens, S. M. 1988. A model of the predatory impact of larval marine fish on the population dynamics of their zooplankton prey. *Journal of Plankton Research*, 10: 887–906.
- Bonnet, D., Richardson, A., Harris, R., Hirst, A., Beaugrand, G., Edwards, M., Ceballos, S., *et al.* 2005. An overview of *Calanus helgolandicus* ecology in European waters. *Progress in Oceanography*, 65: 1–53.
- Borcard, D., Gillet, F., and Legendre, P. 2011. *Numerical ecology with R*. Springer.
- Bouaziz, R., Le Loc'h, F., Rolet, C., Veillet, G., Munaron, J. M., Rabhi, K., Djebar, A. B., *et al.* 2021. Structure and seasonal variability in fish food webs in a small macrotidal estuary (Canche estuary, Eastern English Channel) based on stable carbon and nitrogen isotope analysis. *Regional Studies in Marine Science*, 44: 101694.
- Boyce, D. G., Frank, K. T., and Leggett, W. C. 2015. From mice to elephants: overturning the 'one size fits all' paradigm in marine plankton food chains. *Ecology Letters*, 18: 504–515.

## References

- Bracis, C., Lehuta, S., Savina-Rolland, M., Travers-Trolet, M., and Girardin, R. 2020. Improving confidence in complex ecosystem models: The sensitivity analysis of an Atlantis ecosystem model. *Ecological Modelling*, 431: 109133.
- Brett, M., and Müller-Navarra, D. 1997. The role of highly unsaturated fatty acids in aquatic foodweb processes. *Freshwater Biology*, 38: 483–499.
- Bristow, L. A., Jickells, T. D., Weston, K., Marca-Bell, A., Parker, R., and Andrews, J. E. 2013. Tracing estuarine organic matter sources into the southern North Sea using C and N isotopic signatures. *Biogeochemistry*, 113: 9–22.
- Brooks, J. L., and Dodson, S. I. 1965. Predation, Body Size, and Composition of Plankton. *Science*, 150: 28–35. American Association for the Advancement of Science.
- Brooks, M., E., Kristensen, K., Benthem, K., J., van, Magnusson, A., Berg, C., W., Nielsen, A., Skaug, H., J., *et al.* 2017. glmmTMB Balances Speed and Flexibility Among Packages for Zero-Inflated Generalized Linear Mixed Modeling. *The R Journal*, 9: 378.
- Brosset, P., Ménard, F., Fromentin, J.-M., Bonhommeau, S., Ulses, C., Bourdeix, J.-H., Bigot, J.-L., *et al.* 2015. Influence of environmental variability and age on the body condition of small pelagic fish in the Gulf of Lions. *Marine Ecology Progress Series*, 529: 219–231.
- Brosset, P., Bourg, B. L., Costalago, D., Bănaru, D., Beveren, E. V., Bourdeix, J.-H., Fromentin, J.-M., *et al.* 2016. Linking small pelagic dietary shifts with ecosystem changes in the Gulf of Lions. *Marine Ecology Progress Series*, 554: 157–171.
- Brosset, P., Fromentin, J.-M., Van Beveren, E., Lloret, J., Marques, V., Basilone, G., Bonanno, A., *et al.* 2017. Spatio-temporal patterns and environmental controls of small pelagic fish body condition from contrasted Mediterranean areas. *Progress in Oceanography*, 151: 149–162.
- Brown, J. H., Gillooly, J. F., Allen, A. P., Savage, V. M., and West, G. B. 2004. Toward a metabolic theory of ecology. *Ecology*, 85: 1771–1789.
- Bruce, M., Oyen, F., Bell, G., Asturiano, J. F., Farndale, B., Carrillo, M., Zanuy, S., *et al.* 1999. Development of broodstock diets for the European Sea Bass (*Dicentrarchus labrax*) with special emphasis on the importance of  $n-3$  and  $n-6$  highly unsaturated fatty acid to reproductive performance. *Aquaculture*, 177: 85–97.
- Brussard, P. F., Reed, J. M., and Tracy, C. R. 1998. Ecosystem management: what is it really? *Landscape and Urban Planning*, 40: 9–20.
- Brylinski, J. M., Lagadeuc, Y., Gentilhomme, V., Dupont, J. P., Lafite, R., Dupeuple, P. A., Huault, M. F., *et al.* 1991. Le 'fleuve côtier': Un phénomène hydrologique important en Manche orientale. Exemple du Pas-de-Calais. *Oceanologica Acta*, Special issue.
- Brylinski, J.-M. 2009. The pelagic copepods in the Strait of Dover (Eastern English Channel). A commented inventory 120 years after Eugène CANU. *Cahiers de Biologie Marine*, 50: 251–260. Station Biologique.
- Budge, S. M., Iverson, S. J., and Koopman, H. N. 2006. Studying trophic ecology in marine ecosystems using fatty acids: a primer on analysis and interpretation. *Marine Mammal Science*, 22: 759–801.
- Budge, S. M., Devred, E., Forget, M.-H., Stuart, V., Trzcinski, M. K., Sathyendranath, S., and Platt, T. 2014. Estimating concentrations of essential omega-3 fatty acids in the ocean: supply and demand. *ICES Journal of Marine Science*, 71: 1885–1893.
- Campanella, F., and van der Kooij, J. 2021. Spawning and nursery grounds of forage fish in Welsh and surrounding waters. Cefas Project Report for RSPB.

## References

- Campo, D., Mostarda, E., Castriota, L., Scarabello, M. P., and Andaloro, F. 2006. Feeding habits of the Atlantic bonito, *Sarda sarda* (Bloch, 1793) in the southern Tyrrhenian sea. *Fisheries Research*, 81: 169–175.
- Cardinale, B. J., Duffy, J. E., Gonzalez, A., Hooper, D. U., Perrings, C., Venail, P., Narwani, A., *et al.* 2012. Biodiversity loss and its impact on humanity. *Nature*, 486: 59–67. Nature Publishing Group.
- Casini, M., Cardinale, M., and Arrhenius, F. 2004. Feeding preferences of herring (*Clupea harengus*) and sprat (*Sprattus sprattus*) in the southern Baltic Sea. *ICES Journal of Marine Science*, 61: 1267–1277.
- Cavallo, A., and Peck, L. S. 2020. Lipid storage patterns in marine copepods: environmental, ecological, and intrinsic drivers. *ICES Journal of Marine Science*, 77: 1589–1601.
- Certain, G., Masse, J., Canneyt, O. V., Petitgas, P., Doremus, G., Santos, M. B., and Ridoux, V. 2011. Investigating the coupling between small pelagic fish and marine top predators using data collected from ecosystem-based surveys. *Marine Ecology Progress Series*, 422: 23–39.
- Chatelier, A., McKenzie, D. J., Prinnet, A., Galois, R., Robin, J., Zambonino, J., and Claireaux, G. 2006. Associations between tissue fatty acid composition and physiological traits of performance and metabolism in the seabass (*Dicentrarchus labrax*). *Journal of Experimental Biology*, 209: 3429–3439.
- Checkley, D. 1982. Selective Feeding by Atlantic Herring (*Clupea harengus*) Larvae on Zooplankton in Natural Assemblages. *Marine Ecology Progress Series*, 9: 245–253.
- Checkley Jr, D. M., Ortner, P. B., Settle, L. R., and Cummings, S. R. 1997. A continuous, underway fish egg sampler. *Fisheries Oceanography*, 6: 58–73. Wiley Online Library.
- Chenillat, F., Rivièrè, P., and Ohman, M. D. 2021. On the sensitivity of plankton ecosystem models to the formulation of zooplankton grazing. *PLOS ONE*, 16: e0252033. Public Library of Science.
- Chouvelon, T., Spitz, J., Caurant, F., Mèndez-Fernandez, P., Chappuis, A., Laugier, F., Le Goff, E., *et al.* 2012. Revisiting the use of  $\delta^{15}\text{N}$  in meso-scale studies of marine food webs by considering spatio-temporal variations in stable isotopic signatures – The case of an open ecosystem: The Bay of Biscay (North-East Atlantic). *Progress in Oceanography*, 101: 92–105.
- Christensen, N. L., Bartuska, A. M., Brown, J. H., Carpenter, S., D’Antonio, C., Francis, R., Franklin, J. F., *et al.* 1996. The Report of the Ecological Society of America Committee on the Scientific Basis for Ecosystem Management. *Ecological Applications*, 6: 665–691.
- Chust, G., Allen, J. I., Bopp, L., Schrum, C., Holt, J., Tsiaras, K., Zavatarelli, M., *et al.* 2014. Biomass changes and trophic amplification of plankton in a warmer ocean. *Global Change Biology*, 20: 2124–2139. John Wiley & Sons, Ltd.
- Clark, R. A., and Frid, C. L. 2001. Long-term changes in the North Sea ecosystem. *Environmental Reviews*, 9: 131–187. NRC Research Press.
- Clarke, K. R., and Warwick, R. M. 2001. Change in marine communities. An approach to statistical analysis and interpretation, 2: 1–68. PRIMER-E Ltd Plymouth.
- Cohen, J. E., Pimm, S. L., Yodzis, P., and Saldana, J. 1993. Body Sizes of Animal Predators and Animal Prey in Food Webs. *The Journal of Animal Ecology*, 62: 67.
- Colebrook, J. M. 1984. Continuous plankton records: relationships between species of phytoplankton and zooplankton in the seasonal cycle. *Marine Biology*, 83: 313–323.

## References

- Colebrook, J. M. 1987. Environmental influences on long-term variability in marine plankton. *In* Long-Term Changes in Coastal Benthic Communities. Developments in Hydrobiology, Vol. 38, pp. 309–325. Ed. by C. Heip, B. F. Keegan, and J. R. Lewis. Springer Netherlands, Dordrecht.
- Conway, D. V. P. 2012. Conway, D.V.P. (2012). Marine zooplankton of southern Britain. Part 2: Arachnida, Pycnogonida, Cladocera, Facetotecta, Cirripedia and Copepoda (ed. A.W.G. John). Occasional Publications. Marine Biological Association of the United Kingdom, No 26 Plymouth, United Kingdom 163 pp. Occasional Publications. Marine Biological Association of the United Kingdom, Plymouth, United Kingdom. 138 pp. <http://rgdoi.net/10.13140/2.1.4704.4800>.
- Conway, D. V. P. 2015. Marine zooplankton of southern Britain. Part 3: Ostracoda, Stomatopoda, Nebaliacea, Mysida, Amphipoda, Isopoda, Cumacea, Euphausiacea, Decapoda, Annelida, Tardigrada, Nematoda, Phoronida, Bryozoa, Entoprocta, Brachiopoda, Echinodermata, Chaetognatha, Hemichordata and Chordata. Occasional Publications. Marine Biological Association of the United Kingdom, Plymouth, United Kingdom. 271 pp. <https://plymsea.ac.uk/id/eprint/6360/>.
- Coombs, S. H., Halliday, N. C., Southward, A. J., and Hawkins, S. J. 2005. Distribution and abundance of sardine (*Sardina pilchardus*) eggs in the English Channel from Continuous Plankton Recorder sampling, 1958–1980. *Journal of the Marine Biological Association of the United Kingdom*, 85: 1243–1247. Cambridge University Press.
- Coombs, S. H., Halliday, N. C., Conway, D. V. P., and Smyth, T. J. 2010. Sardine (*Sardina pilchardus*) egg abundance at station L4, Western English Channel, 1988–2008. *Journal of Plankton Research*, 32: 693–697.
- Coppin, F., Curet, L., Dauvin, J.-C., Delavenne, J., Dewarumez, J.-M., Dupuis, L., Foveau, A., *et al.* 2009. Channel Habitat Atlas for marine Resource Management final report / Atlas des Habitats des Ressources Marines de la Manche Orientale, rapport final (CHARM II). INTERREG 3a Programme, IFREMER, Boulogne-sur-Mer. 626 pp.
- Cordier, M., Brichon, G., Weber, J.-M., and Zwingelstein, G. 2002. Changes in the fatty acid composition of phospholipids in tissues of farmed sea bass (*Dicentrarchus labrax*) during an annual cycle. *Roles of environmental temperature and salinity. Comparative Biochemistry and Physiology Part B: Biochemistry and Molecular Biology*, 133: 281–288.
- Corkett, C. J., and McLaren, I. A. 1970. Relationships between Development Rate of Eggs and Older Stages of Copepods. *Journal of the Marine Biological Association of the United Kingdom*, 50: 161–168. Cambridge University Press.
- Corten, A. 2001. Northern distribution of North Sea herring as a response to high water temperatures and/or low food abundance. *Fisheries Research*, 50: 189–204.
- Corten, A. 2013. Recruitment depressions in North Sea herring. *ICES Journal of Marine Science*, 70: 1–15.
- Costalago, D., Garrido, S., and Palomera, I. 2015. Comparison of the feeding apparatus and diet of European sardines *Sardina pilchardus* of Atlantic and Mediterranean waters: ecological implications. *Journal of Fish Biology*, 86: 1348–1362.
- Costanza, R., de Groot, R., Sutton, P., van der Ploeg, S., Anderson, S. J., Kubiszewski, I., Farber, S., *et al.* 2014. Changes in the global value of ecosystem services. *Global Environmental Change*, 26: 152–158.
- Cotonnec, G., Seuront, L., Thoumelin, G., and Fraga-Lago, L. 2003. Fatty acid composition of *Acartia clausi*, *Pseudocalanus elongatus* and *Temora*



## References

- longicornis* associated with their diet in the eastern English Channel during a spring bloom of *Phaeocystis sp.* *La mer*, 41: 37–51.
- Cresson, P., Chouvelon, T., Bustamante, P., Bănaru, D., Baudrier, J., Le Loc'h, F., Mauffret, A., *et al.* 2020. Primary production and depth drive different trophic structure and functioning of fish assemblages in French marine ecosystems. *Progress in Oceanography*, 186: 102343.
- Cury, P., Bakun, A., Crawford, R. J. M., Jarre, A., Quiñones, R. A., Shannon, L. J., and Verheye, H. M. 2000. Small pelagics in upwelling systems: patterns of interaction and structural changes in “wasp-waist” ecosystems. *ICES Journal of Marine Science*, 57: 603–618.
- Cushing, D. H. 1990. Plankton Production and Year-class Strength in Fish Populations: an Update of the Match/Mismatch Hypothesis. *In Advances in Marine Biology*, pp. 249–293. Ed. by J. H. S. Blaxter and A. J. Southward. Academic Press. <https://www.sciencedirect.com/science/article/pii/S0065288108602023>.
- Daewel, U., Hjøllø, S. S., Huret, M., Ji, R., Maar, M., Niiranen, S., Travers-Trolet, M., *et al.* 2014. Predation control of zooplankton dynamics: a review of observations and models. *ICES Journal of Marine Science*, 71: 254–271.
- Daily, G. R. 1997. Nature’s Services: Societal Dependence on Natural Ecosystems. *Environmental Values*, 7: 365–367. White Horse Press.
- Dalsgaard, J., St. John, M., Kattner, G., Müller-Navarra, D., and Hagen, W. 2003. Fatty acid trophic markers in the pelagic marine environment. *In Advances in Marine Biology*, pp. 225–340. Elsevier. <https://linkinghub.elsevier.com/retrieve/pii/S0065288103460057>.
- Daly, E. A., Brodeur, R. D., and Auth, T. D. 2017. Anomalous ocean conditions in 2015: impacts on spring Chinook salmon and their prey field. *Marine Ecology Progress Series*, 566: 169–182.
- Dam, H. G., and Lopes, R. M. 2003. Omnivory in the calanoid copepod *Temora longicornis*: feeding, egg production and egg hatching rates. *Journal of Experimental Marine Biology and Ecology*, 292: 119–137.
- Daufresne, M., Lengfellner, K., and Sommer, U. 2009. Global warming benefits the small in aquatic ecosystems. *Proceedings of the National Academy of Sciences*, 106: 12788–12793.
- Dauvin, J.-C., Thiébaud, E., and Wang, Z. 1998. Short-term changes in the mesozooplanktonic community in the Seine ROFI (Region of Freshwater Influence) (eastern English Channel). *Journal of Plankton Research*, 20: 1145–1167.
- Dauvin, J.-C. 2012. Are the eastern and western basins of the English Channel two separate ecosystems? *Marine Pollution Bulletin*, 64: 463–471.
- Day, L., Brind’Amour, A., Cresson, P., Chouquet, B., and Le Bris, H. 2021. Contribution of estuarine and coastal habitats within nursery to the diets of juvenile fish in spring and autumn. *Estuaries and Coasts*, 44: 1100–1117.
- de Figueiredo, G. M., Nash, R. D. M., and Montagnes, D. J. S. 2005. The role of the generally unrecognised microprey source as food for larval fish in the Irish Sea. *Marine Biology*, 148: 395–404.
- De Leonardis, A., and Macciola, V. 2004. A study on the lipid fraction of Adriatic sardine filets (*Sardina pilchardus*). *Food / Nahrung*, 48: 209–212.
- De Troch, M., Boeckx, P., Cnudde, C., Van Gansbeke, D., Vanreusel, A., Vincx, M., and Caramujo, M. 2012. Bioconversion of fatty acids at the basis of marine food webs: insights from a compound-specific stable isotope analysis. *Marine Ecology Progress Series*, 465: 53–67.

## References

- De Veen, J. F. 1978. On selective tidal transport in the migration of North Sea plaice (*Pleuronectes platessa*) and other flatfish species. *Netherlands Journal of Sea Research*: 115–147.
- Décima, M. 2022. Zooplankton trophic structure and ecosystem productivity. *Marine Ecology Progress Series*, 692: 23–42.
- Denis, J., Vallet, C., Courcot, L., Lefebvre, V., Caboche, J., Antajan, E., Marchal, P., *et al.* 2016. Feeding strategy of Downs herring larvae (*Clupea harengus* L.) in the English Channel and North Sea. *Journal of Sea Research*, 115: 33–46.
- Denis, J., Mahe, K., Tavernier, E., Monchy, S., Vincent, D., Vallet, C., Marchal, P., *et al.* 2017. Ontogenetic changes in the larval condition of Downs herring: use of a multi-index approach at an individual scale. *Marine Biology*, 164: 154.
- Deschamps, M. M., Boersma, M., Meunier, C. L., Kirstein, I. V., Wiltshire, K. H., and Di Pane, J. 2024. Major shift in the copepod functional community of the southern North Sea and potential environmental drivers. *ICES Journal of Marine Science*, 81: 540–552. Oxford University Press (OUP).
- Di Pane, J., Joly, L., Koubbi, P., Giraldo, C., Monchy, S., Tavernier, E., Marchal, P., *et al.* 2019. Ontogenetic shift in the energy allocation strategy and physiological condition of larval plaice (*Pleuronectes platessa*). *PLOS ONE*, 14: e0222261.
- Dickey-Collas, D. M. 2005. Desk Study on the transport of larval herring in the southern North Sea (Downs herring). C031/05. RIVO-Netherlands Institute for Fisheries Research.
- Dickey-Collas, M., Bolle, L., Van Beek, J., and Erftemeijer, P. 2009. Variability in transport of fish eggs and larvae. II. Effects of hydrodynamics on the transport of Downs herring larvae. *Marine Ecology Progress Series*, 390: 183–194.
- Dickey-Collas, M., Nash, R. D. M., Brunel, T., van Damme, C. J. G., Marshall, C. T., Payne, M. R., Corten, A., *et al.* 2010. Lessons learned from stock collapse and recovery of North Sea herring: a review. *ICES Journal of Marine Science*, 67: 1875–1886.
- Doray, M., Petitgas, P., Huret, M., Duhamel, E., Romagnan, J. B., Authier, M., Dupuy, C., *et al.* 2018. Monitoring small pelagic fish in the Bay of Biscay ecosystem, using indicators from an integrated survey. *Progress in Oceanography*, 166: 168–188.
- Dudeck, T., Rohlf, N., Möllmann, C., and Hufnagl, M. 2021. Winter zooplankton dynamics in the English Channel and southern North Sea: trends and drivers from 1991 to 2013. *Journal of Plankton Research*, 43: 244–256.
- Dufrêne, M., and Legendre, P. 1997. Species assemblages and indicator species: The need for a flexible asymmetrical approach. *Ecological Monographs*, 67: 345–366.
- Eberlein, K. 1994. Risk of anthropogenic nitrogen and phosphorus entry into the North Sea ecosystem. *Zentralblatt für Hygiene und Umweltmedizin = International journal of hygiene and environmental medicine*, 196: 285–311.
- Edwards, M., Beaugrand, G., Reid, P. C., Rowden, A. A., and Jones, M. B. 2002. Ocean climate anomalies and the ecology of the North Sea. *Marine Ecology Progress Series*, 239: 1–10.
- Edwards, M., and Richardson, A. J. 2004. Impact of climate change on marine pelagic phenology and trophic mismatch. *Nature*, 430: 881–884. Nature Publishing Group.
- El Mghazli, H., Mounir, A., Znari, M., Naimi, M., El Ouizgani, H., and Aourir, M. 2020. A comparison of spring body condition, maturation status, and diet in the European sardine, *Sardina pilchardus* (Teleostei: Clupeidae) from contrasting

## References

- environments off the Moroccan Atlantic coast. *Marine Biology Research*, 16: 431–445. Taylor & Francis.
- Ellis, J. R., Pawson, M. G., and Shackley, S. E. 1996. The Comparative Feeding Ecology of Six Species of Shark and Four Species of Ray (Elasmobranchii) In The North-East Atlantic. *Journal of the Marine Biological Association of the United Kingdom*, 76: 89–106.
- Eloire, D., Somerfield, P. J., Conway, D. V. P., Halsband-Lenk, C., Harris, R., and Bonnet, D. 2010. Temporal variability and community composition of zooplankton at station L4 in the Western Channel: 20 years of sampling. *Journal of Plankton Research*, 32: 657–679.
- Engel, M., and Hirche, H.-J. 2004. Seasonal variability and inter-specific differences in hatching of calanoid copepod resting eggs from sediments of the German Bight (North Sea). *Journal of Plankton Research*, 26: 1083–1093.
- FAO. 2018. The State of Mediterranean and Black Sea Fisheries 2018. <https://openknowledge.fao.org/items/6c239c3a-49bc-47e2-911d-eb93f7803ba5>.
- FAO. 2019. Report of the FAO Working Group on the Assessment of Small Pelagic Fish Off Northwest Africa. Banjul. The Gambia.
- Farkas, T., Csengeri, I., Majoros, F., and Oláh, J. 1980. Metabolism of fatty acids in fish: III. Combined effect of environmental temperature and diet on formation and deposition of fatty acids in the carp, *Cyprinus carpio* Linnaeus 1758. *Aquaculture*, 20: 29–40.
- Fenaux, R., Bedo, A., and Gorsky, G. 1986. Premières données sur la dynamique d'une population d' *Oikopleura dioica* Fol, 1872 (Appendiculaire) en élevage. *Canadian Journal of Zoology*, 64: 1745–1749.
- Feuilloley, G., Fromentin, J.-M., Stemmann, L., Demarcq, H., Estournel, C., and Saraux, C. 2020. Concomitant changes in the environment and small pelagic fish community of the Gulf of Lions. *Progress in Oceanography*, 186: 102375.
- Figueiredo, G. G. A. A. de, Schwamborn, R., Bertrand, A., Munaron, J.-M., and Le Loch, F. 2020. Body size and stable isotope composition of zooplankton in the western tropical Atlantic. *Journal of Marine Systems*, 212: 103449.
- Fransz, H. G., and van Arkel, W. G. 1983. Fluctuations and succession of common pelagic copepod species in the Dutch Wadden Sea. *Oceanologica Acta*. <https://archimer.ifremer.fr/doc/00247/35793/34306.pdf>.
- Fransz, H. G., Gonzalez, S. R., and Breteler, W. C. M. K. 1990. Fecundity as a factor controlling the seasonal population cycle in *Temora longicornis* (Copepoda, Calanoida). *In* *Reproduction, Genetics and Distribution of Marine Organisms*, Ryland, S.J., Tyler, P.A., pp. 83–90. Olsen & Olsen, Denmark.
- Fransz, H. G., Colebrook, J. M., Gamble, J. C., and Krause, M. 1991. The zooplankton of the North Sea. *Netherlands Journal of Sea Research*, 28: 1–52.
- Frelat, R., Kortsch, S., Kröncke, I., Neumann, H., Nordström, M. C., Olivier, P. E. N., and Sell, A. F. 2022. Food web structure and community composition: a comparison across space and time in the North Sea. *Ecography*, 2022.
- Friedland, K. D., Record, N. R., Asch, R. G., Kristiansen, T., Saba, V. S., Drinkwater, K. F., Henson, S., *et al.* 2016. Seasonal phytoplankton blooms in the North Atlantic linked to the overwintering strategies of copepods. *Elementa: Science of the Anthropocene*, 4: 000099.
- Fry, B. 2006. *Stable Isotope Ecology*. Springer, Berlin.
- Gabaldón, C., Devetter, M., Hejzlar, J., Šimek, K., Znachor, P., Nedoma, J., and Seda, J. 2019. Seasonal strengths of the abiotic and biotic drivers of a zooplankton community. *Freshwater Biology*, 64: 1326–1341.

## References

- Galloway, A. W. E., and Winder, M. 2015. Partitioning the Relative Importance of Phylogeny and Environmental Conditions on Phytoplankton Fatty Acids. *PLOS ONE*, 10: e0130053. Public Library of Science.
- Garrido, S., Marçalo, A., Zwolinski, J., and Lingen, C. D. van der. 2007a. Laboratory investigations on the effect of prey size and concentration on the feeding behaviour of *Sardina pilchardus*. *Marine Ecology Progress Series*, 330: 189–199.
- Garrido, S., Rosa, R., Ben-Hamadou, R., Cunha, M. E., Chícharo, M. A., and van der Lingen, C. D. 2007b. Effect of maternal fat reserves on the fatty acid composition of sardine (*Sardina pilchardus*) oocytes. *Comparative Biochemistry and Physiology Part B: Biochemistry and Molecular Biology*, 148: 398–409.
- Garrido, S., Ben-Hamadou, R., Oliveira, P. B., Cunha, M. E., Chícharo, M. A., and Lingen, C. D. van der. 2008a. Diet and feeding intensity of sardine *Sardina pilchardus*: correlation with satellite-derived chlorophyll data. *Marine Ecology Progress Series*, 354: 245–256.
- Garrido, S., Rosa, R., Ben-Hamadou, R., Cunha, M. E., Chícharo, M. A., and van der Lingen, C. D. 2008b. Spatio-temporal variability in fatty acid trophic biomarkers in stomach contents and muscle of Iberian sardine (*Sardina pilchardus*) and its relationship with spawning. *Marine Biology*, 154: 1053–1065.
- Garrido, S., Silva, A., Pastor, J., Dominguez, R., Silva, A. V., and Santos, A. M. 2015. Trophic ecology of pelagic fish species off the Iberian coast: diet overlap, cannibalism and intraguild predation. *Marine Ecology Progress Series*, 539: 271–285.
- Gaughan, D. J. 1991. Feeding by estuarine and marine fish larvae. *Marine Ecology Progress Series* 51, 51: 19–33.
- Geffen, A. J. 2009. Advances in herring biology: from simple to complex, coping with plasticity and adaptability. *ICES Journal of Marine Science*, 66: 1688–1695.
- Giannoulaki, M., Machias, A., and Tsimenides, N. 1999. Ambient luminance and vertical migration of the sardine *Sardina pilchardus*. *Marine Ecology Progress Series*, 178: 29–38.
- Gibson, R. N., and Ezzi, I. A. 1992. The relative profitability of particulate- and filter-feeding in the herring, *Clupea harengus* L. *Journal of Fish Biology*, 40: 577–590.
- Giraldo, C., Ernande, B., Cresson, P., Kopp, D., Cachera, M., Travers-Trolet, M., and Lefebvre, S. 2017. Depth gradient in the resource use of a fish community from a semi-enclosed sea. *Limnology and Oceanography*, 62: 2213–2226.
- Giraldo, C., Cresson, P., MacKenzie, K., Fontaine, V., Loots, C., Delegrange, A., and Lefebvre, S. 2024. Insights into planktonic food-web dynamics through the lens of size and season. *Scientific Reports*, 14: 1684.
- Girardin, R., Fulton, E. A., Lehuta, S., Rolland, M., Thébaud, O., Travers-Trolet, M., Vermard, Y., *et al.* 2018. Identification of the main processes underlying ecosystem functioning in the Eastern English Channel, with a focus on flatfish species, as revealed through the application of the Atlantis end-to-end model. *Estuarine, Coastal and Shelf Science*, 201: 208–222.
- Gladyshev, M. I., Sushchik, N. N., Makhutova, O. N., Dubovskaya, O. P., Kravchuk, E. S., Kalachova, G. S., and Khromechek, E. B. 2010. Correlations between fatty acid composition of seston and zooplankton and effects of environmental parameters in a eutrophic Siberian reservoir. *Limnologica*, 40: 343–357.
- Gladyshev, M. I., Sushchik, N. N., Tolomeev, A. P., and Dgebuadze, Y. Y. 2018. Meta-analysis of factors associated with omega-3 fatty acid contents of wild fish. *Reviews in Fish Biology and Fisheries*, 28: 277–299.

## References

- Gorsky, G., Ohman, M. D., Picheral, M., Gasparini, S., Stemmann, L., Romagnan, J.-B., Cawood, A., *et al.* 2010. Digital zooplankton image analysis using the ZooScan integrated system. *Journal of Plankton Research*, 32: 285–303.
- Graeve, M., Kattner, G., and Hagen, W. 1994. Diet-induced changes in the fatty acid composition of Arctic herbivorous copepods: Experimental evidence of trophic markers. *Journal of Experimental Marine Biology and Ecology*, 182: 97–110.
- Graham, M., and Harding, J. P. 1938. Some observations of the hydrology and plankton of the North Sea and English Channel. *Journal of the Marine Biological Association of the United Kingdom*, 23: 201.
- Grandremy, N., Romagnan, J.-B., Dupuy, C., Doray, M., Huret, M., and Petitgas, P. 2023. Hydrology and small pelagic fish drive the spatio-temporal dynamics of springtime zooplankton assemblages over the Bay of Biscay continental shelf. *Progress in Oceanography*, 210: 102949.
- Grandremy, N., Bourriau, P., Daché, E., Danielou, M.-M., Doray, M., Dupuy, C., Forest, B., *et al.* 2024. Metazoan zooplankton in the Bay of Biscay: a 16-year record of individual sizes and abundances obtained using the ZooScan and ZooCAM imaging systems. *Earth System Science Data*, 16: 1265–1282.
- Greve, W., Reiners, F., Nast, J., and Hoffmann, S. 2004. Helgoland Roads meso- and macrozooplankton time-series 1974 to 2004: lessons from 30 years of single spot, high frequency sampling at the only off-shore island of the North Sea. *Helgoland Marine Research*, 58: 274–288.
- Grift, R. E., Rijnsdorp, A. D., Barot, S., Heino, M., and Dieckmann, U. 2003. Fisheries-induced trends in reaction norms for maturation in North Sea plaice. *Marine Ecology Progress Series*, 257: 247–257.
- Grosjean, P., Picheral, M., Warembourg, C., and Gorsky, G. 2004. Enumeration, measurement, and identification of net zooplankton samples using the ZOOSCAN digital imaging system. *ICES Journal of Marine Science*, 61: 518–525.
- Groß, E., Di Pane, J., Boersma, M., and Meunier, C. L. 2022. River discharge-related nutrient effects on North Sea coastal and offshore phytoplankton communities. *Journal of Plankton Research*, 44: 947–960.
- Gubiani, É. A., Ruaro, R., Ribeiro, V. R., and Fé, Ú. M. G. D. S. 2020. Relative condition factor: Le Cren's legacy for fisheries science. *Acta Limnologica Brasiliensia*, 32: e3.
- Haberkorn, H., Lambert, C., Le Goïc, N., Guéguen, M., Moal, J., Palacios, E., Lassus, P., *et al.* 2010. Effects of *Alexandrium minutum* exposure upon physiological and hematological variables of diploid and triploid oysters, *Crassostrea gigas*. *Aquatic Toxicology*, 97: 96–108.
- Hagen, W., and Auel, H. 2001. Seasonal adaptations and the role of lipids in oceanic zooplankton. *Zoology*, 104: 313–326.
- Halpern, B. S., Walbridge, S., Selkoe, K. A., Kappel, C. V., Micheli, F., D'Agrosa, C., Bruno, J. F., *et al.* 2008. A Global Map of Human Impact on Marine Ecosystems. *Science*, 319: 948–952. American Association for the Advancement of Science.
- Halsband, C., and Hirche, H. J. 2001. Reproductive cycles of dominant calanoid copepods in the North Sea. *Marine Ecology Progress Series*, 209: 219–229.
- Halsband-Lenk, C., Carlotti, F., and Greve, W. 2004. Life-history strategies of calanoid congeners under two different climate regimes: a comparison. *ICES Journal of Marine Science*, 61: 709–720.
- Hammond, P. S., Hall, A. J., and Prime, J. H. 1994. The Diet of Grey Seals Around Orkney and Other Island and Mainland Sites in North-Eastern Scotland. *Journal of Applied Ecology*, 31: 340–350.

## References

- Harding, D. 1978. The spawning of plaice (*Pleuronectes platessa*) in the southern North Sea and English Channel. Rapp. P.-v. Reun. Cons. Int. Explor. Mer, 172: 102–113.
- Harmelin-Vivien, M., Loizeau, V., Mellon, C., Beker, B., Arlhac, D., Bodiguel, X., Ferraton, F., *et al.* 2008. Comparison of C and N stable isotope ratios between surface particulate organic matter and microphytoplankton in the Gulf of Lions (NW Mediterranean). Continental Shelf Research, 28: 1911–1919.
- Hartig, F. 2022. DHARMA: Residual Diagnostics for Hierarchical (Multi-Level / Mixed) Regression Models. <https://CRAN.R-project.org/package=DHARMA>.
- Hattab, T., Albouy, C., Ben Rais Lasram, F., Le Loc'h, F., Guilhaumon, F., and Leprieur, F. 2015. A biogeographical regionalization of coastal Mediterranean fishes. Journal of Biogeography, 42: 1336–1348.
- Hatton, I. A., Heneghan, R. F., Bar-On, Y. M., and Galbraith, E. D. 2021. The global ocean size spectrum from bacteria to whales. Science Advances, 7: eabh3732. American Association for the Advancement of Science.
- Hawkins, S. J., Southward, A. J., and Genner, M. J. 2003. Detection of environmental change in a marine ecosystem—evidence from the western English Channel. Science of The Total Environment, 310: 245–256.
- Hay, S. 1995. Egg production and secondary production of common North Sea copepods: Field estimates with regional and seasonal comparisons. ICES Journal of Marine Science, 52: 315–327.
- Hay, S. J., Kiørboe, T., and Matthews, A. 1991. Zooplankton biomass and production in the North Sea during the Autumn Circulation experiment, October 1987–March 1988. Continental Shelf Research, 11: 1453–1476.
- Hays, G. C., Kennedy, H., and Frost, B. W. 2001. Individual variability in diel vertical migration of a marine copepod: Why some individuals remain at depth when others migrate. Limnology and Oceanography, 46: 2050–2054.
- Hébert, M.-P., Beisner, B. E., and Maranger, R. 2017. Linking zooplankton communities to ecosystem functioning: toward an effect-trait framework. Journal of Plankton Research, 39: 3–12.
- Hébert, M.-P., Beisner, B. E., Rautio, M., and Fussmann, G. F. 2021. Warming winters in lakes: Later ice onset promotes consumer overwintering and shapes springtime planktonic food webs. Proceedings of the National Academy of Sciences, 118: e2114840118.
- Henderson, R. J. 1993. Fatty acid metabolism in freshwater fish with particular reference to polyunsaturated fatty acids. Archiv für Tierernaehrung, 49. <https://www.tandfonline.com/doi/abs/10.1080/17450399609381859>.
- Heneghan, R. F., Everett, J. D., Blanchard, J. L., Sykes, P., and Richardson, A. J. 2023. Climate-driven zooplankton shifts cause large-scale declines in food quality for fish. Nature Climate Change, 13: 470–477. Nature Publishing Group.
- Hensen, V. 1887. Kapitel 1: Über die Bestimmung des Plankton's oder des im Meere treibenden Materials an Pflanzen und Thieren. Jahresbericht der Commission zur Wissenschaftlichen Untersuchung der Deutschen Meere in Kiel: für die Jahre ..., 12–16: 1–107, I. Parey.
- Hijmans, R. J. 2012. raster: Geographic analysis and modeling with raster data. R package version 2.0-12.
- Hiltunen, M., Strandberg, U., Taipale, S. J., and Kankaala, P. 2015. Taxonomic identity and phytoplankton diet affect fatty acid composition of zooplankton in large lakes with differing dissolved organic carbon concentration. Limnology and Oceanography, 60: 303–317.

## References

- Hiltunen, M., Strandberg, U., Brett, M. T., Winans, A. K., Beauchamp, D. A., Miika, K., and Keister, J. E. 2022. Taxonomic, Temporal, and Spatial Variations in Zooplankton Fatty Acid Composition in Puget Sound, WA, USA. *Estuaries and Coasts*, 45: 567–581. Springer Nature B.V., Port Republic, Netherlands. 567–581 pp.
- Hixson, S. M., and Arts, M. T. 2016. Climate warming is predicted to reduce omega-3, long-chain, polyunsaturated fatty acid production in phytoplankton. *Global Change Biology*, 22: 2744–2755.
- Hjort, J. 1914. Fluctuations in the great fisheries of Northern Europe viewed in the light of biological research. *Rapp. P-V Réun*, 20: 1–228.
- Hoch, T., and Garreau, P. 1998. Phytoplankton dynamics in the English Channel: a simplified three-dimensional approach. *Journal of Marine Systems*, 16: 133–150.
- Holland, M. M., Louchart, A., Artigas, L. F., Ostle, C., Atkinson, A., Rombouts, I., Graves, C. A., *et al.* 2023. Major declines in NE Atlantic plankton contrast with more stable populations in the rapidly warming North Sea. *Science of The Total Environment*, 898: 165505.
- Hooper, D. U., Chapin III, F. S., Ewel, J. J., Hector, A., Inchausti, P., Lavorel, S., Lawton, J. H., *et al.* 2005. Effects of Biodiversity on Ecosystem Functioning: A Consensus of Current Knowledge. *Ecological Monographs*, 75: 3–35.
- Houde, E. D. 2008. Emerging from Hjort's Shadow. *Journal of Northwest Atlantic Fishery Science*, 41: 53–70.
- Houde, E. D. 2016. Recruitment Variability. *In Fish Reproductive Biology*, pp. 98–187. John Wiley & Sons, Ltd. <https://onlinelibrary.wiley.com/doi/abs/10.1002/9781118752739.ch3>.
- Houghton, R. G., and Harding, D. 1976. The plaice of the English Channel: spawning and migration. *ICES Journal of Marine Science*, 36: 229–239.
- Hovenkamp, F. 1990. Growth differences in larval plaice *Pleuronectes platessa* in the Southern Bight of the North Sea as indicated by otolith increments and RNA/DNA ratios. *Mar. Ecol. Prog. Ser.*, 58: 205–215.
- Htun-Han, M. 1978. The reproductive biology of the dab *Limanda limanda* (L.) in the North Sea: Seasonal changes in the ovary. *Journal of Fish Biology*, 13: 351–359.
- Hufnagl, M., and Peck, M. A. 2011. Physiological individual-based modelling of larval Atlantic herring (*Clupea harengus*) foraging and growth: insights on climate-driven life-history scheduling. *ICES Journal of Marine Science*, 68: 1170–1188.
- Hufnagl, M., Peck, M. A., Nash, R. D. M., Pohlmann, T., and Rijnsdorp, A. D. 2013. Changes in potential North Sea spawning grounds of plaice (*Pleuronectes platessa* L.) based on early life stage connectivity to nursery habitats. *Journal of Sea Research*, 84: 26–39.
- Hufnagl, M., Peck, M. A., Nash, R. D. M., and Dickey-Collas, M. 2015. Unravelling the Gordian knot! Key processes impacting overwintering larval survival and growth: A North Sea herring case study. *Progress in Oceanography*, 138: 486–503.
- Hunt, A. Ö., Özkan, F., Engin, K., and Tekelioğlu, N. 2011. The effects of freshwater rearing on the whole body and muscle tissue fatty acid profile of the European sea bass (*Dicentrarchus labrax*). *Aquaculture International*, 19: 51–61.
- Hunter, E., Metcalfe, J. D., and Reynolds, J. D. 2003. Migration route and spawning area fidelity by North Sea plaice. *Proceedings of the Royal Society B: Biological Sciences*, 270: 2097–2103.

## References

- Hunter, E., Metcalfe, J. D., Arnold, G. P., and Reynolds, J. D. 2004. Impacts of Migratory Behaviour on Population Structure in North Sea Plaice. *Journal of Animal Ecology*, 73: 377–385.
- Huynh, M. D., Kitts, D. D., Hu, C., and Trites, A. W. 2007. Comparison of fatty acid profiles of spawning and non-spawning Pacific herring, *Clupea harengus pallasii*. *Comparative Biochemistry and Physiology Part B: Biochemistry and Molecular Biology*, 146: 504–511.
- ICES. 2004. Report of the Herring Assessment Working Group for the Area South of 62°N (HAWG). ICES Scientific Reports. <https://www.ices.dk/sites/pub/CM%20Documents/2004/ACFM/ACFM1804.PDF>.
- ICES. 2007. Report of the Workshop on the Integration of Environmental Information into Fisheries Management Strategies and Advice (WKEFA). report. ICES Expert Group reports (until 2018). [https://ices-library.figshare.com/articles/report/Report\\_of\\_the\\_Workshop\\_on\\_the\\_Integration\\_of\\_Environmental\\_Information\\_into\\_Fisheries\\_Management\\_Strategies\\_and\\_Advice\\_WKEFA\\_/19280237/1](https://ices-library.figshare.com/articles/report/Report_of_the_Workshop_on_the_Integration_of_Environmental_Information_into_Fisheries_Management_Strategies_and_Advice_WKEFA_/19280237/1).
- ICES. 2008. Report of the Working Group on Multispecies Assessment Methods (WGSAM). report. ICES Expert Group reports (until 2018). [https://ices-library.figshare.com/articles/report/Report\\_of\\_the\\_Working\\_Group\\_on\\_Multispecies\\_Assessment\\_Methods\\_WGSAM\\_/19268582/1](https://ices-library.figshare.com/articles/report/Report_of_the_Working_Group_on_Multispecies_Assessment_Methods_WGSAM_/19268582/1).
- ICES. 2017. Report of the Benchmark Workshop on Pelagic Stocks, 6–10 February 2017, Lisbon, Portugal. ICES CM 2017/ACOM, 35: 278.
- ICES. 2018. Report of the Working Group on Southern Horse Mackerel, Anchovy and Sardine (WGHANSA). ICES C. 2018/ACOM17, 659 pp. doi:ICES CM 2011/ACOM:16.
- ICES. 2021. Stock Annex: Plaice (*Pleuronectes platessa*) in Division 7.d (eastern English Channel). ICES Stock Annexes. [https://ices-library.figshare.com/articles/report/Stock\\_Annex\\_Plaice\\_Pleuronectes\\_platessa\\_in\\_Division\\_7\\_d\\_eastern\\_English\\_Channel\\_/18622973/1](https://ices-library.figshare.com/articles/report/Stock_Annex_Plaice_Pleuronectes_platessa_in_Division_7_d_eastern_English_Channel_/18622973/1).
- ICES. 2022a. Stock Annex: Sardine (*Sardina pilchardus*) in Subarea 7 (Southern Celtic Seas and the English Channel). ICES Stock Annexes. [https://ices-library.figshare.com/articles/report/Stock\\_Annex\\_Working\\_Group\\_on\\_Southern\\_Horse\\_Mackerel\\_Anchovy\\_and\\_Sardine\\_WGHANSA\\_/20032127](https://ices-library.figshare.com/articles/report/Stock_Annex_Working_Group_on_Southern_Horse_Mackerel_Anchovy_and_Sardine_WGHANSA_/20032127).
- ICES. 2022b. Working Group on Southern Horse Mackerel, Anchovy and Sardine (WGHANSA). ICES Scientific Reports, 4: 518.
- ICES. 2023a. Herring Assessment Working Group for the Area South of 62°N (HAWG). ICES Scientific Reports, 5: 837.
- ICES. 2023b. Working Group on the Assessment of Demersal Stocks in the North Sea and Skagerrak (WGNSSK). ICES Scientific Reports, 5: 1256.
- ICES. 2024a. Herring (*Clupea harengus*) in Subarea 4 and divisions 3.a and 7.d, autumn spawners (North Sea, Skagerrak and Kattegat, eastern English Channel). ICES Advice: Recurrent Advice. [https://ices-library.figshare.com/articles/report/Herring\\_i\\_Clupea\\_harengus\\_i\\_in\\_Subarea\\_4\\_and\\_divisions\\_3\\_a\\_and\\_7\\_d\\_autumn\\_spawners\\_North\\_Sea\\_Skagerrak\\_and\\_Kattegat\\_eastern\\_English\\_Channel\\_/25019285](https://ices-library.figshare.com/articles/report/Herring_i_Clupea_harengus_i_in_Subarea_4_and_divisions_3_a_and_7_d_autumn_spawners_North_Sea_Skagerrak_and_Kattegat_eastern_English_Channel_/25019285).
- ICES. 2024b. Herring Assessment Working Group for the Area South of 62°N (HAWG). ICES Scientific Reports.
- ICES. 2024c. Sardine (*Sardina pilchardus*) in Subarea 7 (Southern Celtic Seas, English Channel). ICES Advice: Recurrent Advice. [https://ices-library.figshare.com/articles/report/Sardine\\_i\\_Sardina\\_pilchardus\\_i\\_in\\_Subarea\\_7\\_Southern\\_Celtic\\_Seas\\_English\\_Channel\\_/25019285](https://ices-library.figshare.com/articles/report/Sardine_i_Sardina_pilchardus_i_in_Subarea_7_Southern_Celtic_Seas_English_Channel_/25019285).



## References

- library.figshare.com/articles/report/Sardine\_i\_Sardina\_pilchardus\_i\_in\_Subarea\_7\_Southern\_Celtic\_Seas\_English\_Channel\_/21975203.
- ICES. 2024d. Plaice (*Pleuronectes platessa*) in Division 7.d (eastern English Channel). ICES Advice: Recurrent Advice. [https://ices-library.figshare.com/articles/report/Plaice\\_i\\_Pleuronectes\\_platessa\\_i\\_in\\_Division\\_7\\_d\\_eastern\\_English\\_Channel\\_/25019450](https://ices-library.figshare.com/articles/report/Plaice_i_Pleuronectes_platessa_i_in_Division_7_d_eastern_English_Channel_/25019450).
- ICES. 2024e. Plaice (*Pleuronectes platessa*) in Subarea 4 (North Sea) and Subdivision 20 (Skagerrak). ICES Advice: Recurrent Advice. [https://ices-library.figshare.com/articles/report/Plaice\\_i\\_Pleuronectes\\_platessa\\_i\\_in\\_Subarea\\_4\\_North\\_Sea\\_and\\_Subdivision\\_20\\_Skagerrak\\_/25019441](https://ices-library.figshare.com/articles/report/Plaice_i_Pleuronectes_platessa_i_in_Subarea_4_North_Sea_and_Subdivision_20_Skagerrak_/25019441).
- Illing, B., Moyano, M., Berg, J., Hufnagl, M., and Peck, M. A. 2018. Behavioral and physiological responses to prey match-mismatch in larval herring. *Estuarine, Coastal and Shelf Science*, 201: 82–94.
- IPPC (Ed). 2014. Summary for Policymakers. *In* Climate Change 2013 – The Physical Science Basis: Working Group I Contribution to the Fifth Assessment Report of the Intergovernmental Panel on Climate Change, pp. 1–30. Cambridge University Press, Cambridge. <https://www.cambridge.org/core/books/climate-change-2013-the-physical-science-basis/summary-for-policymakers/356E277FD1FBC887845FB9E8CBC90CCD>.
- Ito, M., Halouani, G., Cresson, P., Giraldo, C., and Girardin, R. 2023. Detection of fishing pressure using ecological network indicators derived from ecosystem models. *Ecological Indicators*, 147: 110011.
- Izquierdo, M. S. 1996. Essential fatty acid requirements of cultured marine fish larvae. *Aquaculture Nutrition*, 2: 183–191.
- John, E. H., Batten, S. D., Harris, R. P., and Hays, G. C. 2001. Comparison between zooplankton data collected by the Continuous Plankton Recorder survey in the English Channel and by WP-2 nets at station L4, Plymouth (UK). *Journal of Sea Research*, 46: 223–232.
- Johns, D. G., and Reid, P. C. 2001. An overview of plankton ecology in the North Sea. Sir Alister Hardy Foundation for Ocean Sciences, Plymouth, (UK). 31 pp. [http://www.offshore-sea.org.uk/consultations/SEA\\_2/index.php](http://www.offshore-sea.org.uk/consultations/SEA_2/index.php).
- Joly, L. J., Loots, C., Meunier, C. L., Boersma, M., Collet, S., Lefebvre, V., Zambonino-Infante, J.-L., *et al.* 2021. Maturation of the digestive system of Downs herring larvae (*Clupea harengus*, Linnaeus, 1758): identification of critical periods through ontogeny. *Marine Biology*, 168: 82.
- Jónasdóttir, S. H. 2019. Fatty acid profiles and production in marine phytoplankton. *Marine Drugs*, 17: 151. Multidisciplinary Digital Publishing Institute.
- Kadoya, T., Osada, Y., and Takimoto, G. 2012. IsoWeb: A Bayesian Isotope Mixing Model for Diet Analysis of the Whole Food Web. *PLOS ONE*, 7: e41057.
- Kainz, M., Arts, M. T., and Mazumder, A. 2004. Essential fatty acids in the planktonic food web and their ecological role for higher trophic levels. *Limnology and Oceanography*, 49: 1784–1793.
- Kanstinger, P., and Peck, M. A. 2009. Co-occurrence of European sardine (*Sardina pilchardus*), anchovy (*Engraulis encrasicolus*) and sprat (*Sprattus sprattus*) larvae in southern North Sea habitats: Abundance, distribution and biochemical-based condition. *Scientia Marina*, 73: 141–152.
- Kasapidis, P., Silva, A., Zampicinini, G., and Magoulas, A. 2012. Evidence for microsatellite hitchhiking selection in European sardine (*Sardina pilchardus*) and implications in inferring stock structure. *Scientia Marina*, 76: 123–132.

## References

- Kattner, G., and Krause, M. 1989. Seasonal variations of lipids (wax esters, fatty acids and alcohols) in calanoid copepods from the North Sea. *Marine Chemistry*, 26: 261–275.
- Kattner, G., and Hagen, W. 1995. Polar herbivorous copepods – different pathways in lipid biosynthesis. *ICES Journal of Marine Science*, 52: 329–335.
- Kattner, G., and Hagen, W. 2009. Lipids in Marine Copepods: Latitudinal Characteristics and Perspective to Global Warming. *In* *Lipids in Aquatic Ecosystems*. Ed. by M. Kainz, M. T. Brett, and M. T. Arts. Springer New York, New York, NY. <https://link.springer.com/10.1007/978-0-387-89366-2>.
- Kemp, P., and Smith, M. W. 1970. Effect of temperature acclimatization on the fatty acid composition of goldfish intestinal lipids. *Biochemical Journal*, 117: 9–15.
- Khérifi, S., El Cafsi, M., Masmoudi, W., Castell, J. D., and Romdhane, M. S. 2003. Salinity and Temperature Effects on the Lipid Composition of Mullet Sea Fry (*Mugil cephalus*, Linné, 1758). *Aquaculture International*, 11: 571–582.
- Klein Breteler, W. C. M., Schogt, N., Baas, M., Schouten, S., and Kraay, G. W. 1999. Trophic upgrading of food quality by protozoans enhancing copepod growth: role of essential lipids. *Marine Biology*, 135: 191–198.
- Kléparski, L., Beaugrand, G., and Edwards, M. 2021. Plankton biogeography in the North Atlantic Ocean and its adjacent seas: Species assemblages and environmental signatures. *Ecology and Evolution*, 11: 5135–5149.
- Kopp, D., Lefebvre, S., Cachera, M., Villanueva, M. C., and Ernande, B. 2015. Reorganization of a marine trophic network along an inshore–offshore gradient due to stronger pelagic–benthic coupling in coastal areas. *Progress in Oceanography*, 130: 157–171.
- Kostecki, C., Roussel, J. M., Desroy, N., Roussel, G., Lanshere, J., Bris, H. L., and Pape, O. L. 2012. Trophic ecology of juvenile flatfish in a coastal nursery ground: contributions of intertidal primary production and freshwater particulate organic matter. *Marine Ecology Progress Series*, 449: 221–232.
- Koven, W. M., Tandler, A., Kissil, G. Wm., Sklan, D., Friezlander, O., and Harel, M. 1990. The effect of dietary (n–3) polyunsaturated fatty acids on growth, survival and swim bladder development in *Sparus aurata* larvae. *Aquaculture*, 91: 131–141.
- Kozak, E. R., Franco-Gordo, C., Godínez-Domínguez, E., Suárez-Morales, E., and Ambriz-Arreola, I. 2020. Seasonal variability of stable isotope values and niche size in tropical calanoid copepods and zooplankton size fractions. *Marine Biology*, 167: 37.
- Krause, M., and Martens, P. 1990. Distribution patterns of mesozooplankton biomass in the North Sea. *Helgoländer Meeresuntersuchungen*, 44: 295–327.
- Krause, M., Dippner, J. W., and Beil, J. 1995. A review of hydrographic controls on the distribution of zooplankton biomass and species in the North Sea with particular reference to a survey conducted in January–March 1987. *Progress in Oceanography*, 35: 81–152.
- Krause, M., Fock, H., Greve, W., and Winkler, G. 2003. North Sea zooplankton: a review. *Senckenbergiana maritima*, 33: 71–204.
- Kreft, H., and Jetz, W. 2010. A framework for delineating biogeographical regions based on species distributions: Global quantitative biogeographical regionalizations. *Journal of Biogeography*, 37: 2029–2053.
- Kürten, B., Painting, S. J., Struck, U., Polunin, N. V. C., and Middelburg, J. J. 2013. Tracking seasonal changes in North Sea zooplankton trophic dynamics using stable isotopes. *Biogeochemistry*, 113: 167–187.

## References

- Lacroix, G., Maes, G. E., Bolle, L. J., and Volckaert, F. A. M. 2013. Modelling dispersal dynamics of the early life stages of a marine flatfish (*Solea solea* L.). *Journal of Sea Research*, 84: 13–25.
- Last, J. M. 1978. The food of four species of pleuronectiform larvae in the eastern English Channel and southern North Sea. *Marine Biology*, 45: 359–368.
- Laurent, V., Caneco, B., Magoulas, A., and Planes, S. 2007. Isolation by distance and selection effects on genetic structure of sardines *Sardina pilchardus* Walbaum. *Journal of Fish Biology*, 71: 1–17.
- Le Cren, E. D. 1951. The Length-Weight Relationship and Seasonal Cycle in Gonad Weight and Condition in the Perch (*Perca fluviatilis*). *The Journal of Animal Ecology*, 20: 201.
- Lê, S., Josse, J., and Husson, F. 2008. FactoMineR: A Package for Multivariate Analysis. *Journal of Statistical Software*, 25. <http://www.jstatsoft.org/v25/i01/>.
- Lee, R. F., Hagen, W., and Kattner, G. 2006. Lipid storage in marine zooplankton. *Marine Ecology Progress Series*, 307: 273–306.
- Lefebvre, A., and Devreker, D. 2020. First Comprehensive Quantitative Multi-Parameter Assessment of the Eutrophication Status from Coastal to Marine French Waters in the English Channel, the Celtic Sea, the Bay of Biscay, and the Mediterranean Sea. *Journal of Marine Science and Engineering*, 8: 561. Multidisciplinary Digital Publishing Institute.
- Lefebvre, A., and Devreker, D. 2023. How to learn more about hydrological conditions and phytoplankton dynamics and diversity in the eastern English Channel and the Southern Bight of the North Sea? the SRN data set (1992–2021). <https://essd.copernicus.org/preprints/essd-2022-146/essd-2022-146.pdf>.
- Legendre, L., and Rassoulzadegan, F. 1995. Plankton and nutrient dynamics in marine waters. *Ophelia*, 41: 153–172. Taylor & Francis.
- Legendre, P., and Gallagher, E. D. 2001. Ecologically meaningful transformations for ordination of species data. *Oecologia*, 129: 271–280.
- Legendre, P., and Legendre, L. 2012. *Numerical ecology*. Elsevier, Amsterdam. 990 pp.
- Lelièvre, S., Jérôme, M., Maes, G. E., Vaz, S., Calaivany, S., and Verrez-Bagnis, V. 2012. Integrating molecular identification of pelagic eggs with geostatistical mapping to improve the delineation of North Sea fish spawning grounds. *Marine Ecology Progress Series*, 445: 161–172.
- Lelièvre, S., Vaz, S., Martin, C. S., and Loots, C. 2014. Delineating recurrent fish spawning habitats in the North Sea. *Journal of Sea Research*, 91: 1–14.
- Lenhart, H. J., Pätsch, J., Kühn, W., Moll, A., and Pohlmann, T. 2004. Investigation on the trophic state of the North Sea for three years (1994-1996) simulated with the ecosystem model ERSEM - the role of a sharp NAOI decline. *Biogeosciences Discussions*, 1: 725.
- Lewandowska, A. M., Boyce, D. G., Hofmann, M., Matthiessen, B., Sommer, U., and Worm, B. 2014. Effects of sea surface warming on marine plankton. *Ecology Letters*, 17: 614–623.
- Liénart, C., Savoye, N., Bozec, Y., Breton, E., Conan, P., David, V., Feunteun, E., *et al.* 2017. Dynamics of particulate organic matter composition in coastal systems: A spatio-temporal study at multi-systems scale. *Progress in Oceanography*, 156: 221–239.
- Liénart, C., Savoye, N., Conan, P., David, V., Barbier, P., Bichon, S., Charlier, K., *et al.* 2020. Relationship between bacterial compartment and particulate organic matter (POM) in coastal systems: An assessment using fatty acids and stable isotopes. *Estuarine, Coastal and Shelf Science*, 239: 106720.

## References

- Lindegren, M., Östman, Ö., and Gårdmark, A. 2011. Interacting trophic forcing and the population dynamics of herring. *Ecology*, 92: 1407–1413.
- Lindley, J. A. 1998. Diversity, biomass and production of decapod crustacean larvae in a changing environment. *Invertebrate Reproduction & Development*, 33: 209–219. Taylor & Francis.
- Litchman, E., Ohman, M. D., and Kiørboe, T. 2013. Trait-based approaches to zooplankton communities. *Journal of Plankton Research*, 35: 473–484.
- Litzow, M. A., Bailey, K. M., Prah, F. G., and Heintz, R. 2006. Climate regime shifts and reorganization of fish communities: the essential fatty acid limitation hypothesis. *Marine Ecology Progress Series*, 315: 1–11.
- Llopiz, J. K., Richardson, D. E., Shiroza, A., Smith, S. L., and Cowen, R. K. 2010. Distinctions in the diets and distributions of larval tunas and the important role of appendicularians. *Limnology and Oceanography*, 55: 983–996.
- Lomartire, S., Marques, J. C., and Gonçalves, A. M. M. 2021. The key role of zooplankton in ecosystem services: A perspective of interaction between zooplankton and fish recruitment. *Ecological Indicators*, 129: 107867.
- Lombard, F., Selander, E., and Kiørboe, T. 2011. Active prey rejection in the filter-feeding appendicularian *Oikopleura dioica*. *Limnology and Oceanography*, 56: 1504–1512.
- Longhurst, A. R. 2010. *Ecological Geography of the Sea*. Elsevier. 575 pp.
- Loots, C., Vaz, S., Planque, B., and Koubbi, P. 2010. What controls the spatial distribution of the North Sea plaice spawning population? Confronting ecological hypotheses through a model selection framework. *ICES Journal of Marine Science*, 67: 244–257.
- Luczak, C., and Spilmont, N. 2012. Are the Eastern and Western Basins of the English Channel two separate ecosystems? Get back in line with some cautionary comments. *Marine Pollution Bulletin*, 64: 1318–1319.
- Luo, J. Y., Grassian, B., Tang, D., Irisson, J.-O., Greer, A. T., Guigand, C. M., McClatchie, S., *et al.* 2014. Environmental drivers of the fine-scale distribution of a gelatinous zooplankton community across a mesoscale front. *Marine Ecology Progress Series*, 510: 129–149.
- Lussenhop, J. 1974. Victor Hensen and the development of sampling methods in ecology. *Journal of the History of Biology*, 7: 319–337.
- Maar, M., Butenschön, M., Daewel, U., Eggert, A., Fan, W., Hjøllø, S. S., Hufnagl, M., *et al.* 2018. Responses of summer phytoplankton biomass to changes in top-down forcing: Insights from comparative modelling. *Ecological Modelling*, 376: 54–67.
- Mackas, D., Galbraith, M., Faust, D., Masson, D., Young, K., Shaw, W., Romaine, S., *et al.* 2013. Zooplankton time series from the Strait of Georgia: Results from year-round sampling at deep water locations, 1990–2010. *Progress in Oceanography*, 115: 129–159.
- Maechler, M., Rousseeuw, P., Struyf, A., Hubert, M., and Hornik, K. 2023. cluster: Cluster Analysis Basics and Extensions. <https://CRAN.R-project.org/package=cluster>.
- Maes, J., Tackx, M., and Soetaert, K. 2005. The predation impact of juvenile herring *Clupea harengus* and sprat *Sprattus sprattus* on estuarine zooplankton. *Hydrobiologia*, 540: 225–235.
- Mairesse, G., Thomas, M., Gardeur, J.-N., and Brun-Bellut, J. 2006. Effects of geographic source, rearing system, and season on the nutritional quality of wild and farmed *Perca fluviatilis*. *Lipids*, 41: 221–229.

## References

- Marçalo, A., Nicolau, L., Giménez, J., Ferreira, M., Santos, J., Araújo, H., Silva, A., *et al.* 2018. Feeding ecology of the common dolphin (*Delphinus delphis*) in Western Iberian waters: has the decline in sardine (*Sardina pilchardus*) affected dolphin diet? *Marine Biology*, 165: 44.
- Margalef, R. 1978. Life-forms of phytoplankton as survival alternatives in an unstable environment. *Oceanologica Acta*, 1. <https://archimer.ifremer.fr/doc/00123/23403/21230.pdf>.
- Marques, R., Otto, S. A., Di Pane, J., Boersma, M., Meunier, C. L., Wiltshire, K. H., Möllmann, C., *et al.* 2023. Response of the meso- and macro-zooplankton community to long-term environmental changes in the southern North Sea. *ICES Journal of Marine Science*. Oxford University Press (OUP).
- Marquis, E., Niquil, N., Vézina, A. F., Petitgas, P., and Dupuy, C. 2011. Influence of planktonic foodweb structure on a system's capacity to support pelagic production: an inverse analysis approach. *ICES Journal of Marine Science*, 68: 803–812.
- Martin, C., Sandrine, V., and Lelièvre, S. 2008. Identification of the Spawning Areas in the Dover Strait and adjacent marine areas, Final report of the ISADO project, Interreg IIIa Programme. Canterbury Christ Church University, Canterbury. 114 pp.
- Martin, C. S., Carpentier, A., Vaz, S., Coppin, F., Curet, L., Dauvin, J.-C., Delavenne, J., *et al.* 2009. The Channel habitat atlas for marine resource management (CHARM): an aid for planning and decision-making in an area under strong anthropogenic pressure. *Aquatic Living Resources*, 22: 499–508.
- Mathieu, F., Guo, F., and Kainz, M. J. 2022. Tracking dietary fatty acids in triacylglycerols and phospholipids of zooplankton. *Freshwater Biology*, 67: 1949–1959.
- Mathieu-Resuge, M., Le Grand, F., Brosset, P., Lebigre, C., Soudant, P., Vagner, M., Pecquerie, L., *et al.* 2023. Red muscle of small pelagic fishes' fillets are high-quality sources of essential fatty acids. *Journal of Food Composition and Analysis*: 105304.
- Mathieu-Resuge, M., Brosset, P., Sardenne, F., Soudant, P., Le Grand, F., Schull, Q., and Lebigre, C. 2024. How membrane fatty acids influence sardine size across diverse marine environments. *Progress in Oceanography*, 221: 103209.
- Mayzaud, P., Lacombe, S., and Boutoute, M. 2011. Seasonal and growth stage changes in lipid and fatty acid composition in the multigeneration copepod *Drepanopus pectinatus* from Iles Kerguelen. *Antarctic Science*, 23: 3–17.
- Mayzaud, P., Falk-Petersen, S., Noyon, M., Wold, A., and Boutoute, M. 2016. Lipid composition of the three co-existing *Calanus* species in the Arctic: impact of season, location and environment. *Polar Biology*, 39: 1819–1839.
- McBride, R. S., Somarakis, S., Fitzhugh, G. R., Albert, A., Yaragina, N. A., Wuenschel, M. J., Alonso-Fernández, A., *et al.* 2015. Energy acquisition and allocation to egg production in relation to fish reproductive strategies. *Fish and Fisheries*, 16: 23–57.
- McCutchan Jr, J. H., Lewis Jr, W. M., Kendall, C., and McGrath, C. C. 2003. Variation in trophic shift for stable isotope ratios of carbon, nitrogen, and sulfur. *Oikos*, 102: 378–390.
- McKnight, D. T., Huerlimann, R., Bower, D. S., Schwarzkopf, L., Alford, R. A., and Zenger, K. R. 2019. Methods for normalizing microbiome data: An ecological perspective. *Methods in Ecology and Evolution*, 10: 389–400.

## References

- McLeod, K. L., Lubchenco, J., Palumbi, S. R., and Rosenberg, A. A. 2005. Scientific Consensus Statement on Marine Ecosystem-Based Management. Communication Partnership for Science and the Sea (COMPASS).
- McQuatters-Gollop, A., Atkinson, A., Aubert, A., Bedford, J., Best, M., Bresnan, E., Cook, K., *et al.* 2019. Plankton lifeforms as a biodiversity indicator for regional-scale assessment of pelagic habitats for policy. *Ecological Indicators*, 101: 913–925.
- Megens, L., van der Plicht, J., and de Leeuw, J. W. 2001. Temporal variations in  $^{13}\text{C}$  and  $^{14}\text{C}$  concentrations in particulate organic matter from the southern North Sea. *Geochimica et Cosmochimica Acta*, 65: 2899–2911.
- Menu, C., Pecquerie, L., Bacher, C., Doray, M., Hattab, T., van der Kooij, J., and Huret, M. 2023. Testing the bottom-up hypothesis for the decline in size of anchovy and sardine across European waters through a bioenergetic modeling approach. *Progress in Oceanography*, 210: 102943.
- Meunier, C. L., Boersma, M., Wiltshire, K. H., and Malzahn, A. M. 2016. Zooplankton eat what they need: copepod selective feeding and potential consequences for marine systems. *Oikos*, 125: 50–58.
- Meynier, L., Pusineri, C., Spitz, J., Santos, M. B., Pierce, G. J., and Ridoux, V. 2008. Intraspecific dietary variation in the short-beaked common dolphin *Delphinus delphis* in the Bay of Biscay: importance of fat fish. *Marine Ecology Progress Series*, 354: 277–287.
- Millennium Ecosystem Assessment (Ed). 2005. Ecosystems and human well-being: wetlands and water synthesis: a report of the Millennium Ecosystem Assessment. World Resources Institute, Washington, DC. 68 pp.
- Miller, P. J. 1986. Gobiidae. *In* Fishes of the North-eastern Atlantic and Mediterranean, pp. 1019–1085. Ed. by P. J. P. Whitehead, M. L. Bauchot, J. C. Hureau, J. Nielsen, and E. Tortonese. UNESCO, Paris.
- Miller, T. J., Crowder, L. B., Rice, J. A., and Marschall, E. A. 1988. Larval Size and Recruitment Mechanisms in Fishes: Toward a Conceptual Framework. *Canadian Journal of Fisheries and Aquatic Sciences*, 45: 1657–1670.
- Minagawa, M., and Wada, E. 1984. Stepwise enrichment of  $^{15}\text{N}$  along food chains: Further evidence and the relation between  $\delta^{15}\text{N}$  and animal age. *Geochimica et Cosmochimica Acta*, 48: 1135–1140.
- Mitsuzawa, A., Miyamoto, H., and Ueda, H. 2017. Feeding selectivity of early-stage fish larvae on the nauplii and eggs of different copepod species. *Plankton and Benthos Research*, 12: 115–122.
- Mkadem, H., and Kaanane, A. 2020. Seasonal changes in chemical composition and fatty acids of sardines (*Sardina pilchardus*) from the Dakhla coast (Morocco). *Moroccan Journal of Agricultural Sciences*, 1. <https://agromaroc.com/index.php/MJAS/article/view/853>.
- Mlambo, M. C. 2014. Not all traits are ‘functional’: insights from taxonomy and biodiversity-ecosystem functioning research. *Biodiversity and Conservation*, 23: 781–790.
- Mollet, F. M., Kraak, S. B. M., and Rijnsdorp, A. D. 2007. Fisheries-induced evolutionary changes in maturation reaction norms in North Sea sole *Solea solea*. *Marine Ecology Progress Series*, 351: 189–199.
- Moloney, C. L., and Field, J. G. 1991. The size-based dynamics of plankton food webs. I. A simulation model of carbon and nitrogen flows. *Journal of Plankton Research*, 13: 1003–1038.
- Morote, E., Olivar, M. P., Villate, F., and Uriarte, I. 2010. A comparison of anchovy (*Engraulis encrasicolus*) and sardine (*Sardina pilchardus*) larvae feeding in the

## References

- Northwest Mediterranean: influence of prey availability and ontogeny. *ICES Journal of Marine Science*, 67: 897–908.
- Motoda, S. 1959. Devices of simple plankton apparatus. *Memoirs of the Faculty of fisheries Hokkaido*, 7: 73–94.
- Moyano, M., Illing, B., Peschutter, P., Huebert, K. B., and Peck, M. A. 2016. Thermal impacts on the growth, development and ontogeny of critical swimming speed in Atlantic herring larvae. *Comparative Biochemistry and Physiology Part A: Molecular & Integrative Physiology*, 197: 23–34.
- Munk, P., and Nielsen, T. G. 1994. Trophodynamics of the plankton community at Dogger Bank: predatory impact by larval fish. *Journal of Plankton Research*, 16: 1225–1245.
- Munk, P., and Nielsen, J. G. 2005. Eggs and larvae of North Sea fishes. *Biofolia*, Frederiksberg.
- Munk, P., Huwer, B., van Deurs, M., Kloppmann, M., and Sell, A. 2024. Spatial separation of larval sprat (*Sprattus sprattus*) and sardine (*Sardina pilchardus*) related to hydrographical characteristics in the North Sea. *Fisheries Oceanography*, 33: e12656.
- Murua, H., and Saborido-Rey, F. 2003. Female Reproductive Strategies of Marine Fish Species of the North Atlantic. Northwest Atlantic Fisheries Organization. <https://digital.csic.es/handle/10261/26868>.
- Muus, B. J., and Nielsen, J. G. 1999. Die Meeresfische Europas in Nordsee, Ostsee und Atlantik. Kosmos Verlag, Stuttgart. 336 pp.
- Nahorniak, M., Larsen, D. P., Volk, C., and Jordan, C. E. 2015. Using Inverse Probability Bootstrap Sampling to Eliminate Sample Induced Bias in Model Based Analysis of Unequal Probability Samples. *PLOS ONE*, 10: e0131765.
- Nash, R. D. M., and Dickey-Collas, M. 2005. The influence of life history dynamics and environment on the determination of year class strength in North Sea herring (*Clupea harengus* L.). *Fisheries Oceanography*, 14: 279–291.
- Ndah, A. B., Meunier, C. L., Kirstein, I. V., Göbel, J., Rönn, L., and Boersma, M. 2022. A systematic study of zooplankton-based indices of marine ecological change and water quality: Application to the European marine strategy framework Directive (MSFD). *Ecological Indicators*, 135: 108587.
- Nelson, M. M., Mooney, B. D., Nichols, P. D., and Phleger, C. F. 2001. Lipids of Antarctic Ocean amphipods: food chain interactions and the occurrence of novel biomarkers. *Marine Chemistry*, 73: 53–64.
- Neven, C. J., Giraldo, C., Girardin, R., Lefebvre, A., Lefebvre, S., Loots, C., Meunier, C. L., *et al.* *in press*. Winter distribution of zooplankton and ichthyoplankton assemblages in the North Sea and the English Channel. *PLOS ONE*.
- Neves, J., Silva, A. A., Moreno, A., Veríssimo, A., Santos, A. M., and Garrido, S. 2021. Population structure of the European sardine *Sardina pilchardus* from Atlantic and Mediterranean waters based on otolith shape analysis. *Fisheries Research*, 243: 106050.
- Nielsen, J. G. 1986. Pleuronectidae. *In* *Fishes of the North-eastern Atlantic and the Mediterranean*, p. 1473. Ed. by P. J. P. Whitehead, M. L. Bauchot, J. C. Hureau, J. Nielsen, and E. Tortonese. UNESCO, United Kingdom.
- Nielsen, T., and Richardson, K. 1989. Food chain structure of the North Sea plankton communities: seasonal variations of the role of the microbial loop. *Marine Ecology Progress Series*, 56: 75–87.
- Nielsen, T., Løkkegaard, B., Richardson, K., Bo Pedersen, R., and Hansen, L. 1993. Structure of plankton communities in the Dogger Bank area (North Sea) during a stratified situation. *Marine Ecology Progress Series*, 95: 115–131.

## References

- Nielsen, T., and Sabatini, M. 1996. Role of cyclopoid copepods *Oithona spp.* in North Sea plankton communities. *Marine Ecology Progress Series*, 139: 79–93.
- Nikolioudakis, N., Isari, S., Pitta, P., and Somarakis, S. 2012. Diet of sardine *Sardina pilchardus*: an 'end-to-end' field study. *Marine Ecology Progress Series*, 453: 173–188.
- Nobili, R., Robinson, C., Buitenhuis, E., and Castellani, C. 2013. Food quality regulates the metabolism and reproduction of *Temora longicornis*. *Biogeosciences Discussions*, 10: 3203–3239. Copernicus GmbH.
- Nunes, C., Silva, A., Soares, E., and Gantias, K. 2011. The Use of Hepatic and Somatic Indices and Histological Information to Characterize the Reproductive Dynamics of Atlantic Sardine *Sardina pilchardus* from the Portuguese Coast. *Marine and Coastal Fisheries*, 3: 127–144.
- Ohshimo, S., Hiraoka, Y., Suyama, S., Tsuji, T., Yukami, R., Yasuda, T., and Ando, Y. 2022. Geographical differences in stable isotope ratios and fatty acid and lipid signatures of chub mackerel, *Scomber japonicus*, in waters around Japan. *Bulletin of Marine Science*, 98: 247–270.
- Oksanen, J., Simpson, G. L., Blanchet, F. G., Kindt, R., Legendre, P., Minchin, P. R., O'Hara, R. B., *et al.* 2001, September 6. vegan: Community Ecology Package. <https://CRAN.R-project.org/package=vegan>.
- Olin, A. B., Banas, N. S., Johns, D. G., Heath, M. R., Wright, P. J., and Nager, R. G. 2022. Spatio-temporal variation in the zooplankton prey of lesser sandeels: species and community trait patterns from the Continuous Plankton Recorder. *ICES Journal of Marine Science*, 79: 1649–1661.
- Olsen, R. E., Løvaas, E., and Lie, Ø. 1999. The influence of temperature, dietary polyunsaturated fatty acids,  $\alpha$ -tocopherol and spermine on fatty acid composition and indices of oxidative stress in juvenile Arctic char, *Salvelinus alpinus* (L.). *Fish Physiology and Biochemistry*, 20: 13–29.
- OSPAR Commission, 2000 (Ed). 2000. Quality Status Report 2000, Region 2 - Greater North Sea. London. 136+xiii pp. pp.
- Otto, L., Zimmerman, J. T. E., Furnes, G. K., Mork, M., Saetre, R., and Becker, G. 1990. Review of the physical oceanography of the North Sea. *Netherlands Journal of Sea Research*, 26: 161–238.
- Pacala, S., and Kinzig, A. P. 2013. Introduction to Theory and the Common Ecosystem Model. *In* The Functional Consequences of Biodiversity: Empirical Progress and Theoretical Extensions (MPB-33), pp. 169–174. Ed. by D. Tilman, A. P. Kinzig, and S. Pacala. Princeton University Press. <https://www.degruyter.com/document/doi/10.1515/9781400847303.169/pdf?licenseType=restricted>.
- Paffenhöfer, G.-A., and Harris, R. P. 1976. Feeding, Growth and Reproduction of the Marine Planktonic Copepod *Pseudo-Calanus Elongatus* Boeck. *Journal of the Marine Biological Association of the United Kingdom*, 56: 327–344. Cambridge University Press.
- Parrish, C. C., French, V. M., and Whitticar, M. J. 2012. Lipid class and fatty acid composition of copepods (*Calanus finmarchicus*, *C. glacialis*, *Pseudocalanus sp.*, *Tisbe furcata* and *Nitokra lacustris*) fed various combinations of autotrophic and heterotrophic protists. *Journal of Plankton Research*, 34: 356–375.
- Parrish, R. H., Serra, R., and Grant, W. S. 1989. The Monotypic Sardines, *Sardina* and *Sardinops*: Their Taxonomy, Distribution, Stock Structure, and Zoogeography. *Canadian Journal of Fisheries and Aquatic Sciences*, 46: 2019–2036. NRC Research Press.



## References

- Pauly, D., Christensen, V., Dalsgaard, J., Froese, R., and Torres, F. 1998. Fishing Down Marine Food Webs. *Science*, 279: 860–863.
- Pauly, D., Christensen, V., Gu enette, S., Pitcher, T. J., Sumaila, U. R., Walters, C. J., Watson, R., *et al.* 2002. Towards sustainability in world fisheries. *Nature*, 418: 689–695.
- Pawson, M. G. 1995. Biogeographical identification of English Channel fish and shellfish stocks. Ministry of Agriculture, Fisheries and Food, Directorate of Fisheries Research.
- Payne, M. R., Hatfield, E. M. C., Dickey-Collas, M., Falkenhaus, T., Gallego, A., Gr oger, J., Licandro, P., *et al.* 2009. Recruitment in a changing environment: the 2000s North Sea herring recruitment failure. *ICES Journal of Marine Science*, 66: 272–277.
- Pebesma, E. 2004. Multivariable geostatistics in S: the gstat package. *Computers & Geosciences*, 30: 683–691.
- Pebesma, E., and Bivand, R. 2005. Classes and methods for spatial data in R. *R News*, 5: 9–13.
- Pebesma, E. 2018. Simple Features for R: Standardized Support for Spatial Vector Data. *The R Journal*, 10: 439–446.
- Peck, M. A., Huebert, K. B., and Llopiz, J. K. 2012. Chapter 3 - Intrinsic and Extrinsic Factors Driving Match–Mismatch Dynamics During the Early Life History of Marine Fishes. *In Advances in Ecological Research*, pp. 177–302. Ed. by G. Woodward, U. Jacob, and E. J. O’Gorman. Academic Press.
- Pedersen, E. J., Miller, D. L., Simpson, G. L., and Ross, N. 2019. Hierarchical generalized additive models in ecology: an introduction with mgcv. *PeerJ*, 7: e6876.
- Peltomaa, E., H allfors, H., and Taipale, S. J. 2019. Comparison of Diatoms and Dinoflagellates from Different Habitats as Sources of PUFAs. *Marine Drugs*, 17: 233. Multidisciplinary Digital Publishing Institute.
- Pepin, P., and Dower, J. F. 2007. Variability in the trophic position of larval fish in a coastal pelagic ecosystem based on stable isotope analysis. *Journal of Plankton Research*, 29: 727–737.
- Persson, J., and Vrede, T. 2006. Polyunsaturated fatty acids in zooplankton: variation due to taxonomy and trophic position. *Freshwater Biology*, 51: 887–900.
- Peters, J., Renz, J., van Beusekom, J., Boersma, M., and Hagen, W. 2006. Trophodynamics and seasonal cycle of the copepod *Pseudocalanus acuspes* in the Central Baltic Sea (Bornholm Basin): evidence from lipid composition. *Marine Biology*, 149: 1417–1429.
- Pethybridge, H., Bodin, N., Arsenault-Pernet, E.-J., Bourdeix, J.-H., Brisset, B., Bigot, J.-L., Roos, D., *et al.* 2014. Temporal and inter-specific variations in forage fish feeding conditions in the NW Mediterranean: lipid content and fatty acid compositional changes. *Marine Ecology Progress Series*, 512: 39–54.
- Pethybridge, H. R., Parrish, C. C., Morrongiello, J., Young, J. W., Farley, J. H., Gunasekera, R. M., and Nichols, P. D. 2015. Spatial Patterns and Temperature Predictions of Tuna Fatty Acids: Tracing Essential Nutrients and Changes in Primary Producers. *PLOS ONE*, 10: e0131598. Public Library of Science.
- Pitois, S., and Fox, C. 2006. Long-term changes in zooplankton biomass concentration and mean size over the Northwest European shelf inferred from Continuous Plankton Recorder data. *ICES Journal of Marine Science*, 63: 785–778.
- Pitois, S. G., Lynam, C. P., Jansen, T., Halliday, N., and Edwards, M. 2012. Bottom-up effects of climate on fish populations: data from the Continuous Plankton Recorder. *Marine Ecology Progress Series*, 456: 169–186.

## References

- Post, D. M. 2002. Using Stable Isotopes to Estimate Trophic Position: Models, Methods, and Assumptions. *Ecology*, 83: 703–718.
- Poulet, S. A. 1973. Grazing of *Pseudocalanus minutus* on Naturally Occurring Particulate Matter. *Limnology and Oceanography*, 18: 564–573.
- Purcell, J. E. 1985. Predation on fish eggs and larvae by pelagic cnidarians and ctenophores. *Bulletin of Marine Science*, 37: 739–755.
- Purcell, J. E., Sturdevant, M. V., and Galt, C. P. 2005. A review of appendicularians as prey of fish and invertebrate predators. *In* Response of Marine Ecosystems to Global Change: Ecological Impact of Appendicularians, pp. 359–435. Ed. by G. Gorsky, M. J. Youngbluth, and D. Deibel. Contemporary Publishing International, Paris.
- Queiros, Q., Fromentin, J.-M., Gasset, E., Dutto, G., Huiban, C., Metral, L., Leclerc, L., *et al.* 2019. Food in the sea: size also matters for pelagic fish. *Frontiers in Marine Science*, 6. *Frontiers*. <https://www.frontiersin.org/journals/marine-science/articles/10.3389/fmars.2019.00385/full>.
- Radnaeva, L. D., Popov, D. V., Grahl-Nielsen, O., Khanaev, I. V., Bazarsadueva, S. V., and Käkälä, R. 2017. Fatty acid composition in the white muscle of Cottoidei fishes of Lake Baikal reflects their habitat depth. *Environmental Biology of Fishes*, 100: 1623–1641.
- Rae, K. M., and Fraser, J. H. 1941. The copepoda of the Southern North Sea. 1932-37. *Hull Bulletins of Marine Ecology*, 1: 171–238.
- Rae, K. M., and Rees, C. B. 1947. Continuous Plankton Records: The copepoda in the North Sea, 1938-1939. *Hull Bulletin of Marine Ecology*, 2: 95–132.
- Ratnarajah, L., Abu-Alhaija, R., Atkinson, A., Batten, S., Bax, N. J., Bernard, K. S., Canonico, G., *et al.* 2023. Monitoring and modelling marine zooplankton in a changing climate. *Nature Communications*, 14: 564. Nature Publishing Group.
- Reid, P. C., Edwards, M., Beaugrand, G., Skogen, M., and Stevens, D. 2003. Periodic changes in the zooplankton of the North Sea during the twentieth century linked to oceanic inflow. *Fisheries Oceanography*, 12: 260–269.
- Remize, M., Planchon, F., Loh, A. N., Le Grand, F., Bideau, A., Puccinelli, E., Volety, A., *et al.* 2022. Origin and fate of long-chain polyunsaturated fatty acids in the Kerguelen Islands region (Southern Ocean) in late summer. *Journal of Marine Systems*, 228: 103693.
- REPHY-French Observation And Monitoring Program For Phytoplankton And Hydrology In Coastal Waters. 2023. REPHY dataset - French Observation and Monitoring program for Phytoplankton and Hydrology in coastal waters. Metropolitan data. <https://www.seanoe.org/data/00361/47248/>.
- Reygondeau, G., Molinero, J. C., Coombs, S., MacKenzie, B. R., and Bonnet, D. 2015. Progressive changes in the Western English Channel foster a reorganization in the plankton food web. *Progress in Oceanography*, 137: 524–532.
- Reynolds, C. S. 2006. *The Ecology of Phytoplankton*. Cambridge University Press. 437 pp.
- Richardson, A. J. 2008. In hot water: zooplankton and climate change. *ICES Journal of Marine Science*, 65: 279–295.
- Richirt, J., Schweizer, M., Mouret, A., Quinchar, S., Saad, S., Bouchet, V., Wade, C., *et al.* 2021. Biogeographic distribution of three phylotypes (T1, T2 and T6) of *Ammonia* (foraminifera, Rhizaria) around Great Britain: new insights from combined molecular and morphological recognition. *Journal of Micropalaeontology*, 40: 61–74.
- Rijnsdorp, A. D. 1989. Maturation of male and female North Sea plaice (*Pleuronectes platessa* L.). *ICES Journal of Marine Science*, 46: 35–51.

## References

- Rijnsdorp, A. D., Daan, N., van Beek, F. A., and Heessen, H. J. L. 1991. Reproductive variability in North Sea plaice, sole, and cod. *ICES Journal of Marine Science*, 47: 352–375.
- Rijnsdorp, A. D., and Van Beek, F. A. 1991. Changes in growth of plaice *Pleuronectes platessa* L. and sole *Solea solea* (L.) in the North Sea. *Netherlands Journal of Sea Research*, 27: 441–457.
- Rodríguez, F., Fernández, E., Head, R. N., Harbour, D. S., Bratbak, G., Heldal, M., and Harris, R. P. 2000. Temporal variability of viruses, bacteria, phytoplankton and zooplankton in the western English Channel off Plymouth. *Journal of the Marine Biological Association of the United Kingdom*, 80: 575–586. Cambridge University Press.
- Rolff, C. 2000. Seasonal variation in  $\delta^{13}\text{C}$  and  $\delta^{15}\text{N}$  of size-fractionated plankton at a coastal station in the northern Baltic proper. *Marine Ecology Progress Series*, 203: 47–65.
- Rosa, R., Gonzalez, L., Broitman, B. R., Garrido, S., Santos, A. M. P., and Nunes, M. L. 2010. Bioenergetics of small pelagic fishes in upwelling systems: relationship between fish condition, coastal ecosystem dynamics and fisheries. *Marine Ecology Progress Series*, 410: 205–218.
- Sargent, J. R., and Tocher, D. R. 2002. The lipids. *In* Fish Nutrition, 3rd edn, pp. 154–219. Halver JR Academic Press, San Diego. <https://faculty.ksu.edu.sa/sites/default/files/Fish%20Nutrition.pdf>.
- Sauger, C., Quinquis, J., Berthelin, C., Lepoittevin, M., Elie, N., Dubroca, L., and Kellner, K. 2023. A Quantitative Histologic Analysis of Oogenesis in the Flatfish Species *Pleuronectes platessa* as a Tool for Fisheries Management. *Animals*, 13: 2506. Multidisciplinary Digital Publishing Institute.
- Sautour, B., and Castel, J. 1993. Feeding behaviour of the coastal copepod *Euterpina acutifrons* on small particles.: 13.
- Schlacher, T. A., and Connolly, R. M. 2014. Effects of acid treatment on carbon and nitrogen stable isotope ratios in ecological samples: a review and synthesis. *Methods in Ecology and Evolution*, 5: 541–550.
- Schmidt, J. O., Damme, C. J. G. van, Röckmann, C., and Dickey-Collas, M. 2009. Recolonisation of spawning grounds in a recovering fish stock: recent changes in North Sea herring. *Scientia Marina*, 73: 153–157.
- Schmidt, K., Birchill, A. J., Atkinson, A., Brewin, R. J. W., Clark, J. R., Hickman, A. E., Johns, D. G., *et al.* 2020. Increasing picocyanobacteria success in shelf waters contributes to long-term food web degradation. *Global Change Biology*, 26: 5574–5587.
- Schoo, K. L., Aberle, N., Malzahn, A. M., and Boersma, M. 2012. Food Quality Affects Secondary Consumers Even at Low Quantities: An Experimental Test with Larval European Lobster. *PLOS ONE*, 7: e33550.
- Schoo, K. L., Boersma, M., Malzahn, A. M., Löder, M. G. J., Wiltshire, K. H., and Aberle, N. 2018. Dietary and seasonal variability in trophic relations at the base of the North Sea pelagic food web revealed by stable isotope and fatty acid analysis. *Journal of Sea Research*, 141: 61–70.
- Schramm, M. 2022. echor: Access EPA 'ECHO' Data. R package version 0.1.7.
- Schwamborn, R., and Giarrizzo, T. 2015. Stable isotope discrimination by consumers in a tropical mangrove food web: How important are variations in C/N ratio? *Estuaries and Coasts*, 38: 813–825.
- Segers, F. H. I. D., Dickey-Collas, M., and Rijnsdorp, A. D. 2007. Prey selection by North Sea herring (*Clupea harengus*), with special reference to fish eggs. *ICES Journal of Marine Science*, 64: 60–68.

## References

- Semmouri, I., De Schampelaere, K. A. C., Mortelmans, J., Mees, J., Asselman, J., and Janssen, C. R. 2023. Decadal decline of dominant copepod species in the North Sea is associated with ocean warming: Importance of marine heatwaves. *Marine Pollution Bulletin*, 193: 115159.
- Serra-Pompei, C., Soudijn, F., Visser, A. W., Kiørboe, T., and Andersen, K. H. 2020. A general size- and trait-based model of plankton communities. *Progress in Oceanography*, 189: 102473.
- Sharples, J., Scott, B. E., and Inall, M. E. 2013. From physics to fishing over a shelf sea bank. *Progress in Oceanography*, 117: 1–8.
- Shelbourne, J. E. 1953. The Feeding Habits of Plaice Post-Larvae in the Southern Bight. *Journal of the Marine Biological Association of the United Kingdom*, 32: 149–159.
- Shelbourne, J. E. 1957. The feeding and condition of plaice larvae in good and bad plankton patches. *Journal of the Marine Biological Association of the United Kingdom*, 36: 539–552.
- Shelbourne, J. E. 1962. A predator-prey size relationship for Plaice larvae feeding on *Oikopleura*. *Journal of the Marine Biological Association of the United Kingdom*, 42: 243–252.
- Shideler, A. C., and Houde, E. D. 2014. Spatio-temporal variability in larval-stage feeding and nutritional sources as factors influencing striped bass (*Morone saxatilis*) recruitment success. *Estuaries and Coasts*, 37: 561–575.
- Shirai, N., Terayama, M., and Takeda, H. 2002. Effect of season on the fatty acid composition and free amino acid content of the sardine *Sardinops melanostictus*. *Comparative Biochemistry and Physiology Part B: Biochemistry and Molecular Biology*, 131: 387–393.
- Silva, A., Santos, M. B., Caneco, B., Pestana, G., Porteiro, C., Carrera, P., and Stratoudakis, Y. 2006. Temporal and geographic variability of sardine maturity at length in the northeastern Atlantic and the western Mediterranean. *ICES Journal of Marine Science*, 63: 663–676.
- Silva, A., Carrera, P., Massé, J., Uriarte, A., Santos, M. B., Oliveira, P. B., Soares, E., *et al.* 2008. Geographic variability of sardine growth across the northeastern Atlantic and the Mediterranean Sea. *Fisheries Research*, 90: 56–69.
- Silva, A., Moreno, A., Riveiro, I., Santos, B., Pita, C., Rodriguez, J. G., Villasante, S., *et al.* 2015a. Sardine Fisheries: Resource Assessment and Social and Economic Situation. IP/B/PECH/IC/2015\_133. European Parliament, Directorate-General for Internal Policies Policy Department B: Structural and Cohesion Policies Fisheries, Brussels. [https://www.europarl.europa.eu/thinktank/en/document/IPOL\\_STU\(2015\)5634\\_12](https://www.europarl.europa.eu/thinktank/en/document/IPOL_STU(2015)5634_12).
- Silva, L., Moyano, M., Illing, B., Faria, A. M., Garrido, S., and Peck, M. A. 2015b. Ontogeny of swimming capacity in plaice (*Pleuronectes platessa*) larvae. *Marine Biology*, 162: 753–761.
- Šimat, V., Hamed, I., Petričević, S., and Bogdanović, T. 2020. Seasonal Changes in Free Amino Acid and Fatty Acid Compositions of Sardines, *Sardina pilchardus* (Walbaum, 1792): Implications for Nutrition. *Foods*, 9: 867. Multidisciplinary Digital Publishing Institute.
- Sissener, N. H. 2018. Correction: Are we what we eat? Changes to the feed fatty acid composition of farmed salmon and its effects through the food chain (doi: 10.1242/jeb.161521). *Journal of Experimental Biology*, 221: jeb180976.
- Sissener, N. H., Araujo, P., Sæle, Ø., Rosenlund, G., Stubhaug, I., and Sanden, M. 2020. Dietary 18:2n-6 affects EPA (20:5n-3) and ARA (20:4n-6) content in cell

## References

- membranes and eicosanoid production in Atlantic salmon (*Salmo salar* L.). *Aquaculture*, 522: 735098.
- Skaret, G., Axelsen, B. E., Nøttestad, L., Fernö, A., and Johannessen, A. 2002. Herring as cannibals. *Journal of Fish Biology*, 61: 1050–1052.
- Slotte, A. 1999. Differential utilization of energy during wintering and spawning migration in Norwegian spring-spawning herring. *Journal of Fish Biology*, 54: 338–355.
- Smith, V. H. 2003. Eutrophication of freshwater and coastal marine ecosystems a global problem. *Environmental Science and Pollution Research*, 10: 126–139.
- Sommer, U., and Lewandowska, A. 2011. Climate change and the phytoplankton spring bloom: warming and overwintering zooplankton have similar effects on phytoplankton. *Global Change Biology*, 17: 154–162.
- Sommer, U., Adrian, R., De Senerpont Domis, L., Elser, J. J., Gaedke, U., Ibelings, B., Jeppesen, E., *et al.* 2012. Beyond the Plankton Ecology Group (PEG) Model: Mechanisms Driving Plankton Succession. *Annual Review of Ecology, Evolution, and Systematics*, 43: 429–448.
- Souissi, S., Ibanez, F., Hamadou, R. B., Boucher, J., Cathelineau, A. C., Blanchard, F., and Poulard, J.-C. 2001. A new multivariate mapping method for studying species assemblages and their habitats: Example using bottom trawl surveys in the Bay of Biscay (France). *Sarsia*, 86: 527–542.
- Spalding, M. D., Fox, H. E., Allen, G. R., Davidson, N., Ferdaña, Z. A., Finlayson, M., Halpern, B. S., *et al.* 2007. Marine Ecoregions of the World: A Bioregionalization of Coastal and Shelf Areas. *BioScience*, 57: 573–583.
- Spilling, K., Olli, K., Lehtoranta, J., Kremp, A., Tedesco, L., Tamelander, T., Klais, R., *et al.* 2018. Shifting Diatom-Dinoflagellate Dominance During Spring Bloom in the Baltic Sea and its Potential Effects on Biogeochemical Cycling. *Frontiers in Marine Science*, 5.
- Srivastava, D. S., and Vellend, M. 2005. Biodiversity-Ecosystem Function Research: Is It Relevant to Conservation? *Annual Review of Ecology, Evolution, and Systematics*, 36: 267–294.
- Stanford, R., and Pitcher, T. 2004. Ecosystem simulations of the English Channel: climate and trade-offs. Fisheries Centre Research Reports, 3. Fisheries Centre. University of British Columbia, Vancouver. <https://open.library.ubc.ca/soa/cIRcle/collections/facultyresearchandpublications/52383/items/1.0074799>.
- Sterner, R. W. 1986. Herbivores' Direct and Indirect Effects on Algal Populations. *Science*, 231: 605–607. American Association for the Advancement of Science.
- Sterner, R. W., and Elser, J. J. 2017. Ecological Stoichiometry: The Biology of Elements from Molecules to the Biosphere. *In Ecological Stoichiometry*. Princeton University Press.
- Stock, B. C., Jackson, A. L., Ward, E. J., Parnell, A. C., Phillips, D. L., and Semmens, B. X. 2018. Analyzing mixing systems using a new generation of Bayesian tracer mixing models. *PeerJ*, 6: e5096. PeerJ Inc.
- Strandberg, U., Hiltunen, M., Syväranta, J., Levi, E. E., Davidson, T. A., Jeppesen, E., and Brett, M. T. 2022. Combined effects of eutrophication and warming on polyunsaturated fatty acids in complex phytoplankton communities: A mesocosm experiment. *Science of The Total Environment*, 843: 157001.
- Stratoudakis, Y., Coombs, S., de Lanzós, A. L., Halliday, N., Costas, G., Caneco, B., Franco, C., *et al.* 2007. Sardine (*Sardina pilchardus*) spawning seasonality in European waters of the northeast Atlantic. *Marine Biology*, 152: 201–212.

## References

- Suzuki, K., Nakamura, Y., and Hiromi, J. 1999. Feeding by the small calanoid copepod *Paracalanus* sp. on heterotrophic dinoflagellates and ciliates. *Aquatic Microbial Ecology*, 17: 99–103.
- Svendsen, E., Aglen, A., Iversen, S. A., Skagen, D. W., and Smedstad, O. M. 1991. Influence of climate on recruitment and migration of fish stocks in the North Sea. ICES.
- Tam, J. C., Link, J. S., Rossberg, A. G., Rogers, S. I., Levin, P. S., Rochet, M.-J., Bundy, A., *et al.* 2017. Towards ecosystem-based management: identifying operational food-web indicators for marine ecosystems. *ICES Journal of Marine Science*, 74: 2040–2052.
- Teodosio, M. A., and Barbosa, A. M. B. (Eds). 2020. *Zooplankton Ecology*. CRC Press, Boca Raton.
- Tesán-Onrubia, J. A., Tedetti, M., Carlotti, F., Tenaille, M., Guilloux, L., Pagano, M., Lebreton, B., *et al.* 2023. Spatial variations of biochemical content and stable isotope ratios of size-fractionated plankton in the Mediterranean Sea (MERITE-HIPPOCAMPE campaign). *Marine pollution bulletin*, 189: 114787.
- Thébault, E., and Loreau, M. 2006. The relationship between biodiversity and ecosystem functioning in food webs. *Ecological Research*, 21: 17–25.
- Thomas, H., Bozec, Y., de Baar, H. J. W., Elkalay, K., Frankignoulle, M., Schiettecatte, L.-S., Kattner, G., *et al.* 2005. The carbon budget of the North Sea. *Biogeosciences*, 2: 87–96. Copernicus GmbH.
- Thompson, R. M., Brose, U., Dunne, J. A., Hall, R. O., Hladysz, S., Kitching, R. L., Martinez, N. D., *et al.* 2012. Food webs: reconciling the structure and function of biodiversity. *Trends in Ecology & Evolution*, 27: 689–697.
- Thorpe, R. B. 2024. We need to talk about the role of zooplankton in marine food webs. *Journal of Fish Biology*, n/a: 1–15.
- Tian, R. C., Deibel, D., Thompson, R. J., and Rivkin, R. B. 2003. Modeling of climate forcing on a cold-ocean ecosystem, Conception Bay, Newfoundland. *Marine Ecology Progress Series*, 262: 1–17.
- Timmerman, C.-A., Marchal, P., Denamiel, M., Couvreur, C., and Cresson, P. 2020. Seasonal and ontogenetic variation of whiting diet in the Eastern English Channel and the Southern North Sea. *PLOS ONE*, 15: e0239436. Public Library of Science.
- Tisseyre, B., Leroux, C., Pichon, L., Geraudie, V., and Sari, T. 2018. How to define the optimal grid size to map high resolution spatial data? *Precision Agriculture*, 19: 957–971.
- Tocher, D. R. 2003. Metabolism and Functions of Lipids and Fatty Acids in Teleost Fish. *Reviews in Fisheries Science*, 11: 107–184. Taylor & Francis.
- Tocher, D. R. 2010. Fatty acid requirements in ontogeny of marine and freshwater fish. *Aquaculture Research*, 41: 717–732.
- Turrell, W. R. 1992. New hypotheses concerning the circulation of the northern North Sea and its relation to North Sea fish stock recruitment. *ICES Journal of Marine Science*, 49: 107–123.
- Urban, J., and Alheit, J. 1988. Oocyte development cycle of plaice *Pleuronectes platessa*, and the North Sea sole, *Solea solea*. ICES CM.
- Vagner, M., and Santigosa, E. 2011. Characterization and modulation of gene expression and enzymatic activity of delta-6 desaturase in teleosts: A review. *Aquaculture*, 315: 131–143.
- Vagner, M., Lacoue-Labarthe, T., Infante, J.-L. Z., Mazurais, D., Dubillot, E., Delliou, H. L., Quazuguel, P., *et al.* 2015. Depletion of Essential Fatty Acids in the Food Source Affects Aerobic Capacities of the Golden Grey Mullet *Liza aurata* in a

## References

- Warming Seawater Context. PLOS ONE, 10: e0126489. Public Library of Science.
- Vagner, M., Pante, E., Viricel, A., Lacoue-Labarthe, T., Zambonino-Infante, J.-L., Quazuguel, P., Dubillot, E., *et al.* 2019. Ocean warming combined with lower omega-3 nutritional availability impairs the cardio-respiratory function of a marine fish. *Journal of Experimental Biology*, 222: jeb187179.
- Van Beveren, E., Bonhommeau, S., Fromentin, J.-M., Bigot, J.-L., Bourdeix, J.-H., Brosset, P., Roos, D., *et al.* 2014. Rapid changes in growth, condition, size and age of small pelagic fish in the Mediterranean. *Marine Biology*, 161: 1809–1822.
- Van der Land, M. A. 1991. Distribution of flatfish eggs in the 1989 egg surveys in the southeastern North Sea, and mortality of plaice and sole eggs. *Netherlands Journal of Sea Research*, 27: 277–286.
- van der Veer, H. W., Berghahn, R., Miller, J. M., and Rijnsdorp, A. D. 2000. Recruitment in flatfish, with special emphasis on North Atlantic species: Progress made by the Flatfish Symposia. *ICES Journal of Marine Science*, 57: 202–215.
- Van Ginderdeuren, K., Vandendriessche, S., Prössler, Y., Matola, H., Vincx, M., and Hostens, K. 2014a. Selective feeding by pelagic fish in the Belgian part of the North Sea. *ICES Journal of Marine Science*, 71: 808–820.
- Van Ginderdeuren, K., Van Hoey, G., Vincx, M., and Hostens, K. 2014b. The mesozooplankton community of the Belgian shelf (North Sea). *Journal of Sea Research*, 85: 48–58.
- Varpe, Ø., Fiksen, Ø., and Slotte, A. 2005. Meta-ecosystems and biological energy transport from ocean to coast: the ecological importance of herring migration. *Oecologia*, 146: 443–451.
- Varpe, Ø. 2012. Fitness and phenology: annual routines and zooplankton adaptations to seasonal cycles. *Journal of Plankton Research*, 34: 267–276.
- Véron, M., Duhamel, E., Bertignac, M., Pawlowski, L., and Huret, M. 2020. Major changes in sardine growth and body condition in the Bay of Biscay between 2003 and 2016: Temporal trends and drivers. *Progress in Oceanography*, 182: 102274.
- Voronin, V. P., Nemova, N. N., Ruokolainen, T. R., Artemenkov, D. V., Rolskii, A. Y., Orlov, A. M., and Murzina, S. A. 2021. Into the Deep: New Data on the Lipid and Fatty Acid Profile of Redfish *Sebastes mentella* Inhabiting Different Depths in the Irminger Sea. *Biomolecules*, 11: 704. Multidisciplinary Digital Publishing Institute.
- Voronin, V. P., Artemenkov, D. V., Orlov, A. M., and Murzina, S. A. 2022. Lipids and Fatty Acids in Some Mesopelagic Fish Species: General Characteristics and Peculiarities of Adaptive Response to Deep-Water Habitat. *Journal of Marine Science and Engineering*, 10: 949. Multidisciplinary Digital Publishing Institute.
- Wacquet, G., and Lefebvre, A. 2022. EcoTransLearn: an R-package to easily use transfer learning for ecological studies—a plankton case study. *Bioinformatics*, 38: 5469–5471.
- Wagner, G. N., Balfry, S. K., Higgs, D. A., Lall, S. P., and Farrell, A. P. 2004. Dietary fatty acid composition affects the repeat swimming performance of Atlantic salmon in seawater. *Comparative Biochemistry and Physiology Part A: Molecular & Integrative Physiology*, 137: 567–576.
- Walker, J. C. G. 1980. The Oxygen Cycle. *In The Natural Environment and the Biogeochemical Cycles*, pp. 87–104. Ed. by O. Hutzinger. Springer, Berlin, Heidelberg. [https://doi.org/10.1007/978-3-662-24940-6\\_5](https://doi.org/10.1007/978-3-662-24940-6_5).

## References

- Walve, J., and Larsson, U. 1999. Carbon, nitrogen and phosphorus stoichiometry of crustacean zooplankton in the Baltic Sea: implications for nutrient recycling. *Journal of Plankton Research*, 21: 2309–2321.
- Ward, B. A., Dutkiewicz, S., and Follows, M. J. 2014. Modelling spatial and temporal patterns in size-structured marine plankton communities: top–down and bottom–up controls. *Journal of Plankton Research*, 36: 31–47.
- Werbrouck, E., Tiselius, P., Van Gansbeke, D., Cervin, G., Vanreusel, A., and De Troch, M. 2016. Temperature impact on the trophic transfer of fatty acids in the congeneric copepods *Acartia tonsa* and *Acartia clausi*. *Journal of Sea Research*, 112: 41–48.
- Wesche, A., Wiltshire, K. H., and Hirche, H. J. 2007. Overwintering strategies of dominant calanoid copepods in the German Bight, southern North Sea. *Marine Biology*, 151: 1309–1320.
- White, D., and Gramacy, R. B. 2022. maptree: Mapping, Pruning, and Graphing Tree Models. <https://CRAN.R-project.org/package=maptree>.
- White, D. A., Widdicombe, C. E., Somerfield, P. J., Airs, R. L., Tarran, G. A., Maud, J. L., and Atkinson, A. 2015. The combined effects of seasonal community succession and adaptive algal physiology on lipid profiles of coastal phytoplankton in the Western English Channel. *Marine Chemistry*, 177: 638–652.
- Whitehead, P. J. P. 1985. FAO Species Catalogue Volume 7 Clupeoid fishes of the world. An annotated and illustrated catalogue of the herrings, sardines, pilchards, sprats, shads, anchovies and wolf-herrings. Part 1 Chirocentridae, Clupeidae and Pristigasteridae. FAO Fisheries Synopsis, Rome, 7.
- Whitehead, P. J. P. 1986. Clupeidae. *In* *Fishes of the North-eastern Atlantic and the Mediterranean Volume I*, pp. 268–281. Ed. by M.-L. Bauchot, J. C. Hureau, J. Neilsen, and E. Tortonese. UNESCO, Paris.
- Wickman, H. 2016. ggplot2: Elegant Graphics for Data Analysis. Springer-Verlag New York. <https://ggplot2.tidyverse.org>.
- Widdicombe, C. E., Eloire, D., Harbour, D., Harris, R. P., and Somerfield, P. J. 2010. Long-term phytoplankton community dynamics in the Western English Channel. *Journal of Plankton Research*, 32: 643–655.
- Williams, R., Lindley, J. A., Hunt, H. G., and Collins, N. R. 1993. Plankton community structure and geographical distribution in the North Sea. *Journal of Experimental Marine Biology and Ecology*, 172: 143–156.
- Wiltshire, K. H., and Manly, B. F. J. 2004. The warming trend at Helgoland Roads, North Sea: phytoplankton response. *Helgoland Marine Research*, 58: 269–273.
- Winther, N. G., and Johannessen, J. A. 2006. North Sea circulation: Atlantic inflow and its destination. *Journal of Geophysical Research: Oceans*, 111.
- Wood, S. N. 2011. Fast stable restricted maximum likelihood and marginal likelihood estimation of semiparametric generalized linear models. *Journal of the Royal Statistical Society Series B: Statistical Methodology*, 73: 3–36.
- Wyatt, T. 1973. The biology of *Oikopleura dioica* and *Fritillaria borealis* in the Southern Bight. *Marine Biology*, 22: 137–158.
- Yasuda, T., Oda, M., Tanaka, S., Nanjo, N., Takahashi, M., and Fukuwaka, M. 2021. Selective retention and transfer of long-chain polyunsaturated fatty acids in Japanese sardine. *Marine Biology*, 168: 172.
- Zarauz, L., Irigoien, X., Urtizberea, A., and Gonzalez, M. 2007. Mapping plankton distribution in the Bay of Biscay during three consecutive spring surveys. *Marine Ecology Progress Series*, 345: 27–39.



## References

- Závorka, L., Blanco, A., Chaguaceda, F., Cucherousset, J., Killen, S. S., Liénart, C., Mathieu-Resuge, M., *et al.* 2023. The role of vital dietary biomolecules in eco-evo-devo dynamics. *Trends in Ecology & Evolution*, 38: 72–84.
- Zijlstra, J. J., Dapper, R., and Witte, J. Ij. 1982. Settlement, growth and mortality of post-larval plaice (*Pleuronectes platessa*) in the western Wadden Sea. *Netherlands Journal of Sea Research*, 15: 250–272.
- Zlatanov, S., and Laskaridis, K. 2007. Seasonal variation in the fatty acid composition of three Mediterranean fish – sardine (*Sardina pilchardus*), anchovy (*Engraulis encrasicolus*) and picarel (*Spicara smaris*). *Food Chemistry*, 103: 725–728.
- Zuur, A. F. 2012. A beginner's guide to generalized additive models with R. Highland Statistics Limited. 188 pp.
- Zuur, A. F., Hilbe, J. M., and Ieno, E. N. 2013. A Beginner's Guide to GLM and GLMM with R: A Frequentist and Bayesian Perspective for Ecologists. Highland Statistics Limited. 256 pp.
- Zwolinski, J., Morais, A., Marques, V., Stratoudakis, Y., and Fernandes, P. G. 2007. Diel variation in the vertical distribution and schooling behaviour of sardine (*Sardina pilchardus*) off Portugal. *ICES Journal of Marine Science*, 64: 963–972.

## French Summary - Résumé

Il est nécessaire de comprendre le fonctionnement des écosystèmes pour comprendre l'environnement dans lequel nous vivons et dont nous dépendons. Le fonctionnement des écosystèmes est un terme large qui englobe notamment les propriétés, les services et les biens associés aux écosystèmes. Les propriétés des écosystèmes, également appelées processus écosystémiques, décrivent le stock et le flux d'énergie, ainsi que leur stabilité temporelle. Les services écosystémiques sont définis comme « les conditions et les processus par lesquels les écosystèmes naturels et les espèces qui les composent permettent la vie des êtres humains » (Daily, 1997). Le changement climatique, la pollution, la diminution de la biodiversité, la pêche, l'eutrophisation ou la modification de l'habitat affectent le fonctionnement des écosystèmes ainsi que la fourniture de services écosystémiques (Cardinale et al., 2012 ; Halpern et al., 2008 ; IPPC, 2014 ; Millennium Ecosystem Assessment, 2005 ; Pauly et al., 1998 ; Smith, 2003). Pour adapter et atténuer ces pressions, qui sont liées à des degrés divers aux activités humaines, nous devons comprendre en profondeur le fonctionnement de l'écosystème (Brussard et al 1998).

Le plancton, composé d'organismes vivant en suspension dans la colonne d'eau, joue un rôle central dans le fonctionnement des écosystèmes marins (Richardson, 2008). Constitué de producteurs primaires autotrophes, le phytoplancton séquestre le carbone et produirait 50 à 70 % (Behrenfeld et al., 2001 ; Walker, 1980) de l'oxygène atmosphérique, et constitue la base énergétique et nutritionnelle des océans. En se nourrissant de phytoplancton, le zooplancton régule les cycles biogéochimiques, la qualité de l'eau, la pompe biologique à carbone et le climat. Le zooplancton transfère également de l'énergie et des nutriments, par exemple des protéines et des acides gras polyinsaturés à longue chaîne, à des espèces de niveaux trophiques supérieurs comme les petits poissons pélagiques (Arts et al., 2009 ; De Troch et al., 2012 ; Richardson, 2008). Les petits poissons pélagiques comme le hareng ou la sardine représentent un niveau trophique intermédiaire majeur entre la base planctonique du réseau trophique et les niveaux trophiques supérieurs comme les poissons piscivores, les mammifères marins, les oiseaux de mer et les êtres humains (Beaugrand et al., 2014 ; Cury et al., 2000 ; Olin et al., 2022 ; Richardson, 2008). Comprendre le fonctionnement des communautés de zooplancton au sein de l'écosystème par rapport au phytoplancton et aux

niveaux trophiques supérieurs est dès lors essentiel pour comprendre, prédire et gérer les écosystèmes marins.

Au sein du groupe des organismes zooplanctoniques se cache cependant une diversité complexe en termes de taille (pico à méga), de taxonomie, de traits d'histoire de vie et de comportements (Teodosio et Barbosa, 2020). Cette diversité est source d'interactions complexes au sein de l'écosystème. Ainsi, la compréhension du rôle du zooplancton dans le fonctionnement des écosystèmes, en relation avec les variations spatio-temporelles des facteurs abiotiques et biotiques, est un défi. Les approches de modélisation écosystémique ou les modèles de pêche simplifient souvent à l'excès le compartiment zooplancton, ce qui nuit à la fiabilité des résultats et des prévisions obtenus (Chenillat et al., 2021 ; Ratnarajah et al., 2023 ; Thorpe, 2024, Bracis et al., 2020). Les approches basées sur les traits caractérisant le zooplancton (caractéristiques comportementales, morphométriques, physiologiques ou trophiques) pourraient être un bon compromis entre simplification et représentativité de la diversité du zooplancton. Cependant, rares sont les informations sur les traits pour la plupart des taxons de zooplankton à l'exception des copépodes (Hébert et al., 2021 ; Ratnarajah et al., 2023).

Un cadre théorique permettant d'étudier la diversité du zooplancton en relation avec le fonctionnement de l'écosystème est le Multitrophic Biodiversity Ecosystem Functioning (MBEF) (Thompson et al., 2012). Cette approche vise à connecter l'écologie des communautés et l'écologie des écosystèmes via les interactions trophiques. Elle permet de prendre en compte les interactions entre espèces en ce qui concerne les relations trophiques qui peuvent être quantifiées par des transferts d'énergie ou de nutriments. Lorsque l'on considère le zooplancton comme une proie pour les niveaux trophiques supérieurs, la disponibilité et la qualité de la nourriture ne sont pas seulement déterminées par la composition taxonomique et l'abondance, mais aussi par la composition biochimique et la structuration en taille de la communauté zooplanctonique. Les taxons de zooplancton ont ainsi des teneurs en carbone et des proportions d'acides gras essentiels variables (Heneghan et al., 2023 ; Persson et Vrede, 2006). La taille joue un rôle déterminant dans les interactions prédateur-proie et les taux de mortalité (Anderson, 1988 ; Cohen et al., 1993). Les larves de poisson consomment des proies de taille déterminée, en raison de la taille de leur bouche (Last, 1978). Ainsi, il pourrait être nécessaire de prendre en compte non seulement la diversité taxonomique mais aussi les

diversités de taille et biochimiques dans le contexte du MBEF pour améliorer la compréhension mécaniste de la diversité du zooplancton dans l'écosystème.

L'objectif de cette thèse est de contribuer à une meilleure compréhension du fonctionnement de l'écosystème en étudiant le fonctionnement du zooplancton dans la Manche et le sud de la mer du Nord (SNS) dans le contexte du MBEF. J'ai considéré plusieurs perspectives concernant les compositions taxonomiques, biochimiques et de taille du zooplancton en relation avec les niveaux trophiques inférieurs (phytoplancton) et supérieurs (larves de poisson et sardine adulte), en prenant en compte la variation spatiale et les facteurs abiotiques potentiellement déterminant.

### **Perspective 1 : Composition taxonomique**

Dans le **premier chapitre**, j'ai étudié la composition taxonomique du zooplancton et de l'ichtyoplancton pendant l'hiver dans la Manche orientale (EEC) et le SNS en relation avec les facteurs biotiques et abiotiques dans le but de mieux comprendre et évaluer les assemblages hivernaux de zooplancton et la variabilité spatiale des conditions d'alimentation des larves de poissons nées en hiver.

La principale question du chapitre 1 était : Quels assemblages de mésozooplancton et d'ichtyoplancton sont présents dans le SNS-EEC pendant l'hiver et qu'est-ce qui détermine leur composition et leur distribution ?

Bien que le zooplancton ait été largement étudié en mer du Nord, les connaissances sur les assemblages hivernaux de zooplancton sont encore rares, malgré l'influence potentielle des stocks hivernants de zooplancton sur la succession et la productivité saisonnières du plancton. La taille et la distribution des stocks hivernants de zooplancton influencent les variations annuelles d'abondance et de distribution du zooplancton en mer du Nord (Colebrook, 1987, 1984), à la manière d'une graine (Hay et al., 1991) prête à germer dès que les conditions sont adéquates. Selon la taille et la composition du stock hivernant de zooplancton, la floraison printanière de phytoplancton pourrait être consommée différemment en termes de période, de quantité, de composition spécifique et de taille (Sommer et Lewandowska, 2011). Comme l'ont discuté Nielsen et Richardson (1989), de petites populations hivernantes de zooplancton

## French Summary - Résumé

pourraient laisser une grande partie de la floraison printanière inexploitée. Les stocks initiaux élevés de copépodes hivernants pourraient au contraire exercer un contrôle top-down plus précoce pendant le développement de la floraison printanière, prolongeant ainsi la durée de disponibilité des nutriments pour le phytoplancton par reminéralisation. Cela pourrait avoir d'autres conséquences sur la succession planctonique et la séquestration du carbone (Nielsen et Richardson, 1989 ; Spilling et al., 2018 ; Sterner, 1986). De plus, plusieurs espèces de poissons d'importance économique et écologique se reproduisent pendant l'hiver, contribuant à la communauté zooplanctonique en tant que membres passifs (œufs) ou prédateurs (larves). Pour élucider la distribution, l'abondance et la composition du zooplancton hivernal dans le sud de la mer du Nord et la Manche orientale, nous avons défini des assemblages de mésozoo- et d'ichtyoplancton sur la base de données échantillonnées entre janvier et février 2008 en utilisant des espèces indicatrices et une méthode de fuzzy clustering. Le mésozoo- et l'ichtyoplancton (œufs et larves) ont été intégrés dans une analyse commune en utilisant une grille spatiale adaptée aux ensembles de données et définie au moyen d'une méthode géostatistique développée en agronomie. Les facteurs environnementaux potentiels de la distribution des assemblages ont été évalués au moyen de modèles mixtes linéaires généralisés (GLMM). Une comparaison avec les données de 2022 a permis de mieux comprendre la représentativité interannuelle des assemblages trouvés. Cette étude suggère l'existence de cinq assemblages de zooplancton dans le SNS-EEC pendant l'hiver, qui varient en termes de productivité, d'abondance et de composition des taxons. Les facteurs potentiels de la distribution des assemblages étaient les variables abiotiques (nutriments dissous, salinité, profondeur, température, matière organique en suspension, chlorophylle a) et biotiques (composition du phyto- et du microplancton), les masses d'eau et les frayères des poissons.

## French Summary - Résumé

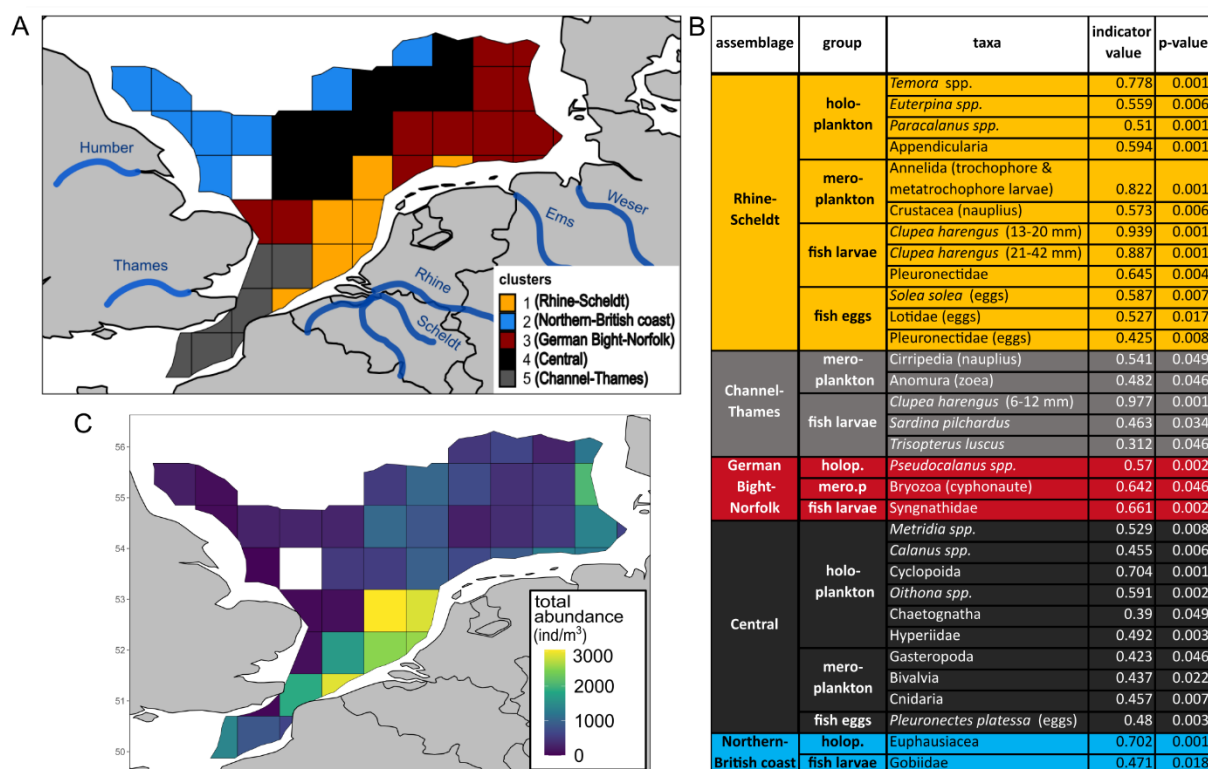


Figure 1 Assemblages et abondance totale du zooplancton. A : Groupes/assemblages basés sur le mésozooplancton et l'ichtyooplancton échantillonnés lors de la campagne IBTS en janvier et février 2008 ; B : Espèces indicatrices par groupe/assemblage avec valeur indicatrice respective et p-value ajustée ; C : Abondance totale du zooplancton (mésozoo- et ichthyoplancton) par cellule de la grille.

La distribution et la composition des assemblages obéissaient à deux schémas globaux liés à la fois à un gradient nord-sud et à l'abondance totale du zooplancton. Le gradient nord-sud était indiqué par la dominance d'*Oithona* spp. dans les assemblages du nord (Northern-British coast et Central) et de *Temora* spp. dans les assemblages du sud (Channel-Thames et Rhine-Scheldt). On peut supposer que les assemblages du nord sont influencés par les eaux du nord et du centre de la mer du Nord, comme l'indique en outre la présence de *Metridia* spp., d'Euphausiacea et de Gobiidae. Les assemblages du sud caractérisés en outre par des larves de hareng (*Clupea harengus*) et de Pleuronectidae étaient très probablement influencés par les eaux de la Manche et du sud de la mer du Nord, qui sont plus riches en azote et en silicate en raison de l'apport fluvial (OSPAR Commission, 2000). La région German Bight-Norfolk n'était pas associée au gradient nord-sud. Elle était caractérisée par *Pseudocalanus* spp. et différait des autres assemblages en terme de phyto-microplancton et de composition en nutriments. Le deuxième schéma était lié à la distribution de l'abondance totale du zooplancton. Les assemblages au large de l'estuaire Rhine-Scheldt et dans le German Bight abritaient les plus grandes abondances de zooplancton, ce qui pourrait influencer la pression

de prédation sur la production printanière de phytoplancton. L'abondance élevée de phyto-microplancton dans la région centrale a indiqué que cet assemblage était central dans la production de plancton au début du printemps. La distribution des taxons d'ichtyoplancton au sein des assemblages correspondait aux frayères et aux voies de migration des espèces de poissons, les assemblages Channel-Thames et Rhine-Scheldt étant d'une grande importance pour les larves de hareng et de plie (*Pleuronectes platessa*).

Bien que d'autres analyses aient suggéré une représentativité interannuelle des assemblages trouvés (2008 vs 2022), la prise en compte d'années supplémentaires serait nécessaire pour évaluer la variabilité interannuelle dans la composition du zooplancton. Les études futures pourraient tirer profit de l'évaluation de microzooplancton, ce qui permettrait de mieux comprendre le potentiel alimentaire des larves de poissons et les stratégies d'hivernage du zooplancton.

### **Perspective 2 : Structure en taille et signature isotopique**

Dans le **deuxième chapitre**, j'ai étudié la structure en taille du plancton par rapport à la signature isotopique, en allant du nano- au mésoplancton, puis la contribution des différentes classes de taille du plancton au régime alimentaire des larves de hareng et de plie en Manche orientale.

Les principales questions du chapitre 2 étaient : Quelle est la structure en taille du plancton de Manche orientale par rapport à sa signature isotopique en hiver ? Quelles classes de taille de plancton sont caractéristiques du régime alimentaire des larves de plie et de hareng ?

Les larves de poisson font partie du réseau alimentaire planctonique en se nourrissant d'une variété d'organismes micro- et méso-planctoniques. Les travaux qui ont exploré les facteurs de survie des larves de poisson ont ainsi souligné l'importance de l'alimentation des larves. Une alimentation réussie permet aux larves de surmonter le passage d'une alimentation interne à une alimentation externe, pendant laquelle la mortalité est particulièrement élevée (hypothèse de la « période critique », Hjort, 1914), et de grandir au-delà de la gamme de taille la plus exposée à la prédation (hypothèse « plus c'est gros, mieux c'est », Anderson, 1988). L'abondance et la biomasse des populations de poissons fluctuent dans le temps, principalement en raison de la variabilité du processus de recrutement (Houde, 2016), au

cours duquel la survie des premiers stades de vie a été déterminée comme un goulot d'étranglement (bottleneck) (Houde, 2008). Les larves de hareng et de plie, deux espèces de poissons importantes sur le plan économique et écologique, font partie du même réseau trophique planctonique en partageant des périodes et des zones de reproduction similaires. Les deux espèces frayent en hiver en Manche orientale et dans le sud de la mer du Nord. Au cours du développement larvaire, plusieurs périodes critiques sont identifiées, comme pour exemple la phase de métamorphose, qui requiert une quantité d'énergie importante (Joly et al., 2021). Ainsi, la compréhension des stratégies alimentaires du hareng et de la plie durant les différents stades de développement est essentielle pour améliorer nos connaissances sur la variabilité de leur recrutement. De telles études sont particulièrement de circonstance pour des stocks tels que le hareng de mer du Nord, qui rencontre une période de faible recrutement depuis 2002 (ICES, 2023), et dans le contexte du changement climatique. Il a été ainsi démontré que le changement climatique influence la composition de la communauté zooplanctonique dans la zone d'étude (Beaugrand et al., 2014 ; Bedford et al., 2020 ; Semmouri et al., 2023), et pourrait donc affecter la quantité et la qualité des proies des larves de poissons. Les larves de hareng et de plie, ainsi que différentes classes de taille de plancton incluant le nano- (> 20  $\mu\text{m}$ ), le micro- (20 – 200  $\mu\text{m}$ ) et le mésozooplancton (200 – 1000  $\mu\text{m}$ ), ont été échantillonnées au cours de la campagne IBTS (International Bottom Trawl Survey) du premier trimestre en Manche orientale en janvier-février 2021. La composition en isotopes stables ( $\delta^{13}\text{C}$ ,  $\delta^{15}\text{N}$ ) de différentes classes de taille de plancton et de larves de poissons a été mesurée pour obtenir des informations sur la structure en taille et les relations trophiques dans la zone d'étude. Des modèles additifs généralisés (GAM) ont été utilisés afin de prédire les valeurs isotopiques des différentes classes de taille de plancton aux stations d'échantillonnage des larves. Sur la base de ces prédictions, des modèles de mélange d'isotopes stables (MixSIAR) ont été utilisés pour évaluer la contribution de différentes classes de taille à la nutrition des larves (Stock et al., 2018). La station d'échantillonnage a été intégrée comme covariable pour évaluer la variabilité spatiale potentielle de la composition du régime alimentaire des larves. Pour les larves de plie, un deuxième modèle utilisant la station d'échantillonnage et le stade de développement comme covariables a permis d'évaluer les différences alimentaires entre les différents stades de développement des larves de plie tout en tenant compte de la variabilité spatiale.



La structure verticale isotopique hivernale du réseau trophique planctonique en Manche orientale était élevée avec  $\delta^{15}\text{N}$  variant entre des valeurs négatives et environ 18‰.

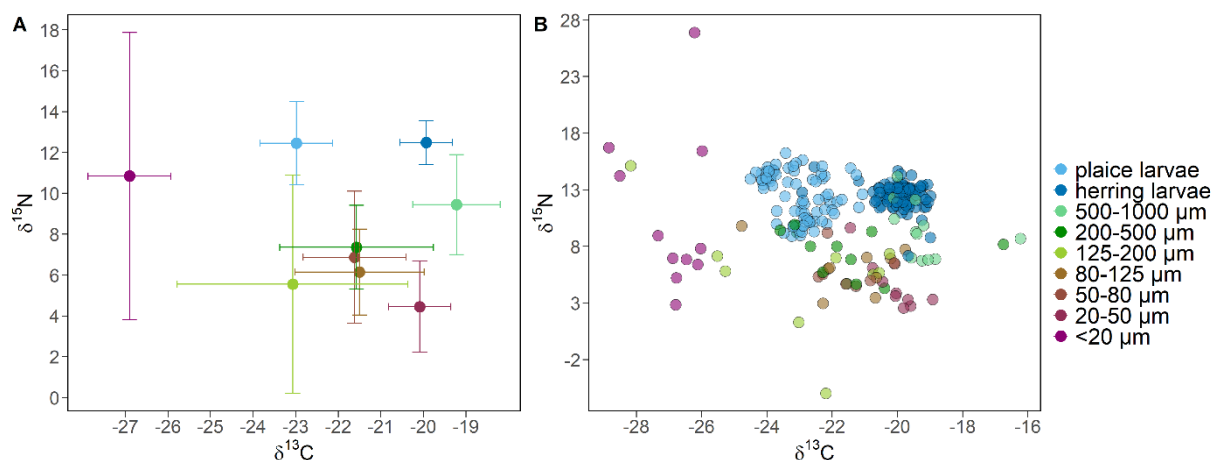


Figure 2 Biplot des signatures en isotopes stables du carbone ( $\delta^{13}\text{C}$ ) et de l'azote ( $\delta^{15}\text{N}$ ) pour différentes classes de taille de plancton et larves de poissons. A : Moyenne et écart type par classe de taille et espèce de larve; B : Valeurs brutes par station d'échantillonnage (un échantillon par station et classe de taille de plancton et entre 8 et 10 larves par station).

En comparaison, la gamme de valeurs de  $\delta^{15}\text{N}$  pour le plancton en Méditerranée (printemps) variait de plus zéro à 5‰ (Tesán-Onrubia et al., 2023). Cependant, la structure en taille verticale était moins prononcée dans la Manche orientale qu'en Méditerranée. Alors qu'en Méditerranée, les signatures isotopiques étaient clairement différenciées dans la gamme de taille 50 – 500 $\mu\text{m}$ , elles étaient similaires en Manche orientale, variant entre -21,5‰ et -23‰ pour  $\delta^{13}\text{C}$ , et entre 6‰ et 8‰ pour  $\delta^{15}\text{N}$ . En plus, les valeurs isotopiques au sein de chaque classe de taille comprise dans cette gamme étaient sujettes à une forte variabilité. Ce manque de structuration en taille pourrait être le résultat d'une faible biomasse de phytoplancton en hiver qui pourrait entraîner une dominance de l'omnivorie pour l'ensemble des classes de taille dans cette gamme (Giraldo et al., 2024 ; Kozak et al., 2020). Les signatures isotopiques de la classe de taille 500 – 1000  $\mu\text{m}$  et des larves de poissons étaient plus distinctes avec des valeurs de  $\delta^{15}\text{N}$  légèrement élevées (~9‰ et 13‰, respectivement) par rapport aux autres classes de taille de plancton (sauf <20  $\mu\text{m}$ ), indiquant l'affiliation à un niveau trophique supérieur et à un mode d'alimentation principalement carnivore.

L'analyse MixSIAR suggère des stratégies d'alimentation différentes pour les larves de hareng et de plie en ce qui concerne la taille des proies. De plus, la contribution des classes de taille du plancton à la nutrition des larves de plie varie spatialement. La signature isotopique des

larves de hareng et de plie était spécifique à l'espèce et n'indiquait aucun chevauchement dans leurs niches isotopiques. Alors que les larves de hareng se nourrissaient préférentiellement de la classe de taille 500 – 1000  $\mu\text{m}$ , les classes de taille 125 – 200  $\mu\text{m}$  et < 20  $\mu\text{m}$  présentaient les contributions les plus élevées dans le régime alimentaire des larves de plie. La contribution de la classe de taille < 20  $\mu\text{m}$  pourrait indirectement étayer les résultats antérieurs signalant *O. dioica* comme proie majeure pour les larves de plie en Manche orientale. La variation spatiale de la composition alimentaire des larves de plie en fonction des apports fluviaux pourrait être liée à la variation spatiale de l'abondance d'*O. dioica*. Cette étude met en outre en l'accent sur l'importance du microplancton dans la nutrition des larves de plie. L'analyse initiale des changements ontogénétiques du régime alimentaire des larves de plie n'a montré aucune variation de la contribution des différentes classes de taille de plancton à leur régime alimentaire du stade 1 au stade 3. Cette étude souligne l'importance de prendre en compte toutes les proies et les classes de taille possibles des proies dans l'analyse MixSIAR, afin d'obtenir des estimations représentatives de la composition du régime alimentaire.

### **Perspective 3 : Composition en acides gras**

Dans le **troisième chapitre**, je me suis concentrée sur la composition biochimique du mésozooplancton en acides gras (AG) et leur transfert vers des niveaux trophiques supérieurs représentés par la sardine (*Sardina pilchardus*). Le profil des acides gras du mésozooplancton et de la sardine a été analysé en combinaison avec la composition taxonomique du zooplancton et du phytoplancton dans toute la Manche.

La principale question posée dans ce chapitre était : Comment le profil des acides gras du zooplancton et de la sardine varie-t-il spatialement dans la Manche et quels sont les facteurs déterminant la variabilité spatiale du transfert trophique de ces nutriments essentiels entre ces deux niveaux trophiques ?

Le phytoplancton joue un rôle crucial dans les réseaux trophiques marins car il fournit des AG essentiels aux niveaux trophiques supérieurs, tels que les petits poissons pélagiques, par l'action intermédiaire du zooplancton. Ainsi, la composition et la valeur nutritionnelle des communautés planctoniques influencent l'abondance et la condition des prédateurs, et

structurent les modalités du transfert trophique dans l'espace. Les AG tels que l'acide docosahexaénoïque (22:6(n-3), DHA), l'acide eicosapentanoïque (20:5(n-3), EPA) et l'acide arachidonique (20:4(n-6), ARA) sont des nutriments essentiels pour la plupart des animaux marins. Ces acides gras sont nécessaires au bon état physiologique (Gladyshev et al., 2018 ; Tocher, 2003) et doivent être obtenus par l'alimentation car ils ne peuvent pas ou seulement dans une moindre mesure être produits par l'animal lui-même (Galloway et Winder, 2015 ; Tocher, 2010). Comprendre la distribution spatiale et la variabilité du transfert trophique des AG est crucial pour une meilleure compréhension du fonctionnement de l'écosystème (Brett et Müller-Navarra, 1997 ; Galloway et Winder, 2015). La sardine européenne est une espèce de poisson planctonivore, qui se nourrit de phyto- et zooplancton (Garrido et al., 2008 ; Nikolioudakis et al., 2012), et représente une proie riche en énergie pour les oiseaux, les mammifères marins et les poissons piscivores (Campo et al., 2006 ; Certain et al., 2011). En me basant sur le profil des AG du zooplancton et de la sardine et sur la composition de la communauté de phytoplancton et de zooplancton, j'ai étudié, (i) la variabilité spatiale à grande échelle du transfert trophique des AG du plancton à la sardine et, (ii) les facteurs influençant ce transfert dans la Manche. À l'aide d'échantillons collectés lors de la campagne CGFS (Channel Ground Fish Survey) dans la Manche à l'automne 2021, nous avons appliqué une analyse en composantes principales au profil en AG du mésozooplancton et de la sardine et aux données taxonomiques du zoo- et du phytoplancton, pour évaluer leur structuration spatiale dans la zone d'étude. Nous avons également utilisé des GLMM et des GAM pour évaluer l'influence des caractéristiques environnementales, morphologiques et physiologiques de la sardine sur le transfert trophique de trois AG essentiels (EPA, DHA et ARA) du zooplancton aux sardines. La proportion d'un AG essentiel chez les sardines a été modélisée en fonction des covariables fixes : proportion de l'AG essentiel respectif dans le zooplancton, indice de condition de Le Cren, activité de ponte et région. La covariable « région » a été utilisée comme proxy de l'état environnemental dans le modèle car les paramètres environnementaux (température, salinité, profondeur) étaient fortement corrélés et différaient significativement entre la Manche occidentale (WEC) et la Manche orientale. Nous avons montré une forte structuration spatiale avec une différence marquée des profils d'AG du zooplancton et de la sardine entre la Manche occidentale et orientale à l'automne 2021. Des patrons spatiaux similaires ont été trouvés dans la composition taxonomique du phyto- et du zooplancton, dans des marqueurs trophiques d'acides gras (FATM) ainsi que dans la

## French Summary - Résumé

corrélation entre les proportions d'AG essentiels du muscle de la sardine et du zooplancton. Ceci indique un fort contrôle bottom-up du transfert trophique des AG essentiels principalement déterminé par la composition taxonomique des proies planctoniques.

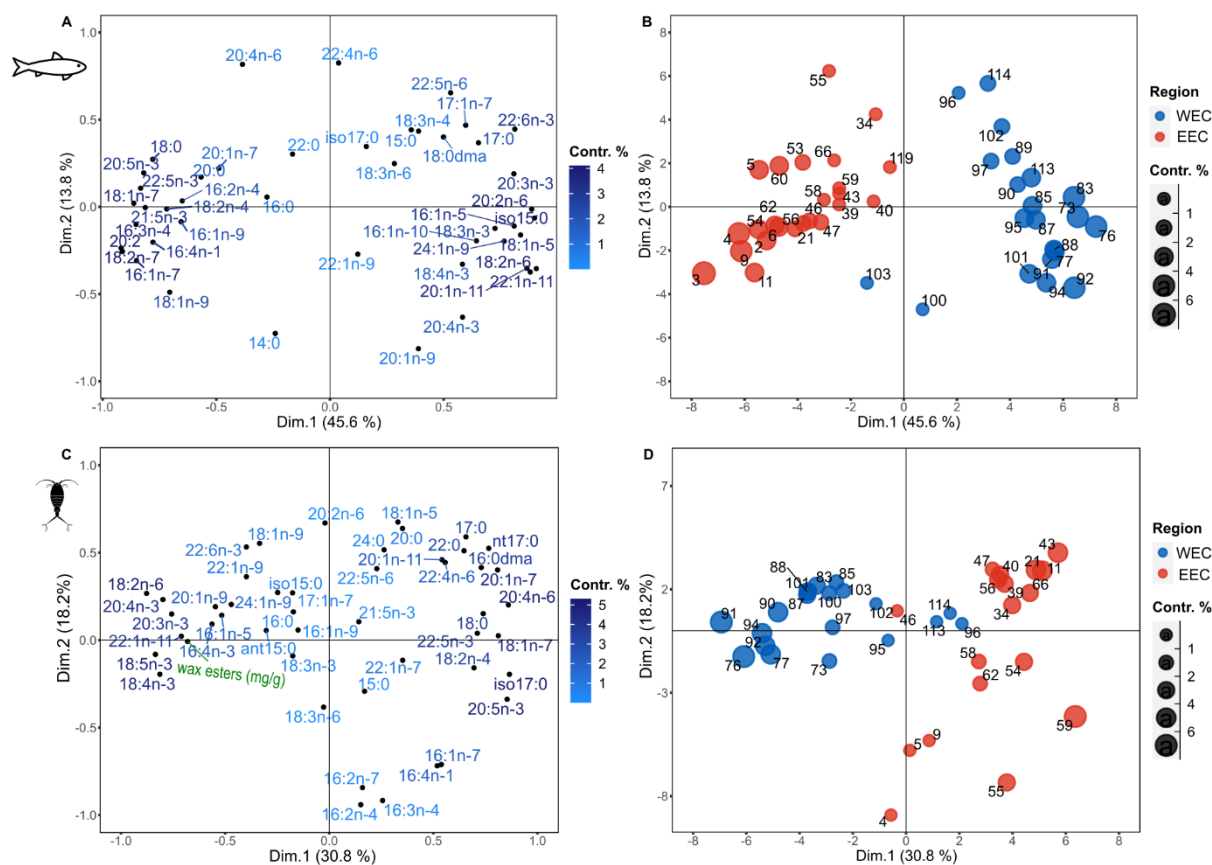


Figure 3 Première et deuxième composantes d'une analyse en composantes principales (ACP) sur les profils d'acides gras des sardines (A, B) et du zooplancton (500 – 1000  $\mu$ m) (C, D) collectés en Manche occidentale (bleu) et en Manche orientale (rouge). Les panneaux A et C affichent les acides gras (plus le taxon est foncé, plus sa contribution à la première composante est élevée). Les panneaux B et D affichent les stations d'échantillonnage (plus le point est gros, plus sa contribution à la première composante est élevée; les nombres représentent l'identifiant de la station d'échantillonnage).

Outre le fort contrôle bottom-up du transfert trophique, l'état physiologique de la sardine en ce qui concerne le stade de maturité, la stratégie d'allocation d'énergie et la condition influence le transfert trophique. L'EPA et l'ARA étaient significativement corrélés aux proportions d'AG du zooplancton, tandis que le DHA ne l'était pas. Cela pourrait être lié à une régulation plus forte de cet AG essentiel et physiologiquement important pour les organismes, ce qui rend le lien avec les sources trophiques plus complexe. L'activité de reproduction était corrélée négativement à la proportion des trois AG essentiels testés. Le DHA, l'EPA et l'ARA sont connus pour être importants pour le développement des embryons et des larves de poissons (Izquierdo, 1996 ; Tocher, 2010) et sont incorporés dans les ovocytes de sardine, ce

qui entraîne une diminution de la concentration de ces AG dans le muscle (Garrido et al., 2008, 2007). Comme l'activité de reproduction et le rapport TAG-ST étaient liés, les individus non reproducteurs ayant un rapport TAG-ST plus faible avaient des réserves en lipides plus faibles que les individus reproducteurs. Donc, la corrélation entre les proportions des trois AG essentiels testés et l'activité de reproduction pourrait également refléter une relation entre les proportions de ces AG avec le TAG-ST.

La structuration spatiale du profil d'AG de la sardine, combinée à l'association du FATM au WEC ou à l'EEC, indique que les sardines n'ont résidé et se sont nourries que d'un côté de la Manche pendant la période d'étude et les semaines précédentes, ce qui correspond au temps d'incorporation du profil en AG. Avec les différences de communautés planctoniques entre les deux bassins, la structuration spatiale des sardines en Manche est en accord avec les études biogéographiques, qui ont affilié la Manche occidentale et la Manche orientale à différentes écorégions, biomes et provinces (Longhurst, 2010 ; Spalding et al., 2007). Des recherches plus approfondies sur le schéma de ségrégation des sardines entre le WEC et l'EEC sont recommandées pour comprendre son origine et en ce qui concerne les modèles écosystémiques et les stratégies de gestion.

Dans cette thèse, nous avons mis en perspective la fonction du zooplancton dans l'écosystème marin de trois manières différentes, toutes basées sur une approche intégrant des niveaux trophiques inférieurs et supérieurs. Nous avons étudié la composition taxonomique et l'abondance du zooplancton dans le sud de la mer du Nord et la Manche orientale, les liens entre structure en taille et signature isotopique du zooplancton en Manche orientale, et les profils en acides gras du zooplancton dans toute la Manche, en tenant compte de la distribution et de la variabilité spatiales des compartiments écosystémiques et environnementaux étudiés.

Toutes les études ont révélé une variabilité spatiale dans le fonctionnement du zooplancton dans l'écosystème, qui semble en partie lié aux niveaux trophiques inférieurs et supérieurs. Ainsi, l'étude du zooplancton, dans le contexte du fonctionnement multitrophique de l'écosystème, a permis une compréhension plus mécaniste de la diversité du zooplancton et de sa relation avec d'autres composantes de l'écosystème. Ces informations seront utiles à la modélisation et à la gestion de l'écosystème marin.

La prise en compte de plusieurs caractéristiques du zooplancton pourrait également être importante dans la compréhension des effets du changement climatique. Il a été suggéré que la diminution de la taille et de l'état des sardines et des anchois observés en Méditerranée et dans le golfe de Gascogne était liés à un stress alimentaire (Brosset et al., 2016 ; Menu et al., 2023 ; Queiros et al., 2019). La prise en compte des différentes caractéristiques de la communauté zooplanctonique était nécessaire pour acquérir une compréhension mécaniste de ce phénomène. La quantité et la qualité de la nourriture peuvent varier en raison de multiples facteurs, tels qu'une diminution de l'abondance globale ou spécifique du zooplancton (Beaugrand et Kirby, 2010 ; Menu et al., 2023), des changements dans la communauté du zooplancton des taxons plus grands vers les taxons plus petits (Brosset et al., 2016), ou une baisse de la qualité des proies, y compris la densité énergétique (Heneghan et al., 2023 ; Menu et al., 2023). L'augmentation de la température due au réchauffement des océans pourrait entraîner une diminution de la taille individuelle du zooplancton en raison d'un effet direct (Daufresne et al., 2009 ; Dudeck et al., 2021) ou indirect via la stratification des masses d'eau (Daufresne et al., 2009 ; Lewandowska et al., 2014). De plus, le changement climatique pourrait également modifier la production d'AG dans le phytoplancton, réduisant potentiellement la disponibilité de ces nutriments essentiels pour les niveaux trophiques supérieurs (Litzow et al., 2006 ; Galloway and Winder, 2015 ; Hixon and Arts, 2016).

Les trois perspectives choisies pour étudier le zooplancton représentent une approche combinant à la fois la taxonomie et les traits biologiques du zooplancton, ceux-ci étant caractérisés par la taille et le profil en AG. La prise en considération de ces traits a permis d'évaluer le lien entre les classes de taille du plancton et le régime alimentaire des larves de hareng et de plie, ainsi que les différences spatiales multitrophiques entre la Manche occidentale et Manche orientale. L'étude combinée de la taxonomie et de la composition en AG du zooplancton en lien avec les niveaux trophiques inférieurs (phytoplancton) et supérieurs (e.g., sardine) propose d'autres caractéristiques du zooplancton qui lient le zooplancton à l'écosystème et qui pourraient ainsi contribuer à une compréhension plus mécaniste du fonctionnement du zooplancton au sein de son écosystème environnant. L'abondance des diatomées, des dino- et nanoflagellés ainsi que la biomasse du phytoplancton se sont révélées être des facteurs déterminant la distribution spatiale des espèces indicatrices d'assemblage (chapitre 1). Ce résultat concordait avec la distribution spatiale du mésozooplancton obtenue

## French Summary - Résumé

dans le golfe de Gascogne, qui présentait également des patrons spatiaux distincts, apparemment liés à la production primaire et aux relations trophiques phyto-zooplancton (Grandremy et al., 2023). Les principales différences dans le profil des AG du zooplancton et de la sardine étaient liées à la proportion de dinoflagellés et de diatomées dans la communauté phytoplanctonique et à la présence de *Calanus spp.* Dans l'ensemble, ce lien entre phytoplancton, zooplancton et sardine semble être lié au transfert des AG, au stockage d'énergie et à l'hibernation, au mode d'alimentation et à la stratégie de reproduction. Selon les taxons de zooplancton, les AG peuvent être soit obtenus quasi-exclusivement à partir du phytoplancton, soit synthétisés et régulés dans une certaine mesure par certains taxons comme *Calanus spp.* qui produisent des réserves de lipides (Dalsgaard et al., 2003 ; Hagen et Auel, 2001 ; Kattner et Hagen, 1995). Il a été suggéré que la production de réserves de lipides sous forme de cires estérifiées était possible chez les espèces capables d'hiberner (Cavallo et Peck, 2020). Alors que *Pseudocalanus spp.* et *Paracalanus spp.* semblent être capables de s'adapter à la forte teneur en matière organique du German Bight en filtrant leur nourriture, les organismes chassant à l'affût ou activement (cruise-feeding) pourraient être désavantagés dans cette région. La reproduction hivernale pourrait permettre à *Temora spp.* de bénéficier de la production primaire dans la région Rhine-Scheldt. Ainsi, la compréhension du lien entre les facteurs déterminants potentiels de la distribution et la composition biochimique du zooplancton permet de mieux interpréter le lien entre les traits du zooplancton et l'écosystème. Litchman et al. (2013) proposent trois groupes de traits du zooplancton liés à l'alimentation, à la reproduction et à la survie, en catégorisant les traits évoqués ci-dessus. Ils suggèrent qu'en raison des compromis d'allocation d'énergie, un organisme ne peut pas maximiser la performance de tous les traits simultanément, ce qui entraîne ce que l'on appelle des compromis de traits et peut générer une combinaison de traits distincts au sein du même organisme. Par exemple, un animal qui investit de l'énergie dans la croissance allouera moins d'énergie à la reproduction. Un animal qui chasse à l'affût connaîtra des taux de rencontre inférieurs avec des partenaires d'accouplement et développera potentiellement des stratégies de reproduction différentes de celles des organismes qui chassent activement. L'utilisation combinée de traits trophiques, de survie et de reproduction résultant de compromis de traits pourrait donc être une voie pertinente pour représenter le zooplancton dans des modèles numériques futurs (Thorpe, 2024), dans la mesure où ces traits représenteraient adéquatement la diversité et le fonctionnement mécaniste du zooplancton au sein de

## French Summary - Résumé

l'écosystème. L'observation du zooplancton dans le contexte du MBEF semble être une approche prometteuse pour évaluer ces traits en association avec des travaux expérimentaux.



## Appendix

### List of Figures Appendix

- Figure A 1 Sampling stations IBTS 2008.** A: Water samples for phyto- and microplankton community analysis; B: Water samples for POM, nitrate, nitrite, ammonium, phosphate, silicate and chlorophyll a; C: Salinity, temperature and depth..... ccxi
- Figure A 2 Empirical and theoretical variograms of species used for the determination of optimal grid cell size.** (A) Small-sized herring larvae (6 – 12 mm), variogram model fitted to raw data; B; medium-sized herring larvae (13 – 20 mm), variogram fitted to raw data; (C) Appendicularia, variogram fitted to residuals of quadratic regression; (D) Acartia, variogram fitted to residuals of linear regression; (E) Calanoida, variogram fitted to residuals of linear regression, (F) Pseudocalanus, variogram fitted to residuals of linear regression; (G) Centropages, variogram fitted to residuals of quadratic regression. .... ccxv
- Figure A 3 Taxon-specific optimal grid cell size (Lopt).** Functions display maximal information content per cell ( $f(v)$ ) depending on grid cell size (length and width in km) calculated for different taxa. PN = proportion of nugget variance removed, PS = proportion of sill variance retained. Lopt indicates taxon-specific optimal grid cell size. The median of the species specific Lopt (91.58 km, 0.83°) produced a single cell of central position not containing sampling stations and was thus accepted without further adjustment. .... ccxvi
- Figure A 4 Statistical methods to determine optimal number of clusters (2008 big spatial extent).** (A) Silhouette width indicating an optimum number of three clusters, (B) Kelly-Gardner-Sutcliffe penalty function proposing an optimal number of four clusters, (C) Mantel correlation indicating an optimal number of four clusters..... ccxvii
- Figure A 5 Statistical methods to determine optimal number of clusters (Comparison 2008 vs 2022, small spatial extent).** (A) Silhouette width indicating an optimum number of three clusters, (B) Kelly-Gardner-Sutcliffe penalty function proposing an optimal number of four clusters, (C) Mantel correlation indicating an optimal number of four clusters. .... ccxvii
- Figure A 6 Relative phyto- microplankton composition per zooplankton assemblage..** ccxviii
- Figure A 7 Distribution of nutrients and chlorophyll a. Maps display mean per grid cell of nutrients sampled during the IBTS 2008.** ..... ccxix

**Figure A 8 Taxa composition of assemblages in 2008 (left) and 2022 (right).** Mean abundance of taxa was calculated with regard to the spatial distribution of clusters in 2008 for both years.

..... CCXX

**Figure A 9 Drivers per assemblage.** Boxplots displaying the variability of a potential driver per assemblage. Beginning in the upper left corner continuing to the right: temperature, salinity, depth, concentration of particulate organic matter, concentration of chlorophyll a, total phyto- and microplankton abundance and Nitrogen/Phosphorus ratio. .... ccxxi

**Figure A 10 Mean abundance of taxa per cluster with individually scaled y-axis.** Mean abundance is therefore not comparable between clusters but gives further insight in community per cluster. .... ccxxii

**Figure A 11 PCA on potential abiotic and biotic drivers.** (A) Abiotic parameters displayed in a two-dimensional space of a PCA. (B) Assemblages/cluster displayed in the same two-dimensional space as in A. Numbers indicate grid cell ID. (C) Phyto- and microplankton groups displayed in a two-dimensional space of a PCA. (D) Assemblages/cluster displayed in the same two-dimensional space as in C. Numbers indicate grid cell ID. ....ccxxiii

**Figure A 12 Boxplots of PCA dimensions per cluster.** (A) First dimension of PCA applied to abiotic parameters. (B) Second dimension of PCA applied to abiotic parameters. (C) First dimension of PCA applied to biotic parameters. ....ccxxiv

**Figure A 13 Clusters received using different k.** (A) Clusters derived using a  $k = 2$ ; (B) Clusters derived using a  $k=3$ .....ccxxiv

**Figure A 14 Inter-annual differences of environmental conditions.** Measurements taken in 2008 were subtracted from measurements taken in 2022 so that positive values indicate an increase in 2022 compared to 2008. Numbers in grid cells indicate grid cell ID. A: Temperature; B: Salinity; C: Chlorophyll a; D: Particulate organic matter. ....ccxxv

**Figure A 15 Carbon (A) and nitrogen (B) stable isotope values at different larval sizes.** ccxxvi

**Figure A 16 TAG-ST ratio model verification using the DHARMA package.** The plot function of the package allows to calculate a quantile regression, which compares the empirical 0.25, 0.5 and 0.75 quantiles with the theoretical 0.25, 0.5 and 0.75 quantiles (dashed black line), and provides a p-value for the deviation from the expected quantile. Red color indicates a significant deviation from the expected quantile. Left: qq-plot to detect deviations from expected distribution, with added tests for correct distribution (KS test), dispersion and outliers. Right: Residuals against predicted values..... ccxxxix

**Figure A 17 Variogram TAG-ST ratio.** To evaluate spatial autocorrelation in the model residuals, variograms were created based on residuals of the glm (upper) not accounting for spatial autocorrelation in the model and on residuals of the glmm (lower) accounting for spatial autocorrelation in the model (lower). ..... ccxl

**Figure A 18 Length model verification using the DHARMA package.** The plot function of the package allows to calculate an quantile regression, which compares the empirical 0.25, 0.5 and 0.75 quantiles with the theoretical 0.25, 0.5 and 0.75 quantiles (dashed black line), and provides a p-value for the deviation from the expected quantile. Red color indicates a significant deviation from the expected quantile. Left: qq-plot to detect deviations from expected distribution, with added tests for correct distribution (KS test), dispersion and outliers. Right: Residuals against predicted values. .... ccxli

**Figure A 19 Variogram Length.** To evaluate spatial autocorrelation in the model residuals, variograms were created based on residuals of the glm (upper) not accounting for spatial autocorrelation in the model and on residuals of the glmm (lower) accounting for spatial autocorrelation in the model (lower). ..... ccxlii

**Figure A 20 Weight model verification using the DHARMA package.** The plot function of the package allows to calculate an quantile regression, which compares the empirical 0.25, 0.5 and 0.75 quantiles with the theoretical 0.25, 0.5 and 0.75 quantiles (dashed black line), and provides a p-value for the deviation from the expected quantile. Red color indicates a significant deviation from the expected quantile. Left: qq-plot to detect deviations from expected distribution, with added tests for correct distribution (KS test), dispersion and outliers. Right: Residuals against predicted values. .... ccxliii

**Figure A 21 Variogram Weight.** To evaluate spatial autocorrelation in the model residuals, variograms were created based on residuals of the glm (upper) not accounting for spatial autocorrelation in the model and on residuals of the glmm (lower) accounting for spatial autocorrelation in the model (lower). ..... ccxliv

**Figure A 22 Le Cren's index model verification using the DHARMA package.** The plot function of the package allows to calculate an quantile regression, which compares the empirical 0.25, 0.5 and 0.75 quantiles with the theoretical 0.25, 0.5 and 0.75 quantiles (dashed black line), and provides a p-value for the deviation from the expected quantile. Red color indicates a significant deviation from the expected quantile. Left: qq-plot to detect deviations from

expected distribution, with added tests for correct distribution (KS test), dispersion and outliers. Right: Residuals against predicted values..... ccxlv

**Figure A 23 Differences of biological parameters of sardine between regions.** A: Comparison of length between sardines caught in the EEC and WEC. Red dots indicate mean; B: Comparison of weight between sardines caught in the EEC and WEC. Red dots indicate mean; C: Comparison of TAG-ST ratio between sardines caught in the EEC and WEC. Red dots indicate mean; D: Comparison of Le Cren’s index between sardines caught in the EEC and WEC. Red dots indicate mean; E: Proportion of spawning and non-spawning individuals per region. .... ccxlvii

**Figure A 24 Environmental conditions in the WEC and EEC during CGFS 2021.** A: Temperature; B: Salinity; C: Depth; P-values of the statistical analysis are indicated in the heading of figures A-C. .... ccxlviii

**Figure A 25 EPA GLMM verification using the DHARMA package.** The plot function of the package allows to calculate a quantile regression, which compares the empirical 0.25, 0.5 and 0.75 quantiles with the theoretical 0.25, 0.5 and 0.75 quantiles (dashed black line), and provides a p-value for the deviation from the expected quantile. Red color indicates a significant deviation from the expected quantile. Left: qq-plot to detect deviations from expected distribution, with added tests for correct distribution (KS test), dispersion and outliers. Right: Residuals against predicted values..... ccxlix

**Figure A 26 EPA GLMM test for over/underdispersion.** If fitted model (red line), is among simulated values no over- or underdispersion is present..... ccl

**Figure A 27 EPA GLMM - Quantile residuals fitted against each covariate.** If second quantile is colored red, a non linear trend was detected and a GAM will be applied in a next step to take into account this non-linear pattern. .... ccli

**Figure A 28 Variogram EPA GLMM.** To evaluate spatial autocorrelation in the model residuals, variograms were created based on residuals of a GLMM (left) not accounting for spatial autocorrelation in the model and on residuals of the GLMM (right) accounting for spatial autocorrelation in the model. .... cclii

**Figure A 29 Convergence plots for GAM on EPA.** The first panel showcases a Q-Q plot, comparing model residuals to a normal distribution. A well-fitted model will exhibit residuals that closely align with a straight line. In the bottom left panel, a histogram of residuals is presented, expected to have a symmetrical bell shape. The top-right panel displays residuals

values, which ideally should be evenly distributed around zero. The final panel in the bottom right shows the response versus fitted values, where a perfect model would yield a straight line. .... cclii

**Figure A 30 EPA GAM verification using the DHARMA package.** The plot function of the package allows to calculate an quantile regression, which compares the empirical 0.25, 0.5 and 0.75 quantiles with the theoretical 0.25, 0.5 and 0.75 quantiles (dashed black line), and provides a p-value for the deviation from the expected quantile. Red color indicates a significant deviation from the expected quantile. Left: qq-plot to detect deviations from expected distribution, with added tests for correct distribution (KS test), dispersion and outliers. Right: Residuals against predicted values. .... ccliii

**Figure A 31 EPA GAM test for over/underdispersion.** If fitted model (red line), is among simulated values no over- or underdispersion is present. .... ccliv

**Figure A 32 Variogram EPA GAM.** To evaluate spatial autocorrelation in the model residuals, variograms were created based on residuals of a GLMM (left) accounting for spatial autocorrelation in the model and on residuals of the GAM (right) not accounting for spatial autocorrelation in the model. .... cclv

**Figure A 33 EPA GAM - Quantile residuals fitted against each covariate.** Is second quantile is colored red, a non linear trend was detected and a GAM will be applied in a next step to take into account this non-linear pattern. .... cclvi

**Figure A 34 Model prediction per covariate for EPA GAM.** .... cclvii

**Figure A 35 DHA GLMM verification using the DHARMA package.** The plot function of the package allows to calculate an quantile regression, which compares the empirical 0.25, 0.5 and 0.75 quantiles with the theoretical 0.25, 0.5 and 0.75 quantiles (dashed black line), and provides a p-value for the deviation from the expected quantile. Red color indicates a significant deviation from the expected quantile. Left: qq-plot to detect deviations from expected distribution, with added tests for correct distribution (KS test), dispersion and outliers. Right: Residuals against predicted values. .... cclix

**Figure A 36 DHA GLMM test for over/underdispersion.** If fitted model (red line), is among simulated values no over- or underdispersion is present. .... cclx

**Figure A 37 Variogram DHA GLMM.** To evaluate spatial autocorrelation in the model residuals, variograms were created based on residuals of a GLMM (left) not accounting for spatial

autocorrelation in the model and on residuals of the GLMM (right) accounting for spatial autocorrelation in the model. .... cclx

**Figure A 38 DHA GLMM - Quantile residuals fitted against each covariate.** Is second quantile is colored red, a non linear trend was detected and a GAM will be applied in a next step to take into account this non-linear pattern. .... cclxi

**Figure A 39 Convergence plots for GAM on DHA.** The first panel showcases a Q-Q plot, comparing model residuals to a normal distribution. A well-fitted model will exhibit residuals that closely align with a straight line. In the bottom left panel, a histogram of residuals is presented, expected to have a symmetrical bell shape. The top-right panel displays residuals values, which ideally should be evenly distributed around zero. The final panel in the bottom right shows the response versus fitted values, where a perfect model would yield a straight line. .... cclxii

**Figure A 40 DHA GAM verification using the DHARMA package.** The plot function of the package allows to calculate an quantile regression, which compares the empirical 0.25, 0.5 and 0.75 quantiles with the theoretical 0.25, 0.5 and 0.75 quantiles (dashed black line), and provides a p-value for the deviation from the expected quantile. Red color indicates a significant deviation from the expected quantile. Left: qq-plot to detect deviations from expected distribution, with added tests for correct distribution (KS test), dispersion and outliers. Right: Residuals against predicted values. .... cclxiii

**Figure A 41 DHA GAM test for over/underdispersion.** If fitted model (red line), is among simulated values no over- or underdispersion is present. .... cclxiv

**Figure A 42 Variogram DHA GAM.** To evaluate spatial autocorrelation in the model residuals, variograms were created based on residuals of a GLMM (left) accounting for spatial autocorrelation in the model and on residuals of the GAM (right) not accounting for spatial autocorrelation in the model. .... cclxiv

**Figure A 43 DHA GAM - Quantile residuals fitted against each covariate.** Is second quantile is colored red, a non linear trend was detected and a GAM will be applied in a next step to take into account this non-linear pattern. .... cclxv

**Figure A 44 Model prediction per covariate for DHA (GAM).** .... cclxvi

**Figure A 45 ARA GLMM verification using the DHARMA package.** The plot function of the package allows to calculate an quantile regression, which compares the empirical 0.25, 0.5 and 0.75 quantiles with the theoretical 0.25, 0.5 and 0.75 quantiles (dashed black line), and

provides a p-value for the deviation from the expected quantile. Red color indicates a significant deviation from the expected quantile. Left: qq-plot to detect deviations from expected distribution, with added tests for correct distribution (KS test), dispersion and outliers. Right: Residuals against predicted values.....cclxviii

**Figure A 46 ARA GLMM test for over/underdispersion.** If fitted model (red line), is among simulated values no over- or underdispersion is present..... cclxix

**Figure A 47 Variogram ARA GLMM.** To evaluate spatial autocorrelation in the model residuals, variograms were created based on residuals of a GLMM (left) not accounting for spatial autocorrelation in the model and on residuals of the GLMM (right) accounting for spatial autocorrelation in the model. .... cclxx

**Figure A 48 ARA GLMM - Quantile residuals fitted against each covariate.** Is second quantile is colored red, a non linear trend was detected and a GAM will be applied in a next step to take into account this non-linear pattern. .... cclxxi

**Figure A 49 Model prediction per covariate for ARA (GLMM).** .....cclxxii

**Figure A 50 Correlation between spawning activity, TAG-ST ratio, length and region.** Points represent sardine individuals. ....cclxxiii

**Figure A 51 Relation between sardines EFA and TAG-ST ratio. Colors indicate western or eastern English Channel.** .....cclxxiv

**Figure A 52 Differences of biological parameters of sardine between sex.** A: Comparison of length between sex. Red dots indicate mean independent of region; B: Comparison of weight between sex. Red dots indicate mean independent of region; C: Comparison of TAG-ST ratio between sex independent of region; D: Comparison of Le Cren’s index between sex independent of region. E: PCA on FA of females (green dots) and males (gray triangle); F: Proportion of females and males per region. ....cclxxv

**Figure A 53 PCA taxonomic composition zooplankton (entire size spectrum sampled: 300 – 1000+  $\mu\text{m}$ ).** A: Taxa displayed in two-dimensional space of first and second principal component. The darker the taxon, the higher its contribution to the first component. Displayed are all taxa with a higher contribution than 1.5%; B: Sampling stations displayed in a two-dimensional space of first and second principal component. The bigger the dot the higher its contribution to the first component. Blue dots were located in the WEC, red dots in the EEC. Numbers represent sampling station id. ....cclxxvi

**Figure A 54 Phytoplankton size-structure.** A: Mean median size per basin; B: mean median size per station. Turquoise indicating stations located in the WEC, red indicating locations in EEC; C: mean median size per taxonomic group; D: Location of sampling stations of phytoplankton.....cclxxx

**Figure A 55 Taxonomic composition phytoplankton.** A: Relative abundance and composition of phytoplankton in the EC. Size of pie charts represent abundance in cells/l and colored fractions represent the contribution of diatoms and dinoflagellates to the total abundance collected per station. B: Taxonomic composition and mean abundance with standard deviation per taxa in the WEC (turquoise) and EEC (red). Colored boxes mark taxa belonging to dinoflagellates and diatoms. Colors thereby corresponding to figure A.....cclxxx

## List of Tables Appendix

**Table A 1 Taxa determined in 2008 sorted by taxonomic level**..... ccxii

**Table A 2 Taxa determined in 2022 sorted by taxonomic level**..... ccxiii

**Table A 3 Posterior distribution of global model.** .....ccxxvii

**Table A 4 Posterior distribution of spatial model.** .....ccxxvii

**Table A 5 Posterior distribution of stage-space model run for plaice larvae**.....ccxxxi

**Table A 6 Results GLMM testing inter-regional differences of sardines.** Estimates with standard error (S.E.) indicate significant and non-significant positive or negative correlation between a covariate and the proportion of the respective parameter of sardines. Significance: \*\*\* (P<0.001), \*\* (P<0.01), \* (P<0.05). AIC (Akaike’s Information Criteria). n indicates the number of individuals used in the model. .... ccxlv

**Table A 7 Factors influencing trophic transfer including sex.** Estimates indicate significant and non-significant positive or negative correlation between a covariate and the proportion of the respective FA in sardine. Significance: \*\*\* (P<0.001), \*\* (P<0.01), \* (P<0.05). Type indicates the type of model used. N indicates the number of sampling stations used in the model. (s) indicate the parameters not displaying a linear relationship and thus integrated in the model with a spatial smoother.....cclxxiv

**Table A 8 Lipids and fatty acids (FA) in sardine.** Values are reported as mean ± standard deviation by region (Eastern English Channel, Western English Channel). n corresponds to the individuals sampled per region. ....cclxxvi



Appendix

**Table A 9 Lipids and fatty acids (FA) in mesozooplankton (500-1000  $\mu\text{m}$ ).** Values are reported as mean  $\pm$  standard deviation by region (Eastern English Channel, Western English Channel).

.....cclxxviii

## Appendix I – Chapter 1

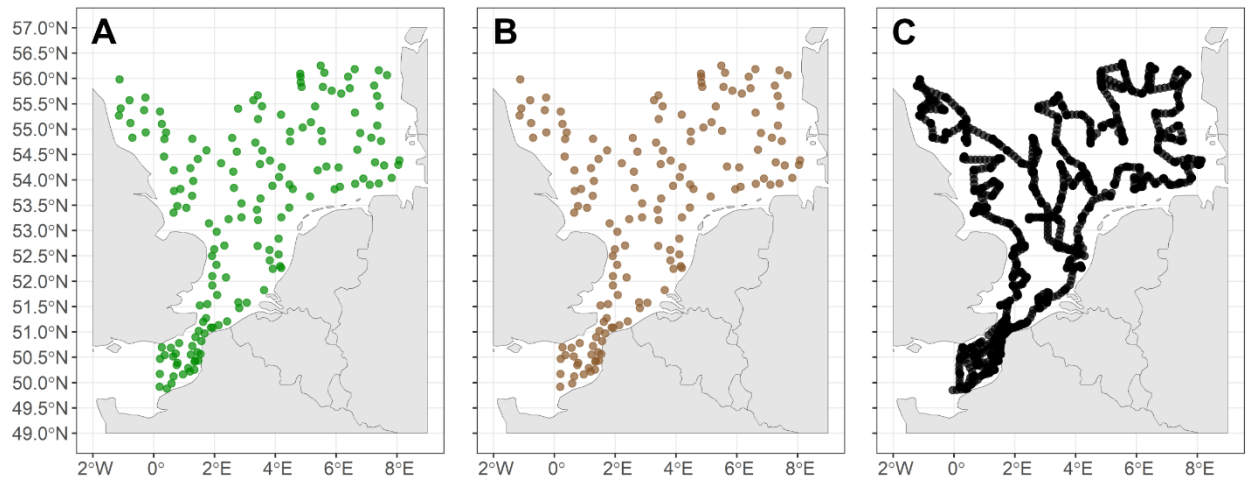


**Figure A 1 Sampling stations IBTS 2008.** A: Water samples for phyto- and microplankton community analysis; B: Water samples for POM, nitrate, nitrite, ammonium, phosphate, silicate and chlorophyll a; C: Salinity, temperature and depth.

Appendix I – Chapter 1

**Table A 1 Taxa determined in 2008 sorted by taxonomic level.**

Mesozooplankton	Fish larvae	Fish eggs	classification
Annelida	Ammodytidae	Gadidae	Phylum
Annelida (trochophore & metatrochophore larvae)	Gobiidae	Pleuronectidae	Subphylum
Chaetognatha	Pleuronectidae	Lotidae	Classe
Cnidaria	Syngnathidae	<i>Trisopterus spp.</i>	Infraclass
Echinodermata	Gadidae	<i>Solea solea</i>	Subclass
Crustacea	<i>Liparis liparis</i>	<i>Scophthalmus rhombus</i>	Order
Crustacea (nauplius larvae)	<i>Clupea harengus</i>	<i>Pleuronectes platessa</i>	Infraorder
Crustacea (cyprid larvae)	<i>Sardina pilchardus</i>	<i>Sprattus sprattus</i>	Suborder
Bryozoa (cyphonaute larvae)			Family
Gasteropoda			Genus
Bivalvia			Species
Asteroida (brachiolaria larvae)			
Appendicularia			
Cirripeda (nauplius larvae)			
Copepoda			
Calanoida			
Cyclopoida			
Harpacticoida			
Amphipoda			
Cumacea			
Euphausiacea			
Isopoda			
Mysidacea			
Siphonophora			
Anomura (zoea larvae)			
Brachyura (zoea larvae)			
Brachyura (megalopa larvae)			
Caridea (zoea)			
Cladocera			
Hyperidae			
<i>Acartia spp.</i>			
<i>Calanus spp.</i>			
<i>Candacia spp.</i>			
<i>Centropages spp.</i>			
<i>Corycaeus spp.</i>			
<i>Euterpina spp.</i>			
<i>Metridia spp.</i>			
<i>Paracalanus spp.</i>			
<i>Pseudocalanus spp.</i>			
<i>Temora spp.</i>			
<i>Clione spp.</i>			
<i>Aglantha spp.</i>			
<i>Tomopteris spp.</i>			

Appendix I – Chapter 1

**Table A 2 Taxa determined in 2022 sorted by taxonomic level.**

Mesozooplankton	Fish larvae	classification
Annelida	Ammodytidae	Phylum
Chaetognatha	Syngnathidae	Subphylum
Cnidaria	<i>Pomatoschistus sp</i>	Classe
Cnidaria (ephyra)	<i>Agonus cataphractus</i>	Infraclass
Annelida (larvae)	<i>Aphia minuta</i>	Subclass
Echinodermata (larvae)	<i>Crystallogobius linearis</i>	Order
Crustacea (megalopa)	<i>Pomatoschistus minutus</i>	Infraorder
Crustacea (nauplii)	<i>Clupea harengus</i>	Suborder
Bryozoa (cyphonaute)	<i>Liparis liparis</i>	Family
Bivalvia	<i>Microstomus kitt</i>	Genus
Mollusca	<i>Pleuronectes platessa</i>	Species
Ostracoda	<i>Sardina pilchardus</i>	
Echinoidea (pluteus)	<i>Solea solea</i>	
Ophiuroidea (pluteus)	<i>Syngnathus acus</i>	
Cirripedia (cypris)		
Cirripedia (naulius)		
Copepoda (nauplii)		
Amphipoda		
Calanoida		
Euphausiacea (calytopis larvae)		
Calanoida (copepodite)		
Cumacea		
Cyclopoida		
Decapoda		
Euphausiacea		
Harpacticoida		
Isopoda		
Mysidacea		
Mysidacea (larvae)		
Siphonostomatoida		
Decapoda (zoea)		
Brachyura (zoea)		
Brachyura		
Anomura		
Peltidiidae		
Calanidae		
Caprellidae		
Caridea		
Centropagidae		
Calanidae (copepodite)		
Gnathiidae		
Oithonidae		
<b>Continued</b>		

Appendix I – Chapter 1

Mesozooplankton	Fish larvae	classification
Paguridae		
Porcellanidae		
<i>Acartia spp.</i>		
<i>Calanus spp.</i>		
<i>Candacia spp.</i>		
<i>Centropages spp.</i>		
<i>Corycaeus spp.</i>		
<i>Evadne spp.</i>		
<i>Labidocera spp.</i>		
<i>Obelia spp.</i>		
<i>Ophiura spp.</i>		
<i>Podon spp.</i>		
<i>Paracalanus.Pseudocalanus</i>		
<i>Pseudodiaptomus spp.</i>		
<i>Temora longicornis</i>		
<i>Euterpina acutifrons</i>		
<i>Pseudocalanus elongatus</i>		
<i>Pleurobrachia pileus</i>		
<i>Paracalanus parvus</i>		
<i>Oikopleura dioica</i>		

Appendix I – Chapter 1

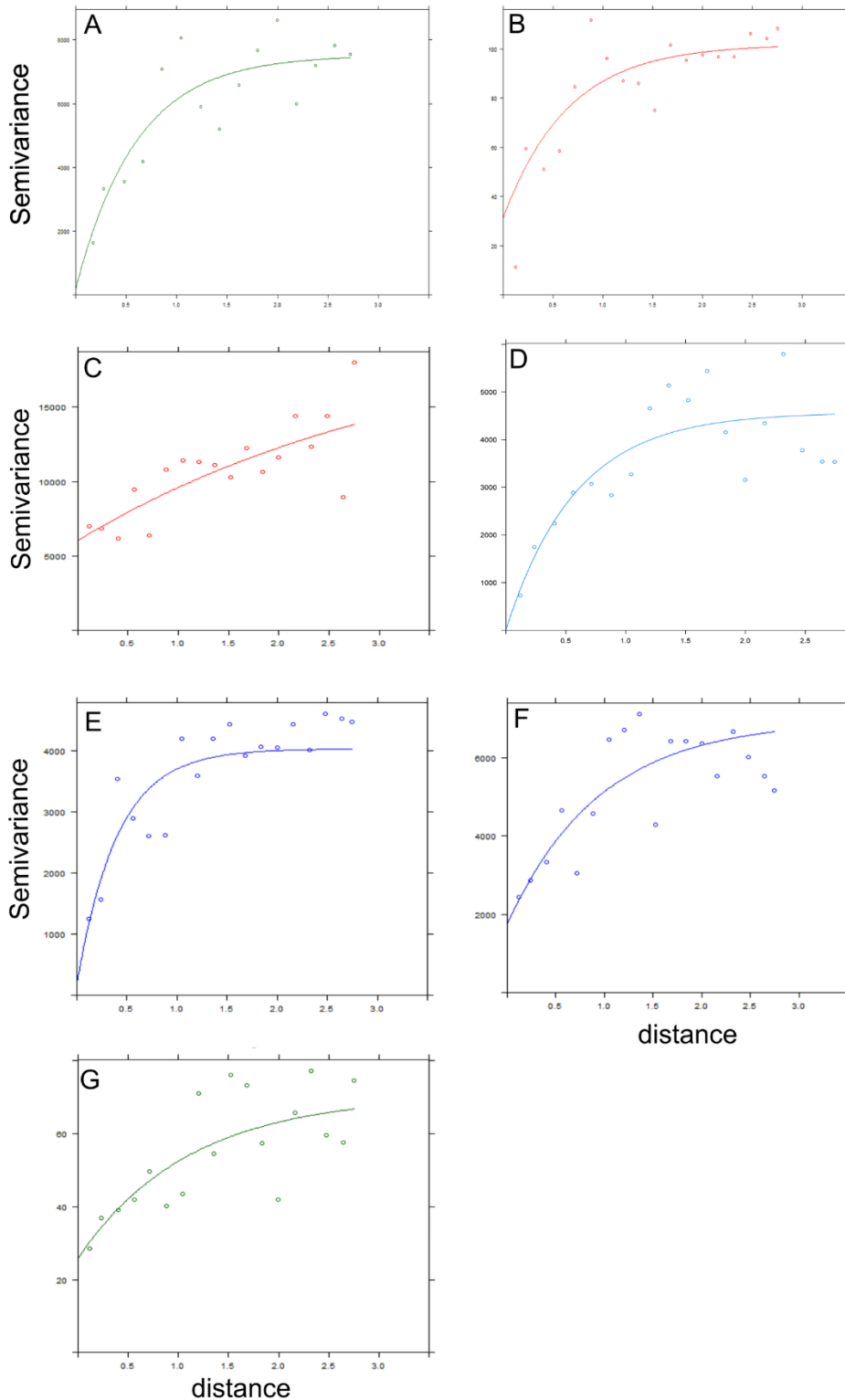


**Figure A 2 Empirical and theoretical variograms of species used for the determination of optimal grid cell size.** (A) Small-sized herring larvae (6–12 mm), variogram model fitted to raw data; (B) medium-sized herring larvae (13–20 mm), variogram fitted to raw data; (C) Appendicularia, variogram fitted to residuals of quadratic regression; (D) Acartia, variogram fitted to residuals of linear regression; (E) Calanoida, variogram fitted to residuals of linear regression; (F) Pseudocalanus, variogram fitted to residuals of linear regression; (G) Centropages, variogram fitted to residuals of quadratic regression.

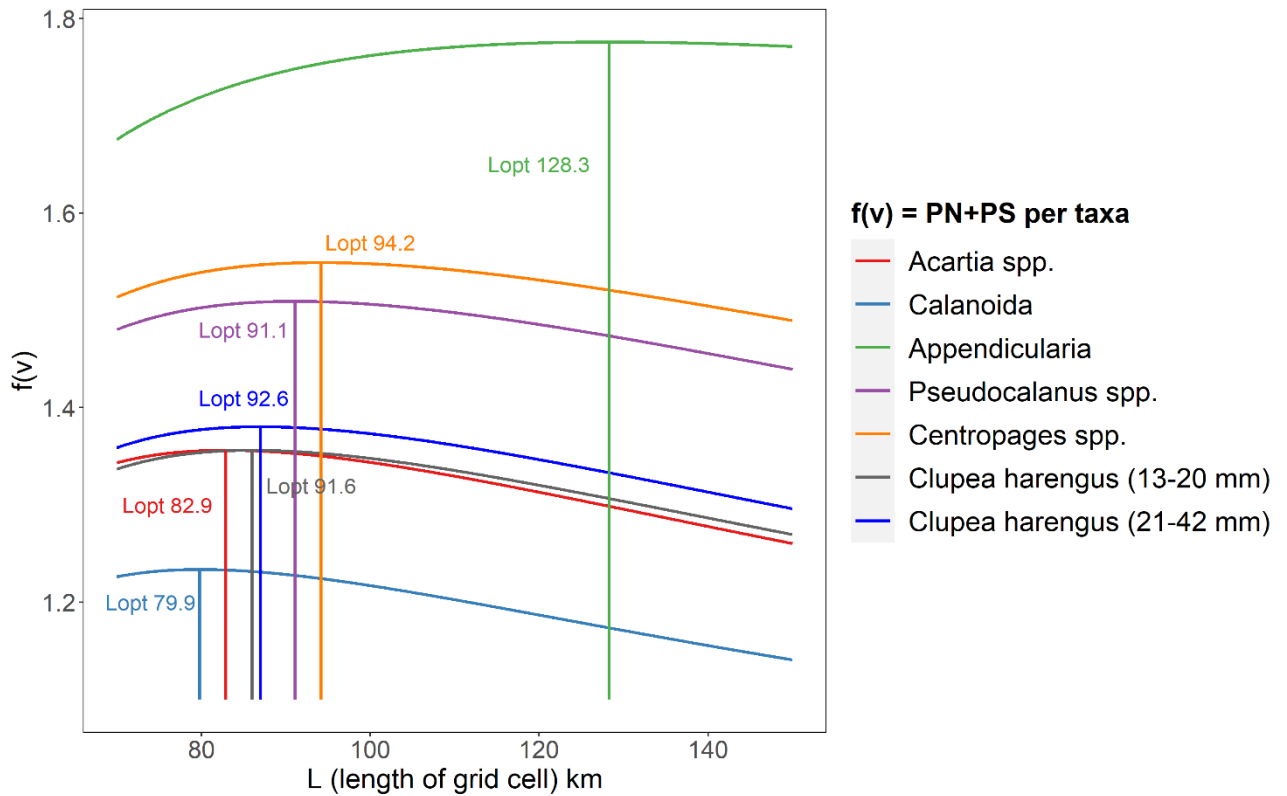


**Figure A 3 Taxon-specific optimal grid cell size (Lopt).** Functions display maximal information content per cell ( $f(v)$ ) depending on grid cell size (length and width in km) calculated for different taxa. PN = proportion of nugget variance removed, PS = proportion of sill variance retained. Lopt indicates taxon-specific optimal grid cell size. The median of the species specific Lopt (91.58 km, 0.83°) produced a single cell of central position not containing sampling stations and was thus accepted without further adjustment.

## Appendix I – Chapter 1

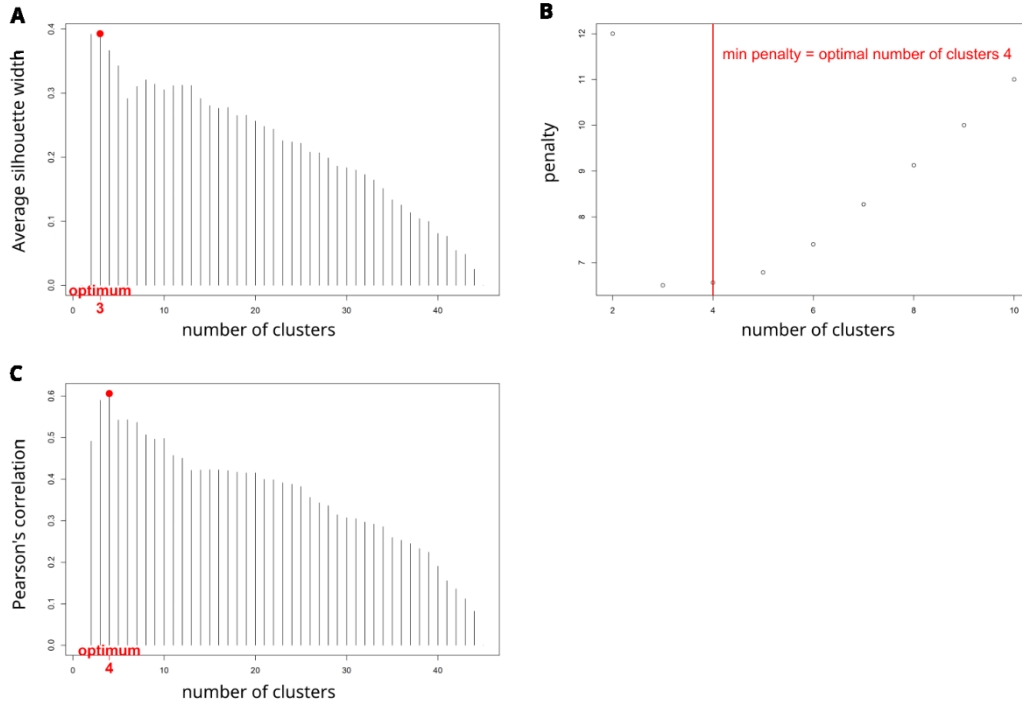


**Figure A 4 Statistical methods to determine optimal number of clusters (2008 big spatial extent).** (A) Silhouette width indicating an optimum number of three clusters, (B) Kelly-Gardner-Sutcliffe penalty function proposing an optimal number of four clusters, (C) Mantel correlation indicating an optimal number of four clusters.

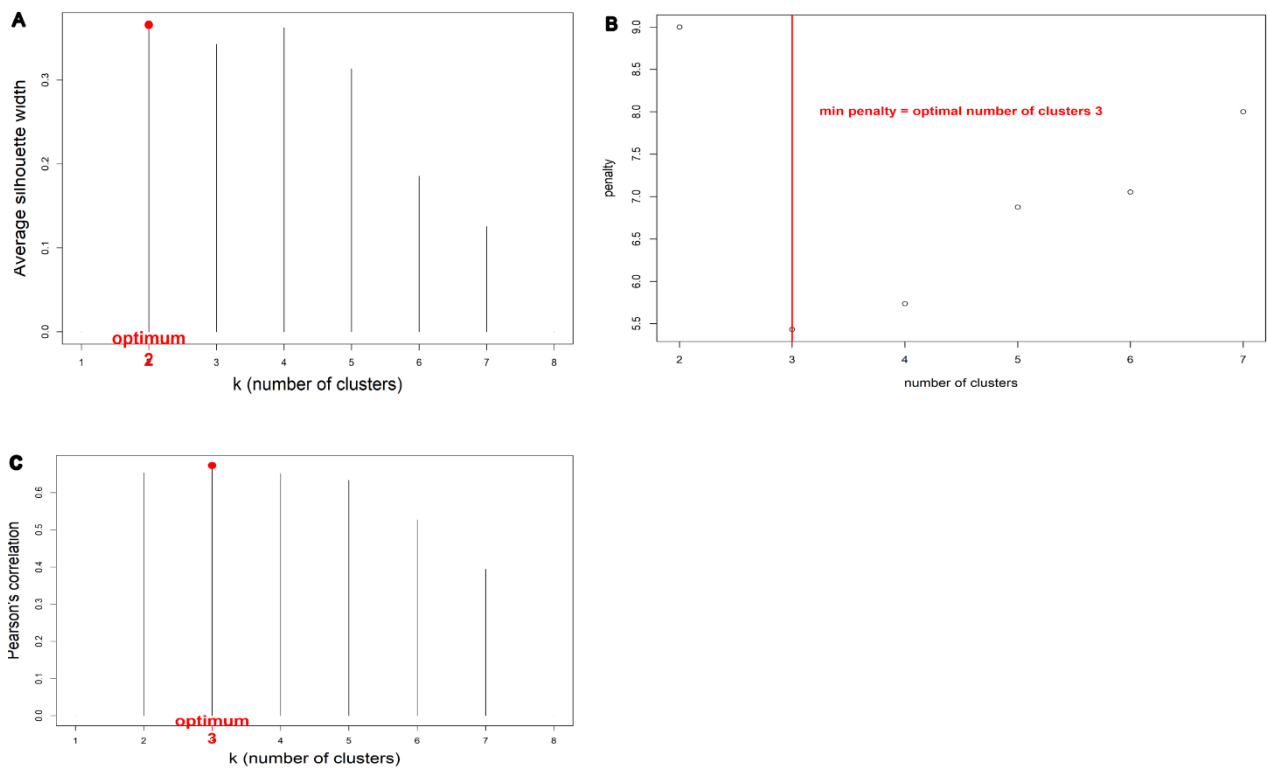


**Figure A 5 Statistical methods to determine optimal number of clusters (Comparison 2008 vs 2022, small spatial extent).** (A) Silhouette width indicating an optimum number of three clusters, (B) Kelly-Gardner-Sutcliffe



penalty function proposing an optimal number of four clusters, (C) Mantel correlation indicating an optimal number of four clusters.

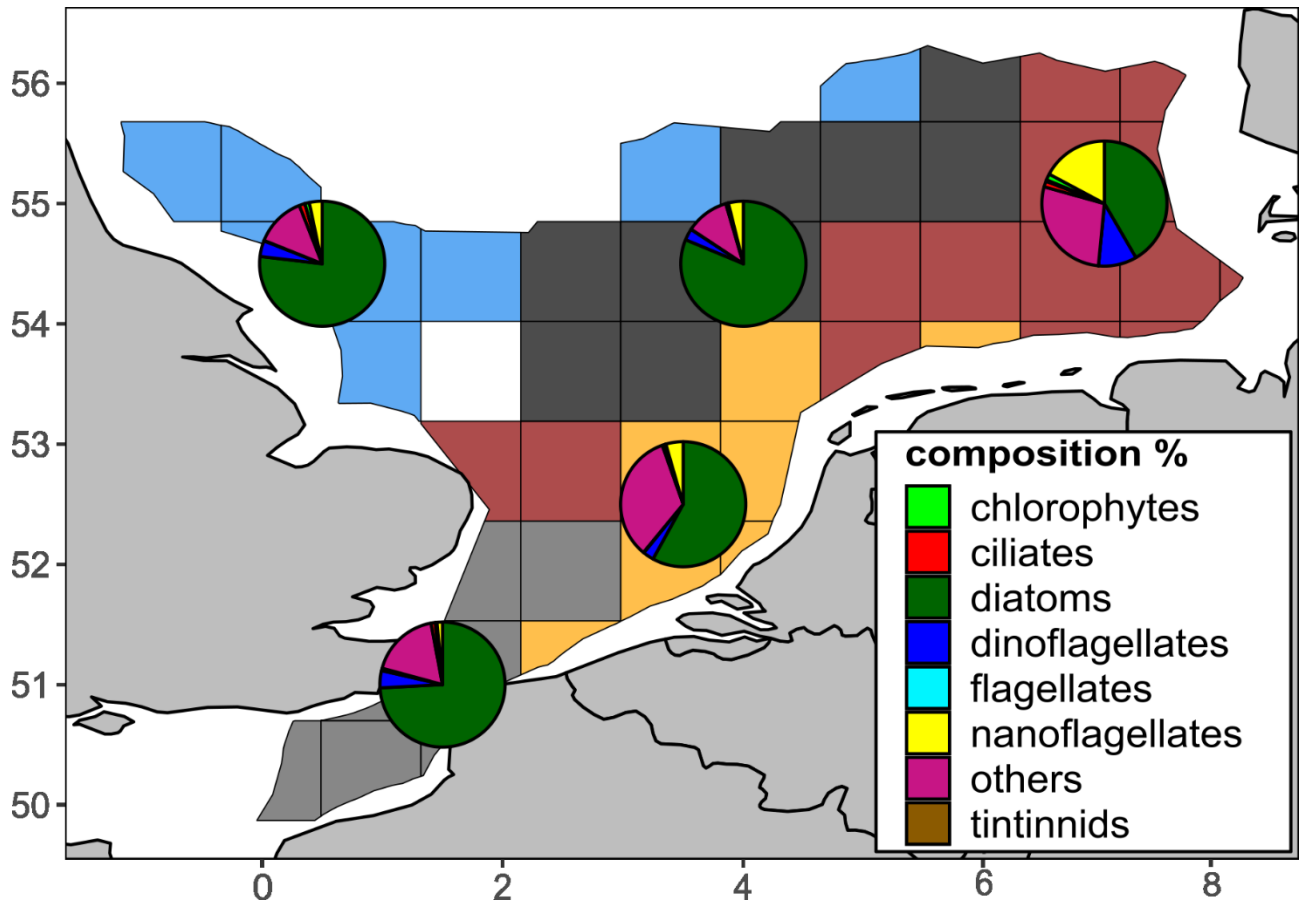
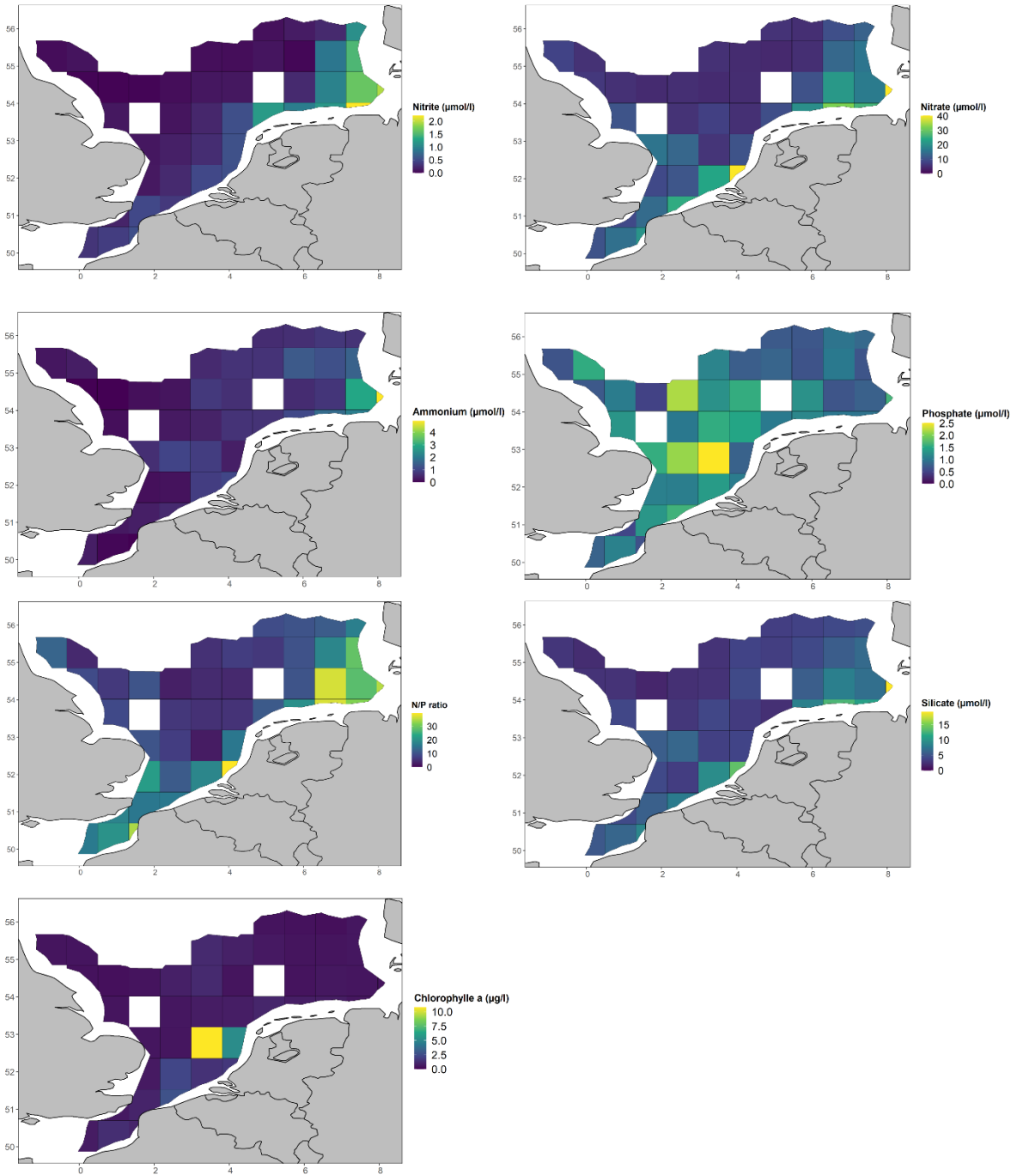


Figure A 6 Relative phyto- microplankton composition per zooplankton assemblage.

Appendix I – Chapter 1



**Figure A 7** Distribution of nutrients and chlorophyll a. Maps display mean per grid cell of nutrients sampled during the IBTS 2008.

# Appendix I – Chapter 1

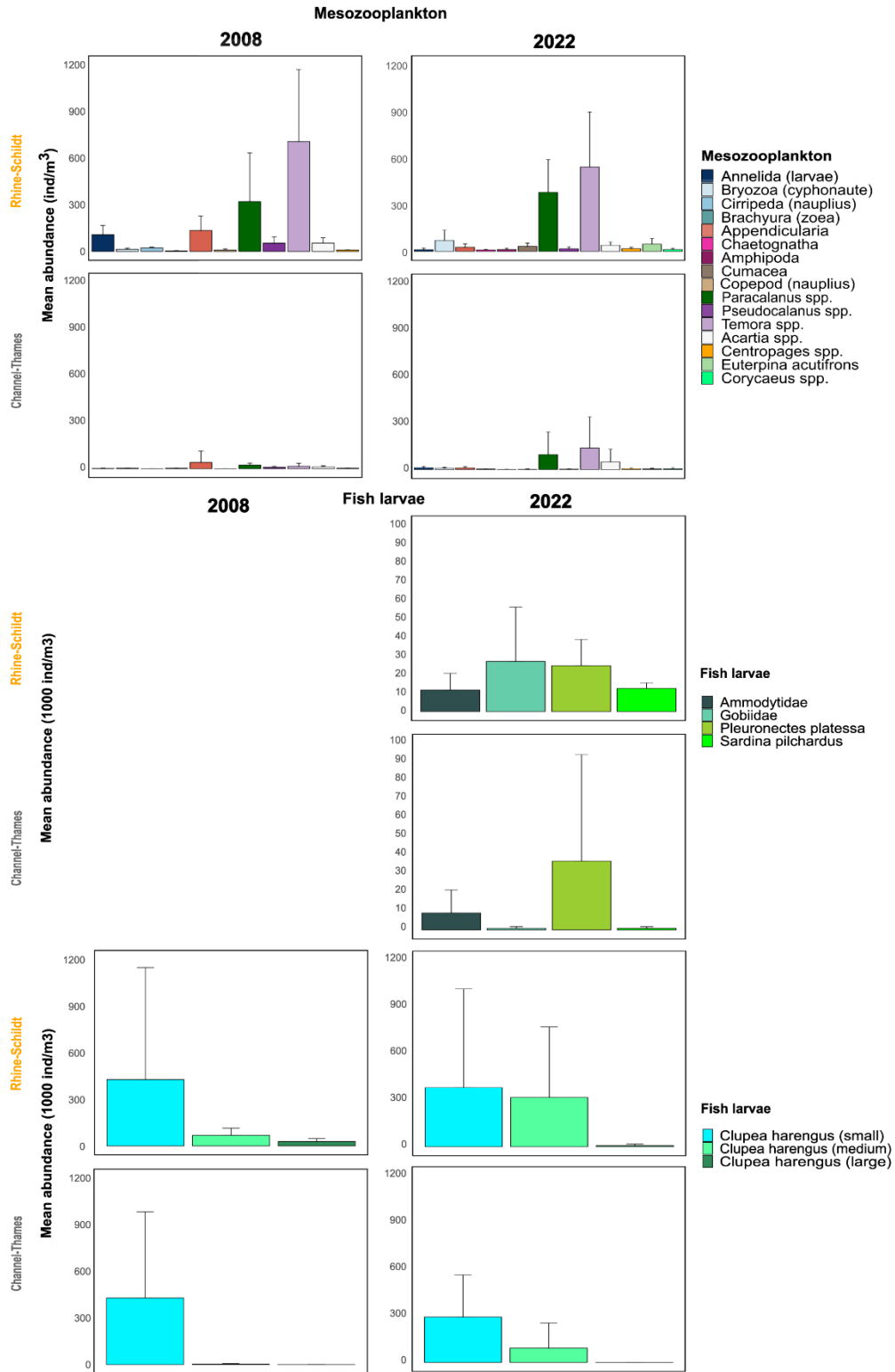
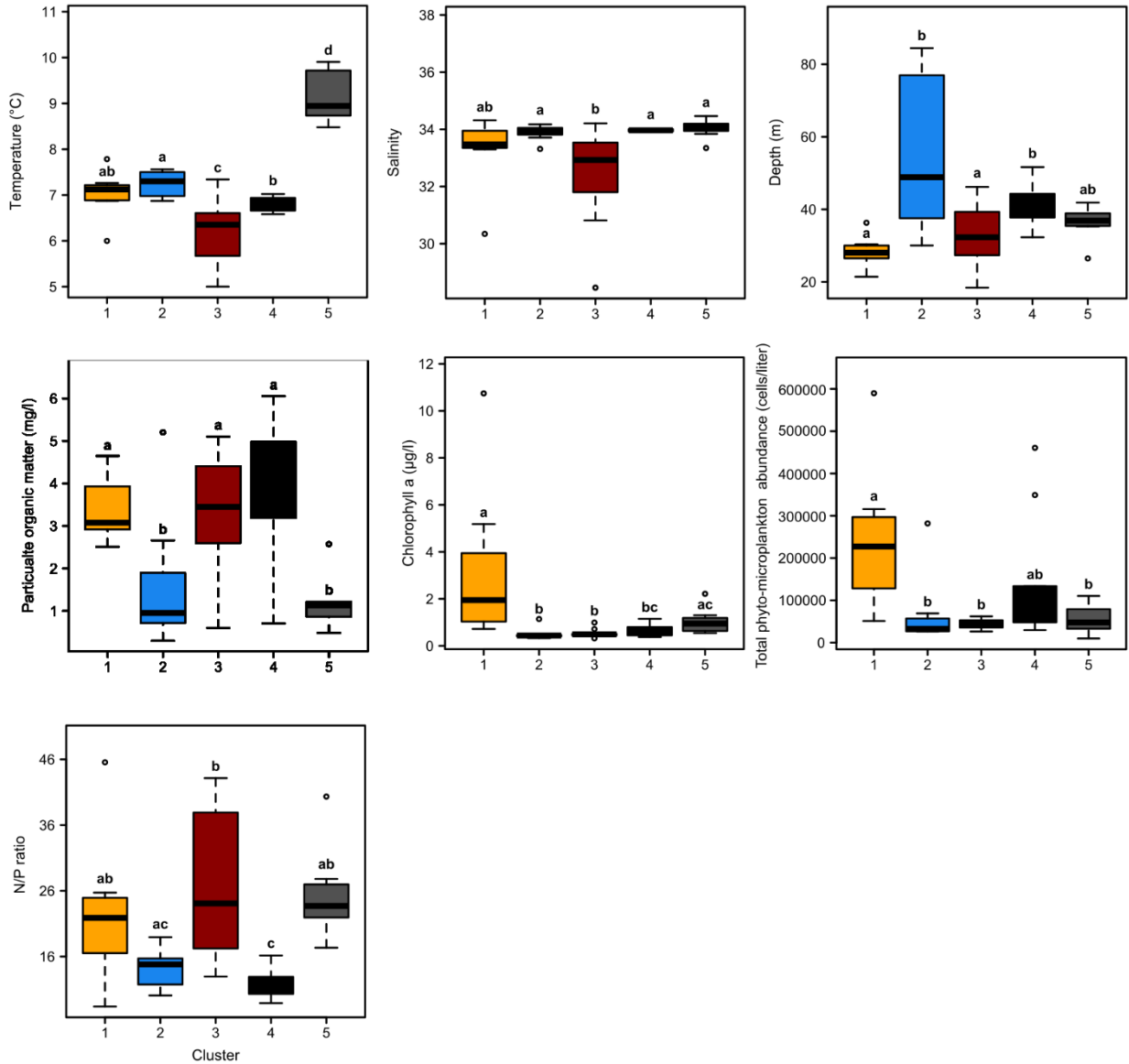


**Figure A 8 Taxa composition of assemblages in 2008 (left) and 2022 (right).** Mean abundance of taxa was calculated with regard to the spatial distribution of clusters in 2008 for both years.

## Appendix I – Chapter 1



# Appendix I – Chapter 1

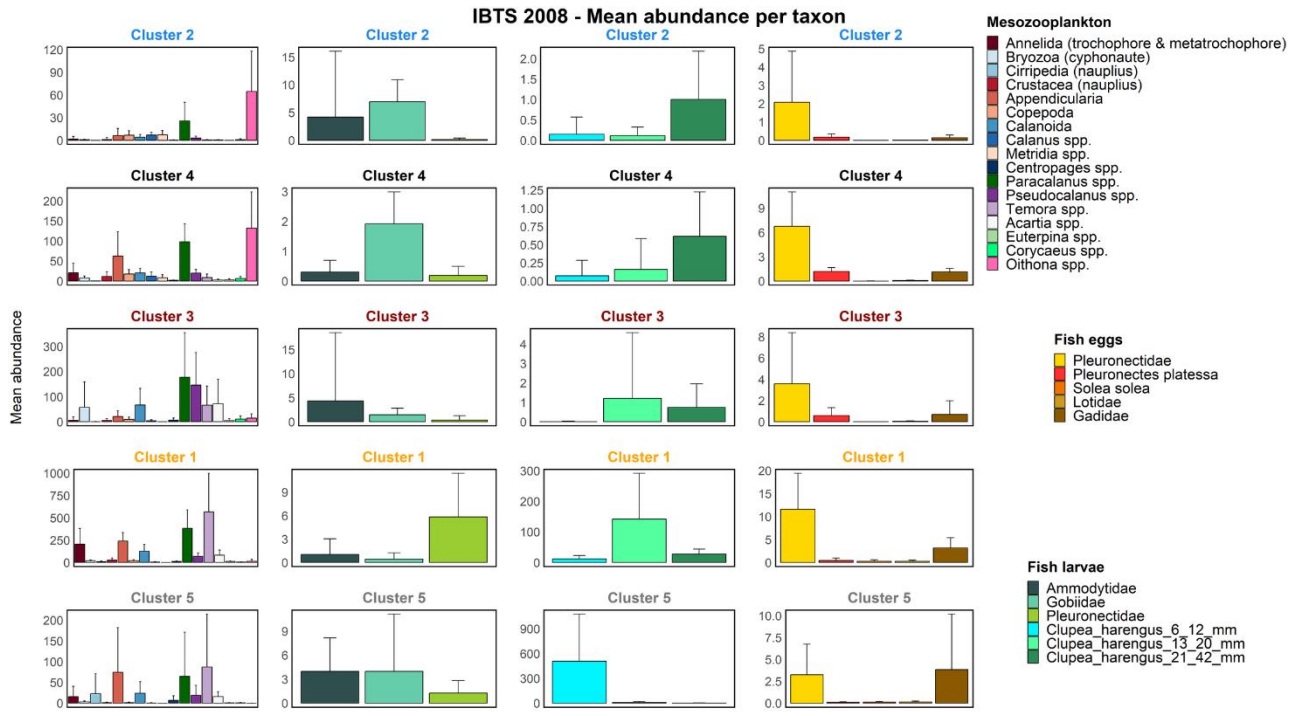


**Figure A 10 Mean abundance of taxa per cluster with individually scaled y-axis. Mean abundance is therefore not comparable between clusters but gives further inside in community per cluster.**

## Appendix I – Chapter 1

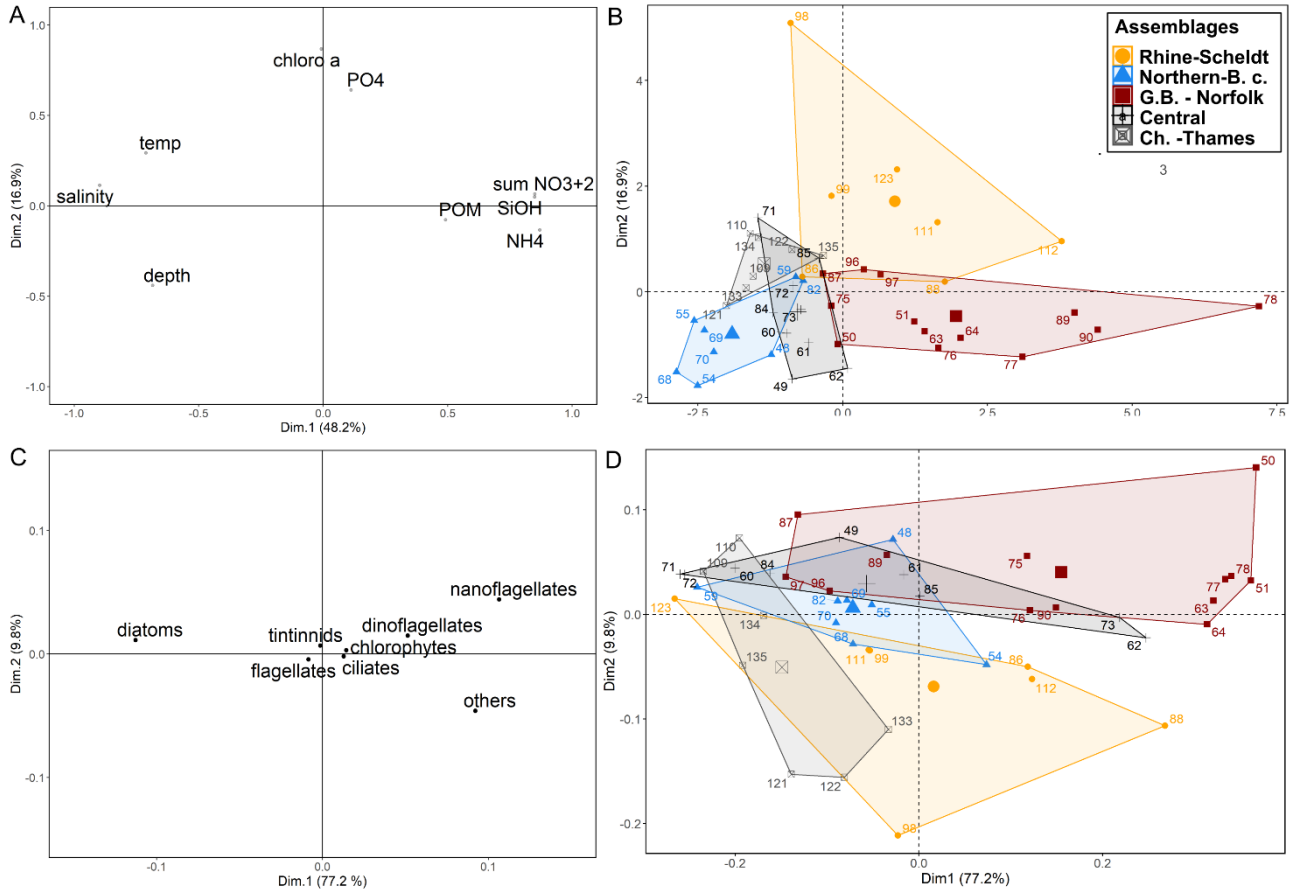


**Figure A 11** PCA on potential abiotic and biotic drivers. (A) Abiotic parameters displayed in a two-dimensional space of a PCA. (B) Assemblages/cluster displayed in the same two-dimensional space as in A. Numbers indicate grid cell ID. (C) Phyto- and microplankton groups displayed in a two-dimensional space of a PCA. (D) Assemblages/cluster displayed in the same two-dimensional space as in C. Numbers indicate grid cell ID.

Appendix I – Chapter 1

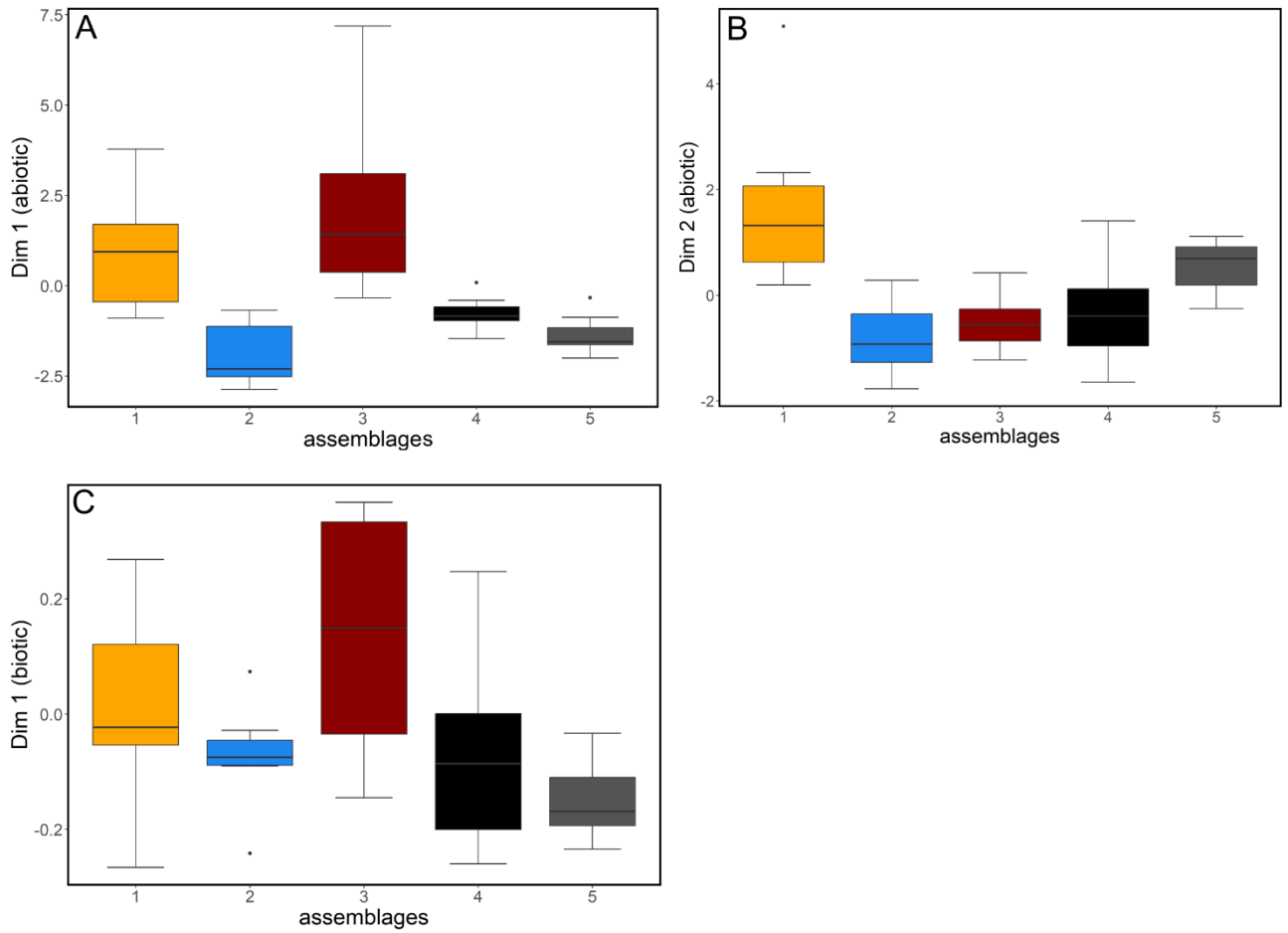


**Figure A 12** Boxplots of PCA dimensions per cluster. (A) First dimension of PCA applied to abiotic parameters. (B) Second dimension of PCA applied to abiotic parameters. (C) First dimension of PCA applied to biotic parameters.

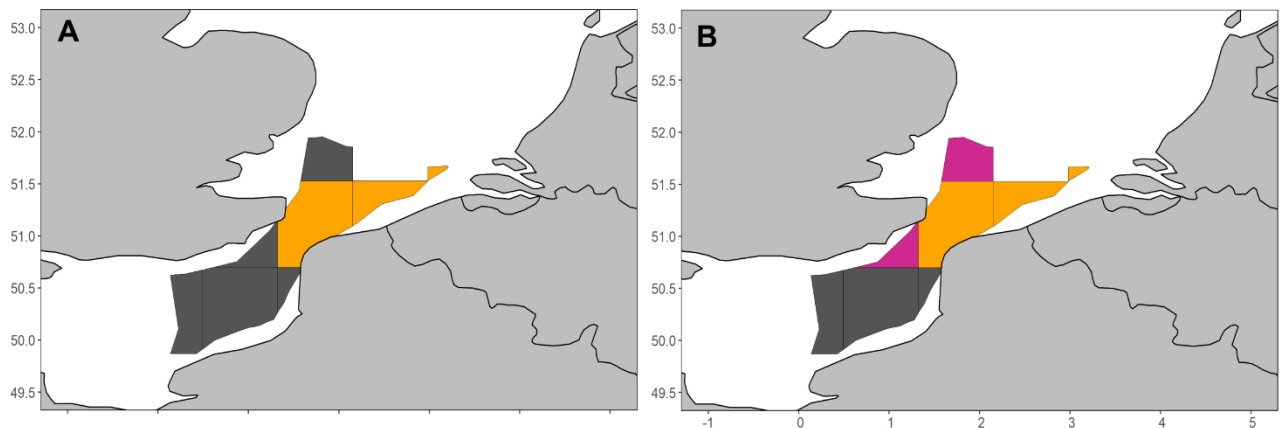


**Figure A 13** Clusters received using different  $k$ . (A) Clusters derived using a  $k = 2$ ; (B) Clusters derived using a  $k = 3$ .

Appendix I – Chapter 1

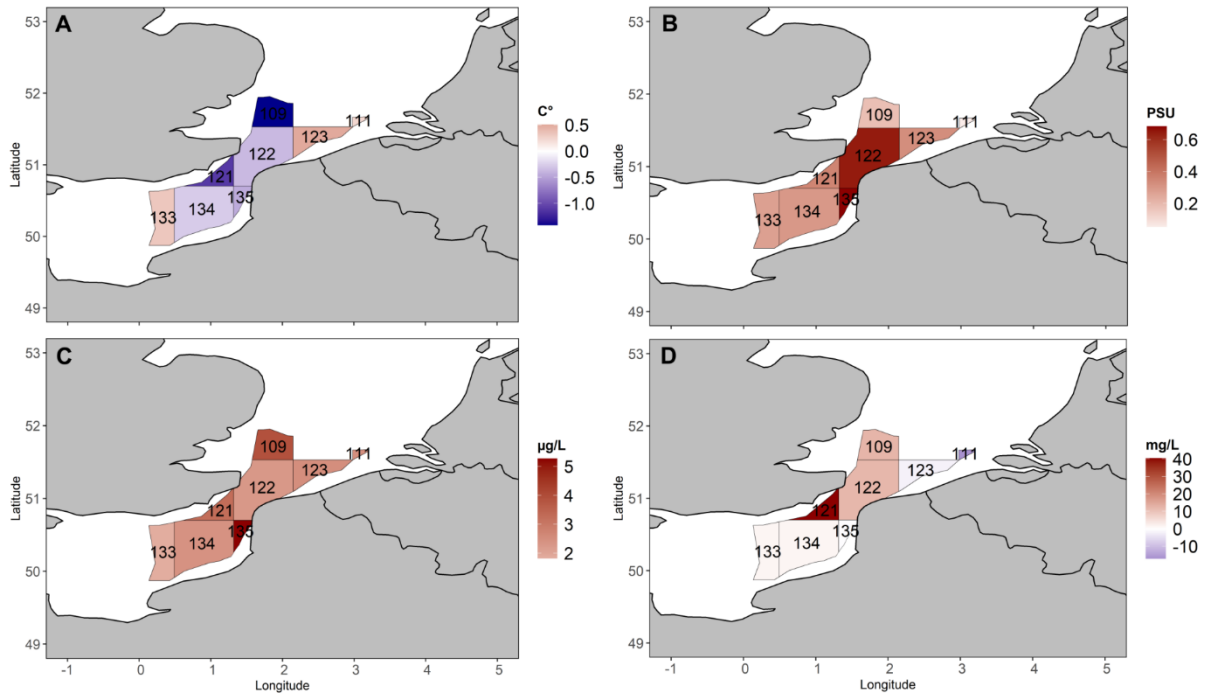


**Figure A 14 Inter-annual differences of environmental conditions.** Measurements taken in 2008 were subtracted from measurements taken in 2022 so that positive values indicate an increase in 2022 compared to 2008. Numbers in grid cells indicate grid cell ID. A: Temperature; B: Salinity; C: Chlorophyll a; D: Particulate organic matter.



## Appendix II – Chapter 2

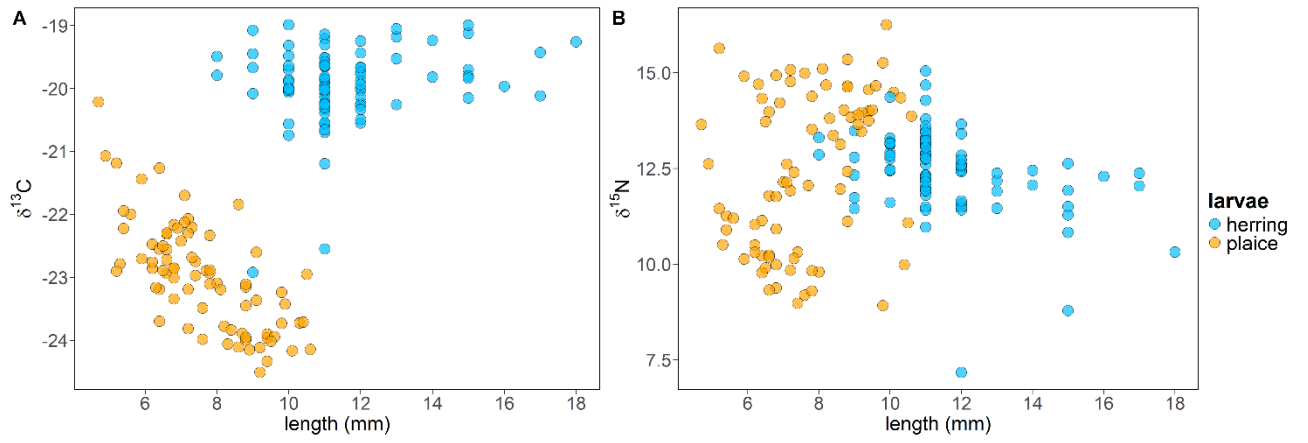


**Figure A 15 Carbon (A) and nitrogen (B) stable isotope values at different larval sizes.**

Appendix II – Chapter 2

*Table A 3 Posterior distribution of global model.*

species.sizeclass	Mean	SD	2.5%	5%	25%	50%	75%	95%	97.5%
p.herring.0_20	0.231	0.047	0.133	0.150	0.203	0.231	0.260	0.307	0.324
p.plaice.0_20	0.508	0.060	0.376	0.400	0.471	0.513	0.551	0.599	0.614
p.herring.125_200	0.034	0.029	0.002	0.003	0.012	0.027	0.048	0.091	0.109
p.plaice.125_200	0.111	0.117	0.001	0.002	0.017	0.065	0.182	0.351	0.396
p.herring.20_125	0.031	0.027	0.001	0.002	0.011	0.023	0.043	0.086	0.101
p.plaice.20_125	0.078	0.091	0.001	0.002	0.012	0.040	0.113	0.286	0.330
p.herring.200_500	0.040	0.035	0.001	0.002	0.013	0.030	0.057	0.111	0.131
p.plaice.200_500	0.099	0.114	0.001	0.002	0.014	0.051	0.148	0.352	0.404
p.herring.500_1000	0.664	0.062	0.538	0.560	0.625	0.667	0.706	0.760	0.785
p.plaice.500_1000	0.203	0.080	0.063	0.078	0.144	0.199	0.255	0.348	0.372

*Table A 4 Posterior distribution of spatial model.*

species.station.sizeclass	Mean	SD	2.5%	5%	25%	50%	75%	95%	97.5%
p.herring.0_20	0.130	0.059	0.039	0.048	0.085	0.123	0.169	0.236	0.262
p.plaice.0_20	0.396	0.077	0.257	0.274	0.343	0.392	0.442	0.533	0.565
p.herring.125_200	0.038	0.022	0.009	0.012	0.022	0.034	0.051	0.080	0.091
p.plaice.125_200	0.365	0.095	0.181	0.210	0.304	0.362	0.431	0.520	0.545
p.herring.20_125	0.018	0.020	0.000	0.001	0.004	0.011	0.024	0.057	0.072
p.plaice.20_125	0.026	0.035	0.000	0.000	0.004	0.013	0.032	0.095	0.129
p.herring.200_500	0.029	0.029	0.001	0.002	0.009	0.020	0.039	0.085	0.106
p.plaice.200_500	0.040	0.049	0.001	0.002	0.008	0.022	0.052	0.142	0.179
p.herring.500_1000	0.785	0.077	0.620	0.649	0.736	0.794	0.843	0.897	0.909
p.plaice.500_1000	0.174	0.061	0.060	0.075	0.133	0.169	0.211	0.282	0.302

Continued

Appendix II – Chapter 2

<b>species.station.sizeclass</b>	<b>Mean</b>	<b>SD</b>	<b>2.5%</b>	<b>5%</b>	<b>25%</b>	<b>50%</b>	<b>75%</b>	<b>95%</b>	<b>97.5%</b>
p.herring.Z0147.0_20	0.086	0.041	0.025	0.030	0.053	0.079	0.116	0.158	0.174
p.herring.Z0147.125_200	0.037	0.021	0.008	0.010	0.021	0.033	0.048	0.077	0.087
p.herring.Z0147.20_125	0.022	0.033	0.000	0.000	0.003	0.009	0.028	0.085	0.123
p.herring.Z0147.200_500	0.033	0.041	0.001	0.001	0.007	0.018	0.045	0.116	0.146
p.herring.Z0147.500_1000	0.822	0.073	0.661	0.691	0.776	0.831	0.878	0.925	0.937
p.herring.Z0153.0_20	0.119	0.054	0.029	0.038	0.077	0.116	0.160	0.209	0.224
p.herring.Z0153.125_200	0.100	0.041	0.032	0.038	0.068	0.097	0.126	0.174	0.189
p.herring.Z0153.20_125	0.020	0.023	0.000	0.001	0.004	0.011	0.027	0.068	0.087
p.herring.Z0153.200_500	0.033	0.034	0.001	0.001	0.008	0.021	0.045	0.105	0.125
p.herring.Z0153.500_1000	0.728	0.083	0.563	0.587	0.672	0.730	0.790	0.859	0.879
p.herring.Z0154.0_20	0.093	0.045	0.024	0.030	0.056	0.087	0.125	0.174	0.187
p.herring.Z0154.125_200	0.070	0.033	0.019	0.025	0.046	0.066	0.090	0.130	0.147
p.herring.Z0154.20_125	0.018	0.023	0.000	0.000	0.003	0.010	0.024	0.064	0.084
p.herring.Z0154.200_500	0.029	0.033	0.001	0.001	0.007	0.018	0.040	0.098	0.125
p.herring.Z0154.500_1000	0.790	0.073	0.637	0.660	0.740	0.795	0.845	0.902	0.911
p.herring.Z0155.0_20	0.080	0.043	0.018	0.022	0.044	0.074	0.110	0.158	0.170
p.herring.Z0155.125_200	0.063	0.034	0.015	0.019	0.037	0.056	0.083	0.124	0.141
p.herring.Z0155.20_125	0.027	0.036	0.000	0.000	0.004	0.013	0.036	0.102	0.130
p.herring.Z0155.200_500	0.047	0.056	0.001	0.001	0.009	0.026	0.066	0.170	0.201
p.herring.Z0155.500_1000	0.783	0.088	0.599	0.629	0.723	0.791	0.850	0.912	0.926
p.herring.Z0162.0_20	0.152	0.053	0.058	0.070	0.110	0.149	0.192	0.241	0.257
p.herring.Z0162.125_200	0.016	0.011	0.002	0.003	0.008	0.013	0.021	0.037	0.044
p.herring.Z0162.20_125	0.013	0.019	0.000	0.000	0.002	0.007	0.016	0.049	0.067
p.herring.Z0162.200_500	0.020	0.024	0.000	0.001	0.005	0.012	0.027	0.065	0.084
p.herring.Z0162.500_1000	0.799	0.065	0.667	0.690	0.756	0.801	0.847	0.901	0.912
p.herring.Z0163.0_20	0.136	0.049	0.052	0.063	0.098	0.133	0.173	0.218	0.232
p.herring.Z0163.125_200	0.015	0.011	0.002	0.003	0.008	0.013	0.020	0.035	0.042
p.herring.Z0163.20_125	0.013	0.019	0.000	0.000	0.002	0.006	0.016	0.051	0.068
p.herring.Z0163.200_500	0.019	0.024	0.000	0.001	0.005	0.012	0.024	0.063	0.084

Continued

Appendix II – Chapter 2

<b>species.station.sizeclass</b>	<b>Mean</b>	<b>SD</b>	<b>2.5%</b>	<b>5%</b>	<b>25%</b>	<b>50%</b>	<b>75%</b>	<b>95%</b>	<b>97.5%</b>
<b>p.herring.Z0163.500_1000</b>	0.816	0.060	0.689	0.714	0.777	0.820	0.860	0.905	0.919
<b>p.herring.Z0164.0_20</b>	0.187	0.055	0.085	0.099	0.147	0.187	0.227	0.275	0.290
<b>p.herring.Z0164.125_200</b>	0.041	0.023	0.010	0.012	0.024	0.036	0.053	0.084	0.096
<b>p.herring.Z0164.20_125</b>	0.019	0.025	0.000	0.000	0.004	0.011	0.025	0.068	0.090
<b>p.herring.Z0164.200_500</b>	0.031	0.035	0.001	0.001	0.008	0.020	0.041	0.099	0.123
<b>p.herring.Z0164.500_1000</b>	0.722	0.069	0.580	0.604	0.677	0.723	0.771	0.827	0.845
<b>p.herring.Z0165.0_20</b>	0.151	0.057	0.042	0.059	0.111	0.151	0.194	0.244	0.256
<b>p.herring.Z0165.125_200</b>	0.030	0.023	0.003	0.005	0.013	0.024	0.041	0.074	0.086
<b>p.herring.Z0165.20_125</b>	0.015	0.019	0.000	0.000	0.003	0.009	0.020	0.050	0.068
<b>p.herring.Z0165.200_500</b>	0.025	0.028	0.000	0.001	0.006	0.015	0.033	0.079	0.107
<b>p.herring.Z0165.500_1000</b>	0.779	0.074	0.632	0.656	0.728	0.783	0.832	0.895	0.914
<b>p.herring.Z0166.0_20</b>	0.092	0.052	0.021	0.025	0.048	0.079	0.129	0.188	0.205
<b>p.herring.Z0166.125_200</b>	0.010	0.009	0.001	0.001	0.004	0.007	0.012	0.027	0.035
<b>p.herring.Z0166.20_125</b>	0.011	0.017	0.000	0.000	0.002	0.005	0.014	0.044	0.063
<b>p.herring.Z0166.200_500</b>	0.022	0.034	0.000	0.001	0.003	0.010	0.026	0.087	0.122
<b>p.herring.Z0166.500_1000</b>	0.865	0.082	0.665	0.702	0.819	0.887	0.927	0.960	0.967
<b>p.herring.Z0175.0_20</b>	0.071	0.043	0.009	0.013	0.036	0.064	0.101	0.150	0.166
<b>p.herring.Z0175.125_200</b>	0.045	0.037	0.003	0.005	0.017	0.035	0.062	0.121	0.140
<b>p.herring.Z0175.20_125</b>	0.023	0.035	0.000	0.000	0.003	0.010	0.027	0.096	0.130
<b>p.herring.Z0175.200_500</b>	0.038	0.051	0.000	0.001	0.006	0.019	0.049	0.140	0.189
<b>p.herring.Z0175.500_1000</b>	0.823	0.085	0.641	0.671	0.766	0.831	0.889	0.947	0.960
<b>p.plaice.Z0147.0_20</b>	0.299	0.040	0.222	0.234	0.272	0.298	0.326	0.367	0.379
<b>p.plaice.Z0147.125_200</b>	0.404	0.087	0.212	0.254	0.352	0.410	0.463	0.534	0.555
<b>p.plaice.Z0147.20_125</b>	0.035	0.053	0.000	0.000	0.004	0.014	0.042	0.148	0.199
<b>p.plaice.Z0147.200_500</b>	0.051	0.068	0.001	0.001	0.008	0.025	0.067	0.192	0.243
<b>p.plaice.Z0147.500_1000</b>	0.211	0.067	0.080	0.097	0.166	0.211	0.256	0.323	0.342
<b>p.plaice.Z0153.0_20</b>	0.224	0.042	0.141	0.154	0.196	0.224	0.251	0.295	0.309
<b>p.plaice.Z0153.125_200</b>	0.620	0.075	0.456	0.490	0.581	0.629	0.669	0.726	0.744

Continued

Appendix II – Chapter 2

<b>species.station.sizeclass</b>	<b>Mean</b>	<b>SD</b>	<b>2.5%</b>	<b>5%</b>	<b>25%</b>	<b>50%</b>	<b>75%</b>	<b>95%</b>	<b>97.5%</b>
p.plaice.Z0153.20_125	0.021	0.038	0.000	0.000	0.003	0.008	0.023	0.090	0.125
p.plaice.Z0153.200_500	0.032	0.051	0.000	0.001	0.005	0.014	0.037	0.130	0.169
p.plaice.Z0153.500_1000	0.103	0.043	0.034	0.043	0.074	0.097	0.125	0.181	0.205
p.plaice.Z0154.0_20	0.229	0.042	0.144	0.159	0.202	0.229	0.257	0.297	0.312
p.plaice.Z0154.125_200	0.569	0.074	0.412	0.446	0.525	0.574	0.618	0.677	0.696
p.plaice.Z0154.20_125	0.023	0.035	0.000	0.000	0.003	0.009	0.027	0.093	0.124
p.plaice.Z0154.200_500	0.034	0.051	0.001	0.001	0.006	0.016	0.042	0.128	0.175
p.plaice.Z0154.500_1000	0.145	0.051	0.052	0.067	0.111	0.141	0.176	0.234	0.255
p.plaice.Z0155.0_20	0.207	0.042	0.125	0.139	0.180	0.207	0.235	0.277	0.292
p.plaice.Z0155.125_200	0.535	0.103	0.280	0.346	0.481	0.549	0.606	0.676	0.696
p.plaice.Z0155.20_125	0.038	0.062	0.000	0.000	0.003	0.013	0.042	0.166	0.231
p.plaice.Z0155.200_500	0.061	0.088	0.001	0.001	0.007	0.025	0.076	0.239	0.328
p.plaice.Z0155.500_1000	0.159	0.064	0.049	0.063	0.113	0.153	0.199	0.274	0.299
p.plaice.Z0162.0_20	0.568	0.047	0.469	0.487	0.539	0.571	0.600	0.642	0.652
p.plaice.Z0162.125_200	0.174	0.078	0.040	0.055	0.117	0.170	0.224	0.310	0.339
p.plaice.Z0162.20_125	0.020	0.027	0.000	0.000	0.003	0.010	0.026	0.076	0.100
p.plaice.Z0162.200_500	0.030	0.037	0.000	0.001	0.006	0.017	0.040	0.105	0.138
p.plaice.Z0162.500_1000	0.207	0.058	0.088	0.107	0.167	0.209	0.247	0.300	0.313
p.plaice.Z0163.0_20	0.543	0.047	0.447	0.465	0.513	0.546	0.576	0.615	0.628
p.plaice.Z0163.125_200	0.184	0.078	0.046	0.064	0.129	0.181	0.233	0.317	0.343
p.plaice.Z0163.20_125	0.020	0.025	0.000	0.000	0.003	0.010	0.027	0.075	0.092
p.plaice.Z0163.200_500	0.029	0.034	0.000	0.001	0.006	0.017	0.041	0.098	0.121
p.plaice.Z0163.500_1000	0.223	0.057	0.103	0.127	0.186	0.226	0.262	0.311	0.328
p.plaice.Z0164.0_20	0.493	0.049	0.394	0.410	0.460	0.495	0.526	0.572	0.584
p.plaice.Z0164.125_200	0.321	0.080	0.150	0.181	0.272	0.323	0.375	0.447	0.470
p.plaice.Z0164.20_125	0.022	0.031	0.000	0.000	0.003	0.010	0.028	0.085	0.113
p.plaice.Z0164.200_500	0.035	0.044	0.000	0.001	0.006	0.018	0.045	0.125	0.158
p.plaice.Z0164.500_1000	0.129	0.041	0.053	0.066	0.100	0.128	0.157	0.197	0.212
p.plaice.Z0166.0_20	0.442	0.043	0.356	0.370	0.413	0.441	0.471	0.514	0.529

Continued

Appendix II – Chapter 2

species.station.sizeclass	Mean	SD	2.5%	5%	25%	50%	75%	95%	97.5%
p.plaice.Z0166.125_200	0.146	0.080	0.027	0.036	0.086	0.135	0.191	0.289	0.335
p.plaice.Z0166.20_125	0.028	0.049	0.000	0.000	0.003	0.011	0.030	0.123	0.178
p.plaice.Z0166.200_500	0.050	0.078	0.000	0.001	0.006	0.019	0.053	0.234	0.311
p.plaice.Z0166.500_1000	0.335	0.114	0.079	0.111	0.265	0.355	0.421	0.492	0.512

Table A 5 Posterior distribution of stage-space model run for plaice larvae.

stage.station.size class	Mean	SD	2.5%	5%	25%	50%	75%	95%	97.5%
	0.840	0.277	0.450	0.491	0.647	0.790	0.977	1.337	1.510
1.0_20	0.379	0.089	0.224	0.247	0.317	0.371	0.434	0.536	0.568
2.0_20	0.377	0.094	0.213	0.236	0.311	0.371	0.437	0.542	0.574
3.0_20	0.381	0.097	0.213	0.231	0.312	0.374	0.445	0.550	0.583
1.125_200	0.271	0.114	0.059	0.091	0.192	0.267	0.348	0.462	0.501
2.125_200	0.333	0.140	0.059	0.100	0.235	0.332	0.427	0.567	0.611
3.125_200	0.349	0.149	0.056	0.095	0.245	0.350	0.453	0.595	0.629
1.20_125	0.066	0.060	0.002	0.004	0.021	0.048	0.093	0.181	0.219
2.20_125	0.067	0.070	0.001	0.002	0.014	0.043	0.097	0.211	0.255
3.20_125	0.062	0.068	0.001	0.002	0.013	0.037	0.089	0.197	0.247
1.200_500	0.101	0.094	0.003	0.006	0.033	0.073	0.138	0.299	0.353
2.200_500	0.117	0.121	0.001	0.003	0.026	0.078	0.172	0.372	0.462
3.200_500	0.100	0.115	0.001	0.003	0.020	0.058	0.138	0.341	0.439
1.500_1000	0.184	0.082	0.053	0.069	0.125	0.175	0.230	0.333	0.370
2.500_1000	0.106	0.064	0.020	0.026	0.060	0.093	0.138	0.229	0.264
3.500_1000	0.110	0.068	0.017	0.024	0.059	0.097	0.146	0.242	0.277
1.Z0147.0_20	0.318	0.052	0.218	0.235	0.283	0.317	0.351	0.405	0.425
1.Z0147.125_200	0.293	0.145	0.023	0.045	0.186	0.299	0.399	0.527	0.557
1.Z0147.20_125	0.093	0.101	0.002	0.003	0.018	0.059	0.131	0.311	0.372
Continued									

Appendix II – Chapter 2

<b>stage.station.size class</b>	<b>Mean</b>	<b>SD</b>	<b>2.5%</b>	<b>5%</b>	<b>25%</b>	<b>50%</b>	<b>75%</b>	<b>95%</b>	<b>97.5%</b>
<b>1.Z0147.200_500</b>	0.154	0.151	0.002	0.004	0.033	0.102	0.236	0.469	0.533
<b>1.Z0147.500_1000</b>	0.142	0.084	0.015	0.026	0.078	0.132	0.198	0.298	0.330
<b>1.Z0153.0_20</b>	0.207	0.048	0.116	0.132	0.175	0.208	0.240	0.285	0.301
<b>1.Z0153.125_200</b>	0.506	0.147	0.111	0.233	0.427	0.527	0.610	0.703	0.728
<b>1.Z0153.20_125</b>	0.063	0.075	0.001	0.002	0.012	0.034	0.084	0.223	0.273
<b>1.Z0153.200_500</b>	0.107	0.143	0.002	0.003	0.019	0.053	0.139	0.398	0.561
<b>1.Z0153.500_1000</b>	0.116	0.069	0.013	0.021	0.064	0.106	0.160	0.242	0.270
<b>1.Z0154.0_20</b>	0.225	0.046	0.137	0.150	0.194	0.225	0.255	0.303	0.316
<b>1.Z0154.125_200</b>	0.492	0.149	0.067	0.180	0.423	0.518	0.592	0.685	0.707
<b>1.Z0154.20_125</b>	0.064	0.074	0.001	0.002	0.012	0.037	0.087	0.215	0.262
<b>1.Z0154.200_500</b>	0.114	0.148	0.002	0.003	0.020	0.062	0.142	0.455	0.604
<b>1.Z0154.500_1000</b>	0.105	0.062	0.013	0.021	0.058	0.096	0.144	0.221	0.246
<b>1.Z0155.0_20</b>	0.201	0.043	0.118	0.132	0.172	0.200	0.229	0.272	0.291
<b>1.Z0155.125_200</b>	0.414	0.140	0.059	0.130	0.339	0.430	0.509	0.609	0.643
<b>1.Z0155.20_125</b>	0.071	0.085	0.001	0.003	0.014	0.040	0.096	0.252	0.315
<b>1.Z0155.200_500</b>	0.123	0.150	0.002	0.004	0.022	0.064	0.162	0.457	0.570
<b>1.Z0155.500_1000</b>	0.192	0.090	0.029	0.045	0.123	0.191	0.255	0.343	0.372
<b>1.Z0162.0_20</b>	0.555	0.052	0.448	0.466	0.520	0.557	0.592	0.638	0.654
<b>1.Z0162.125_200</b>	0.143	0.087	0.013	0.023	0.076	0.130	0.198	0.303	0.335
<b>1.Z0162.20_125</b>	0.049	0.050	0.001	0.002	0.012	0.032	0.070	0.152	0.186
<b>1.Z0162.200_500</b>	0.070	0.070	0.001	0.003	0.018	0.047	0.102	0.218	0.255
<b>1.Z0162.500_1000</b>	0.182	0.079	0.037	0.055	0.124	0.181	0.239	0.308	0.329
<b>1.Z0166.0_20</b>	0.416	0.044	0.329	0.343	0.387	0.417	0.446	0.486	0.500
<b>1.Z0166.125_200</b>	0.091	0.062	0.009	0.013	0.043	0.079	0.128	0.207	0.238
<b>1.Z0166.20_125</b>	0.047	0.053	0.001	0.002	0.012	0.029	0.064	0.153	0.195
<b>1.Z0166.200_500</b>	0.067	0.071	0.001	0.003	0.018	0.045	0.092	0.210	0.269
<b>1.Z0166.500_1000</b>	0.378	0.090	0.170	0.214	0.327	0.387	0.442	0.505	0.528
<b>2.Z0147.0_20</b>	0.294	0.049	0.2	0.217	0.263	0.293	0.327	0.376	0.394
<b>Continued</b>									

Appendix II – Chapter 2

<b>stage.station.size class</b>	<b>Mean</b>	<b>SD</b>	<b>2.5%</b>	<b>5%</b>	<b>25%</b>	<b>50%</b>	<b>75%</b>	<b>95%</b>	<b>97.5%</b>
2.Z0147.125_200	0.339	0.177	0.024	0.046	0.200	0.342	0.476	0.622	0.658
2.Z0147.20_125	0.103	0.129	0.001	0.001	0.010	0.042	0.151	0.399	0.451
2.Z0147.200_500	0.182	0.193	0.001	0.002	0.020	0.101	0.311	0.568	0.635
2.Z0147.500_1000	0.082	0.065	0.005	0.009	0.032	0.065	0.116	0.215	0.243
2.Z0153.0_20	0.196	0.052	0.097	0.113	0.160	0.195	0.233	0.284	0.298
2.Z0153.125_200	0.580	0.155	0.106	0.281	0.514	0.608	0.683	0.771	0.794
2.Z0153.20_125	0.053	0.064	0.001	0.001	0.009	0.030	0.072	0.183	0.239
2.Z0153.200_500	0.108	0.151	0.001	0.002	0.016	0.054	0.137	0.404	0.624
2.Z0153.500_1000	0.062	0.043	0.006	0.009	0.029	0.053	0.085	0.146	0.167
2.Z0154.0_20	0.206	0.053	0.109	0.124	0.169	0.205	0.241	0.296	0.314
2.Z0154.125_200	0.555	0.173	0.047	0.177	0.475	0.589	0.673	0.764	0.791
2.Z0154.20_125	0.061	0.080	0.000	0.001	0.008	0.029	0.080	0.229	0.298
2.Z0154.200_500	0.123	0.169	0.001	0.002	0.015	0.056	0.163	0.504	0.697
2.Z0154.500_1000	0.056	0.041	0.005	0.008	0.025	0.046	0.077	0.135	0.155
2.Z0155.0_20	0.197	0.050	0.106	0.120	0.163	0.196	0.230	0.279	0.299
2.Z0155.125_200	0.499	0.167	0.049	0.142	0.415	0.532	0.618	0.714	0.744
2.Z0155.20_125	0.067	0.084	0.001	0.001	0.010	0.034	0.090	0.246	0.304
2.Z0155.200_500	0.132	0.169	0.001	0.002	0.021	0.066	0.172	0.523	0.675
2.Z0155.500_1000	0.105	0.060	0.014	0.022	0.060	0.096	0.140	0.218	0.244
2.Z0162.0_20	0.581	0.064	0.451	0.470	0.537	0.582	0.627	0.683	0.700
2.Z0162.125_200	0.181	0.106	0.014	0.027	0.099	0.171	0.253	0.373	0.405
2.Z0162.20_125	0.049	0.052	0.001	0.001	0.010	0.030	0.072	0.155	0.193
2.Z0162.200_500	0.080	0.081	0.001	0.002	0.017	0.052	0.120	0.245	0.286
2.Z0162.500_1000	0.110	0.061	0.016	0.023	0.062	0.102	0.151	0.222	0.244
2.Z0163.0_20	0.552	0.062	0.428	0.447	0.510	0.554	0.595	0.651	0.669
2.Z0163.125_200	0.201	0.114	0.014	0.029	0.112	0.194	0.281	0.398	0.438
2.Z0163.20_125	0.055	0.063	0.001	0.001	0.010	0.032	0.079	0.186	0.228
2.Z0163.200_500	0.090	0.094	0.001	0.002	0.017	0.057	0.137	0.283	0.327
2.Z0163.500_1000	0.102	0.065	0.009	0.015	0.050	0.091	0.144	0.222	0.247
Continued									



Appendix II – Chapter 2

stage.station.size class	Mean	SD	2.5%	5%	25%	50%	75%	95%	97.5%
2.Z0164.0_20	0.451	0.059	0.331	0.351	0.412	0.451	0.489	0.546	0.565
2.Z0164.125_200	0.275	0.148	0.018	0.041	0.159	0.273	0.386	0.510	0.553
2.Z0164.20_125	0.077	0.099	0.000	0.001	0.008	0.032	0.106	0.308	0.350
2.Z0164.200_500	0.128	0.144	0.001	0.001	0.016	0.062	0.208	0.436	0.487
2.Z0164.500_1000	0.070	0.059	0.004	0.008	0.027	0.052	0.098	0.189	0.221
2.Z0166.0_20	0.483	0.052	0.382	0.394	0.449	0.484	0.521	0.565	0.579
2.Z0166.125_200	0.129	0.087	0.010	0.017	0.062	0.112	0.179	0.296	0.339
2.Z0166.20_125	0.052	0.060	0.001	0.001	0.010	0.029	0.073	0.178	0.222
2.Z0166.200_500	0.085	0.090	0.001	0.002	0.017	0.051	0.126	0.274	0.326
2.Z0166.500_1000	0.251	0.094	0.056	0.086	0.186	0.256	0.318	0.397	0.419
3.Z0147.0_20	0.303	0.053	0.204	0.218	0.266	0.301	0.339	0.393	0.408
3.Z0147.125_200	0.362	0.186	0.018	0.043	0.222	0.371	0.513	0.649	0.678
3.Z0147.20_125	0.093	0.121	0.001	0.001	0.010	0.038	0.131	0.368	0.443
3.Z0147.200_500	0.156	0.180	0.001	0.002	0.017	0.076	0.251	0.545	0.601
3.Z0147.500_1000	0.085	0.069	0.005	0.008	0.032	0.067	0.121	0.223	0.256
3.Z0153.0_20	0.193	0.060	0.085	0.103	0.152	0.187	0.233	0.297	0.322
3.Z0153.125_200	0.590	0.177	0.088	0.215	0.504	0.628	0.714	0.806	0.828
3.Z0153.20_125	0.055	0.077	0.001	0.001	0.007	0.023	0.069	0.222	0.285
3.Z0153.200_500	0.099	0.153	0.001	0.001	0.011	0.038	0.114	0.413	0.620
3.Z0153.500_1000	0.063	0.048	0.005	0.008	0.027	0.052	0.086	0.160	0.186
3.Z0162.0_20	0.581	0.061	0.461	0.478	0.541	0.584	0.625	0.675	0.693
3.Z0162.125_200	0.190	0.112	0.014	0.025	0.100	0.178	0.268	0.386	0.423
3.Z0162.20_125	0.046	0.053	0.001	0.001	0.008	0.026	0.066	0.164	0.192
3.Z0162.200_500	0.069	0.078	0.001	0.002	0.012	0.039	0.098	0.238	0.281
3.Z0162.500_1000	0.114	0.066	0.012	0.019	0.061	0.106	0.158	0.232	0.255
3.Z0163.0_20	0.555	0.056	0.443	0.458	0.516	0.558	0.596	0.640	0.655
3.Z0163.125_200	0.208	0.116	0.016	0.028	0.118	0.198	0.292	0.410	0.436
3.Z0163.20_125	0.053	0.062	0.000	0.001	0.009	0.028	0.075	0.183	0.230
Continued									

Appendix II – Chapter 2

<b>stage.station.size class</b>	<b>Mean</b>	<b>SD</b>	<b>2.5%</b>	<b>5%</b>	<b>25%</b>	<b>50%</b>	<b>75%</b>	<b>95%</b>	<b>97.5%</b>
<b>3.Z0163.200_500</b>	0.079	0.091	0.001	0.002	0.013	0.042	0.115	0.280	0.329
<b>3.Z0163.500_1000</b>	0.106	0.070	0.007	0.012	0.049	0.095	0.154	0.232	0.257
<b>3.Z0164.0_20</b>	0.495	0.057	0.380	0.398	0.456	0.496	0.534	0.586	0.605
<b>3.Z0164.125_200</b>	0.289	0.127	0.027	0.053	0.204	0.297	0.379	0.490	0.524
<b>3.Z0164.20_125</b>	0.055	0.061	0.001	0.002	0.011	0.034	0.077	0.188	0.235
<b>3.Z0164.200_500</b>	0.092	0.102	0.001	0.002	0.017	0.055	0.129	0.313	0.380
<b>3.Z0164.500_1000</b>	0.069	0.048	0.007	0.011	0.033	0.059	0.095	0.164	0.186



## Appendix III – Chapter 3

### 3.1 Phytoplankton community composition

**FlowCam.** Samples were digitized using an 8-bit grayscale Benchtop B2 Series FlowCam® Model VS-IV (Yokogawa Fluid Imaging Technologies, Inc., Scarborough, ME, USA). This is an image acquisition system building on optical microscopy. It can generate high-resolution images of particles in the flow, in the size range 2  $\mu\text{m}$ -1000  $\mu\text{m}$  (depending on the magnification/flow cell depth combination). For our study, a 4X objective (40X overall magnification) coupled with a 300  $\mu\text{m}$ -depth flow-cell was used and samples were run in “AutoImage” operation mode. In this way, as described by Zarauz et al. (2007), all particles in the field-of-view of the camera (phytoplankton, zooplankton and inorganic particles) are captured and imaged at a regular user-defined interval, which allows an accurate estimation of imaged volume and consequently of particle concentration.

A database representative of each plankton community met in the English Channel and North Sea, was built using samples taken throughout 2013 (in the frame of the IFREMER Phytoplankton and Phycotoxins monitoring network, REPHY (REPHY-French Observation And Monitoring Program For Phytoplankton And Hydrology In Coastal Waters, 2023) and the SRN (Suivi Régional de Nutriments) monitoring programme (Lefebvre and Devreker, 2023)). A total of 31700 images were manually classified in 20 plankton groups. Moreover, instead of manually removing inorganic particles and artefacts as is commonly done (Zarauz *et al.*, 2007), we added 6 groups for floating dark and light dead particles, bubbles, fibers, etc. to the 20 plankton groups in order to automatically identify and then eliminate them from the statistics.

**EcoTransLearn.** “EcoTransLearn” is an R-package that facilitates the use of Transfer Learning methods to automatically classify digital images for ecological studies (Wacquet and Lefebvre, 2022). This tool includes some Convolutional Neural Networks models, widely used in Deep Learning, for many applications, and in particular for image recognition.

All models were pre-trained on the *ImageNet* dataset, which is an image database, organized according to the WordNet hierarchy, and composed of approximately 1.4 M images sorted into 1000 classes. *EcoTransLearn* uses the Python Deep Learning toolbox *Keras* for both model construction step and automated classification process thanks to the R-package “reticulate”. For our study, the model used is the *VGG16* adapted with the plankton dataset built from images acquired with the FlowCam (Wacquet and Lefebvre, 2022).

## 3.2 GLMM sardine morphological and physiological parameters.

### 3.2.1 Verification

For each parameter a glm without a spatial component and a glmm with a spatial component were run to assess reduction of spatial autocorrelation by using a spatial term as random effect. Presented is only the outcome of the glmm because these models were the more appropriate because they either reduced the spatial autocorrelation or the AIC.

#### TAG-ST ratio:

```
Family: gaussian ( identity )
Formula: TAG_ST ~ region + region:Sexe + exp(pos + 0 | group)
Data: dat_v
```

AIC	BIC	logLik	deviance	df.resid
2632.0	2656.5	-1309.0	2618.0	238

Number of obs: 245, groups: group, 1

Dispersion estimate for gaussian family (sigma<sup>2</sup>): 2.32e+03

Conditional model:

	Estimate	Std. Error	z value	Pr(> z )
(Intercept)	72.342	9.103	7.947	1.91e-15 ***
regionE	9.953	12.208	0.815	0.415
regionW:SexeM	-10.297	8.789	-1.172	0.241
regionE:SexeM	-5.011	9.657	-0.519	0.604

---  
Signif. codes: 0 '\*\*\*' 0.001 '\*\*' 0.01 '\*' 0.05 '.' 0.1 ' ' 1

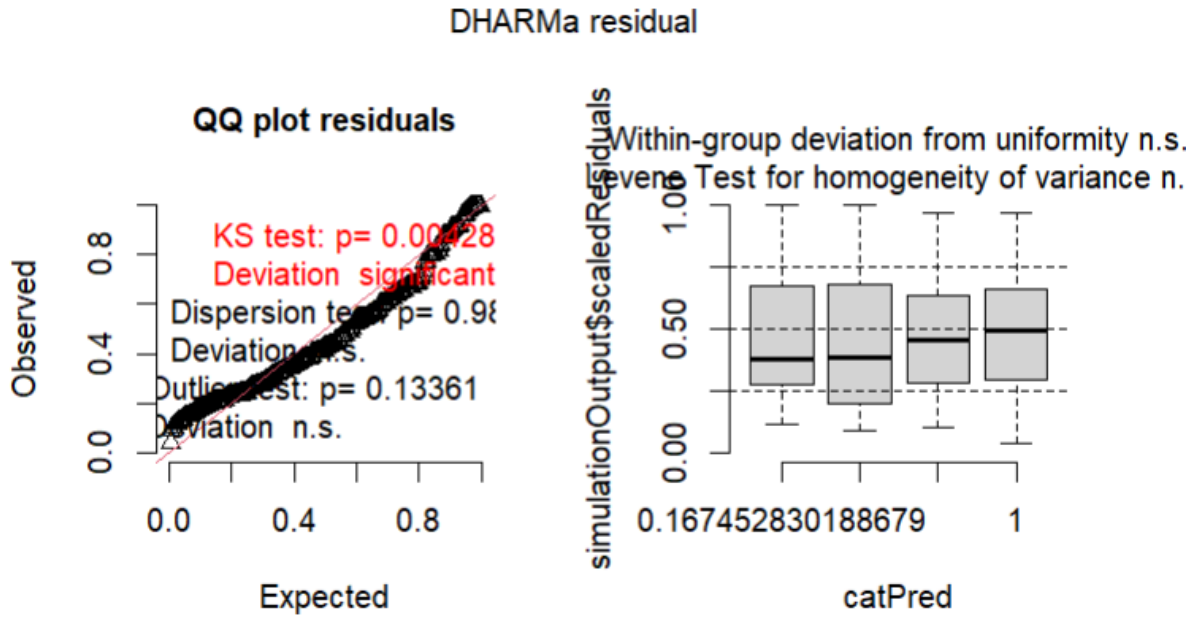


**Figure A 16 TAG-ST ratio model verification using the DHARMA package.** The plot function of the package allows to calculate an quantile regression, which compares the empirical 0.25, 0.5 and 0.75 quantiles with the theoretical 0.25, 0.5 and 0.75 quantiles (dashed black line), and provides a p-value for the deviation from the expected quantile. Red color indicates a significant deviation from the expected quantile. Left: qq-plot to detect deviations from expected distribution, with added tests for correct distribution (KS test), dispersion and outliers. Right: Residuals against predicted values.

Moran I test under randomisation

```
data: residuals
weights: nb2listw(spdep::dnearneigh(coordinates(datsp), 0, 1))
```

Moran I statistic standard deviate = -0.88432, p-value = 0.8117  
 alternative hypothesis: greater

sample estimates:

Moran I statistic	Expectation	Variance
-0.013995953	-0.004098361	0.000125267

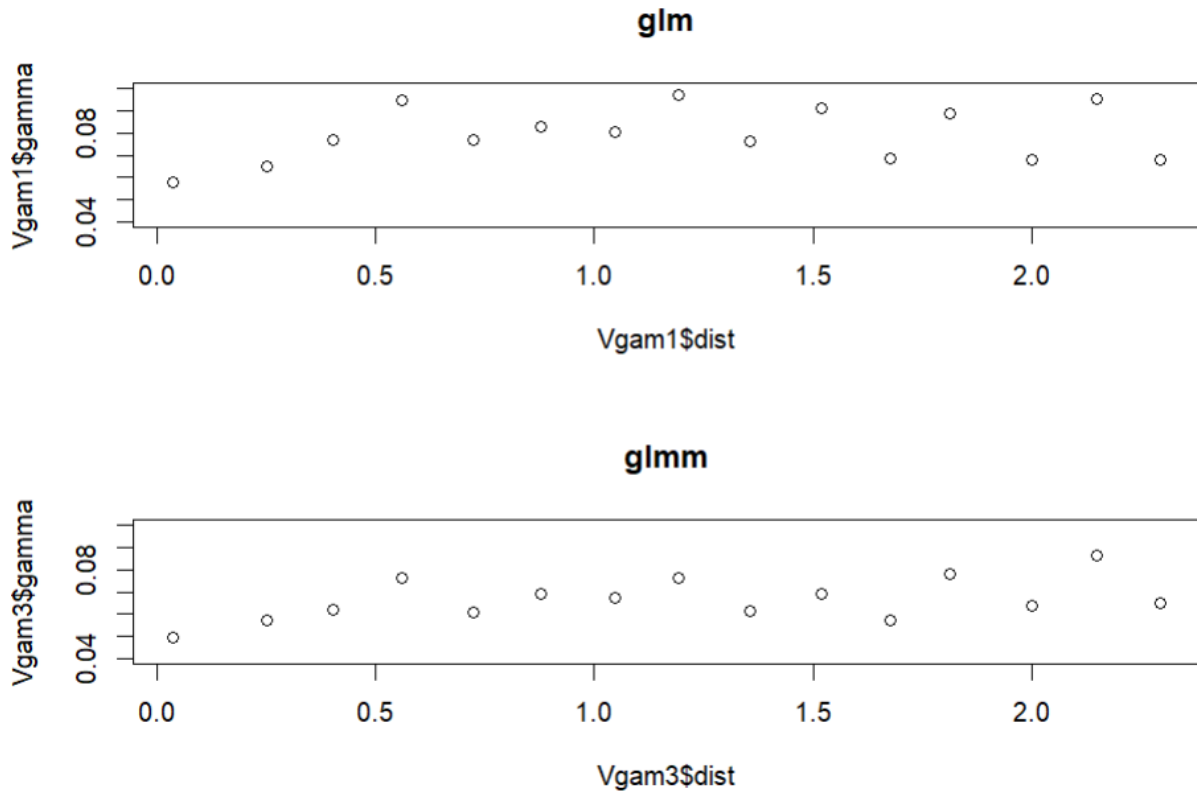


**Figure A 17 Variogram TAG-ST ratio.** To evaluate spatial autocorrelation in the model residuals, variograms were created based on residuals of the *glm* (upper) not accounting for spatial autocorrelation in the model and on residuals of the *glmm* (lower) accounting for spatial autocorrelation in the model (lower).

**Length:**

Family: gaussian ( identity )  
 Formula: Length ~ region + region:Sexe + exp(pos + 0 | group)  
 Data: dat\_v

AIC	BIC	logLik	deviance	df.resid
1057.9	1082.4	-521.9	1043.9	238

Number of obs: 245, groups: group, 1

Dispersion estimate for gaussian family (sigma<sup>2</sup>): 2.81

Conditional model:

	Estimate	Std. Error	z value	Pr(> z )
(Intercept)	19.0691	0.4901	38.91	< 2e-16 ***
regionE	2.5631	0.6803	3.77	0.000165 ***
regionW:SexeM	-1.1992	0.3160	-3.80	0.000148 ***
regionE:SexeM	-0.8093	0.3772	-2.15	0.031916 *

---  
 Signif. codes: 0 '\*\*\*' 0.001 '\*\*' 0.01 '\*' 0.05 '.' 0.1 ' ' 1

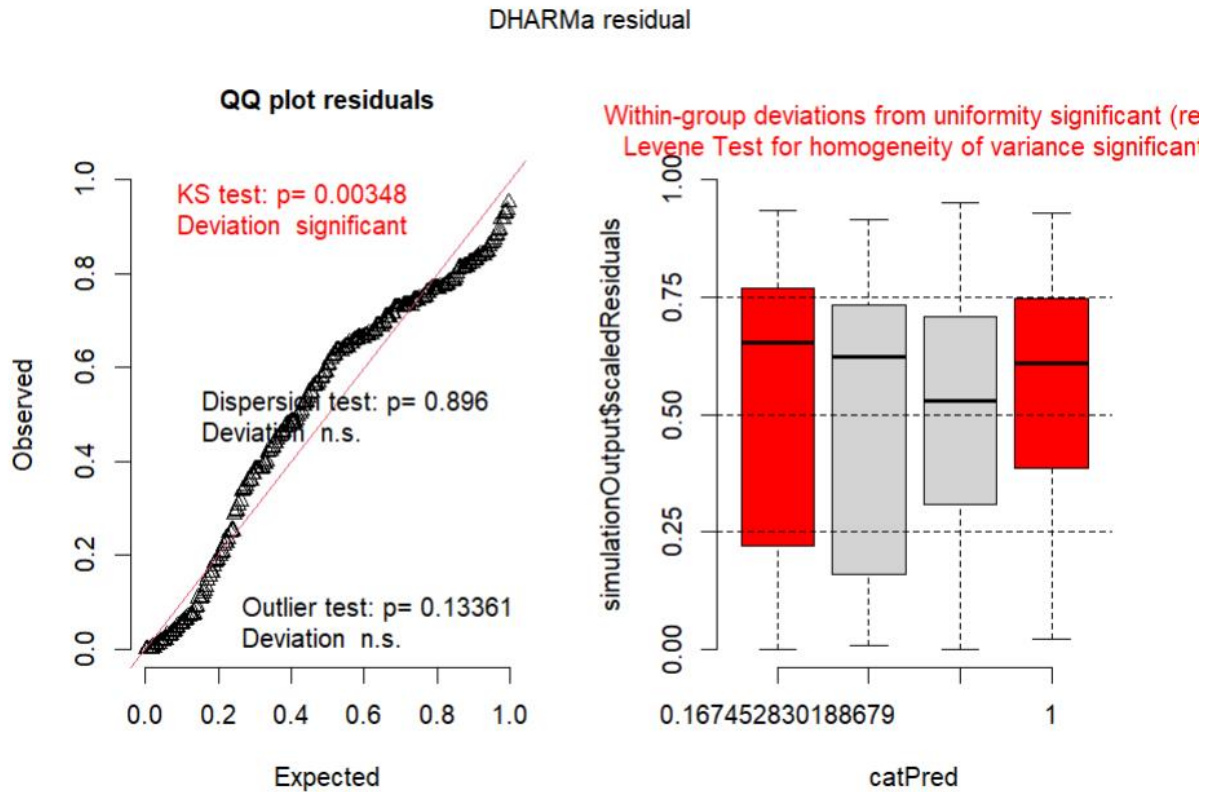


**Figure A 18 Length model verification using the DHARMA package.** The plot function of the package allows to calculate an quantile regression, which compares the empirical 0.25, 0.5 and 0.75 quantiles with the theoretical 0.25, 0.5 and 0.75 quantiles (dashed black line), and provides a p-value for the deviation from the expected quantile. Red color indicates a significant deviation from the expected quantile. Left: qq-plot to detect deviations from expected distribution, with added tests for correct distribution (KS test), dispersion and outliers. Right: Residuals against predicted values.

Moran I test under randomisation

```
data: residuals
weights: nb2listw(spdep::dnearneigh(coordinates(datsp), 0, 1))
```

```
Moran I statistic standard deviate = -1.1928, p-value = 0.8835
alternative hypothesis: greater
```

```
sample estimates:
Moran I statistic      Expectation      Variance
-0.017749914         -0.004098361      0.000130987
```



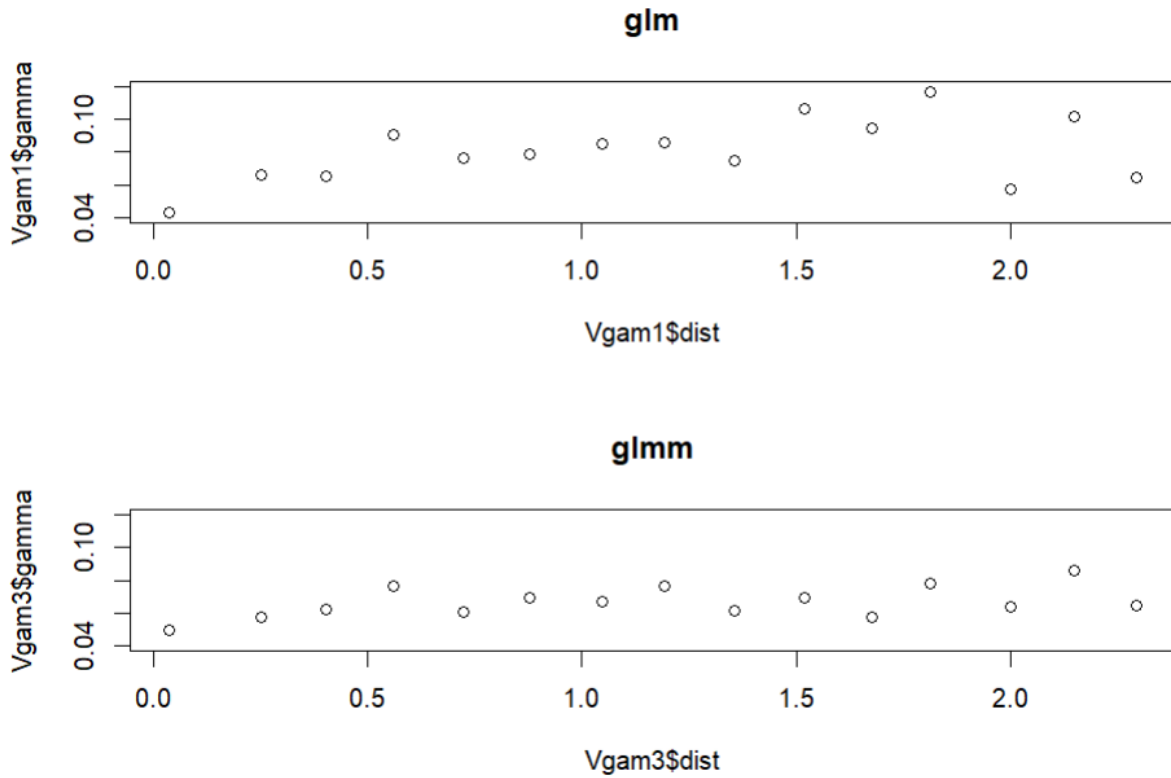


**Figure A 19 Variogram Length.** To evaluate spatial autocorrelation in the model residuals, variograms were created based on residuals of the glm (upper) not accounting for spatial autocorrelation in the model and on residuals of the glmm (lower) accounting for spatial autocorrelation in the model (lower).

**Weight**

Family: gaussian ( log )  
 Formula: weight ~ region + region:Sexe + exp(pos + 0 | group)  
 Data: dat\_v

AIC	BIC	logLik	deviance	df.resid
2150.7	2175.3	-1068.4	2136.7	238

Number of obs: 245, groups: group, 1

Dispersion estimate for gaussian family (sigma^2): 245

Conditional model:

	Estimate	Std. Error	z value	Pr(> z )	
(Intercept)	3.99712	0.07014	56.99	< 2e-16	***
regionE	0.48675	0.09224	5.28	1.31e-07	***
regionW:SexeM	-0.18857	0.05825	-3.24	0.00121	**
regionE:SexeM	-0.12209	0.04024	-3.03	0.00241	**

---  
 Signif. codes: 0 '\*\*\*' 0.001 '\*\*' 0.01 '\*' 0.05 '.' 0.1 ' ' 1

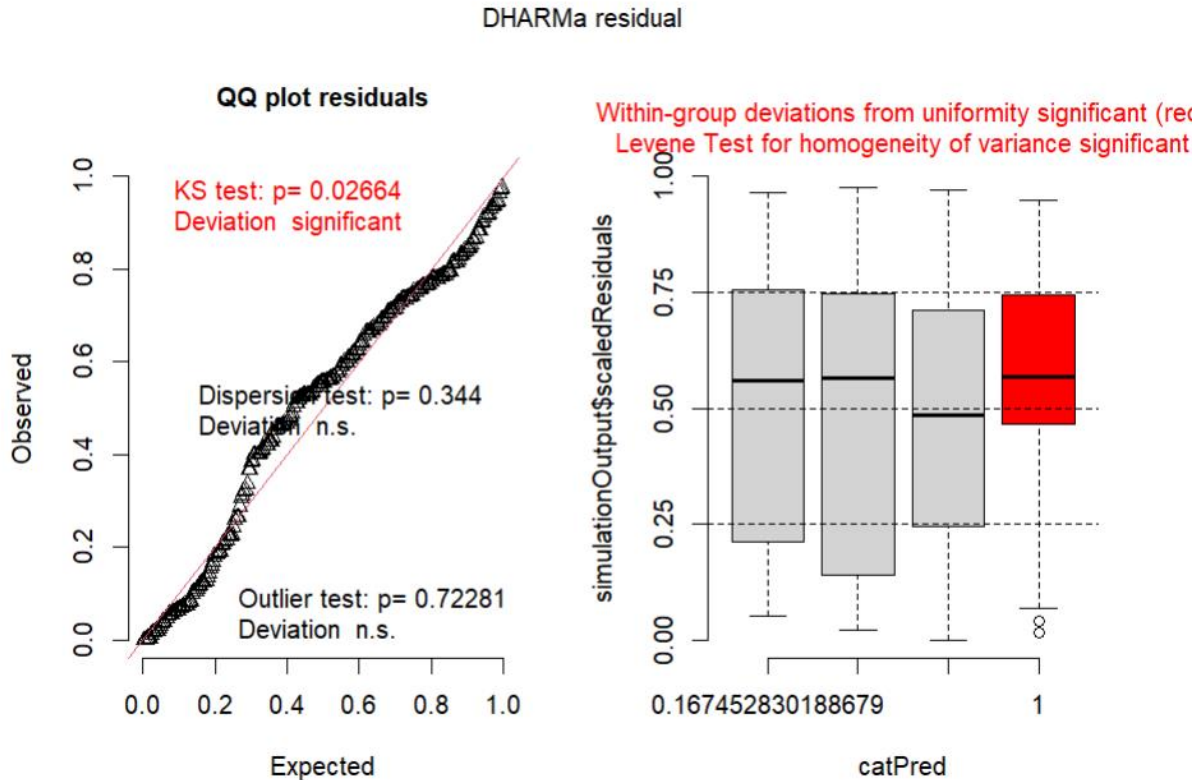


**Figure A 20 Weight model verification using the DHARMa package.** The plot function of the package allows to calculate an quantile regression, which compares the empirical 0.25, 0.5 and 0.75 quantiles with the theoretical 0.25, 0.5 and 0.75 quantiles (dashed black line), and provides a p-value for the deviation from the expected quantile. Red color indicates a significant deviation from the expected quantile. Left: qq-plot to detect deviations from expected distribution, with added tests for correct distribution (KS test), dispersion and outliers. Right: Residuals against predicted values.

Moran I test under randomisation

```

data: residuals
weights: nb2listw(spdep::dnearneigh(coordinates(datsp), 0, 1))

Moran I statistic standard deviate = -1.1744, p-value = 0.8799
alternative hypothesis: greater
sample estimates:
Moran I statistic      Expectation      Variance
-0.0175417143      -0.0040983607      0.0001310302
    
```

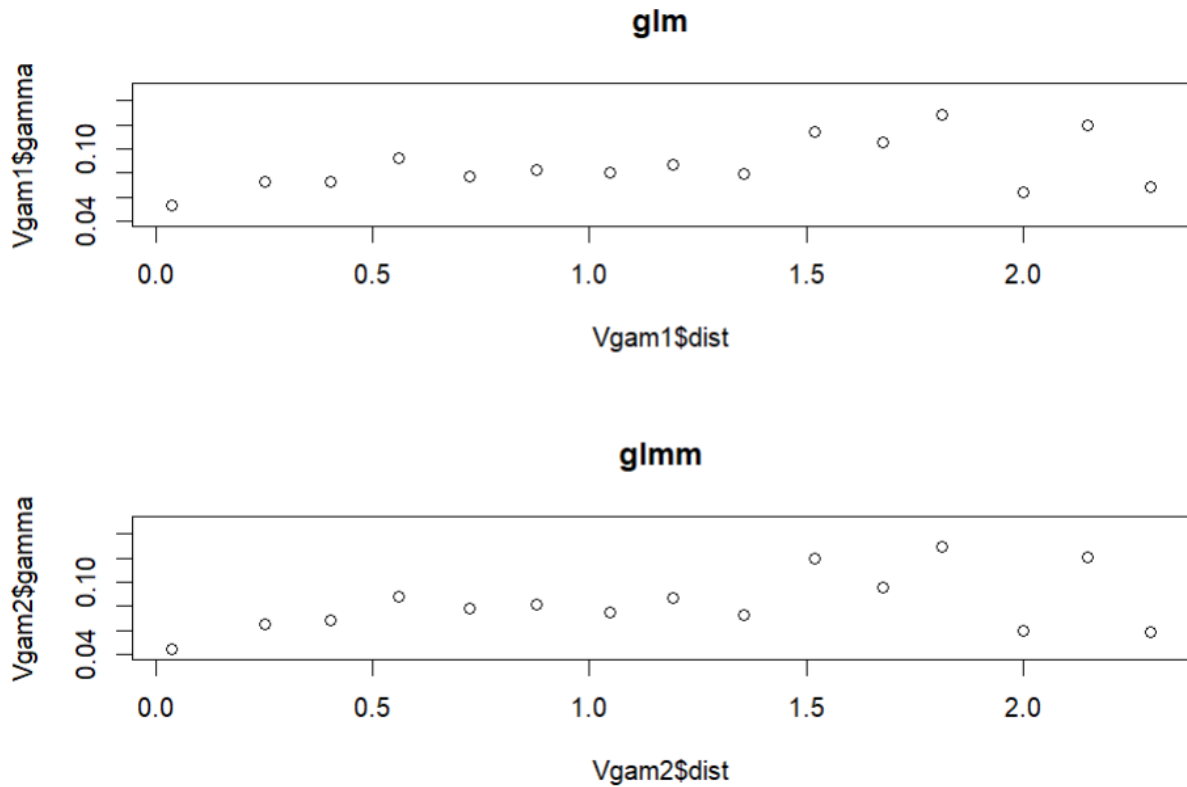


**Figure A 21 Variogram Weight.** To evaluate spatial autocorrelation in the model residuals, variograms were created based on residuals of the glm (upper) not accounting for spatial autocorrelation in the model and on residuals of the glmm (lower) accounting for spatial autocorrelation in the model (lower).

**Le Cren’s condition index**

Family: gaussian ( log )  
 Formula: condition ~ region + region:Sexe + exp(pos + 0 | group)  
 Data: dat\_v

AIC	BIC	logLik	deviance	df.resid
-429.3	-404.8	221.7	-443.3	238

Number of obs: 245, groups: group, 1

Dispersion estimate for gaussian family (sigma^2): 0.00874

Conditional model:

	Estimate	Std. Error	z value	Pr(> z )
(Intercept)	0.01703	0.01417	1.202	0.229
regionE	-0.03080	0.01967	-1.566	0.117
regionW:SexeM	0.01558	0.01657	0.941	0.347
regionE:SexeM	-0.02899	0.01933	-1.499	0.134



Appendix III – Chapter 3

the respective parameter of sardines. Significance: \*\*\* ( $P < 0.001$ ), \*\* ( $P < 0.01$ ), \* ( $P < 0.05$ ). AIC (Akaike's Information Criteria). *n* indicates the number of individuals used in the model.

		length	weight	TAG-ST ratio	Le Cren's index
Intercept (S.E.)		19.07 (0.5) ***	4.0 (0.07) ***	72.34 (9.10) ***	0.02 (0.01)
Estimates (S.E.)	region	2.56 (0.68) ***	0.49 (0.09) ***	9.95 (12.21)	-0.03 (0.02)
	regionWEC:sex	-1.2 (0.31) ***	-0.19 (0.06) **	-10.3 (8.79)	0.02 (0.02)
	regionEEC:sex	-0.81 (0.38) *	0.12 (0.04) **	-5.01 (9.66)	-0.03 (0.02)
AIC		1058	2151	2632	-429
n		245	245	245	245

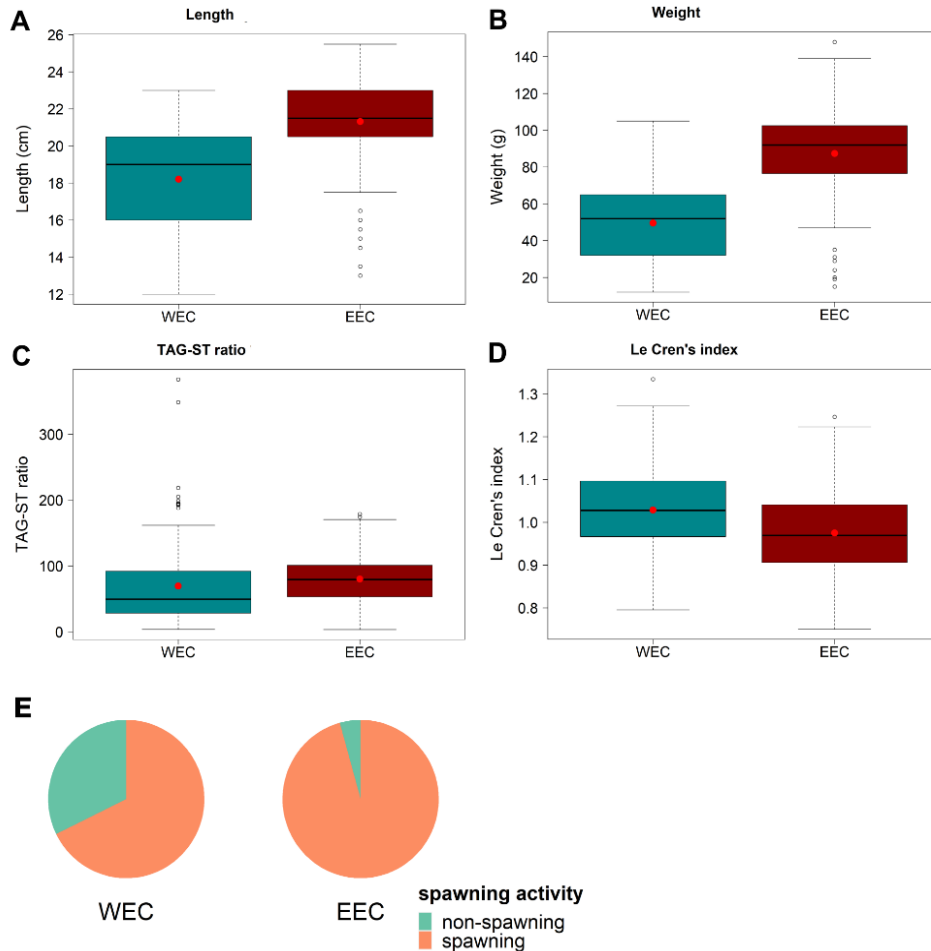


**Figure A 23 Differences of biological parameters of sardine between regions.** A: Comparison of length between sardines caught in the EEC and WEC. Red dots indicate mean; B: Comparison of weight between sardines caught in the EEC and WEC. Red dots indicate mean; C: Comparison of TAG-ST ratio between sardines caught in the EEC and WEC. Red dots indicate mean; D: Comparison of Le Cren's index between sardines caught in the EEC and WEC. Red dots indicate mean; E: Proportion of spawning and non-spawning individuals per region.

### 3.3 Differences in environmental parameters between the basins

The prevailing environmental conditions during the study period corresponded to the known conditions in the study area during autumn (Stanford and Pitcher, 2004). The WEC was significantly more saline (p-value: <0.01, WEC:  $35.1 \pm 0.2$ , EEC:  $34.3 \pm 0.5$ ), deeper (p-value: <0.01, WEC:  $80.9 \pm 23$  m, EEC:  $37.6 \pm 16$  m) and colder than the EEC (p-value: 0.01, WEC:  $16.6 \pm 0.9$  °C, EEC:  $17 \pm 0.5$  °C) (Figure A 24).

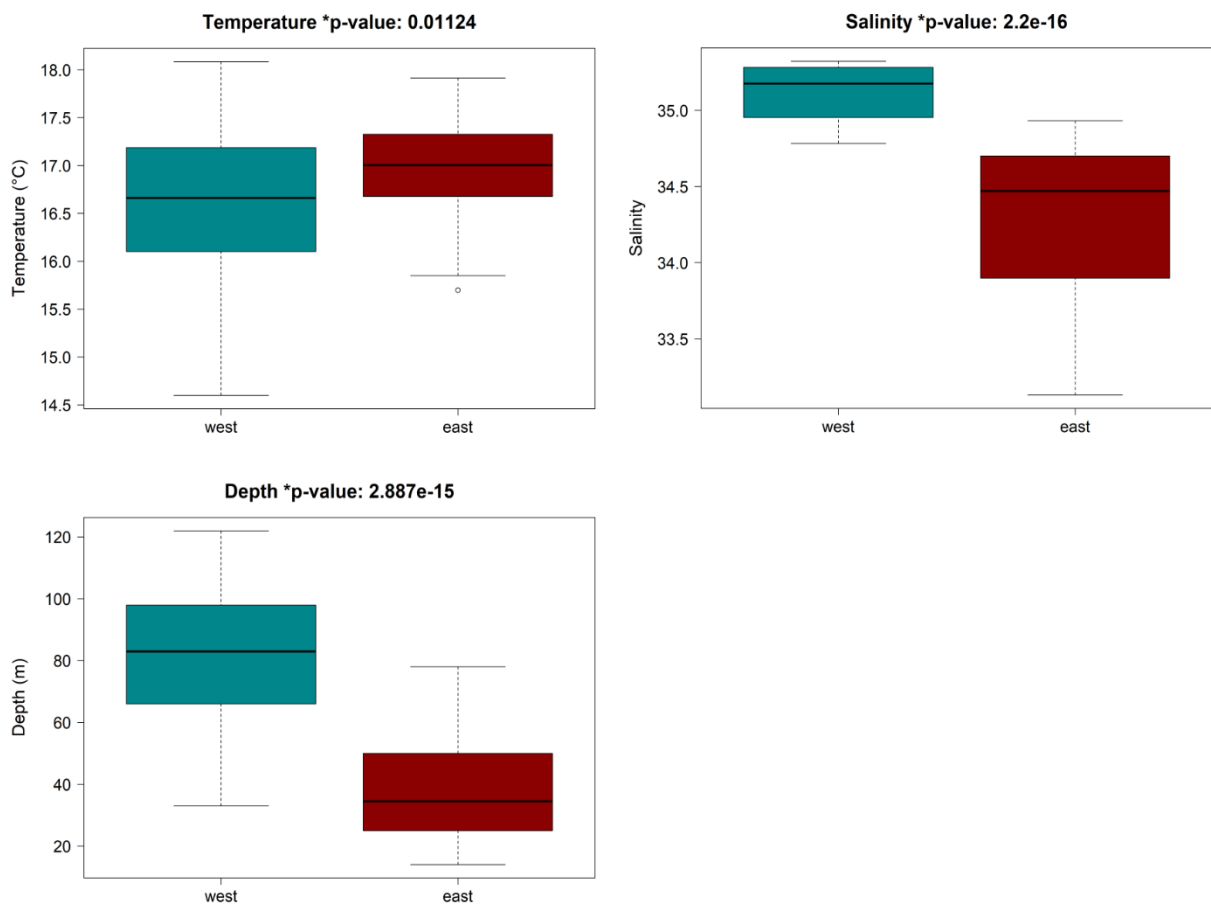


**Figure A 24 Environmental conditions in the WEC and EEC during CGFS 2021. A: Temperature; B: Salinity; C: Depth; P-values of the statistical analysis are indicated in the heading of figures A-C.**

## 3.4 GLMM and GAM to evaluate factors influencing trophic transfer - Model selection process

### 3.4.1 EPA

#### 3.4.1.1 GLMM

```
Family: beta ( logit )
Formula:          s20_5n3 ~ z20_5n3 + condition + region + Mat
urity + exp(pos + 0 | group)
Data: dat_transformed
```

```
      AIC      BIC   logLik deviance df.resid
-1234.7 -1207.1   625.4  -1250.7     225
Number of obs: 233, groups:  group, 2
```

Dispersion parameter for beta family (): 418

Conditional model:

	Estimate	Std. Error	z value	Pr(> z )	
(Intercept)	-2.230669	0.202561	-11.012	<2e-16	***
z20_5n3	0.017411	0.007102	2.451	0.0142	*
condition	0.156365	0.109843	1.424	0.1546	
regionw	-0.171999	0.115890	-1.484	0.1378	
Maturity	-0.252890	0.029697	-8.516	<2e-16	***

---  
Signif. codes: 0 '\*\*\*' 0.001 '\*\*' 0.01 '\*' 0.05 '.' 0.1 ' ' 1

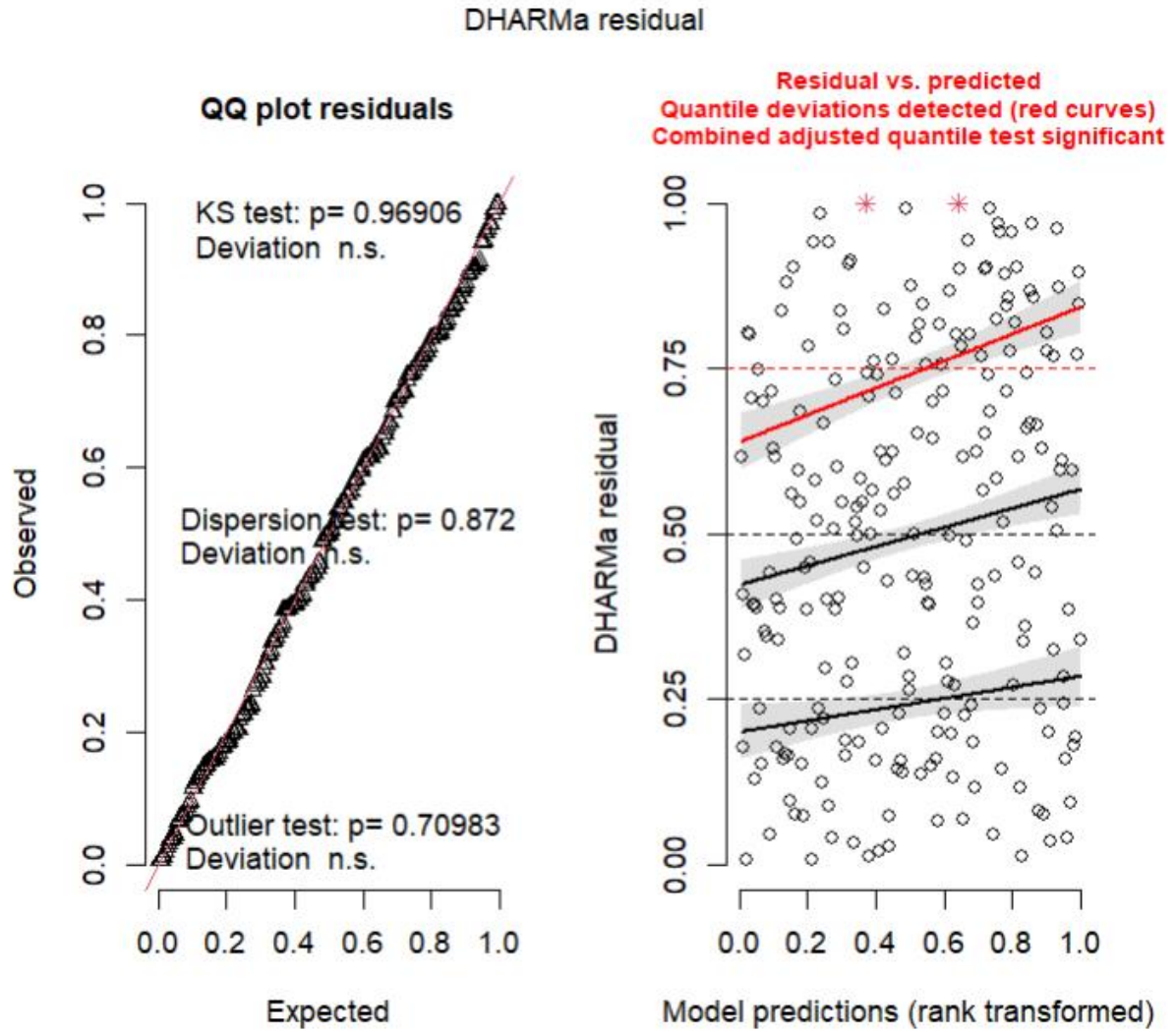


**Figure A 25 EPA GLMM verification using the DHARMa package.** The plot function of the package allows to calculate an quantile regression, which compares the empirical 0.25, 0.5 and 0.75 quantiles with the theoretical 0.25, 0.5 and 0.75 quantiles (dashed black line), and provides a p-value for the deviation from the expected quantile. Red color indicates a significant deviation from the expected quantile. Left: qq-plot to detect deviations from expected distribution, with added tests for correct distribution (KS test), dispersion and outliers. Right: Residuals against predicted values.



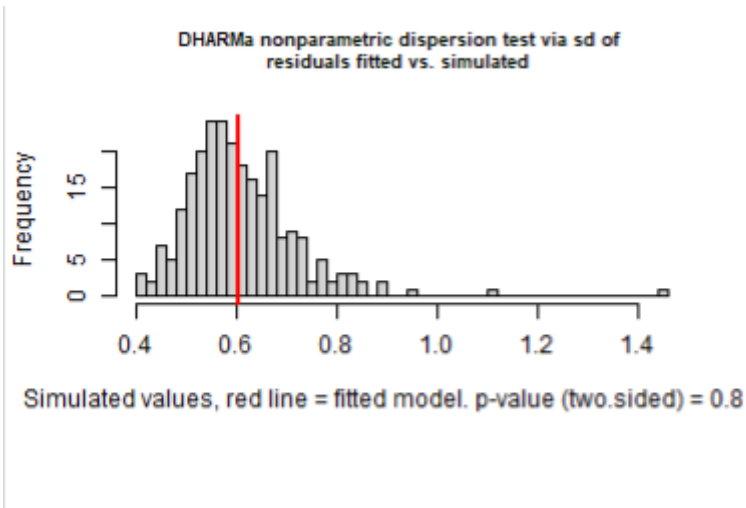


**Figure A 26 EPA GLMM test for over/underdispersion.** If fitted model (red line), is among simulated values no over- or underdispersion is present.

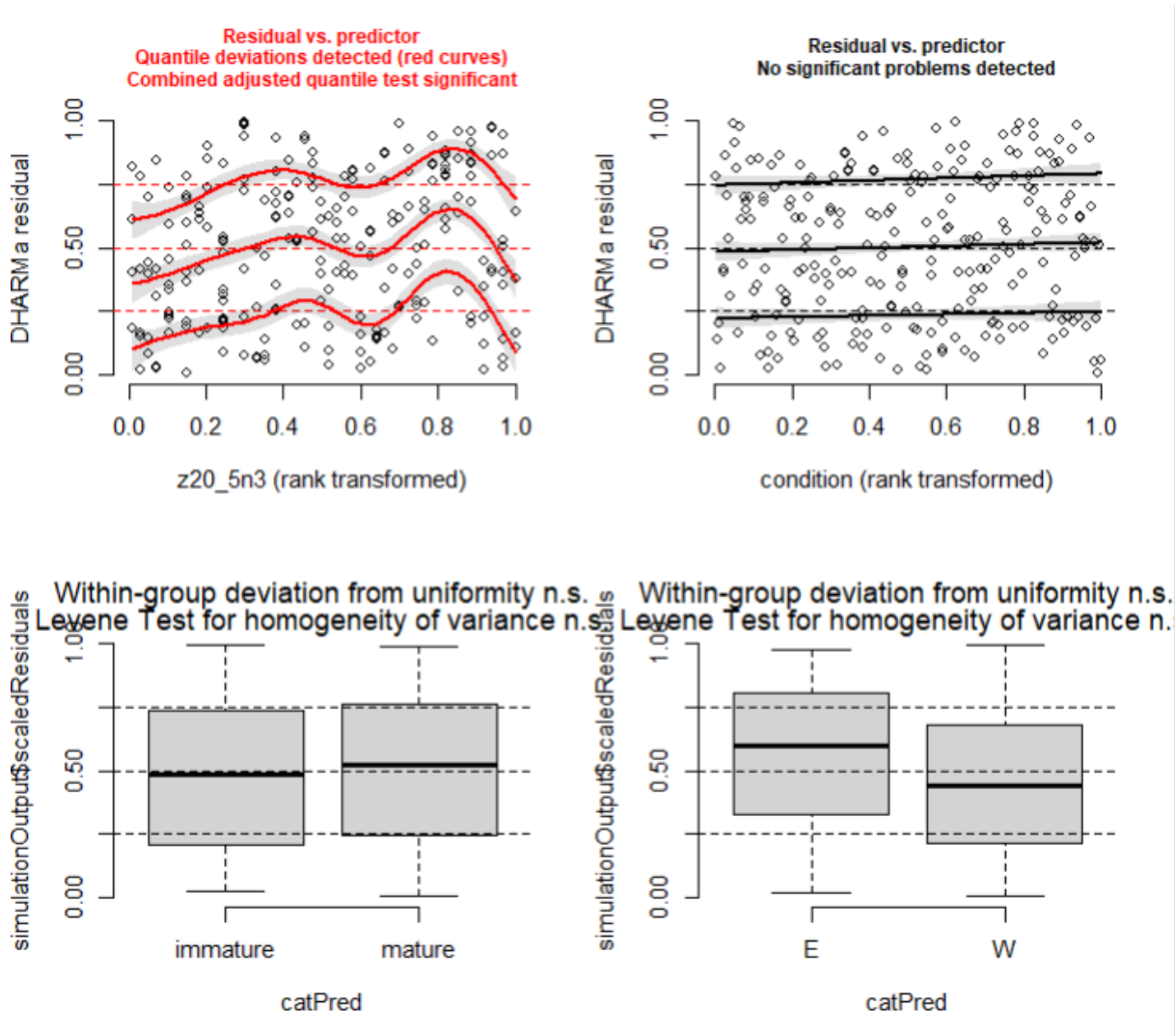


**Figure A 27 EPA GLMM - Quantile residuals fitted against each covariate.** Is second quantile is colored red, a non linear trend was detected and a GAM will be applied in a next step to take into account this non-linear pattern.

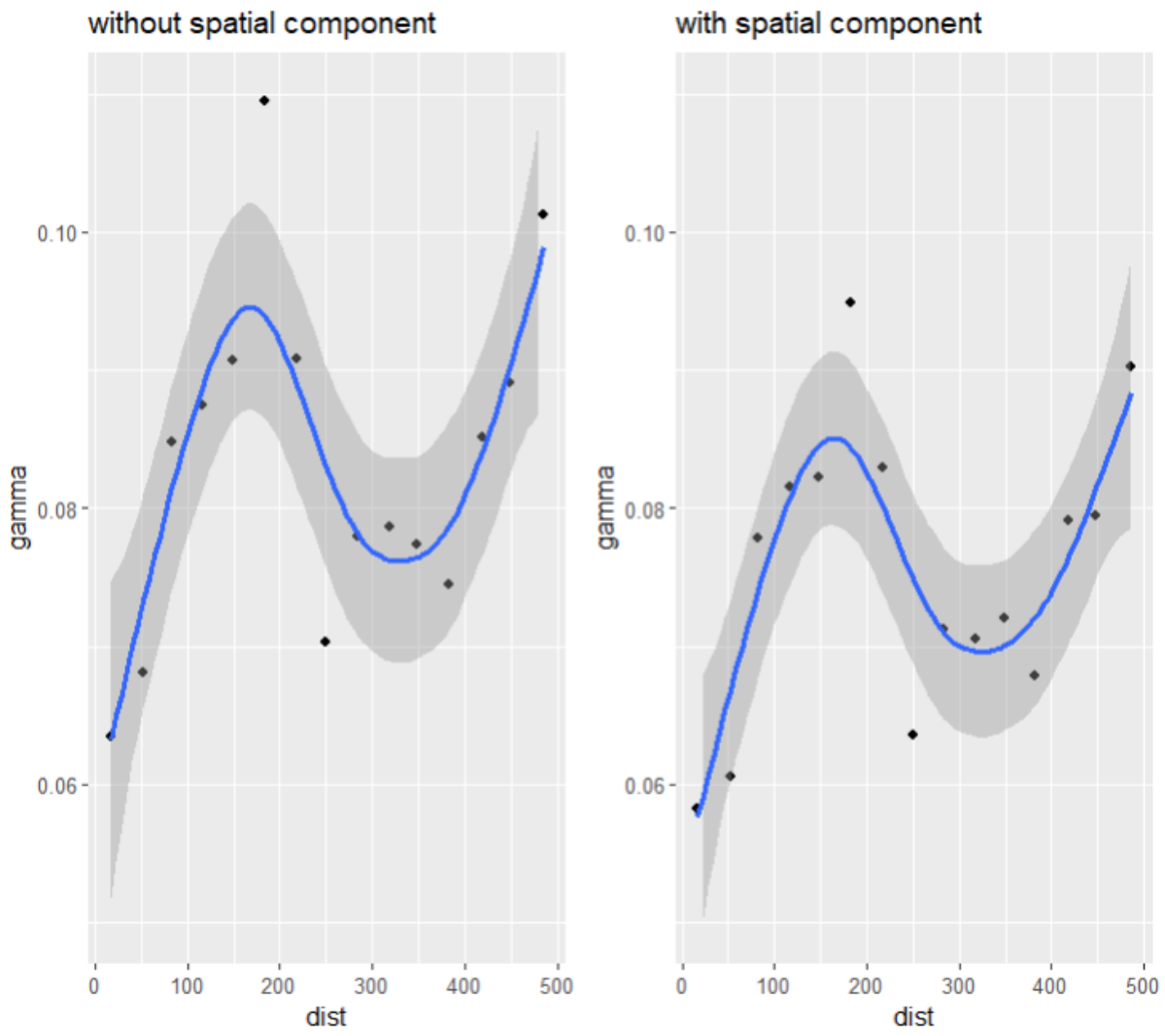


**Figure A 28 Variogram EPA GLMM.** To evaluate spatial autocorrelation in the model residuals, variograms were created based on residuals of a GLMM (left) not accounting for spatial autocorrelation in the model and on residuals of the GLMM (right) accounting for spatial autocorrelation in the model.

### 3.4.1.2 GAM

Family: Beta regression(322.038)  
Link function: logit

Formula:  
s20\_5n3 ~ s(z20\_5n3) + Maturity + condition + region

Parametric coefficients:

	Estimate	Std. Error	z value	Pr(> z )	
(Intercept)	-1.97253	0.11877	-16.608	< 2e-16	***
Maturity	-0.26037	0.03030	-8.593	< 2e-16	***
condition	0.23234	0.11700	1.986	0.0471	*
regionW	-0.18806	0.03949	-4.762	1.91e-06	***

---  
Signif. codes: 0 '\*\*\*' 0.001 '\*\*' 0.01 '\*' 0.05 '.' 0.1 ' ' 1

Approximate significance of smooth terms:

	edf	Ref.df	Chi.sq	p-value	
s(z20_5n3)	2.932	3.694	21.53	0.000199	***

---

Signif. codes: 0 '\*\*\*' 0.001 '\*\*' 0.01 '\*' 0.05 '.' 0.1 ' ' 1

R-sq.(adj) = 0.449 Deviance explained = 47.4%

-REML = -598.74 Scale est. = 1 n = 233

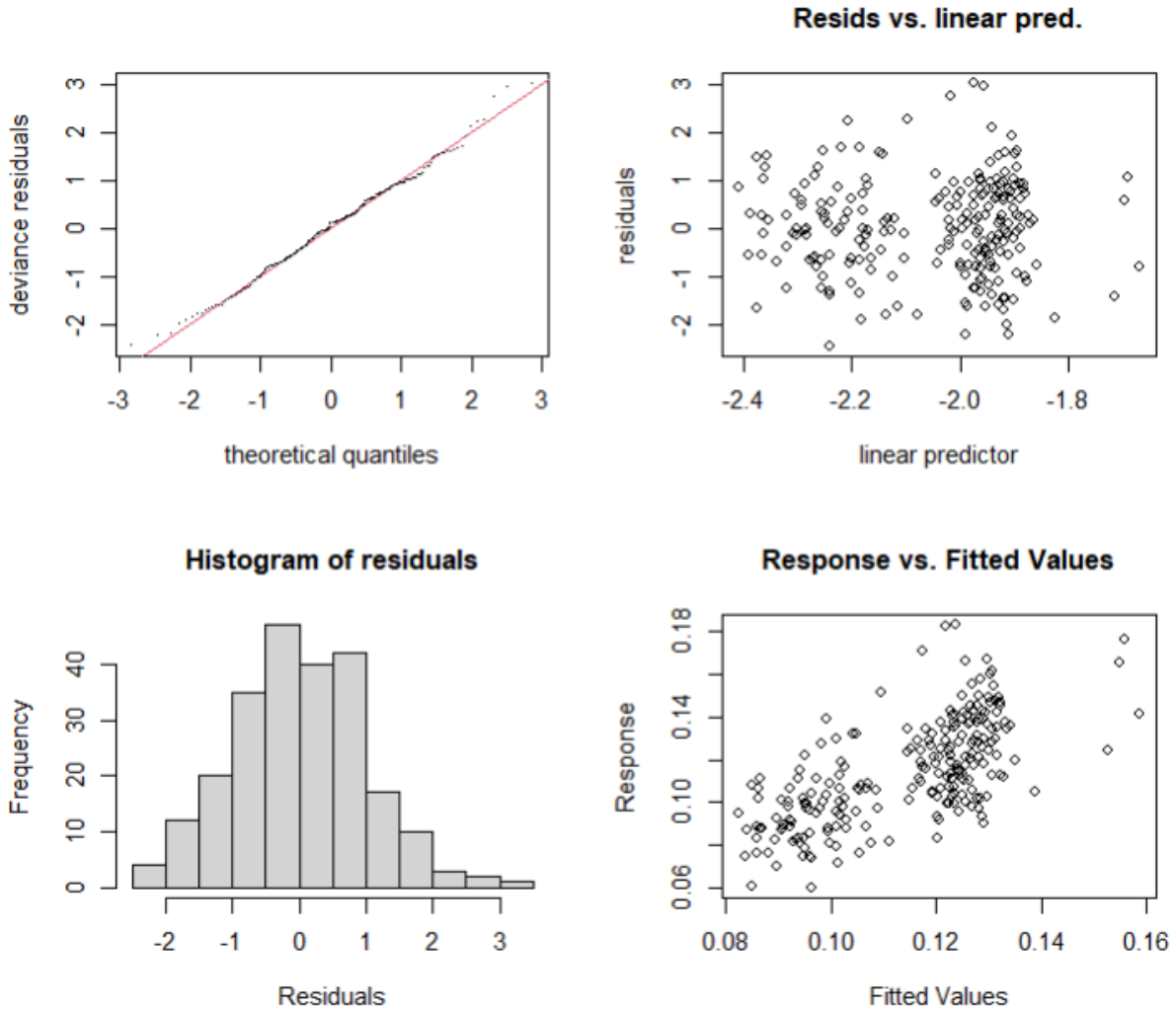


**Figure A 29 Convergence plots for GAM on EPA.** The first panel showcases a Q-Q plot, comparing model residuals to a normal distribution. A well-fitted model will exhibit residuals that closely align with a straight line. In the bottom left panel, a histogram of residuals is presented, expected to have a symmetrical bell shape. The top-right panel displays residuals values, which ideally should be evenly distributed around zero. The final panel in the bottom right shows the response versus fitted values, where a perfect model would yield a straight line.

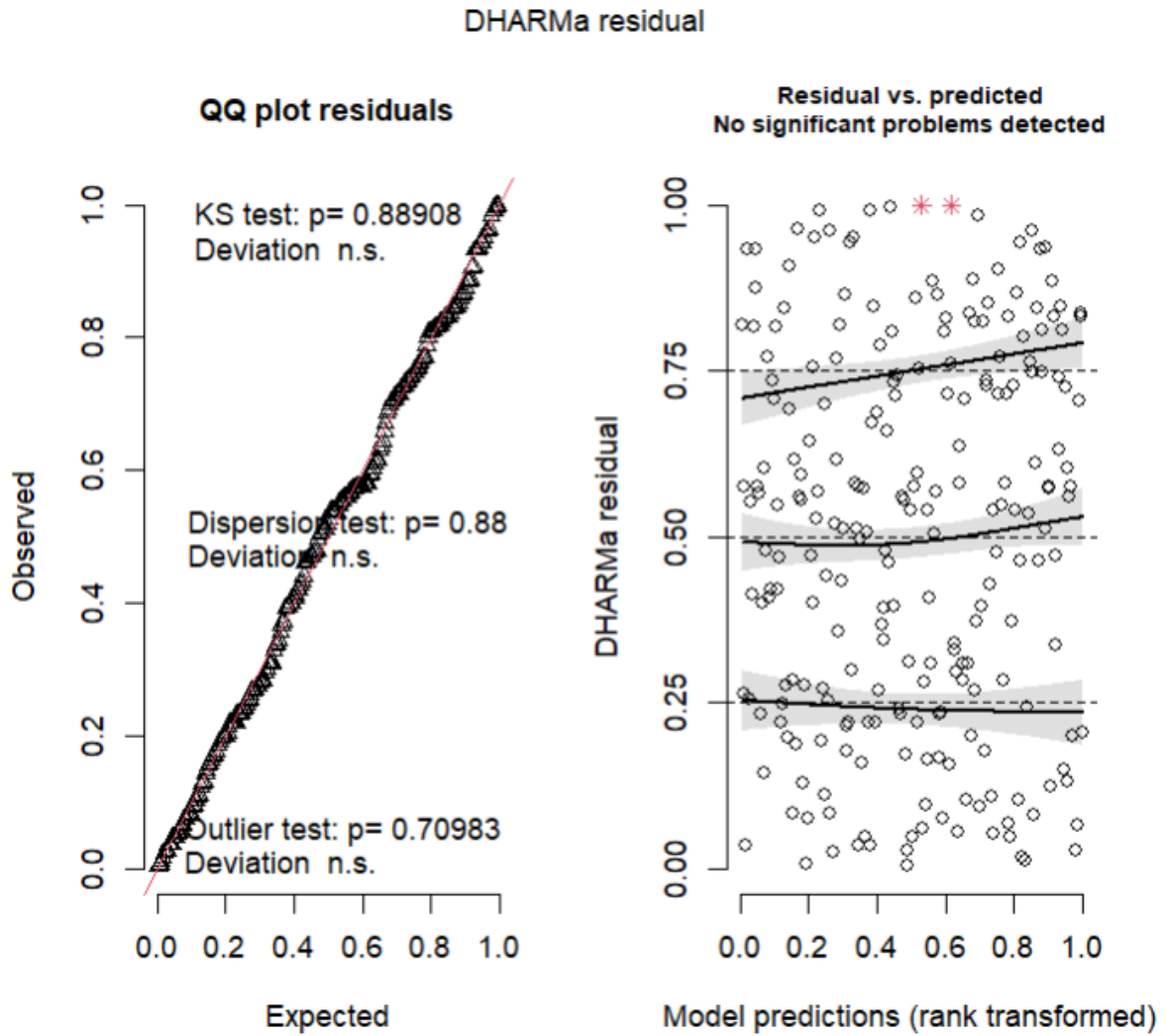


**Figure A 30 EPA GAM verification using the DHARMA package.** The plot function of the package allows to calculate an quantile regression, which compares the empirical 0.25, 0.5 and 0.75 quantiles with the theoretical 0.25, 0.5 and 0.75 quantiles (dashed black line), and provides a p-value for the deviation from the expected quantile. Red color indicates a significant deviation from the expected quantile. Left: qq-plot to detect deviations from expected distribution, with added tests for correct distribution (KS test), dispersion and outliers. Right: Residuals against predicted values.

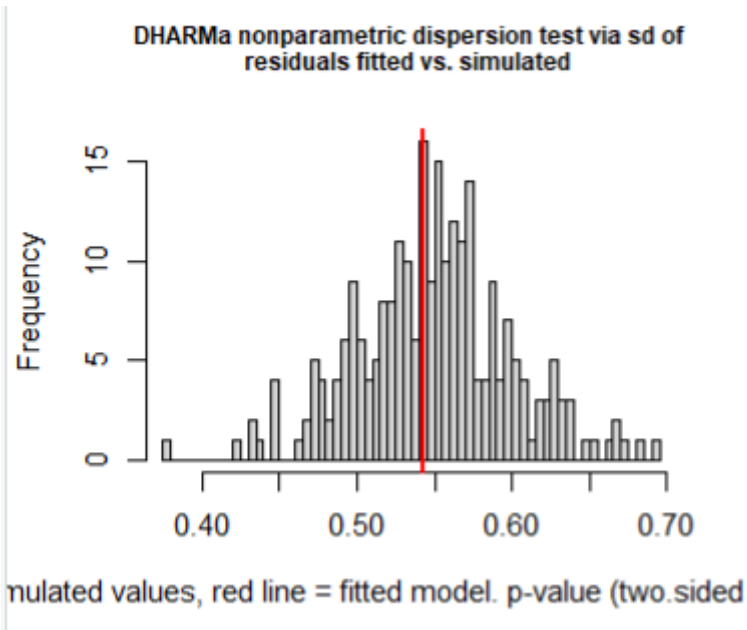


**Figure A 31 EPA GAM test for over/underdispersion.** If fitted model (red line), is among simulated values no over- or underdispersion is present.

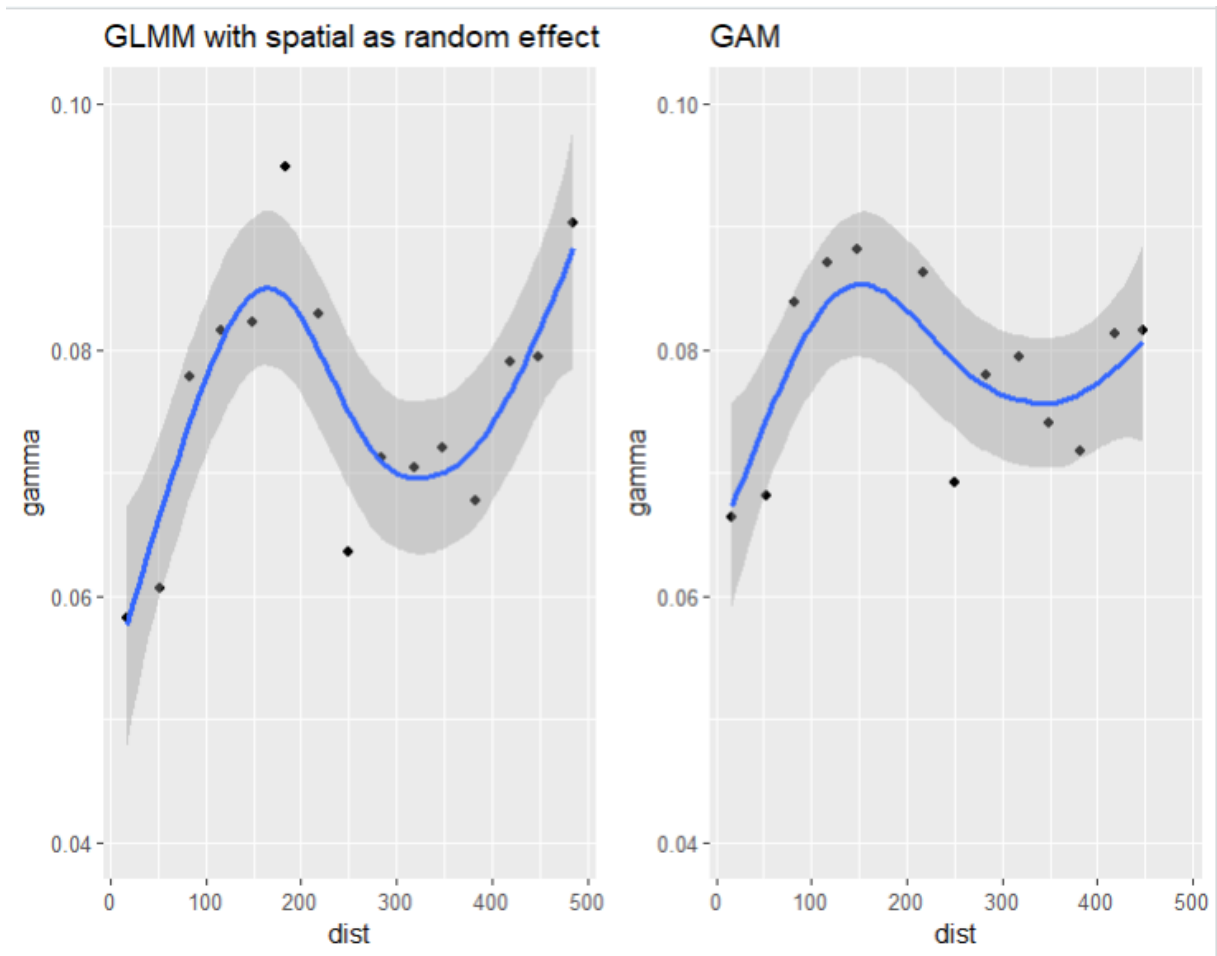


**Figure A 32 Variogram EPA GAM.** To evaluate spatial autocorrelation in the model residuals, variograms were created based on residuals of a GLMM (left) accounting for spatial autocorrelation in the model and on residuals of the GAM (right) not accounting for spatial autocorrelation in the model.

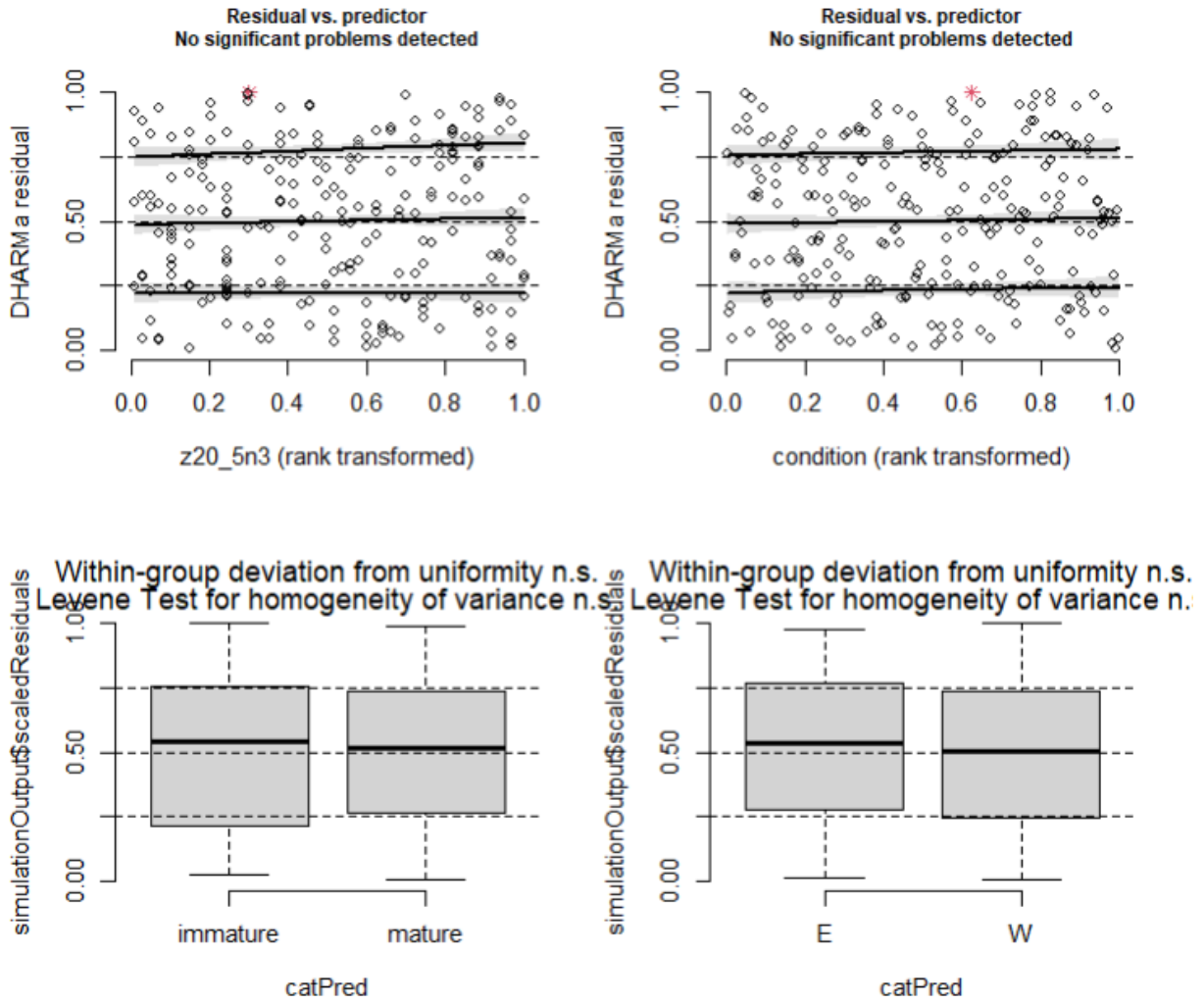


**Figure A 33 EPA GAM - Quantile residuals fitted against each covariate.** Is second quantile is colored red, a non linear trend was detected and a GAM will be applied in a next step to take into account this non-linear pattern.

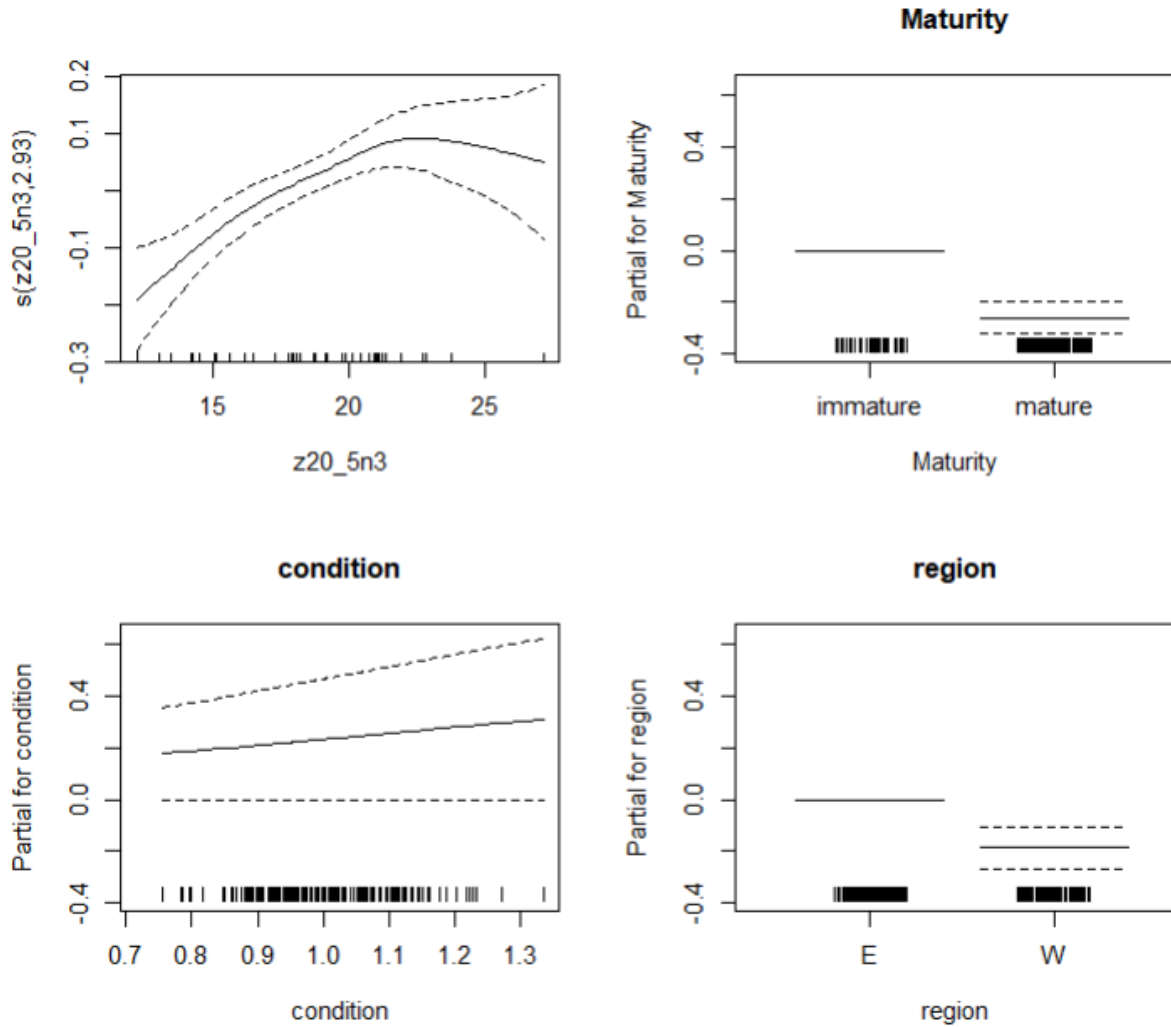


Figure A 34 Model prediction per covariate for EPA GAM.

### 3.4.1.3 Conclusion models EPA

AIC of glmm with spatial component (modelEPA1), glmm without spatial component (modelEPA\_V) and of gam (gameEPA):

	df	AIC
modelEPA1	8.000000	-1234.728
modelEPA_V	7.000000	-1204.992
gameEPA	8.694339	-1212.164

Including a spatial term in the model did enhance the AIC (modelEPA1 vs modelEPA\_V). The gam not taking into account spatial autocorrelation had still a lower AIC than the glmm without spatial autocorrelation. As the variogram of the gam and the glmm (with spatial



component) is similar and the gam allows taking into account the non-linear relationship between sardine and zooplankton EPA and shows non remaining patterns in the residuals in contrast to the glmm (modelEPA1) the gam was chosen as final model although it had a higher AIC than the glmm.

### 3.4.2 DHA

First a glmm was tried to take into account spatial autocorrelation of the samples:

#### 3.4.2.1 GLMM

```
Family: beta (logit)
Formula: s22_6n3 ~ z22_6n3 + condition + region + Maturity + exp(p
os + 0 | group)
Data: dat_transformed
```

```
      AIC      BIC   logLik deviance df.resid
-671.7  -644.1   343.8  -687.7     225
Number of obs: 233, groups: group, 2
```

Dispersion parameter for beta family (): 60.3

Conditional model:

	Estimate	Std. Error	z value	Pr(> z )
(Intercept)	-1.069236	0.301324	-3.548	0.000387 ***
z22_6n3	0.001606	0.008776	0.183	0.854763
condition	-0.254578	0.219564	-1.159	0.246264
regionw	0.345105	0.195454	1.766	0.077453 .
Maturitymature	-0.194178	0.057048	-3.404	0.000665 ***

---  
Signif. codes: 0 '\*\*\*' 0.001 '\*\*' 0.01 '\*' 0.05 '.' 0.1 ' ' 1

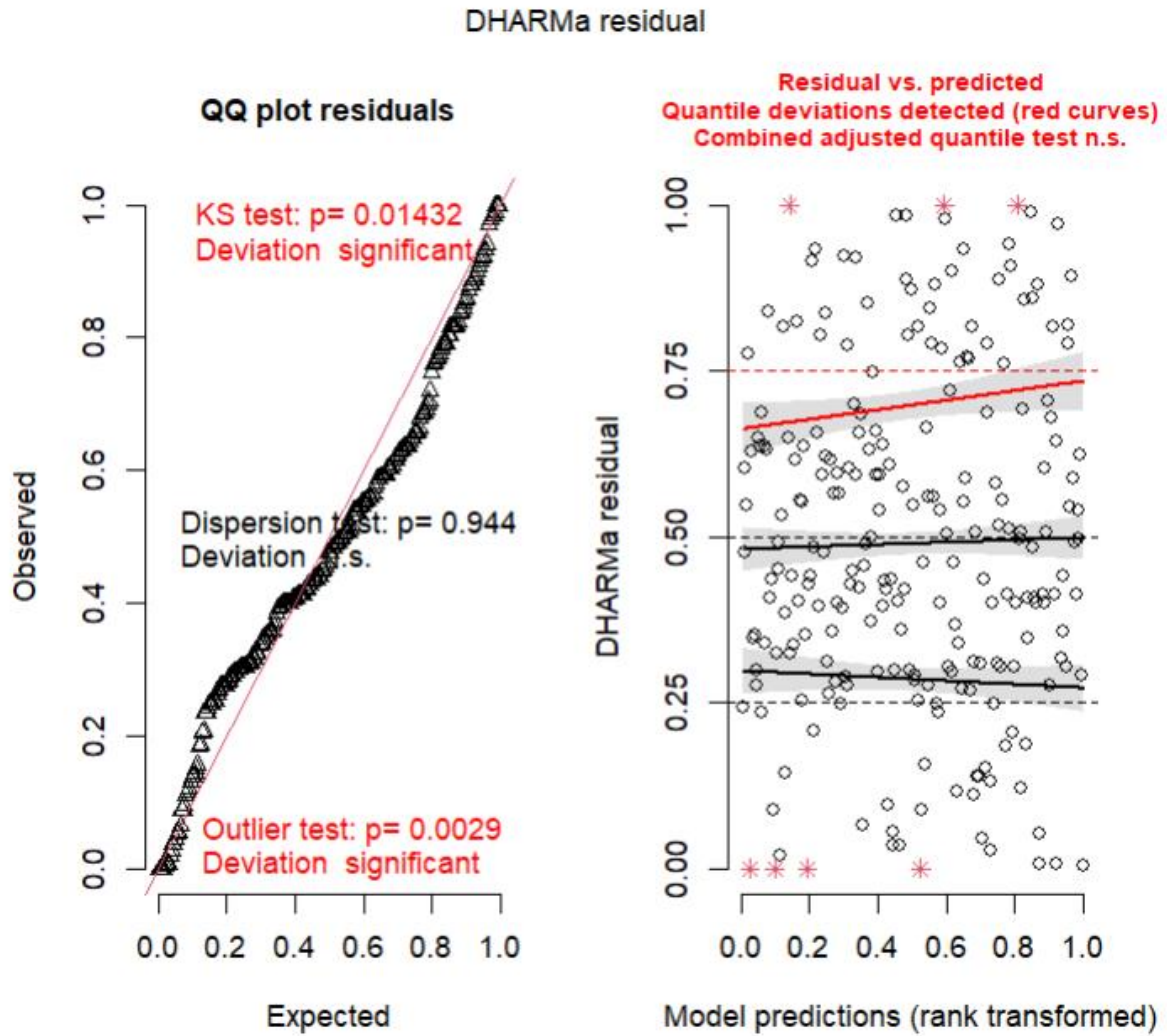
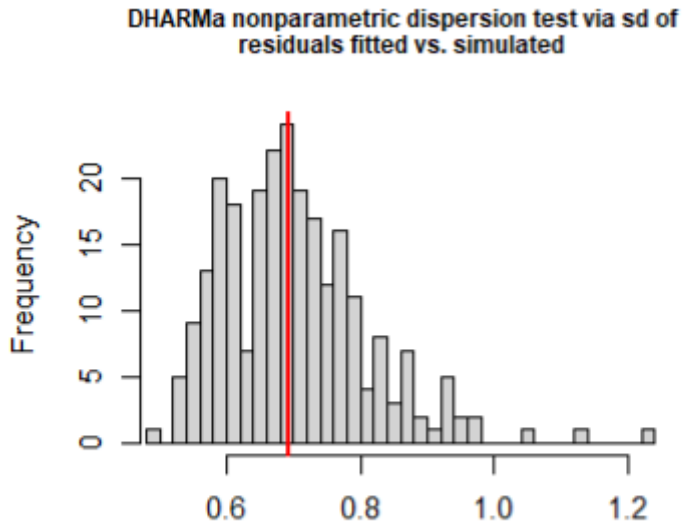


**Figure A 35 DHA GLMM verification using the DHARMA package.** The plot function of the package allows to calculate an quantile regression, which compares the empirical 0.25, 0.5 and 0.75 quantiles with the theoretical 0.25, 0.5 and 0.75 quantiles (dashed black line), and provides a p-value for the deviation from the expected quantile. Red color indicates a significant deviation from the expected quantile. Left: qq-plot to detect deviations from expected distribution, with added tests for correct distribution (KS test), dispersion and outliers. Right: Residuals against predicted values.



simulated values, red line = fitted model. p-value (two.sided)

**Figure A 36 DHA GLMM test for over/underdispersion.** If fitted model (red line), is among simulated values no over- or underdispersion is present.

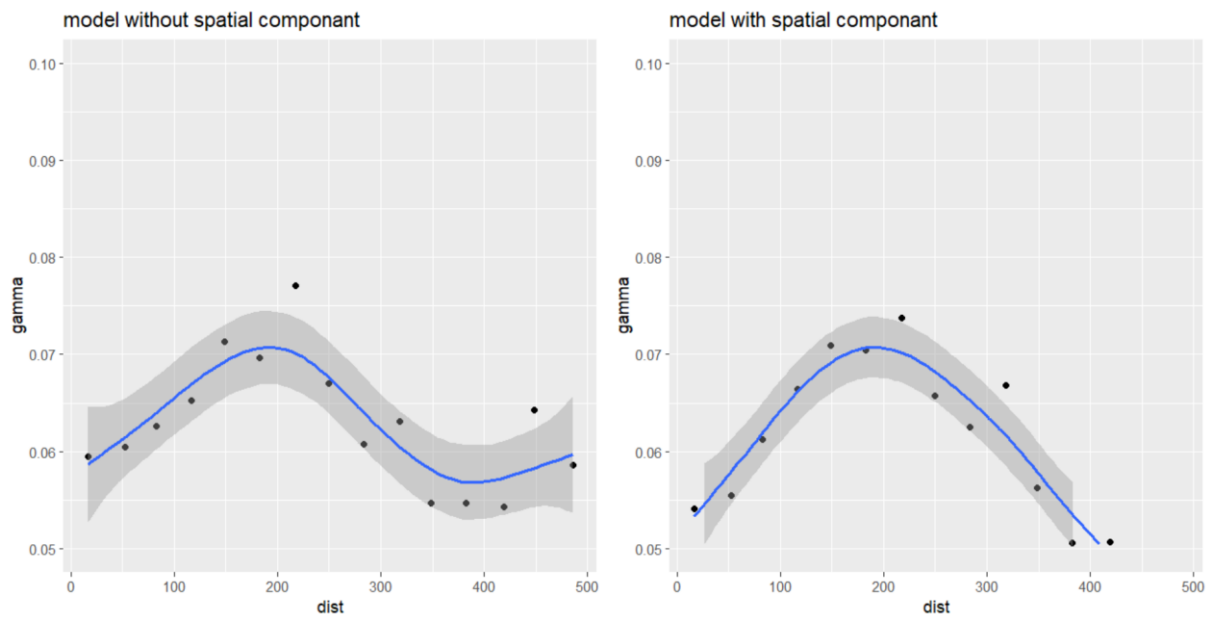


**Figure A 37 Variogram DHA GLMM.** To evaluate spatial autocorrelation in the model residuals, variograms were created based on residuals of a GLMM (left) not accounting for spatial autocorrelation in the model and on residuals of the GLMM (right) accounting for spatial autocorrelation in the model.

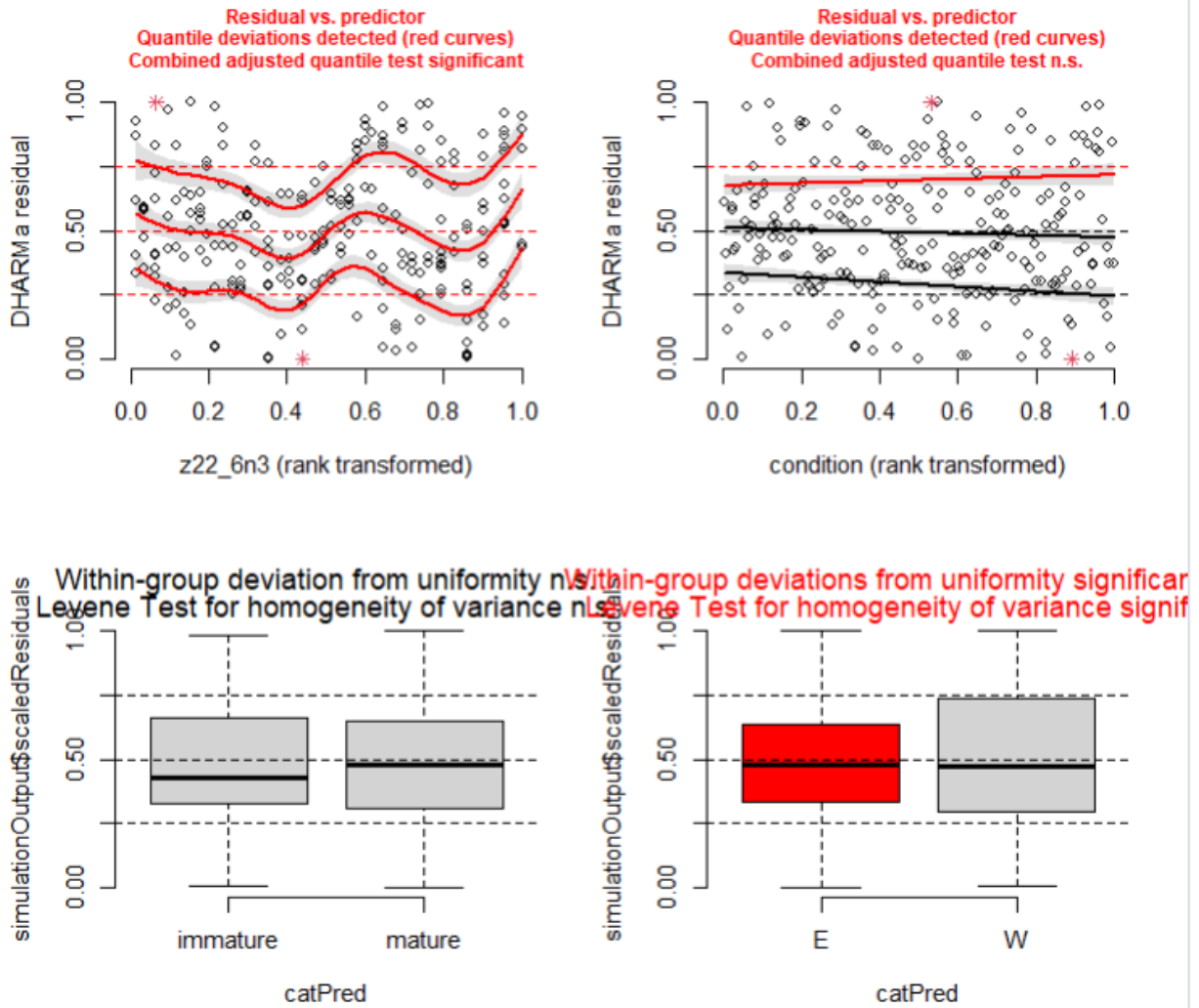


**Figure A 38 DHA GLMM - Quantile residuals fitted against each covariate.** Is second quantile is colored red, a non linear trend was detected and a GAM will be applied in a next step to take into account this non-linear pattern.

The spatial component in the model could not remove all spatial autocorrelation but it enhanced the AIC of the model (-671) compared to the same model not including a spatial component (AIC -640). When plotting residuals against each covariate non linear patterns in the residuals were detected for zooplankton DHA. Thus, a gam was applied to model these non linear patterns by using a smooth term.

### 3.4.2.2 GAM

Family: Beta regression(47.067)  
Link function: logit

Formula:  
s22\_6n3 ~ s(z22\_6n3) + condition + region + Maturity

Parametric coefficients:

Appendix III – Chapter 3

	Estimate	Std. Error	z value	Pr(> z )	
(Intercept)	-0.98704	0.23761	-4.154	3.27e-05	***
condition	-0.37008	0.23287	-1.589	0.1120	
regionw	0.41698	0.06127	6.806	1.01e-11	***
Maturity <span>mature</span>	-0.15814	0.05767	-2.742	0.0061	**

---  
 Signif. codes: 0 '\*\*\*' 0.001 '\*\*' 0.01 '\*' 0.05 '.' 0.1 ' ' 1

Approximate significance of smooth terms:

	edf	Ref.df	Chi.sq	p-value
s(z22_6n3)	1	1	0.847	0.358

R-sq.(adj) = 0.272    Deviance explained = 28.9%  
 -REML = -321.81    Scale est. = 1                    n = 233

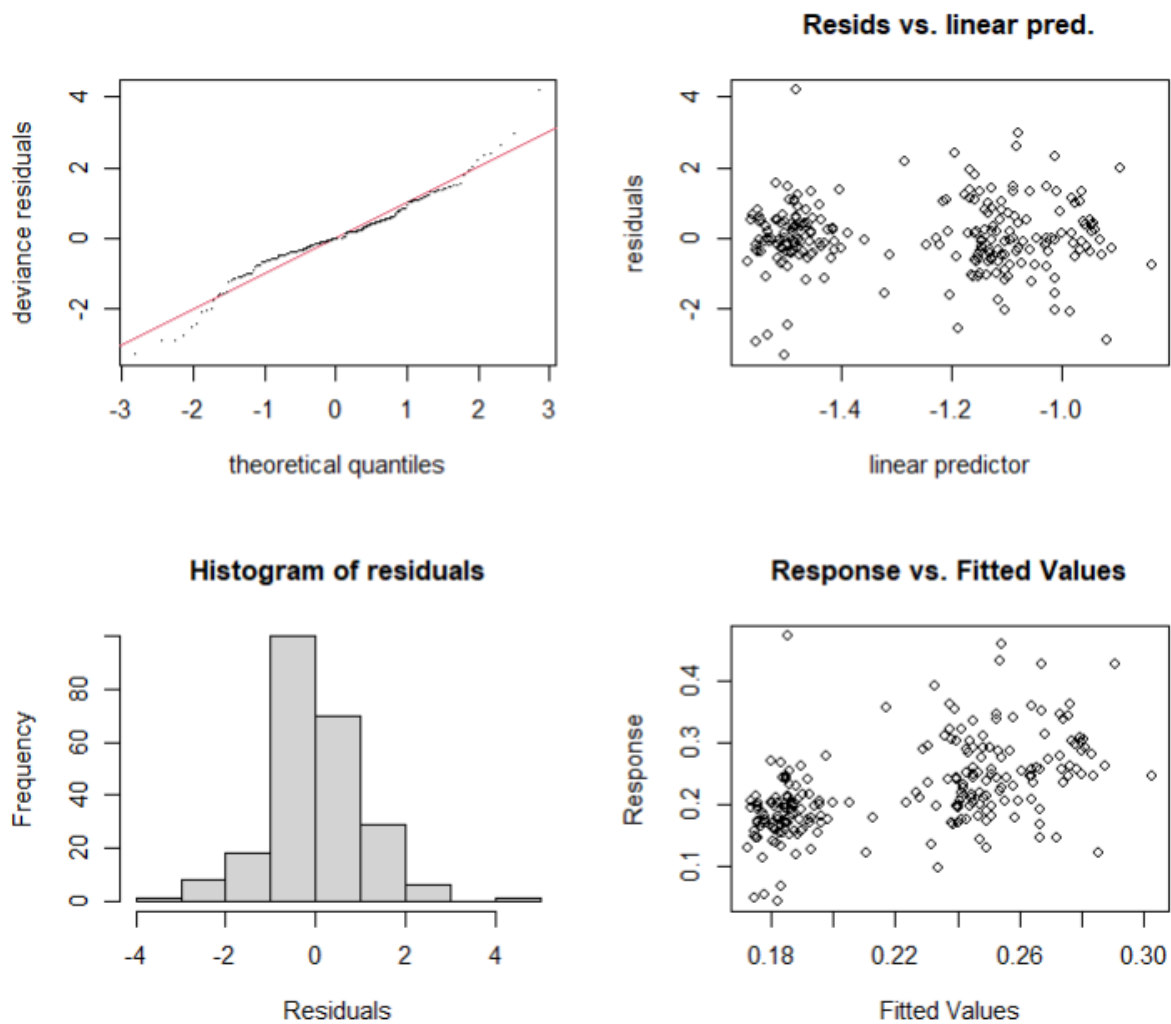


**Figure A 39 Convergence plots for GAM on DHA.** The first panel showcases a Q-Q plot, comparing model residuals to a normal distribution. A well-fitted model will exhibit residuals that closely align with a straight line. In the bottom left panel, a histogram of residuals is presented, expected to have a symmetrical bell shape. The top-right panel displays residuals values, which ideally should be evenly distributed around zero. The final panel in the bottom right shows the response versus fitted values, where a perfect model would yield a straight line.

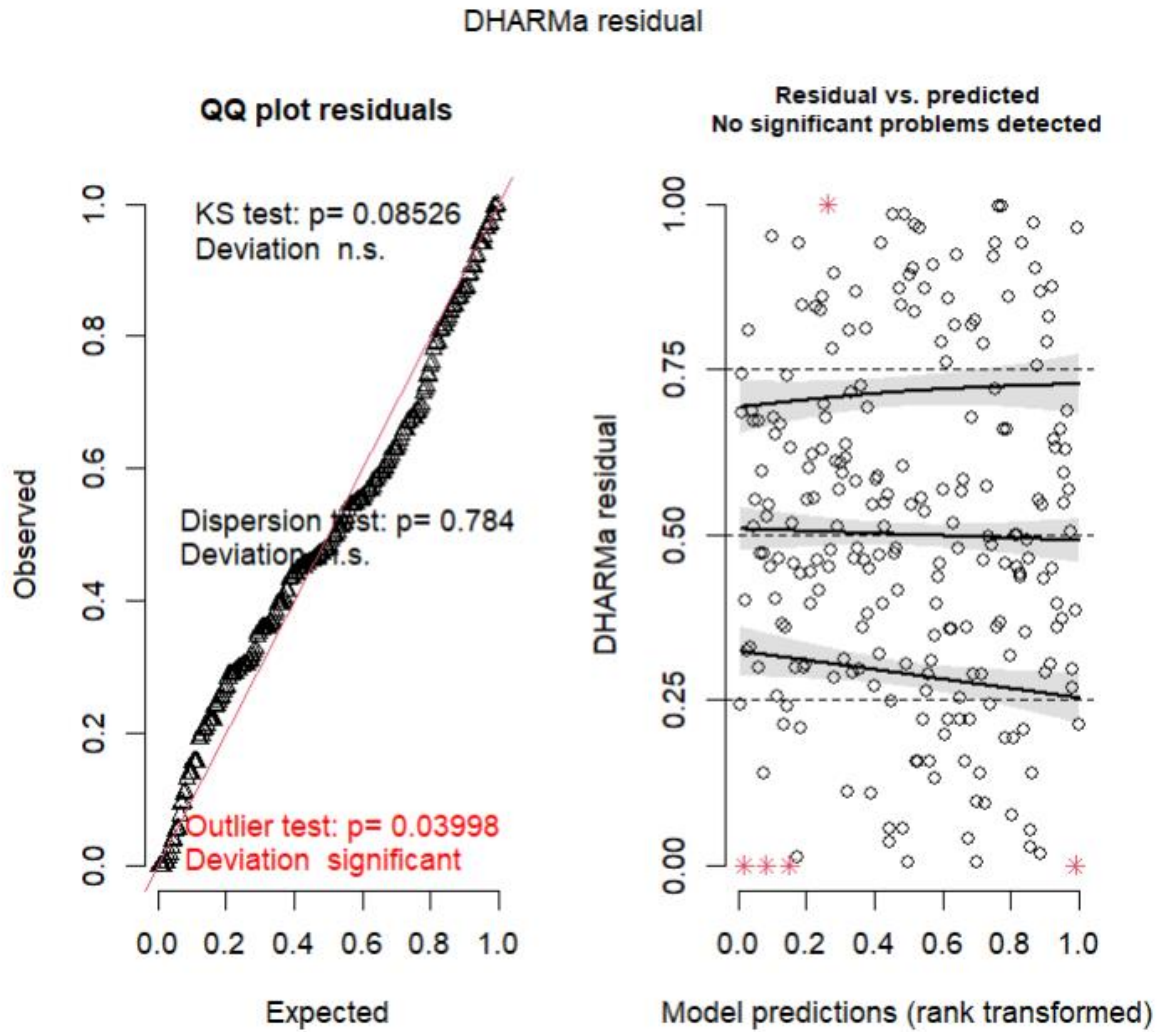
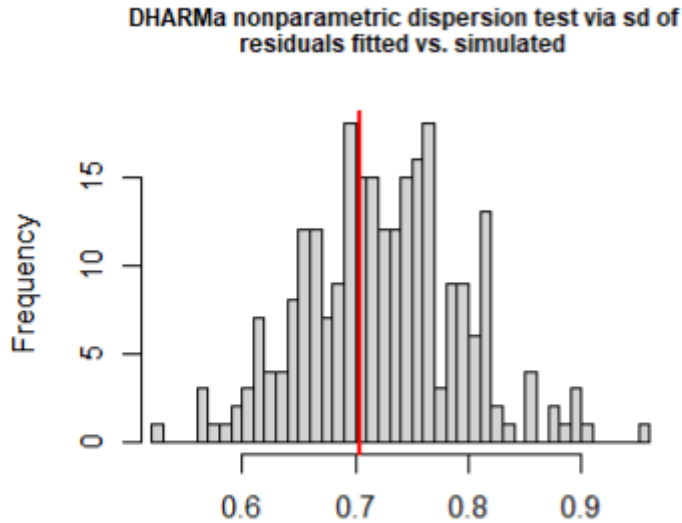


**Figure A 40 DHA GAM verification using the DHARMA package.** The plot function of the package allows to calculate an quantile regression, which compares the empirical 0.25, 0.5 and 0.75 quantiles with the theoretical 0.25, 0.5 and 0.75 quantiles (dashed black line), and provides a p-value for the deviation from the expected quantile. Red color indicates a significant deviation from the expected quantile. Left: qq-plot to detect deviations from expected distribution, with added tests for correct distribution (KS test), dispersion and outliers. Right: Residuals against predicted values.



ulated values, red line = fitted model. p-value (two.sided)

**Figure A 41 DHA GAM test for over/underdispersion.** If fitted model (red line), is among simulated values no over- or underdispersion is present.

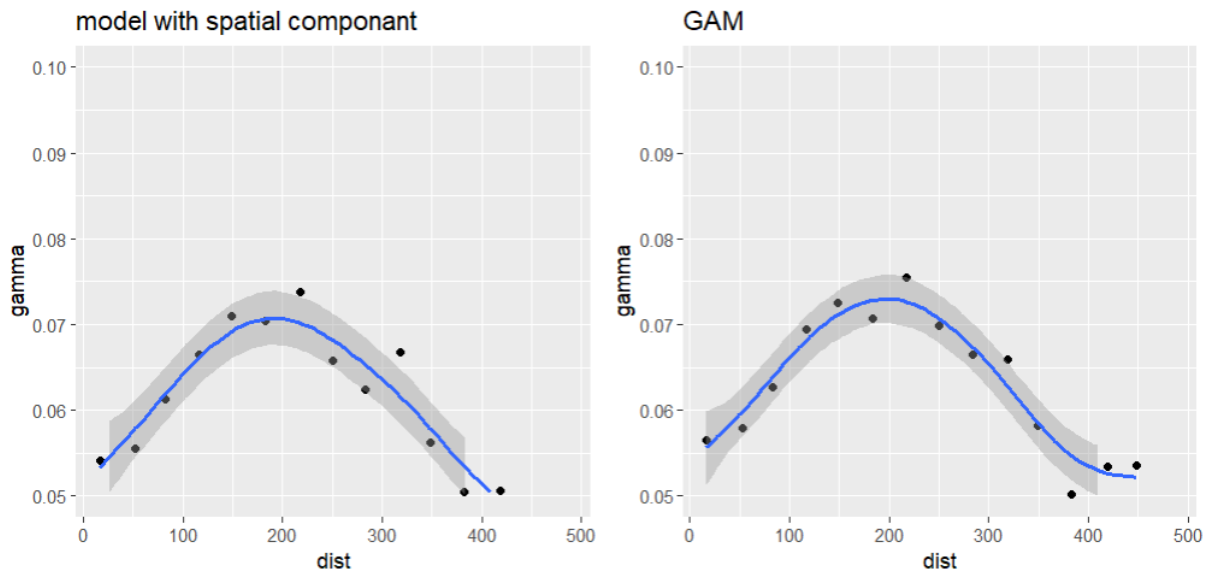


**Figure A 42 Variogram DHA GAM.** To evaluate spatial autocorrelation in the model residuals, variograms were created based on residuals of a GLMM (left) accounting for spatial autocorrelation in the model and on residuals of the GAM (right) not accounting for spatial autocorrelation in the model.

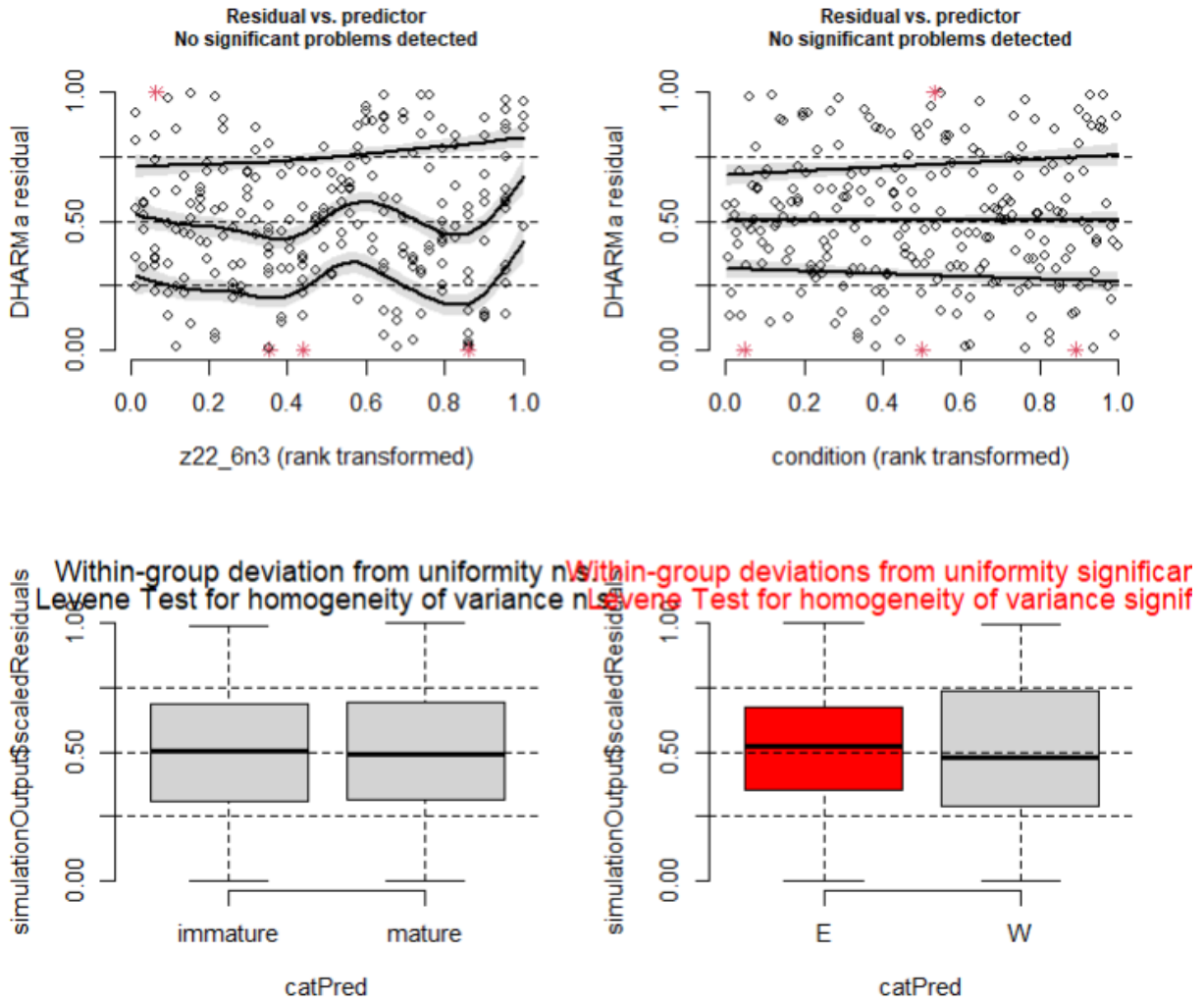


Figure A 43 DHA GAM - Quantile residuals fitted against each covariate. Is second quantile is colored red, a non linear trend was detected and a GAM will be applied in a next step to take into account this non-linear pattern.



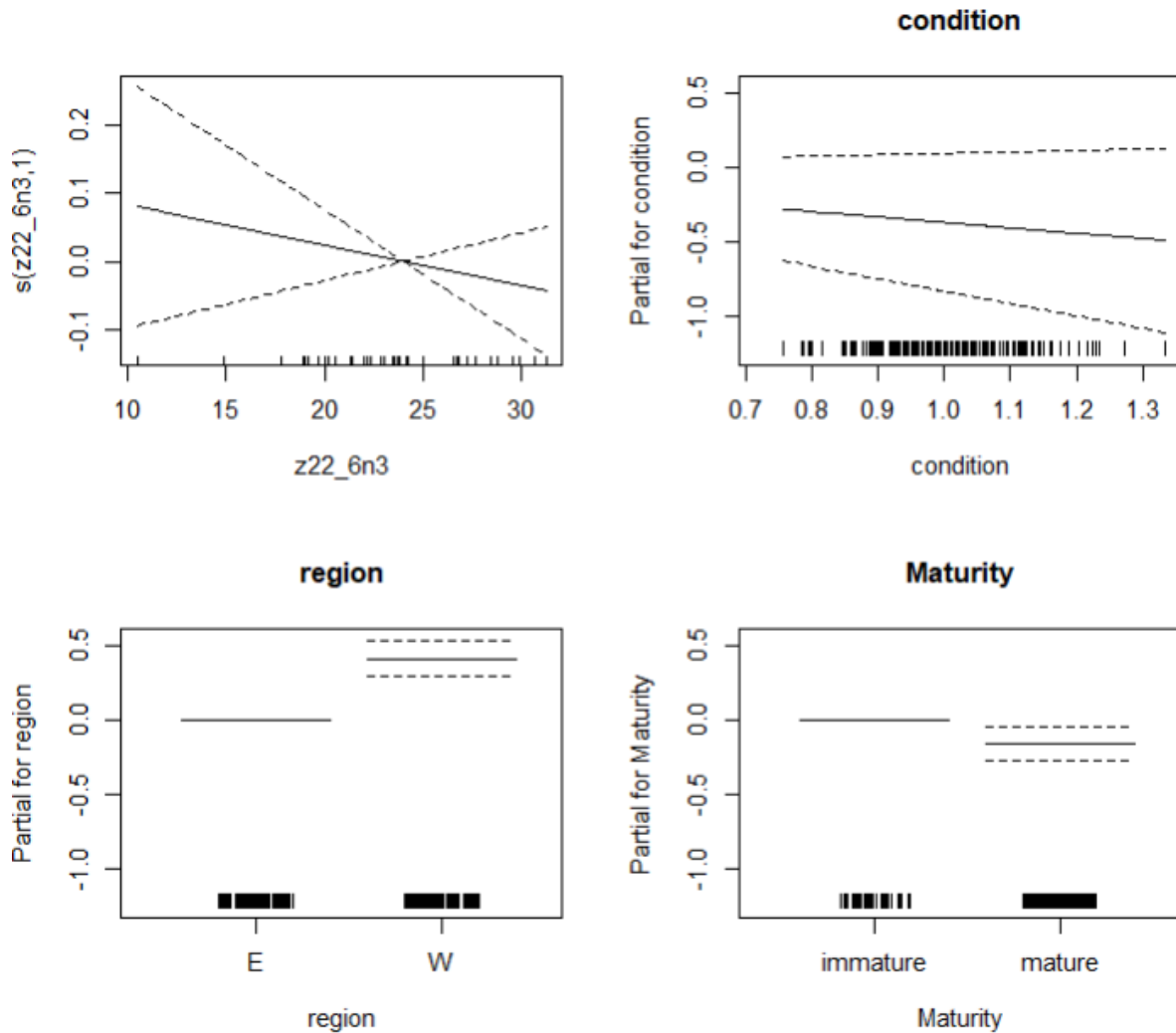


Figure A 44 Model prediction per covariate for DHA (GAM).

### 3.4.2.3 Conclusion model DHA

AIC of glmm with spatial component (modelDHA), glmm without spatial component (modelDHA\_V) and of gam (gamDHA):

	df	AIC
modelDHA	8.000000	-671.6912
modelDHA_V	6.000000	-640.3781
gamDHA	6.000415	-651.8730

As the relationship of sardine and zooplankton DHA in the GAM model turned out to be linear (edf = 1), and the glmm taking into account spatial autocorrelation had a smaller AIC the glmm (modelDHA) was chosen as the most appropriate model.

### 3.4.3 ARA

#### 3.4.3.1 GLMM

Family: beta ( logit )

Formula: s20\_4n6 ~ z20\_4n6 + condition + region + Maturity

Data: dat\_transformed

AIC	BIC	logLik	deviance	df.resid
-2075.5	-2054.8	1043.7	-2087.5	227

Dispersion parameter for beta family (): 1.5e+03

Conditional model:

	Estimate	Std. Error	z value	Pr(> z )	
(Intercept)	-4.26261	0.16762	-25.430	< 2e-16	***
z20_4n6	0.17162	0.04037	4.251	2.13e-05	***
condition	-0.03625	0.15771	-0.230	0.818225	
regionw	-0.14545	0.04304	-3.380	0.000726	***
Maturity <span>mature</span>	-0.29070	0.03977	-7.310	2.67e-13	***

---  
 Signif. codes: 0 '\*\*\*' 0.001 '\*\*' 0.01 '\*' 0.05 '.' 0.1 ' ' 1

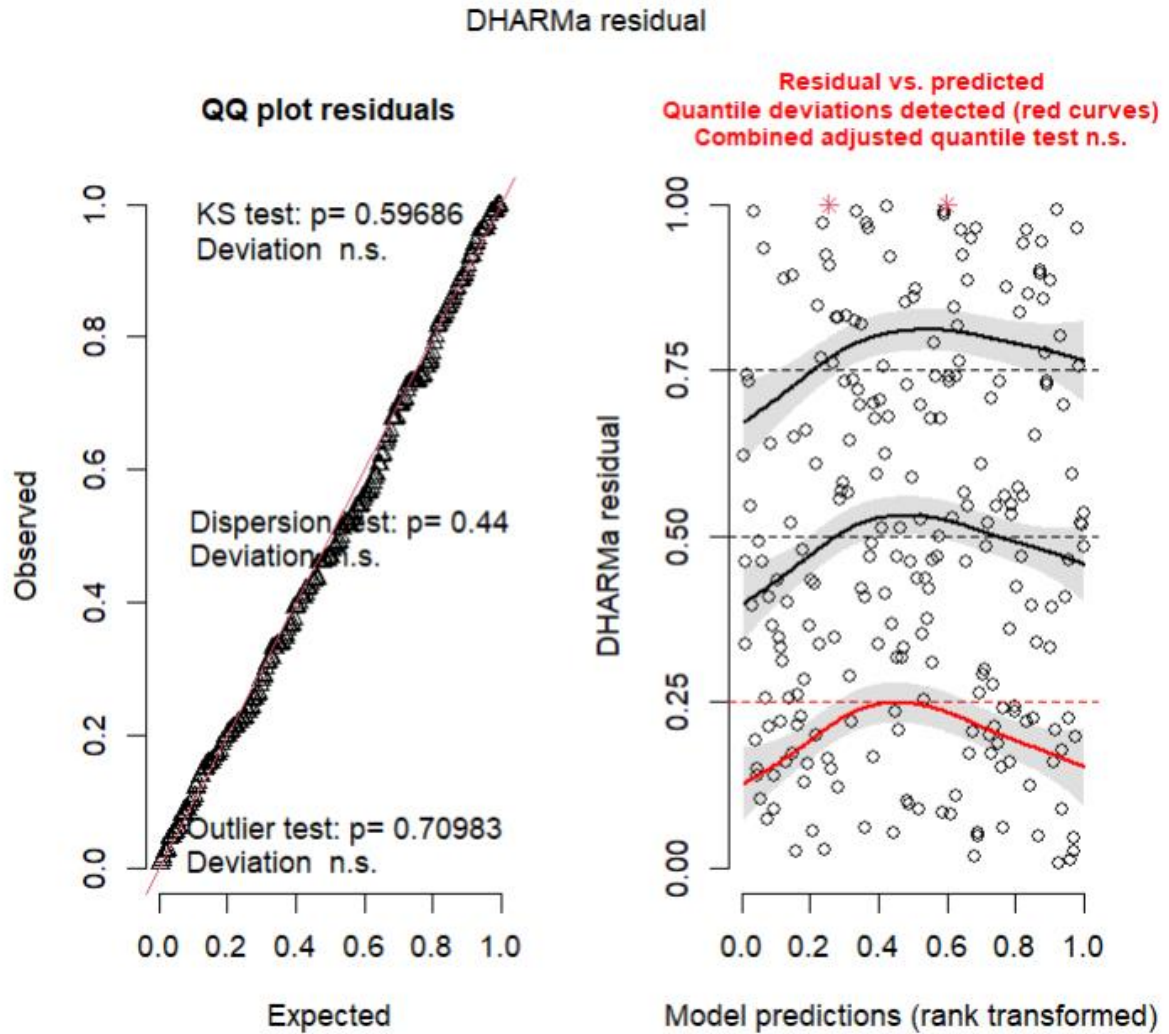


**Figure A 45 ARA GLMM verification using the DHARMA package.** The plot function of the package allows to calculate an quantile regression, which compares the empirical 0.25, 0.5 and 0.75 quantiles with the theoretical 0.25, 0.5 and 0.75 quantiles (dashed black line), and provides a p-value for the deviation from the expected quantile. Red color indicates a significant deviation from the expected quantile. Left: qq-plot to detect deviations from expected distribution, with added tests for correct distribution (KS test), dispersion and outliers. Right: Residuals against predicted values.

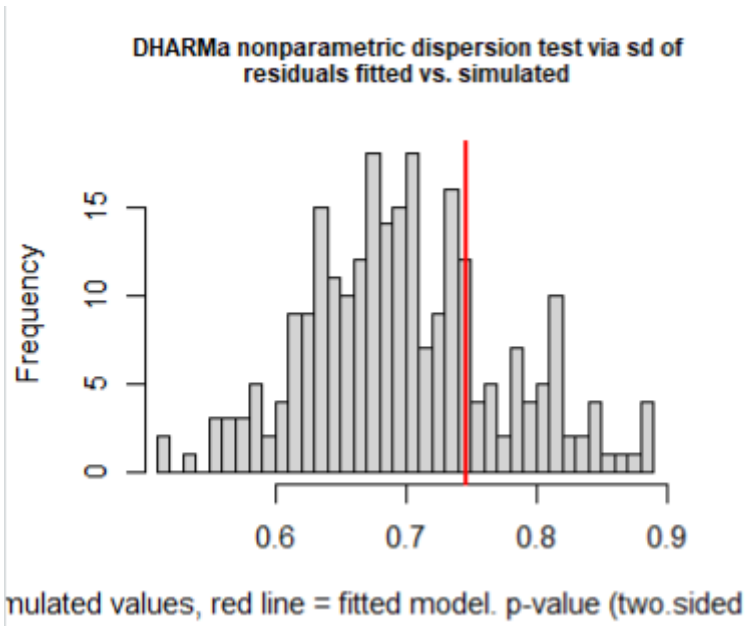


**Figure A 46 ARA GLMM test for over/underdispersion.** If fitted model (red line), is among simulated values no over- or underdispersion is present.

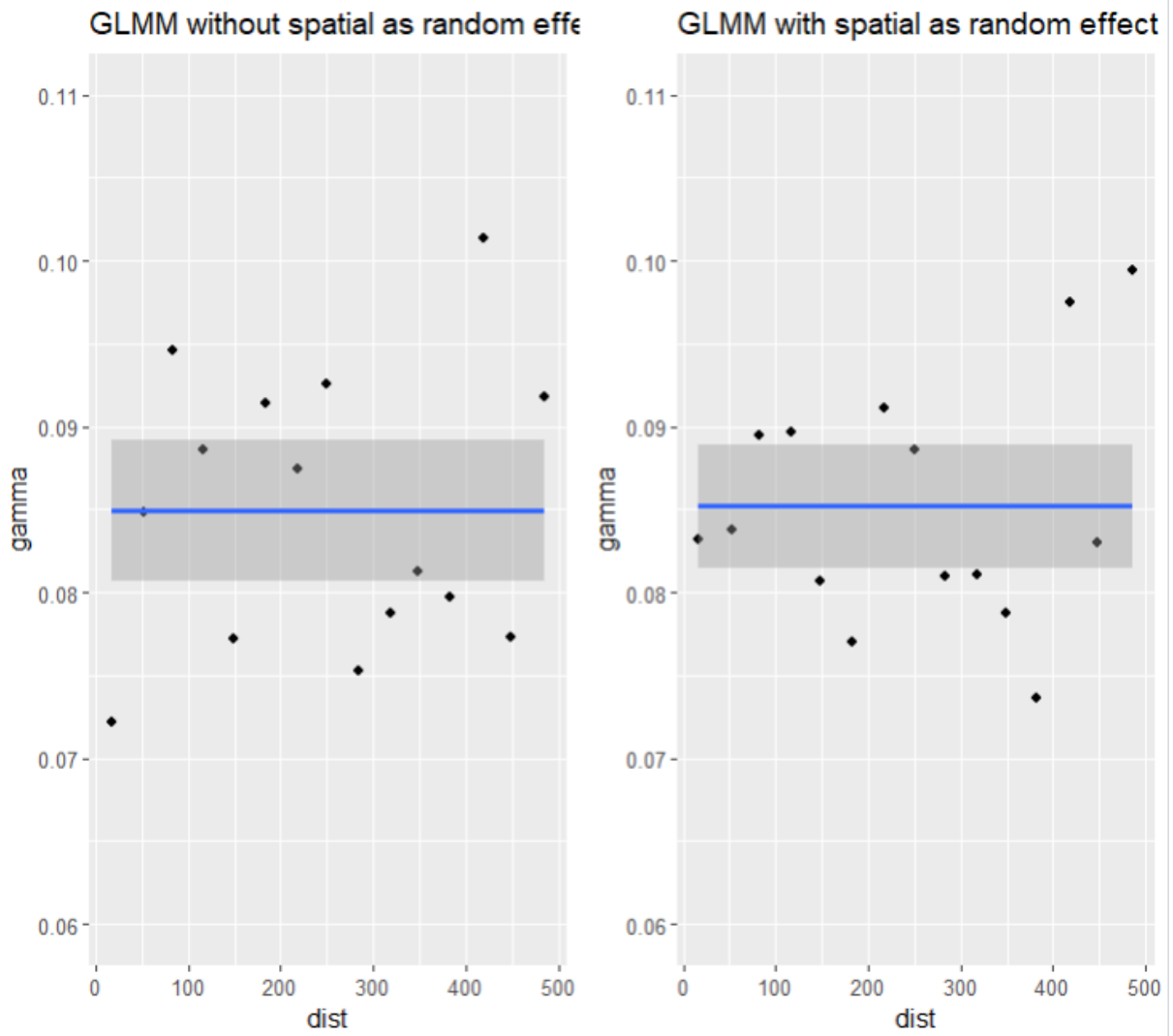


**Figure A 47 Variogram ARA GLMM.** To evaluate spatial autocorrelation in the model residuals, variograms were created based on residuals of a GLMM (left) not accounting for spatial autocorrelation in the model and on residuals of the GLMM (right) accounting for spatial autocorrelation in the model.

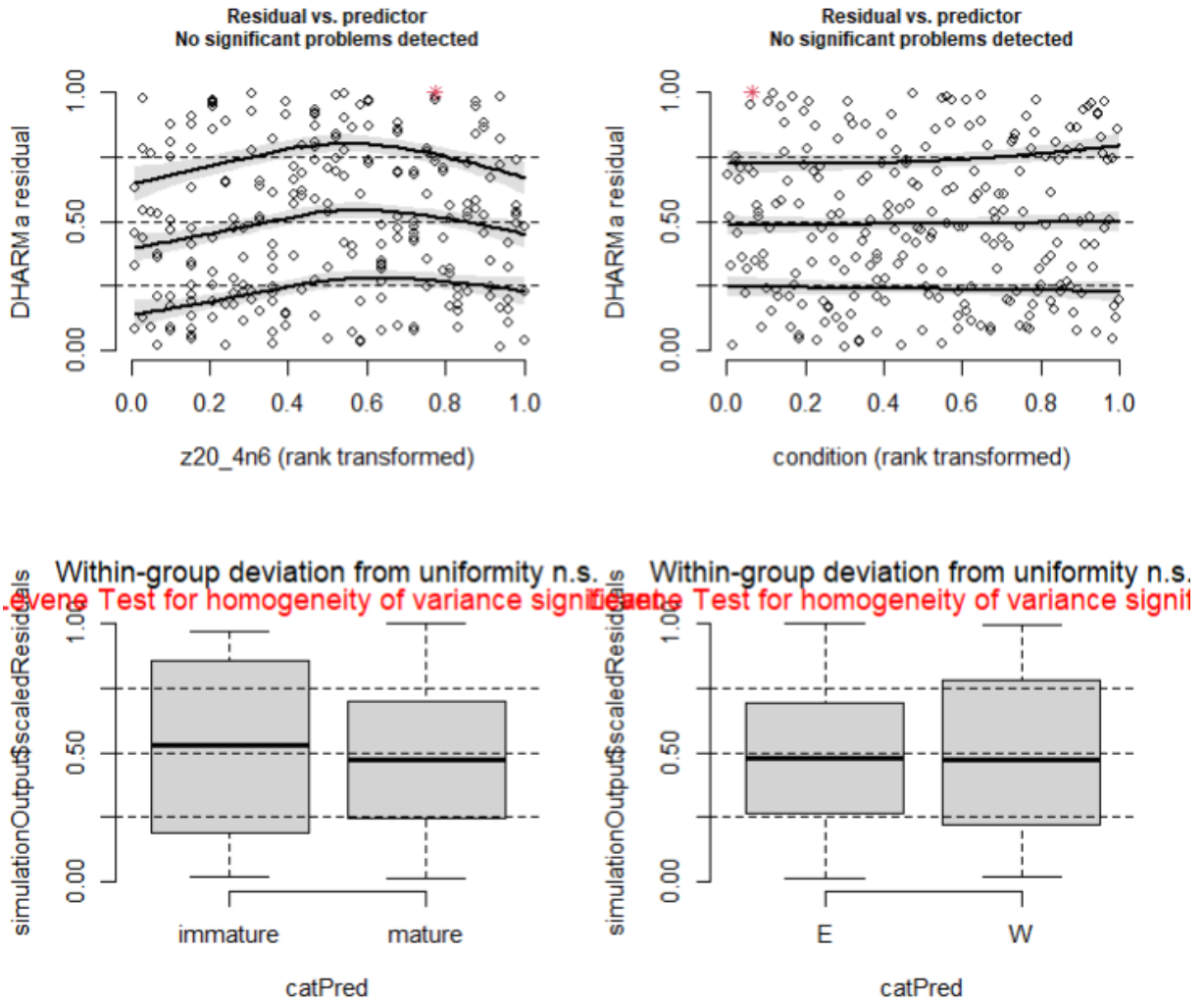


**Figure A 48 ARA GLMM - Quantile residuals fitted against each covariate.** Is second quantile is colored red, a non linear trend was detected and a GAM will be applied in a next step to take into account this non-linear pattern.

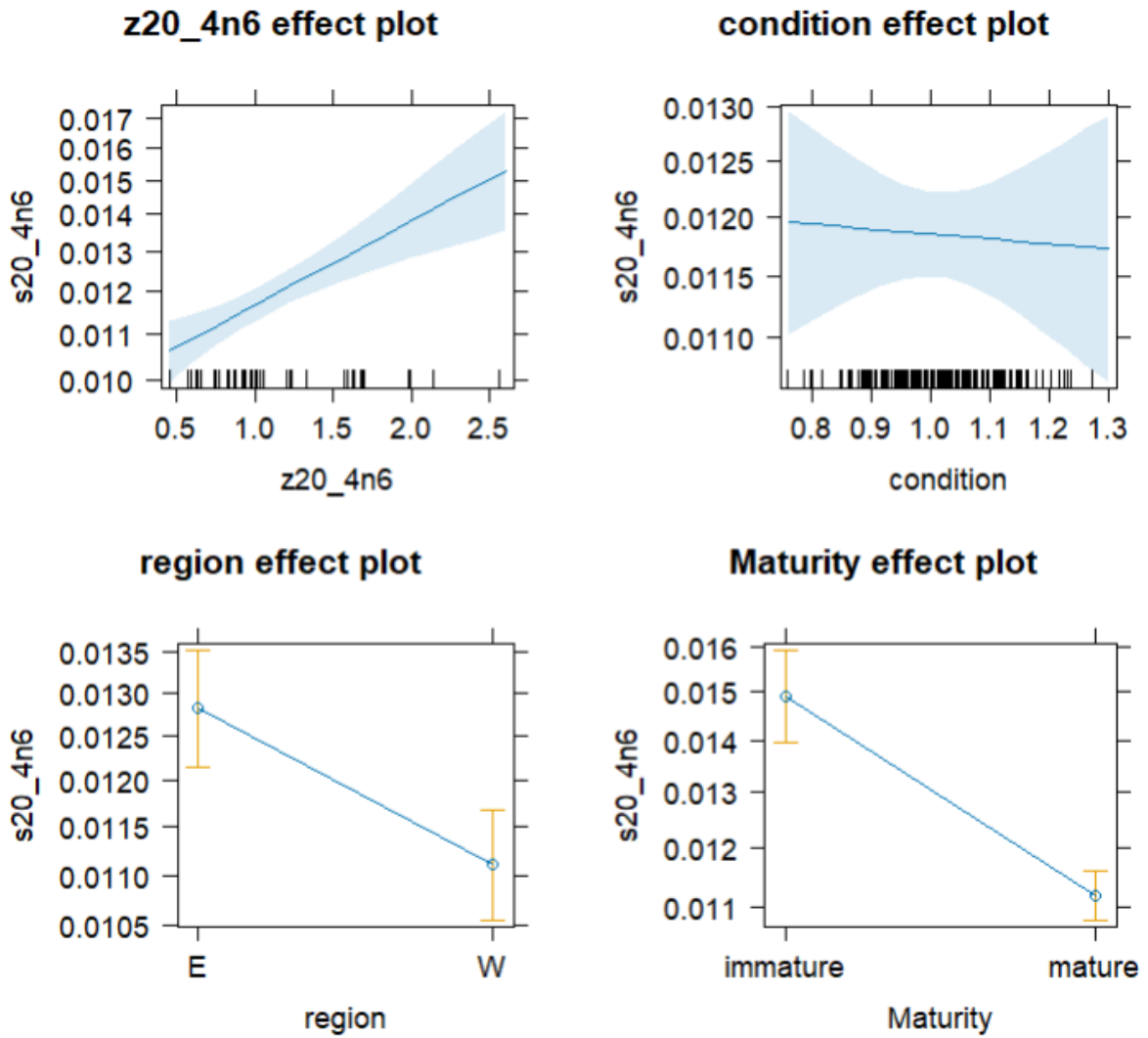
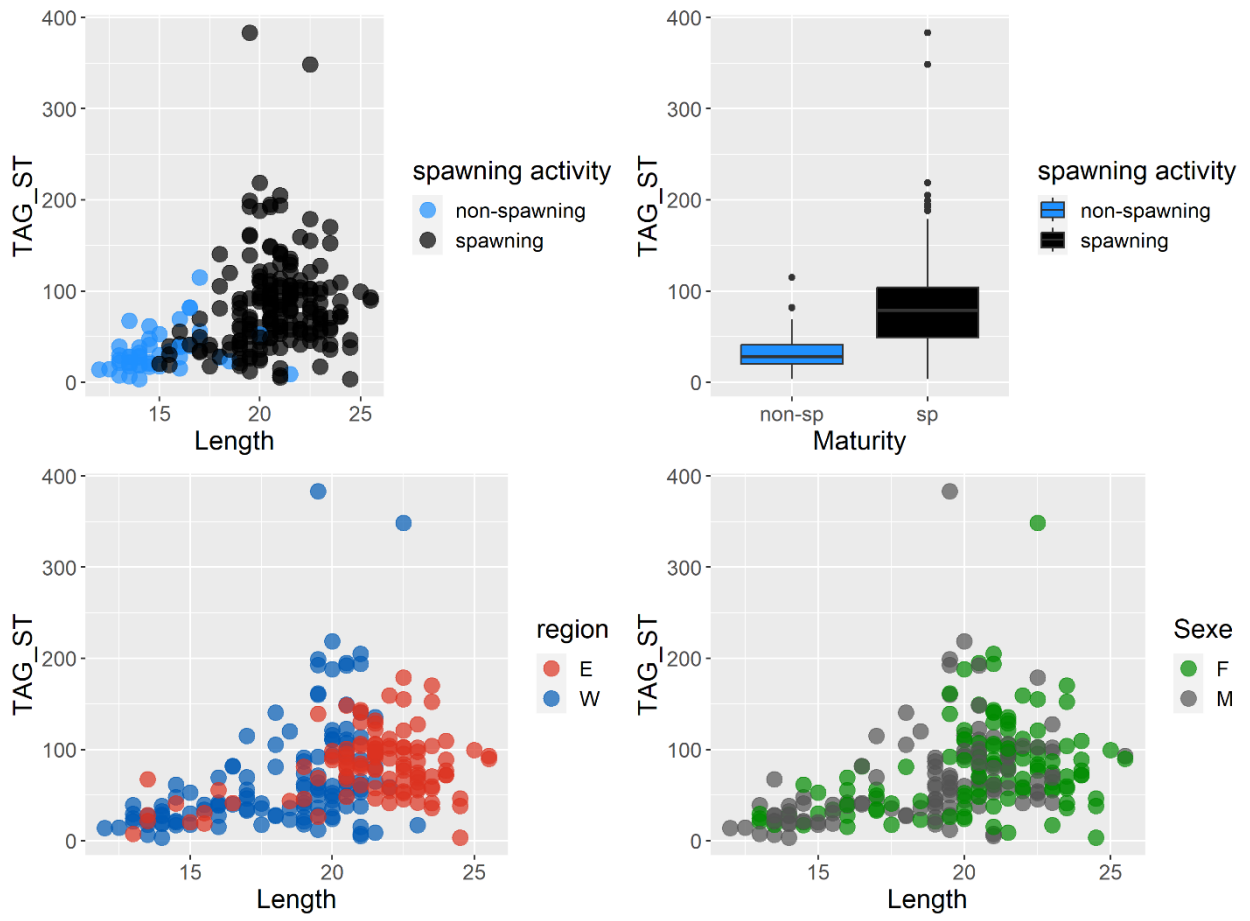


Figure A 49 Model prediction per covariate for ARA (GLMM).

### 3.4.3.2 Conclusion model ARA

As the variograms of a glmm with a spatial component and without did not indicate spatial autocorrelation, the glmm without a spatial component as random effect was chosen. As no non-linear relationships between sardine ARA and the covariates was found in the residuals a glmm without spatial component as random effect was chosen.



**Figure A 50** Correlation between spawning activity, TAG-ST ratio, length and region. Points represent sardine individuals.



Appendix III – Chapter 3

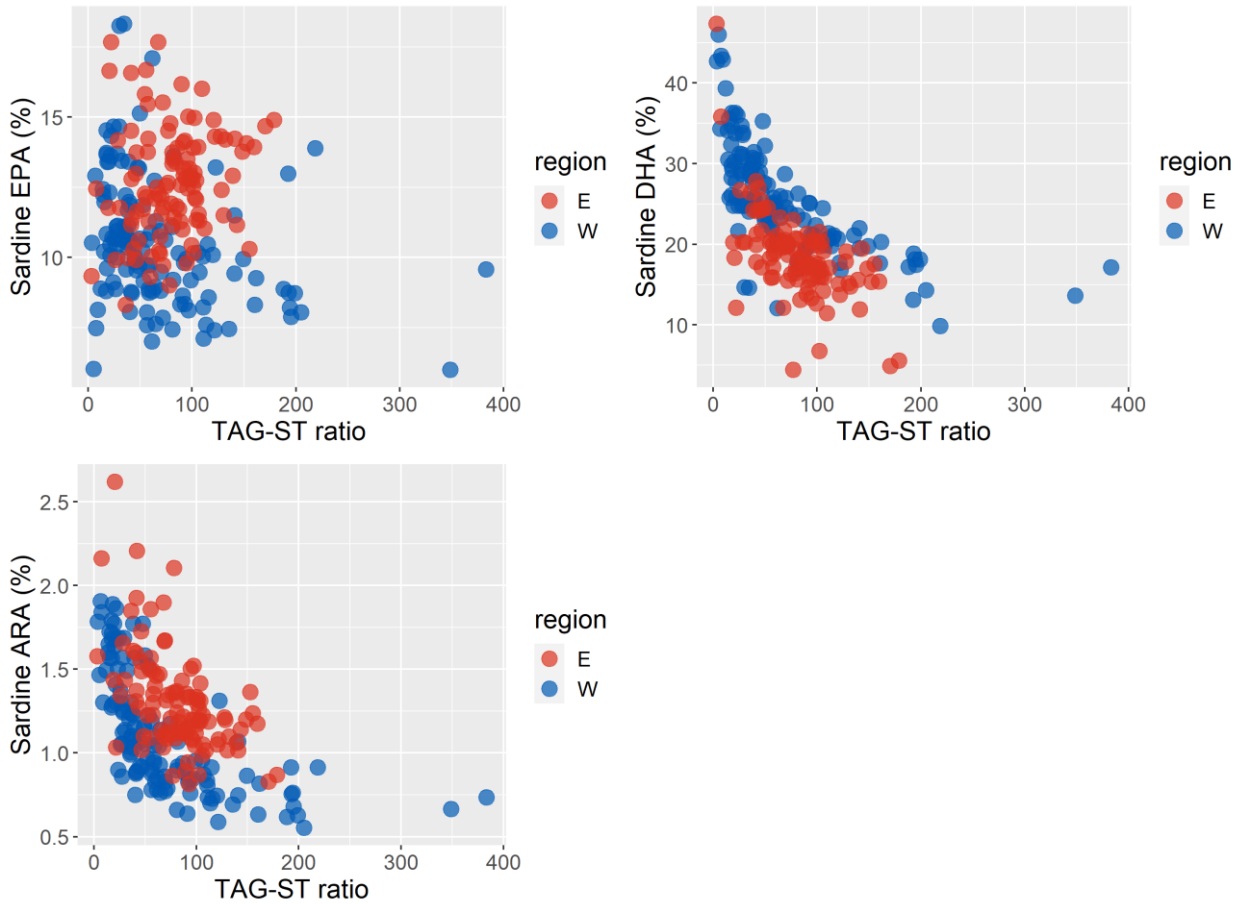


**Figure A 51** Relation between sardines EFA and TAG-ST ratio. Colors indicate western or eastern English Channel.

**Table A 7** Factors influencing trophic transfer including sex. Estimates indicate significant and non-significant positive or negative correlation between a covariate and the proportion of the respective FA in sardine. Significance: \*\*\* ( $P < 0.001$ ), \*\* ( $P < 0.01$ ), \* ( $P < 0.05$ ). Type indicates the type of model used. N indicates the number of sampling stations used in the model. (s) indicate the parameters not displaying a linear relationship and thus integrated in the model with a spatial smoother.

Fatty acid	Intercept	Estimates					type	N
		zooplankton FA	Le Cren's index	spawning	region	sex		
EPA	-1.98483	(s)***	0.23373*	-0.25823***	-0.18878***	0.01947	GAM	233
DHA	1.0145	(s)	-0.37257	-0.15466**	0.40958***	0.06258	GAM	233
ARA	-4.29442	0.17503***	-0.03282	-0.28696***	-0.14667***	0.0448	GLMM	234

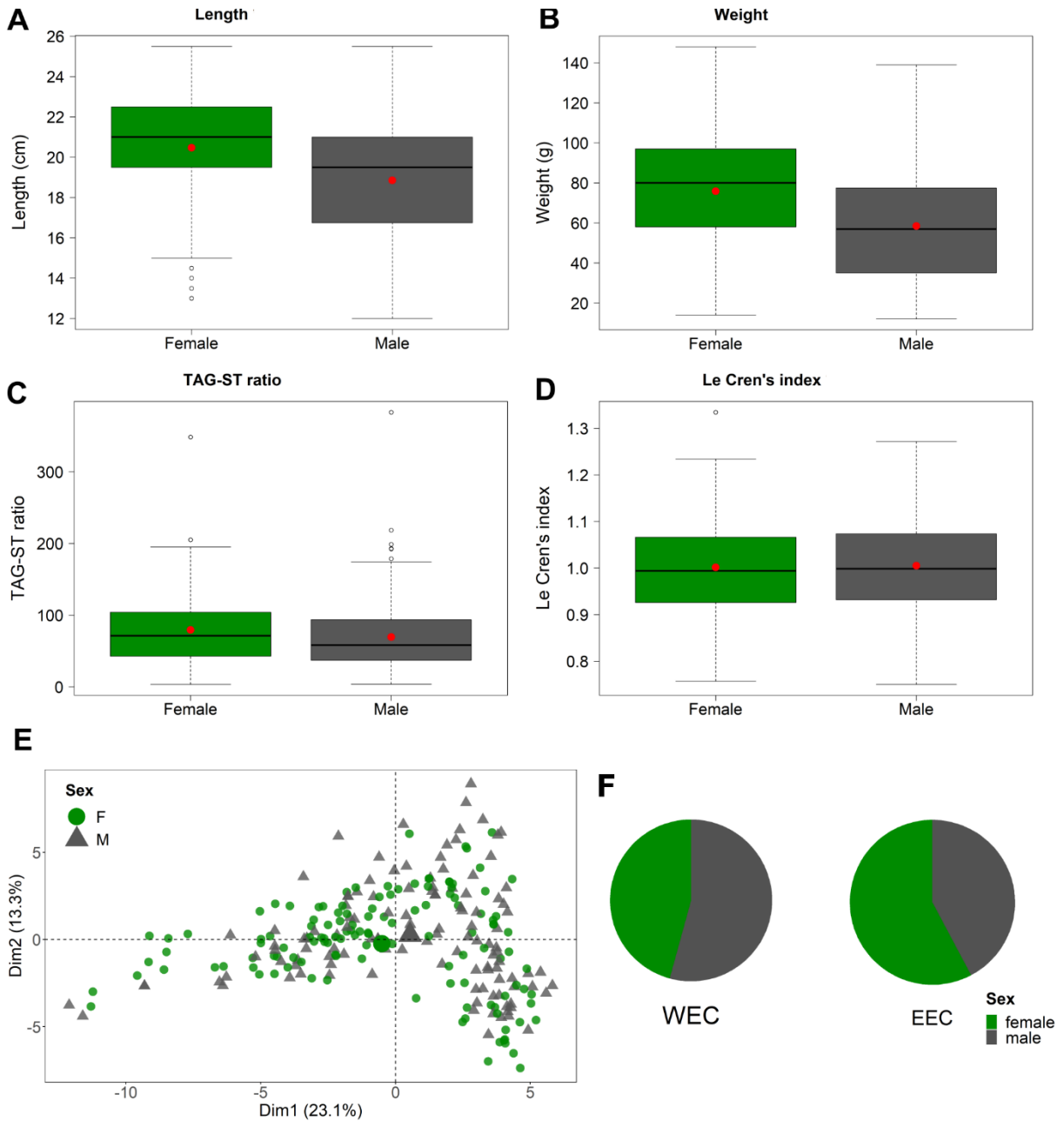


**Figure A 52 Differences of biological parameters of sardine between sex.** A: Comparison of length between sex. Red dots indicate mean independent of region; B: Comparison of weight between sex. Red dots indicate mean independent of region; C: Comparison of TAG-ST ratio between sex independent of region; D: Comparison of Le Cren's index between sex independent of region. E: PCA on FA of females (green dots) and males (gray triangle); F: Proportion of females and males per region.

### 3.5 Principal Component Analysis Zooplankton (PCA)

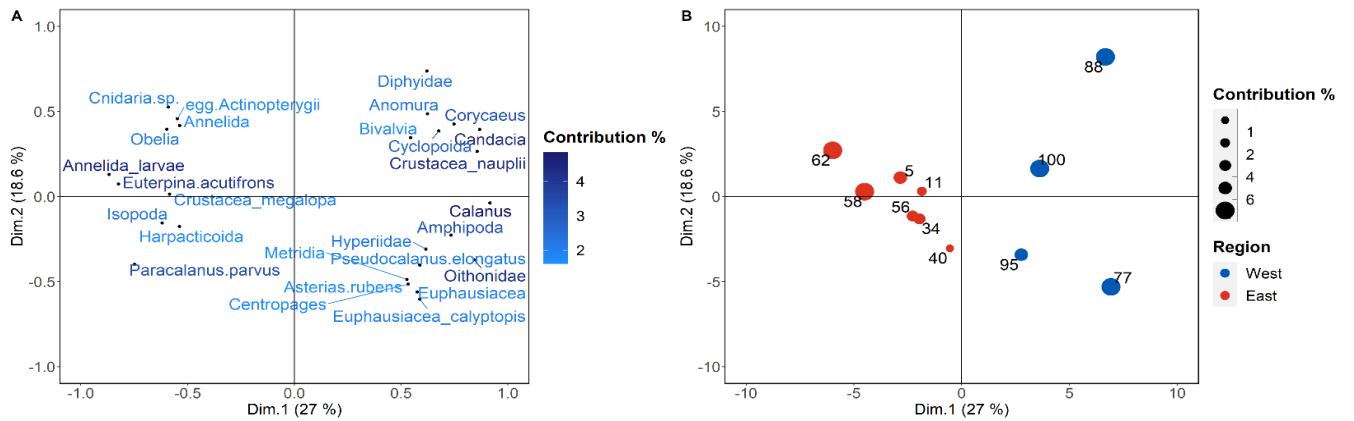


**Figure A 53 PCA taxonomic composition zooplankton (entire size spectrum sampled: 300 – 1000+  $\mu\text{m}$ ).** A: Taxa displayed in two-dimensional space of first and second principal component. The darker the taxon, the higher its contribution to the first component. Displayed are all taxa with a higher contribution than 1.5%; B: Sampling stations displayed in a two-dimensional space of first and second principal component. The bigger the dot the higher its contribution to the first component. Blue dots were located in the WEC, red dots in the EEC. Numbers represent sampling station id.

### 3.6 Complete FA profiles of zooplankton and sardine

**Table A 8 Lipids and fatty acids (FA) in sardine.** Values are reported as mean  $\pm$  standard deviation by region (Eastern English Channel, Western English Channel). n corresponds to the individuals sampled per region.

	%	
	WEST n = 129 mean $\pm$ S.D.	EAST n = 117 mean $\pm$ S.D.
<b>Saturated FA</b>		
iso15:0	0.13 $\pm$ 0.09	0.01 $\pm$ 0.03
iso17:0	0.26 $\pm$ 0.10	0.25 $\pm$ 0.14
14:0	3.69 $\pm$ 0.95	3.88 $\pm$ 1.07
15:0	0.60 $\pm$ 0.12	0.55 $\pm$ 0.14
16:0	20.88 $\pm$ 2.11	21.54 $\pm$ 1.24
17:0	0.63 $\pm$ 0.11	0.53 $\pm$ 0.17
18:0	4.95 $\pm$ 0.61	5.97 $\pm$ 0.80
20:0	0.28 $\pm$ 0.14	0.51 $\pm$ 0.28
22:0	0.20 $\pm$ 0.17	0.24 $\pm$ 0.19
<b>Monounsaturated FA</b>		
16:1n-10	0.55 $\pm$ 0.16	0.40 $\pm$ 0.20
<b>Continued</b>		
	%	
	WEST	EAST

Appendix III – Chapter 3

16:1n-9	0.32± 0.10	0.40± 0.10
16:1n-7	3.72± 0.99	5.08± 1.37
16:1n-5	0.22± 0.09	0.07± 0.09
17:1n-7	0.12± 0.12	0.05± 0.09
18:1n-9	7.92± 3.19	11.45± 2.92
18:1n-7	2.35± 0.54	3.25± 0.59
18:1n-5	0.23± 0.16	0.03± 0.07
20:1n-11	0.31± 0.19	0.08± 0.05
20:1n-9	2.05± 1.21	1.70± 0.49
20:1n-7	0.21± 0.12	0.31± 0.17
22:1n-11	1.92± 1.58	0.11± 0.20
22:1n-9	0.52± 0.23	0.52± 0.32
24:1n-9	0.83± 0.27	0.65± 0.17
<b>Polyunsaturated FA</b>		
16:2n-4	0.23± 0.17	0.38± 0.26
16:3n-4	0.12± 0.17	0.37± 0.30
16:4n-1	0.24± 0.29	0.54± 0.42
18:2n-7	0.05± 0.14	0.37± 0.30
18:2n-6	1.23± 0.38	0.59± 0.20
18:2n-4	0.04± 0.08	0.13± 0.14
18:3n-6	0.06± 0.09	0.04± 0.08
18:3n-4	0.04± 0.08	0.02± 0.08
18:3n-3	1.12± 0.32	0.72± 0.26
18:4n-3	2.13± 0.56	1.58± 0.46
20:2	0.09± 0.17	0.51± 0.30
20:2n-6	0.33± 0.11	0.15± 0.12
20:4n-6	1.11± 0.35	1.33± 0.34
20:3n-3	0.18± 0.11	0.06± 0.09
20:4n-3	0.95± 0.24	0.80± 0.15
20:5n-3	10.49± 2.29	12.70± 1.94
21:5n-3	0.38± 0.11	0.49± 0.13
22:4n-6	0.23± 0.16	0.25± 0.20
22:5n-6	0.57± 0.17	0.50± 0.20
22:5n-3	1.42± 0.24	1.73± 0.28
22:6n-3	25.65± 6.77	18.85± 5.33
18:0dma	0.09± 0.14	0.00± 0.01
Total SFA	31.56± 0.91	33.49± 0.91
Total MUFA	21.43± 3.30	24.07± 2.51
Total PUFA	46.34± 3.69	41.75± 2.46
Total PUFA w/ 16C	0.57± 0.28	1.28± 0.52
<b>Continued</b>		
	%	
	WEST	EAST

Appendix III – Chapter 3

Total PUFA n-3	41.30± 3.71	36.13± 2.48
Total PUFA n-6	3.55± 0.31	2.88± 0.46
n-3/n-6	11.67± 0.77	12.79± 1.66
DHA / EPA	2.57± 0.51	1.52± 0.37

**Table A 9 Lipids and fatty acids (FA) in mesozooplankton (500-1000 µm).** Values are reported as mean ± standard deviation by region (Eastern English Channel, Western English Channel).

	%			
	West n = 20		East n = 19	
	mean	± S.D.	mean	± S.D.
<b>Saturated FA</b>				
iso15:0	0.28	± 0.04	0.25	± 0.07
iso17:0	0.31	± 0.09	0.56	± 0.11
14:0	6.67	± 2.30	4.58	± 1.88
15:0	0.69	± 0.11	0.76	± 0.19
16:0	15.96	± 1.01	15.63	± 1.25
17:0	0.82	± 0.14	1.01	± 0.24
18:0	3.55	± 1.12	5.23	± 1.00
20:0	0.24	± 0.13	0.26	± 0.13
22:0	0.11	± 0.03	0.18	± 0.10
<b>Monounsaturated FA</b>				
16:1n-7	3.61	± 0.99	5.36	± 1.52
16:1n-5	0.35	± 0.08	0.24	± 0.07
17:1n-7	0.54	± 0.51	0.23	± 0.24
18:1n-9	4.26	± 1.30	3.34	± 1.34
18:1n-7	1.32	± 0.49	3.03	± 1.28
18:1n-5	0.16	± 0.03	0.18	± 0.10
20:1n-11	0.14	± 0.05	0.46	± 0.42
20:1n-9	0.79	± 0.53	0.31	± 0.19
20:1n-7	0.10	± 0.08	0.29	± 0.16
22:1n-11	1.84	± 1.57	0.10	± 0.06
22:1n-9	0.20	± 0.10	0.11	± 0.10
22:1n-7	0.06	± 0.06	0.13	± 0.10
24:1n-9	0.54	± 0.13	0.40	± 0.20
<b>Continued</b>				

	West	East	
<b>Polyunsaturated FA</b>			

Appendix III – Chapter 3

16:2n-7	0.06 ± 0.06	0.11 ± 0.11
16:2n-4	0.41 ± 0.18	0.68 ± 0.51
16:3n-4	0.24 ± 0.13	0.73 ± 0.73
16:4n-3	0.33 ± 0.08	0.21 ± 0.11
16:4n-1	0.68 ± 0.25	1.37 ± 0.65
18:2n-6	1.91 ± 0.59	0.89 ± 0.17
18:2n-4	0.07 ± 0.06	0.22 ± 0.11
18:3n-6	0.11 ± 0.08	0.11 ± 0.08
18:3n-3	1.15 ± 0.83	1.19 ± 0.63
18:4n-3	4.65 ± 2.21	2.66 ± 1.26
18:5n-3	0.27 ± 0.17	0.08 ± 0.10
20:2n-6	0.33 ± 0.10	0.30 ± 0.13
20:4n-6	0.85 ± 0.34	1.47 ± 0.42
20:3n-3	0.46 ± 0.17	0.30 ± 0.09
20:4n-3	0.75 ± 0.21	0.44 ± 0.07
20:5n-3	16.08 ± 2.43	20.95 ± 2.15
21:5n-3	0.47 ± 0.08	0.52 ± 0.14
22:4n-6	0.13 ± 0.10	0.23 ± 0.14
22:5n-6	0.65 ± 0.14	0.65 ± 0.10
22:5n-3	0.72 ± 0.07	0.99 ± 0.25
22:6n-3	25.76 ± 3.72	20.82 ± 3.40
Total SFA	28.63 ± 1.24	28.46 ± 1.94
Total MUFA	13.90 ± 2.93	14.17 ± 2.80
Total PUFA	56.08 ± 3.26	54.92 ± 2.52
Total PUFA w/ 16C	1.40 ± 0.55	2.89 ± 1.91
Total PUFA n-3	50.64 ± 3.41	48.16 ± 2.89
Total PUFA n-6	3.98 ± 0.62	3.65 ± 0.67
n-3/n-6	13.02 ± 2.04	13.68 ± 2.86
DHA / EPA	1.62 ± 0.24	1.02 ± 0.22

### 3.7 Phytoplankton community

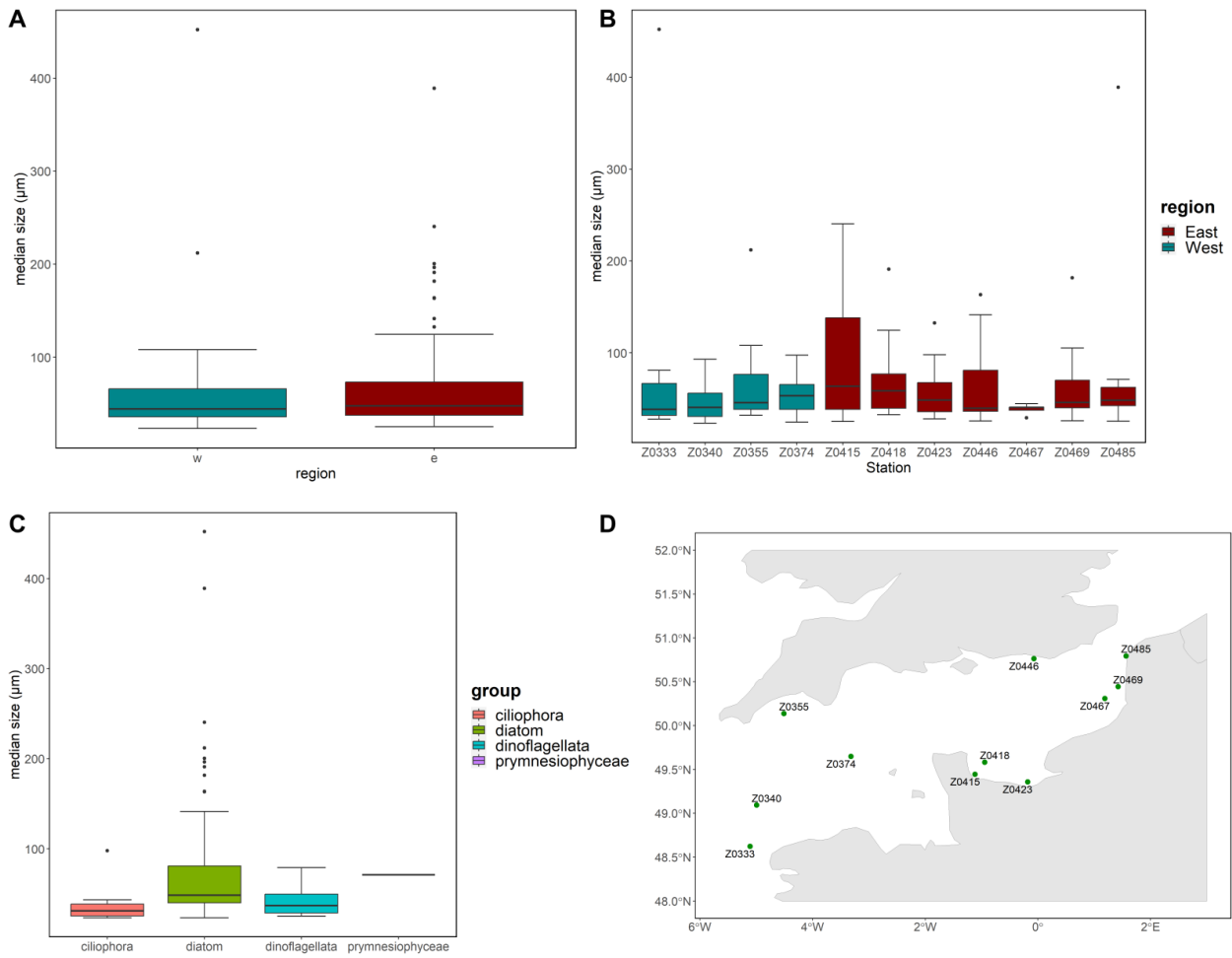


**Figure A 54 Phytoplankton size-structure.** A: Mean median size per basin; B: mean median size per station. Turquoise indicating stations located in the WEC, red indicating locations in EEC; C: mean median size per taxonomic group; D: Location of sampling stations of phytoplankton.

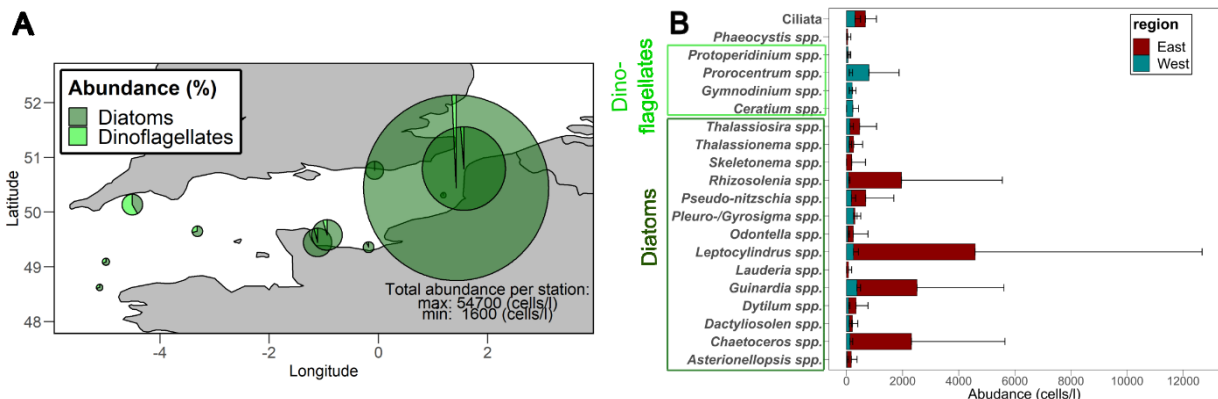


**Figure A 55 Taxonomic composition phytoplankton.** A: Relative abundance and composition of phytoplankton in the EC. Size of pie charts represent abundance in cells/l and colored fractions represent the contribution of diatoms and dinoflagellates to the total abundance collected per station; B: Taxonomic composition and mean abundance with standard deviation per taxa in the WEC (turquoise) and EEC (red). Colored boxes mark taxa belonging to dinoflagellates and diatoms. Colors thereby corresponding to figure A.

## Abstract

Understanding ecosystem functioning is important to predict, manage and protect the ecosystems in which we live and on which we depend. Intending to contribute to a better ecosystem understanding the present thesis focused on zooplankton that play a crucial role in the functioning of marine ecosystems with regard to biogeochemical cycles and trophic transfer. Despite their central role, zooplankton are to-date not adequately represented in ecosystem-models, potentially affecting ecosystem-management. The present thesis explores three different perspectives on zooplankton functioning namely taxonomical composition (chapter 1), size-structure (chapter 2) and biochemical composition (chapter 3) using an integrated approach that considers both lower and higher trophic levels within the context of *Multitrophic Biodiversity Ecosystem Functioning*. Chapter 1 revealed the existence of five zooplankton assemblages in the Southern North Sea and Eastern English Channel (EEC) during winter that varied with regard to productivity, taxa abundance and composition. Assemblage composition and distribution was driven by abiotic (e.g., dissolved nutrients, salinity, depth, temperature) and biotic variables (e.g., phyto- and microplankton composition), including water masses and fish spawning grounds. Chapter 2 revealed a weak size structuration of plankton between 20 and 500  $\mu\text{m}$  regarding their isotopic signature indicating omnivory was the dominant feeding strategy of this plankton size class during winter. Herring (*Clupea harengus*) and plaice (*Pleuronectes platessa*) larvae displayed species-specific isotopic signatures and different prey size preferences. Additionally, spatial differences in prey size composition were observed among plaice larvae sampled at river influenced stations compared to those collected at stations in the center of the EEC. The fatty acid (FA) profile of zooplankton and sardine (*Sardina pilchardus*) differed between the western and the eastern side of the English Channel alongside with differences in the taxonomical composition of phytoplankton and zooplankton, indicating a bottom-up control of the trophic transfer of these essential nutrients. Independent of the perspective, all chapters revealed spatial patterns in ecosystem functioning, as spatial variability in zooplankton characteristics seemed to be related to both lower and higher trophic levels. The combined investigation of zooplankton taxonomy and traits (size and FA composition) in relation to lower and higher trophic levels revealed additional zooplankton characteristics related to trophic strategy, reproduction and survival further connecting zooplankton to ecosystem functioning. Thus, investigating zooplankton in a multitrophic context considering different aspects of their



diversity contributed to a more mechanistic understanding of zooplankton as part of, and in relation to the ecosystem. It further facilitated the development of hypotheses to explain the observed patterns and relationships. Consequently, the approach used in the present study appears promising to acquire information needed to enhance the representation of zooplankton in ecosystem models and ecosystem-based management.

## Résumé

La compréhension du fonctionnement des écosystèmes est importante pour prédire, gérer et protéger les écosystèmes dans lesquels nous vivons et dont nous dépendons. Cette thèse y apporte une contribution en scrutant le compartiment zooplanctonique, qui joue un rôle crucial – quoiqu'encore largement méconnu – dans le fonctionnement des écosystèmes marins, et plus particulièrement les cycles biogéochimiques et le transfert trophique. La présente thèse propose trois perspectives différentes sur le fonctionnement du zooplancton, centrées sur la composition taxonomique (chapitre 1), la structuration en taille (chapitre 2) et la composition biochimique (chapitre 3), en utilisant une approche intégrée qui prend en compte les niveaux trophiques inférieurs et supérieurs dans le contexte du *Multitrophic Biodiversity Ecosystem Functioning*. Le chapitre 1 a révélé l'existence de cinq assemblages de zooplancton dans le sud de la mer du Nord et l'est de la Manche (EEC) pendant l'hiver, qui variaient en termes de productivité, d'abondance des taxons et de composition. La composition et la distribution des assemblages étaient déterminées par des variables abiotiques (nutriments dissous, salinité, profondeur, température, matière organique en suspension, chlorophylle a) et biotiques (composition du phyto- et du microplancton), des masses d'eau et des frayères de poissons. Le chapitre 2 a révélé une faible structuration de la taille du plancton entre 20 et 500 µm en ce qui concerne leur signature isotopique. Cela indique que l'omnivorie est la stratégie alimentaire dominante de cette classe de taille de plancton en hiver. Les larves de hareng (*Clupea harengus*) et de plie (*Pleuronectes platessa*) présentaient des signatures isotopiques spécifiques et différentes préférences de taille de proie. Des différences spatiales ont ainsi été observées dans la composition de la taille des proies des larves de plie échantillonnées dans les stations influencées par les rivières et dans les stations situées au centre de la Manche orientale. Le profil en acides gras (AG) du zooplancton et de la sardine différait entre la partie ouest et est de la Manche, ainsi que des différences dans la composition taxonomique du phytoplancton et du zooplancton, indiquant

un contrôle ascendant du transfert trophique de ces nutriments essentiels. Tous les chapitres ont révélé une structuration spatiale dans le fonctionnement de l'écosystème, car la variabilité spatiale des caractéristiques du zooplancton semblait être liée aux niveaux trophiques inférieurs et supérieurs. L'étude combinée de la taxonomie et des traits du zooplancton (taille et composition en AG) en relation avec les niveaux trophiques inférieurs et supérieurs a révélé des caractéristiques supplémentaires du zooplancton liées à la stratégie trophique, à la reproduction et à la survie reliant le zooplancton à l'écosystème. Ainsi, l'étude du zooplancton dans un contexte multitrophique prenant en compte différents aspects de sa diversité a contribué à une compréhension plus mécaniste du zooplancton en tant que partie et en relation avec d'autres composants de l'écosystème et a facilité l'élaboration d'hypothèses pour expliquer les schémas et les relations observés. Par conséquent, l'approche utilisée dans cette thèse semble prometteuse pour acquérir les informations nécessaires pour améliorer la représentation du zooplancton dans les modèles écosystémiques et la gestion écosystémique.